



UNIVERSITY OF
LEICESTER

Graduate School

**CARDIOVASCULAR MAGNETIC RESONANCE IMAGING IN
THE ASSESSMENT OF THE MANAGEMENT OF
MULTIVESSEL CORONARY ARTERY DISEASE IN ACUTE ST-
SEGMENT ELEVATION MYOCARDIAL INFARCTION**

Thesis submitted for the degree of
Doctor of Philosophy
at the University of Leicester

by

Dr Jamal Nasir Khan MRCP (Lond), MBChB (Hons), BMedSci (Hons)
Clinical Research Fellow
Department of Cardiovascular Sciences
University of Leicester

June 2016

Acknowledgements

My research fellowship has given me the opportunity to contribute to academic cardiology. This has been a privilege and provided me with four of the most stimulating, challenging and rewarding years of my career.

It has been a pleasure working alongside the Cardiac Research Team, MRI Radiographers, University of Leicester Clinical Wing, and Department of Cardiology at Glenfield Hospital, who have helped me at the coalface of cardiac research.

My supervisor, Dr Gerry McCann has been a continued source of guidance, encouragement, support, good humour and good company. I would like to thank him for opening my eyes to the exciting world of Cardiac MRI and inspiring me to pursue a career in cardiac imaging and lifelong involvement in academia.

Professor Anthony Gershlick, my co-supervisor has been a constant source of guidance and encouragement, and provided invaluable support for the angiographic components of my work and critique of submitted manuscripts.

I would like to thank Anvesha Singh, Sheraz Nazir and Prathap Kanagala for their support with my work and for the friendships that we have developed during our PhD fellowships and countless hours spent analysing MRIs in the 'little research room'!

I would like to thank the Cardiac Research teams at Southampton Hospital, Leeds General Hospital, Royal Derby Hospital, Kettering General Hospital, Harefield Hospital and Bournemouth Hospital; the Clinical Trials Unit at the Royal Brompton Hospital, and all members of the CvLPRIT trial steering committee for their invaluable input.

Last but not least, I am indebted to my father Nasim, mother Raazia and sisters Amina and Sadiyah. Words cannot describe how important you have been during my research period and there is no way that any of this would have been possible without your constant encouragement, understanding and good humour.

Academic outputs resulting from this thesis

The work in this thesis has contributed to the following publications and presentations at scientific conferences. They are listed most recent first.

Prizes

Best UK abstract: American College of Cardiology Scientific Sessions 2015 (San Diego, USA): CvLPRIT-CMR substudy.

Young Investigator Finalist: British Society of Cardiovascular Magnetic Resonance Annual Meeting 2015 (London, UK): CvLPRIT-CMR substudy.

Awarded Regional Scholarship (Europe): Society of Cardiovascular Magnetic Resonance / European Association of Cardiovascular Magnetic Resonance (SCMR/Euro-CMR) Scientific Sessions 2015 (Nice, France).

Publications

Publications arising from this thesis

Khan JN, Nazir SN, Singh A, Shetye A, Lai FY, Peebles C, Wong J, Greenwood JP, McCann GP. Relationship of myocardial strain and markers of myocardial injury to predict segmental recovery following acute ST-segment elevation myocardial infarction. Jun 2016. Circulation: Cardiovascular Imaging. doi: 10.1161/CIRCIMAGING.115.003457.

McCann GP*; **Khan JN***, Greenwood JP, Nazir S, Dalby M, Curzen N, Hetherington S, Kelly DJ, Blackman D, Ring A, Peebles C, Wong J, Sasikaran T, Flather M, Swanton H, Gershlick AH. The Randomized Complete vs. Lesion Only Primary PCI Trial-Cardiac MRI substudy. JACC. Dec 2015. 66:2713-24. (*= joint first authorship).

McCann GP*; **Khan JN***, Greenwood JP, Nazir S, Dalby M, Curzen N, Hetherington S, Kelly DJ, Blackman D, Ring A, Peebles C, Wong J, Sasikaran T, Flather M, Swanton H, Gershlick AH. The Randomized Complete vs. Lesion Only Primary PCI Trial-Cardiac MRI substudy. NIHR Journals. (*= joint first authorship).

Khan JN, Singh A, Nazir SA, Kanagala P, Gershlick AH, McCann GP. Comparison of cardiovascular magnetic resonance feature tracking and tagging for the assessment of left ventricular systolic strain in acute myocardial infarction. European Journal of Radiology. May 2015. 84(5):840-8. doi: 10.1016/j.ejrad.2015.02.002.

Khan JN, Nazir SA, Horsfield MA, Singh A, Kanagala P, Greenwood JP, Gershlick AH, McCann GP. Comparison of semi-automated methods to quantify infarct size and area at risk by cardiovascular magnetic resonance imaging at 1.5T and 3.0T field strengths. BMC Res Notes. Feb 2015. 8:52 doi: 10.1186/s13104-015-1007-1. 1-12.

Manuscripts arising from this thesis currently under review

Khan JN, Nazir SA, Greenwood JP, Dalby M, Curzen N, Hetherington S, Kelly DJ, Blackman D, Ring A, Peebles C, Wong J, Sasikaran T, Flather M, Swanton H, Gershlick AH, McCann GP. Infarct size following complete revascularization in patients presenting with STEMI: a comparison of immediate and staged in-hospital non-infarct related artery PCI subgroups in the CvLPRIT study. May 2016 (submitted to JCMR).

Publications related to this thesis

Khan JN, Greenwood JP, Nazir SA, Lai FY, Dalby M, Curzen N, Hetherington S, Kelly DJ, Blackman D, Peebles C, Wong J, Flather M, Swanton H, Gershlick AH, McCann GP. Infarct size following treatment with second-generation versus third-generation P2Y₁₂ antagonists in patients with multivessel coronary disease at STEMI in the CvLPRIT study. JAMA. May 2016. 31;5(6). doi: 10.1161/JAHA.116.003403.

Gershlick AH, **Khan JN**, Kelly DJ, Greenwood JP, Sasikaran T, Curzen N, Blackman DJ, Dalby M, Fairbrother KL, Banya W, Wang D, Flather M, Hetherington SL, Kelion AD, Talwar S, Gunning M, Hall R, Swanton H, McCann GP. Reply: Complete Revascularization in Patients Undergoing Primary Percutaneous Coronary Intervention for STEMI: Is It Really What We Should Be Doing? (Letter). JACC. Jul 2015. 66(3):332-3. doi:10.1016/j.jacc.2015.04.067.

Gershlick AH, **Khan JN**, Kelly DJ, Greenwood JP, Sasikaran T, Curzen N, Blackman DJ, Dalby M, Fairbrother KL, Banya W, Wang D, Flather M, Hetherington SL, Kelion AD, Talwar S, Gunning M, Hall R, Swanton H, McCann GP. Randomized trial of complete versus lesion-only revascularization in patients undergoing primary percutaneous coronary intervention for STEMI and multivessel disease: the CvLPRIT trial. JACC. Mar 2015. 65(10):963-72. doi: 10.1016/j.jacc.2014.12.038.

Khan JN, Razvi N, Nazir SA, Singh A, Masca NG, Gershlick AH, Squire I, McCann GP¹. Prevalence and extent of infarct and microvascular obstruction following different reperfusion therapies in ST-elevation myocardial infarction. JCMR. May 2014. 16:38. doi: 10.1186/1532-429X-16-38.

Kelly DJ, McCann GP, Blackman D, Curzen NP, Dalby M, Greenwood JP, Fairbrother K, Shipley L, Kelion A, Hetherington S, **Khan JN**, Nazir S, Alahmar A, Flather M, Swanton H, Schofield P, Gunning M, Hall R, Gershlick AH. Complete Versus culprit-Lesion only PRimary PCI Trial (CVLPRIT): a multicentre trial testing management strategies when multivessel disease is detected at the time of primary PCI: rationale and design. Feb 2013. Eurointervention. 8(10):1190-8. doi: 10.4244/EIJV8I10A183.

Presentations

International

Khan JN, Greenwood JP, Nazir SA, Dalby M, Curzen N, Hetherington S, Kelly DJ, Blackman D, Peebles C, Wong J, Swanton H, Flather M, Gershlick AH, McCann GP.

Infarct size in staged versus immediate complete revascularisation for multivessel disease in the Complete Versus Lesion-only PRImary PCI Trial Cardiovascular Magnetic Resonance substudy (CvLPRIT-CMR). Moderated poster presented at European Society of Cardiology Congress 2015 (London, UK).

Khan JN, Greenwood JP, Nazir S, Dalby M, Curzen N, Hetherington S, Kelly DJ, Blackman D, Ring A, Peebles C, Wong J, Sasikaran T, Flather M, Swanton H, Gershlick AH, McCann GP. The Randomized Complete vs. Lesion Only Primary PCI Trial-Cardiac MRI substudy. JACC. Dec 2015. 66:2713-24. Moderated Poster presented at American College of Cardiology Scientific Sessions 2015 (Chicago, USA)

Khan JN, Greenwood JP, Nazir, Singh A, Peebles C, Wong J, Gershlick AH, McCann GP. Relationship of myocardial strain and markers of myocardial injury to predict segmental recovery following acute ST-segment elevation myocardial infarction. Oral presentation at Society of Cardiovascular Magnetic Resonance / European Association of Cardiovascular Magnetic Resonance (SCMR/Euro-CMR) Scientific Sessions 2015 (Nice, France).

Khan JN, Singh A, Nazir SA, Kanagala P, Gershlick AH, McCann GP. Comparison of cardiovascular magnetic resonance feature tracking and tagging for the assessment of left ventricular systolic strain in acute myocardial infarction. Moderated Poster presented at Society of Cardiovascular Magnetic Resonance / European Association of Cardiovascular Magnetic Resonance (SCMR/Euro-CMR) Scientific Sessions 2015 (Nice, France).

National

Khan JN, Greenwood JP, Nazir SA, Dalby M, Curzen N, Hetherington S, Kelly DJ, Blackman D, Peebles C, Wong J, Swanton H, Flather M, Gershlick AH, McCann GP. Predictors of final left ventricular ejection fraction <35% and medium-term clinical outcomes in patients with multivessel disease at STEMI. Moderated poster presented at British Cardiovascular Society Congress 2015 (London, UK).

Khan JN, Greenwood JP, Nazir S, Dalby M, Curzen N, Hetherington S, Kelly DJ, Blackman D, Ring A, Peebles C, Wong J, Sasikaran T, Flather M, Swanton H, Gershlick AH. The Randomized Complete vs. Lesion Only Primary PCI Trial-Cardiac MRI substudy. Young Investigator Finalist Oral presentation presented at British Society of Cardiovascular Magnetic Resonance Annual Meeting 2015 (London, UK)

Khan JN, Greenwood JP, Nazir, Singh A, Peebles C, Wong J, Gershlick AH, McCann GP. Relationship of myocardial strain and markers of myocardial injury to predict segmental recovery following acute ST-segment elevation myocardial infarction. Poster presented at British Society of Cardiovascular Magnetic Resonance Annual Meeting 2015 (London, UK).

Khan JN, Nazir SA, Horsfield MA, Singh A, Kanagala P, Greenwood JP, Gershlick AH, McCann GP. Comparison of semi-automated methods to quantify infarct size and area at risk by cardiovascular magnetic resonance imaging at 1.5T and 3.0T field strengths. Poster presented at British Society of Cardiovascular Magnetic Resonance Annual Meeting 2014 (Manchester, UK) and at British Society of Cardiovascular Magnetic Resonance Annual Meeting 2014 (Southampton, UK).

Table of Contents

I. ABSTRACT.....	14
1. INTRODUCTION	15
1.1 MULTIVESSEL DISEASE AT STEMI	16
1.1.1 Management of MVD at STEMI	16
1.2 CMR SURROGATE MARKERS OF OUTCOMES FOLLOWING PPCI	24
1.2.1 Assessment of LV ejection fraction and volumes in acute STEMI.....	25
1.2.2 Assessment of myocardial strain in acute STEMI	30
1.2.3 Assessment of infarct size (IS) in acute STEMI.....	33
1.2.4 Assessment of microvascular obstruction (MVO) in acute STEMI	45
1.2.5 Assessment of intramyocardial haemorrhage (IMH) in acute STEMI.....	51
1.2.6 Assessment of ischaemic area at risk (oedema) and myocardial salvage in acute STEMI.....	55
1.2.7 T1, T2 and T2* quantification and mapping in acute STEMI.....	63
1.2.8 Assessment of right ventricular involvement in acute STEMI	65
1.2.9 When is the optimal time to undertake CMR assessment post acute STEMI?.....	66
1.3 SUMMARY.....	67
1.4 AIMS AND ORIGINAL HYPOTHESES.....	72
1.4.1 Assessment of IS.....	72
1.4.2 Assessment of MSI, MVO and IMH.....	72
1.4.3 Assessment of LV function.....	73
1.4.4 Assessment of ischaemic burden	73
1.4.5 Assessment of clinical outcomes	73
1.4.6 Assessment of infarct characteristics using semi-automated quantification methods.....	73
1.4.7 Assessment of LV strain using novel quantification methods	74
1.4.8 Assessment of predictors of improvement in segmental function.....	74
1.4.9 Assessment of IS following staged and immediate in-hospital CR strategies.....	75
2. METHODS	76
2.1 STUDY OVERVIEW	77
2.1.1 Study design.....	77
2.1.2 Study population	78
2.1.3 Recruitment.....	78
2.1.4 Treatment.....	80
2.1.5 Trial management and governance	82
2.1.6 Ethics.....	82
2.1.7 Patient and Public Involvement (PPI)	83
2.2 HISTORY TAKING	83
2.3 INVESTIGATIONS AND ANALYSES	83
2.3.1 Angiographic analysis	84
2.3.2 Creatine kinase and clinical bloods.....	86
2.3.3 Electrocardiography.....	87
2.4 CARDIOVASCULAR MAGNETIC RESONANCE	87
2.4.1 Acute CMR	87
2.4.2 Follow-up CMR	92
2.4.3 CMR analysis.....	95
2.5 STUDY OUTCOMES AND DATA HANDLING.....	106
2.5.1 Data handling.....	106
3. SEMI-AUTOMATED CMR METHODS OF ASSESSING INFARCT CHARACTERISTICS	107
3.1 BACKGROUND	108

3.2	METHODS	108
3.2.1	Study cohort	108
3.2.2	CMR image acquisition	109
3.2.3	IS and AAR Quantification.....	109
3.2.4	Statistical analysis	112
3.3	RESULTS.....	112
3.3.1	Baseline characteristics	112
3.3.2	Infarct size.....	114
3.3.3	Area At Risk extent	119
3.4	DISCUSSION.....	123
3.4.1	Infarct size.....	123
3.4.2	Area At Risk.....	126
3.4.3	Limitations	128
3.4.4	Conclusions	128
3.4.5	Original contribution to knowledge.....	129
3.4.6	My contribution	129
4.	FEATURE-TRACKING AND TAGGING ASSESSMENT OF STRAIN IN ACUTE STEMI	130
4.1	BACKGROUND	131
4.2	METHODS	131
4.2.1	Study population	131
4.2.2	Cardiovascular MRI	131
4.2.3	MRI analysis	132
4.2.4	Statistical analysis	133
4.3	RESULTS.....	134
4.3.1	Baseline characteristics	134
4.3.2	Global strain on FT and tagging	135
4.3.3	Association with infarct extent.....	135
4.3.4	Association with oedema	138
4.3.5	Association with myocardial salvage index	141
4.3.6	Interobserver and intraobserver agreement of strain assessment	141
4.4	DISCUSSION	141
4.4.1	Limitations	146
4.4.2	Conclusions	147
4.4.3	Original contribution to knowledge.....	147
4.4.4	My contributions	148
5.	THE CVLPRIT-CMR SUBSTUDY	149
5.1	BACKGROUND	150
5.2	METHODS.....	150
5.2.1	Study design.....	150
5.2.2	Analysis	151
5.2.3	Study outcomes	151
5.2.4	Statistical analysis	152
5.3	RESULTS.....	154
5.3.1	Main CvLPRIT study	154
5.3.2	CvLPRIT-CMR substudy	155
5.4	DISCUSSION.....	171
5.4.1	Limitations	174
5.4.2	Conclusions	174
5.4.3	Original contribution to knowledge.....	174
5.4.4	My contribution	174
6.	CMR PREDICTORS OF SEGMENTAL FUNCTIONAL RECOVERY IN STEMI.....	176

6.1	BACKGROUND	177
6.2	METHODS	178
6.2.1	Study population	178
6.2.2	Cardiovascular MRI	178
6.3	RESULTS.....	180
6.3.1	Baseline characteristics	180
6.3.2	Segmental systolic function post STEMI	181
6.3.3	Predictors of segmental recovery in dysfunctional segments post STEMI	184
6.3.4	SEE and Ecc as predictors of segmental functional recovery where SEE $\geq 50\%$	185
6.3.5	CMR predictors of segmental functional recovery stratified by revascularisation strategy.....	185
6.4	DISCUSSION	189
6.4.1	Prediction of segmental functional recovery with LGE.....	189
6.4.2	Prediction of segmental functional recovery with strain	191
6.4.3	Limitations	192
6.4.4	Clinical Summary	192
6.4.5	Conclusions.....	193
6.4.6	Original contribution to knowledge.....	193
6.4.7	My contribution	193
7.	CMR FINDINGS IN STAGED VERSUS IMMEDIATE COMPLETE REVASCULARISATION.....	194
7.1	BACKGROUND	195
7.2	METHODS	195
7.2.1	Study design, data acquisition/analysis.....	195
7.2.2	Outcome measures.....	196
7.2.3	Statistical analysis	196
7.3	RESULTS.....	197
7.3.1	Baseline characteristics	197
7.3.2	Angiographic and PCI details	198
7.3.3	CMR data	200
7.3.4	Clinical outcomes.....	203
7.4	DISCUSSION	204
7.4.1	Infarct size, MVO and myocardial salvage	205
7.4.2	Non-IRA MI	206
7.4.3	Clinical outcomes.....	207
7.4.4	Limitations	207
7.4.5	Conclusions.....	208
7.4.6	Original contribution to knowledge.....	208
7.4.7	My contribution	208
8.	THESIS CONCLUSIONS AND RECOMMENDATIONS FOR FURTHER RESEARCH	209
8.1	THESIS CONCLUSIONS AND RECOMMENDATIONS FOR FUTURE STUDY	210
8.1.1.	Semi-automated CMR methods of assessing infarct characteristics.....	210
8.1.2	Feature-Tracking and Tagging assessment of strain in acute STEMI	210
8.1.3	The CvLPRIT-CMR substudy	210
8.1.4	CMR predictors of segmental functional recovery in STEMI	211
8.1.5	CMR findings in staged vs. immediate complete revascularisation	211
9.	APPENDICES	213
SUPPLEMENTAL DATA.....	213	
Supplemental Data 1:	Prospective registry studies investigating MVD revascularisation at PPCI	213
Supplemental Data 2:	Retrospective studies investigating MVD revascularisation at PPCI	215
Supplemental Data 3:	Bland-Altman Plots for Infarct Size (IS) Quantification at 1.5T	217
Supplemental Data 4:	Bland-Altman Plots for Infarct Size (IS) Quantification at 3.0T	218
Supplemental Data 5:	Bland-Altman Plots for Area At Risk (AAR) Quantification at 1.5T.....	219
Supplemental Data 6:	Bland-Altman Plots for Area At Risk (AAR) Quantification at 3.0T.....	220

Supplemental Data 7: Bland-Altman Plots for Myocardial Salvage (MSI) Quantification at 1.5T	221
Supplemental Data 8: Bland-Altman Plots for Myocardial Salvage (MSI) Quantification at 3.0T	222
Supplemental Data 9: Bland-Altman Plots of Intraobserver Variability for Global Strain	223
Supplemental Data 10: Bland-Altman Plots of Interobserver Variability for Global Strain	224
Supplemental Data 11: Bland-Altman Plots of Intraobserver Variability for Segmental Strain	225
Supplemental Data 12: Bland-Altman Plots of Interobserver Variability for Segmental Strain	226
Supplemental Data 13: Patients with ≥ 2 'acute' MI: infarct characteristics (CvLPRIT-CMR).....	227
Supplemental Data 14: CMR data excluding patients with chronic infarcts on acute CMR	228
Supplemental Data 15: SEE and Ecc as predictors of segmental recovery where SEE $\geq 50\%$	229
Supplemental Data 16: Segmental function and predictors of segmental recovery by treatment.....	230
Supplemental Data 17: Patients with ≥ 2 'acute' MI: infarct characteristics (Staged vs Immediate) ...	233
Supplemental Data 18: CMR data excluding patients with chronic infarcts on acute CMR	234
Appendix 1: Verbal assent document inviting study participation.....	236
Appendix 2: Interim DSMB approval letter.....	237
Appendix 3: Full Statistical Analysis Plan for CvLPRIT-CMR	238
Appendix 4: REDCAP database lock confirmation for CvLPRIT-CMR	252
PUBLICATIONS ARISING FROM THIS THESIS	253
Paper 1: Circulation: Cardiovascular Imaging (June 2016)	253
Paper 2: JACC (December 2015)	262
Paper 3: Eur J Radiol (March 2015)	274
Paper 4: BMC Research Notes (Feb 2015)	283
10. REFERENCES	298

List of Tables

Table 1:	Key studies demonstrating the medium-term prognostic importance of MVD in STEMI	17
Table 2:	Multicentre prospective randomised interventional studies of revascularisation for MVD at PPCI.....	18
Table 3:	Single-centre prospective randomised interventional studies of revascularisation for MVD at PPCI.....	19
Table 4:	Potential risks and benefits of a CR strategy for MVD at PPCI	22
Table 5:	CMR studies illustrating the prognostic importance of LVEF in acute STEMI.....	28
Table 6:	Studies illustrating the prognostic importance of LV volumes and adverse LV remodelling in STEMI ...	29
Table 7:	Studies illustrating the prognostic importance of LV strain in acute STEMI.....	33
Table 8:	Temporal changes in CMR-derived infarct size in STEMI	39
Table 9:	CMR studies illustrating importance of segmental LGE extent and functional recovery in STEMI	42
Table 10:	CMR studies illustrating importance of infarct size on LV function and remodelling in STEMI	43
Table 11:	CMR studies illustrating the prognostic importance of infarct in acute STEMI.....	44
Table 12:	Temporal changes in CMR-derived late MVO in acute STEMI.....	47
Table 13:	CMR studies illustrating the importance of Late MVO on LV function and remodelling in STEMI.....	48
Table 14:	CMR studies illustrating the prognostic importance of Late MVO in acute STEMI	50
Table 15:	CMR studies illustrating the importance of IMH on LV function and remodelling in STEMI.....	54
Table 16:	Temporal changes in CMR-derived area at risk and myocardial salvage index in acute STEMI	59
Table 17:	CMR studies showing importance of myocardial salvage on LV function and remodelling in STEMI ...	61
Table 18:	CMR studies illustrating the prognostic importance of myocardial salvage index in acute STEMI	62
Table 19:	CMR studies illustrating the prognostic importance of right ventricular infarction in acute STEMI	66
Table 20:	Key studies illustrating the independent predictive value of CMR markers for LV remodelling	69
Table 21:	Key studies illustrating the independent predictive value of CMR markers for prognosis	70
Table 22:	Summary and order of investigations	84
Table 23:	TIMI and Rentrop visual angiographic scoring systems.....	85
Table 24:	CMR scanners used at the centres	87
Table 25:	CMR image quality grading scale.....	95
Table 26:	Baseline demographics by CMR field strength cohort	113
Table 27:	Infarct size (IS) results at 1.5T by quantification method and corresponding reproducibilities.....	115
Table 28:	Infarct size (IS) results at 3.0T by quantification method and corresponding reproducibilities.....	116
Table 29:	Time taken per patient for Infarct Size (IS) and Area at risk (AAR) quantification	118
Table 30:	Area at risk (AAR) by field strength and quantification method and corresponding reproducibility..	122
Table 31:	Patient characteristics and MRI data: quality and analysis time.....	134
Table 32:	Myocardial tracking and quantification time by method	135
Table 33:	Agreement of peak systolic strain by feature tracking and tagging	136
Table 34:	Correlation between strain by FT and tagging and infarct size, area at risk and myocardial salvage.	137
Table 35:	Peak strain by FT and tagging and segmental transmural late gadolinium enhancement.....	139
Table 36:	Interobserver and intraobserver agreement of strain measured by FT and tagging	142
Table 37:	Recruitment at the study centres.....	156
Table 38:	Baseline characteristics of main CVLPRIT and CMR substudy cohort.....	157
Table 39:	Baseline characteristics of the IRA-only and CR CMR substudy	158
Table 40:	Periprocedural details in the complete revascularization and infarct related artery-only groups	159
Table 41:	Acute CMR image quality	160
Table 42:	Intra and interobserver variability of CMR measurements	161
Table 43:	Acute CMR data.....	162
Table 44:	Follow-up CMR image quality.....	165
Table 45:	Follow-up CMR data	166
Table 46:	Volumetric data at in those undergoing both CMR scans	167
Table 47:	Infarct characteristics in patients undergoing both CMR scans	168
Table 48:	Safety profile: Inpatient clinical events	169
Table 49:	Twelve-month clinical outcomes (time to first event MACE)	170
Table 50:	Baseline demographics and CMR characteristics	180
Table 51:	Segmental extent of myocardial injury according to degree of dysfunction at acute CMR	182
Table 52:	CMR predictors of segmental improvement and normalisation in dysfunctional segments	186
Table 53:	Baseline characteristics of the CvLPRIT and immediate vs. staged CR CMR substudy participants.....	197
Table 54:	Periprocedural details in the Immediate and staged in-hospital complete revascularisation groups	199
Table 55:	Acute CMR data.....	201
Table 56:	Follow-up CMR data	203
Table 57:	Clinical outcomes	204

List of Figures

Figure 1:	CMR markers are ideal surrogate biomarkers for the assessment of revascularisation in STEMI.....	25
Figure 2:	The three planes of LV strain assessment.....	31
Figure 3:	CMR assessment of strain using tissue tagging.....	31
Figure 4:	Mechanism of late gadolinium enhancement (LGE)	34
Figure 5:	Late gadolinium enhancement of acute infarct	35
Figure 6:	Modifications to the standard 2D segmented, magnitude LGE sequence for infarct size analysis.....	37
Figure 7:	Validation of late gadolinium enhancement imaging on animal models.....	38
Figure 8:	Replacement of infarct by collagenous scar in canine myocardium	41
Figure 9:	Early and Late Microvascular Obstruction on CMR.....	46
Figure 10:	Intramycardial haemorrhage on CMR.....	52
Figure 11:	Alternative CMR sequences to dark-blood T2w spin echo for visualising oedema.....	57
Figure 13:	Importance of quantifying area at risk (AAR)	58
Figure 14:	Effect of cardiac motion on T2w-STIR and T2 maps.....	64
Figure 15:	T2* mapping for assessment of intramycardial haemorrhage (IMH)	64
Figure 16:	The Complete Versus Lesion-only PRimary PCI pilot (CvLPRIT) study	77
Figure 17:	MVD at PPCI managed with CR (complete revascularisation) [Patient X708].....	81
Figure 18:	2D Quantitative Coronary Angiography (QCA) [Patient X642].....	86
Figure 19:	MRI protocol for the acute CMR scan (CMR 1)	88
Figure 20:	SSFP Cine imaging in the long-axis planes [Patient X797]	89
Figure 21:	SSFP Cine imaging in a contiguous short-axis stack [Patient X797].....	90
Figure 22:	T2w-STIR imaging showing myocardial oedema (area-at-risk) [X797].....	90
Figure 23:	Myocardial tissue tagging images acquired using SPAMM [Patient X797]	91
Figure 24:	Late gadolinium enhancement imaging (LGE) showing infarction [X797]	92
Figure 25:	MRI protocol for the follow-up CMR scan (CMR 2).....	94
Figure 26:	Myocardial contouring for ventricular volumetric analysis [Patient X797].....	96
Figure 27:	Exclusion of blood-pool artefact from oedema quantification	97
Figure 28:	Oedema quantification on T2w-STIR imaging [Patient X797]	98
Figure 29:	Manual inclusion of IMH and MVO in area at risk and infarct size [Patient X670]	99
Figure 30:	Tagging strain assessment using <i>Intag</i> software [Patient X596]	100
Figure 31:	Feature Tracking strain assessment [Patient X596]	101
Figure 32:	Calculation of ascending aortic distensibility [Patient X797]	102
Figure 33:	Full-Width Half-Maximum infarct quantification method on LGE [Patient X797]	104
Figure 34:	The range of perfusion patterns possible [Patients (1) X589, (2) X623, (3) X512]	106
Figure 35:	Otsu's Automated Thresholding (OAT) method.....	111
Figure 36:	Mean Infarct Size (IS) by Quantification Method.....	117
Figure 37:	Mean Area-At-Risk (AAR) by Quantification Method.....	120
Figure 38:	Infarct size and Area-At-Risk quantification at 3.0T.....	121
Figure 39:	Hyperenhancement with OAT without obvious Infarct	125
Figure 40:	Hyperenhancement and hypoenhancement on cine imaging	135
Figure 41:	Peak systolic strain by feature tracking and tagging in infarct, adjacent and remote segments.....	140
Figure 42:	CVLPRIT-CMR recruitment	155
Figure 43:	Reasons for non-participation in CMR substudy and follow-up CMR	156
Figure 44:	Median total infarct size at acute CMR in the treatment arms.....	163
Figure 45:	Examples of patients with more than one 'acute' MI on CMR.	165
Figure 46:	Kaplan-Meier survival curves for 12-month clinical outcomes	171
Figure 47:	Wall-motion scoring at acute and follow-up CMR by segmental extent of enhancement	182
Figure 48:	Recovery in dysfunctional segments at follow-up CMR by segmental extent of enhancement.....	183
Figure 49:	Recovery in dysfunctional segments at follow-up CMR by segmental myocardial salvage	183
Figure 50:	CMR predictors of segmental improvement assessed using Receiver Operator Curves	187
Figure 51:	CMR predictors of segmental normalisation assessed using Receiver Operator Curves	188
Figure 52:	CONSORT diagram for patient recruitment	196
Figure 53:	Examples of patients with >1 'acute' MI on CMR.	202

i. ABSTRACT

Background: Cardiovascular Magnetic Resonance (CMR) comprehensively assesses myocardial injury in ST-segment elevation myocardial infarction (STEMI). Complete revascularization (CR) may improve outcomes compared to an infarct-related artery (IRA)-only strategy in patients with multivessel disease at primary percutaneous coronary intervention (PPCI). However, CR could cause additional non-IRA infarcts.

Objectives: To determine optimal techniques for quantifying infarct characteristics and myocardial strain in STEMI. To assess whether in-hospital CR was associated with increased myocardial injury compared to an IRA-only strategy in the CvLPRIT-CMR substudy. To investigate differences in myocardial injury associated with staged and immediate in-hospital CR. To assess CMR predictors of segmental myocardial functional recovery post-STEMI.

Methods: Multicentre PROBE-design trial in STEMI patients with multivessel disease and ≤ 12 hours symptom duration. Patients were randomized to IRA-only PCI or in-hospital CR. Contrast-enhanced CMR was performed at 3 days post-PPCI and stress CMR at 9 months. The pre-specified primary endpoint was infarct size (IS) on acute CMR. Accuracy, feasibility and observer variability for semi-automated CMR methods of quantifying infarct size and area-at-risk (AAR) were assessed. Strain quantification using Feature Tracking and tagging was assessed. Functional recovery in dysfunctional segments was assessed at follow-up CMR on wall-motion scoring.

Results: 205 of 296 patients in the main trial participated in CvLPRIT-CMR and 203 (105 IRA, 98 CR) completed acute CMR. There was a strong trend towards reduced AAR in the CR group ($p=0.06$). Total IS was similar with IRA-only PCI: 13.5% (6.2-21.9%) and CR: 12.6% (7.2-22.6) of LV mass, $p=0.57$. The CR group had an increased incidence of non-IRA MI at acute CMR (22/98 vs. 11/105, $p=0.02$). There was no difference in total IS or ischemic burden between the groups at follow-up CMR. Full-width half-maximum, Otsu's Automated Thresholding and Feature Tracking were used for IS, AAR and strain analysis. Immediate CR was associated with reduced IS.

Conclusions: In-hospital CR for multivessel disease in STEMI leads to a small increase in CMR non-IRA MI but total IS was not different from an IRA-only PCI strategy. The comparable ischaemic burden in the groups suggests that the similarly improved medium-term clinical outcomes seen in the CvLPRIT, PRAMI and DANAMI-3-PRIMULTI studies are unlikely to be ischaemia-driven and instead may result from stabilization of unstable plaques and improved collateral flow to the ischaemic AAR.

CHAPTER ONE

1. INTRODUCTION

1.1 Multivessel disease at STEMI

Coronary artery disease is the commonest cause of adult mortality worldwide. In Europe, its impact is huge, with acute myocardial infarction accounting for 17% of annual mortality in males, and 14% in females¹. ST-segment elevation myocardial infarction (STEMI) is at the extreme of the coronary artery disease spectrum and results from complete occlusion or critically impaired coronary flow due to plaque rupture and subsequent thrombus formation in a main epicardial coronary artery or one of its side-branches, deemed the infarct related artery (IRA). Primary percutaneous coronary angioplasty (PPCI) offers direct visualisation of the occlusive lesion and revascularisation and has replaced thrombolysis as the preferred treatment strategy in STEMI^{2, 3}. Multivessel disease (MVD) is typically defined as the presence of $\geq 70\%$ stenosis in ≥ 1 non-infarct related artery (N-IRA) at PPCI. Occurring in approximately 50% of STEMI^{4, 5}, MVD is an independent predictor (IP) of medium-term prognosis as summarised in Table 1.⁴⁻¹⁰ Presence of a chronic total occlusion (CTO) in the N-IRA confers particularly poor prognosis and was an independent predictor of mortality at 3.1 years and impaired left ventricular ejection fraction (LVEF $< 40\%$) at 12 months post-STEMI after correcting for the higher risk baseline profile of CTO patients and cardiogenic shock¹¹.

1.1.1 Management of MVD at STEMI

1.1.1.1 Evidence base for revascularisation strategies for MVD at PPCI

The evidence base for the management of MVD at PPCI is currently weak, and at the time that this study (The Randomized Complete vs. Lesion Only Primary PCI Trial: Cardiovascular MRI substudy [CvLPRIT-CMR]) commenced in May 2011, it was based on small prospective studies, small retrospective studies and moderate-to-large registry studies. The retrospective studies suffer from selection bias, non-matched treatment arms and unrecorded confounding variables. Until recently, prospective studies have been limited by a lack of adequately powered, large-scale randomised trials of revascularisation strategies with hard clinical endpoints.

Table 1: Key studies demonstrating the medium-term prognostic importance of MVD in STEMI

Study	Year	n	Main findings	Mean F/U
Tarantini ⁹	2010	288	MVD was IP of non-fatal MI (OR 5.7), combined death/MI (OR 4.8) and combined MACE (OR 4.7). MVD also IP for LV remodelling (OR 2.2)	32m
Dziewierz ⁴	2010	1598	MVD was IP (HR 1.58) for mortality at 12 months in a model including left anterior descending artery IRA, Killip class	12m
Corpus ¹⁰	2004	820	Significantly higher non-fatal MI, target vessel revascularisation, mortality, MACE at 30 days in MVD. MVD was IP of mortality at 12 months (OR 3.3) in model including age, renal function and LV ejection fraction (LVEF)	12m
Sorajja ⁵	1997	2082	Increasing composite MACE at 12 months with number of diseased vessels. MVD was strongest IP for MACE (HR 1.9), mortality (HR 2.6)	12m
Jaski ¹²	1992	151	MVD was only IP for prediction of angioplasty success (75 vs. 92%, p<0.005) on stepwise logistic regression	Inpatient
Muller ⁶	1991	236	Reduced LVEF and increased mortality in MVD group. MVD was strongest IP of inpatient mortality in model including LVEF, age, TIMI post lysis.	Inpatient

IP= independent predictor, OR= odds ratio, HR= hazard ratio, MACE= major adverse cardiovascular events

Prospective interventional studies are summarised in Tables 2 and 3. Registry and retrospective studies are summarised in Supplemental Data 1 and 2 respectively. Studies to date have provided conflicting data on the safety and efficacy of complete (CR) versus infarct-related artery (IRA)-only revascularisation, with registry data suggesting increased risk with complete revascularisation and prospective studies demonstrating equipoise between the strategies. The resulting lack of consensus regarding management of MVD at PPCI was reflected by the US Cardiovascular Data Registry, which demonstrated wide variation in practice, with 0-38% of MVD patients undergoing complete revascularisation at PPCI on registry studies^{13, 14}.

Table 2: Multicentre prospective randomised interventional studies of revascularisation for MVD at PPCI

Study	Year	n	Inclusion criteria	Exclusion criteria	Median F/U	IRA (%)	CR (%)	SR (%)	Outcomes (primary [PO], secondary [SO])	Main findings
Engstrom ¹⁵ (DANAMI-3)	2015	627	MVD >50%,	Shock, CABG, ST, bleed risk	27m	50	50	0	PO: combined MACE. SO: individual MACE, CV death, HF/ACS, angina, 90d CMR: MSI, 12m echo: LVEF	CR: ↓ PO (HR 0.56, 13 vs. 22%) driven by ↓ N-IRA revasc (5% vs. 17%). SO similar. CR arm: 31% FFR >0.8 and no N-IRA PCI
Wald ¹⁶ (PRAMI)	2014	465	MVD >50%	Shock, CABG, LMS, only N-IRA is CTO	23m	50	50	0	PO: combined MACE (cardiac death, re-MI, refractory angina) and individual MACE. SO: non-cardiac death, repeat revasc	↓ Combined MACE in CR arm (HR 0.35, 14% ARR). Similar individual MACE reduction (HR~0.35). Similar complications rate, LOS. ↓ Need stress testing with CR
Di Mario ¹⁷	2005	69	MVD >70%, TTR <12h	CABG, LMS, shock	12m	25	75	0	PO: 12m revasc. SO: 12m MACE combined (death, MI), 12m cost	Weak trend ↓ revasc in IRA (35% vs. 15%, p=0.1). 12m MACE and cost similar.

(Studies highlighted in blue favour in-hospital CR; yellow favour IRA-only PCI; pink favour Staged PCI; white no consensus)

IRA= Infarct-related artery only, CR= complete in-hospital revascularisation, SR= staged complete revascularisation (outpatient N-IRA PCI)

Inclusion criteria: MVD= multivessel disease, LMS= left-main stem disease >50% stenosis, TTR= symptom time. *Exclusion criteria:* CABG= coronary artery bypass surgery, CTO= chronic total occlusion, CKD= chronic kidney disease, AF= atrial fibrillation, ST= stent thrombosis, valve= severe valve disease. *Outcomes:* MACE= major adverse cardiovascular events, re-MI = reinfarction, CVA= cerebrovascular accident, ACS= acute coronary syndrome, HF= heart failure, LVEF= left ventricular ejection fraction. *Main findings:* IRA= infarct-related artery only revascularisation, ARR= absolute risk reduction, FFR= fractional flow reserve, LVEF= left ventricular ejection fraction, LOS= in-hospital length of stay.

Table 3: Single-centre prospective randomised interventional studies of revascularisation for MVD at PPCI

Study	Year	n	Inclusion criteria	Exclusion criteria	Median F/U	IRA (%)	CR (%)	SR (%)	Outcomes (primary [PO], secondary [SO])	Main findings
Tarasov ¹⁸	2014	89	MVD >70%	Shock, LMS	6m	0	48	52	PO: combined mortality, MI, revasc	Staged PCI d8. No difference PO, SO, ST.
Ghani ¹⁹	2012	121	MVD >50%	CTO, CABG, LMS, AF, >80	6m	33	0	67	PO: combined 3y MACE (mortality, re-MI, repeat revasc)	Similar mortality, combined MACE. ↑Re-MI, TVR with CR. Non-TVR ↑in IRA.
Maamoun ²⁰	2011	78	MVD >70%, TTR <12h	Shock, LMS	12m	0	54	46	PO: combined MACE (death, re-MI, ACS, repeat revasc, CVA)	Staged PCI d7. No difference in PO (19% vs. 26%, p=0.06)
Politi ²¹	2010	214	MVD >70% TTR <12h	Shock, LMS, CABG, valve	30m	39	30	31	PO: combined MACE (death, ACS hospitalisation, repeat revasc)	IRA ↑PO, similar in CR and SR, driven by in-hospital death, revasc, ACS. Similar LOS
Dambrink ²²	2010	121	MVD >50%	CTO, CABG, LMS, AF, >80	6m	33	0	67 FFR	PO: 6m nuclear LVEF. SO: 6m MACE (death, re-MI, revasc)	FFR-staged <7d of PPCI. 40% N-IRA needed no PCI on FFR. No in PO or SO
Khattab ²³	2008	73	MVD >70%	LMS, prev MI	12m	62	38	0	PO: Combined MACE (death, MI, CVA)	No difference PO (28% IRA, 24% CR). CR safe
Ochala ²⁴	2004	92	MVD >70%, TTR <12h	LMS, shock, CABG, valve	6m	0	52	48	PO: 6m ΔLVEF, ↑5% LVEF. SO: combined MACE (death, MI, revasc)	Staged PCI d27. CR ↑6m LVEF increase, ↑% with +>5% LVEF at 6m. MACE similar

(Studies highlighted in **blue** favour in-hospital CR; **yellow** favour IRA-only PCI; **pink** favour Staged PCI; white no consensus)

IRA= Infarct-related artery only, CR= complete in-hospital revascularisation, SR= staged complete revascularisation (outpatient N-IRA PCI)

Inclusion criteria: MVD= multivessel disease. *Exclusion criteria:* CABG= coronary artery bypass surgery, CTO= chronic total occlusion, AF= atrial fibrillation, valve= severe valve disease, LMS= left-main stem disease >50% stenosis. *Outcomes:* MACE= major adverse cardiovascular events, re-MI = reinfarction, CVA= cerebrovascular accident, ACS= acute coronary syndrome, LVEF= left ventricular ejection fraction. *Main findings:* IRA= infarct-related artery only revascularisation, FFR= fractional flow reserve, LVEF= left ventricular ejection fraction.

The largest meta-analysis of prospective RCTs comparing CR at the index PPCI procedure with staged and IRA-only revascularisation included 7 studies (n=1303)²⁵. The primary outcome was combined 12-month MACE (mortality, recurrent MI and repeat revascularisation). CR at PPCI was associated with reduced combined MACE (OR 0.59) driven by a reduced incidence of recurrent MI (OR 0.48) and repeat revascularisation (OR 0.51), and trend towards reduced mortality (OR 0.54, p=0.09). The largest meta-analysis to date²⁶ included 2 prospective and 17 retrospective studies (n=61764). It demonstrated reduced 30-day MACE (OR 0.68) with CR during the index admission compared with IRA-only revascularisation, driven by reduced repeat revascularisation. Two-year MACE was 40% lower with CR, driven by a 33% reduction in mortality and 43% reduction in repeat PCI. These meta-analyses suggest that CR is a safe and potentially more effective strategy for MVD at PPCI and indicate a need for larger prospective RCTs and re-evaluation of current guidelines.

The largest two RCTs to date have been published since the commencement of CvLPRIT-CMR and have shown improved medium-term clinical outcomes with CR.

DANAMI-3-PRIMULTI (2015, n=627)

The recent Third Danish Study of Optimal Acute Treatment of Patients with STEMI (DANAMI-3-PRIMULTI)¹⁵ compared FFR-guided CR at ≥48hr post PPCI with IRA-only PPCI. It showed a 45% relative risk reduction in the primary outcomes of combined all-cause mortality, reinfarction and N-IRA revascularisation with FFR-guided CR (HR 0.56, p=0.004), driven by reduced N-IRA revascularisation (HR 0.31, p<0.001). It concluded that FFR-guided CR during the index admission improves prognosis. There are however important limitations of this study warranting discussion:

- The study does not evaluate the efficacy of CR at the index procedure.
- Patients were randomised after IRA PCI. Selection bias may result from preferential inclusion of patients with technically attractive N-IRA disease.
- Time to reperfusion, a crucial determinant of outcome, was not presented.
- There was a strong trend (p=0.1) towards higher prevalence of diabetes in the IRA PCI arm, however this was not adjusted for in the assessment of clinical outcomes.

- No imaging of ventricular function or myocardial damage was performed during the index admission. This could have provided important prognostic information.
- The definition of significant N-IRA disease of $\geq 50\%$ stenosis in any angiographic projection is less severe than the majority of studies, which use a $\geq 70\%$ cut-off.
- Of the patients randomised to CR, 39% of patients did not receive this treatment, of which 31% were due to FFR > 0.80 at the second procedure.
- CR was FFR-guided, which is not in keeping with current clinical practice and hence the results are less generalizable to contemporary practice.
- There is no information about objective methods demonstrating ischaemia in patients who underwent outpatient N-IRA revascularisation.

PRAMI (2014, n=465)

The Preventative Angioplasty in Myocardial Infarction (PRAMI)¹⁶ study is the second-largest prospective RCT. PRAMI compared CR at the index procedure with IRA-only PPCI and demonstrated a 65% relative risk reduction in the primary outcome of combined (cardiac death, reinfarction, refractory angina) and individual MACE with CR (HR 0.35, $p < 0.001$) at a mean of 23-months follow-up. Repeat revascularisation was reduced (HR 0.30) and non-invasive ischaemia testing was required in fewer patients (16.7% vs. 33.3%) in the CR arm. It concluded that CR at the index procedure improves prognosis. This study also has important limitations warranting discussion:

- There were more patients with diabetes and anterior infarcts in the IRA-only arm. These are known to adversely affect prognosis post MI^{27, 28}.
- Time to reperfusion data was not presented.
- The study does not evaluate whether CR at the index procedure is a more appropriate strategy compared with staged in-hospital PCI of N-IRAs.
- Patients were randomised after IRA PCI, with the potential for selection bias.
- No imaging of ventricular function or myocardial damage was performed.
- The definition of significant N-IRA disease of $\geq 50\%$ stenosis in any angiographic projection is less severe than the majority of studies, which use a $\geq 70\%$ cut-off.
- A range of non-invasive ischaemia assessment techniques were used in patients with refractory angina. There are no data on the number of patients undergoing

each method or rationale behind modality selection. This could affect the secondary endpoint of repeat revascularisation due to varying sensitivities of the modalities. In addition, ischaemia testing was used twice as commonly in the IRA-only arm, which could have contributed to their increased repeat revascularisation.

- Infarction was defined by elevated serum troponin >99th centile. Since there was no direct infarct visualisation using non-invasive imaging (i.e. CMR late gadolinium [LGE] imaging), this could result in an inability to detect peri-PCI infarcts during CR at PPCI, and an overestimation of peri-PCI infarcts during elective outpatient PCI.

1.1.1.2 Potential mechanisms relating CR and prognosis

The potential risks and benefits of CR are summarised in Table 4.

Table 4: Potential risks and benefits of a CR strategy for MVD at PPCI

Potential Benefits of CR strategy	Potential Risks of CR strategy
Limitation of infarct size and increased myocardial salvage by improving collateral flow to infarct and peri-infarct zones	Infarct size may be increased through peri-procedural infarcts (see 1.1.3.1) ^{29, 30}
Improved blood flow to remote myocardial regions, which are known to be implicated in left ventricular remodelling ^{9, 31}	Increased risk of contrast-induced nephropathy due to increased contrast load ³²
Manage unstable N-IRA lesions ^{33, 34}	Increased procedural time and radiation exposure during potential haemodynamic and clinical instability seen in acute STEMI ^{8, 32}
Reduced overall hospital stay and total cost of care through single procedure	Prothrombotic and inflammatory milieu during STEMI increase risks of stent thrombosis and restenosis ³⁵
Reduced ischaemia burden post MI, which could improve clinical outcomes. There are no data on CR at PPCI but this has been shown to improve outcomes in acute MI in the subsequent 3 months with silent ischaemia on functional testing ³⁶	Vasospasm and endothelial dysfunction can overestimate N-IRA lesion severity, resulting in PCI of lesions that would neither cause ischaemia or symptoms. ^{22, 37}
Reduced need for outpatient non-invasive ischaemia testing and revascularisation ¹⁶	Limited ability to discuss treatment of N-IRA lesions with patient and family ³⁴
Reduced risk of vascular complications through single vascular access site	Complications of N-IRA PCI could be catastrophic during PPCI ('double myocardial jeopardy') ³⁴

Peri-procedural (PCI-related) MI

Of particular interest is peri-procedural MI (PMI), defined as new myocardial injury directly resulting from revascularisation procedures. PMI related to PCI can result from microvascular damage (emboli, spasm, platelet activation) seen in distal injury, or dissection and side-branch occlusion injury adjacent to stent placement^{29, 38}. The recent European Society of Cardiology (ESC) Third Universal Definition of Myocardial Infarction defines PMI related to PCI as 'Type 4a MI' based on Troponin values >5 x 99th percentile within 24 hours of PCI in patients with normal troponin levels pre-PCI, or a >20% increase in patients with pre-existing troponin elevation³⁹. A large meta-analysis demonstrated an incidence of Type 4a MI of 15% and resultant increased in-hospital and 18-month MACE (OR 2.25)⁴⁰. MVD independently predicted PCI-related PMI in acute coronary syndromes⁴⁵ and elective PCI^{41, 42} on enzymatic criteria.

Cardiovascular MRI-based infarct is increasingly being used as the primary marker of PMI. It is more accurate as the extent and location of injury can be assessed due to the high spatial resolution of LGE imaging. CMR-based studies illustrate an incidence of PMI related to PCI for stable coronary artery disease^{29, 43} of ~30%. Studies have revealed a mean PMI size of 2.0–6.0g, or 1.5-5.0% of LV mass^{29, 30, 44}. Rahimi showed that new LGE post-PCI was the strongest IP of MACE at 29 months (HR 3.1), with each gram of new myocardial injury resulting in a 10% increased MACE risk³⁰.

1.1.1.3 Current guidelines

European Society of Cardiology (ESC)² and American Heart Association (AHA)³ guidelines recommend **PCI of the infarct-related artery only ('IRA-only')** at PPCI unless the patient is in cardiogenic shock, where complete revascularisation is permitted for critical (>90% stenosis) or unstable lesions (ESC/AHA: Class IIa, level of evidence B). The two alternative options at PPCI are **complete revascularisation during the index admission (of all significant lesions, including in N-IRAs ['CR'])** and planned outpatient PCI of the N-IRA at a later date (usually <6 weeks) as a **staged** procedure³⁴. Where outpatient revascularisation to N-IRAs is being considered, this should be preceded by non-invasive ischaemia assessment (e.g. myocardial perfusion

scintigraphy, stress cardiovascular MRI) (ESC: Class I, level of evidence A; AHA: Class IIa, level of evidence B)^{2, 3}. Fractional flow reserve (FFR) assessment of N-IRAs at PPCI is not currently undertaken since it is felt that potential microvascular dysfunction in N-IRA territories could render FFR inaccurate. Indeed, 31% of patients in DANAMI-3-PRIMULTI¹⁵ deemed to have significant N-IRA at PPCI did not undergo FFR-guided N-IRA PCI when assessed at 48 hours.

1.2 CMR surrogate markers of outcomes following PPCI

Prognostic studies using clinical outcomes, in particular mortality require large sample sizes in order to achieve statistical power due to their relatively low incidence post STEMI. **Surrogate biomarkers** of outcome are directly measured alternative endpoints used as a substitute for biological processes and clinical outcomes^{45, 46}. CMR is the gold standard modality for assessment of cardiac volumes and function and it uniquely characterises myocardial and microvascular injury in acute MI due to its accuracy, reliability and validity (Figure 1)^{46, 47, 48}. CMR data are thus strong surrogate markers of outcome following PPCI, and a significant proportion of contemporary STEMI studies hence use CMR outcomes. The accuracy, reliability and validity in turn improve the reproducibility of CMR-based surrogate markers of outcome, significantly increasing the statistical power of studies, allowing sample size requirements to be reduced.

Understanding the mechanisms underlying prognostic differences of the treatment strategies for MVD at PPCI requires an appreciation of their effects on LV function and structure. The only imaging assessment of the LV in studies to date has been assessment of LVEF on echocardiography in 2 studies^{24, 49} and on nuclear imaging in 1 study²². A study investigating MVD PPCI strategies using CMR-based outcomes would be a novel, important addition to the evidence base. These outcomes and their current evidence base are discussed in this review.

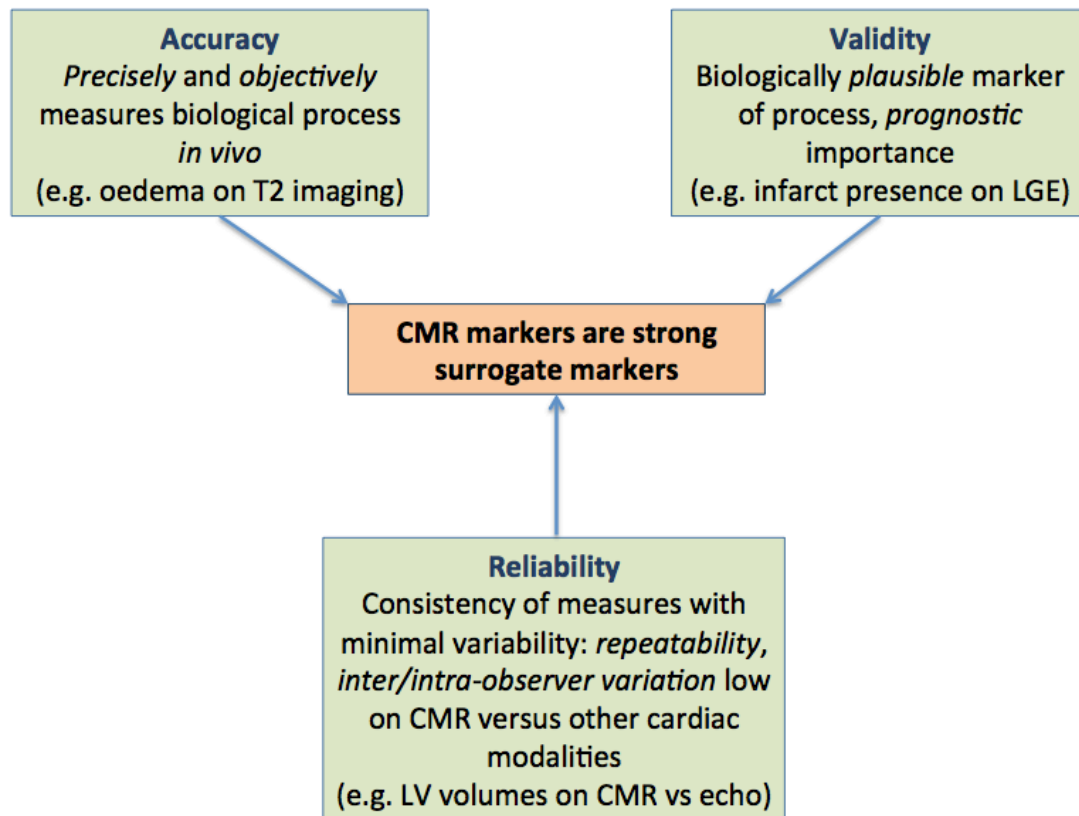


Figure 1: CMR markers are ideal surrogate biomarkers for the assessment of revascularisation in STEMI
(from references⁴⁶⁻⁴⁸)

1.2.1 Assessment of LV ejection fraction and volumes in acute STEMI

1.2.1.1 Background

In the medium-term following STEMI, the LV end-diastolic volume (LVEDV) increases, the LV end-systolic volume (LVESV) decreases⁵⁰⁻⁵² and there can be compensatory hypertrophy of remote myocardium^{53, 54} in order to preserve LV stroke volume and LVEF. Excessive LV dilatation is termed ‘adverse remodelling’. This results from an inability of the heart to maintain its geometry post MI in the context of large infarcts and increased wall stresses affecting infarct, peri-infarct and remote regions^{31, 55}. There is no consensus on the degree of LV dilatation post STEMI defining adverse remodelling, with an increase in LVEDVI >20%^{56, 57} and increase in LVESVI >15%⁵⁸ at follow-up the most commonly used criteria.

1.2.1.2 CMR assessment of LV volumes and ejection fraction

CMR is the gold standard modality for assessment of ventricular function and volumes. The absence of radiation makes it ideal for serial assessments. It has higher spatial resolution than nuclear single-photon emission computed tomography (SPECT) imaging ($\sim 1.8 \times 1.8 \times 8 \text{ mm}$ vs. $10 \times 10 \times 10 \text{ mm}$)⁵⁹, and suffers from little subjectivity or reliance on patient body habitus, and thus the variability associated with echocardiography⁶⁰.

Volumes and mass are assessed on analysis of a 3D cine stack of short-axis biventricular contiguous slices. End-diastolic and end-systolic endocardial and epicardial contours are traced onto slices allowing calculation of volumes via summation of disks, and mass by converting myocardial volume within epicardial and endocardial contours into mass ($\text{mass [g]} = \text{volume [ml]} \times 1.05$). Modern cine sequences use breath-hold, segmented steady-state free precession (SSFP) to produce high spatial resolution images with excellent contrast between blood and myocardium. Retrospective electrocardiographic gating is used, however arrhythmia rejection algorithms, prospective gating, free-breathing (using multiple signal averages) and parallel imaging can provide high quality images in patients with irregular heart rhythms and suboptimal breath holding. Regional analysis of systolic function can alternatively be assessed using wall motion scoring based on the American Heart Association 16-segment model⁶¹.

CMR studies have demonstrated that recovery of LVEF occurs relatively early post STEMI. Ripa showed that improvement in LVEF and systolic wall thickening occurred by 1 month, with no further change at 6 months⁵⁰. The majority of improvement in LVEF occurred between day 2 and 1 week in the study by Mather⁶², with no further significant improvement at 1 month but a final increase by 3 months. Beek showed that 55% of segments with initially impaired systolic wall thickness improved at 13-weeks⁶³. Ganame⁶⁴ and Dall'Armellina⁶⁵ however showed that LVEF underwent no significant change by 6 and 12 months post PPCI respectively. This may be because patients in their studies sustained less myocardial damage, represented by relatively

preserved LVEFs and thus lower potential for improvement (e.g. LVEF 59±9% at CMR 24-hours post STEMI⁶⁵).

Volumetric changes occur more slowly. Ripa⁵⁰ showed a continued increase in LVEDV and reduction in LVESV at all time points to 6 months. Engblom⁵² demonstrated similar sequelae to 12-months. Ganame showed progressive significant changes in LVEDV and LVESV and resulting LV sphericity at all timepoints to 12 months⁶⁴. These studies have important implications for optimising timing of follow-up CMR studies assessing remodelling.

The degree of impairment of LVEF and changes in volume depend on a number of CMR-based markers including IS⁶⁶, microvascular obstruction (MVO)^{67, 68}, intramyocardial haemorrhage (IMH)⁶⁹ and myocardial salvage (non-infarcted proportion of ischaemic area at risk)^{70, 71}. Anterior STEMI results in larger IS and lower LVEF due to the greater ischaemic area at risk (AAR) supplied by the left anterior descending artery⁷².

1.2.1.3 Prognostic importance of LVEF and volumes in acute STEMI

Norris⁷³ and White⁷⁴ first illustrated the prognostic importance of LVEF (strongest independent predictor of survival at 3.5 years) and LVESV (only independent predictor of long-term mortality at 6 years) respectively, using invasive ventriculography. Burns first demonstrated the prognostic importance of LVEF, LVEDVI (LVEDV indexed to body surface area) and LVESVI and their strong correlation with each other, using SPECT and radionuclide analysis⁷⁵.

The last 10 years has seen a large evidence base emerge for the negative prognostic impact of impaired systolic function based on reduced CMR-derived LVEF, as summarised in Table 5.

Table 5: CMR studies illustrating the prognostic importance of LVEF in acute STEMI

Study	Year	n	CMR time	Main findings	Mean/median F/U
El Aidi ⁷⁶	2014	25497	N/A	Meta analysis of CMR studies of prognostic value of surrogate markers. LVEF was the only IP for MACE (HR 1.05 per 5% decrease)	N/A
Husser ⁷⁷	2012	304	7d	LVEF IP for combined MACE (HR 0.95 for each % increase in LVEF)	140w
Eitel ⁷⁸	2011	208	3d	LVEF IP for combined MACE (HR 0.95 for each % increase in LVEF)	18.5m
Amabile ⁷⁹	2010	114	6d	LVEF at CMR scan was IP for combined 12 month MACE (HR 0.96 with each % increase in LVEF)	12m
De Waha ⁸⁰	2010	438	3d	LVEF IP for combined MACE (OR 1.63) and all-cause mortality (OR 2.51)	19m
Cochet ⁸¹	2009	127	3-7d	LVEF <40% IP for combined MACE (OR 1.20)	12m
Hombach ⁵¹	2005	110	6d	LVEF IP for combined 9m MACE post STEMI (p=0.006)	225d

MACE= major adverse cardiovascular events, IP= independent predictor, LVEF= left ventricular ejection fraction. *CMR time*: mean/median time of CMR post acute STEMI, d= days, m=months, y= years

In addition to LVEF-based global systolic function, Bodi demonstrated that the number of dysfunctional segments on CMR at 1-week post STEMI was an independent predictor of combined MACE at a median follow-up of 553 days²⁸. The evidence base for the prognostic importance of LV volumes is largely historical, based on large echocardiographic and radionuclide studies, demonstrating the negative prognostic impact of ventricular dilatation and remodelling as summarised in Table 6.

Negative LV remodelling has demonstrated prognostic importance in two studies, based on the cut-off of LVEDVI dilation of >20% at 6-months follow-up^{56, 57}.

Table 6: Studies illustrating the prognostic importance of LV volumes and adverse LV remodelling in STEMI

Study	Year	n	Modality	Main findings	Mean/median F/U
Ahn ⁵⁷	2013	135	Echo	Adverse LV remodelling (>20% inc. LVEDV) at 6m IP for combined 3y MACE. MACE rate ~25% in patients with adverse LV remodelling vs. ~6% in non-remodelled patients	981d
Hombach ⁵¹	2005	110	CMR	LVEDV at baseline CMR was IP for combined MACE (p=0.038)	225d
St John Sutton ⁸²	2003	512	Echo	Percentage change in LV area (surrogate for LV volume) between baseline echo and follow-up at 12m was IP for ventricular ectopy (>10/hour) and VT at 1 and 2y	2y
Bolognese ⁵⁶	2002	284	Echo	Baseline LVESV IP for cardiac death and combined MACE. Combined and individual components of 5y MACE higher in patients with adverse remodelling (>20% inc. LVEDV) at 6m (mortality 14% vs. 5%, MACE 18% vs. 10%)	5y
Otterstad ⁸³	2001	712	Echo	Increase in LVESV between baseline scan at 7d and follow-up echo at 3m strongest IP for combined MACE	24m
St John Sutton ⁸⁴	1994	512	Echo	LV end-diastolic area (RR1.1) and LV end-systolic area (RR 1.1) on baseline echo, and % change in LV area at 12m echo (RR 1.55) (surrogates for LV volumes) strongest IPs for combined MACE	12m
White ⁷⁴	1987	605	LV gram	LV gram angio 4-8w post STEMI (lysis). LVESV strongest IP long-term mortality (mean FU 78m, p<0.0001).	78m

MACE= major adverse cardiovascular events, IP= independent predictor, LVEDV= left ventricular end-diastolic volume, LVESV= left ventricular end-systolic volume.

Modality: modality of LV volume assessment (CMR= cardiovascular MRI, Echo= echocardiography, LV gram= LV contrast angiography), d= days, m=months, y= years

Recently, the left ventricular global performance index has been proposed as a CMR marker of cardiac performance, incorporating LVEF, LV volumes and mass. It has been assessed in one study in STEMI and correlated strongly with IS, MSI, MVO and IMH extent, and had incremental prognostic value to LVEF in predicting 12-month MACE⁸⁵. Further work is needed to investigate its prognostic value in STEMI.

1.2.2 Assessment of myocardial strain in acute STEMI

Early recognition and management of myocardial dysfunction is important. CMR-measured myocardial strain (tissue deformity) is the gold standard non-invasive measure of systolic and diastolic myocardial function⁸⁶. Circumferential strain (*Ecc*) describes shortening of fibres (contraction) in a short-axis plane tangential to the epicardium; longitudinal strain (*Ell*) describes shortening in the long axis, and radial strain (*Err*) describes lengthening (thickening) of fibres towards the centre of the ventricle. Torsion is the wringing motion of the ventricle caused by clockwise rotation at the base, and anticlockwise at the apex (Figure 2).

Strain offers greater accuracy in detecting myocardial dysfunction compared with global (LVEF) and regional (visual wall-motion scoring, segmental wall thickening)⁸⁷ measures of function.

1.2.2.1 CMR assessment of myocardial strain

In 1988, Zerhouni developed a T1 spoiled gradient echo sequence, creating 'tags' formed by saturation of thin myocardial lines perpendicular to the slice plane⁸⁸. This was modified by Axel with the tag lines running in perpendicular directions in-plane to form a myocardial grid⁸⁹. These tagging lines act as tissue markers, accurately tracking myocardial deformation (strain) as shown in Figure 3. Peak systolic strain and peak diastolic strain rate (relaxation of strain over time) provide objective and sensitive measures of systolic and diastolic function respectively, compared with SSFP CMR-based cine and echocardiographic assessment. Its accuracy has been validated on comparison with sonomicrometry.^{90, 91} Strain analysis can objectively detect subtle and subclinical systolic dysfunction. Harmonic Phase Analysis (HARP) is currently the most widely used method for analysis of CMR tissue tagging⁸⁶.

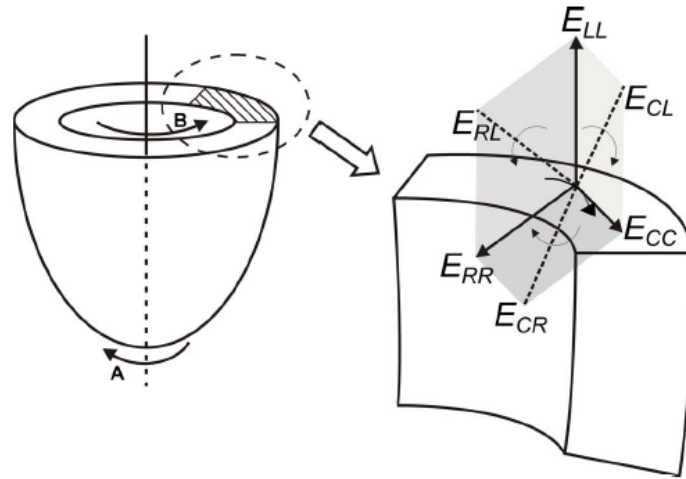


Figure 2: The three planes of LV strain assessment

E_{cc} = circumferential strain, E_{ll} = longitudinal strain, E_{rr} = radial strain (figure from Shehata *et al*⁹²). Torsion is the wringing motion of the ventricle.

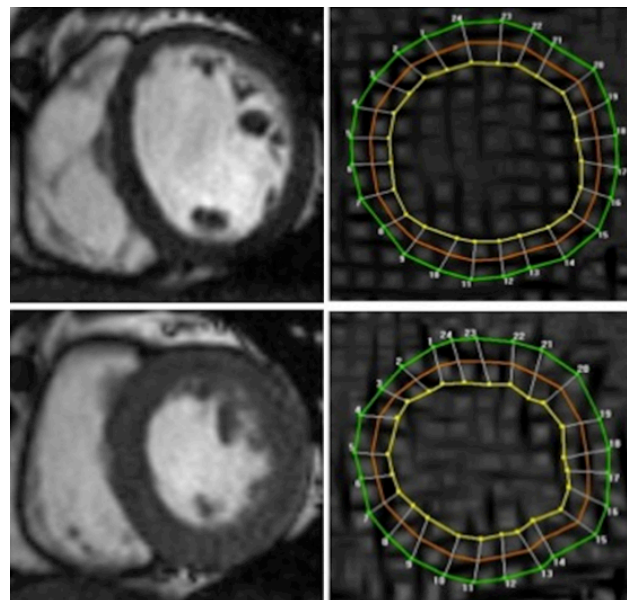


Figure 3: CMR assessment of strain using tissue tagging

Cine SSFP images in end-diastole (top left) and end-systole (bottom left), with corresponding Spatial Modulation of Motion (SPAMM) tagged images (right). Grid lines (tags) are visible and contours drawn at 3 levels within the myocardium (green [epicardial], red [mid myocardial], yellow [endocardial]) allow accurate tracking of myocardial motion and strain (circumferential), here using HARP.

Feature Tracking (FT) has been introduced as an alternative method to tagging for assessing strain on CMR. FT tracks anatomical features of interest along contour lines on routinely acquired SSFP cine images analogous to echocardiographic Speckle Tracking, thus obviating the need for additional tagging sequences⁹³. FT-derived strain has been compared to tagging in muscular dystrophy patients⁹³ and normal volunteers⁹⁴ showing reasonable agreement.

1.2.2.2 CMR LV strain as a predictor of LV function and remodelling in acute STEMI

Tagging-derived LV strain accurately and reliably assesses regional function, and could improve our understanding of the mechanics underlying LV systolic dysfunction associated with prognostic CMR surrogate markers of myocardial damage during STEMI (e.g. MVO, IMH, oedema).

The work of Gotte and Neitzel showed that systolic function is not only affected in infarcted and adjacent regions, but also in remote (non-infarcted) segments, and that LV mechanics outside of the infarct zone are also affected during infarction and contribute to remodelling^{87, 95, 96}. Gerber demonstrated that the presence of MVO had the highest predictive value for persistent dysfunction on circumferential strain analysis at 7-months post STEMI, and that MVO may result in systolic dysfunction due to direct mechanical effects (myocardial stiffness)⁹⁷. Wong showed that baseline segmental circumferential strain was the strongest predictor of segmental functional recovery at 3-months in a model containing infarct transmuralty and MVO⁹⁸. Buss recently demonstrated that FT-derived global circumferential strain assessed acutely post PPCI (median d3) correlated strongly with acute IS on LGE ($r=0.75$) and final LVEF at 6 months ($r=-0.71$). Global circumferential strain was a stronger predictor of functional recovery (LVEF >50%) at 6 months than global longitudinal strain, age, diabetes and baseline LVEF, and was of similar predictive value to acute IS (AUC 0.86 [Ecc] vs. 0.92 [IS])⁹⁹.

1.2.2.3 Prognostic importance of LV strain in acute STEMI

The evidence base for the prognostic importance of LV strain post STEMI is currently based on echocardiographic studies demonstrating that global longitudinal predicts medium and long-term using Speckle Tracking analysis as summarised in Table 7.

Table 7: Studies illustrating the prognostic importance of LV strain in acute STEMI

Study	Year	n	Modality	Main findings	Mean/ median F/U
Ersboll ¹⁰⁰	2014	1048	TTE	(E-prime divided by peak early diastolic strain rate) was the strongest IP for combined MACE (HR 1.5) and death (HR 2.5) on multivariate analysis	29m
Ersboll ¹⁰¹	2013	849	TTE	GLS was IP for combined MACE (HR 1.14) and individual MACE on multivariate analysis	30m
Hung ¹⁰²	2010	610	TTE	GLS and strain-rate, and global circumferential strain and strain-rate were IPs for combined MACE in a model including wall-motion score index, LVEF	24.7m
Antoni ¹⁰³	2010	659	TTE	GLS (HR 1.2) IPs for mortality. LVEF, wall-motion score and Tissue Doppler mitral valve inflow not	21m

TTE= transthoracic echocardiography, GLS= global longitudinal strain, MACE= major adverse cardiovascular events, IP= independent predictor, HR= hazard ratio

1.2.3 Assessment of infarct size (IS) in acute STEMI

1.2.3.1 Background

The 'ischaemic cascade' defines the sequence of pathophysiological effects developing immediately following myocardial ischaemia due to coronary occlusion. Aerobic respiration loses efficiency due to reduced oxygen availability and increased ATP demand, resulting in cellular oedema due to inactivation of sodium and water cell-membrane pumps. With increasing ischaemic time, cell membranes rupture which results in cell death. Following healing, necrotic cells are replaced by extracellular deposition of collagen (scar). Therefore, both the acute and chronic phases are characterised by an increase myocardial extracellular volume¹⁰⁴⁻¹⁰⁶. The acute stage is due to membrane rupture and in the chronic phase due to scar tissue

predominantly consisting of collagen, which is extracellular with only a small amount of cells (fibroblasts) compared to normal myocardium.

1.2.3.2 CMR assessment of infarct size in acute STEMI

Gadolinium based contrast agents have an extracellular distribution, being too large to cross intact cell membranes (Figure 4). Infarct can be visualised on T1-weighted imaging after ~10 minutes post intravenous administration of gadolinium-based contrast agents and was initially named delayed contrast enhancement (DCE), but **late gadolinium enhancement (LGE)** is now the preferred terminology.

In acute infarct, LGE results from gadolinium entering ruptured cell membranes. In chronic infarction, LGE results from increased extracellular space due to collagen deposition and prolonged washout due to reduced capillary density within myocardium^{104, 107}. Gadolinium shortens T1, causing infarcted myocardium to appear bright, and normal myocardium to appear black (Figure 5)^{107, 108}. Normal myocardium is progressively nulled using the appropriate inversion time to provide optimal contrast between infarct and normal myocardium. T1 levels and contrast-to-noise between myocardium and infarct are stable between 5-20 minutes post gadolinium based contrast in animal models of acute STEMI¹⁰⁹.

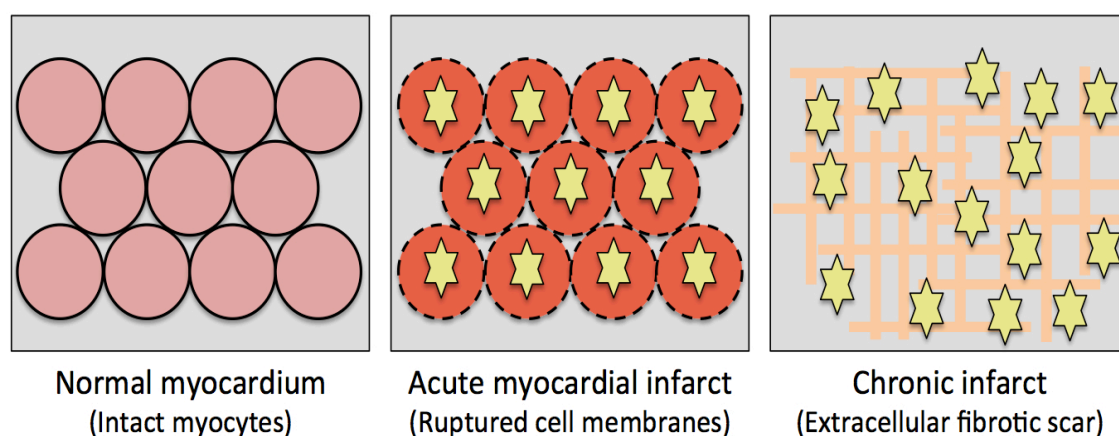


Figure 4: Mechanism of late gadolinium enhancement (LGE)

Gadolinium is extracellular. Left: in normal myocardium, gadolinium washes out ~10 minutes post administration and there is no LGE. Middle: in acute infarction,

gadolinium (yellow stars) enters ruptured cell membranes and causes LGE. Right: in chronic infarct, LGE results from increased extracellular space due to fibrotic scar deposition.

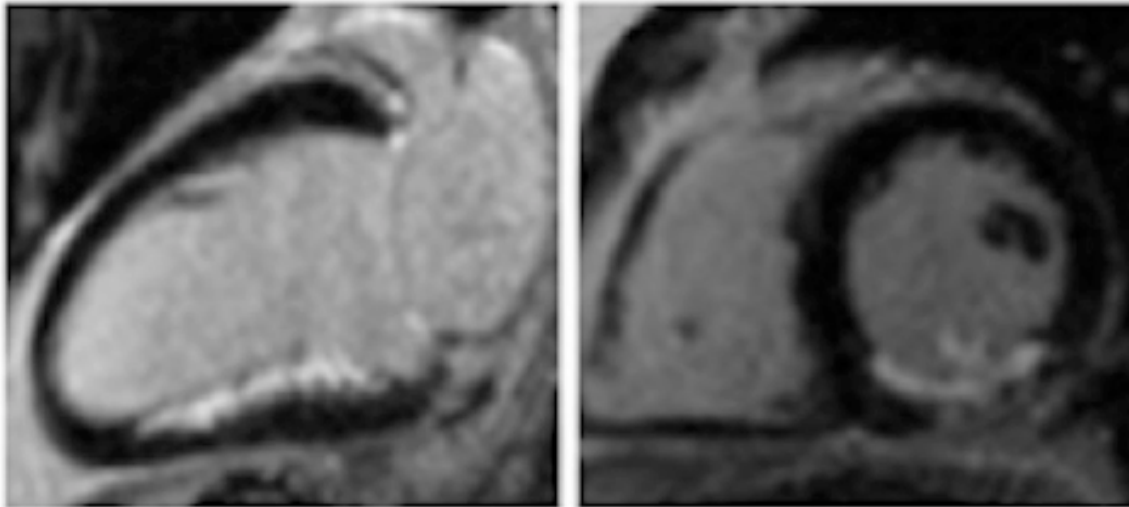


Figure 5: Late gadolinium enhancement of acute infarct

Infarct appearing white (enhanced) in the inferior wall, with unaffected myocardium black (nulled). Left: 2-chamber long-axis view. Right: short-axis view at mid left ventricular level. Of note, the posteromedial papillary muscle is also infarcted in the short-axis view.

Typically, a high spatial resolution of $\sim 1.4 \times 1.6 \times 6\text{-}8\text{mm}$ is achieved⁵⁹. IS is typically expressed as a percentage of total LV mass. Delineation of infarct can be performed visually (manual quantification)^{51, 54, 66}, however most groups use semi-automated methods in order to reduce observer variability. These include enhancing myocardium exceeding a pre-defined signal intensity (SI) threshold, typically $>2\text{-}6$ standard deviations above that of remote (non-infarcted) myocardium^{46, 110}.

Currently, the semi-automated **full-width at half-maximum (FWHM) method** is commonly used¹¹¹⁻¹¹⁵, defining infarct as myocardium with SI $>50\%$ of the peak SI in the infarct core. Amado demonstrated that FWHM had the highest interobserver agreement and closest correlation with TTC-stained infarct in a dog model of acute infarction ($r^2=0.94$), compared with $>1\text{-}6$ standard deviation methods¹¹¹. This may be

because FWHM is less prone to IS overestimation due to oedema (increased water content increasing the volume of distribution in areas without membrane disruption) and partial volume effects giving rise to intermediate signal intensities^{62, 116}. A comparison of techniques in 20 acute and 20 chronic STEMI patients showed that the FWHM technique had the lowest intraobserver and interobserver variability, and in paired analysis could lead to a subsequent reduction of 60% in required sample sizes¹¹⁷. It is likely that this is because selection of the brightest region of infarct core is more reproducible than selection of a remote region of interest in thresholding-based techniques, and since the FWHM region of interest is unaffected by inadequate nulling of remote myocardium.

The segmented, standard 2D breath-hold LGE sequence provides high spatial resolution. However it can be affected by arrhythmias, suboptimal breath holding, inadequate nulling, and acquisition of a full set of LGE images can take up to 10 minutes. Modifications have been developed and are undergoing assessment, summarised in Figure 6.

There are no studies comparing IS at different field strengths. Almost all STEMI studies have been done at 1.5T. The higher field strength at 3T could potentially improve LGE imaging since the increased signal to noise ratio¹¹⁸ could be used to shorten breath hold durations (by increasing parallel imaging factor), or be offset to improve spatial or temporal resolution.

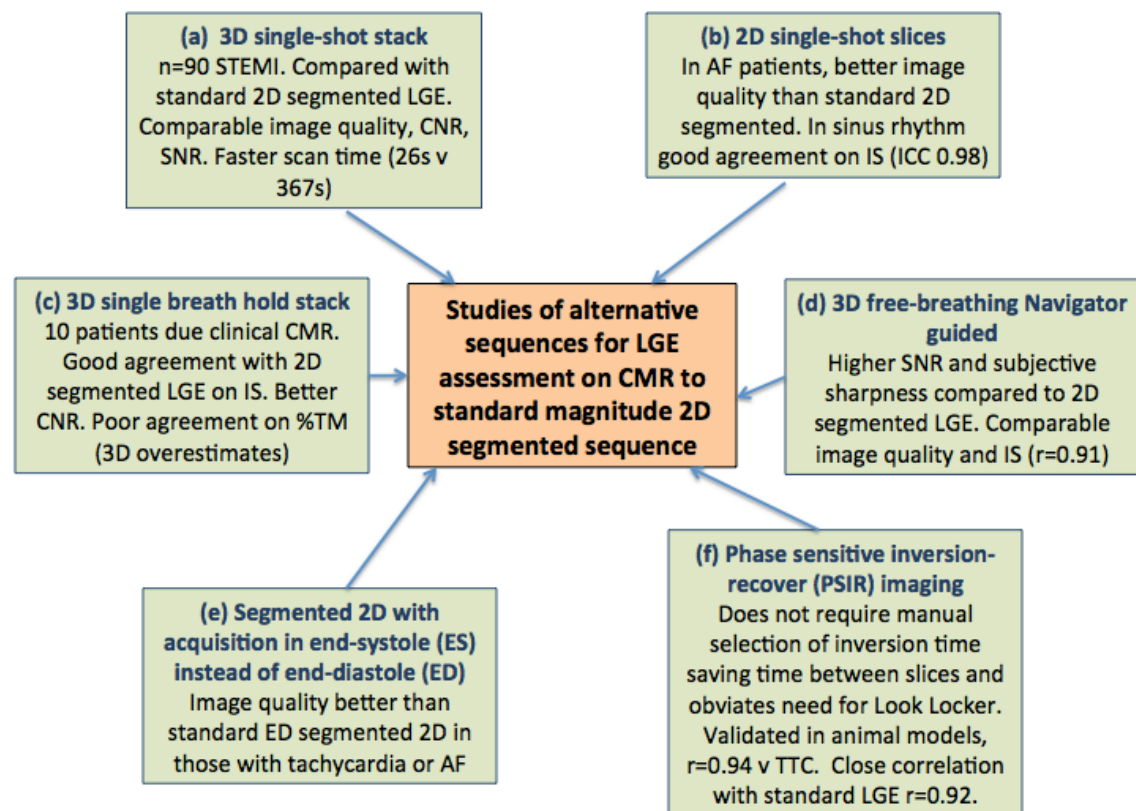


Figure 6: Modifications to the standard 2D segmented, magnitude LGE sequence for infarct size analysis

(from references¹¹⁹⁻¹²⁶)

CMR measurement of IS on LGE is well validated^{107, 108}. Kim demonstrated that IS in dog myocardium on *ex-vivo* CMR corresponded closely with IS derived from tetrazolium (TTC) staining ($r=0.99$ for comparisons undertaken at 24 hours to 8 weeks post infarct, Figure 7), but also that infarct shrinkage occurred over the 8 weeks^{59, 108}. IS derived from LGE correlates with the area of infarct suggested on ECG. LGE has dramatically higher sensitivity for the detection of MI compared to SPECT. In an experimental model of MI, CMR LGE detected 92% of all segments with subendocardial infarction (<50% transmural) compared with only 28% with SPECT⁵⁹. In patients presenting with MI, SPECT only detects ~50% of the infarcts seen on LGE. The superior sensitivity is almost certainly due to the vastly increased spatial resolution of CMR, but LGE also has greater test-retest reproducibility in humans¹⁰⁴.

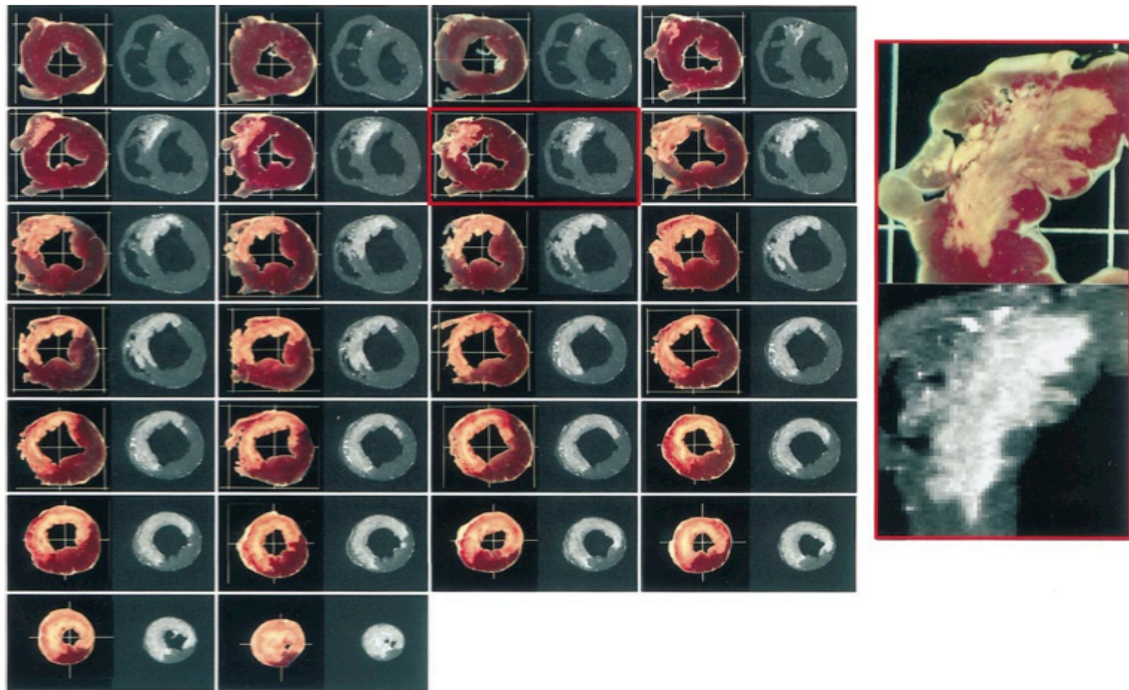


Figure 7: Validation of late gadolinium enhancement imaging on animal models

Validation of LGE imaging of infarct was first achieved by Kim who demonstrated extremely close correlation of ex-vivo CMR images (right columns) with TTC-stained slices (left columns) from dog myocardium in experimental models of acute infarction. Slices arranged from base to apex (top to bottom row) (from Kim *et al*)¹⁰⁸.

Since gadolinium is distributed throughout the extracellular space, gadolinium-based contrast agents are not exclusively specific to necrosis. In the acute stage, the area of hyperenhancement (LGE) is a mixture of viable (oedematous) and necrotic cells and thus has the potential to overestimate true IS. This is amplified by quantification techniques with lower signal intensity thresholds^{111, 127}. Studies of IS chronology in humans corroborate this, as summarised in Table 8. Indeed, it has been demonstrated that severely dysfunctional segments with minimal myocardial salvage (<25% of oedematous area non-infarcted) early post STEMI can show significant functional improvement at follow-up¹²⁸.

Table 8: Temporal changes in CMR-derived infarct size in STEMI

Study	Year	n	CMR Timepoints post STEMI	Total LGE IS Reduction	LGE Method	Main findings
Carrick ¹²⁹	2016	30	8h → 3d → 10d → 7m	26%	Automated	Significant decrease 3d to 10d (20±13% to 14±10 LVM). No change at 7m (14±10% LVM).
Dall'Armeline ⁶⁵	2011	30	2d → 6m	22%	>2SD	IS significantly reduced at all timepoints from 27±15% of LV mass at 24h post PPCI, to 21±11 at 6m
Mather ⁶²	2011	48	2d → 1w → 30d → 3m	37%	>2SD	27% IS drop between d2 and d7 post PPCI, no significant change at 3m
Ganame ⁶⁴	2011	58	3d → 4m → 12m	45%	Manual	33% decrease IS between d3 and 4m then no further decrease at 12m
Ibrahim ⁵⁴	2010	17	1d → 1w → 1m → 6m	37%	Manual	34% reduction in IS from d2 to 1w, then no further change at 1 and 6m
Engblom ⁵²	2009	22	1d → 1w → 6w → 12m	40%	Automated	28% reduction in IS between d1 and 1w. Greatest reduction in IS and % transmural in first week
Ripa ⁵⁰	2007	58	2d → 1m → 6m	30%	Manual	14% % reduction in IS from d2 to 1m
Hombach ⁵¹	2005	110	6d → 9m	28%	Manual	28% reduction in IS from d6 to 9m

Timepoints: d= days, w= weeks, m= months. LGE method: SD= standard deviations.
Total LGE IS Overest= relative overestimation of final IS (last timepoint) on acute CMR.

Dall'Armeline⁶⁵ and Mather⁶² used a >2SD threshold for LGE quantification, which itself may have overestimated IS somewhat relative to other studies¹¹⁷. The majority

of IS reduction occurs relatively early post STEMI, particularly by 1 week. Thus in studies where IS was assessed at 1 week, it closely correlated with final IS in all but one study^{52, 54, 62}. Mather also showed that IS at 1-week predicted final LVEF at 3-months, and Ibrahim demonstrated that IS measured at 1-week closely correlated with IS derived by SPECT and with improvement in segmental wall thickening⁵⁴.

The overestimation of necrosis by LGE-derived IS early post STEMI is likely to be predominantly due to a combination of oedema, infarct resorption and partial volume effects. Oedema results in an overestimation of LGE IS due to increased extracellular water content and thus volume of distribution of contrast agent^{111, 130}. Evidence for the contribution of oedema includes the 15% reduction in AAR accompanying the IS reduction in the first week shown by Mather⁶². In addition, the major temporal decline in LGE appears to be in terms of transmural rather than circumferential extent^{54, 131}. Epicardially, the probability of LGE representing true necrosis rather than oedema is lowest, due to the wavefront spread of necrosis in STEMI¹³².

Infarct resorption results from the healing process where collagenous scar tissue is produced in order to provide stability and tensile strength to necrotic myocardium^{31, 52}. This leads to infarct shrinkage and contraction and was confirmed in a canine model where a 3.4-fold decrease in infarct volume was seen between day 3 and 8-weeks post infarct on ex-vivo LGE and TTC-stained slices¹⁰⁸ (Figure 8). The degree of infarct resorption has been shown to be proportional to initial infarct size ($r=0.65$) and presence of LV remodelling ($r=0.41$)⁵⁵. The greater degree of infarct resorption relative to total myocardial mass and volume results in an inability to maintain LV geometry in light of mechanical stresses post STEMI, resulting in adverse LV remodelling and sphericity^{55, 133}. Infarct resorption is hence a known contributor to adverse LV remodelling³¹. Finally, partial volume effects proportional to slice thickness are known to overestimate LGE IS^{111, 134}.

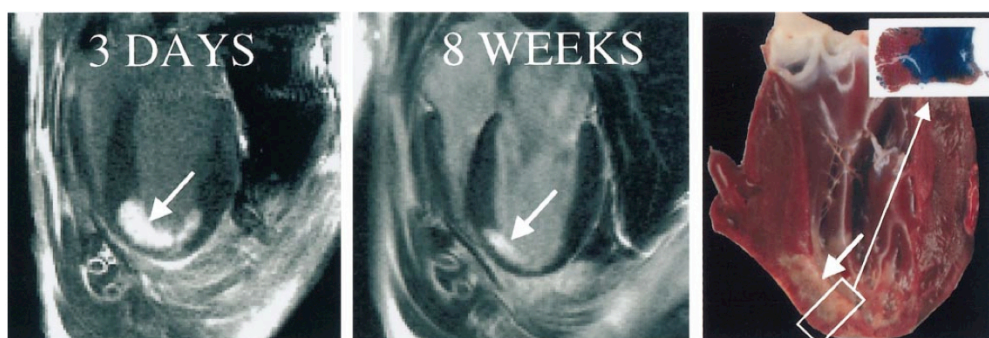


Figure 8: Replacement of infarct by collagenous scar in canine myocardium

In-vivo CMR showed significant reduction in IS (arrow) on LGE between day 3 (*left*) and 8-weeks (*middle*) post MI, confirmed pathologically (*right*) (from Kim *et al*)¹⁰⁸

Factors known to affect absolute IS include AAR extent (highest in anterior STEMI) which has been shown to account for up to 77% of variation in IS^{132, 135, 136}; collateral flow to the AAR^{132, 137}; MVO¹³⁸; time to reperfusion¹³⁹, and hyperglycaemia¹⁴⁰.

1.2.3.3 CMR infarct size as a predictor of LV function and remodelling in acute STEMI

Segmental function

In 2000, Kim illustrated in stable patients awaiting revascularisation, that LGE transmural extent strongly predicted recovery of systolic function in dysfunctional segments. Only 2% of segments with >75% transmural extent improved after revascularisation¹⁴¹. Since then, segmental extent of LGE has also been shown to negatively predict functional recovery in dysfunctional segments following PPCI for acute STEMI, as summarised in Table 9.

Global function

Infarct size is a powerful independent predictor of global LV function and adverse LV remodelling in the medium to long-term post STEMI. Greater IS and degree of infarct transmural extent strongly predicts impaired LV systolic function (reduced LVEF) and negative remodelling as summarised in Table 10.

Table 9: CMR studies illustrating importance of segmental LGE extent and functional recovery in STEMI

Study	Year	n	LGE Method	Cutoff (LGE)	Main findings	Time of MRI 1	Time of MRI 2
Wong ⁹⁸	2014	45	FWHM	50% SEE	Inverse relationship between TEE and likelihood of functional recovery on WMS at 24w (area under curve 0.68)	8d	13w
Natale ¹⁴²	2011	46	2SD	50% TEE	Inverse relationship between TEE and likelihood of functional recovery on SWT at 24w (93% sens, 75% spec)	5d	20w
Engblom ⁵²	2008	22	Manual	50% TEE	Inverse relationship between TEE and likelihood functional recovery on WMS	7d	24w
Shapiro ¹⁴³	2007	17	Manual	50% SEE	Inverse relationship between TEE and likelihood of functional recovery on WMS at 26w. Odds-ratio of functional recovery 0.2 with each SEE quartile	6d	26w
Kitagawa ¹⁴⁴	2007	18	2SD	50% TEE	Inverse relationship between TEE and likelihood of functional recovery at 24w. 31% of dysfunctional segments >50% TEE still improved	5d	39w
Janssen ¹⁴⁵	2006	67	Manual	50% TEE	Inverse relationship between TEE and likelihood of functional recovery on WMS at 12w (51-75%: 39% segments improved, 76%+: 21% improved)	4d	12w
Motoyasu ¹⁴⁶	2004	23	2SD	50% TEE	Inverse relationship between SEE and likelihood of functional recovery on SWT at 24w (area under curve for TEE in predicting functional recovery 0.78)	25d	24w
Beek ⁶³	2003	30	6SD	50% SEE	Inverse relationship between SEE and likelihood of functional recovery WMS	7d	13w

WMS= wall motion scoring, SWT= systolic wall thickening, TEE= transmural extent of enhancement, SEE= segmental extent of enhancement, SD= standard deviations

Table 10: CMR studies illustrating importance of infarct size on LV function and remodelling in STEMI

Study	Year	n	LGE Method	Main findings	Time post STEMI of predictive CMR	Mean/Median F/U CMR
Ahn ⁵⁷	2013	135	Manual	IS strongest IP of LV remodelling (>+20% LVEDVI, OR 1.06) in model with LVEF and MI location	7d	6m (echocardiogram)
Husser ⁷⁷	2012	304	>2SD	IS extent IP (OR 1.05) of LV remodelling (>LVESVI >normal) in model incl. LVEF, IS, LV vols, MVO	6d	189d
Monmeneu ¹⁴⁷	2012	118	>2SD	No. segments >50% transmural IP for LV remodelling (LVESVI at FU > LVESVI at baseline, OR 1.51)	6d	6m
Ezekowicz ¹⁴⁸	2010	64	Manual	IS extent strongest IP of LVEF at 3m in model with MVO, troponins	7d	3m
Ganame ⁶⁹	2009	98	Manual	IS strongest IP of LV remodelling (>LVESVI at follow-up; stronger IP than MVO, AAR, Troponin-I)	2d	6m
Bodi ¹⁴⁹	2009	214	>2SD	Extent of transmural necrosis (no. of segments >50% transmural) was strongest IP (OR 0.8) for LVEF recovery (>+5% LVEF at follow-up)	7d	6m
Wu ¹⁵⁰	2008	122	Manual	IS extent only IP for LVEF and LV remodelling (>+20% LVEDVI)	2d	4m
Hombach ⁵¹	2005	110	Manual	IS extent IP of LV remodelling (>+20% LVEDVI) in model with MVO, % transmural	6d	225d

IS= infarct size, IP= independent predictor, LVEDVI= left-ventricular end-diastolic volume index, LVESVI= left-ventricular end-systolic volume index, LVEF = left ventricular ejection fraction, MVO= microvascular obstruction, SD= standard deviation

1.2.3.4 Prognostic importance of CMR-derived infarct size in acute STEMI

The goal of STEMI management is early reperfusion in order to minimise IS and thus maximise myocardial salvage². There is a strong evidence base for the prognostic importance of CMR-derived infarct size post STEMI, as summarised in Table 11. Infarct size is a strong independent predictor of medium to long-term clinical outcomes post STEMI.

Table 11: CMR studies illustrating the prognostic importance of infarct in acute STEMI

Study	Year	n	LGE Method	Main findings	Time of prognostic CMR post STEMI	Mean/median F/U
Husser ¹⁵¹	2013	250	>2SD	Extent of transmural infarction (no. of segments >50% transmural) only IP for MACE at 6m (HR 1.31)	7d	163w
Izquierdo ¹⁵²	2013	440	>2SD	IS was IP for AACEs (arrhythmic cardiac events: sudden death, VT, VF, ICD shock) (OR 1.06) in model including LVEF, hypertension	7d	123w
Eitel ⁷⁸	2011	208	>5SD	IS was IP of MACE at 19m (HR 1.06), in model including MVO, LVEF, MSI, Killip class on admission and TIMI flow post-PPCI	3d	18.5m
Miszalski-Jamka ¹⁵³	2010	77	Manual	LV transmural index IP (HR 1.03) and IS (HR 1.03) IPs for MACE in a model containing RVEF and RV IS	'3-5d'	1150d
Larose ¹¹²	2010	103	FWHM	IS strongest IP for MACE (HR 1.36) in model containing LVEF, CK. LGE>23% had HR 6.1 for MACE.	4.5h	2y
Bodi ²⁸	2009	214	>2SD	Extent of transmural infarction (no. of segments >50% transmural) IP for MACE (HR 1.35 if >5 segs)	7d	553d
Wu ¹⁵⁴	2008	122	Manual	IS only IP of 2y MACE in model containing LVEF, LVESVI (HR 1.06)	2d	538d

LGE= late gadolinium enhancement, FWHM= full-width half-maximum, SD= standard deviations, MACE= major adverse cardiovascular events, LVEF= left ventricular ejection fraction, PPCI= primary percutaneous coronary intervention, LGE method (LGE quantification method): SD= standard deviations, FWHM= full-width half-maximum

1.2.4 Assessment of microvascular obstruction (MVO) in acute STEMI

1.2.4.1 Background

Despite prompt recanalization of the IRA, perfusion of the microcirculatory bed does not always ensue. Histopathological studies have demonstrated that the infarct core (endocardial) perishes first due to its distance from the epicardial IRA. Necrosis spreads transmurally towards the epicardium. This phenomenon is known as the ‘**wavefront theory**’, as first described by Reimer¹⁵⁵. Due to the profound ischaemia occurring at this core, necrosis occurs rapidly, with myocardial and capillary endothelial cells perishing simultaneously. Capillaries can become obstructed by resultant cellular debris, resulting in non-perfusion of the infarct core, despite patency of the IRA¹⁵⁶. This process is known as **microvascular obstruction (MVO)** and can be indicated at angiography, as ‘no reflow’. This phenomenon was first described by Kloner in 1974 in canine reperfused myocardium¹⁵⁶. Rochitte extended these findings by providing the first insight into the time-course of MVO and histopathological confirmation of MVO by directly measuring coronary blood flow and tissue microperfusion using radiolabelled microspheres and thioflavin-S staining respectively¹⁵⁷.

1.2.4.2 CMR assessment of microvascular obstruction in acute STEMI

Three CMR methods demonstrate MVO (Figure 9). Its extent is typically expressed as a percentage of LV mass.

- (1). Qualitative **first-pass rest perfusion**. A modified version involves quantification of myocardial blood flow (SI-time curve) and time to 50% of maximal SI^{157, 158}.
- (2). Hypoperfusion on inversion recovery images between 1-3 minutes post contrast. A fixed inversion time of ~440ms nulls MVO and retains intermediate signal in normal myocardium. This is known as ‘**early MVO (E-MVO)**’^{72, 159}.

- (3). Hypointensity within infarct core on LGE due to absence contrast perfusion, known as '**late MVO (L-MVO)**'. L-MVO is seen in up to 60% of patients on CMR within the first week post STEMI^{50, 51, 62, 64}. This is the preferred method of MVO demonstration in contemporary clinical practice and research.

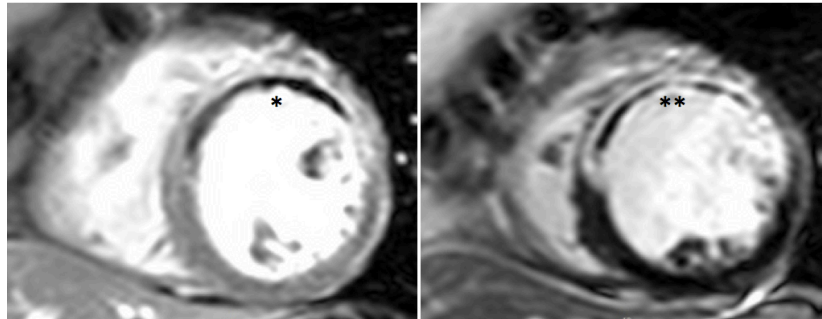


Figure 9: Early and Late Microvascular Obstruction on CMR

Left: Early gadolinium imaging at 1-minute post contrast with hypoperfusion in anteroseptal, anterior and anterolateral segments, consistent with early MVO (E-MVO, *). *Right:* Corresponding late gadolinium image showing transmural infarction with a hypointense late MVO core (L-MVO, **) co-localising with E-MVO.

The extent of E-MVO is approximately 70% greater than L-MVO, due to slow diffusion of contrast into areas with less severe MVO, and thus L-MVO may reflect more severe microvascular damage^{72, 80, 160, 161}. E-MVO could be considered to be a more sensitive measure of microvascular obstruction.

Other non-CMR techniques used to detect MVO include angiographic assessment (myocardial blush grade [MBG]¹⁶², TIMI score post-PPCI¹⁶³, intracoronary systolic resistance to flow¹³⁸); ECG markers (degree of residual ST-elevation, degree of ST-resolution)^{67, 72, 160}, SPECT⁷²; clinical bedside scoring systems⁷⁹ and myocardial contrast echocardiography⁷². CMR assessment is superior since it does not need to be done at the time of PPCI (cf. MBG, TIMI, SRF); has stronger prognostic value^{51, 80, 81, 164}; and can be undertaken during a routine multimodal non-stress CMR study allowing assessment of ventricular function and volumes, infarct, oedema, haemorrhage and valvular function within a single scan.

The presence and extent of L-MVO is dynamic⁶³. L-MVO extent is maximal at 48 hours post infarct^{53, 62}, and then decreases. It has been shown to exist for at least 1 week, and for up to 1 month^{53, 62} and then resolves in the medium-term in humans (Table 12). Animal models corroborate these findings. Wu showed that MVO extent is unchanged between days 2 and 9 post reperfusion in canines¹⁶⁵. Gerber also demonstrated progressively increasing MVO extent at 4, 6 and 48 hours in canines, followed by a decrease by day 10¹⁶⁶. Ghugre demonstrated that in pigs, L-MVO extent was greatest at day 2 then significantly decreased at subsequent time points (1/2/4/6-weeks). No L-MVO was present at 6 weeks⁵³.

Table 12: Temporal changes in CMR-derived late MVO in acute STEMI

Study	Year	n	CMR Timepoints post STEMI	LGE Method	Main findings
Carrick ¹²⁹	2016	30	8h → 3d → 10d → 7m	Auto	L-MVO in 20%, peaked early at 8h and stable at d3. Decreased by d10, absent at 7m
Mather ⁶²	2011	48	2d → 1w → 30d → 3m	>2SD	L-MVO in 60% patients, peak at d2. Decrease at subsequent points. L-MVO absent at 3m.
Ganame ⁶⁴	2011	58	3d → 4m → 12m	Manual	L-MVO in 64% patients. L-MVO absent at 4m.
Ripa ⁵⁰	2007	58	2d → 6m	Manual	L-MVO in 42% patients. L-MVO absent at 6m.
Hombach ⁵¹	2005	110	6d → 9m	Manual	46% had L-MVO (2.8% LV mass, 16% of IS) on acute CMR. L-MVO absent at 6m.

MVO= microvascular obstruction. *Timepoints*: d= days, w= weeks, m= months. *LGE Method*: SD= standard deviations. IS= infarct size, LV= left ventricle

The extent of MVO on CMR has been shown to correlate with IS^{139, 150, 161, 167}, oedema, IMH, TIMI-flow pre PCI^{79, 168} and time to reperfusion^{79, 139, 169}.

1.2.4.3 CMR microvascular obstruction as a predictor of LV function and remodelling in acute STEMI

A growing evidence base demonstrates that L-MVO is a strong independent predictor of medium-term LV function and adverse remodelling, as summarised in Table 13. It

is likely that this is because L-MVO reflects more severe microvascular damage than E-MVO and is thus more likely to result in long-term myocardial damage^{72, 80}. In the majority of studies demonstrating the independent predictive value of L-MVO on LV function and remodelling, E-MVO was not an IP on multivariate analysis^{158, 160, 170}. L-MVO remained an IP when baseline IS was entered into the model^{51, 64, 148, 160, 170, 171}. Recently it was seen that monocyte recruitment, which is important in cellular debris removal and scar formation post infarct, is impaired in areas of L-MVO in rat myocardium and may contribute to the adverse remodelling associated with MVO¹⁷².

Table 13: CMR studies illustrating the importance of Late MVO on LV function and remodelling in STEMI

Study	Year	n	LGE Method	Main findings	Time post STEMI of predictive CMR	Mean/Median F/U CMR
Kidambi ¹⁷³	2013	39	>2SD	L-MVO presence (+/-IMH) only IP for impaired infarct Ecc. Model with IS, TIMI pre and post, DM, transmural	3d	3m
Wong ¹⁵⁸	2012	40	Manual	L-MVO extent only IP for LVEF at 3m in model including E-MVO, IS and myocardial blood flow on perfusion	3d	3m
Ezekowitz ¹⁴⁸	2010	64	Manual	L-MVO extent was IP of LVEF at 3m in model including IS and NT-proBNP	7d	4m
Weir ¹⁷⁰	2010	100	Manual	L-MVO extent was only IP of LV remodelling (>LVESVI at follow-up) in model with TIMI post PCI, E-MVO, IS	4d	6m
Ganame ⁶⁹	2009	98	Manual	L-MVO extent was IP of LV remodelling (>LVESVI at follow-up) in model with IS, troponin-I, TTR	2d	6m
Nijveldt ¹⁶⁰	2008	60	Manual	L-MVO presence strongest IP of LVEF change and remodelling (LVESVI) in model with TTR, IS, LVEF, E-MVO	5d	4m
Hombach ⁵¹	2005	110	Manual	L-MVO extent IP for LV remodelling (>20% LVEDVI) in model with baseline IS, infarct transmural	6d	225d

MVO= microvascular obstruction, IS= infarct size, IP= independent predictor, TTR= time to revascularisation, LVEF= left ventricular ejection fraction, LVEDVI= left-ventricular end diastolic volume index, LVESVI= left-ventricular end systolic volume index

1.2.4.4 Prognostic importance of CMR-derived microvascular obstruction in acute STEMI

An increasing evidence base demonstrates the strong adverse prognostic value of L-MVO following STEMI in the short to medium term, in addition to that from IS and LVEF^{51, 80, 81, 164}, as summarised in Table 14.

The 2 studies featuring both L-MVO and E-MVO showed that L-MVO was a stronger prognostic indicator^{80, 81}, Regenfus¹⁷⁴ and colleagues demonstrated that L-MVO was the strongest IP of long-term combined MACE at 6 years follow-up in a model including CMR-assessed LVEF and IS (HR 3.9), and hence provides incremental prognostic value over traditional CMR markers of myocardial damage. A meta-analysis¹⁷⁵ of studies with n>60 (8 studies, n=1025) demonstrated that L-MVO presence was the strongest independent predictor of medium-term combined MACE (HR 3.7) and cardiovascular death (HR 13.2) at 2 years. Infarct size and LV volumes were not independent predictors.

The strong adverse prognostic value of L-MVO may be due to its negative effects on LV function, wall thickness and stiffness, and remodelling, and subsequent risk of heart failure and arrhythmias^{51, 64, 148, 160, 170, 171}.

Table 14: CMR studies illustrating the prognostic importance of Late MVO in acute STEMI

Study	Year	n	LGE Method	Main findings	Time of prognostic CMR post STEMI	Mean/median F/U
Regenfus ¹⁷⁴	2015	249	Manual	L-MVO extent strongest IP (HR 3.9) for combined MACE in model including IS, LVEF, TIMI pre and post PPCI and no. diseased vessels	3.7d	72m
Eitel ¹⁷⁶	2014	738	>5SD	Largest multicentre study of L-MVO in PPCI. L-MVO >1.4% LVM and TIMI risk score only IPs of combined MACE. Adding L-MVO to model with clinical predictors, LVEF and IS increased c-statistic (0.78 0.80).	7d	6m
De Waha ¹⁷⁷	2012	438	Manual	L-MVO extent IP for combined MACE in model including IS, LV volumes (only other IP was LVEF). L-MVO/IS strongest IP in model including L-MVO extent, LVEF, IS, LV volumes	3d	19m
De Waha ⁸⁰	2010	438	Manual	Presence and extent of L-MVO were strongest IPs for MACE and mortality in models with IS, LVEF, ST-res, TIMI-flow post PCI. E-MVO was not an IP	3d	19m
Cochet ⁸¹	2009	184	Manual	L-MVO strongest IP for MACE, in models including GRACE score, IS, LVEF. L-MVO stronger IP than E-MVO (OR 8.7 vs. 2.5).	'3-7d'	12m
Bruder ¹⁶⁴	2008	143	Manual	Only extent of L-MVO >0.5% LV mass was IP for MACE; model included IS, LVEF, age, DM, sex	4.5d	12m
Hombach ⁵¹	2005	110	Manual	L-MVO IP for MACE (p=0.04) in model including LV end-diastolic volume and LVEF	6d	268d

MVO= microvascular obstruction, LVEF= left ventricular ejection fraction, IS= infarct size, PCI= percutaneous coronary intervention, MACE= major adverse cardiovascular events, IP= independent predictor

1.2.5 Assessment of intramyocardial haemorrhage (IMH) in acute STEMI

1.2.5.1 Background

Intramyocardial haemorrhage (IMH) is seen in up to 80% of subjects with MVO^{68, 178}. It is thought to be a reperfusion injury occurring exclusively in the presence of MVO^{114, 129}, where restored blood flow into damaged capillaries extravasates erythrocytes into myocardium^{178, 179}. CMR-derived IMH was first described in reperfused canine myocardium where it was visualised on *ex-vivo* T2-weighted (T2w) spin-echo imaging with excellent agreement with histology ($r=0.96$ for IMH extent)¹⁸⁰. The 3 non-reperfused dogs in this study developed no IMH on MRI or histology.

1.2.5.2 CMR assessment of intramyocardial haemorrhage in acute STEMI

Paramagnetic haemoglobin breakdown products shorten T2 relaxation times^{180, 181}. Thus IMH is seen as hypointense zones within hyperintense oedematous myocardium on T2-weighted spin-echo (T2w-TSE) sequences. It has shown good histological correlation in canine myocardium (*ex-vivo* MRI, $r=0.96$)¹⁸⁰ and in an autopsy case series in humans (*in-vivo* MRI, $r=0.97$)¹⁸¹. IMH shows very close correlation with L-MVO (r^2 for co-localisation ~ 0.9) (Figure 10)^{69, 77, 182, 183}. Spin-echo refocusing pulses however reverse the loss of SI and phase accompanying paramagnetic iron products, and thus can reduce the T2-lowering potential and CNR of IMH^{184, 185}, and the relatively thick slices typically used in T2w-TSE imaging can lead to partial volume effects and failure to detect small areas of IMH^{184, 185}.

Newer sequences based on direct quantification of T2 and T2* values (commonly using T2* <20 ms) to detect IMH have been developed^{129, 183, 184, 186, 187}. These allow IMH to be quantified and mapped without the limitations of T2w-TSE imaging. IMH is hypointense on T2 and T2* mapping. The main limitation of T2* mapping is susceptibility to off-resonance artefacts manifesting as hypointensity¹⁸⁶.

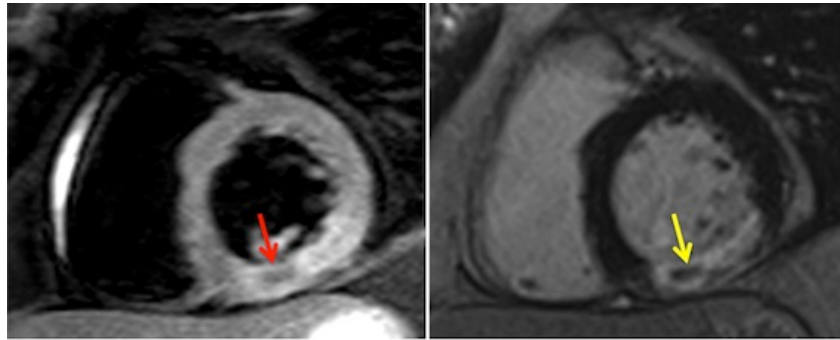


Figure 10: Intramyocardial haemorrhage on CMR

Left: T2-weighted spin-echo image with hypointensity corresponding with IMH within the hyperintense oedematous region in the inferior wall (red arrow). *Right:* corresponding LGE image showing co-localisation of IMH and L-MVO (yellow arrow).

Initial studies have been promising and shown that these sequences are reproducible and appear more sensitive and accurate than T2w-TSE for IMH detection^{183, 188, 189}.

O'Regan showed that T2* had 100% sensitivity for IMH detection compared to 90% for T2w-TSE, where the 'gold standard' was co-localisation with L-MVO¹⁸³. In canines, T2* in haemorrhagic infarcts closely correlates with iron levels on spectrometry, and T2*-detected IMH co-localises with iron deposition on Perl's staining¹⁸⁵ and extravasated erythrocytes on Haematoxylin-Eosin staining¹⁸⁴. In pigs, regions of IMH on T2* imaging showed vessel degeneration and iron deposition⁵³. A recent porcine study¹⁹⁰ showed that hyperintensity on pre-contrast T1w-IR imaging due to IMH may be visualised easier than hypointensity on T2*. The study suggested that T1w-IR had higher sensitivity, specificity and agreement with histology than T2* and T2w-TSE.

There is a paucity of data regarding temporal changes in CMR-detected IMH.

Mather⁶² showed that IMH on T2w-TSE was present in 33% of patients, with maximal extent at 48 hours post PPCI and progressively decreased at 1 week and 1 month with complete resolution by 3 months. Ghugre⁵³ demonstrated lowest T2* values at 48 hours suggesting maximal extent of IMH (corresponded with maximal iron content on Perl's staining), higher T2* values at 1 week and resolution of IMH at 1 month.

Carrick¹²⁹ recently demonstrated that the incidence and extent of IMH on T2* increased between 8 hours and 3 days post PPCI. Its extent was significantly lower at

10 days and was seen in only 13% of patients at 7 months. The authors also found that MVO was present in all patients with IMH, and its extent peaked earlier at 8 hours suggesting that IMH is an ensuing reperfusion injury in regions of MVO.

1.2.5.3 CMR intramyocardial haemorrhage as a predictor of LV function and remodelling in acute STEMI

There is a small evidence base demonstrating that IMH is a strong univariate predictor of medium-term impaired LV function and adverse remodelling, however multivariate analysis reveals mixed results, with some studies suggesting that IMH offers no incremental predictive value over MVO and IS. Studies are summarised in Table 15.

1.2.5.4 Prognostic importance of CMR-derived intramyocardial haemorrhage in acute STEMI

Multivariate analyses including IMH as a prognostic indicator also show mixed results. Amabile¹⁹¹ demonstrated that IMH on T2w-TSE at 4 days post STEMI was the strongest independent predictor of MACE at 1-year (HR 2.8) in a model including LVEF, ST-resolution and 'lone MVO' (L-MVO but no IMH). However this study had a relatively low incidence of IMH (10%)^{182, 188} and did not provide the number of patients with 'lone MVO', suggesting potential for a Type I error. Husser⁷⁷ showed that only LVEF and IMH extent on T2w-TSE independently predicted MACE at 140 weeks follow-up in a model containing LV volumes, AAR, IS and L-MVO. However IMH and MVO extent showed strong correlation ($r=0.95$) and adding T2w imaging to a model containing LGE and cine imaging did not improve the predictive power for MACE, supporting a strong concordance of IMH and MVO. Eitel¹⁸² demonstrated that IMH presence on T2w-TSE and LVEF <53% were the only CMR independent predictors of MACE at 6 months in a model containing lone MVO. In this study however, adding T2w imaging increased the prognostic value of a model containing LGE and cine imaging. Carrick¹²⁹ recently demonstrated that IMH on T2* mapping was the strongest independent predictor of cardiac death and heart failure hospitalisation at 830 days follow-up. In their multivariate model, L-MVO was not a predictor suggesting that IMH reflects extreme microvascular injury.

Table 15: CMR studies illustrating the importance of IMH on LV function and remodelling in STEMI

Study	Year	n	IMH CMR Method	Main findings	CMR time post MI	Mean/Median F/U CMR
Carrick ¹²⁹	2016	245	T2*	IMH strongest IP (OR 2.64) for LV remodelling in model with patient and angio characteristics, and LVEDVI. IMH associated with lower LVEF and greater volumes	3d	7m
Kidambi ¹⁷³	2013	39	T2w-TSE and T2*	IMH associated with further attenuation of follow-up infarct <i>Ecc</i> in addition to MVO. MVO+IMH strongest IP for decreased infarct <i>Ecc</i> . Model included IS, TIMI pre and post, diabetes, infarct transmural	3d	3m
Husser ⁷⁷	2012	304	T2w-TSE	IMH strongest IP for LV remodelling in model with LVEF, IS, LV vol, L-MVO	6d	189d
Mather ¹⁸⁹	2011	48	T2w-TSE and T2*	IMH presence strongest IP of LV remodelling (>LVESVI) in model with IS, LVEF, LV volumes, E-MVO, MSI	2d	3m
Beek ⁶⁸	2010	45	T2w-TSE	IMH in 49% of patients. IMH was a univariate predictor of LVEF. However no prognostic significance beyond baseline LVEF and presence of MVO in predicting final LVEF	5d	4m
Bekkers ¹⁷⁸	2010	90	T2w-TSE	Acute MSI and LVEF increase at follow-up lowest if IMH present. But IMH no prognostic significance beyond MVO in predicting LVEF	5d	103d
O' Regan ¹⁸³	2010	50	T2*	IMH presence univariate predictor of LVEF and LV volumes. However only IS independently predicted LVEF.	3d	N/A
Ganame ⁶⁹	2009	98	T2w-TSE	IMH extent strongest IP of LV remodelling (increase in LVESVI) in model with IS, Early-MVO, Troponin-I, AAR, TTR and infarct transmural	2d	4m

IS= infarct size, IP= independent predictor, MVO= late microvascular obstruction, LVEF= left ventricular ejection fraction, LVESVI= left-ventricular end systolic volume index, T2w-TSE= T2-weighted turbo spin-echo, AAR=area at risk, MSI= myocardial salvage index

1.2.6 Assessment of ischaemic area at risk (oedema) and myocardial salvage in acute STEMI

1.2.6.1 Background

Oedema is seen in acute cardiac inflammation. In STEMI, it signifies reversible myocardial injury in the ischaemic cascade. The area of oedematous myocardium defines the ischaemic area at risk (AAR) supplied by the occluded IRA^{105, 192}.

1.2.6.2 CMR assessment of ischaemic area at risk (oedema) and myocardial salvage

The T2 (transverse) relaxation time is increased by regional water content. Higgins first demonstrated the linear relationship between increased myocardial water volume on histological assessment of canine acute MI and T2 values¹⁹³.

T2w sequences illustrate oedema as hyperintensity¹⁹² and are currently the mainstay of CMR oedema imaging, in particular turbo spin-echo sequences (T2w-TSE). Most commonly used is the black-blood T2-weighted short-tau inversion-recovery sequence (T2w-STIR). This uses two initial inversion pulses (90° excitation pulse followed by 180° refocusing pulse) to null moving blood. This is followed by a third inversion pulse, which nulls tissues with short T1 times (fat) to provide high contrast between blood (nulled) and myocardium^{192, 194}. T2w imaging of myocardial oedema was first validated by Garcia-Dorado¹⁹⁵, who demonstrated close correlation between T2 values, T2 signal intensity, myocardial water volume and histological assessment in pig myocardial infarction. Aletras¹³⁵ and Tilak¹⁹⁶ then demonstrated in canine myocardium that the AAR on T2w CMR showed close concordance with that on fluorescent microspheres and first-pass perfusion MRI, respectively. T2w oedema assessment is well validated with SPECT¹⁹⁷⁻¹⁹⁹ and angiographic markers of AAR

(BARI²⁰⁰, APPROACH²⁰¹ scoring). T2w imaging was also more accurate at detecting AAR compared with the ECG-based Aldrich criteria, using LGE as a reference²⁰². AAR on T2w can be assessed accurately for upto 1-week post-PPCI unlike SPECT, which requires radionuclide tracer administration during coronary occlusion and analysis within hours; it delivers no radiation, and has higher spatial resolution and thus ability to detect subendocardial injury¹⁹⁷.

However black-blood T2w-TSE imaging has inherent disadvantages that can compromise image quality and oedema detection. Indeed up to 30% of datasets have been deemed non-analysable in studies^{68, 203, 204}. Hence new T2w sequences have been studied, with encouraging results as illustrated in Figure 11. Most extensively investigated is bright-blood T2w-TSE imaging. In the largest study to date (n=54), Payne²⁰⁵ demonstrated greater observer agreement of AAR and myocardial salvage quantification, lower underestimation of AAR extent and more accurate identification of the culprit vessel with bright-blood compared with dark-blood T2w-TSE imaging.

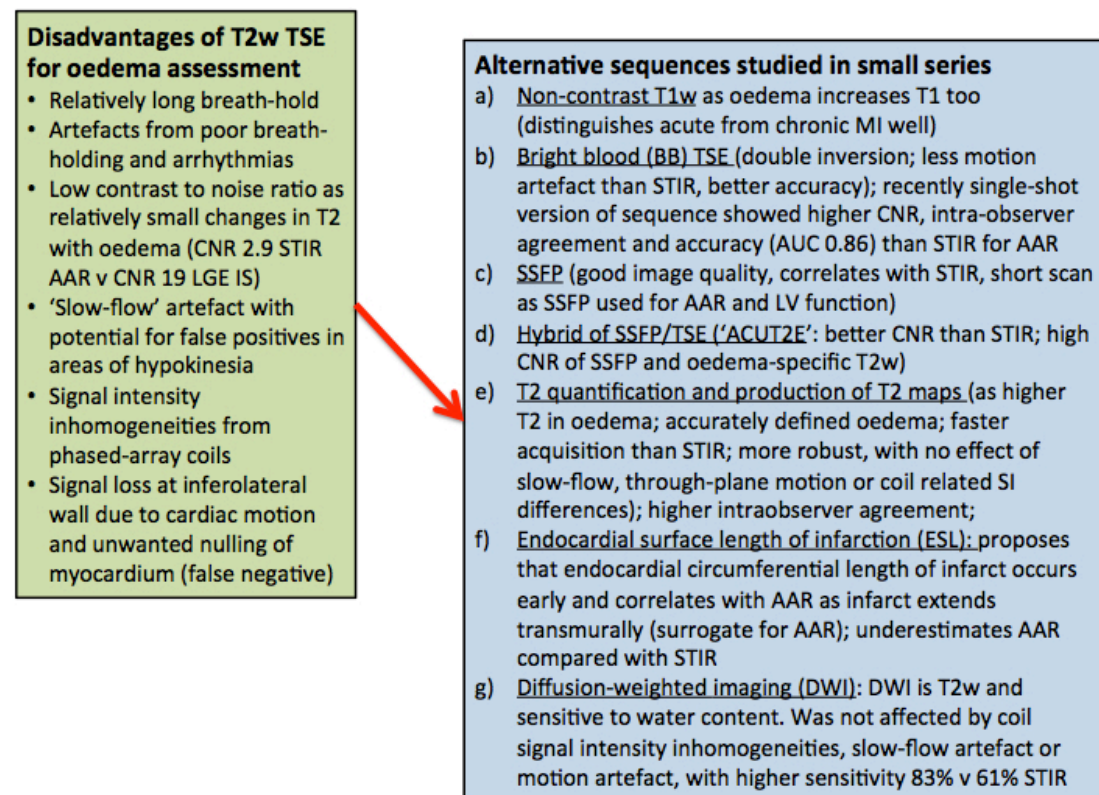


Figure 11: Alternative CMR sequences to dark-blood T2w spin echo for visualising oedema

Left: inherent disadvantages of T2w-TSE^{192, 204, 206-208}. *Right:* alternative sequences studied in small series and compared with T2w-TSE [references for studies: (a)²⁰⁶, (b)^{200, 201, 204, 205}, (c)^{209, 210}, (d)²⁰⁴, (e)^{211, 212}, (f)^{213, 214}, (g)²¹⁵]

The aim of prompt reperfusion is to limit IS by minimizing the conversion of reversibly injured myocardial cells (AAR) into necrotic, infarcted tissue (IS)^{2, 3} since time to revascularisation (TTR) is crucial determinant of IS^{139, 198, 216, 217}. An important predictors of IS is also AAR extent^{58, 70, 218}. Lowe¹³⁶ and Reimer¹³² demonstrated that AAR extent accounted for 81% and 77% of IS variability respectively on animal studies. Indeed, anterior infarction typically results in larger IS due to the larger coronary bed supplied by the left anterior descending artery^{58, 137, 139}. Thus, simply using IS as an endpoint following reperfusion may introduce bias, since a major confounding factor, AAR cannot be assumed to be equal in different treatment arms. A more accurate assessment of revascularisation strategies can be provided by adjusting IS for the AAR. The resulting **myocardial salvage index (MSI)** defines the proportion of reversibly injured tissue (AAR) that does not progress to infarction (IS). It is calculated using Equation 1 below, where MSI is expressed as percentage of the initial AAR (0% is no salvage, 100% is complete salvage [aborted STEMI])²¹⁹ and is illustrated in Figures 12 and 13.

Equation 1: Myocardial salvage index (MSI)

$$\text{Myocardial salvage index (MSI, \%)} = 100 \times \left(\frac{\text{(AAR-IS)}}{\text{AAR}} \right)$$

AAR= area at risk, IS=infarct size

Desch demonstrated excellent intraobserver and interobserver agreement for MSI assessment using T2w-STIR and LGE (coefficients of variation: 4.8%, 5.4% respectively) and excellent test-retest reproducibility in a study of 20 patients with acute STEMI²²⁰.

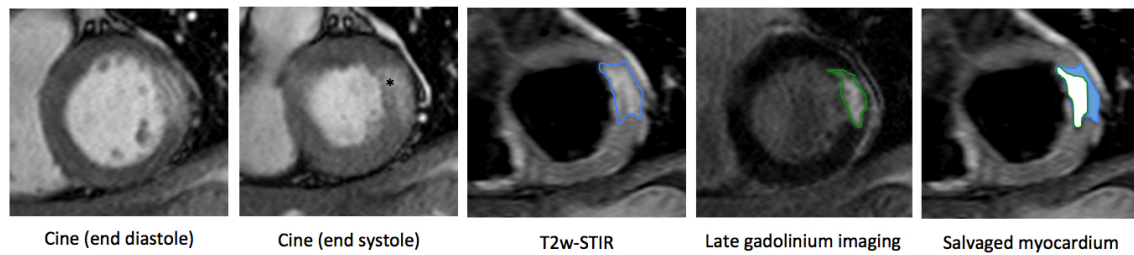


Figure 12: Calculation of salvaged myocardium (MSI) [Patient X504]

Left: SSFP end-diastolic cine image. *Second left:* SSFP end-systolic cine image showing hypokinesia of basal anterolateral segment (*). *Middle:* T2w-STIR image showing oedema (AAR) in anterolateral wall consistent with circumflex artery occlusion. *Second from right:* Corresponding LGE image with near-transmural infarction. *Right:* calculation of salvaged myocardium in blue (MSI)

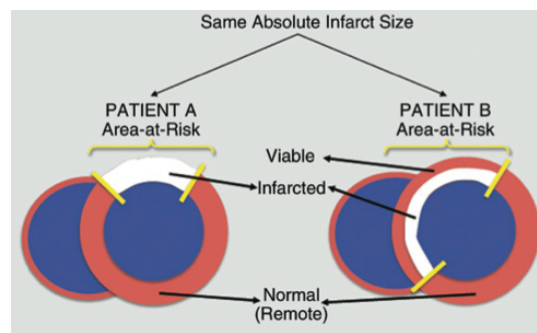


Figure 13: Importance of quantifying area at risk (AAR)

Area at risk (AAR, red within yellow boundaries). Patients A and B have the same IS (white, % of LV mass) post PPCI. However Patient A has transmural infarction with no salvaged myocardium, suggesting prolonged ischaemia and little benefit from reperfusion. Patient B however has subendocardial infarction with a myocardial salvage index of ~60% (from Croisille *et al*)²⁰⁷

Other determinants of AAR include TTR^{147, 188, 221-224}, extent of collateralised blood flow to the IRA territory^{50, 137, 221, 225}, TIMI-flow pre PPCI, LAD IRA and diabetes¹⁴⁷. Phrommintikal demonstrated a moderate correlation between MVO extent and AAR ($r=0.363$, $p<0.01$)²²⁶. Oedema has also been postulated in the pathophysiology of MVO mediated through increased capillary cell stress and volume, and ischaemia²²⁶.

Studies of the chronology of oedema suggest that it occurs very early in the ischaemic cascade. Abdel-Aty confirmed the presence of transmural oedema in canines on *in-vivo* T2w imaging at 28 minutes post LAD occlusion at which point LGE and troponin release were absent, indicating reversible injury²²⁷. Ghugre⁵³ demonstrated that on quantitative T2 mapping in pigs, infarct zone T2 values progressively increased from day 2 to 1 month post infarct, after which they were significantly lower at 6 weeks. Fernandez-Jiminez²²⁸ however recently demonstrated a bimodal pattern of AAR extent in pigs with T2-mapping CMR and histological water quantification. They showed peak values at 2 hours thought to be a direct result of reperfusion, followed by a return to baseline at 2 days and then progressive increase towards peak values at 7 days, with the latter peak felt due to water replacement of cleared cellular debris. Studies of temporal changes in AAR and MSI in humans are summarised in Table 16. Correct timing of oedema imaging is crucial in accurate calculation of AAR and MSI.

Table 16: Temporal changes in CMR-derived area at risk and myocardial salvage index in acute STEMI

Study	Year	n	CMR Timepoints post STEMI when AAR, IS measured	AAR, IS Method (for MSI)	Main findings
Mather ⁶²	2011	48	2d → 1w → 30d → 3m	>2SD T2w-STIR, >2SD LGE	100% had oedema at d2. AAR reduction at successive timepoints, 1-3m (-75%). No change MSI at d2 or 1w as IS and AAR decreased proportionally.
Dall'Armeline ⁶⁵	2011	30	2d → 1w → 2w → 6m	>2SD T2p-BB, >2SD LGE	100% had oedema at d2. AAR stable over 1 st week (37% v 39% LV). Decreased by 2w and nearly resolved at 6m.
Carlsson ¹⁹⁷	2009	16	1d → 1w → 6w → 6m	Manual T2w-STIR, and LGE	AAR on CMR at all timepoints; IS (MSI) at 1w. AAR stable in 1 st week, correlated with 1w SPECT. Dec by 1m (10% LV), nearly gone 6m
Ripa ⁵⁰	2007	58	2d → 1m → 6m	Manual T2w-STIR and LGE	All had oedema at d2. AAR significantly decreased at all time points. No data on MSI in this study.

AAR= area at risk, MSI= myocardial salvage index. *Timepoints*: d= days, w= weeks, m= months. *AAR, LGE Method*: SD= standard deviations, T2w-STIR= T2-weighted short-tau inversion recovery imaging, T2p-SS-BB= T2-prepared single-shot bright-blood, 3T= 3.0 tesla field strength. IS= infarct size

The near-resolution of oedema by 6 months^{50, 62, 65, 147, 197} allows distinction between acute and chronic infarcts when combined with LGE imaging. In a study of 57 infarcts (33 acute, 24 chronic), the combined use of T2w-STIR and LGE imaging demonstrated no difference in SNR or CNR between infarcted and remote myocardium on T2w-STIR in chronic infarcts, whereas acute infarcts demonstrated transmural oedema regardless of reperfusion status²²⁹.

1.2.6.3 CMR myocardial salvage index (MSI) as a predictor of LV function and remodelling in acute STEMI

Myocardial salvage is a strong univariate predictor of medium-term LV function^{58, 226, 230} and adverse LV remodelling post STEMI^{58, 71, 147, 223}. Multivariate analysis however demonstrates mixed results. MSI independently predicted LV remodelling in the work of Mather¹⁸⁹ (Table 17). However MSI was not an IP once IS was added into multivariate models in studies by Monmeneu¹⁴⁷ and Masci⁵⁸, suggesting that IS was a better predictor in these studies. This, in conjunction with the correlation between MSI and IS, and AAR and IS⁷⁰ questions whether MSI and IS are truly independent of each other in predicting LV remodelling and prognosis post STEMI. It could be argued that since MSI adjusts IS for the extent of AAR, it may have less inherent variability than IS. Since up to 30% of AAR datasets have been deemed non-diagnostic in previous studies^{68, 203, 204}, this may impact on the robustness of MSI quantification whereas IS datasets are exceptionally rarely excluded based on image quality. It is therefore not clear currently whether IS or MSI is the better measure of revascularisation success post PPCI.

Table 17: CMR studies showing importance of myocardial salvage on LV function and remodelling in STEMI

Study	Year	n	AAR, IS Method (for MSI)	Main findings	Time post STEMI of predictive CMR	Mean/Median F/U CMR
Mather ¹⁸⁹	2011	48	>2SD T2w-STIR, >2SD LGE	MSI was IP for LV remodelling (>LVESVI at 3m vs. baseline) (OR 0.95) in model including LV volumes, LVEF, IS, IMH, MVO	2d	3m
Monmeneu ¹⁴⁷	2012	118	>2SD T2w-STIR, >2SD LGE	MSI was strong univariate predictor of LV remodelling (>LVESVI at 3m vs. baseline) and final LVEF. However not IP of remodelling in model including IS, LVESVI, no. of transmurally enhanced segments	6d	6m
Masci ⁵⁸	2011	260	>2SD T2w-STIR, >5SD LGE	MSI was strong univariate predictor of LV remodelling (+LVESVI>15%) and final LVEF. However not IP of either in model including IS, MVO extent	1w	4m
Masci ⁷⁰	2010	137	>2SD T2w-STIR, >5SD LGE	MSI strongest IP for LV remodelling (+LVESVI>15%, OR 0.64 per +10% MSI). However IS and MSI (r=-0.72) and IS and AAR (r=0.85) closely correlated. Hence IS excluded from multivariate model, with infarct transmural, AAR, MVO, LVEF	1w	4m

IS= infarct size, IP= independent predictor, MVO= microvascular obstruction, LVEF= left ventricular ejection fraction, LVESVI= left-ventricular end systolic volume index, T2w-STIR= T2-weighted short-tau inversion-recovery, LGE= late gadolinium enhancement

1.2.6.4 Prognostic importance of CMR-derived myocardial salvage index (MSI) in acute STEMI

Historically, the prognostic value of MSI was demonstrated using SPECT. Ndrepapa first showed that MSI was the strongest independent predictor of 6-month mortality²³¹. MSI was an independent prognostic indicator in the medium term post STEMI in two studies^{78, 223}. Although the studies are from the same patient cohort, they have both been included in Table 18 due to their differing primary findings. Interestingly in the first study, MSI (but not IS) was an IP of MACE and mortality at 6 months²²³. However in the second study, MSI was an IP of mortality, but not MACE, whereas IS was now an IP for MACE⁷⁸. Only one of IS and MSI was an IP in the models in the studies, which is again likely to be due to the correlation between MSI and IS.

Table 18: CMR studies illustrating the prognostic importance of myocardial salvage index in acute STEMI

Study	Year	n	AAR, IS Method (for MSI)	Main findings	Time of prognostic CMR post STEMI	Mean/median clinical follow up
Eitel ⁷⁸	2011	208	>2SD T2w-STIR, >5SD LGE	MSI was only CMR-based IP of mortality (OR 0.93) in model with age, IS, MVO, LVEF, TIMI-flow post PPCI, diabetes, age (IS not IP). MSI however not IP of MACE (only IPs were IS, LVEF, age)	3d	19m
Eitel ²²³	2010	208	>2SD T2w-STIR, >5SD LGE	MSI was only IP for MACE and mortality in model including LVEF, MVO, IS, ST-resolution and TIMI-grade post PCI	3d	6m

IS= infarct size, PCI= percutaneous coronary intervention, MACE= major adverse cardiovascular events, IP= independent predictor, MVO= microvascular obstruction, LVEF= left ventricular ejection fraction

1.2.7 T1, T2 and T2* quantification and mapping in acute STEMI

The current mainstay of LGE and T2w assessment for infarct and oedema relies on semi-quantitative threshold-based quantification, automated algorithms or manual planimetry. There is no consensus on the optimal quantification method for IS or AAR. This can lead to subjectivity and dependence upon optimal myocardial nulling.

T1, T2 and T2* quantification present an exciting and complementary approach to LGE and T2w imaging. They allow not only the location and extent of infarction, oedema, MVO and IMH to be determined from parametric maps, but also the severity of these pathologies to be assessed through the magnitude of values obtained^{232, 233}. In addition these methods are not reliant on reference regions of interest and do not suffer from the artefacts associated with T2w-TSE imaging.

1.2.7.1 T1 mapping (longitudinal relaxation)

The currently used curve-fitting sequences for T1 time calculation include MOLLI (Modified Look-Locker Inversion Recovery), ShMOLLI (Shortened MOLLI), SASHA (SATuration recovery single-SHOT Acquisition) and SAPPHIRE (Saturation Pulse Prepared Heart rate independent Inversion REcovery)¹²⁷. Infarcted and oedematous myocardium demonstrate prolonged pre-contrast (native) T1 values and reduced post-contrast T1 values^{232, 234-236}. Messroghli showed that this technique had high test-retest reproducibility²³⁷, was stable within the range of commonly encountered heart rates and showed comparable sensitivity for IS quantification to LGE^{234, 235, 238}.

1.2.7.2 T2 mapping (transverse relaxation)

T2 values are generated using log-transformed curve fitting on T2-SSFP sequences. T2 mapping has demonstrated excellent reproducibility and no effect of slow-flow, through-plane movement (Figure 14), SI loss, or effects of coil SI inhomogeneities^{211, 239}. T2 mapping accurately assessed oedema in 96% of patients, whereas T2w-STIR detected oedema in only 67% of patients²¹¹. High intraobserver and interobserver agreement, and close agreement between T1 ($r^2=0.94$) and T2 maps ($r^2=0.96$), and fluorescent microspheres for AAR detection were shown in canine myocardium²⁴⁰.

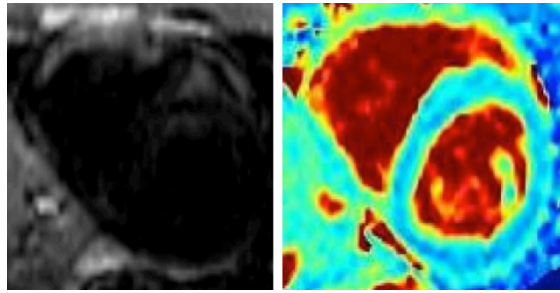


Figure 14: Effect of cardiac motion on T2w-STIR and T2 maps

Left: Non-diagnostic T2w STIR image with signal loss due to cardiac through-plane motion. This can be improved by increasing the dark-blood inversion slab thickness but at a cost of increased slow-flow artefact. *Right:* Corresponding T2 map with no effect of cardiac motion, and high quality parametric T2 map (from Giri *et al*)²³⁹

1.2.7.3 T2* mapping (transverse relaxation in presence of field inhomogeneities)

T2* mapping allows visualisation and quantification of IMH due to the presence of paramagnetic haemoglobin breakdown products using a cut-off value of $<20\text{ms}$ ²⁴¹. O'Regan demonstrated that it has greater sensitivity than T2w-STIR imaging (100% vs. 90%) for IMH (Figure 15). Kali showed good correlation between *in-vivo* T2* values and histological assessment of IMH and iron levels in canine myocardium^{184, 186}. T2* mapping may improve the specificity of IMH detected on CMR¹⁸⁹.

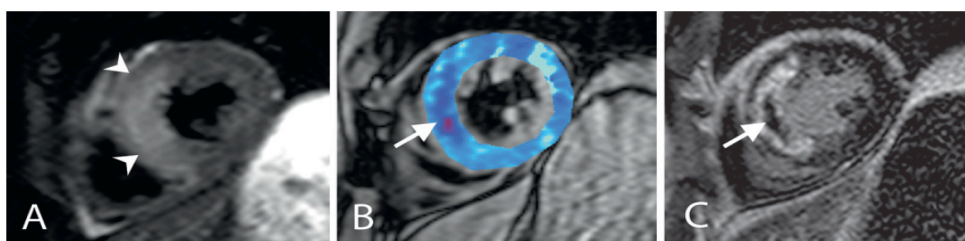


Figure 15: T2* mapping for assessment of intramyocardial haemorrhage (IMH)

IMH only visible on T2* mapping demonstrating greater sensitivity than T2w-TSE imaging. *Left:* (A) T2w-SPIR (spectrally selective inversion-recovery) demonstrates oedema (AAR) in the arrowed area but no IMH. *Middle:* (B) T2* map demonstrates area of reduced T2* within the septum consistent with IMH arrowed. *Right:* (C) this is confirmed by the co-localisation of L-MVO on LGE imaging (from O'Regan *et al*)¹⁸³

T1, T2 and T2* surrogate markers hold promise for improving the accuracy of detection of infarct, oedema and IMH respectively, and improving the statistical power of STEMI studies. However, due to the importance of protocol standardisation, these techniques are rarely used in multicentre studies at present.

1.2.8 Assessment of right ventricular involvement in acute STEMI

1.2.8.1 CMR assessment of right ventricular infarction in acute STEMI

CMR is the gold standard imaging modality for the assessment of right ventricular (RV) volumes, function, oedema²⁴² and infarction (RVI)²⁴³. CMR has been shown to identify RVI on manual quantification with greater sensitivity than echocardiography, ECG (V4_R ST-segment elevation) and clinical examination^{244, 245} and demonstrate RV L-MVO^{246, 247}. There is good interobserver and intraobserver agreement for the identification of RV oedema ($\kappa=0.62$, $\kappa=0.62$, respectively) and very good agreement for RVI ($\kappa=0.70$, $\kappa=0.70$, respectively)²⁴². The high MSI in RVI often >90%^{248, 249} is thought to be due the relatively low RV nutrient needs, direct endocardial diffusion of oxygen and good collateral blood supply^{249, 250}. There is little data on temporal changes in RVI. Kumar²⁵¹ undertook CMR on day 3 and 13-months post STEMI with RVI persisting in 93% of patients, whereas Masci²⁴² demonstrated persistent RVI at 4-months in only 18% of patients. The contrasting findings may be due to the fact that over 60% of patients in the Kumar study had large RVIs (>25% RV mass)²⁵¹.

1.2.8.2 Prognostic importance of CMR-derived right ventricular infarction in acute STEMI

RVI confers adverse short-term prognosis, with a large meta-analysis (n=7136) demonstrating that RVI assessed on ECG, echocardiography or radionuclide ventriculography predicted 30-day mortality (RR 2.59) and in-hospital MACE²⁵². Shah first demonstrated the prognostic importance of right ventricular infarction diagnosed on imaging, where RVEF <38% on radionuclide ventriculography post STEMI was a strong independent predictor of 1-year mortality²⁵³. Right ventricular infarction has been shown to be a strong independent predictor of medium to long-term prognosis in a small number of CMR studies, as summarised in Table 19.

Table 19: CMR studies illustrating the prognostic importance of right ventricular infarction in acute STEMI

Study	Year	n	RV LGE analysis method	Main findings	Time of prognostic CMR post STEMI	Mean/median F/U
Jensen ²⁴⁵	2010	50	Manual	RVI only IP of MACE in model with age, sex, LVEF, LV IS	3d	32m
Miszalski-Jamka ¹⁵³	2010	99	Manual	RVEF (HR 1.46) and RVI extent (HR 1.50) IP for MACE	'3-5d'	1150d
Grothoff ²⁴⁸	2012	450	Manual	RVI was IP of MACE (HR 6.70)	'1-4d'	20m

MACE= major adverse cardiovascular events, IP= independent predictor, HR= hazard ratio, RV= right ventricle, LVEF= left ventricular ejection fraction

1.2.9 When is the optimal time to undertake CMR assessment post acute STEMI?

In acute STEMI, IS, AAR and MSI are best imaged at 7 days post PPCI due to overestimation of necrosis on LGE, and IS at 7 days best predicts final IS, LV remodelling and function and prognosis^{50-52, 54, 62, 64, 65}. Human studies suggest that AAR is stable during the first week^{65, 197}. Although Fernandez-Jimenez²²⁸ demonstrated a bimodal AAR peak in pigs, their drop in AAR extent on T2w CMR at 2 days post-reperfusion may be due to a high incidence of IMH in pigs and peak IMH extent at 2 days¹²⁹. Indeed the drop in AAR extent on the gold standard of histological water analysis in their study at 2 days was much less pronounced, and at 7 days AAR extent had returned to stable peak levels. In addition, studies demonstrating close agreement between T2w-derived AAR and the reference non-invasive modality of SPECT^{197, 198} were undertaken at 7 days post STEMI. MVO and IMH extent peak at 48 hours then decrease⁶² but are present at 7 days^{54, 62}. Although undertaking CMR at 7-days may potentially underestimate MVO and IMH extent^{54, 62, 129}, this may be minimised by expressing MVO and IMH extent as a proportion of IS rather than LV mass, to correct for the corresponding reduction in IS. Thus, **acutely post STEMI** for the assessment of IS, MSI, MVO and IMH, imaging at **7 days** may

provide the best compromise in relation to their temporal changes^{50-52, 54, 62, 64, 65} for accurate quantification and prediction of LV function, remodelling and prognosis. This needs to be balanced with contemporary clinical practice where patients are typically discharged at 3-4 days post-PPCI, and the risk of early attrition. Using final IS at follow-up as a primary outcome risks underestimating potential differences in treatment strategies due to greater infarct resorption with the larger infarcts.

Data on the chronology of IS suggests that infarct resorption is essentially complete by 3 months post MI^{54, 62, 64, 129}. However a key objective of follow-up CMR is to assess LV geometry and remodelling and hence must allow the relatively slower adaptations of ventricular volumes (~12 months), compared with changes in IS and LVEF to complete. LVEF shows no significant change after 1-month post STEMI. Follow-up CMR at 3 and 6-months may fail to provide an accurate assessment of LV volumes and remodelling. The current evidence base suggests that in order to allow completion of the trio of IS, LVEF *and* LV volumetric changes, follow-up CMR should be performed at **12-months** post STEMI^{50, 52, 62, 64, 65}. When correlating CMR and clinical outcomes, the longer timepoint of 12-months also permits more reliable clinical follow-up.

Standardisation of LGE, AAR and IMH sequences and quantification methods is equally important in light of newer T1, T2 and T2*-mapping sequences and inherent image quality issues associated with T2w-TSE.

1.3 Summary

Contrast-enhanced CMR offers robust, validated and reproducible surrogate markers, providing an accurate representation of pathophysiology, assessment of myocardial function and injury, and predictive value for medium to long-term LV function, remodelling and prognosis following PPCI for STEMI. Tables 20 and 21 summarise the key prospective studies illustrating the independent predictive value of CMR markers for LV remodelling (studies where n>100, follow-up CMR ≥3 months post PPCI) and prognosis (studies where n>100, ≥6 months follow-up) respectively.

Current areas for focus include ascertainment of whether MSI and MVO offer incremental predictive value for LV remodelling and prognosis over IS, whether MVO and IMH are separate entities and offer independent predictive value for LV remodelling and prognosis, and a need for large multicentre studies and standardisation of quantification methods and acute and follow-up CMR timing.

In the acute phase, CMR can be performed accurately for up to 7 days post PPCI. CMR delivers no radiation to the patient and this makes it ideal for serial studies. The multimodal nature of CMR allows a multiparametric study of cardiac function, structure and volumes within a single study, which can be undertaken within ~45 minutes in the majority of patients. It is likely that CMR will become the mainstay of cardiac imaging, providing an important role in risk stratification and treatment post STEMI. Focus needs to be continued in translating findings on the prognostic importance of surrogate markers to development of therapeutic targets post STEMI.

The accuracy, reliability, reproducibility and prognostic importance of CMR-based surrogate markers of outcome post STEMI significantly increases statistical power of studies, and thus allows the required sample size to be reduced. There is a real need for an adequately powered, prospective, randomised-controlled study investigating the current treatment strategies for managing MVD at PPCI **with non-invasive imaging** assessment to provide a mechanistic understanding of differences in efficacy, safety and outcomes between the groups. A study investigating MVD PPCI strategies using CMR-based outcomes would be a novel, vital addition to the evidence base, and help tackle the current lack of consensus. The recent DANAMI-3-PRIMULTI¹⁵ and PRAMI¹⁶ studies are a welcome addition to the current evidence base as the largest prospective, randomised study to date, but as discussed earlier, it has a number of important limitations and features no cardiac imaging.

Table 20: Key studies illustrating the independent predictive value of CMR markers for LV remodelling

CMR marker	Study	Year	n	CMR quantification	Main findings	Acute CMR Time	F/U CMR Time
IS	Husser ⁷⁷	2012	304	>2SD	IS extent IP for LV remodelling in model with LVEF, IS, LV volumes, MVO	6d	189d
IS	Monmeneu ¹⁴⁷	2012	118	>2SD	Number of segments >50% transmural IP for LV remodelling	6d	6m
IS	Wu ¹⁵⁰	2008	122	Manual	IS extent at 2d only IP for LVEF and LV remodelling	2d	4m
IS	Hombach ⁵¹	2005	110	Manual	IS extent at 6d was an IP for LV remodelling in model with MVO, % transmural	6d	225d
L-MVO	Weir ¹⁷⁰	2010	100	Manual	L-MVO extent was only IP of LV remodelling in model with TIMI post PCI, E-MVO, IS	4d	6m
L-MVO	Hombach ⁵¹	2005	110	Manual	L-MVO extent IP of LV remodelling in model with baseline IS, infarct transmural	6d	225d
IMH	Carrick ¹²⁹	2016	245	T2*	IMH strongest IP of LV remodelling in model with patient/angio characteristics, LVEDVI	3d	7m
IMH	Husser ⁷⁷	2012	304	T2w-TSE	IMH strongest IP for LV remodelling in model with LVEF, IS, LV volumes, L-MVO	6d	189d
MSI	Monmeneu ¹⁴⁷	2012	118	>2SD STIR, >2SD LGE	MSI univariate but not IP of remodelling in model with IS, LVESVI, no. of segments >50%	6d	6m
MSI	Masci ⁵⁸	2011	260	>2SD STIR, >5SD LGE	MSI univariate predictor of LV remodelling and final LVEF. However not IP of either in model including IS, MVO extent	1w	4m
MSI	Masci ⁷⁰	2010	137	>2SD T2w-STIR, >5SD LGE	MSI strongest IP for LV remodelling. However IS and MSI and IS and AAR correlated. Thus IS excluded from multivariate model, containing transmural, AAR, MVO, LVEF	1w	4m

Criteria were individual studies with $n \geq 100$ and follow-up CMR ≥ 3 months post-PPCI. IS= infarct size, L-MVO= late microvascular obstruction, IMH= intramyocardial haemorrhage, MSI= myocardial salvage index, SD= standard deviations, STIR= T2-weighted short-tau inversion recovery, LGE= late gadolinium enhancement, IP= independent predictor, LV= left ventricular, LVEF= left ventricular ejection fraction, AAR= area at risk, LVEDVI= left ventricular end-diastolic volume

Table 21: Key studies illustrating the independent predictive value of CMR markers for prognosis

CMR marker	Study	Year	n	CMR quantification	Main findings	Acute CMR Time	F/U Duration
IS	Husser ¹⁵¹	2013	250	>2SD	Extent of transmural infarction (no. of segments >50% transmural) only IP for MACE	7d	163w
IS	Izquierdo ¹⁵²	2013	440	>2SD	IS was IP for arrhythmic cardiac events in model including LVEF, hypertension	7d	123w
IS	Eitel ⁷⁸	2011	208	>5SD	IS was IP of MACE at 19m, in model with MVO, LVEF, MSI, Killip class TIMI flow post-PPCI	3d	18.5m
IS	Larose ¹¹²	2010	103	FWHM	IS strongest IP for MACE in model containing LVEF, CK. LGE>23% had HR 6.1 for MACE.	4.5h	2y
IS	Bodi ²⁸	2009	214	>2SD	Extent of transmural infarction (no. of segments >50% transmural) IP for MACE	7d	553d
IS	Wu ¹⁵⁴	2008	122	Manual	IS only IP of 2y MACE in model containing LVEF, LVESVI (HR 1.06)	2d	538d
L-MVO	Regenfus ¹⁷⁴	2015	249	Manual	MVO extent strongest IP for MACE in model with IS, LVEF, TIMI and no. of diseased vessels	3.7d	72m
L-MVO	Eitel ¹⁷⁶	2014	738	>5SD	L-MVO >1.4% LVM IP of MACE in model with LVEDVI, LVEF and clinical markers	7d	6m
L-MVO	De Waha ¹⁷⁷	2012	438	Manual	L-MVO extent IP for MACE in model with IS, LV volumes. L-MVO/IS strongest IP	3d	19m
L-MVO	De Waha ⁸⁰	2010	438	Manual	L-MVO strongest IP of MACE and mortality in models with IS, LVEF, STR, TIMI post PPCI.	3d	19m
L-MVO	Cochet ⁸¹	2009	184	Manual	L-MVO strongest IP for MACE, in models with GRACE, IS, LVEF. E-MVO weaker IP	'3-7d'	12m
L-MVO	Bruder ¹⁶⁴	2008	143	Manual	Only extent of L-MVO >0.5% LV mass was IP for MACE in model with IS, LVEF, age, DM, sex	4.5d	12m
L-MVO	Hombach ⁵¹	2005	110	Manual	L-MVO IP for MACE (p=0.04) in model including LV end-diastolic volume and LVEF	6d	268d
IMH	Carrick ¹²⁹	2016	245	T2*	IMH strongest IP of CV death and HF. In multivariate model, L-MVO not a predictor	3d	830d
IMH	Amabile ¹⁹¹	2012	114	T2w-TSE	IMH presence was strongest predictor of MACE in model with MVO, LVEF, STR	4d	12m
IMH	Husser ⁷⁷	2012	304	T2w-TSE	IMH IP for MACE in model with AAR, IS, L-MVO. T2w no inc. value of model with LGE, cine	6d	140w
IMH	Eitel ¹⁸²	2011	346	T2w-TSE	IMH was IP of MACE in model with L-MVO. T2w inc. value of model with LGE and cine	3d	6m
MSI	Eitel ⁷⁸	2011	208	>2SD / >5SD	MSI only CMR IP of mortality in model with age, IS, MVO, LVEF, TIMI post PCI, DM. IS not IP	3d	19m
MSI	Eitel ²²³	2010	208	>2SD / >5SD	MSI was only IP for MACE and mortality in model with LVEF, MVO, IS, STR, TIMI post PPCI	3d	6m

Criteria were individual studies with $n \geq 100$ and follow-up CMR ≥ 6 months follow-up. IS= infarct size, L-MVO= late microvascular obstruction, IMH= intramyocardial haemorrhage, MSI= myocardial salvage index, SD= standard deviations, STIR= T2-weighted short-tau inversion recovery, LGE= late gadolinium enhancement, IP= independent predictor, LV= left ventricular, LVEF= left ventricular ejection fraction, AAR= area at risk, LVEDVI= left ventricular end-diastolic volume, CK= creatine kinase, T2w-TSE= T2-weighted turbo spin echo, MACE= major adverse cardiovascular events, CV= cardiovascular

1.4 Aims and original hypotheses

This thesis aims to investigate the mechanisms by which differences in clinical outcomes between patients participating in the CvLPRIT trial comparing a CR and IRA-only PCI strategy may arise ('CvLPRIT-CMR substudy')²⁵⁴. Multiparametric contrast-enhanced CMR imaging was undertaken in the acute and chronic phases post-PPCI for MVD in STEMI. This formed the main results chapter of this thesis. In addition, using this unique dataset, several other hypotheses were tested as outlined below.

1.4.1 Assessment of IS

Aim(s): The primary aim of the CvLPRIT-CMR substudy was to assess whether a CR strategy, due to causing additional infarcts in non-IRA territories was associated with increased total IS at acute and follow-up CMR than an IRA-only strategy in patients randomized in CvLPRIT.

- H_0 : There will be no difference in total IS in patients in the CR and IRA-only revascularisation groups.
- H_A : Total IS will be increased in the CR revascularisation group compared with the IRA-only revascularisation group.
- H_0 : There will be no difference in non-IRA myocardial injury post index STEMI (non-IRA acute IS, proportion of patients with >1 acute infarcts on LGE).
- H_A : Non-IRA myocardial injury post index STEMI (non-IRA acute IS, proportion of patients with >1 acute infarcts on LGE) will be increased in patients having CR.

1.4.2 Assessment of MSI, MVO and IMH

Aim(s): To examine whether myocardial salvage and microvascular injury (MVO, IMH) differ in the CR versus IRA-only revascularisation strategies.

- H_0 : There will be no difference in MSI, MVO and IMH in patients in the CR and IRA-only revascularisation groups.
- H_A : MSI will be reduced and MVO and IMH will be increased in the CR revascularisation group

1.4.3 Assessment of LV function

Aim(s): To determine whether LV function and volumes differs following the CR versus IRA-only revascularisation strategies.

- H_0 : There will be no difference in LVEF in patients in the CR and IRA-only revascularisation groups.
- H_A : LVEF will be reduced in the CR revascularisation group compared with the IRA-only revascularisation group.

1.4.4 Assessment of ischaemic burden

Aim: To determine whether CR reduces ischaemic burden in the medium-term.

- H_0 : There will be no difference in ischaemic burden at 9-months post PPCI in patients in the CR and IRA-only revascularisation groups.
- H_A : CR patients will have lower ischaemic burden than those undergoing IRA-only revascularisation at 9-months post PPCI.

1.4.5 Assessment of clinical outcomes

Aim: To determine whether medium-term (12 month) clinical outcomes differ in the CvLPRIT-CMR substudy following CR versus IRA-only revascularisation strategies.

- H_0 : There will be no difference in 12-month combined MACE (time to first event) in patients in the CR and IRA-only revascularisation groups.
- H_A : CR patients will have lower 12-month combined MACE (time to first event) burden than an IRA-only at 9-months post PPCI.

1.4.6 Assessment of infarct characteristics using semi-automated quantification methods

Aim(s): To compare the feasibility, accuracy and reproducibility of existing FWHM and standard-deviation based quantification methods with the newer Otsu's Automated Thresholding technique in the assessment of IS and AAR, where manual

quantification is taken as the reference method.

- H_0 : There will be no difference in the time taken for quantification, interobserver and intraobserver agreement, correlation with IS, or agreement with manual quantification of IS and AAR and MSI measures using FWHM, Otsu's Automated Thresholding and standard-deviation based quantification methods.
- H_A : Otsu's Automated Thresholding will have higher (i) interobserver and (ii) intraobserver agreement, (iii) require shorter analysis times and (iv) demonstrate closer agreement with manual quantification and (v) LVEF for the assessment of IS and AAR compared with established semi-automated established methods.

1.4.7 Assessment of LV strain using novel quantification methods

Aim(s): To compare the feasibility and observer agreement of FT and tissue-tracking analysis for the measurement of global and segmental LV peak systolic circumferential and longitudinal strain in acute STEMI.

- H_0 : There will be no difference in the interobserver and intraobserver agreement, time taken for quantification, or number of non-analysable datasets for the quantification of global and segmental peak systolic LV circumferential (E_{cc}) and longitudinal strain (E_{ll}) using FT and tissue-tagging analysis methods.
- H_A : FT quantification of global and segmental peak systolic LV circumferential (E_{cc}) and longitudinal strain (E_{ll}) will have greater interobserver and intraobserver agreement, require shorter analysis times and have fewer non-analysable datasets compared with tissue-tagging analysis methods.

1.4.8 Assessment of predictors of improvement in segmental function

Aim(s): To assess whether FT-derived E_{cc} , MSI, late MVO and IMH predict segmental functional recovery in acute STEMI and whether this was of additive value to the known predictor of segmental extent of LGE.

1.4.9 Assessment of IS following staged and immediate in-hospital CR strategies

Aim(s): To assess IS and LV function in patients who underwent immediate compared with staged in-hospital CR, in order to gain insight into potential likely mechanisms to explain differences in clinical outcomes seen in CvLPRIT-CMR.

- H_0 : There will be no difference in IS or LVEF in patients undergoing immediate versus staged in-hospital CR.
- H_A : Patients undergoing immediate in-hospital CR will have smaller IS and resultant higher LVEF compared with those undergoing staged in-hospital CR.

CHAPTER TWO

2. METHODS

2.1 Study overview

2.1.1 Study design

The Complete Versus Lesion-only Primary PCI pilot (CvLPRIT) study was a multicentre, open, RCT comparing in-patient IRA-only and complete revascularisation (CR) for the management of MVD at PPCI for STEMI (Figure 16).

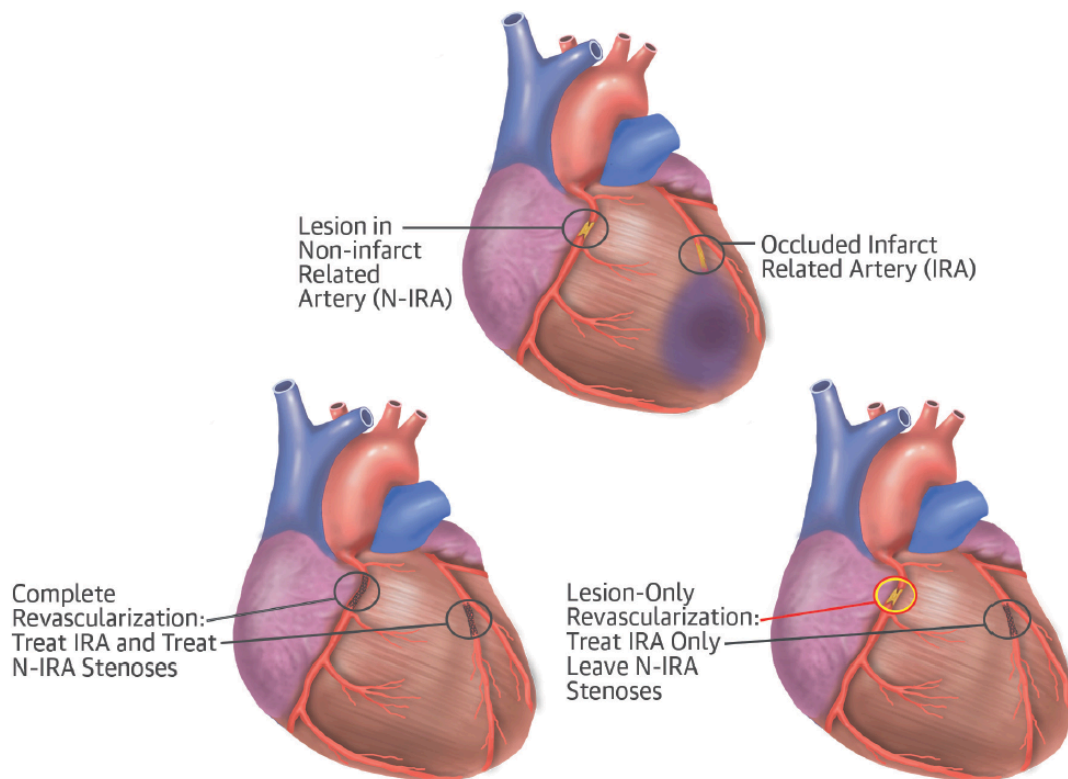


Figure 16: The Complete Versus Lesion-only Primary PCI pilot (CvLPRIT) study

Schematic illustrating the main CvLPRIT study randomisation strategy.

IRA= infarct-related artery, N-IRA= non infarct-related artery (from Gershlick *et al*)²⁵⁵

The trial was funded by the British Heart Foundation in 2010 as a pilot study aiming to recruit 250 patients in 4 centres (Leicester, Leeds, Harefield and Southampton).

The embedded CMR substudy (CvLPRIT-CMR) was funded by the MRC-NIHR EME programme following a fast track application in August 2010. The design was a pragmatic, multicentre, prospective, randomized-controlled, open, clinical trial with blinded end-point (CMR) analysis (PROBE design)²⁵⁶. It was intended to complete recruitment, follow-up and data analysis within 2 years of study initiation.

2.1.2 Study population

Patients presenting to the participating centres with acute STEMI and MVD at PPCI.

2.1.3 Recruitment

Recruitment started in May 2011 and was slower than anticipated. The study was rolled out to three additional centres with support from the NIHR Comprehensive Local research Networks. The BHF awarded a one-year extension in 2013 to allow the recruitment target to be extended (285 patients, ensuring) and 12-month follow-up to be completed. The NIHR EME also awarded a 9-month time extension with a small cost extension. The participating hospitals and recruitment dates are as follows:

The 7 centres undertaking 24/7 PPCI in this multicentre study were:

1. Glenfield Hospital (recruited May 2011-April 2013)
2. Southampton General Hospital (recruited August 2011-April 2013)
3. Leeds General Hospital (recruited September 2011-April 2013)
4. Harefield Hospital (recruited November 2011- April 2013)
5. Kettering General Hospital (recruited July 2012-April 2013)
6. Royal Derby Hospital (recruited August 2012- April 2013)
7. Royal Bournemouth Hospital (recruited February 2013- April 2013)

2.1.3.1 Inclusion criteria

- Suspected acute STEMI: ST elevation (≥ 2 mm in ≥ 2 adjacent chest leads, ≥ 1 mm in ≥ 2 adjacent limb leads, ≥ 1 mm in leads V7-V9) or left bundle branch block on 12-lead ECG
- <12 hrs symptom duration^{3, 257}
- Scheduled for PPCI
- Verbal assent followed by written informed consent
- MVD: defined as IRA plus ≥ 1 N-IRA with significant disease ($>70\%$ stenosis in 1 plane or $>50\%$ in 2 planes). The N-IRA must be an stentable epicardial coronary artery or major branch of >2 mm diameter²⁵⁸

2.1.3.2 Exclusion criteria

- <18 years age
- Clear indication for or against CR according to operator
- Previous Q-wave MI
- Previous CABG
- Cardiogenic shock
- Ventricular septal defect or moderate/severe mitral regurgitation
- Severe chronic kidney disease (eGFR<30ml/min)
- Stent thrombosis
- Where the only significant N-IRA lesion is a chronic total occlusion (CTO)
- Standard MRI contraindications (pacemaker, ICD/CRT, intracranial implant incompatible with magnetic field, severe claustrophobia, weight >200kg)

2.1.3.3 Initial assessment (pre-PPCI)

The coronary care unit at each centre was alerted by paramedics of incoming STEMI patients. On arrival to hospital, the CvLPRIT Research Team discussed the study with patients once acute STEMI of <12 hours duration was confirmed on history and ECG. Prior to PPCI, an ethically approved, short study narrative was read to the patient (Appendix 1). Where eligible patients provided verbal agreement (assent) to enter the RCT, this was documented in the medical records. Assent allowed delivery of key information to patients within expected time constraints during STEMI and sufficient opportunity for patients to ask questions. Verbal information is understood and retained significantly better by patients, compared with written information in acute MI trials²⁵⁹⁻²⁶¹. The assent procedure was successfully used in the STREAM²⁶² and ReFLO-STEMI²⁶³ multicenter acute STEMI studies. If patients met inclusion criteria after angiography they were asked to give further verbal assent before randomisation.

2.1.3.4 Randomisation

Patients were randomised on-table, pre-PCI, via a dedicated 24/7-telephone service to **in-hospital IRA-only revascularisation** or **CR**. Randomisation was stratified using minimization, by anterior or non-anterior STEMI (ECG-guided), and symptom time

(time to reperfusion) \leq or >3 hrs, since these are strong prognostic indicators post STEMI²⁶⁴. Randomisation was run through an independent company ('Sealed Envelope'TM [London, UK]) and took <90 seconds.

2.1.3.5 Consent

Randomised patients were given full patient information leaflets within 24 hours, assuming medically fit, and asked to provide full written informed consent to continued study participation, including the optional CMR substudy. At all times, patients were informed that they were under no obligation to continue study participation.

2.1.4 Treatment

2.1.4.1 IRA-only revascularisation (IRA-only)

PPCI to the IRA-only was regarded as the standard of care and was performed according to ACCF/AHA³ and ESC² guidelines. Multiple orthogonal angiograms of the left and right coronary artery systems were acquired in standard radiographic projections using digital fluoroscopic angiography systems at 15 frames per second.

Peri-PCI adjuncts were administered at the operator's discretion as follows:

- Dual antiplatelet loading with Aspirin plus Clopidogrel, Prasugrel (Daiichi-Sankyo, Japan) or Ticagrelor (Astra-Zeneca, UK) for P2Y12 inhibition pre-angiography.
- Heparin, Bivalirudin (Medicines Company, USA), glycoprotein IIb/IIIa inhibitors e.g. Abciximab (Lilly, USA), thrombus aspiration devices e.g. Export (Medtronic USA), vasodilators e.g. adenosine and isosorbide dinitrate during PPCI.

The choice of stent and stent implantation technique were at the operator's discretion but drug-eluting stent use was strongly encouraged.

2.1.4.2 Complete revascularisation (CR)

Complete revascularisation was the investigational intervention. It was recommended that revascularisation be completed during the index PPCI procedure (Figure 17). Where this was not possible, N-IRA PCI was performed during the index admission, within 36 hours of PPCI and prior to CMR.

All patients were treated with optimal medical treatment as per ESC and ACCF/AHA guidelines (dual antiplatelet therapy, ACE-inhibition, beta-blockade, high dose statin)^{2,3}. Repeat coronary angiography was recommended only for (a) recurrent ischaemic symptoms with confirmation on non-invasive imaging (e.g. stress CMR, SPECT) or (b) at the discretion of the local investigator following a positive non-invasive test at 6-8 weeks post PPCI.

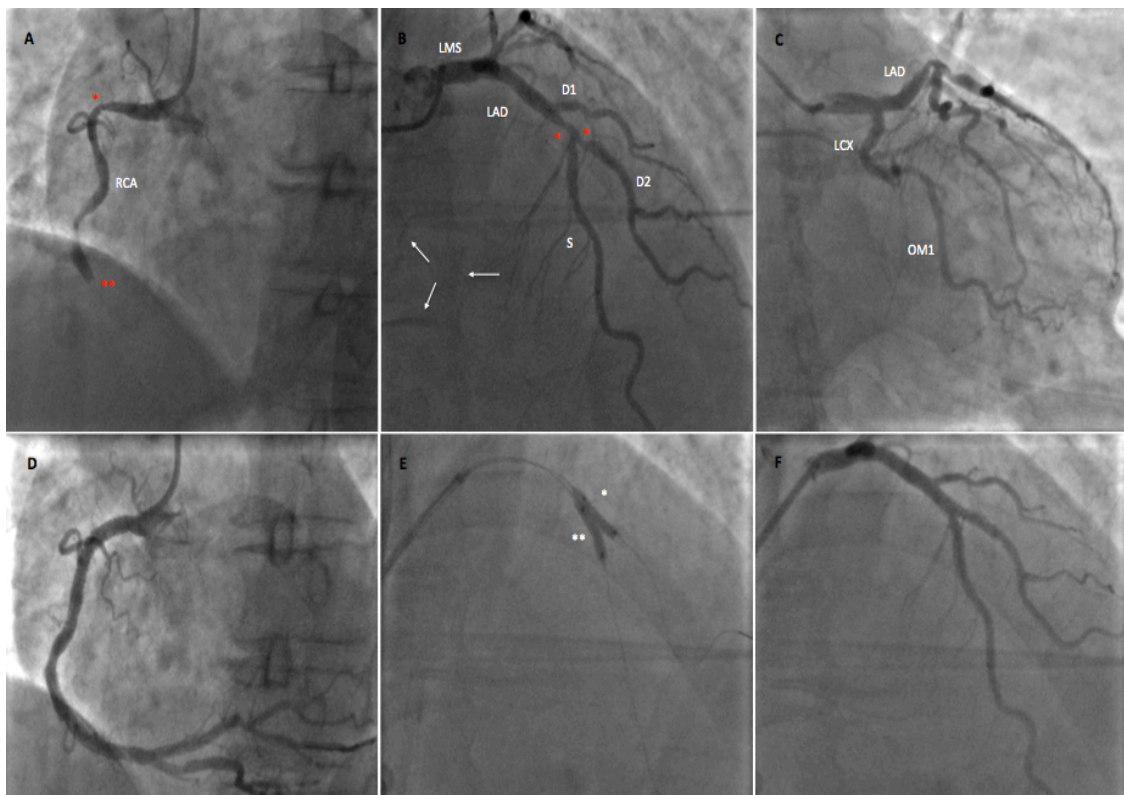


Figure 17: MVD at PPCI managed with CR (complete revascularisation) [Patient X708]

A: RCA is IRA in this patient with inferior MI. Two significant stenoses (* = ~70% stenosis in proximal RCA and ** = complete occlusion). B: Angiogram of left coronary

system with 2 stenosis of >70% (*) in mid LAD and ostium of second diagonal branch of LAD (D2) constituting N-IRA disease and confirming MVD. White arrows show collateral flow from septal branches of LAD to territory of RCA C: No significant LCX disease. D: RCA after PPCI with both lesions successfully stented. E: Post stent dilatation (* in D2 and ** in mid-LAD). F: Both lesions in LAD system successfully treated, confirming CR angiographic success. LMS = left main stem, LAD = left anterior descending artery, LCX = left circumflex artery, OM1 = obtuse marginal branch 1 of LCX, RCA = right coronary artery, S = septal branches of LAD.

2.1.5 Trial management and governance

CvLPRIT was sponsored by University Hospitals of Leicester NHS Trust. The main study was managed by the Royal Brompton CTEU and the University of Leicester was the coordinating centre responsible for CMR substudy management. The latter included production of final protocols, Case Record Forms, Standard Operating Procedures, data handling, quality assurance and statistical reporting. Regular progress reports were provided to relevant parties. Close liaison with the Royal Brompton CTEU occurred throughout the study. The main trial and CMR substudy were overseen by a Trial Steering Committee (TSC) and an independent Data and Safety Monitoring Board (DSMB). An interim data review performed by the DSMB in October 2012 (16 months after recruitment started, at which point 147 patients had been recruited into the CMR substudy and 36 had undergone 9-month follow-up CMR) was satisfied with progress to date and for the trial to continue (Appendix 2).

This CMR sub-study was funded by the Medical Research Council (MRC) through the Efficacy and Mechanism Evaluation (EME) Board (project number 09/150/28) and managed by the National Institute for Health Research (NIHR) on behalf of the MRC-NIHR partnership. The main trial was funded by the British Heart Foundation.

2.1.6 Ethics

The studies were approved by Trent Research Ethics Committee, conducted according to the Declaration of Helsinki and all participants provided written

informed consent²⁶⁵. Trial protocols, patient information leaflets and consent forms were approved by the National Research Ethics Service and each site was granted Site Specific Approval from their NHS R&D department before trial commencement.

2.1.7 Patient and Public Involvement (PPI)

As the grant application for CvLPRIT-CMR (NIHR) went through a fast-track application there was limited time to involve service users. However, the study was presented, before initiation, to the PPI group of the NIHR Leicester Cardiovascular Biomedical Research Unit, and was welcomed. One patient with a history of MI and previous PCI volunteered to join the trial steering committee and regularly attended these meetings. The study progress was presented to the PPI group on two further occasions and the chief investigator spoke to regional PPI meetings on active CMR studies in heart disease, including CvLPRIT CMR.

2.2 History taking

Patients were interviewed once clinically stable post PPCI to ascertain their past medical history, cardiac risk factors and medications history. Particular attention was paid to determining the presence or absence of the following:

1. Diabetes Mellitus
2. Hypercholesterolemia
3. Hypertension
4. Prior MI or PCI
5. Smoking history

2.3 Investigations and analyses

Consenting patients were allocated an anonymised study number allowing blinded CMR analysis. Investigations performed relevant to CvLPRIT-CMR are summarised in Table 22.

Table 22: Summary and order of investigations

Events	Order	Timepoint	Investigation
Inpatient	1	Immediately	Angiography and PPCI
Inpatient	2	Pre PPCI	Biomarker assessment (Creatinine, eGFR, CK)
Inpatient	3	90 mins post PPCI	Electrocardiogram (ECG)
Inpatient	4	12 hours post PPCI	Biomarker assessment (Creatinine, eGFR, CK)
Inpatient	5	24 hours post PPCI	Biomarker assessment (CK)
Inpatient	6	Pre-discharge	History taking
Inpatient	7	Pre-discharge	Acute CMR scan
9-month F/U	9	9 months post PPCI	Follow-up CMR scan
12-month F/U	11	12 months post PPCI	History taking/Case note review

PPCI= primary percutaneous coronary intervention, CK= creatinine kinase, eGFR= estimated glomerular filtration rate, F/U= follow up

2.3.1 Angiographic analysis

2.3.1.1 Visual assessment

Pre and post-PPCI epicardial coronary flow was assessed using Thrombolysis In Myocardial Infarction (TIMI) scoring²⁶⁶. Collateral flow to the IRA pre-PPCI was graded using the Rentrop system (Table 23)²⁶⁷. The degree of stenosis in each significant IRA and N-IRA lesion was graded visually on a 5-point scale (1 = 1-49%, 2 = 50-74%, 3 = 75-94%, 4 = 95-99%, 5 = 100%). The complexity of coronary artery disease pre PPCI was measured using the validated SYNTAX score (sum of SYNTAX scores for each lesion) by two experienced observers (JNK, SAN)^{268, 269}

Table 23: TIMI and Rentrop visual angiographic scoring systems

Perfusion analysed	Scoring system	Definition
Epicardial coronary flow	TIMI Grade 0	No perfusion: no antegrade flow post occlusion
Epicardial coronary flow	TIMI Grade 1	Penetration without perfusion: contrast passes beyond occlusion, but fails to opacify entire distal coronary bed
Epicardial coronary flow	TIMI Grade 2	Partial reperfusion: contrast passes occlusion and opacifies distal coronary bed but rate of entry and exit of contrast slower than in unaffected vessels (N-IRAs)
Epicardial coronary flow	TIMI Grade 3	Complete reperfusion: contrast passes occlusion, opacifies distal coronary bed; rate of contrast entry and clearance as in N-IRAs
Collateral flow to IRA territory (AAR) pre-PPCI	Rentrop Grade 0	Absent visible collateral flow
Collateral flow to IRA territory (AAR) pre-PPCI	Rentrop Grade 1	IRA side-branches only filled
Collateral flow to IRA territory (AAR) pre-PPCI	Rentrop Grade 2	Partial filling of main IRA vessel
Collateral flow to IRA territory (AAR) pre-PPCI	Rentrop Grade 3	IRA completely filled by collaterals

(N)-IRA= (non)-infarct related artery, AAR= area at risk

2.3.1.2 Quantitative coronary angiography

The percentage diameter stenosis of lesions was also assessed by 2D Quantitative Coronary Angiography (QCA) using *QAngioXA v1.0* software (Medis, Leiden, Netherlands) (Figure 18).

2.3.1.3 SYNTAX scoring

The complexity of coronary artery disease was calculated using the SYNTAX (Synergy between PCI with Taxus and Cardiac Surgery) scoring system²⁷⁰. This takes into account the location, length, dominance, branching, calcification, thrombus burden, severity and number of lesions. The validated SYNTAX score online calculator v2.11 (<http://www.syntaxscore.com>, SYNTAX score working group, Rotterdam,

Netherlands) was used to calculate the total SYNTAX score, which was deemed as the sum of SYNTAX scores for all significant coronary lesions.

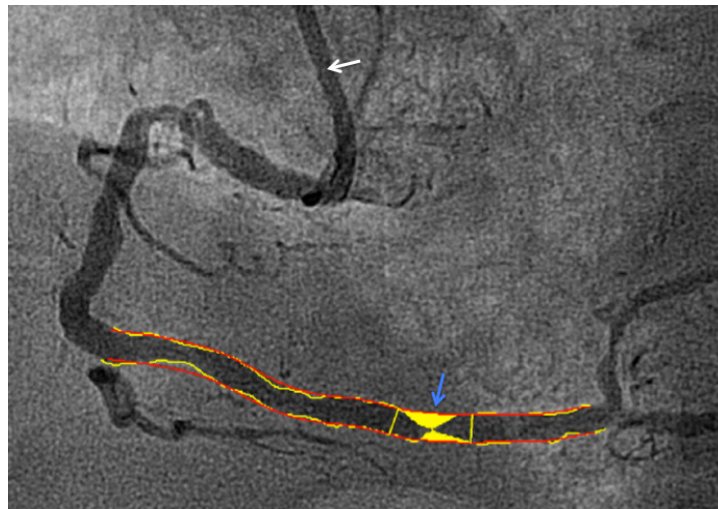


Figure 18: 2D Quantitative Coronary Angiography (QCA) [Patient X642]

Percentage diameter stenosis of lesions was assessed by 2D QCA using *QAngioXA v1.0*. The artery diameter is quantified by comparison with the reference catheter (white arrow, here 6 French, 2.0mm). Loci proximal and distal to the lesion under assessment are manually identified. The software then automatically contours the artery and lesion. Manual adjustment of contours can be performed if needed. Here, the distal RCA lesion (blue arrow) is of 80% stenosis in a segment of 2.4mm diameter.

2.3.2 Creatine kinase and clinical bloods

Twenty millilitres of venous blood was collected with the patient lying semi-recumbent. For the assessment of serum creatinine, estimated glomerular filtration rate (eGFR) and Creatinine Kinase (CK), blood was collected in Clot Activator tubes (BD Diagnostics, USA) as summarised in Table 22. These were routine clinical bloods analysed using Clinical Pathology Accreditation Service (CPA) accredited (United Kingdom Accreditation Service, Middlesex, UK) laboratories at each centre, which were to ISO 15189 standard (International Organisation for Standardization, UK).

2.3.3 Electrocardiography

A 12-lead surface ECG was taken on arrival of the patient to hospital to confirm STEMI. This was repeated at 90 minutes post-PPCI to assess the degree of ST-segment resolution, quantified as the sum of ST-segment elevation at 60ms after the J-point in the infarct-related leads. ST-segment resolution was defined as complete (>70%), partial (30-70%) or absent (<30%)²⁷¹ compared with the initial ECG.

2.4 Cardiovascular magnetic resonance

CMR was performed on 1.5T scanners (Table 24) as close to 72 hours post-PPCI as possible (acute CMR) during the index admission, and at 9 months (follow-up CMR). CMR was permitted at 24-48 hours in patients due for weekend discharge, and could be delayed if required due to the patient's clinical condition. Prior to CMR, patients completed a safety questionnaire. At the 9-month CMR, an additional stress questionnaire was completed to ensure suitability for adenosine and caffeine abstinence.

Table 24: CMR scanners used at the centres

Recruitment centre	CMR centre	1.5T Scanner used
Bournemouth	Bournemouth	Siemens Avanto (Erlangen, Germany)
Derby, Glenfield, Kettering	Glenfield	Siemens Avanto (Erlangen, Germany)
Harefield	Harefield	Siemens Avanto (Erlangen, Germany)
Leeds	Leeds	Philips Intera (Best, Netherlands)
Southampton	Southampton	Siemens Avanto (Erlangen, Germany)

2.4.1 Acute CMR

The detailed protocol for the acute CMR scan is summarised in Figure 19 and explained in subsequent sections. All imaging was performed with retrospective electrocardiographic gating using dedicated cardiac receiver coils, unless atrial fibrillation or frequent ectopy was present, or for tagging images, where prospective gating was used. Parallel imaging (factor 2) was used to shorten breath-holds for all imaging, except T2w-STIR.

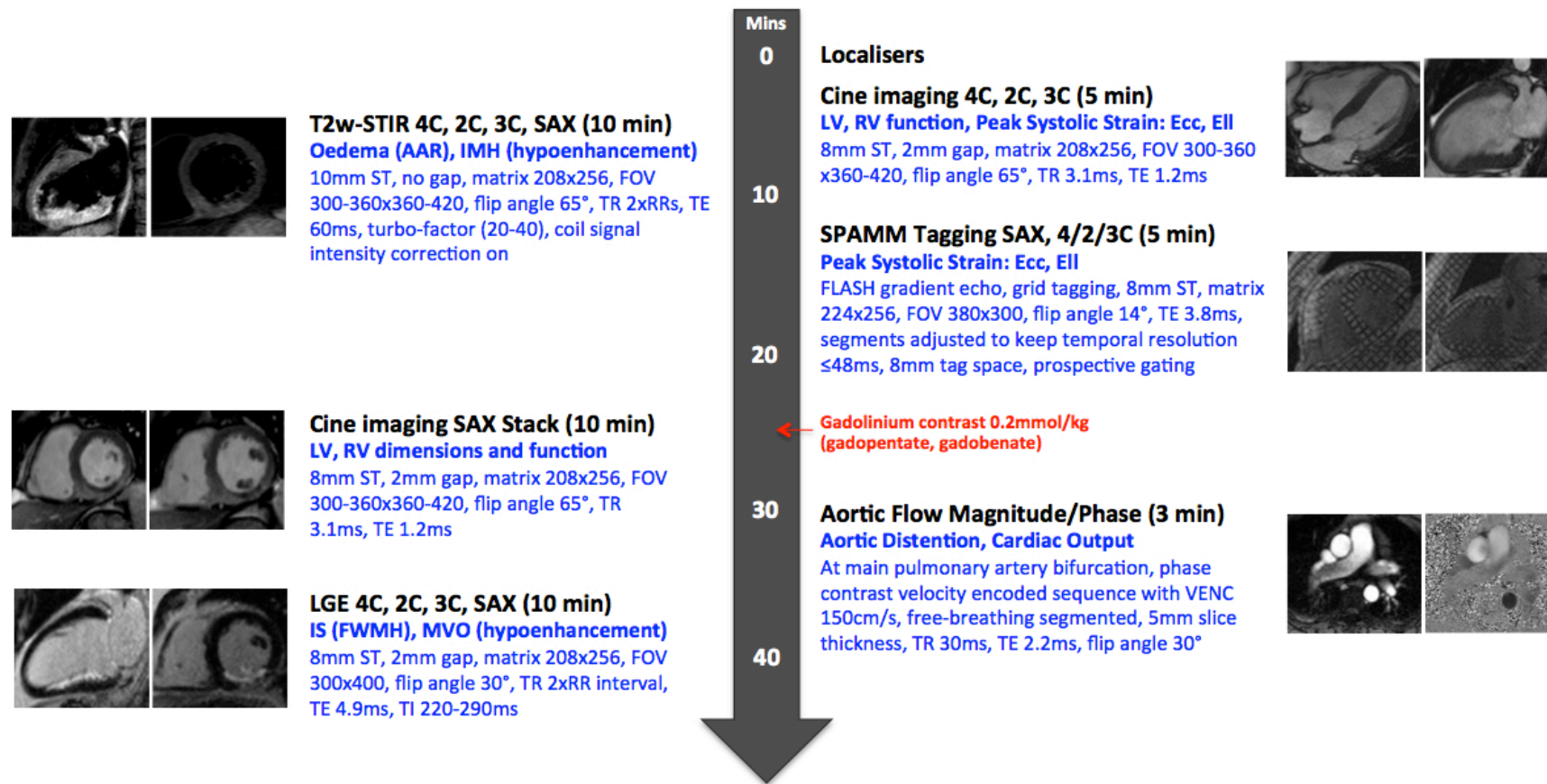


Figure 19: MRI protocol for the acute CMR scan (CMR 1)

TE= echo time, TR= repetition time, SAX= short-axis, 4/3/2C= 4/3/2-chamber, LV= left ventricle, RV= right ventricle, Ecc= circumferential strain, Ell= longitudinal strain, FOV= field of view, IS= infarct size, FWHM= full-width half-maximum, MVO= microvascular obstruction, AAR= area at risk, IMH= intramyocardial haemorrhage,

2.4.1.1 Cine imaging

After the acquisition of localising images, balanced steady-state free precession cine imaging (bSSFP) was performed in 4, 2 and 3-chamber long-axis views (Figure 20).

The field-of-view was optimised to achieve in-plane spatial resolution of $\sim 1.1\text{-}1.7\text{mm} \times 1.3\text{-}1.9\text{mm}$. The number of segments was adjusted according to heart rate (HR <50bpm: 17 segments, HR 50-70bpm: 15 segments, HR 71-90bpm: 13 segments, HR >90bpm: 11 segments) at the discretion of the supervising investigator.

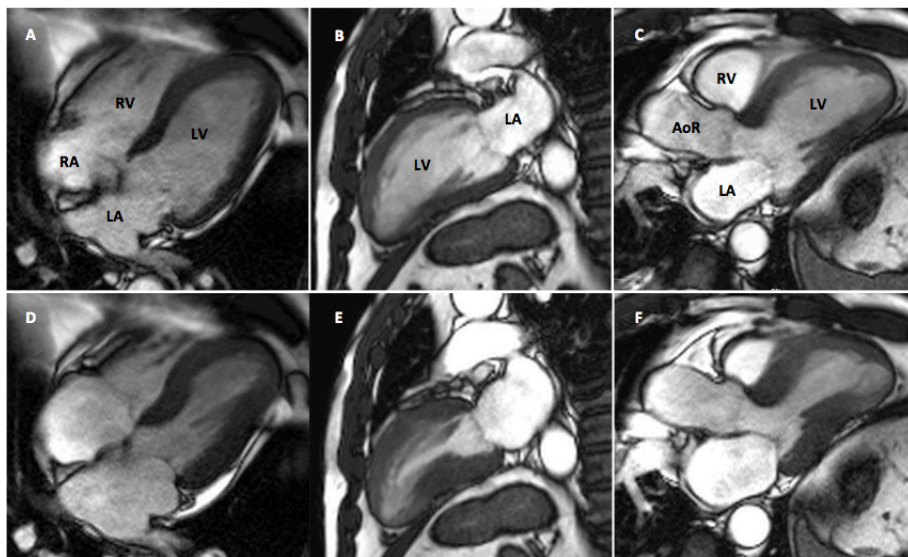


Figure 20: SSFP Cine imaging in the long-axis planes [Patient X797]

Top row (A-C) in end-diastole, bottom row (D-F) corresponding end-systolic image. A: 4-chamber view. B: 2-chamber view. C: 3-chamber view. LV= left ventricle, LA= left atrium, RV= right ventricle, RA= right atrium, RV= right ventricle, AoR= aortic root.

Intravenous contrast (0.2mmol/kg gadolinium-diethylenetriaminepentacetate [Gd-DTPA, Magnevist®, Bayer, Germany] was administered before short-axis cine stack acquisition to minimise scan time before acquiring the LGE images (primary endpoint). Cine imaging was performed in contiguous short-axis slices covering the entire LV and RV (Figure 21). The basal short-axis slice was planned at the mitral valve annulus perpendicular to the interventricular septum to minimize partial volume at the atrioventricular boundary.

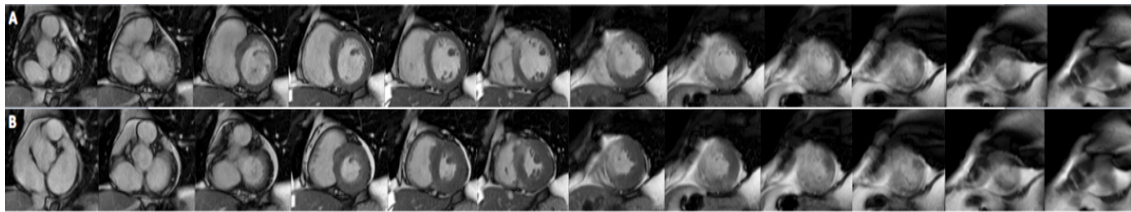


Figure 21: SSFP Cine imaging in a contiguous short-axis stack [Patient X797]

Top row (A) in end-diastole, bottom row (B) corresponding end-systolic image.

Left to right: basal to apical complete left and right ventricular coverage.

2.4.1.2 Oedema (area-at-risk) imaging

Area-at-risk was assessed using black-blood T2w-STIR imaging. This sequence is explained in detail in section 1.2.6.2. T2w-STIR imaging was performed using coil signal intensity correction in 4, 2 and 3-chamber long-axis views and contiguous short-axis slices covering the entire LV (Figure 22). Ten millimeter slices were acquired to optimize signal-to-noise ratio. The echo train length (ETL) was adjusted with heart rate (HR) (HR <50bpm: ETL 40, HR 50-70bpm: ETL 30, HR 71-90bpm: ETL 25, HR >90bpm: ETL 20).

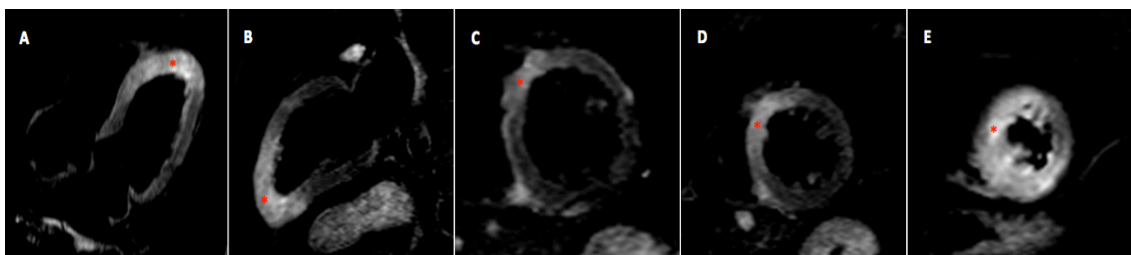


Figure 22: T2w-STIR imaging showing myocardial oedema (area-at-risk) [X797]

Myocardial oedema seen as hyperintensity on T2w-STIR imaging in the anteroseptal segments (left anterior descending artery IRA) as indicated by *. A, B: 4, 2-chamber long-axis views. C-E: Basal, mid and apical LV short-axis views respectively

2.4.1.3 Myocardial strain imaging

Myocardial strain was assessed on cine images using Feature Tracking (*Tomtec Image Arena v4.5*, Tomtec, Munich, Germany) and on pre-contrast myocardial tissue tagging images. The latter were acquired in 4, 2 and 3-chamber long-axis views and three short-axis views (base, mid, apical) using a prospectively gated spatial modulation of magnetization (SPAMM) gradient-echo sequence to obtain images in a single breath-hold (Figure 23). This sequence is explained in detail in section 1.2.2.2. Short-axis images were planned in mid-systole to avoid the LV outflow tract, with the middle 3 of 5 slices spaced from the mitral valve annulus to apex acquired. The number of segments was set at 11, to achieve temporal resolution of <50ms and breath-hold tolerability. In-plane spatial resolution was ~1.3mm x 1.3mm for tagging and ~1.4mm x 1.4mm for Feature Tracking.

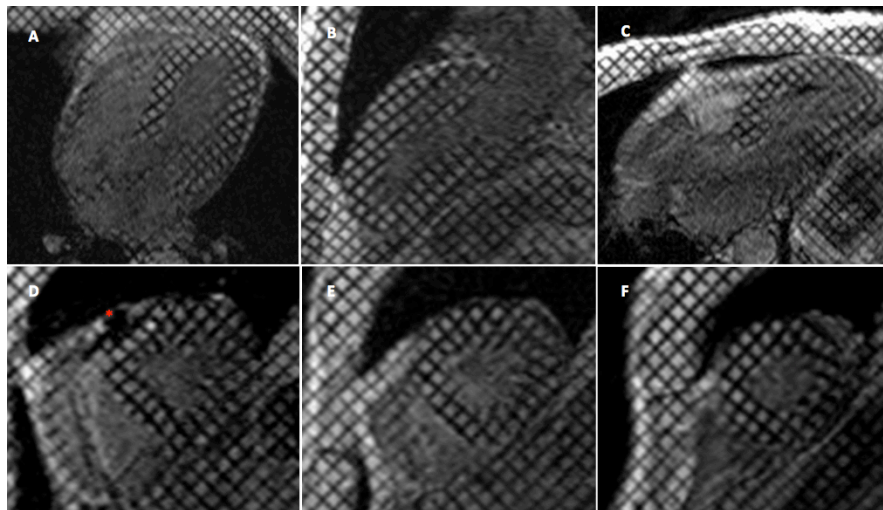


Figure 23: Myocardial tissue tagging images acquired using SPAMM [Patient X797]

Tissue tags in a grid-like configuration throughout the left ventricle. Imaging in end-systole demonstrates deformation of myocardium and tissue tags. Top row (A-C): 4, 2 and 3-chamber long-axis views. Bottom row (D-F): Basal, mid and apical LV short-axis views respectively. * = Susceptibility due to stent in proximal LAD

2.4.1.4 Aortic distension

Phase-contrast velocity-encoding and magnitude SSFP cine imaging were performed perpendicular to the ascending and descending thoracic aorta at the level of the

pulmonary artery bifurcation, allowing calculation of through-plane flow, cardiac output and stroke volume, and a surrogate of aortic distensibility respectively (Equation 2).

2.4.1.5 Late gadolinium enhancement (LGE) imaging

LGE imaging was commenced 10 minutes after intravenous administration of 0.2mmol/kg gadolinium-DTPA (Magnevist, Bayer, Germany) using a segmented inversion-recovery gradient-echo sequence with a 2-beat trigger. This was preceded by a bSSFP Look-Locker inversion time (TI) scout to determine the optimal TI to null unaffected myocardium. The TI was progressively adjusted to maintain nulling of unaffected myocardium. The LGE sequence is explained in detail in section 1.2.3.2. LGE imaging was performed in 4, 2 and 3-chamber long-axis views and contiguous short-axis slices covering the entire LV (Figure 24). T2w-STIR, cine and LGE short-axis images were acquired at identical slice positions. The number of segments was adjusted with heart rate (HR <50bpm: 40 segments, HR 50-70bpm: 30 segments, HR 71-90bpm: 25 segments, HR >90bpm: 20 segments).

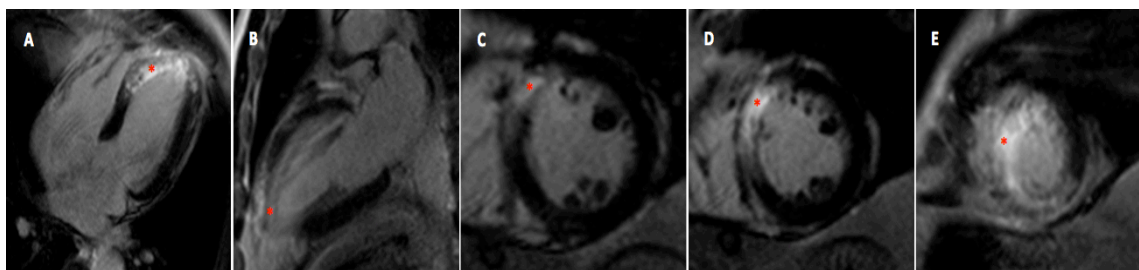


Figure 24: Late gadolinium enhancement imaging (LGE) showing infarction [X797]

Antero-septal infarction seen as hyperenhancement on LGE imaging as indicated by * in the oedematous territory (area at risk) seen in Figure 22. A, B: 4, 2-chamber long-axis views. C-E: Basal, mid and apical LV short-axis views respectively

2.4.2 Follow-up CMR

The detailed imaging protocol for the follow-up CMR scan is summarised in Figure 25. Cine, myocardial tissue tagging, aortic stiffness and cardiac output, and LGE imaging

were performed as per the acute CMR. T2w-STIR imaging was omitted at follow-up CMR. Perfusion imaging was performed only during follow-up CMR.

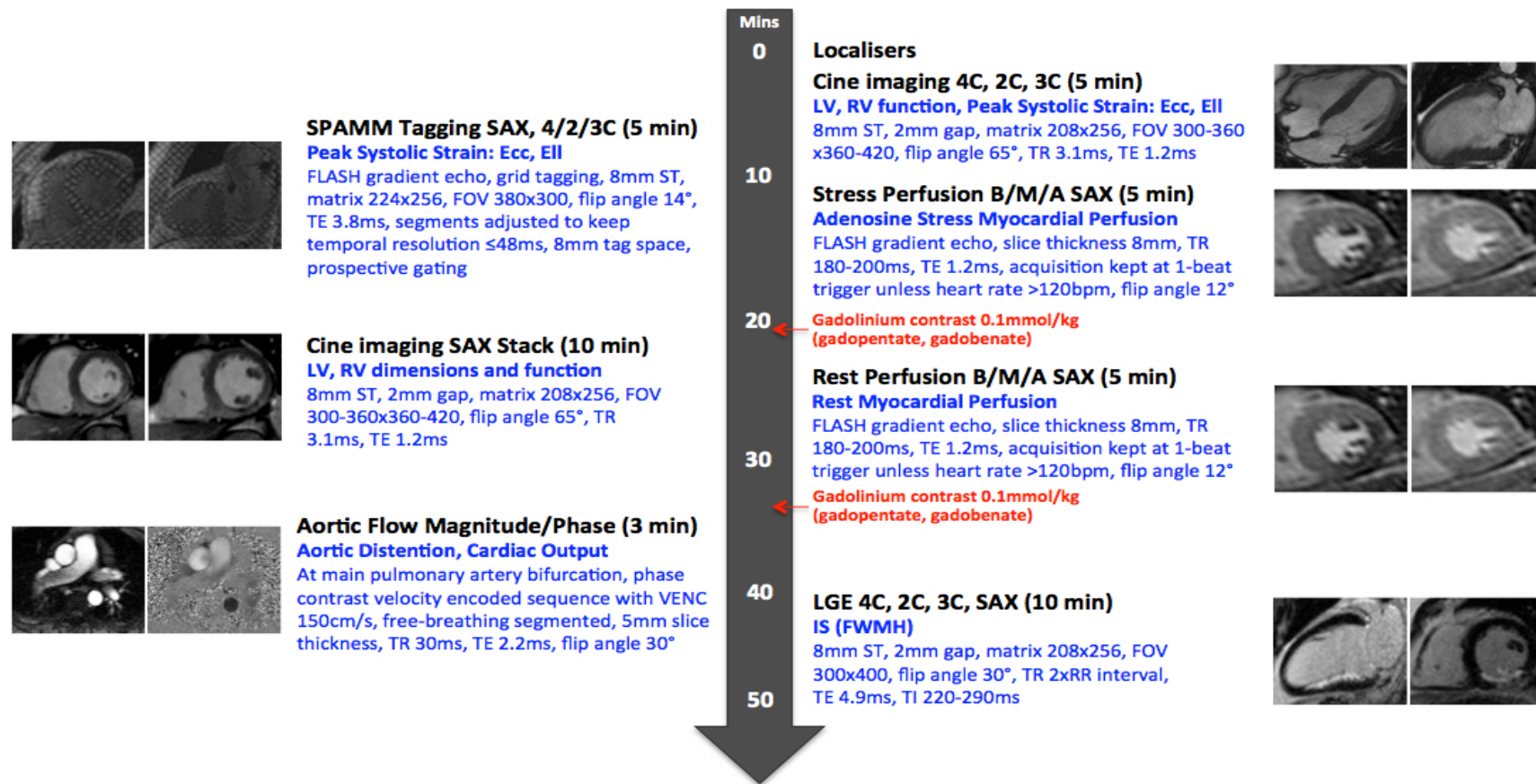


Figure 25: MRI protocol for the follow-up CMR scan (CMR 2)

TR= repetition time, TE= echo time, ST= slice thickness, SAX= short-axis, 4/3/2C= 4/3/2-chamber, LV= left ventricular, RV= right ventricular, Ecc= circumferential strain, Ell= longitudinal strain, FOV= field of view, IS= infarct size, FWHM= full-width half-maximum, FLASH= fast low-angle shot

2.4.2.1 Perfusion imaging

Stress perfusion imaging was performed following pharmacological vasodilator stress using intravenous adenosine infusion at 140µt/kg/min for 3 minutes. Heart rate and blood pressure and symptoms were closely monitored during stress at one-minute intervals. A radiographer was present within the scanner room with the patient during stress. First-pass perfusion imaging was performed following intravenous administration of 0.1mmol/kg gadolinium-DTPA (Magnevist, Bayer, Germany) using a breath-hold, saturation recovery gradient-echo sequence at basal, mid-ventricular and apical short-axis LV slices, planned as per myocardial tagging (Figure 25). Acquisition was undertaken every heart beat to optimise visual assessment of contrast wash-in. Where the heart rate was >110 bpm, phase resolution was reduced to 70% to increase temporal resolution. In the rare situation where heart rate was >125 bpm, acquisition was undertaken every other heart beat. Rest perfusion imaging was performed 10 minutes after stress imaging using identical parameters.

2.4.3 CMR analysis

All CMR analysis was performed offline, blinded to patient details by the candidate (3 years experience). Image quality was graded by 2 experienced observers (JNK, GPM) as summarised in Table 25.

Table 25: CMR image quality grading scale

Sequence	Grade	1.5T Scanner used
All	N/A	Sequence not performed
	0	Non-analysable
	1	Minor artefact in area of interest may affect analysis, however analysable
	2	Minimal artefact, does not affect images analysis
	3	Good quality, no artefact
Oedema	'ONS'	No artefact however no oedema seen (no CNR between oedema and unaffected myocardium)

2.4.3.1 Volumetric analysis

Volumetric analysis was performed using *QMass* v7.1 (Medis, Leiden, Netherlands). LV and RV endocardial and epicardial borders were manually contoured onto

contiguous short-axis cine slices at end-diastole and end-systole, excluding papillary muscles, trabeculae and epicardial surfaces. This method has superior reproducibility²⁷² compared to inclusion of papillary muscles and trabeculae in mass assessment. This allowed calculation of LV/RV end-diastolic volume (LVEDV, RVEDV), LV/RV end-systolic volume (LVESV, RVESV), LV/RV stroke volume (LVSV, RVSV), LV/RV ejection fraction (LVEF, RVEF) and LV end-diastolic mass (LVM) (Figure 26). Volumes and LVM were indexed for body surface area.

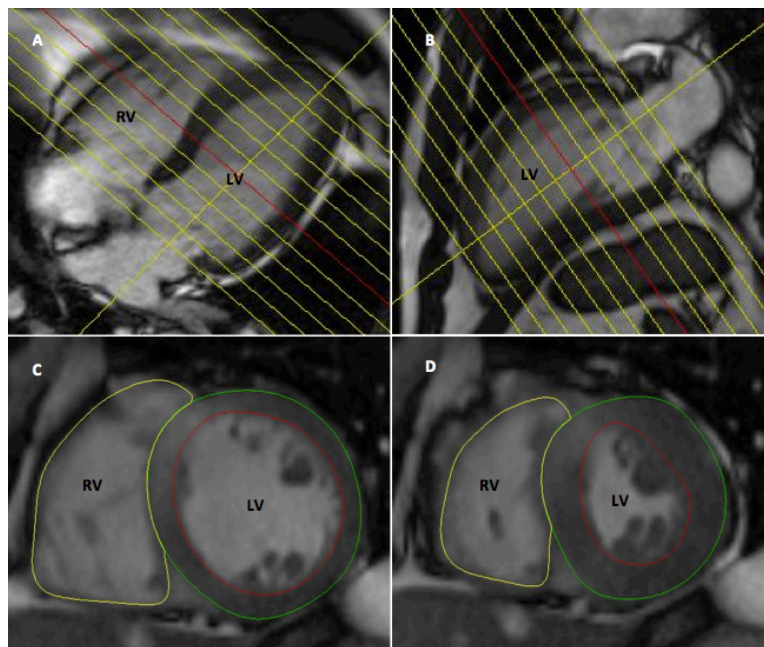


Figure 26: Myocardial contouring for ventricular volumetric analysis [Patient X797]

Left ventricular (LV) contours (green epicardial, red endocardial) endocardial right ventricular contours (yellow). A, B: demonstrate slice positions of short-axis cine slices. C: end-diastole, D: end-systole.

2.4.3.2 Wall motion scoring analysis

Wall motion and systolic thickening in each of the 16 American Heart Association myocardial segments was graded on visual assessment where: 1= normokinesis, 2= hypokinesis, 3= akinesis, 4= dyskinesis and 5= aneurysmal. The wall motion score (WMS) was the sum of segmental wall motion and was also expressed as the wall motion score index (WMS/number of segments analysed)²⁷³.

2.4.3.3 Oedema (area at risk) quantification

Oedema (AAR) was quantified as hyperenhancement on T2w-STIR imaging using *cmr42* (Circle Cardiovascular Imaging, Calgary, Canada) using Otsu's Automated Method (OAT). Endocardial and epicardial borders were manually contoured on contiguous LV short-axis slices, excluding papillary muscles, trabeculae, epicardial surfaces and blood-pool artefact (Figure 27) and OAT applied.

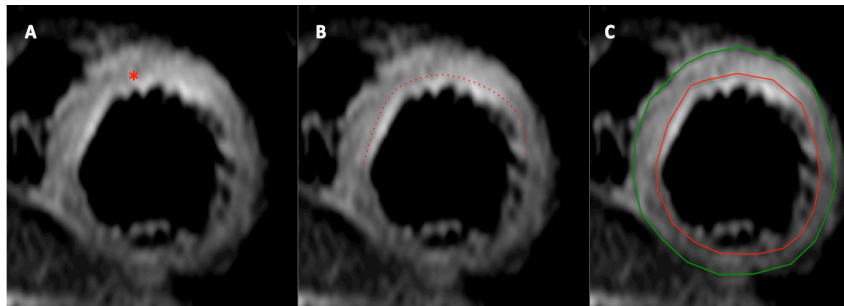


Figure 27: Exclusion of blood-pool artefact from oedema quantification

Blood-pool artefact (hyperenhancement) is caused since stagnant blood in regions of severe hypokinesia receives all inversion pulses in T2w-STIR imaging, and needs to be excluded from LV myocardium during endocardial contouring. A: T2w-STIR image showing oedema (hyperenhancement) in the anteroseptal segments (*). B: Hyperenhancement on the cavity side of the endocardial contour (red) is blood-pool artefact and is, C: correctly excluded from LV myocardial contours.

OAT automatically calculates a unique signal intensity threshold for each slice by dividing the greyscale signal intensity histogram into 2 groups (enhanced, normal) based on the threshold giving the least intraclass variance within each group²⁷⁴, without the need for a user-defined region of interest (ROI). Oedema was calculated as a percentage area for each of the 16 AHA segments⁶¹ (Figure 28). Total AAR was expressed as percentage of LVM. The most apical T2w-STIR slice was excluded to minimize partial volume.

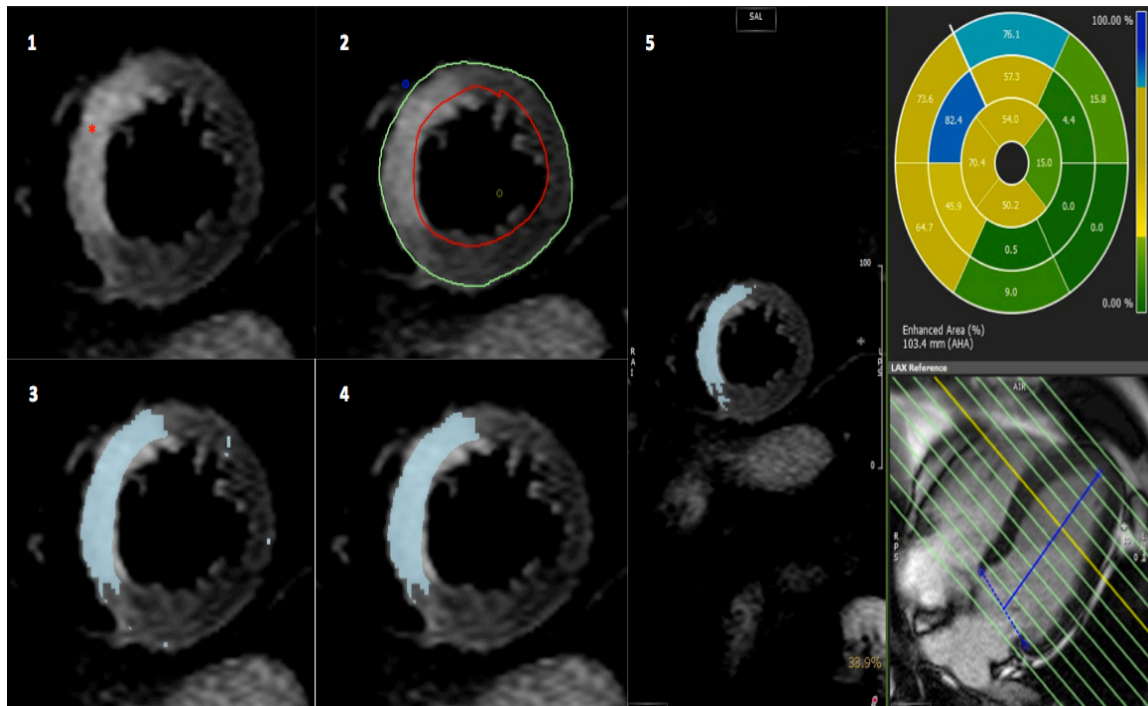


Figure 28: Oedema quantification on T2w-STIR imaging [Patient X797]

1: T2w-STIR image showing basal anteroseptal and anterior wall oedema (*). 2: Endocardial (green) and epicardial contours (red) drawn. 3: Otsu's Automated Method automatically highlights enhanced myocardium (oedema) in blue. 4: Final image after noise artefact excluded. 5: Percentage segmental area extent of oedema

Two manual corrections were applied to AAR measurements: inclusion of hypointensity within enhancement corresponding to IMH⁷⁸, and exclusion of small isolated enhanced regions without interslice continuity in N-IRA territories deemed noise artefact (Figure 29).

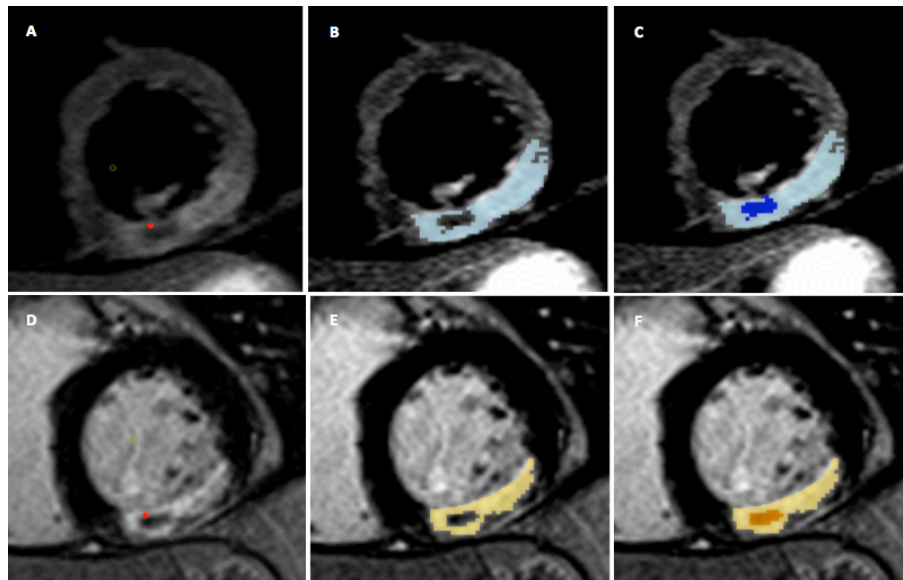


Figure 29: Manual inclusion of IMH and MVO in area at risk and infarct size [Patient X670]

Top row: T2w-STIR images demonstrating oedema in inferolateral segments. *A, B*: Region of hypoenhancement within oedema corresponding to IMH (*). *C*: IMH manually included in total area at risk and labelled as IMH. Bottom row: *D-F*: corresponding images demonstrating MVO on LGE imaging in the same patient.

2.4.3.4 Myocardial strain quantification

Myocardial strain was quantified using Feature Tracking (cine imaging-based) and tissue tagging. Global peak systolic circumferential (*Ecc*) and longitudinal (*Ell*) strain were calculated as an average of values obtained in the three short-axis (basal, mid, apical) and long-axis views respectively. Segmental *Ecc* was assessed as per AHA 16-segment nomenclature⁶¹.

Tagging analysis

Strain was measured using dedicated software (*inTag*, CREATIS, Lyon, France run as a plug-in for OsiriX v3.8, Pixmeo, Switzerland) as described previously²⁷⁵ and illustrated in Figure 30. OsiriX functions only on Apple Mac (Cupertino, California, USA) computers. *Intag* uses the SinMod technique. Endocardial and epicardial contours

were manually drawn onto the end-systolic image and automatically propagated through the cardiac cycle. Numerical data was outputted for further post-processing.

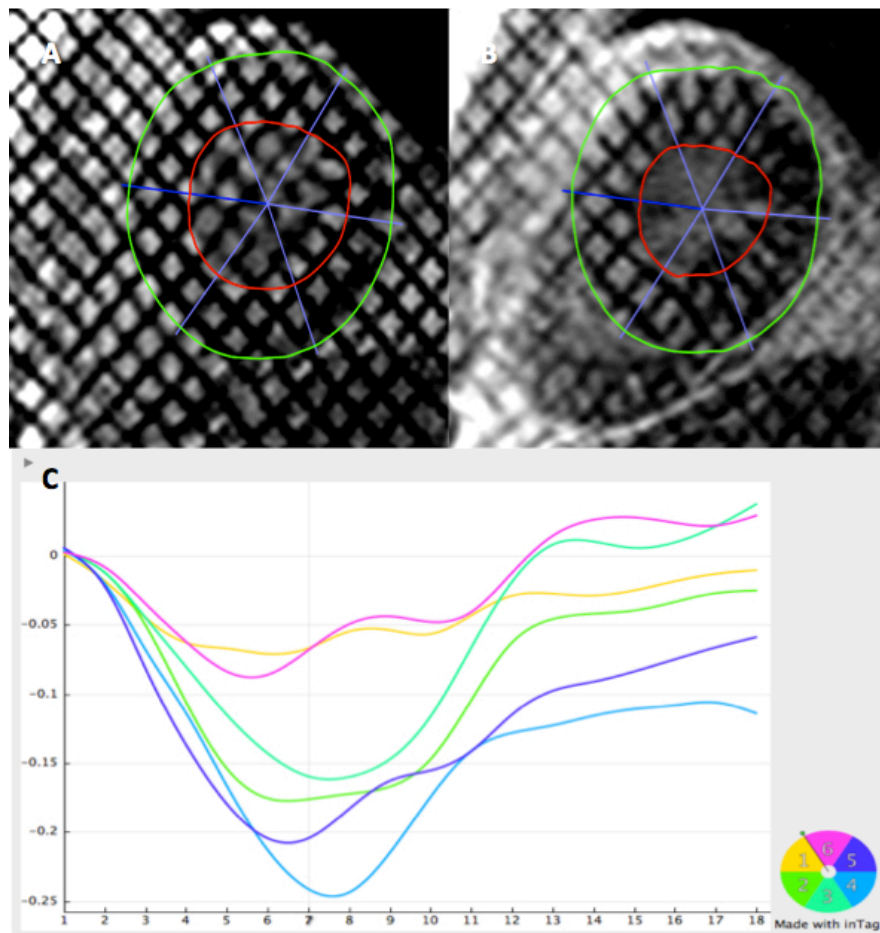


Figure 30: Tagging strain assessment using *Intag* software [Patient X596]

A: End-diastolic tagged image (basal short-axis) with endocardial and epicardial contours manually drawn and automatically propagated along the cardiac cycle. B: Corresponding end-systolic image. C: Segmental circumferential strain curves.

Feature Tracking (FT) analysis

Strain was measured using *2D Cardiac Performance Analysis MR v1.0* run as a plug-in *Tomtec Image Arena v4.5* (Tomtec, Munich, Germany). Feature Tracking tracks features of interest (tissue-cavity interfaces, tissue dishomogeneities, anatomic landmarks) along contour lines on routinely acquired bSSFP cine images, analogous to echocardiographic speckle tracking⁹³. Endocardial contours were manually drawn

onto end-diastolic image and propagated. The software automatically places 8-12 optimally tracking points of interest along contours (Figure 31).

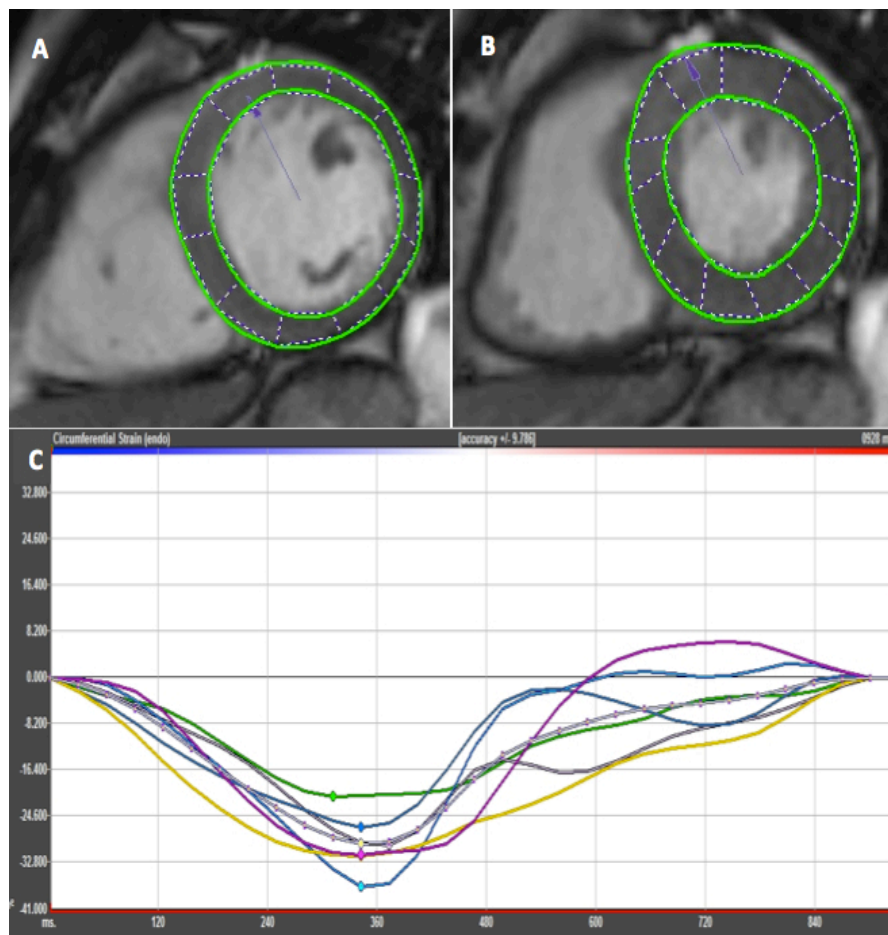


Figure 31: Feature Tracking strain assessment [Patient X596]

A: Manually drawn endocardial contours are automatically propagated; here end-diastolic image with 12 analysis points generated as indicated by vertical dotted lines from epicardium to endocardium. B: Corresponding end-systolic image. C: Segmental Ecc strain curves

Poorly tracking segments using both techniques were manually adjusted and excluded from analysis if the movement of contours deviated from true myocardial motion by >50%.⁹⁴

2.4.3.5 Aortic stiffness assessment

A manually drawn contour of the ascending aorta on the axial magnitude cine at pulmonary artery bifurcation level was propagated through the cardiac cycle using *cvi42* (Figure 32). Ascending aortic stiffness was assessed by calculating a surrogate of aortic distensibility as described in Equation 2 (surrogate as the denominator uses aortic forward flow instead of pulse pressure):²⁷⁶

Equation 2: Calculation of surrogate of aortic distensibility

A = aortic cross-sectional area. Aortic forward flow = stroke volume in ascending aorta calculated from phase-contrast velocity-encoded imaging (Figure 32).

$$\text{Aortic compliance (10}^{-3}\text{ml}^{-1}) = \frac{(A_{\max} - A_{\min})}{A_{\min} \times \text{Aortic forward flow}}$$

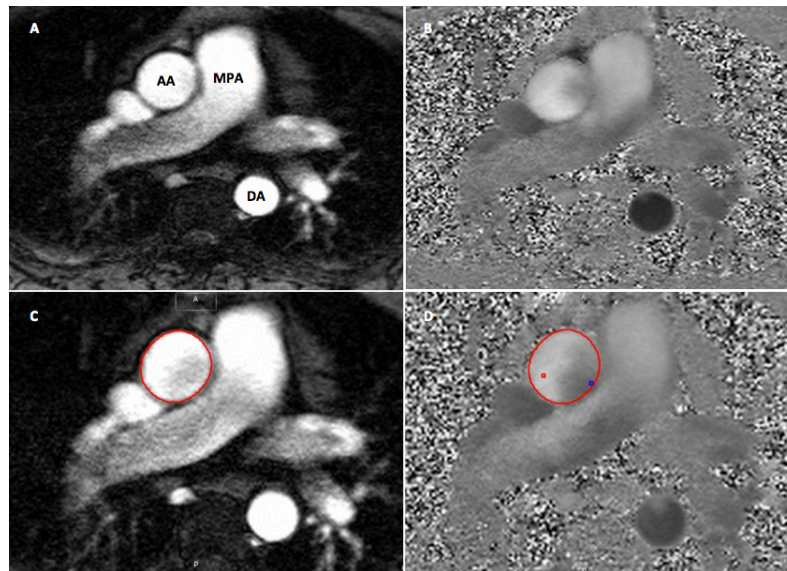


Figure 32: Calculation of ascending aortic distensibility [Patient X797]

A = Axial magnitude image at level of pulmonary artery bifurcation. B: Corresponding phase-contrast velocity-encoded image. C, D: Ascending aortic contour drawn and propagated throughout cardiac cycle in magnitude and phase-contrast images allows calculation of aortic distension and ascending aortic forward flow, respectively, and

derivation of compliance. AA = ascending aorta, DA = descending aorta, MPA = main pulmonary artery.

2.4.3.6 Late gadolinium enhancement

Infarct was defined semi-automatically on magnitude LGE images using *cvi42*. Endocardial and epicardial borders were manually contoured on contiguous short-axis LV slices, excluding papillary muscles, trabeculae and epicardial surfaces and the FWHM technique¹¹¹ applied. Here, a 2cm² ROI was manually drawn in the infarct core and enhancement calculated as pixels of >50% of the automatically determined maximum signal intensity in the ROI (Figure 33). Total infarct size was expressed as a percentage of LVM and segmental area extent of LGE was calculated⁶¹. The apical LGE slice was excluded to minimize partial volume effect. Total IS was manually corrected by including hypointensity within enhancement (MVO) to total infarct size, and exclusion of noise artefact as per AAR quantification (Figure 29).

If infarction was seen in more than one coronary territory in the acute CMR, this was recorded as being in the IRA territory (associated edema and/or MVO) or the non-IRA territory with the consensus of three observers (JNK, GPM, JPG). Non-IRA infarcts were additionally classified as likely to be acute or chronic (presence of wall thinning and no edema/MVO). Infarct size was recorded for both IRA and non-IRA LGE and total infarct size was the sum of all LGE. Segmental extent of enhancement (SEE) was assessed as percentage area of enhancement.

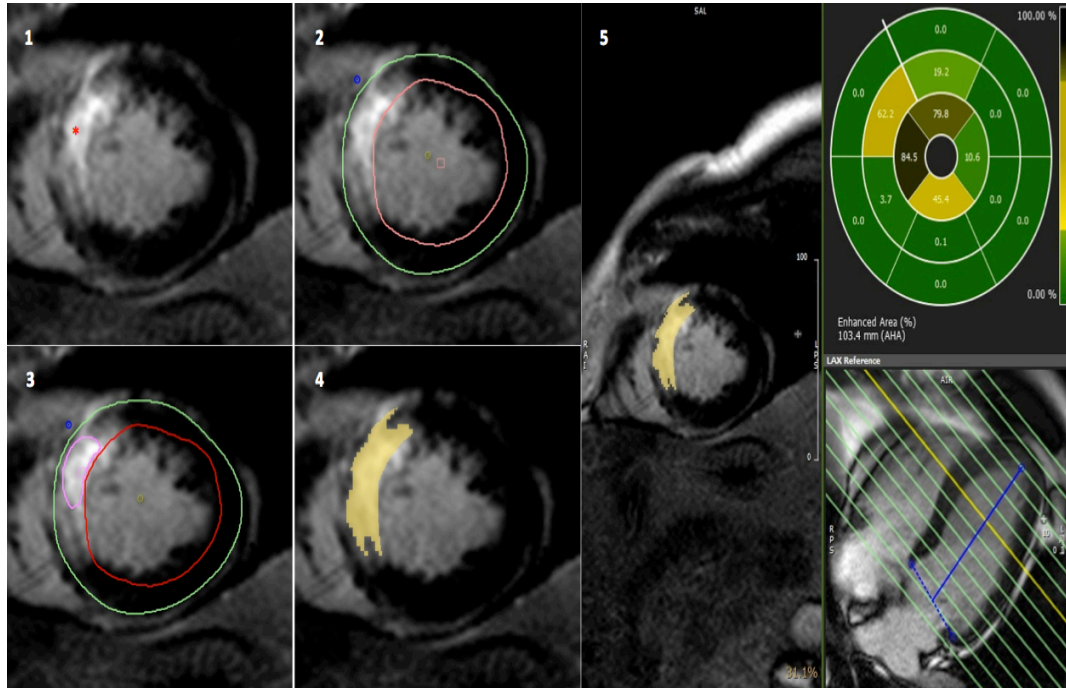


Figure 33: Full-Width Half-Maximum infarct quantification method on LGE [Patient X797]

1: LGE image showing infarct (*) in basal anteroseptum and anterior segments. 2: Endocardial (green) and epicardial contours (red) drawn. 3: A 2cm² region of interest (pink) drawn in infarct core. 4: FWHM enhancement with signal intensity threshold >50% maximum in infarct core. 5: Percentage area of each segment with infarct.

2.4.3.7 Myocardial salvage index quantification

MSI²¹⁹ is the proportion of the area at risk that does not progress to infarction. It was expressed as 'acute MSI' using total IS at acute CMR and 'final MSI' using final total IS at follow-up CMR, and calculated as defined in Equation 1.

2.4.3.8 Perfusion analysis

Perfusion images were visually, semi-quantitatively assessed for perfusion defects (visible defect for ≥ 5 heartbeats) by the consensus of two experienced observers (JNK, GPM). Stress perfusion, rest perfusion and LGE images were compared to allow accurate assessment based on all available data. Three perfusion patterns were possible: (a) no perfusion defect: normal perfusion of myocardium during stress and rest; (b) reversible perfusion defect: perfusion defect seen only during stress

perfusion, in viable, non-infarcted myocardium; (c) matched perfusion defect: stress perfusion defect in infarcted myocardium (Figure 34). Where a perfusion defect or infarct were present on stress perfusion or LGE respectively, they were defined as subendocardial ($\leq 50\%$ transmural) or transmural ($>50\%$ transmural) and given a score of 1 or 2 respectively per segment, whereas normal myocardium was scored 0. Global perfusion was expressed as the Summed Difference Score (SDS, maximum 32), defined as the difference between the sum of segmental stress perfusion defects and LGE²⁷⁷. The SDS was also expressed as the global ischaemic burden (%).

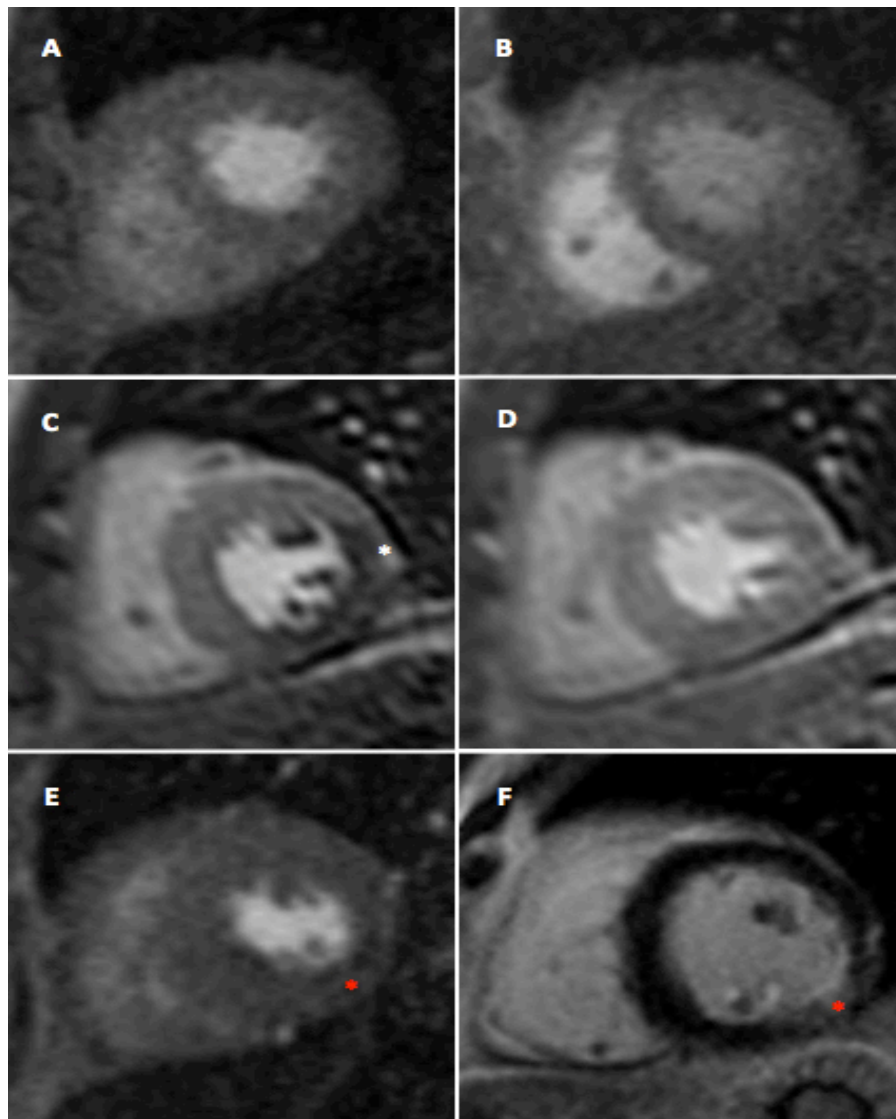


Figure 34: The range of perfusion patterns possible [Patients (1) X589, (2) X623, (3) X512]

A, B: Stress and rest perfusion imaging respectively, no perfusion defect (SDS=0 for segments in image). *C, D*: Stress and rest perfusion imaging, with reversible transmural defect in anterolateral and inferolateral segments (■, SDS=2 for both segments). *E, F*: Matched subendocardial perfusion defect in infarcted basal inferior/inferolateral segments (*, SDS=0 for segment).

2.5 Study outcomes and data handling

Study outcomes and statistical methods employed in this thesis are described in each of the six results chapters. The main results chapter ('CvLPRIT-CMR substudy') also has a dedicated statistical analysis plan, which forms Appendix 3.

2.5.1 Data handling

CMR data were recorded in a lockable, validated²⁷⁸ Research Electronic Data Capture v5.0 (REDCap) database (Vanderbilt University, USA). No clinical data was released to the candidate until the database was complete, checked for errors and a locked copy provided to the CTEU. The CMR database was locked on 13th June 2014 (Appendix 4). Data entry into the REDCap database was automated, using data transposition from automatically produced data-files from CMR analysis software. Complete datasets for 5% of randomly selected patients were manually checked and 100% of this data was correct compared with raw data files from CMR software.

CHAPTER THREE

3. SEMI-AUTOMATED CMR METHODS OF ASSESSING INFARCT CHARACTERISTICS

Comparison of semi-automated methods to quantify infarct size and area at risk by cardiovascular magnetic resonance imaging at 1.5T and 3.0T field strengths

Published:

Khan JN, Nazir SA, Horsfield MA, Singh A, Kanagala P, Greenwood JP, Gershlick AH, McCann GP. Comparison of semi-automated methods to quantify infarct size and area at risk by cardiovascular magnetic resonance imaging at 1.5T and 3.0T field strengths. BMC Res Notes. Feb 2015. 8:52 doi: 10.1186/s13104-015-1007-1. 1-12.

3.1 Background

Cardiovascular magnetic resonance (CMR)-measured IS^{51, 279} and MSI^{70, 78} are important measures of reperfusion success and predictors of remodelling and prognosis post acute STEMI. MSI is the proportion of reversibly injured ischaemic AAR visualised as myocardium with high signal intensity on T2w images.^{70, 78, 280}

There is currently no gold standard technique for the quantification of IS and AAR on LGE and T2w-STIR imaging respectively.¹¹⁷ Semi-automated standard deviation (SD)-based thresholding techniques^{78, 108}, manual (visual) contouring of enhancement^{51, 279}, the FWHM method^{111, 117}, and recently, automated techniques have been used.^{281, 282} The heterogeneity of techniques and resulting IS and AAR values hinders comparisons between studies.

Otsu's Automated Thresholding (OAT) automatically identifies hyperenhanced areas by selecting the grayscale signal intensity threshold giving minimal intraclass variance within enhanced and normal myocardium and is largely user-independent.²⁷⁴ There are very scarce published data using OAT quantification, of IS²⁸³ and AAR.^{284, 285} There are no published studies assessing IS or AAR quantification at 3.0T, or using 7SD and 8SD infarct quantification thresholding at any field strength.

This study aimed to compare the accuracy and observer variability of IS and AAR quantification on LGE and T2w-STIR using OAT with the currently used quantification methods at 1.5T and 3.0T.

3.2 Methods

3.2.1 Study cohort

Ten patients were retrospectively, randomly selected using a random number generator²⁸⁶ from the acute CMR cohort of the CvLPRIT-CMR study²⁵⁴. Ten further patients were identically selected from a separate multicentre study at 3.0T

(Randomized Controlled Trial Comparing Intracoronary Administration of Adenosine or Sodium Nitroprusside to Control for Attenuation of Microvascular Obstruction During Primary Percutaneous Coronary Intervention)²⁶³.

3.2.2 CMR image acquisition

CMR was performed during the index admission on a 1.5T scanner (Siemens Avanto, Erlangen, Germany [n=4] or Philips Intera, Best, The Netherlands [n=6]) or 3.0T scanner (Siemens Skyra, Erlangen, Germany [n=5]; Philips Achieva TX, Best, Netherlands [n=4] or GE Signa HDxt, Little Chalford, UK [n=1]) with retrospective electrocardiographic gating and dedicated cardiac receiver coils. The imaging protocol is outlined in Figure 19. T2w-STIR imaging with coil SI correction, cine imaging with steady state free precession and Late Gadolinium Enhancement (LGE) imaging were performed in long-axis views and contiguous short-axis slices covering the entire LV. LGE images were acquired 10-15 minutes after administration of 0.15mmol/kg (3.0T) or 0.2mmol/kg (1.5T) gadolinium-DTPA (Magnevist, Bayer, Germany) using a segmented inversion-recovery gradient-echo sequence. The inversion time was progressively adjusted to null unaffected myocardium.

3.2.3 IS and AAR Quantification

Image quality was graded according to a 4-point scale before analysis: 3= excellent, 2= good, 1= moderate and 0= unanalysable. To remove the confounding variable of image quality on AAR quantification, 26% of studies from the total study population, where T2w-STIR images were deemed non-analysable were excluded from the random number study selection pool. Analysis was performed offline in a central core lab, blinded to patient details using *cvi42* v4.1 (Circle Cardiovascular Imaging, Calgary, Canada). LGE, T2w-STIR and cine images were studied together and co-registered to allow accurate quantification based on all available data. For the assessment of LV volumes and function, IS and AAR, endocardial and epicardial borders were manually contoured on contiguous short-axis LV slices, excluding papillary muscles, trabeculae, epicardial surfaces and blood-pool artefact, and the

quantification method applied. The most apical LGE and T2w-STIR slice was excluded to minimize partial volume effect. IS and AAR were expressed as percentage of LVM.

3.2.3.1 IS quantification

IS was quantified on LGE magnitude images as hyperenhancement using 5/6/7/8 SD thresholding, FWHM¹¹¹ and OAT by 2 experienced readers (JNK, SN: 3 years experience each). Mean IS was compared using the techniques and with manual (visual) quantification. As there is no gold standard technique for *in vivo* IS quantification, we used the mean of 6 analyses (manual quantification undertaken twice each by observers JNK and SAN, and by an SCMR Level 3 trained reader [GPM: 10 years experience]). Manual quantification has been used in this capacity in the majority of studies comparing quantification methods for IS^{117, 287, 288} and AAR^{284, 289, 290}, and has high intraobserver and interobserver agreement and reproducibility^{117, 285}. For 5/6/7/8 SD thresholding, a region of interest (ROI) was manually drawn in remote (no enhancement, oedema or wall-motion abnormality) myocardium and the area of enhancement automatically calculated as the region with signal intensity 5/6/7/8 SD above the mean within the ROI respectively. For the FWHM technique, an ROI was manually drawn in the infarct core and enhancement calculated as pixels where signal intensity exceeded 50% of the automatically determined maximum signal intensity in the infarct core. Where it was not obvious which ROI in the infarct core had the highest maximum signal intensity, ROIs were drawn in potential regions and the ROI with the highest signal intensity selected. The ROI size for the 5/6/7/8 SD and FWHM methods was set at 2cm². The FWHM method is unaffected by ROI size as it selects the threshold based on the single pixel with highest signal intensity. The same signal intensity threshold was set for all slices on 5/6/7/8 SD and FWHM thresholding. OAT automatically calculates a unique signal intensity threshold for each slice by dividing the greyscale signal intensity histogram in each slice into 2 groups (enhanced, normal) based on the signal intensity threshold giving the least intraclass variance (lowest sum of variances) and thus most homogeneity of signal intensities within each group (Figure 35)^{274, 283}. The only user input, and thus potential sources of variation are the endocardial and epicardial contours, and

manual correction of noise artefact. OAT requires no ROI selection and is thus largely user-independent compared with SD-based, FWHM and manual quantification.

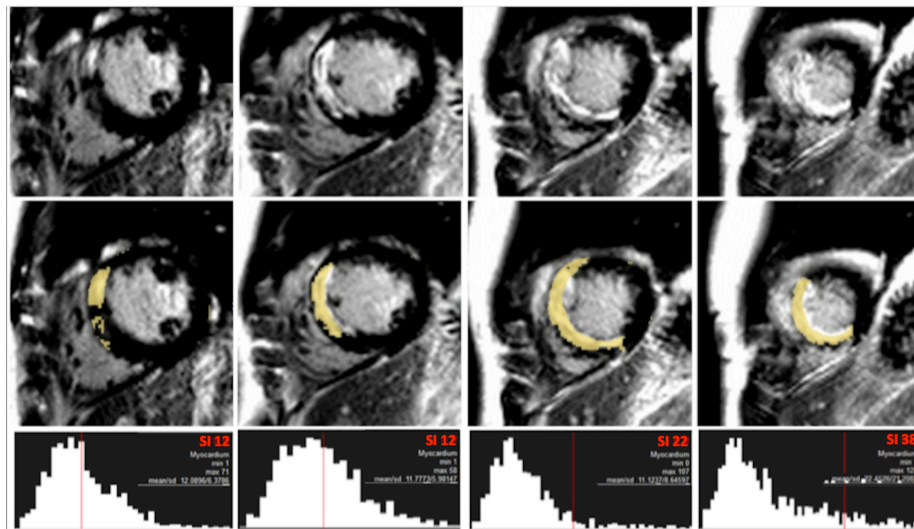


Figure 35: Otsu's Automated Thresholding (OAT) method

Top row: Short-axis late gadolinium images from basal to apical (left to right). Middle row: Enhancement (yellow) signifying infarct, designated on a slice-by-slice basis by OAT method. Bottom row: OAT automatically identifies hyperenhanced areas by selecting the grayscale signal intensity threshold (red) on a slice-by-slice basis that gives the minimal intraclass variance within enhanced and normal myocardium

3.2.3.2 AAR quantification

AAR was quantified on T2w-STIR as hyperenhancement using 2SD thresholding and OAT by 2 blinded readers (JNK, SAN). The ROI size for 2SD was set at 2cm^2 . Mean AAR was compared across the techniques and with manual quantification as described above for IS quantification.

Two manual corrections were applied to IS and AAR measurements: [a] inclusion of hypointense regions within enhancement corresponding to microvascular obstruction and intramyocardial haemorrhage in total IS and AAR respectively^{78, 117}; [b] exclusion of small isolated regions of enhancement without interslice continuity, in non-infarct related artery territories deemed to be noise artefact.

To assess intraobserver variability of the techniques, all images were re-quantified by a single observer after a 2-month interval. We also recorded the time taken to quantify IS and AAR using each of the methods once the endocardial and epicardial contours had been drawn (time taken for [a] quantification of AAR or IS using chosen technique + [b] inclusion of IMH or MVO where appropriate + [c] exclusion of noise artefact).

3.2.4 Statistical analysis

Normality was assessed using the Shapiro-Wilk test, histograms and Q-Q plots. Normally distributed data were expressed as mean±standard deviation. IS and AAR by each quantification method were normally distributed and thus compared using paired t-tests, and the accuracy of each method was assessed by comparison with manual assessment using paired t-testing, two-way mixed-effect intraclass correlation coefficient for absolute agreement ICC (three, one)²⁹¹ and Bland-Altman analysis²⁹². On ICC, agreement was defined as excellent (ICC≥0.75), good (ICC 0.6-0.74), fair (ICC 0.4-0.59), or poor (ICC<0.40)²⁹³. Interobserver and intraobserver variabilities were expressed using ICC (three, one) and Bland-Altman analysis. The significance of differences in reproducibility was assessed using Wilcoxon rank comparison of the squared differences¹¹⁷. Statistical tests were performed using SPSS v20 (IBM, USA). $p<0.05$ was considered significant.

3.3 Results

3.3.1 Baseline characteristics

Baseline characteristics are summarised in Table 26. Twenty patients were studied (1.5T n=10, 3.0T n=10). CMR was undertaken 3.7 ± 1.3 days post STEMI in the 1.5T group and 3.4 ± 2.1 days post STEMI in the 3.0T group. In total, 171 slices were analysed for IS and AAR (89 at 1.5T, at 82 at 3.0T). All LGE and STIR slices were of diagnostic image quality.

Table 26: Baseline demographics by CMR field strength cohort

	<u>1.5T</u>	<u>3.0T</u>
n	10	10
Age (years)	56.6±14.0	52.6±10.6
LAD IRA (n, %)	3 (30%)	4 (40%)
LCX IRA (n, %)	2 (20%)	2 (20%)
RCA IRA (n, %)	5 (50%)	4 (40%)
Treatment strategy	IRA-only PCI: n=3 (30%), CR: n=7 (70%)	Vasodilator treatment: n=7 (70%), Control: n=3 (30%)
CMR time post STEMI (d)	3.7±1.3	3.4±2.1
LVEDM (g)	111.6±21.9	107.1±23.1
LVEDV (ml)	179.9±33.8	169.3±35.2
LVESV (ml)	94.7±20.9	94.4±32.3
LVEF (%)	47.2±7.8	45.4±8.1
LGE image quality	2.5±0.6	2.2±0.6
T2w-STIR image quality	2.6±0.5	2.1±0.3

Data expressed as mean±standard deviation. CMR= cardiovascular magnetic resonance, STEMI= ST-segment elevation myocardial infarction, LVEDM= Left ventricular end-diastolic mass, LVEDV= Left ventricular end-diastolic volume, LVESV= Left-ventricular end-systolic volume, LVEF= Left ventricular ejection fraction, PCI= percutaneous coronary intervention, IRA= infarct-related artery

3.3.2 Infarct size

3.3.2.1 Infarct size using the quantification methods

IS varied significantly with the quantification method (Tables 27, 28 and Figures 36, 38). FWHM, 7SD and 8SD closely agreed with manual quantification at 1.5T, and 6SD showed weak agreement. FWHM and 8SD closely agreed with manual quantification at 3.0T. At both field strengths, IS was significantly greater with OAT and 5SD compared with manual quantification. IS was also greater with 6SD and 7SD at 3.0T. Bland-Altman plots for agreement with manual quantification are shown in Supplemental Data 3 and 4.

There was a strong trend towards reduced IS quantification time using FWHM compared with all SD-based methods at both field strengths. The reduction in quantification time with FWHM was highly significant when compared with manual quantification at both field strengths, and when compared with 5SD and 8SD at 1.5T. There was no difference in quantification time using FWHM and OAT (Table 29).

3.3.2.2 Interobserver and intraobserver variability of IS quantification

Results are displayed in Tables 27-28. FWHM and OAT demonstrated extremely high interobserver and intraobserver agreement at both field strengths, with all ICC values >0.922 and mean bias $<+1.84\%$. SD-based techniques demonstrated good interobserver and intraobserver agreement at both field strengths, however lower than for FWHM and OAT, with ICC values >0.888 and mean bias $<+4.43\%$. Interobserver and intraobserver agreement for manual quantification were very high at both field strengths apart from interobserver agreement at 1.5T, which was good (ICC 0.793). Bland-Altman charts for IS are shown in Supplemental Data 3 and 4.

Interobserver agreement for IS at 3.0T was significantly better with FWHM vs. manual quantification ($p=0.037$). Intraobserver agreement for IS was significantly better at 1.5T with FWHM vs. 6SD ($p=0.013$), 7SD ($p=0.022$) and 8SD ($p=0.037$), and at 3.0T for FWHM vs. manual ($p=0.047$). There was a strong trend towards higher intraobserver agreement for IS at 1.5T with FWHM vs. manual ($p=0.093$).

Table 27: Infarct size (IS) results at 1.5T by quantification method and corresponding reproducibilities

1.5T	IS (FWHM)	IS (5SD)	IS (6SD)	IS (7SD)	IS (8SD)	IS (OAT)	IS (MANUAL)
Mean IS (%LVM)	18.3±10.7	25.9±16.1 ^b	22.0±15.8 ^a	19.8±15.3	17.7±14.4	28.2±11.8 ^b	16.5±10.3
ICC v Manual	0.909	0.667	0.759	0.804	0.832	0.621	
Mean bias v Manual (±1.96SD LoA)	+1.84 (+10.30, -6.62)	+9.39 (+25.58, -6.81)	+5.57 (+21.65, -10.52)	+3.28 (+18.86, -12.30)	+1.21 (+15.92, -13.50)	+11.71 (+17.39, +6.03)	
Interobserver ICC	0.922	0.952	0.904	0.906	0.888	0.976	0.793
Interobserver mean bias (±1.96SD LoA)	+0.37 (+9.17, -8.43)	+2.54 (+11.62, -6.54)	+4.43 (+16.01, -7.16)	+4.00 (+15.48, -7.47)	+4.01 (+16.02, -8.01)	+0.55 (+5.82, -4.73)	+5.34 (+14.96, -4.28)
Intraobserver ICC	0.991	0.957	0.954	0.938	0.925	0.991	0.983
Intraobserver mean bias (±1.96SD LoA)	+0.36 (+3.34, -2.61)	-0.81 (+9.37, -10.99)	+0.01 (+10.28, -10.27)	+0.07 (+11.76, -11.62)	+0.42 (+13.00, -12.17)	+0.81 (+4.21, -2.50)	-1.92 (+0.64, -4.49)

IS expressed as mean±standard deviation. FWHM = full-width half maximum, 5SD= >5 standard deviation, OAT= Otsu's Automated Thresholding, LVM= Left Ventricular Mass, ICC= Intraclass Correlation Coefficient, LoA= Limits of Agreement (Bland-Altman).

^a - p<0.05 vs. manually quantified IS. ^b – p<0.01 vs. manually quantified IS.

Table 28: Infarct size (IS) results at 3.0T by quantification method and corresponding reproducibilities

3T	IS (FWHM)	IS (5SD)	IS (6SD)	IS (7SD)	IS (8SD)	IS (OAT)	IS (MANUAL)
Mean IS (%LVM)	10.8±8.2	17.0±11.2 ^b	14.77±10.4 ^b	13.0±9.7 ^a	11.4±9.0	21.6±9.8 ^b	11.5±9.0
ICC v Manual	0.964	0.780	0.874	0.937	0.966	0.505	
Mean bias v Manual (±1.96SD LoA)	+0.22 (+5.09, -4.65)	+6.42 (+14.93, -2.09)	+4.17 (+11.05, -2.71)	+2.38 (+7.92, -3.16)	+0.81 (+5.62, -4.01)	+11.03 (+22.20, -0.15)	
Interobserver ICC	0.990	0.957	0.937	0.916	0.888	0.977	0.913
Interobserver mean bias (±1.96SD LoA)	-0.49 (+1.74, -2.72)	+0.44 (+7.23, -6.35)	+1.14 (+8.51, -6.23)	+1.40 (+9.25, -6.44)	+1.50 (+9.99, -6.98)	-0.05 (+4.35, -4.44)	+1.97 (+9.48, -5.54)
Intraobserver ICC	0.988	0.992	0.992	0.993	0.993	0.986	0.972
Intraobserver mean bias (±1.96SD LoA)	+0.20 (+1.49, -1.10)	+0.43 (+2.90, -2.03)	-0.04 (+2.42, -2.50)	+0.10 (+2.19, -1.98)	+0.32 (+2.08, -1.45)	+0.15 (+3.50, -3.21)	+1.14 (+4.35, -2.07)

IS expressed as mean±standard deviation. FWHM= full-width half maximum, 5SD= >5 standard deviation, OAT= Otsu's Automated Thresholding, LVM= Left Ventricular Mass, ICC= Intraclass Correlation Coefficient, LoA= Limits of Agreement (Bland-Altman).

^a - p<0.05 vs. manually quantified IS. ^b – p<0.01 vs. manually quantified IS.

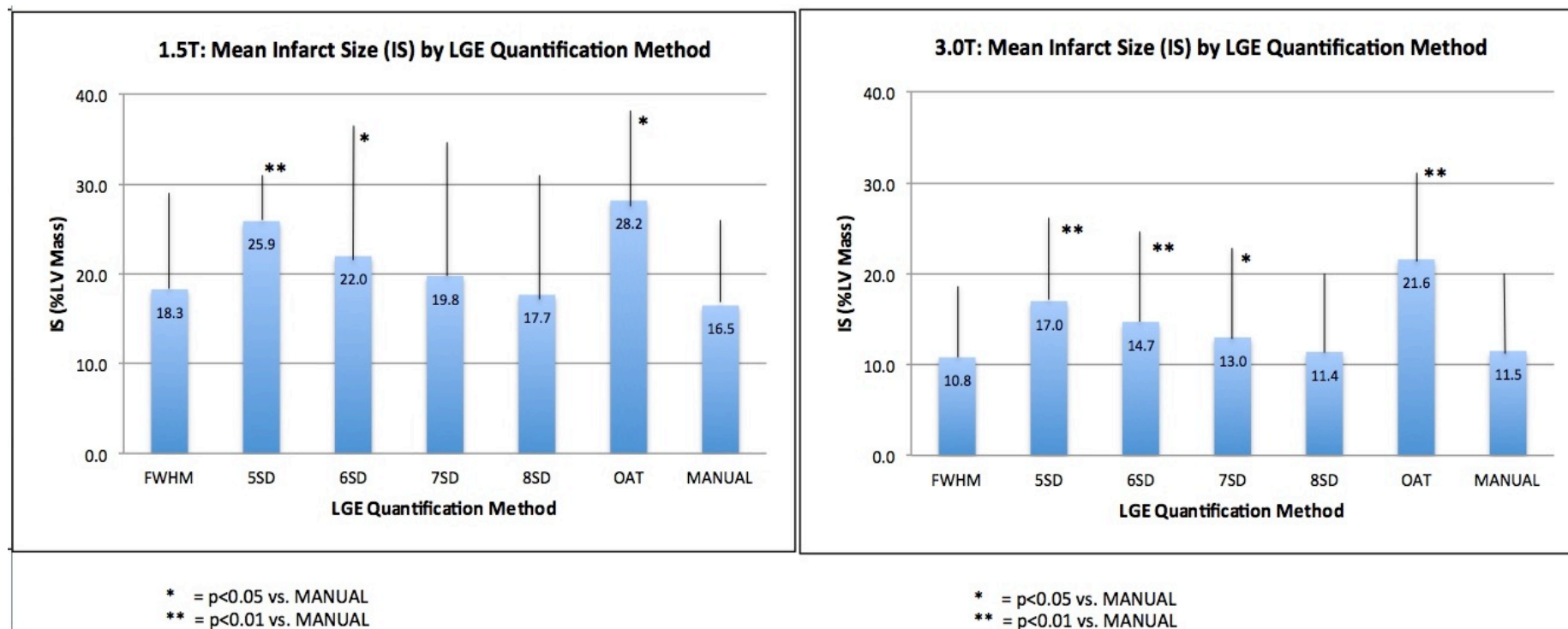


Figure 36: Mean Infarct Size (IS) by Quantification Method

Left panel 1.5T and right panel 3.0T. IS using OAT, 5-8SD, FWHM and manual quantification.

IS= infarct size, FWHM= full-width half maximum, 5-8SD= >5-8 standard deviations, OAT= Otsu's Automated Thresholding.

Table 29: Time taken per patient for Infarct Size (IS) and Area at risk (AAR) quantification

	Time (minutes)	p
1.5T: FWHM v 5SD (IS)	17.1±2.4 vs. 20.9±5.5	0.04
1.5T: FWHM v 6SD (IS)	17.1±2.4 vs. 19.4±3.1	0.09
1.5T: FWHM v 7SD (IS)	17.1±2.4 vs. 19.1±3.7	0.13
1.5T: FWHM v 8SD (IS)	17.1±2.4 vs. 19.6±3.2	<0.01
1.5T: FWHM v OAT (IS)	17.1±2.4 vs. 18.0±2.6	0.45
1.5T: FWHM v MANUAL (IS)	17.1±2.4 vs. 21.1±4.7	0.01
1.5T: 5SD v OAT (IS)	20.9±5.5 vs. 18.0±2.6	0.21
1.5T: 2SD v OAT (AAR)	17.1±2.4 vs. 16.7±2.6	0.73
1.5T: 2SD v MANUAL (AAR)	17.1±2.4 vs. 18.3±2.6	0.14
1.5T: OAT v MANUAL (AAR)	16.7±2.6 vs. 18.3±2.6	0.07
3T: FWHM v 5SD (IS)	18.9±2.7 vs. 24.7±9.1	0.08
3T: FWHM v 6SD (IS)	18.9±2.7 vs. 22.2±5.2	0.07
3T: FWHM v 7SD (IS)	18.9±2.7 vs. 22.5±5.3	0.07
3T: FWHM v 8SD (IS)	18.9±2.7 vs. 21.2±3.0	0.08
3T: FWHM v OAT (IS)	18.9±2.7 vs. 20.7±3.2	0.11
3T: FWHM v MANUAL (IS)	18.9±2.7 vs. 24.0±3.7	<0.01
3T: 5SD v OAT (IS)	24.7±9.1 vs. 20.7±3.2	0.25
3T: 2SD v OAT (AAR)	19.6±2.7 vs. 18.5±2.6	0.26
3T: 2SD v MANUAL (AAR)	19.6±2.7 vs. 18.3±2.6	0.31
3T: OAT v MANUAL (AAR)	18.5±2.6 vs. 18.3±2.6	0.83

Results illustrated by field strength and quantification method. FWHM= full-width half maximum, 5/6/7/8SD= >5/6/7/8 standard deviation, OAT= Otsu's Automated Thresholding, 2SD= >2 standard deviations. p<0.05 taken as statistically significant

3.3.2.3 Correlation of myocardial injury with LV ejection fraction

At 1.5T, FWHM and manual quantification demonstrated a strong inverse correlation between IS and LVEF (FWHM: $r=-0.745$, $p=0.013$; manual $r=-0.709$, $p=0.022$). All other methods demonstrated moderate inverse correlation and did not reach statistical significance. At 3.0T, FWHM IS showed a significant, moderate correlation with LVEF ($r=-0.673$, $p=0.033$). The correlation using all other techniques was weaker and not statistically significant.

3.3.3 Area At Risk extent

3.3.3.1 AAR extent using the quantification methods

AAR varied with the quantification method used (Table 30, Figures 37-38). There was no significant difference between 2SD, OAT and manually quantified AAR at 1.5T. At 3.0T, AAR quantified with OAT was larger than that manually contoured ($p=0.004$) and similar to that on 2SD. Agreement with manual quantification at 1.5T tended to be higher for OAT than 2SD, with ICC 0.920 and narrower limits of agreement on Bland-Altman analysis (Supplemental Data 5 and 6).

There was no difference in AAR quantification time using OAT, 2SD or manual quantification at 1.5T or 3.0T (Table 29).

3.3.3.2 Interobserver and intraobserver variability of AAR quantification

OAT had extremely high interobserver and intraobserver agreement for AAR quantification at both field strengths, with all ICC values >0.976 . Good interobserver agreement was seen for 2SD quantification of AAR at both field strengths. Manual quantification demonstrated excellent interobserver agreement at 3.0T. Interobserver agreement at 1.5T and intraobserver agreement at both field strengths was good with manual quantification (ICC >0.716)

Interobserver agreement at 3.0T was significantly better for OAT vs. manual quantification ($p=0.017$), and at 1.5T was borderline significantly higher for OAT vs. manual ($p=0.059$). Intraobserver agreement at 3.0T was significantly better for OAT vs. manual quantification ($p=0.007$).

Bland-Altman charts for AAR and MSI are shown in Supplemental Data 5 and 6 (AAR) and Supplemental Data 7 and 8 (MSI).

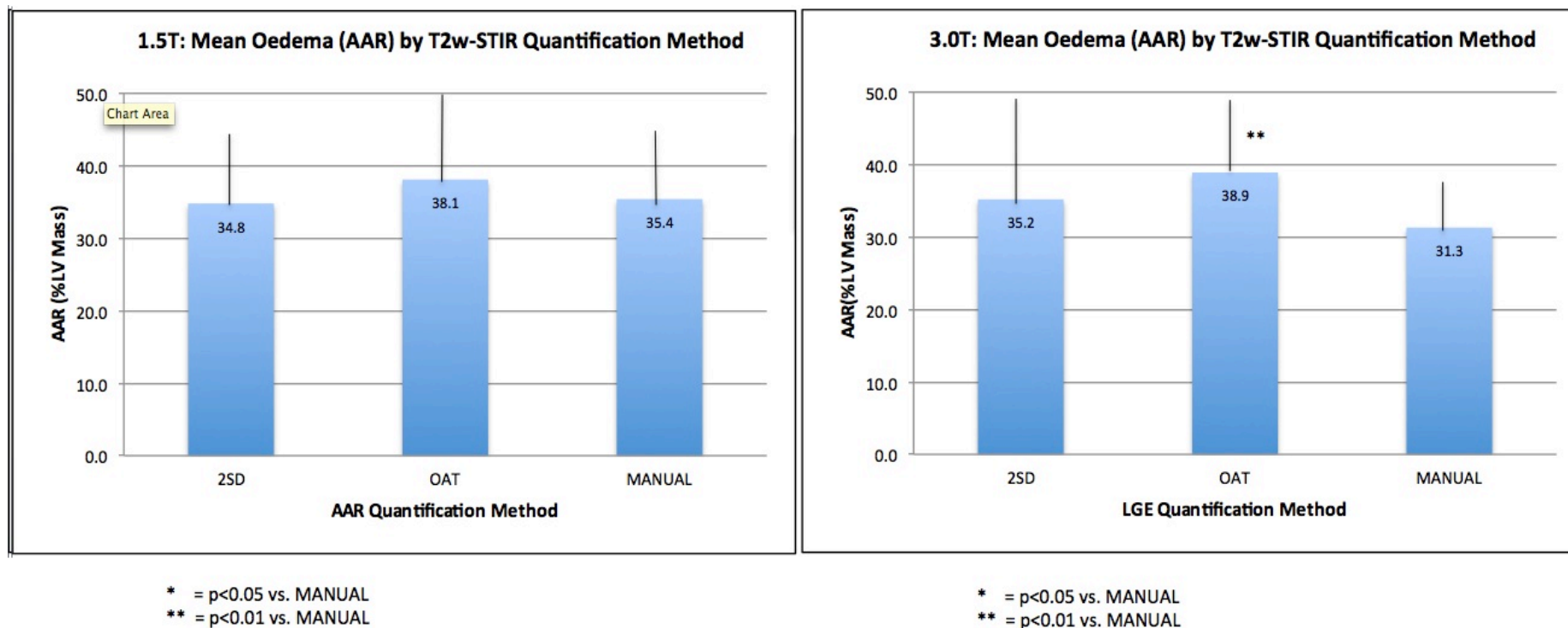


Figure 37: Mean Area-At-Risk (AAR) by Quantification Method

Left panel 1.5T and right panel 3.0T. AAR compared using 2SD, OAT and manual quantification.

IS= infarct size, OAT= Otsu's Automated Thresholding, 2SD= >2 standard deviations.

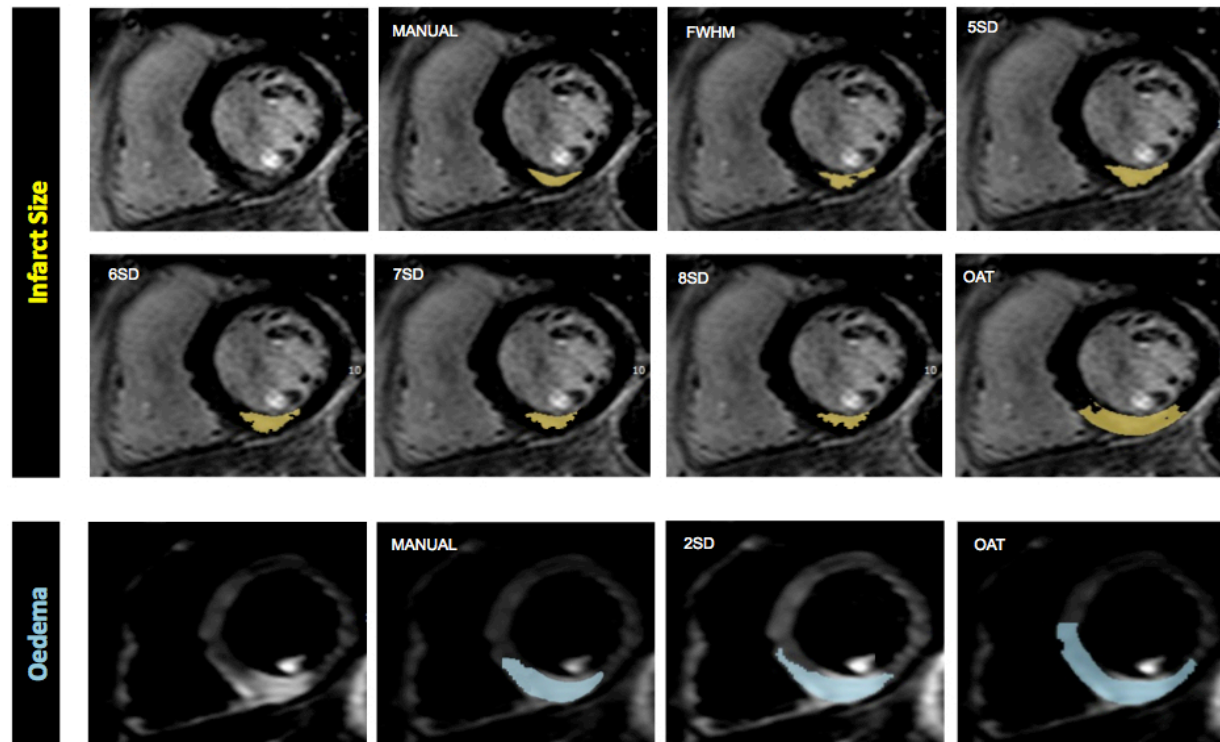


Figure 38: Infarct size and Area-At-Risk quantification at 3.0T

Top/middle rows: IS on a single patient at 3.0T demonstrating increasing IS using FWHM, 5SD and OAT, and decreasing IS from 5-8 SD. FWHM and 8SD closely correlated with the reference standard of manual quantification. Bottom row: AAR in the same patient using OAT and 2SD thresholding was non-significantly greater than the reference standard of manual quantification.

FWHM= full-width half maximum, 2/5/6/7/8SD= $>2/5/6/7/8$ standard deviations, OAT= Otsu's Automated Thresholding

Table 30: Area at risk (AAR) by field strength and quantification method and corresponding reproducibility

	1.5T			3.0T		
	AAR (2SD)	AAR (OAT)	AAR (MANUAL)	AAR (2SD)	AAR (OAT)	AAR (MANUAL)
Mean value (AAR [% LVM])	34.8±9.8	38.1±13.0	35.4±11.2	35.2±14.4	38.9±9.9 ^a	30.0±8.2
ICC v Manual	0.865	0.920		0.649	0.465	
Mean bias v Manual (±1.96SD LoA)	+0.31 (+12.20, -11.57)	+3.62 (+11.24, -4.00)		+5.13 (+22.76, -12.50)	+8.92 (+23.15, -5.31)	
Interobserver ICC	0.908	0.976	0.825	0.869	0.981	0.716
Interobserver mean bias (±1.96SD LoA)	+3.38 (+9.12, -2.37)	+1.26 (+7.20, -4.68)	+1.31 (+17.11, -14.49)	-0.34 (+15.36, -16.03)	-1.35 (+1.64, -4.33)	-5.20 (+9.54, -19.95)
Intraobserver ICC	0.948	0.995	0.977	0.987	0.990	0.826
Intraobserver mean bias (±1.96SD LoA)	+2.80 (+7.28, -1.68)	+0.58 (+3.31, -2.16)	-0.01 (+5.62, -5.64)	+1.00 (+5.50, -3.51)	+0.04 (+2.82, -2.74)	+1.46 (+14.84, -11.93)

AAR and MSI expressed as mean±standard deviation. 2SD= >2 standard deviations, OAT= Otsu's Automated Thresholding, LVM= Left Ventricular Mass, ICC= Intraclass Correlation Coefficient, LoA= Limits of Agreement (Bland-Altman).

^a - p<0.05 vs. manually quantified AAR.

3.4 Discussion

In this study we assessed IS and AAR quantification in acute STEMI patients with currently used semi-automatic techniques at 1.5T and 3.0T. FWHM and 8SD closely agreed with the reference standard of manual IS quantification at both field strengths, whereas 5SD and OAT led to higher IS values compared to manual quantification. AAR measured by OAT and 2SD were similar to manual quantification only at 1.5T. Interobserver and intraobserver agreement for IS and AAR quantification were better with FWHM and OAT compared with manual quantification respectively, and tended to be better than with SD-based methods. There was an inverse correlation between IS and LVEF for all quantification methods and this was strongest and most significant for FWHM. Our study is the first to assess IS quantification methods using 7SD and 8SD thresholding and to assess IS and AAR quantification at 3.0T.

3.4.1 Infarct size

3.4.1.1 Mean IS using the quantification techniques

LGE IS quantification in acute MI has been validated in a small number of animal studies. FWHM¹¹¹ and manual quantification²⁸¹ of *in-vivo* images closely correlated with IS on tetrazolium chloride stained canine hearts. Kim et al (1999) demonstrated good agreement of 2SD thresholding with tetrazolium chloride stained canine myocardium. However this was on *ex-vivo* slices with high spatial resolution and in the absence of rhythm and motion artefacts, and may not be generalizable to humans¹⁰⁸. Indeed, 2SD has been shown to overestimate IS in humans based on functional improvement and IS reduction in enhanced areas.^{62, 65} There is no histological validation in humans and hence no 'gold standard' quantification. We thus used manual assessment as has been used previously^{117, 283}, however derived from the mean of repeated analyses by three experienced CMR cardiologists to increase the robustness of our reference standard.

FWHM and 8SD were the only methods in our substudy showing good agreement with manual quantification at both field strengths. This may be because they are less

prone to IS overestimation resulting from oedema and partial volume effects giving rise to intermediate signal intensities^{62, 116}. This resulted in negligible requirements for manual exclusion of noise artefact with FWHM and 8SD. This in conjunction with the relative ease in identification of the brightest infarct core compared with deciding on a representative remote ROI is likely to explain the shorter time required for IS quantification using FWHM compared with SD-based techniques.

The greater IS using 5SD compared with manual quantification in our study is in agreement with previous results at 1.5T¹¹⁷. These findings indicate that the good agreement between 5SD and manual quantification in chronic ischaemic heart disease²⁹⁴, where infarct tends to have a higher and more homogenous SI¹¹⁷, cannot be extrapolated to acute STEMI patients. The close correlation of 5SD and in particular OAT with manual assessment shown by Vermes²⁸³ is in contrast to our findings. IS quantification was only performed on slices with infarct seen visually in that study, thus potentially underestimating IS. In addition, the small remote ROI used for 5SD thresholding (0.5-1cm²) by Vermes et al may not adequately represent remote myocardium signal intensity, thus leading to underestimation or overestimation of IS if an excessively bright or dark, isolated region of myocardium is taken as the remote ROI respectively. By setting the ROI size at 2cm² for all SD-based methods in our study, we aimed to ensure that the ROI was large enough to represent remote myocardium accurately. Using the same remote ROI for all SD-based methods in our substudy ensured consistency and removed the effect of ROI size and location when comparing IS between 5-8 SD thresholds. Hence, 6 and 5-SD and 7, 6 and 5-SD quantification overestimated IS at 1.5T and 3.0T respectively due to their intrinsically progressively lower signal intensity thresholds and not due to differences in remote ROI.

OAT has the potential to overestimate LGE IS because it calculates an individual SI threshold, and thus enhancement on every slice, regardless of the presence of infarct (Figure 39). Whilst small areas of enhancement in the non-infarct region were manually excluded, it is likely that OAT leads to higher values due to near transmural enhancement in the infarct area, in the presence of peri-infarct oedema.²⁷⁴

We studied IS and AAR quantification early after STEMI. IS decreases with time post PPCI with a reduction of ~30% demonstrated within the first week in some studies^{54, 62}. The extent of necrosis is overestimated by LGE early post STEMI due to cellular disruption and oedema. As scar resorbs and remodels, IS reduces and scar may become more homogenous in signal intensity and brighter. The relative overestimation of IS by lower standard deviation thresholds and OAT compared with FWHM, 8SD and manual quantification may thus be more significant in acute compared with in chronic infarcts. We chose an early time point to minimise drop-out in the study and most importantly, all the data relating infarct size to subsequent prognosis following STEMI has been based on early measurement of infarct size (usually within 1 week)^{78, 154}. Whether AAR varies in the first week after STEMI has shown conflicting results^{62, 65}. As we have only scanned the patients in this study on a single occasion we cannot comment on how the results would have varied if performed at later dates following presentation.

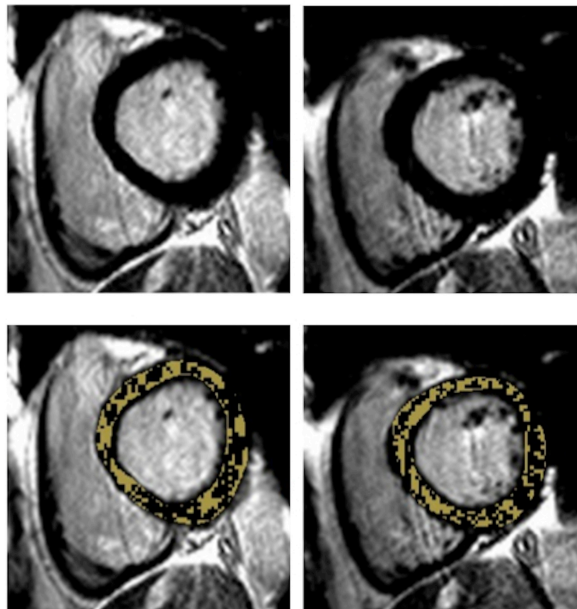


Figure 39: Hyperenhancement with OAT without obvious Infarct

In this case there is no infarct present (top row), whereas OAT has calculated a significant infarct volume (bottom row). OAT = Otsu's Automated Thresholding

2SD thresholding was not assessed for IS as it has been shown to overestimate IS^{117, 283} and had the lowest correlation with histological IS on tetrazolium chloride staining using Bland-Altman analysis¹¹¹ compared with all other quantification methods used in studies of IS in acute STEMI (5SD, FWHM, manual quantification).

3.4.1.2 Interobserver and intraobserver variability of IS quantification

The excellent interobserver and intraobserver agreement for FWHM, 5SD and OAT quantification of IS in our study at both field strengths is in agreement with previous studies at 1.5T: FWHM, 5SD^{65, 117} and FWHM, OAT²⁸³. Consistent with the work of Flett et al (2011)¹¹⁷, we found that the FWHM technique had greater interobserver and intraobserver reproducibility compared with SD-based and manual quantification. This is expected when considering that for each patient there is a single brightest core of infarct. This is in contrast to the remote ROI, which could be drawn on any slice without complete LGE in SD-based quantification, or manual contouring of enhancement, which is completely user-dependent and in the acute phase post STEMI could potentially be affected by partial volume in infarct boundaries and oedematous myocardium.

3.4.2 Area At Risk

3.4.2.1 Mean AAR and MSI using the quantification techniques

T2w-STIR AAR is typically quantified using 2SD thresholding. Validation studies are limited. 2SD-derived AAR on T2w images *in vivo* correlated with microsphere-assessed AAR in canine myocardium ($r=0.84$).¹³⁵ There is no gold standard AAR quantification method on T2w-STIR, hence we used manual assessment.

The close agreement between OAT and manually contoured AAR at 1.5T is consistent with the work of McAlindon.²⁸⁵ OAT however demonstrated greater AAR compared with manual quantification at 3.0T. This is in keeping with Sjogren²⁸⁴ who showed overestimation of AAR using OAT with a mean bias of $+5.3 \pm 9.6\%$ compared with manual quantification²⁸⁴. The determination of an optimal threshold and quantification of enhancement on every slice with OAT, regardless of oedema is likely to contribute to this. The risk of overestimation of AAR will be greatest in slices with

minimal oedema since OAT will deem a proportion of pixels enhanced. This may potentially have contributed to the overestimation of AAR at 3.0T in our study with OAT, since our 3.0T cohort had a smaller AAR than the 1.5T patients. IS was also smaller in our 3.0T cohort and may have contributed to the greater overestimation of IS using OAT at 3.0T compared with 1.5T. Conversely, underestimation of AAR is more likely in slices with complete enhancement since OAT will deem a proportion of pixels unenhanced²⁸⁴. Mean AAR image quality grade was slightly lower at 3.0T (2.1 ± 0.3 [3T] vs. 2.6 ± 0.5 [1.5T], $p=0.05$) and may have potentially contributed to the overestimation of OAT-derived AAR if there was more noise artefact in the AAR or signal intensity drop-out in remote regions by reducing the threshold. More work into automated quantification methods is required, in particular at 3.0T. Newer automated techniques, taking into account *a priori* information about the culprit artery²⁸⁴ and including noise and false positive artefact exclusion^{282, 289} algorithms may improve the accuracy of automated IS and AAR quantification.

The relative degree of AAR overestimation in our study was however, considerably less than for IS. The predominantly transmural pattern of OAT enhancement for IS and AAR may cause less overestimation of AAR compared with IS, since oedema has been shown to be predominantly transmural in 70-100% of oedematous segments^{224, 295}.

FWHM quantification of AAR was not undertaken due to the lower CNR of T2w-STIR imaging, since the vast majority of myocardium would have signal intensity >50% of the maximum at the AAR core, leading to potentially extreme overestimation of AAR and MSI. Indeed, McAlindon et al demonstrated that FWHM significantly overestimated AAR compared to all other quantification methods tested at 1.5T (2,3,5 SD, OAT, manual quantification)²⁸⁵. 5SD thresholding was not assessed for AAR as it has never been validated or correlated with clinical outcomes and the only study to feature it demonstrated that it significantly overestimated AAR compared to all other quantification methods tested at 1.5T (2,3 SD, FWHM, OAT, manual quantification)²⁸⁵.

3.4.2.2 Interobserver and intraobserver variability of AAR quantification

The relatively low interobserver and intraobserver agreement using 2SD compared with OAT at both field strengths is likely to result from varying manual definition of the remote ROI. The extremely high ICC's obtained with OAT are remarkable considering that these figures still take account differences in manual correction and contouring of endocardial and epicardial borders. Given these results, quantification of AAR with OAT could minimise variability in measurement in multi-centre trials.

3.4.3 Limitations

The main limitation of our and previous similar studies is the lack of a gold standard for IS and AAR quantification. Test-retest reproducibility was not assessed and should be considered in future studies. Infarct heterogeneity and identification of peri-infarct zone (greyzone) was not assessed in this study and may be of interest to assess in future studies using OAT. We deliberately studied patients imaged at different field strengths and with different scanner vendors to represent the situation in multi-centre clinical trials and this should make the results more generalizable. Our small sample size (total n=20) is a limitation, however is comparable to similar studies in myocardial infarction^{111, 281-283, 285, 288} and our findings are supported by their consistency at both field strengths. T2w-STIR AAR imaging was non-diagnostic in 26% of patients, which calls into question the use of this method of AAR imaging in clinical practice, and hence recent studies of AAR are increasingly using the more robust T2-mapping derived sequences. Finally our results may not be generalizable to if patients are scanned at different time points following STEMI.

3.4.4 Conclusions

Inter- and intraobserver variability for the quantification of IS with FWHM are excellent at 1.5 and 3.0T and better than when using manual quantification. Only FWHM and 8SD closely agreed with manual delineation of IS at both field strengths. FWHM had better reproducibility, shorter quantification time and closer correlation with LVEF and may be the preferred method for IS quantification in future studies. AAR is similar when assessed with OAT, 2SD and manual quantification at 1.5T,

however OAT has excellent intra and interobserver variability and thus has potential in quantification of AAR at 1.5T, especially in multi-centre studies. OAT overestimated AAR at 3.0T compared with manual quantification and thus cannot currently be recommended as the preferred method for AAR quantification at 3.0T. **FWHM and OAT will hence be used for IS and AAR quantification respectively in the CvLPRIT-CMR substudy.**

3.4.5 Original contribution to knowledge

At the time of writing, this is the first study assessing IS quantification methods using 7SD and 8SD thresholding and assessing IS and AAR quantification at 3.0T.

3.4.6 My contribution

I conceived the idea for this study. I recruited patients and was present at study visits. I and SAN performed the CMR analyses. I performed the statistical analysis and wrote the manuscript, which all authors critically reviewed for content.

CHAPTER 4

4. FEATURE-TRACKING AND TAGGING ASSESSMENT OF STRAIN IN ACUTE STEMI

Comparison of cardiovascular magnetic resonance feature tracking and tagging for the assessment of left ventricular systolic strain in acute myocardial infarction

Published:

Khan JN, Singh A, Nazir SA, Kanagala P, Gershlick AH, McCann GP. Comparison of cardiovascular magnetic resonance feature tracking and tagging for the assessment of left ventricular systolic strain in acute myocardial infarction. *European Journal of Radiology*. May 2015. 84(5):840-8. doi: 10.1016/j.ejrad.2015.02.002.

4.1 Background

Contractile dysfunction following acute STEMI predicts prognosis⁷⁴. Cardiovascular MRI measured myocardial strain is the gold standard measure of myocardial function⁸⁶. It offers greater accuracy in detecting dysfunctional myocardium compared with global (ejection fraction) and regional (wall-motion scoring, wall thickening) measures of function⁸⁷. Global strain is also an independent predictor of medium-term prognosis post STEMI.¹⁰³

Myocardial tissue tagging creates saturated lines perpendicular to the slice plane and act as tissue markers in a grid, tracking myocardial motion. Various tagging analysis techniques are available, including local sine-wave modelling (SinMod) and HARP, which have demonstrated close agreement.^{275, 296} Tagging requires the acquisition of additional sequences and time-consuming post-processing. Feature tracking (FT) tracks features of interest (tissue-cavity interfaces, tissue dishomogeneities, anatomic landmarks) along contour lines on routinely acquired SSFP cine images, analogous to echocardiographic speckle tracking^{93, 297}. FT-derived strain has been compared to tagging in muscular dystrophy patients⁹³ and normal volunteers⁹⁴ showing reasonable agreement although we have recently shown that FT overestimates systolic strain compared to tagging.²⁹⁸

This study aimed to assess the feasibility of FT measured global and segmental peak *Ecc* and *Ell* strain assessment post acute STEMI and compare strain values to those obtained with tagging.

4.2 Methods

4.2.1 Study population

Twenty-four patients were retrospectively, randomly selected using a random number generator²⁸⁶ from the acute CMR cohort of the CvLPRIT-CMR study²⁵⁴.

4.2.2 Cardiovascular MRI

MRI was performed at a median of 2.2 days following STEMI presentation on a 1.5T

scanner (Siemens Avanto, Erlangen, Germany) with dedicated cardiac receiver coils. SSFP cine, T2-weighted short-tau inversion recovery (T2w-STIR) and Late Gadolinium Enhancement (LGE) imaging were performed in long-axis (2/3/4-chamber) views and contiguous short-axis slices covering the left ventricle (LV). LGE images were acquired 10 minutes after 0.2mmol/kg gadolinium-DTPA (Magnevist, Bayer, Germany) using a segmented inversion-recovery gradient-echo sequence. The inversion time was progressively adjusted to null unaffected myocardium. Three pre-contrast short-axis (base, mid, apical) and long-axis tagged images were acquired using a prospectively gated spatial modulation of magnetization (SPAMM) gradient-echo sequence. In-plane spatial resolution was ~1.3mm x 1.3mm for tagging and ~1.4mm x 1.4mm for Feature Tracking. The imaging protocol is detailed in Figure 19.

4.2.3 MRI analysis

4.2.3.1 Volumetric and LGE analysis

Analysis was performed using *cvi42* v4.1 (Circle Cardiovascular Imaging, Calgary, Canada). LV volumes and function were calculated as previously described.²⁹⁹ Oedema (area-at-risk, AAR) and infarct size (IS) were quantified on T2w-STIR and LGE imaging using Otsu's Automated Method²⁸⁴ and Full-Width Half-Maximum technique respectively.¹¹⁷ Myocardial salvage index (MSI) defines the proportion of the AAR that does not progress to infarction and was calculated as $[(\text{AAR} - \text{infarct size}) / \text{AAR}] \times 100$. Total oedema and infarct size were expressed as a percentage of LV end-diastolic mass. Segmental oedema, infarct and MSI were calculated as a percentage area for each of the 16 segments in the American Heart Association model^{61, 98}. Transmural enhancement was defined as >50% segmental enhanced area. Segments with <1% area of oedema or LGE were classed as having no oedema or infarct respectively. 'Infarct' segments had LGE and oedema, 'adjacent' ('at risk') segments had oedema but no LGE, and 'remote' segments had no oedema or LGE¹⁶⁶.

4.2.3.2 Circumferential and longitudinal strain analysis

Global peak *Ecc* and *Ell* strain were calculated as the average of values obtained in the three short-axis slices and long-axis views respectively. We recorded the time taken to: (a) analyse images, (b) post-process numerical data (generate and extract

strain data on a segmental, slice and long-axis basis and paste into a spreadsheet where segmental data are illustrated for the 16 segments in numerical order as per American Heart Association nomenclature)⁶¹ and (c) total analysis time (sum of a and b). A detailed description of the strain quantification method using Tagging and FT is described in Section 2.4.3.4. Interobserver and intraobserver variability of global and segmental strain analysis for both techniques was performed by two observers (JNK, AS) on a subset of 10 patients and repeated by a single observer (JNK) after 4 weeks.

4.2.4 Statistical analysis

Normality was assessed using Shapiro-Wilk tests, histograms and Q-Q plots. Normally distributed data were expressed as mean±standard deviation. Non-parametric data were expressed as median (25%-75% interquartile range). Global and segmental *Ecc* and *EII* using FT and tagging were compared using paired t-testing, two-way mixed-effect intraclass correlation coefficient for absolute agreement (ICC)²⁹¹ and Bland-Altman analysis²⁹². Interobserver and intraobserver variabilities were expressed using ICC, coefficient of variation (COV) and Bland-Altman analysis. On ICC, agreement was defined as excellent (ICC≥0.75), good (ICC0.6-0.74), fair (ICC 0.4-0.59), or poor (ICC<0.40)²⁹³. Strain was correlated with infarct and MSI using Spearman's Ranked Correlation Coefficient (r_s) and with oedema using Pearson's Correlation Coefficient (r). The sample size was chosen according to the table of Critical Values of the Spearman's Ranked Correlation Coefficient for $r_s \sim 0.40$ with $p < 0.05$, based on an initial pilot of 10 patients³⁰⁰. The correlation between global strain and number of transmurally-enhanced segments after correction for total IS was assessed using multiple regression. Independent t-testing compared segmental strain according to the presence of infarct, transmural infarction and oedema. Receiver Operating Curve (ROC) Area Under the Curve (AUC) analysis assessed the accuracy of each method in predicting transmural infarction. Statistical tests were performed using SPSS V20. $p < 0.05$ was considered significant.

4.3 Results

4.3.1 Baseline characteristics

CMR data for the 24 patients are summarised in Table 31. All segments tracked satisfactorily with FT despite hypoenhancement (MVO) or hyperenhancement (contrast enhancement) in the infarct territory on cine imaging (Figure 40). The number of segments excluded from tagging analysis was significantly higher than for FT. The time taken to contour, post-process and fully analyse each patient was significantly shorter with FT ($p < 0.001$ for all steps) (Table 32).

Table 31: Patient characteristics and MRI data: quality and analysis time

Number of patients (male/female)	24 (22/2)
Age (years)	63.0±9.5
Timing of CMR (days post PPCI)	2.2 (1.8-3.2)
Left ventricular end-diastolic mass (g/m ²) ^a	43.7 (38.3-49.8)
Left ventricular end-diastolic volume (ml/m ²) ^a	96.4 (84.1-121.8)
Left-ventricular end-systolic volume (ml/m ²) ^a	45.9 (36.7-69.6)
Left ventricular ejection fraction (%)	49.6±7.5
Infarct size (% left ventricular mass)	13.2 (8.2-21.1)
Anterior infarct	8 (35%)
Number of segments with infarction	170
Total segments analysed	384

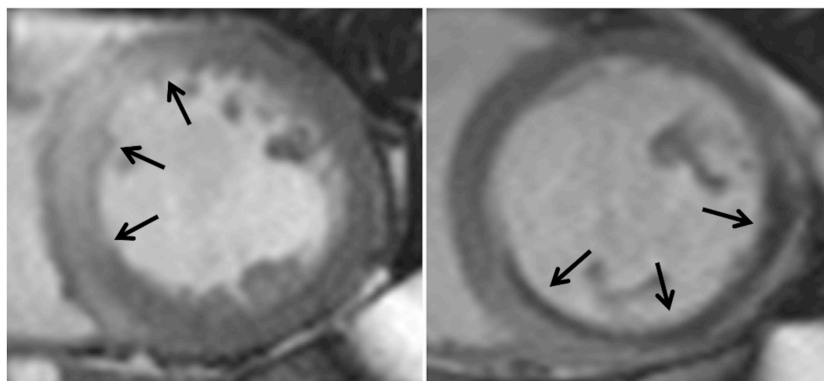


Figure 40: Hyperenhancement and hypoenhancement on cine imaging

All segments tracked satisfactorily with FT despite hyperenhancement (contrast enhancement, *left*) or hypoenhancement (microvascular obstruction, *right*) in the infarct related territory

Table 32: Myocardial tracking and quantification time by method

	FT	Tagging	p
SAX cine segments excluded	0 (0%) ^a	18 (5%)	<0.001
LAX cine segments excluded	0 (0%) ^a	81 (21%)	<0.001
Number of excluded SAX segments in infarct core	0 (0%) ^a	3/18 (17%)	<0.001
Number of excluded LAX segments in infarct core	0 (0%) ^a	14/81 (17%)	<0.001
Analysis time per patient (min)	25.3±3.7 ^a	33.4±5.6	<0.001
Post-processing time per patient (min)	12.9±2.0 ^a	30.3±5.9	<0.001
Total analysis time (min)	38.2±3.8 ^a	63.7±10.3	<0.001

FT= Feature tracking, SAX= short-axis, LAX= long-axis.

a – p<0.001 compared with tagging. Infarction defined where ≥1% segmental LGE.

4.3.2 Global strain on FT and tagging

Global strain varied significantly with the quantification technique (Table 33). On FT, *Ecc* and *EII* were highest using endocardial contours only, followed by the mean of endocardial and epicardial contours, and lowest using epicardial contours only (p<0.01 for all comparisons). FT-derived global *Ecc* using endocardial contours only was higher than that derived with tagging, and lower using epicardial contours only (p<0.05). Global *Ecc* derived using the mean of endocardial and epicardial contoured values on FT moderately agreed with tagging but showed poor agreement using results generated from either of epicardial or endocardial contours. Global *EII* was higher for all FT methods compared with tagging (p<0.05).

4.3.3 Association with infarct extent

4.3.3.1 Total infarct size

There was a moderate correlation between total IS and global *Ecc* using all methods but statistically significant only with endocardial contours on FT (Table 34).

Table 33: Agreement of peak systolic strain by feature tracking and tagging

	<i>Ecc</i> FT Endo	<i>Ecc</i> FT Epi	<i>Ecc</i> FT Mean	<i>Ell</i> FT Endo	<i>Ell</i> FT Epi	<i>Ell</i> FT Mean	<i>Ecc</i> Tagging	<i>Ell</i> Tagging
Global strain (%)	-18.57±5.4 ^a	-8.33±3.0 ^a	-13.45±4.1	-15.39±4.5 ^b	-12.35±3.7 ^b	-13.87±4.0 ^b	-13.85±3.9	-9.17±2.4
ICC (FT v tagging)	0.271	0.159	0.417	0.137	0.297	0.200	n/a	n/a
Mean bias (%) v tagging (LoA)	+4.7 (+14.9, -5.4)	-5.5 (+2.3, -13.3)	-0.4 (+8.2, -9.0)	+6.2 (+14.2, -1.8)	+3.2 (+9.6, -3.2)	+4.7 (+11.7, -2.3)	n/a	n/a

Ecc= Circumferential strain, *Ell*= Longitudinal strain, FT= Feature-Tracking derived, Endo= Endocardial contoured, Epi= Epicardial contoured, IS= infarct size. *Ecc* (or *Ell*) FT Mean= *Ecc* (or *Ell*) from mean of endocardial and epicardial strain values, LoA = 95% Bland-Altman limits of agreement. ^a – p<0.05 compared with *Ecc* tagging PSS, ^b - p<0.05 compared with *Ell* tagging PSS

Table 34: Correlation between strain by FT and tagging and infarct size, area at risk and myocardial salvage

	<i>Ecc</i> FT Endo	<i>Ecc</i> FT Epi	<i>Ecc</i> FT Mean	<i>EII</i> FT Endo	<i>EII</i> FT Epi	<i>EII</i> FT Mean	<i>Ecc</i> Tagging	<i>EII</i> Tagging
Correlation global strain vs. total IS	0.438 (p=0.03)	0.385 (p=0.06)	0.395 (p=0.06)	0.314 (p=0.14)	0.326 (p=0.12)	0.368 (p=0.08)	0.303 (p=0.15)	0.396 (p=0.06)
Correlation segmental strain vs. segmental IS	0.437 (p<0.01)	0.368 (p<0.01)	0.445 (p<0.01)	0.176 (p=0.01)	0.171 (p=0.01)	0.184 (p<0.01)	0.266 (p<0.01)	0.078 (p=0.17)
PSS in 209 segments without infarct (%)	-24.53±10.8	-11.63±7.1	-18.08±8.2	-19.89±12.2	-16.57±10.3	-17.83±10.7	-16.19±5.8	-11.67±5.4
PSS in 175 segments with infarct (%)	-14.68±10.5 ^a	-7.30±6.0 ^a	-10.99±7.7 ^a	-15.24±11.0 ^a	-13.38±9.8 ^a	-14.04±9.4 ^a	-13.21±7.1 ^a	-10.36±5.3 ^a
Correlation global strain vs. total AAR	0.260 (p=0.27)	0.145 (p=0.54)	0.224 (p=0.34)	0.231 (p=0.33)	0.215 (p=0.36)	0.227 (p=0.34)	0.260 (p=0.27)	0.559 (p=0.01)
Correlation segmental strain vs segmental AAR	0.376 (p<0.01)	0.274 (p< 0.01)	0.363 (p<0.01)	0.114 (p=0.04)	0.099 (p=0.08)	0.103 (p=0.07)	0.257 (p<0.01)	0.073 (p=0.24)
PSS in 99 segments without oedema (%)	-24.81±9.4	-11.47±5.8	-18.13±6.8	-17.75±11.7	-15.87±9.7	-16.61±10.3	-15.64±5.5	-11.43±5.8
PSS in 221 segments with oedema (%)	-17.51±11.1 ^b	-8.75±6.5 ^b	-13.13±8.3 ^b	-16.85±11.3	-14.18±10.3	-15.01±10.0	-13.56±6.4 ^b	-10.81±5.1
Correlation global strain vs. total MSI	-0.304 (p=0.19)	-0.260 (p=0.27)	-0.294 (p=0.21)	-0.108 (p=0.65)	-0.299 (p=0.20)	-0.284 (p=0.23)	-0.224 (p=0.34)	-0.105 (p=0.66)
Correlation segmental strain vs. segmental MSI	-0.409 (p<0.01)	-0.332 (p<0.01)	-0.406 (p<0.01)	-0.216 (p<0.01)	-0.201 (p<0.01)	-0.226 (p<0.01)	-0.273 (p<0.01)	-0.063 (p=0.39)

^a – p<0.05 compared with segments without infarct, ^b – p<0.05 compared with segments without oedema. Spearman's Ranked Correlation Coefficient used for non-parametrically distributed IS and MSI. Pearson's Correlation Coefficient used for normally distributed AAR.

4.3.3.2 Segmental extent of infarct and transmural

Segmentally, *Ecc* and LGE moderately correlated for all FT *Ecc* methods, but only weakly using tagging-derived *Ecc*. FT and tagging-derived segmental *EII* weakly correlated with segmental LGE (Table 34). The number of transmurally-enhanced segments moderately correlated with global strain (Table 35). This was significant for all FT strain methods, but only for tagging-derived *EII*. After correction for total IS, this correlation remained for FT methods but not for tagging-derived strain. Strain was significantly lower in transmurally-enhanced (>50%) compared with non-transmural segments using all techniques. The relative reduction in strain in transmurally-enhanced segments, and accuracy (AUC) in predicting transmural enhancement were greatest for FT-derived *Ecc* using endocardial contours only and FT *Ecc* using the mean of endocardial and epicardial contours.

4.3.3.3 Infarct, adjacent and remote segments

Ecc and *EII* were significantly lower in segments with infarct than in segments without, on FT and tagging. The relative reduction was greatest for FT *Ecc* using endocardial contours only (40% lower *Ecc*, Table 34). *Ecc* and *EII* were significantly lower ($p < 0.01$ for all techniques) in 'infarct' compared with 'adjacent' segments using all techniques, except tagging-derived *EII* ($p = 0.22$) (Figure 41). The relative reduction in segmental strain was greatest for FT *Ecc* using endocardial contours only (41% lower *Ecc* in infarct vs. adjacent segments). Strain in adjacent and remote segments was similar using all techniques.

4.3.4 Association with oedema

Only tagging-derived global *EII* significantly correlated with total oedema (AAR) (Table 34). Segmentally, there was a significant moderate correlation between *Ecc* and oedema for all methods (Table 34). There was no significant correlation between segmental *EII* and oedema. The relative reduction in *Ecc* in oedematous segments was greatest for FT *Ecc* using endocardial contours (29% lower in oedematous vs. non-oedematous segments).

Table 35: Peak strain by FT and tagging and segmental transmural late gadolinium enhancement

	<i>Ecc</i> FT Endo	<i>Ecc</i> FT Epi	<i>Ecc</i> FT Mean	<i>EII</i> FT Endo	<i>EII</i> FT Epi	<i>EII</i> FT Mean	<i>Ecc</i> Tagging	<i>EII</i> Tagging
Correlation of global strain vs. no. of transmurally enhanced segments	0.463 (p=0.023)	0.442 (p=0.030)	0.436 (p=0.033)	0.397 (p=0.055)	0.414 (p=0.044)	0.441 (p=0.031)	0.334 (p=0.110)	0.487 (p=0.016)
Beta value for correlation between number of transmurally enhanced segments and global strain independent of total IS (p)*	+2.01 (p=0.088)	+1.17 (p=0.077)	+1.59 (p=0.076)	+2.00 (p=0.038)	+1.58 (p=0.049)	+1.79 (p=0.038)	+0.42 (p=0.619)	+0.49 (p=0.171)
PSS in 39 segments with transmural LGE (%)	-11.61±12.1 ^a	-5.90±7.3 ^a	-8.76±9.3 ^a	-16.03±11.8 ^b	-12.32±9.2 ^b	-14.21±10.2 ^b	-11.77±6.6 ^b	-10.63±5.1 ^b
PSS in 345 segments without transmural LGE (%)	-20.99±11.3	-10.08±6.8	-15.54±8.4	-17.97±11.9	-15.43±10.3	-16.32±10.3	-15.18±6.5	-11.13±5.4
Relative reduction in strain in transmural LGE segments (%)	-44.7	-41.5	-43.6	-10.8	-20.2	-12.9	-22.4	-4.5
Accuracy in predicting segmental transmural LGE (ROC AUC)	0.763	0.736	0.772	0.558	0.601	0.572	0.662	0.534

^a – p<0.001 compared with segments without transmural LGE.

^b – p<0.05 compared with segments without transmural LGE.

* - Beta value defines change in PSS (+ is reduction in strain) with each transmurally-enhanced segment

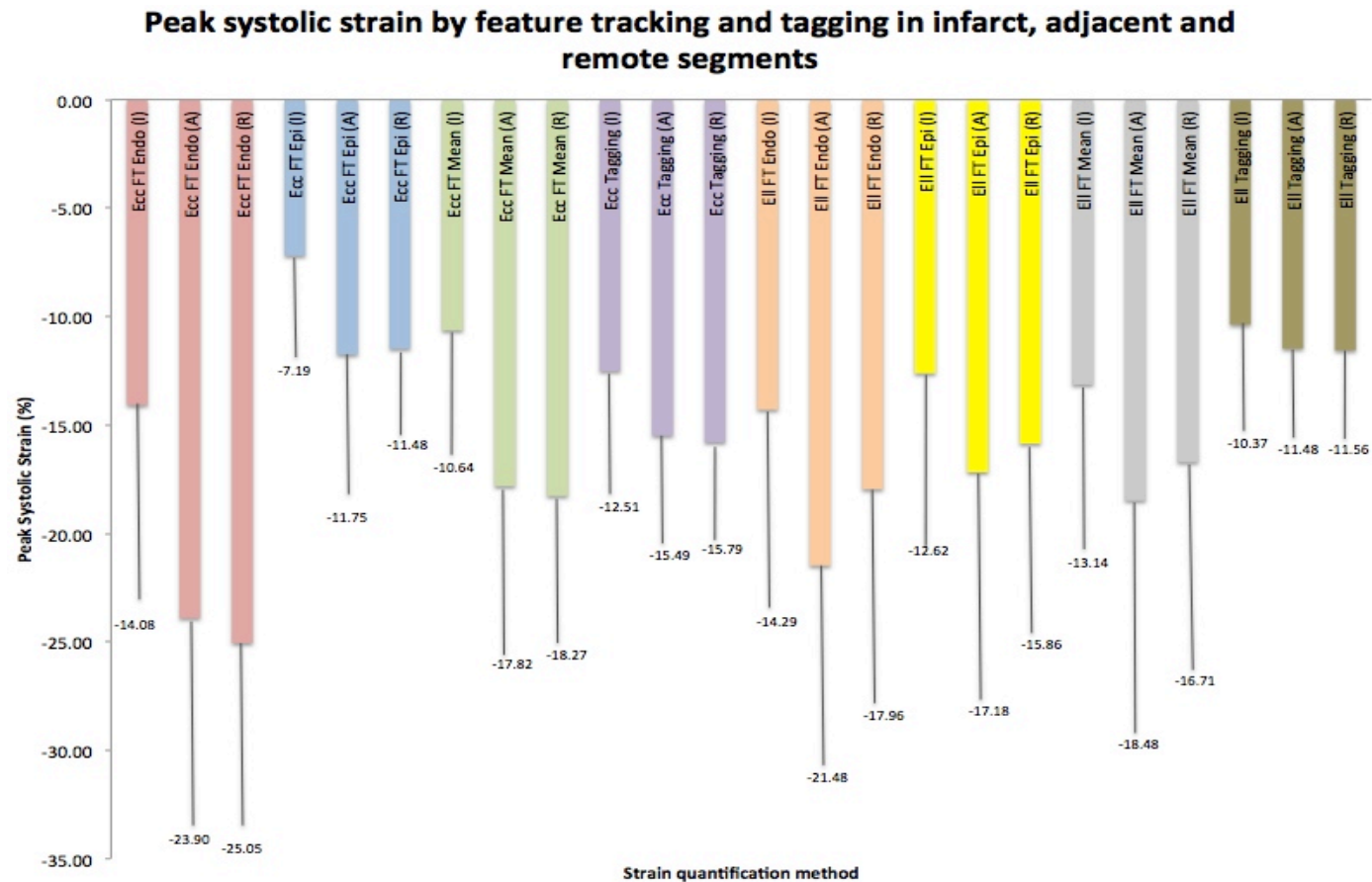


Figure 41: Peak systolic strain by feature tracking and tagging in infarct, adjacent and remote segments

Ecc= peak circumferential systolic strain, *EII*= peak longitudinal systolic strain, Endo= endocardial Feature-Tracking, Epi= epicardial Feature-Tracking, Mean= mean of endocardial and epicardial Feature-Tracking strain, (I)= infarct, (A)= adjacent, (R)= remote

4.3.5 Association with myocardial salvage index

There was a non-significant moderate correlation between global strain and total MSI using all techniques, apart from endocardially-derived FT *EII* and tagging-derived *EII* where there was no correlation (Table 34). Segmental strain and MSI moderately correlated using all methods, excluding tagging-derived *EII*. The correlation was strongest for FT *Ecc* using endocardial contours only ($r_s=-0.406$) and FT *Ecc* using the mean of endocardial and epicardial contours ($r_s=-0.402$).

4.3.6 Interobserver and intraobserver agreement of strain assessment

4.3.6.1 Global strain

All FT techniques for *Ecc* and *EII* had excellent interobserver and intraobserver agreement (Table 36). FT strain derivation from a mean of endocardial and epicardial contours did not improve interobserver or intraobserver agreement above endocardial contouring alone. Intraobserver agreement for tagging-derived *Ecc* and *EII* was excellent, however interobserver agreement was lower than with FT.

4.3.6.2 Segmental strain

Interobserver and intraobserver agreement were lower for segmental compared with global strain for FT and tagging. Interobserver and intraobserver agreement were good for all techniques except for tagging-derived *EII* where interobserver agreement was very poor (ICC 0.150, COV 58.6%). There was a trend for higher interobserver and intraobserver agreement for *Ecc* than with *EII* with FT (Table 36).

Bland-Altman plots for intra and interobserver agreement for global and segmental strain using the techniques are in Supplemental Data 9-12.

4.4 Discussion

This is the first study to date assessing the robustness of FT for the quantification of global and segmental systolic strain in acute MI. Strain was higher with FT than tagging. There was excellent intraobserver agreement with FT and tagging for

Table 36: Interobserver and intraobserver agreement of strain measured by FT and tagging

	<i>Ecc</i> FT Endo	<i>Ecc</i> FT Epi	<i>Ecc</i> FT Mean	<i>EII</i> FT Endo	<i>EII</i> FT Epi	<i>EII</i> FT Mean	<i>Ecc</i> Tagging	<i>EII</i> Tagging
Global strain								
<u>Inter-observer</u>								
ICC	0.979	0.906	0.971	0.942	0.936	0.949	0.765	0.733
Mean bias (%)	+0.6	+0.2	0.4	-0.5	+0.1	-0.2	+0.2	-0.2
LOA ($\pm 1.96SD$)	(+2.6, -1.3)	(+2.3, -1.9)	(+2.1, -1.3)	(+2.7, -3.8)	(+3.1, -2.8)	(+2.6, -3.1)	(+6.3, -22.2)	(+5.4, -5.9)
CoV (%)	4.8	12.1	6.0	10.0	11.6	9.9	22.2	28.8
<u>Intra-observer</u>								
ICC	0.989	0.963	0.988	0.990	0.911	0.973	0.920	0.936
Mean bias, (%)	-0.7	-0.5	-0.6	-0.2	0.0	-0.1	+0.9	+0.5
LOA ($\pm 1.96SD$)	(+0.4, -1.7)	(+0.7, -1.7)	(0.0, -1.2)	(+1.3, -1.6)	(+3.7, -3.7)	(+2.1, -2.2)	(+4.4, -2.5)	(+1.9, -1.0)
CoV (%)	2.5	6.5	2.1	4.5	14.5	7.6	13.1	7.7
Segmental strain								
<u>Inter-observer</u>								
ICC	0.796	0.824	0.829	0.726	0.780	0.739	0.735	0.150
Mean bias (%)	+0.6	0.0	+0.3	-0.4	+0.6	-0.7	+0.3	+1.6
LOA ($\pm 1.96SD$)	(+15.0, -13.9)	(+7.6, -7.7)	(+9.9, -9.4)	(+16.8, -17.7)	(+14.3, -13.2)	(+14.2, -15.7)	(+10.2, -9.7)	(+14.7, -11.4)
CoV (%)	34.5	38.8	31.4	46.7	44.2	44.9	34.7	58.6
<u>Intra-observer</u>								
ICC	0.872	0.859	0.887	0.826	0.771	0.822	0.813	0.864
Mean bias (%)	-0.6	-0.4	-0.5	-0.5	+0.7	+0.3	+0.8	+0.5
LOA ($\pm 1.96SD$)	(+10.8, -12.0)	(+7.1, -8.0)	(+7.5, -8.6)	(+13.6, -14.5)	(+15.8, -14.3)	(+13.2, -12.6)	(+9.2, -7.6)	(+6.3, -5.3)
CoV (%)	26.4	37.5	25.6	38.0	48.7	40.0	29.9	24.7

Ecc= Circumferential strain, *Ell*= Longitudinal strain, FT= Feature-Tracking derived, Endo= Endocardial contoured, Epi= Epicardial contoured, IS= infarct size, ICC= intraclass correlation coefficient, LoA= Limits of Agreement (Bland-Altman), *Ecc* (or *Ell*) FT Mean= *Ecc* (or *Ell*) derived from mean of endocardial and epicardial strain values.

global strain, whereas interobserver agreement using tagging was good but remained excellent for FT. Segmental strain analysis had markedly poorer interobserver and intraobserver agreement using both techniques and was particularly poor for *EII*. FT-derived strain correlated more strongly with IS, AAR, MSI and infarct transmuralilty.

Our results may have significant implications for future research studies. Firstly, FT proved robust in our study with no non-analysable segments and a shorter analysis time compared with tagging. This was despite hypoenhancement and in particular hyperenhancement on post-contrast SSFP images, which reduces the contrast-to-noise ratio between blood-pool and myocardium. The significant number of poorly tracking, and consequently excluded tagged segments is most likely the result of image degradation due to suboptimal breath-holding and ectopy, often seen in acute STEMI. Tag fading was not a major issue as we only assessed peak systolic strain. FT requires no additional sequences to routinely acquired SSFP images, which require shorter breath-holds than tagged images. Our findings are consistent with published literature in which ~11% of tagged images have been excluded³⁰¹, whereas the majority of FT studies report no non-analysable segments.^{302, 303} FT thus allows faster scan times, faster post-processing and less data are excluded due to poor contour tracking compared to tagging. In this report we quantified strain using FT by three different methods: (1) endocardial contours only, (2) epicardial contours only and (3) using the average results generated from 1 and 2. Using only one FT method dramatically speeds up the process⁹⁴.

Secondly, the method used to derive FT strain is important and investigators should be clear on which technique was used and be cautious when comparing results directly with other studies. Global *Ecc* using the average of endocardial and epicardial values moderately correlated with tagging in our study. We have again shown²⁹⁸ that strain measured with endocardial only contouring on FT results in markedly increased values compared to the average of endocardial and epicardial values, which were similar to tagging for *Ecc* (with wide limits of agreement) but higher than *EII*. Strain values were also higher with FT than tagging in a study of

healthy volunteers⁹⁴, and anteroseptal, inferior and inferoseptal *Ecc* were higher with FT in hypertrophic cardiomyopathy³⁰⁴. It is surprising that FT and tagging strain were reported to be very similar in patients with muscular dystrophy since it appears that endocardial contours only were used in that analysis⁹³. It may be that the results of such comparisons will vary with the population and methods used, although differences in tagging analysis software are unlikely to be significant since SinMod and HARP have shown close agreement for global strain²⁷⁵. The close temporal relationship between acquisition of tagged and cine images makes true physiological differences unlikely and the temporal resolution of tagged and SSFP cine images was also very similar (~50ms). The lower average global strain with tagging may partly result from the exclusion of segments, which contained normal non-infarcted myocardium, and this effect is likely to be greater for *EII* (21% of segments excluded and 83% of those non-infarcted tissue) than for *Ecc* (5% of segments excluded). Our global strain *Ecc* values on tagging are similar to those reported previously post STEMI.⁸⁷

Thirdly, the moderate correlation between FT *Ecc* and infarct globally and segmentally, combined with significant differences in *Ecc* in segments with and without infarct provide some internal validation in the absence of 'true' strain in this clinical population. This was especially the case with FT-derived *Ecc* using endocardial contours only and may be because scarring and dysfunction post STEMI is greatest endocardially¹³². The moderate correlation between *Ecc* and infarct size may in part be explained by the limited sample size of 24 patients. *Ecc* has correlated better with infarct size than *EII* and *Err* on previous FT³⁰⁵ (in chronic infarction) and tagging studies^{87, 306} and been shown to be similarly higher in adjacent and remote segments compared with infarct.³⁰⁷

Furthermore, the ability of FT-derived *Ecc* to identify transmural enhancement offers potential for predicting functional improvement post STEMI. *Ecc* has also been shown to distinguish segmental transmural enhancement better than *EII* using Strain-Encoded Imaging (SENC)³⁰⁶. Our findings are consistent with the only published study to date studying the influence of MSI on baseline segmental function, where O'Regan

demonstrated lower *Ecc* on CSPAMM tagging with reducing MSI quartiles.¹²⁸ Given that quantifying strain with FT endocardial contours only is quick, requires minimal post-processing, and demonstrates moderately good agreement between *Ecc* and infarct size and excellent intra and interobserver agreement, this method of analysis may be preferred, even though strain values compared to tagging are markedly increased. We observed no significant relationship between segmental tagging-derived *EII* and infarct. This is likely to be contributed to by the fact that 21% of long-axis tagged segments were unanalysable.

Given the tendency for LGE early after STEMI to underestimate the potential for functional recovery^{65, 128}, it remains to be determined whether strain assessment combined with LGE more accurately predicts viable segments and clinical outcomes¹⁰¹.

The excellent intraobserver agreement for global *Ecc* and *EII* using FT and tagging is in agreement with published data, with COVs ranging from 2.8%⁹⁴ to 11.8%³⁰⁵ using FT and ICCs of >0.8 using tagging²⁹³. The higher interobserver agreement seen with FT compared with tagging is likely related to variations in manual adjustment of poorly tracking contours, especially in end-systole where tagging may not differentiate trabeculae and papillary muscles from compact myocardium. Our interobserver and intraobserver agreement using *Intag* is lower than described by Miller²⁷⁵, however they studied stable cardiomyopathy and healthy subjects who usually have good breath holding and gating. Segmental interobserver and intraobserver agreement was much poorer for FT and tagging. Our data is consistent with published literature, with reported COVs of 24-46% for FT^{303, 308} and ICC ~0.75 for tagging.²⁷⁵ This aspect needs improving, especially when assessing changes in regional contractile function at follow-up post STEMI and it is unclear whether segmental strain assessment offers any major advantages over semi-quantitative visual wall motion scoring.

4.4.1 Limitations

This study has a number of limitations. We have compared a single tagging sequence with FT on a single platform and the results may not be generalizable to other

sequences, field strength and manufacturers. The use of a CSPAMM sequence is likely to have resulted in better tag persistence⁸⁶ but we choose to use a SPAMM sequence because of widespread availability and the likely use in multicentre clinical trials. We did not attempt to quantify diastolic strain rate due to tag fading in most patients and did not study *Err* since it is established that this is significantly less reproducible than *Ecc* and *Ell*. Test-retest reproducibility was not assessed and should be considered in future studies. Finally, our sample size of 24 patients was limited, however was chosen according to the table of Critical Values of the Spearman's Ranked Correlation Coefficient for $r_s \sim 0.40$ with significance value of $p < 0.05$. Additionally the detailed segmental analysis in this sample size provided 384 myocardial segments for analysis, dramatically increasing the power for analyses.

4.4.2 Conclusions

In conclusion, global *Ecc* and *Ell* are higher measured using FT than with tagging in patients early after STEMI. FT is more robust than SPAMM tagging in acute STEMI with better myocardial tracking, greater interobserver agreement, faster analysis and stronger correlation with IS, AAR, MSI and infarct transmural. FT strain assessment using the mean of endocardial and epicardial contours does not add to the robustness, observer agreement or correlation with IS, AAR and MSI of FT strain assessment derived from endocardial contours alone. FT strain assessment is feasible in acute STEMI and is likely to become the preferred quantification method.

FT-derived endocardial *Ecc* and *Ell* will hence be used for strain assessment in the CvLPRIT-CMR substudy.

4.4.3 Original contribution to knowledge

At the time of writing, this is the first study to date assessing the robustness, feasibility and observer agreement of FT for the quantification of global and segmental systolic strain in acute MI.

4.4.4 My contributions

I and GPM conceived the idea for this study. I recruited patients and was present at study visits. I and AS performed the CMR analyses. I performed the statistical analysis and wrote the manuscript, which all authors critically reviewed for content.

CHAPTER 5

5. THE CVLPRIT-CMR SUBSTUDY

The Randomized Complete vs. Lesion Only Primary PCI Trial:

Cardiovascular MRI substudy

Published:

McCann GP*; **Khan JN***, Greenwood JP, Nazir S, Dalby M, Curzen N, Hetherington S, Kelly DJ, Blackman D, Ring A, Peebles C, Wong J, Sasikaran T, Flather M, Swanton H, Gershlick AH. The Randomized Complete vs. Lesion Only Primary PCI Trial-Cardiac MRI substudy. JACC. Dec 2015. 66:2713-24. (*= **joint first authorship**).

5.1 Background

The recent DANAMI-3-PRIMULTI¹⁵ and PRAMI¹⁶ RCTs, which compared a strategy of complete versus IRA-only in-hospital revascularization in PPCI patients with multivessel disease, showed a reduction in major adverse cardiovascular events (MACE) with complete revascularization.

The mechanisms leading to improved clinical outcomes are currently unclear. However there is concern that PCI to non-IRAs may be associated with additional procedural-related infarction⁴². These well-described Type 4a MI³⁹ cannot be detected by conventional enzymatic markers at the time of PPCI because the associated increases are relatively small compared to the large rise in enzymes caused by the STEMI itself. CMR is able to precisely characterize areas of myocardial injury following myocardial ischemia. Infarct size³⁰⁹ and MVO⁸⁰ measured on CMR are both strong medium term prognostic markers following PPCI. There are no CMR data as yet in the literature in patients undergoing complete revascularization for multivessel disease at the time of PPCI.

The primary aim of this current pre-specified substudy of CvLPRIT was to assess whether a complete revascularization strategy, due to causing additional infarcts in the non-IRA territories, was associated with greater infarct size than an IRA-only strategy in patients randomized in CvLPRIT. Additionally, we aimed to assess whether LV systolic function, myocardial salvage, microvascular damage and myocardial ischemia at were different in the two groups.

5.2 Methods

5.2.1 Study design

The design and rationale of the main CvLPRIT study have been published previously.²⁵⁴ Study design (2.1.1), patient randomisation (2.1.2, 2.1.3), treatment (2.1.5) and ethics (2.1.6) for the CvLPRIT-CMR substudy have been described in detail in the main Methods chapter of this thesis. A separate, nuclear (Single Photon Emission Computed Tomography [SPECT]) substudy³¹⁰ was undertaken based on

analysis of SPECT imaging performed at 6-weeks post PPCI. All SPECT data was blinded and clinicians and members of the CvLPRIT-CMR group had no access to this data during the CvLPRIT or CvLPRIT-CMR study durations.

5.2.2 Analysis

5.2.2.1 Angiographic, biomarker and electrocardiographic analysis

Angiographic (2.3.1), biomarker (2.3.2) and ECG (2.3.3) analyses employed in the CvLPRIT-CMR substudy are described in detail in the Methods chapter of this thesis.

5.2.2.2 CMR analysis

CMR image acquisition (acute scan: 2.4.1 and follow-up scan: 2.4.2) and analysis (2.4.3) are described in detail in the Methods chapter of this thesis. In light of the findings of Chapter 3 (Results Chapter One), infarct was quantified as hyperenhancement on LGE imaging using the FWHM technique³¹¹, and oedema (AAR) was quantified as hyperintensity on T2w-STIR imaging using Otsu's Automated Technique²⁸⁴. CMR analysis was performed using *cvi42* (Cardiovascular Imaging, Calgary, Canada) software. Subsequent to the findings of Chapter 4 (Results Chapter Two), LV systolic strain was assessed using the FT method with endocardial tracking.

5.2.3 Study outcomes

5.2.3.1 CMR outcomes

Primary outcome

The primary outcome of the CMR substudy was total IS (% LVM) on acute CMR.

Secondary CMR outcomes

The following outcomes were compared in the treatment arms at both CMR scans, except for those solid-underlined (at acute CMR scan only [pre-discharge]) or dotted-underlined (at follow-up scan only):

- IMH and MVO (% LVM)
- AAR (% LVM).
- Infarct size (% LVM) at 9-months

- New MI (CMR-detected) at 9 months compared to acute CMR
- Proportion of patients with ischaemia, and global ischaemic burden (% LV)
- Number of discrete infarcts on CMR
- LV volumes, LVEF and RVEF.
- Baseline and final MSI
- Visual presence of RV infarction, LV thrombus.

5.2.3.2 Clinical outcomes

The following clinical endpoints were recorded (time points in brackets):

- Contrast-induced nephropathy (inpatient)
- Vascular access injury requiring surgical repair (inpatient)
- All-cause mortality (all: inpatient, 6-week, 6-month, 12-month)
- MI (all)
- Planned or repeat revascularisation (CABG or PCI) (all)
- Heart failure admission (all)
- Transient ischaemic attack/cerebrovascular event (all)
- Major bleed (TIMI)³¹² (all)

The primary clinical outcome for the main CvLPRIT study was *first combined MACE at 12-months* (composite of all-cause mortality, MI, planned or repeat revascularisation, heart failure admission) and this was assessed for all patients in the CMR substudy. Secondary outcomes included *individual clinical endpoints* at 12-months, and *inpatient events* (cerebrovascular accident, major bleeding, major vascular injury and contrast-induced nephropathy). The latter formed the safety analysis. Data were collected by an independent clinical trials unit (Royal Brompton Hospital, London) and events adjudicated by blinded clinicians.

5.2.4 Statistical analysis

For the full statistical analysis plan for the CvLPRIT-CMR substudy, please refer to Appendix 3. This section contains a detailed summary of the statistical methods employed.

5.2.4.1 CMR outcomes

Statistical analysis was performed using SPSS v20 (IBM, USA). Primary and secondary outcomes were analysed according to an **Intention To Treat** basis. Normality was assessed using Q-Q plots, Kolmogorov-Smirnov and Shapiro-Wilk tests. Logarithmic transformations were made to non-normally distributed continuous variables, including the right-skewed primary CMR outcome of IS (% LVM). Categorical variables were summarised with the number and proportion of participants in each category and compared using Chi-squared testing or Fisher's exact test as appropriate. Normally distributed continuous variables were expressed as mean±standard deviation and compared with Student's t-tests. Non-normally distributed data were expressed as median (25th and 75th quartiles) and analysed using independent t-testing where log transformation normalised data, and using Mann-Whitney testing where the degree of skew rendered data non-transformable.

Primary analysis was on an intention-to-treat basis of all randomized patients according to treatment group who completed the acute CMR. The primary outcomes of IS was adjusted for known predictors of infarct size (age, anterior MI, time to revascularization, diabetes, AAR, Rentrop grade and TIMI flow pre-PPCI), using Generalised Linear Models (Generalised Estimating Equations [GEE]). GEEs were used since they provide a very robust standard error and allow correction for covariates of a range of distributions and data types. No adjustments for multiplicity were performed for secondary endpoints. One hundred patients in each arm had 81% power to detect a 4% absolute difference in infarct size, assuming a mean of 20% of left ventricular mass and standard deviation of 10%^{55, 313}, using a two-tailed test with alpha=0.05. New infarct comprising 4% of LV mass is associated with adverse prognosis in patients with revascularization-related injury³⁰.

5.2.4.2 Clinical outcomes

Twelve-month clinical outcomes were assessed using time-to-first event survival analysis (log-rank test with right-censoring) and Cox proportional hazard models were fitted to estimate hazard ratios and 95% confidence intervals for treatment

comparisons. The Schoenfeld residuals output test was used to confirm the validity of the proportional hazards model. Kaplan-Meier survival curves were produced for the subgroups. Inpatient safety outcomes were compared in the two treatment arms using Chi-squared testing and results were presented as odds ratios (OR) with 95% confidence intervals.

5.2.4.3 Interobserver and intraobserver variability

Inter and intraobserver agreement were assessed on 10 randomly selected acute CMR scans using two-way mixed-effect intraclass correlation coefficient for absolute agreement (ICC)²⁹¹ and Bland-Altman analysis²⁹². On ICC, agreement was defined as excellent (ICC \geq 0.75), good (ICC 0.6-0.74), fair (ICC 0.4-0.59) or poor (ICC $<$ 0.40)²⁹³.

5.2.4.4. Sample Size

There are no published CMR data comparing the revascularisation strategies. There are however considerable data on unselected patients undergoing PPCI and CMR IS^{55, 154, 314} which are similar to that seen in our centre. One hundred patients in each arm had 81% power to detect a 4% absolute difference in IS, assuming IS \sim 20% of LVM, standard deviation of 10%, alpha=0.05 and 2-tailed given that either strategy may be associated with larger IS. New IS of 4% of LV mass is associated with adverse prognosis in CAD patients with revascularisation-related injury.³⁰

5.3 Results

5.3.1 Main CvLPRIT study

The main trial screened 850 STEMI patients of whom 296 were randomized. The main trial results were presented at the European Society of Cardiology congress in Barcelona, August 2014 and published in JACC in March 2015.³¹⁵ Patient groups were well matched for baseline clinical characteristics. The primary endpoint of 12-month combined MACE occurred in 10.0% of the CR group versus 21.2% in the IRA-only revascularization group (HR 0.45 [0.24 to 0.84], p=0.009). A trend towards benefit was seen early following CR (p=0.055 at 30 days). A non-significant reduction in all

primary endpoint components was seen. There was no reduction in ischemic burden on SPECT or in the safety endpoints.³¹⁵

5.3.2 CvLPRIT-CMR substudy

5.3.2.1 Patient recruitment

The proportion of patients randomized and completing study aspects are shown in the CONSORT diagram in Figure 42.

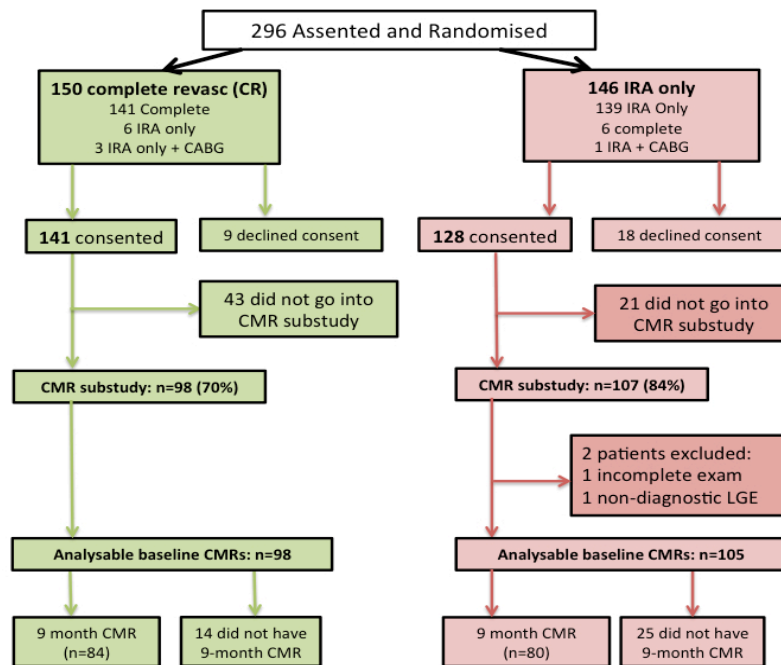


Figure 42: CVLPRIT-CMR recruitment

CONSORT diagram of recruitment into main CVLPRIT study and CMR substudy

Ninety-one percent (n=269) of the 296 randomised patients consented to ongoing participation in CVLPRIT, of which 76% (n=205) entered the CMR substudy. LGE images from 1 patient were unanalysable and 1 patient did not complete the acute CMR scan, resulting in 203 acute CMR scans analysable for the primary CMR outcome. The recruitment target of 200 was exceeded as 4 patients were recruited on the final day. The reasons for non-participation in the CMR substudy and drop out from the second CMR scan are shown in Figure 43. Eighty-one percent (164/203) of eligible patients had follow-up CMR as per Figure 42. Those who did not have a

second CMR had similar baseline characteristics to those who completed both scans. CvLPRIT-CMR completed recruitment 1 month before the main trial and hence 13 patients randomized were not approached to participate in the CMR substudy. Recruitment in the main trial and substudy at each centre is shown in Table 37.

Reasons for patients consenting to enter CVLPRIT not entering CMR substudy	
Patient declined consent to enter CMR substudy	9
Claustrophobia	14
Renal failure	2
CMR Contraindicated	4
Too unwell for CMR/Death	7
After CMR substudy	13
No CMR available at centre at time of consent into CVLPRIT	10
Other	2
Repatriated to district general hospital	3
	64
Reasons for patients in CMR substudy not returning for follow-up CMR	
Patient withdrawn from CVLPRIT study	3
Patient declined follow-up CMR scan	26
Death	3
Implantable Cardioverter-Defibrillator	1
Other severe illness	1
Follow-up CMR due after end of CMR substudy period	3
Claustrophobia	2
	39

Figure 43: Reasons for non-participation in CMR substudy and follow-up CMR

Table 37: Recruitment at the study centres

Centre	Patients randomised (% of total)	Patients in CMR substudy (%)
Glenfield	99 (33.4)	78 (78.8)
Southampton	35 (11.8)	26 (77.1)*
Leeds	57 (19.3)	32 (56.1)
Harefield	38 (12.8)	26 (68.4)
Kettering	32 (10.8)	26 (81.3)
Derby	20 (6.8)	12 (60.0)
Bournemouth	15 (5.1)	3 (26.7)**
Total	296	203 diagnostic

* 1 patient excluded from CMR substudy due to unanalysable LGE images

** 1 patient excluded from CMR substudy as unable to complete acute CMR scan

5.3.2.2 Baseline characteristics

The CMR substudy cohort closely represented the overall CVLPRIT group, with similar baseline characteristics, comorbidities and important prognostic predictors including symptom time (TTR), infarct location and Killip class (Table 38).

Table 38: Baseline characteristics of main CVLPRIT and CMR substudy cohort

Variable	Overall CVLPRIT group (n=296)	CMR substudy cohort (n=203)	p
Age (y)	64.9±11.6	63.6±11.0	0.21
Male sex (n, %)	240/296 (81.1)	172/205 (83.9)	0.42
BME (%)	33/293 (11.3)	22/200 (11.0)	0.93
BMI (kg/m ²)	27.3 (24.4-30.2)	27.5 (24.7-30.1)	0.62*
Systolic BP (mmHg)	137.6±27.1	137.5±27.7	0.96
Hypertension (n, %)	105/287 (36.6)	73/203 (36.0)	0.89
Hypercholestromia (n, %)	75/287 (26.1)	56/203 (27.6)	0.72
Diabetes Mellitus (n, %)	39/287 (13.6)	28/203 (13.8)	0.95
Current smoker (n, %)	87/285 (30.5)	66/204 (32.4)	0.67
Previous MI (n, %)	12/287 (4.2%)	8/203 (3.9%)	0.90
Previous PCI (n, %)	9/287 (3.1%)	7/203 (3.4%)	0.85
Symptom-PCI time (TTR, min)	184 (131-304)	177 (130-292)	0.49*
Peak CK (IU/L)	1010 (423.3-1740)	997 (429.8-1740)	0.98*
Anterior infarct (n, %)	106/296 (35.8)	72/203 (35.5)	0.94
Killip II-III on arrival (n, %)	24/286 (8.4)	16/203 (7.9)	0.84

BME= black or minority ethnicity, BMI= body mass index, CK= creatinine kinase, PCI= percutaneous coronary intervention, TTR= time to revascularisation

Baseline characteristics and comorbidities were closely matched in the IRA and CR arms of the CvLPRIT-CMR substudy cohort (Table 39). There was a slight, non-significant increase in males in the CR arm. The proportion of anterior infarcts in each arm was closely matched as a result of stratified randomisation.

Table 39: Baseline characteristics of the IRA-only and CR CMR substudy

Variable	CR (n=98)	IRA-only (n=105)	p
<u>Anthropometrics</u>			
Age (y)	63.1±11.3	64.1±10.8	0.53
Male sex (n, %)	87/98 (88.8)	83/105 (79.0)	0.06
BME (n, %)	13/97 (13.4)	9/103 (8.7)	0.29
BMI (kg/m ²)	27.5 (24.6-29.7)	27.5 (24.7-30.6)	0.36
Systolic BP (mmHg)	134.7±27.3	140.0±28.0	0.18*
Anterior infarct (n, %)	35/98 (35.7)	37/105 (37.2)	0.94
Killip Class II-III on arrival (%)	6/98 (6.1)	10/105 (9.5)	0.37
<u>Biochemical</u>			
eGFR (ml/min/1.73)	98.2±34.3	93.49±30.7	0.36
Peak CK (IU/L)	1025 (628-1660)	1057 (614-1834)	0.37*
<u>Past medical history</u>			
Hypertension (n, %)	36/98 (36.7)	37/105 (35.2)	0.82
Hypercholesterolemia (n,%)	28/98 (28.6)	28/105 (26.7)	0.76
Diabetes Mellitus (n, %)	15/98 (15.3)	13/105 (12.4)	0.55
Current smoker (n, %)	36/98 (36.7)	28/105 (28.0)	0.12
Previous MI (n, %)	4/98 (4.1)	4/105 (3.8)	0.92
Previous PCI (n, %)	4/98 (4.1)	3/105 (2.9)	0.63

BME= black or minority ethnicity, BMI= body mass index, CK= creatinine kinase, PCI= percutaneous coronary intervention, IRA= IRA-only revascularisation, CR= complete revascularisation, eGFR= estimated glomerular filtration rate. *Log10 transformed.

5.3.2.3 Angiographic and PCI details

Data are shown in Table 40. Thirty patients in the CR group had a staged procedure, 1.43 (1.03-2.04) days after the PPCI. Coronary artery disease severity and complexity was similar in the groups although the IRA-territory collateralization grade was higher in the CR group. Total screening time, contrast dose, procedure length and number of implanted stents were significantly greater in CR patients. The vast majority of patients in both arms received drug-eluting stents, although this was slightly higher in CR patients.

Table 40: Periprocedural details in the complete revascularization and infarct related artery-only groups

Variable	CR (n=98)	IRA-only (n=105)	p
Radial access (%)	81/97 (83.5)	82/105 (78.1)	0.33
Symptom to PCI time (min)	192 (131-302)	172 (127-268)	0.20*
Glycoprotein IIb/IIIa inhibitor (%)	34/97 (35.1)	36/104 (34.6)	0.95
Bivalirudin (%)	52/92 (56.5)	43/94 (45.7)	0.14
Thrombectomy catheter (%)	67/97 (69.1)	79/105 (75.2)	0.33
Contrast dose (ml)	300 (220-400)	190 (150-230)	<0.001*
Screening time (min)	17 (12-23)	9 (7-13)	<0.001*
Procedure length (min)	66 (43-84)	42 (30-55)	<0.001*
Vessels with ≥70% stenosis (n)	1.8±0.6	1.7±0.6	0.82
Left anterior descending IRA (%)	34/98 (34.7)	39/105 (36.2)	0.82
Left circumflex artery IRA (%)	20/98 (20.4)	18/105 (37.1)	0.55
Right coronary artery IRA (%)	44/98 (44.9)	48/105 (45.7)	0.91
Rentrop grade n (%)			
0-1	88/98 (89.8)	102/105 (97.1)	0.033
2-3	10/98 (10.2)	3/105 (2.9)	0.033
SYNTAX score (Total)	17.3 (13-23.5)	18 (14-22)	0.81
SYNTAX score (IRA)	8 (6-11.5)	9 (6-14.5)	0.75
SYNTAX score (NIRAs)	7 (4-10)	7 (3-11)	0.51
TIMI grade pre PCI	0 (0-1)	0 (0-1)	0.56
TIMI grade post PCI	3 (3-3)	3 (3-3)	0.31
IRA no-reflow (n, %)	8/98 (8.2)	3/107 (2.8)	0.09
Total number of stents (n)	3 (2-4)	1 (1-2)	<0.001
Drug-eluting stent use (n, %)	97/98 (99)	96/105 (91.4)	0.013
Aspirin (n, %)	97/98 (99.0)	105/105 (100)	0.30
2 nd anti-platelet agent (n, %)	98/98 (100)	105/105 (100)	1.00
Clopidogrel	34/98 (34.7)	36/105 (34.3)	0.95
Prasugrel	49/98 (50.0)	53/104 (51.0)	0.89
Ticagrelor	15/98 (15.3)	16/105 (14.3)	0.91
Beta-blocker (n, %)	93/98 (94.9)	97/105 (92.4)	0.46
ACEi or ARB (n,%)	95/98 (96.9)	101/105 (96.2)	0.77
Additional antianginal medication (n, %)	6/98 (6.1)	17/105 (16.2)	0.024
Statin (n,%)	98/98 (100)	104/105 (99.1)	0.33
Loop diuretic (n, %)	9/98 (9.2)	13/105 (12.4)	0.46
Aldosterone inhibitor (n,%)	5/98 (5.1)	5/105 (4.8)	0.91

CR= complete revascularization, IRA= Infarct related artery, PCI= percutaneous coronary intervention, TIMI= thrombolysis in myocardial infarction, ACEi= angiotensin converting enzyme inhibitor, ARB= angiotensin receptor blocker. Additional antianginal medication includes calcium channel blockers, nitrates or nicorandil.

*= non-normally distributed data: analysed after log10 transformation.

Symptom to PCI times, anti-platelet, anticoagulant use and post-PPCI creatine kinase rise were similar in both arms. There was a non-significant trend for no-reflow to be more common in the CR than the IRA-only group. There was greater usage of a second anti-anginal agent in patients in the IRA-only group.

5.3.2.4 Acute CMR results

CMR image quality

Acute CMR was undertaken at a median of 3 days post-PPCI in both groups. All cine and LGE images in the final 203 CMR subjects were of very good quality (Table 41). Fifty-two patients' (26%) STIR datasets were non-diagnostic (no artefact but no oedema discernable [n=33], STIR not performed due to arrhythmia or suboptimal breath-holding [n=14], severe artefact [n=5]). Image quality was similar in both arms.

Table 41: Acute CMR image quality

Variable	CR (n=98)	IRA-only (n=105)	p
Time to acute CMR (d)	3.0 (2.0-4.3)	2.8 (1.8-3.4)	0.13
Cine imaging quality score	2.5±0.7	2.4±0.8	0.31
Oedema imaging diagnostic (n, %)	75/98 (76.5)	76/105 (72.4)	0.50
Oedema image quality score	1.4±0.9	1.3±0.9	0.53
Late gadolinium image quality score	2.0±0.6	1.9±0.7	0.13

Intra and interobserver variability of LV volumetrics and infarct characteristics

Ten acute and follow-up scans were randomly selected and analyzed twice by the same observer after 4 weeks (JNK) and once by a further observer (SAN). All

intraclass correlation coefficients (ICCs) for intraobserver and interobserver agreement for CMR quantitative data exceeded 0.92 (Table 42).

Table 42: Intra and interobserver variability of CMR measurements

	<i>Intra-observer agreement</i>			<i>Inter-observer agreement</i>		
	ICC	Mean bias	±95% LoA	ICC	Mean bias	±95% LoA
LV mass index	0.986	-0.3	+6.3, -6.8	0.995	+0.5	+4.4, -3.5
LV end diastolic volume index	0.996	+1.2	+6.4, -4.0	0.995	+1.3	+7.9, -5.3
LV end systolic volume index	0.988	-0.9	+4.6, -6.4	0.996	+0.8	+6.4, -4.8
LV ejection fraction (%)	0.976	+1.0	+3.8, -1.8	0.996	-0.1	+1.4, -1.6
Infarct size	0.988	+0.2	+1.5, -1.1	0.990	-0.5	+1.7, -2.7
Area at risk	0.948	+2.8	+7.3, -1.7	0.908	+3.4	+9.1, -2.4

LV= left ventricular, ICC= intraclass correlation coefficient, LoA= limits of agreement.

Ventricular function and volumes

LV volumes, LVM, LVEF and peak systolic strains (*Ecc*, *Ell*) were similar in both groups. RV injury, and LV thrombus were similarly prevalent in both arms (Table 43).

Myocardial and microvascular injury and salvage

Acute CMR data are presented in Table 41. There was no statistical difference in the primary endpoint of total IS between the groups: IRA-only (13.5% [6.2-21.9%] of LVM) versus CR (12.6% [7.2-22.6] of LVM, $p=0.57$) (Figure 44). The ratio of the geometric means for total IS in the IRA-only ($15.9 \pm 13.2\%$) and CR ($16.3 \pm 13.0\%$) arms was 0.98 (95% CI: 0.82, to 1.41), confirming no difference between the treatment arms. When corrected for covariates (age, sex, anterior MI, time to revascularization, TIMI flow pre-PCI, diabetic status, Rentrop grade and AAR) there remained no difference in median IS ($\beta=0.02$, $p=0.68$) between the two groups. There was a trend towards smaller AAR with CR but no difference in MSI in the groups.

The prevalence of multiple territory infarcts in the CR group was double that of the IRA-only group and the number of acute non-IRA infarcts was increased three-fold in those undergoing CR (Table 43).

Table 43: Acute CMR data

Acute CMR variable	CR (n=98)	IRA-only (n=105)	p
Ventricular volumes and function			
LVMI (g/m ²)	52.3 (46.8-62.0)	52.2 (44.7-59.2)	0.33*
LVEDVI (ml/m ²)	89.7 (80.7-102)	90.7 (80.4-102)	0.64*
LVESVI (ml/m ²)	47.0 (38.0-58.4)	49.8 (39.7-62.1)	0.56*
LVEF (%)	45.9±9.9	45.1±9.5	0.60
Number of dysfunctional segments (WMS>1)	5.0 (3-7)	5.0 (3-7)	0.64
Wall motion score	22.0 (19-26)	23.0 (19-26)	0.71
Peak global LV <i>Ecc</i>	-18.6±6.1	-18.1±6.0	0.86
Peak global LV <i>EII</i>	-14.7±5.2	-13.7±5.3	0.16
RVEDVI (ml/m ²)	84.8 (73.3-95.0)	82.2 (73.0-94.5)	0.47
RVESVI (ml/m ²)	42.4 (36.8-50.9)	41.2 (34.0-50.3)	0.38
RVEF (%)	48.4±7.3	49.0±7.3	0.53
Infarct characteristics			
Total IS (% LV Mass) [Mean±SD]	12.6 (7.2-22.6) [16.3±13.0]	13.5 (6.2-21.9) [15.9±13.2]	0.57*
Time from PPCI (days)	3.0 (2.0-4.3)	2.8 (1.8-3.4)	0.13*
Infarct on LGE (%)	95 (96.9)	95 (90.5)	0.06
Patients with >1 infarct (%)	22 (22.4)	11 (10.5)	0.02
Patients >1 acute infarct	17 (17.1)	5 (4.8)	0.004
Number of acute infarcts in those with >1 infarct	2 (2-2) [2.2±0.4]	2 (2-2) [2.0±0.0]	0.60**
IRA IS (% LV Mass) Mean±SD	12.1 (7.0-21.4) [15.2±12.1]	12.2 (6.2-21.2) [15.3±13.2]	0.68*
Total acute IS (% LV Mass) Mean±SD	12.5 (7.0-22.0) [15.8±12.4]	12.4 (6.2-21.6) [15.4±13.2]	0.60*
Acute NIRA IS (% LV Mass) where >1 infarct Mean±SD	2.5 (0.54-4.5) [3.2±3.3]	2.1 (0.81-4.5) [2.5±1.9]	0.004**
Acute NIRA IS (% LV Mass) per infarct Mean±SD	1.4 (0.3-2.3) [1.6±1.5]	1.0 (0.4-2.2) [1.3±1.0]	0.94**
Transmural LGE area extent >50% (segs)	0 (0-1)	0 (0-1)	0.96
Area at risk (% LV Mass) [§]	32.2±11.8	36.0±12.9	0.06
Acute MSI (%) [§]	58.5 (32.8-74.9)	60.5 (40.6-81.9)	0.14
MVO present (%)	57/98 (58.2)	54/105 (51.4)	0.34
MVO (% LV Mass)	0.19 (0.00-2.00)	0.08 (0.00-1.05)	0.63**
IMH present (%) [§]	22/75 (29.3)	17/77 (22.1)	0.31
RV infarction (n, %)	7/98 (7.1)	4/105 (3.8)	0.29
LV thrombus (n, %)	1/80 (1.2)	1/84 (1.2)	0.97
Aortic distensibility (%/ml)	15.1 (10.7-19.8)	17.0 (11.9-22.4)	0.60

CR= complete revascularization, IRA= Infarct related artery, IS= infarct size, LVMI= left ventricular mass index, LVEDVI= left ventricular end-diastolic volume index, LVESVI= left ventricular end-systolic volume index, LVEF= left ventricular ejection fraction, LGE= late gadolinium enhancement, *Ecc*= circumferential strain, *Ell*= longitudinal strain, NIRA= non-infarct related artery, IS=infarct size, MVO= microvascular obstruction; IMH= Intramyocardial haemorrhage, MSI= myocardial salvage index

[§] Analyzable oedema imaging in 75 of the CR group and 77 of the IRA-only group.

*= non-normally distributed data (log10 transformed)

**= non-normally distributed data (Mann-Whitney analysis)

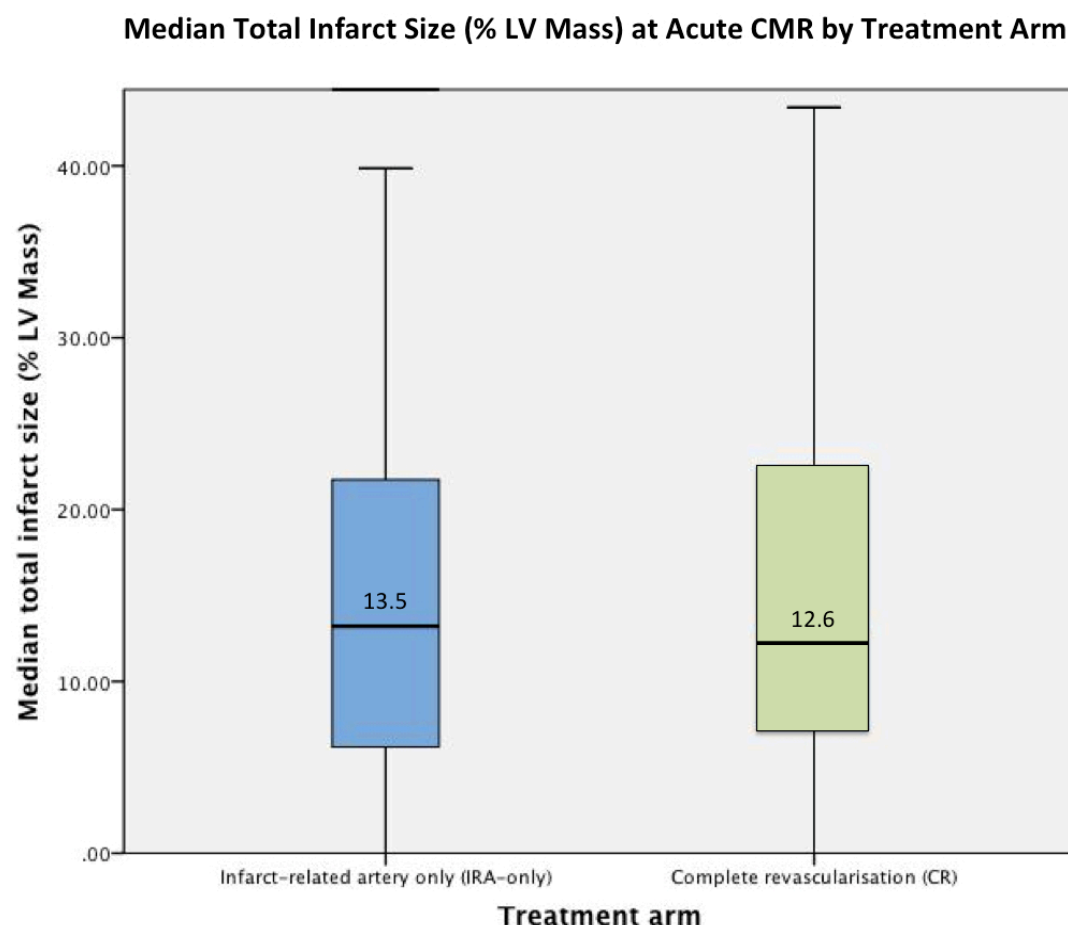


Figure 44: Median total infarct size at acute CMR in the treatment arms

There was no difference in the primary CMR outcome of median acute total IS. Box demonstrates median (thick line), interquartile range (top and bottom of box), minimum (bottom of whisker, 0% in both arms) and maximum value (top of whisker)

Acute NIRA infarct extent was greater and there was a trend towards a higher prevalence of acute NIRA infarcts >4% LVM with CR. Examples, with corresponding edema images, are shown in Figure 45 and the location, size of infarct, expected coronary artery territory and whether the individual patients had an additional non-IRA PCI are shown in Supplemental Data 13. Eighteen of 20 acute non-IRA infarcts in patents in the CR group concurred with additional PCI in the relevant non-IRA coronary territory. Five patients randomised to the IRA-only group also had non-IRA acute MI. Two of these patients had treatment crossover and received non-IRA PCI. The first crossover followed ongoing ischaemia post PPCI and was associated with non-IRA MI in the relevant territory. The second crossover resulted from human error and this patient had a small non-IRA acute MI in the anteroseptum but had non-IRA PCI of the circumflex artery. Six patients in the IRA-only and five in the CR group had chronic infarcts (evidenced by wall thinning). Excluding these patients from analysis did not affect results (Supplemental Data 14).

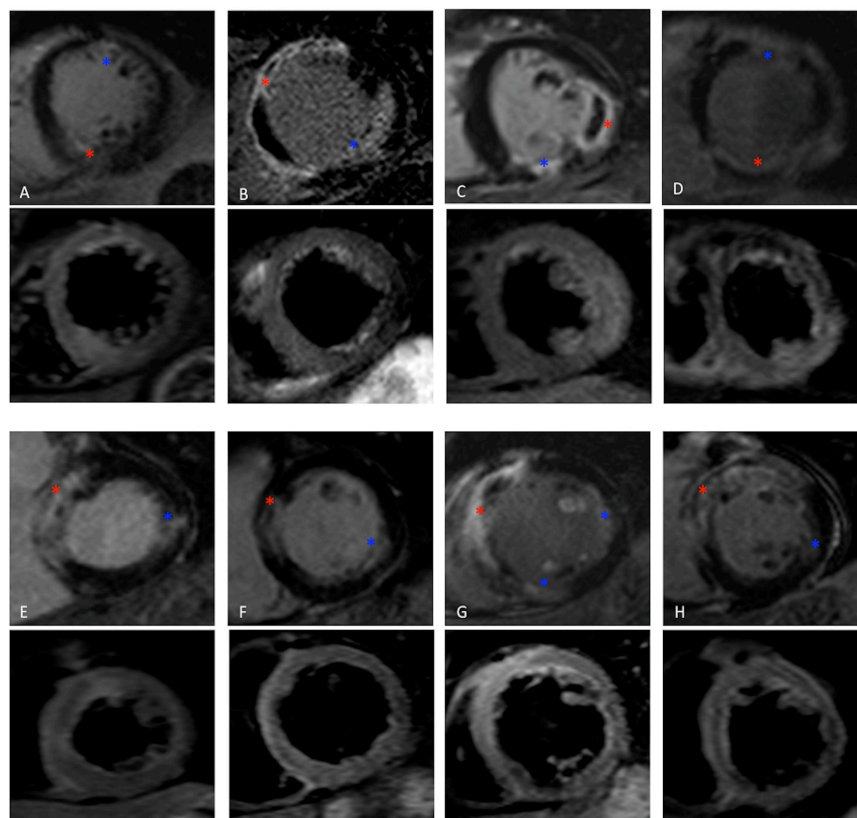


Figure 45: Examples of patients with more than one ‘acute’ MI on CMR.

Late gadolinium enhanced short-axis images (Top and 3rd row) and corresponding co-localised oedema images (2nd and 4th row). * IRA-related infarct; * NIRA-related infarct(s). A (X511), B (X612), C (X665), D (X709), E (X757), F (X791), G (X798), H (X808). IRA infarct size and non-IRA PCI are shown in Supplemental Data 13.

MVO was present in more than half of all patients, although quantitatively the amount was very low (median <0.2% of LV mass). In 52 patients (26%), AAR could not be quantified: no artefact but no oedema discernable (n=33), not performed due to arrhythmia or suboptimal breath-holding (n=14) or severe artefact (n=5). Area-at-risk and myocardial salvage index were lower, but not significantly, in the CR group.

3.2.5 Follow-up CMR

CMR image quality

Follow-up CMR was completed in 84 patients in the CR group and 80 patients in the IRA-only group (Table 44). There were no differences in baseline characteristics or acute CMR between those who completed and did not attend the follow-up CMR.

Table 44: Follow-up CMR image quality

Variable	CR (n=84)	IRA-only (n=80)	p
Time to follow-up CMR (CMR2, mth)	9.4 (9.0-10)	9.3 (8.9-9.9)	0.20
Cine imaging quality score	2.7±0.6	2.8±0.6	0.58
Late gadolinium image quality score	2.3±0.7	2.2±0.7	0.74
Stress perfusion diagnostic (n, %)	82/84 (97.6)	76/79 (96.2)	0.60
Stress perfusion quality score	2.4±0.8	2.4±0.7	0.70
Rest perfusion diagnostic (n, %)	82/84 (97.6)	76/79 (96.2)	0.60
Rest perfusion quality score	2.5±0.7	2.5±0.6	0.82

Of the 39 patients who did not have a repeat CMR, 29 patients declined, 3 had died, 2 cited claustrophobia, 1 had an implantable cardioverter defibrillator, 1 had a severe non-cardiovascular illness and in 3 there were logistical reasons. Follow-up CMR was undertaken at approximately 9.4 months post-PPCI in both treatment arms and all scans were analysable for the primary outcome of IS. Image quality for all sequences

was very good. Three patients were unable to undertake adenosine stress perfusion due to airways disease (2 IRA-only, 1 in CR group). Perfusion imaging was unanalysable in 2 patients due to severe dark-rim artefact (1 IRA-only, 1 in CR group).

Ventricular function and volumes

Left ventricular volumes, mass and systolic function were similar in the groups at follow-up CMR (Table 45). Left ventricular function was mildly impaired on LVEF.

Table 45: Follow-up CMR data

Follow-up CMR variable	CR (n=84)	IRA-only (n=80)	p
Ventricular volumes and function			
Time to CMR (months)	9.4 (9.0-10)	9.3 (8.9-9.9)	0.20
LVMI (g/m ²)*	47.4(40-52.6)	43.4 (38.0-49.3)	0.33
LVEDVI (ml/m ²)*	93.3 (82.2-110)	95.0 (82.7-107)	0.63
LVESVI (ml/m ²)*	45.1 (37.8-58)	43.6 (34.8-57.9)	0.33
LVEF (%)	49.7±9.4	50.8±8.7	0.42
Number of dysfunctional segments (WMS>1)	3.0 (1-5)	2.0 (1-4)	1.00
Wall motion score	19 (17-21)	18 (17-21)	0.55
Peak global Ecc	-22.5±6.3	-23.6±6.3	0.28
Peak global EII	-17.1±4.7	-17.1±4.8	0.98
RVEDVI (ml/m ²)	90.4 (80.7-100)	89.4 (81-101.3)	0.93
RVESVI (ml/m ²)	45.1 (37.8-58)	43.5 (34.8-57.9)	0.49
RVEF (%)	51.8±5.8	52.6±5.8	0.35
Infarct characteristics			
Infarct on LGE (n,%)	82/84 (97.6)	71/80 (88.8)	0.023
Patients with >1 infarct (%)	20/84 (23.8)	9/80 (11.2)	0.035
Total IS (% LV Mass)	7.3 (3.0-14.4)	7.6 (3.2-15.1)	0.41*
Final MSI (%)	82.1 (63.0-90.3)	79.4 (71.6-93.3)	0.20*
Presence of ischaemia (n, %) in all pats	17/82 (20.7)	16/77 (20.8)	0.99
Global ischaemic burden (%) in all pats Mean±SD	0.0 (0-0), [3.4±8.9]	0.0 (0-0), [4.3±11.3]	0.81
Global ischaemic burden (%) in pats with ischaemia	15.5±13.7	20.4±17.1	0.37
Pats (n, %) with ischaemic burden > 20%	6/82 (7.3)	6/77 (7.8)	0.91
Mean ischaemic burden (%) in pats with post PPCI revascularisation	3.1 (n=1)	6.3 (n=2)	0.67
Mean ischaemic burden (%) in pats without post PPCI revascularisation	3.4 (n=78)	4.4 (n=71)	0.54

CR= complete revascularization, IRA= Infarct related artery, IS= infarct size, LVMI= left ventricular mass index, LVEDVI= left ventricular end-diastolic volume index, LVESVI= left ventricular end-systolic volume index, LVEF= left ventricular ejection fraction, RVEF= right ventricular ejection fraction, LGE= late gadolinium enhancement, *Ecc*= circumferential strain, *E//*= longitudinal strain, IS=infarct size, MSI= myocardial salvage index. *= non-normally distributed (log10 transformed)

In patients undergoing both scans, there was a similar, significant improvement in global LV systolic function based on LVEF, WMS and strain, and RV function on RVEF between acute and follow-up CMR in both treatment arms (Table 46). Left ventricular mass decreased, LVEDVI increased and there was a trend towards decreased LVESVI between acute and follow-up CMR in both groups. LV remodelling was present in 15.0% of IRA and 14.3% of CR patients (p=0.90).

Table 46: Volumetric data at in those undergoing both CMR scans

Volumetric Variable	CR Acute CMR (n=84)	CR Follow-up CMR (n=84)	IRA Acute CMR (n=80)	IRA Follow-up CMR (n=80)
No. of dysfunctional segments	5.0 (3-7)	3.0 (1-5) ^{^^}	5.0 (3-7)	2.0 (1-4) ^{^^}
Wall motion score	19 (22-30)	19 (17-21) ^{^^}	19 (22-30)	18 (17-21) ^{^^}
LVMI (g/m ²)	51.8 (46.9-61.7)	47.4 (40-52.6) ^{^^}	52.5 (44.9-59.9)	43.4 (38-49.3) ^{^^}
LVEDVI (ml/m ²)	89.7 (80.8-102)	93.3 (82.2-110) ^{^^}	89.2 (80.2-101)	95.0 (82.7-107) [^]
LVESVI (ml/m ²)	47.0 (38.0-56.9)	45.1 (37.8-58.0)	48.8 (39.7-59.5)	43.6 (34.8-57.9)
LVEF (%)	46.1±9.5	49.7±9.4 ^{^^}	46.0±8.9	50.8±8.7 ^{^^}
RVEF (%)	49.2 (44.5-51.8)	51.7 (49-55.5) ^{^^}	49.2 (46.1-53.7)	53.2 (48.4-57.1) ^{^^}
Peak global <i>Ecc</i>	-18.8±6.0	-22.5±6.3 ^{^^}	-18.6±6.0	-23.6±6.3 ^{^^}
Peak global <i>E//</i>	-15.0±5.1	-17.1±4.7 ^{^^}	-13.7±5.3	-17.1±4.8 ^{^^}

LVMl= left ventricular mass index, LVEDVI= left ventricular end-diastolic volume index, LVESVI= left ventricular end-systolic volume index, LVEF= left ventricular ejection fraction, RVEF= right ventricular ejection fraction,

^ p<0.05 for change between CMR 1 and 2

^^ p<0.01 for change between CMR 1 and 2

Myocardial and microvascular injury and salvage

The prevalence of infarct and multiple infarcts were greater in the complete revascularization group. However there was no significant difference in total infarct size and final myocardial salvage index between the groups (Table 45). At follow-up CMR, there was a similar, significant reduction in median final IS in both groups. Total IS was reduced by approximately one-third (-35.5% relative reduction [IRA], -40.7% [CR], p=0.91) and remained similar in the treatment groups (Table 47). Two new infarcts were seen in the IRA-only group (0.8% and 2.2% LVM) and 1 in the CR group (3.7% LVM, p=0.53). Infarct in 4 IRA-only patients and 1 CR patient had resolved at follow-up CMR. Infarct transmuralities decreased similarly in both groups, and LV thrombus in 1 IRA-only patient had cleared at follow-up CMR.

Table 47: Infarct characteristics in patients undergoing both CMR scans

Tissue characterisation variable	CR Acute CMR (n=84)	CR Follow- up CMR (n=84)	IRA Acute CMR (n=80)	IRA Follow- up CMR (n=80)
Infarct present on LGE (n, %)	82/84 (97.6)	82/84 (97.6)	73/80 (91.2)	71/80 (88.8)
Total IS (% LVM)	12.4 (7.1-22.7)	7.3 (3.0-14)^^	13.2 (6.8-21.2)	7.6 (3.2-15.1)^^
NIRA-related IS (% LVM)	4.0 (1.0-5.2)	4.2 (1.9-6.1)	3.2 (0.8-5.3)	4.1 (2.3-8.1)^
Transmural LGE SEE >50% (segments)	1 (0-3)	0 (0-1)^^	1 (0-2)	0 (0-1)^^
Patients with >1 infarct	19/84 (22)	20/84 (24)	8/80 (13.2)	9/80 (11.2)
RV infarction (n, %)	6/84 (7.1)	5/84 (6.0)	4/80 (5.0)	0/80 (0.0)
LV thrombus (n, %)	1/84 (1.2)	1/84 (1.2)	2/80 (2.5)	1/80 (1.2)

LGE= late gadolinium enhancement, IS= infarct size, NIRA= non-infarct related artery,

LVM= left ventricular mass, SEE= segmental extent of enhancement

[^] p<0.05 for change between CMR 1 and 2

^{^^} p<0.01 for change between CMR 1 and 2

Perfusion analysis

Reversible perfusion defects were seen in 21% of patients in both groups and overall ischemic burden was small (Table 45). When the extent of ischemia was assessed only in patients with reversible perfusion defects, the ischemic burden was not statistically different in complete revascularization and IRA-only groups.

5.3.2.6 Clinical outcomes

Follow-up

Median follow-up length was 372 days (IRA 378d, CR 366d, p=0.37). One hundred and ninety-eight (98%) patients attended 12-month clinical follow-up (3 patients died before this and 2 patients withdrew consent for follow-up at days 7 and 220).

Safety endpoints

Length of inpatient stay and incidence of in-hospital clinical events were similar in the treatment arms (Table 48). There were no adverse effects on safety with CR.

Table 48: Safety profile: Inpatient clinical events

Inpatient clinical events	CR (n=98)	IRA (n=105)	Hazard Ratio (95% CI)	p
Length of inpatient stay (d)	3 (2-4) 3.5±2.6	3 (2-4) 3.9±2.8		0.13
Contrast nephropathy (n, %)	1/98 (1.0)	0/105 (0.0)	**	0.30
Vascular access injury needing repair (n, %)	0/98 (0.0)	0/105 (0.0)	**	1.00
Death (n, %)	1/98 (1.0)	1/105 (0.9)	1.07 (0.07, 17.4)	0.96
Recurrent myocardial infarction (n, %)	0/98 (0.0)	1/05 (0.9)	**	0.33
Cerebrovascular accident (n, %)	0/98 (0.0)	0/105 (0.0)	**	1.00
Heart failure (n, %)	2/98 (2.0)	1/105 (1.0)	2.17 (0.19, 24.3)	0.52
Repeat revascularisation (n, %)	2/98 (2.0)	3/105 (2.9)	0.71 (0.12, 4.3)	0.71
Major bleed (n, %)	3/98 (3.1)	1/105 (1.0)	3.29 (0.34, 32.1)	0.28

** Unable to calculate HR as ≥ 1 treatment arms had 0 events.

Twelve-month clinical outcomes

The primary clinical outcome of first combined MACE at 12-months was borderline significantly reduced in patients undergoing CR and the corresponding events rates and hazard ratio were similar to that seen in the main trial (Table 49, Figure 46). This was driven primarily by reduced revascularisation events (4.1% vs. 9.5%, $p=0.13$) and recurrent MI (0% vs. 2.9%, $p=0.09$). In the IRA-only group, all but one revascularisation procedures were to the non-IRAs (1 patient had acute stent thrombosis of the IRA on day 0 and had repeat PCI.) The indications for repeat revascularisation in the overall cohort (14 events) were as follows: acute coronary syndrome 7 (3 NSTEMI); 6 refractory symptoms (1 CABG) and 1 patient underwent elective PCI at the discretion of the responsible physician. There was 1 death in each arm (both cardiovascular) and two-thirds of MI were Type I NSTEMI.

Table 49: Twelve-month clinical outcomes (time to first event MACE)

Time to first event (MACE)	CR (n=98)	IRA (n=105)	Hazard Ratio (95% CI)	p
MACE (n, %)	8/98 (8.2)	18/105 (17.1)	0.43 (0.18, 1.04)	0.055
All-cause mortality (n, %)	1/98 (1.0)	1/105 (1.0)	1.07 (0.07, 17.4)	0.96
• CV mortality	1/98 (1.0)	1/105 (1.0)	1.07 (0.07, 17.4)	0.96
• Non-CV mortality	0/98 (0.0)	0/105 (0.0)	**	1.00
Recurrent MI (n, %)	0/98 (0.0)	3/105 (2.9)	**	0.09
• Type I (de novo)	0/98 (0.0)	2/105 (1.9)	**	0.17
• Type 4b (stent thrombosis)	0/98 (0.0)	1/105 (1.0)	**	0.33
Heart failure (n, %)	3/98 (3.1)	4/105 (3.8)	0.80 (0.17, 3.7)	0.77
Repeat revascularisation (n, %)	4/98 (4.1)	10/105 (9.5)	0.40 (0.12, 1.3)	0.13

** Unable to calculate HR as ≥ 1 treatment arms had 0 events.

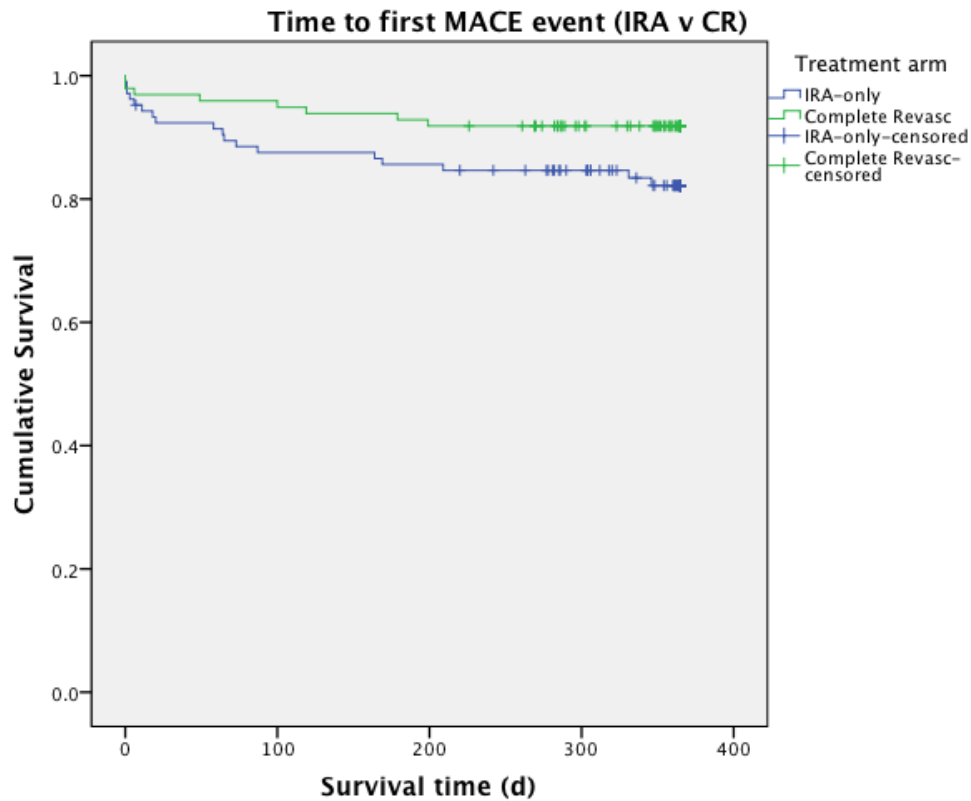


Figure 46: Kaplan-Meier survival curves for 12-month clinical outcomes

Primary clinical outcome of first combined MACE ($p=0.055$).

5.4 Discussion

This is the first detailed study of acute and follow-up CMR outcomes in a randomized study of IRA-only versus CR in multivessel coronary disease at PPCI. The data have confirmed that non-IRA PCI is associated with additional infarction. However, these type 4a MI³⁹ are relatively infrequent, generally small and did not result in an increase in total infarct size. There is mounting evidence from randomized trials that treating multivessel disease with CR^{16, 255} leads to a reduction in MACE after PPCI compared to an IRA-only strategy.

The patients in the CMR substudy had similar baseline characteristics to those in the main trial. As time to revascularization²⁵⁵ and anterior MI⁵⁸ are strongly associated with infarct size, randomization was stratified by these variables. There was a similar reduction in the hazard ratio for MACE in the CR CMR subgroup as that seen in the

main study compared to IRA-only revascularization and we believe that the CMR substudy population is representative of those in the main study.

It is well recognized that elective PCI can cause a troponin rise in approximately 30% of patients and approximately 50% undergoing PCI for unstable angina³¹⁶. Such type 4a MI³⁹ can be detected on CMR and have been associated with adverse prognosis^{29, 30}. In this substudy of CvLPRIT, the prevalence of >1 CMR-detected infarct in patients receiving complete revascularization was double that in the IRA-only arm (23.8% v 11.2%), and more than three-fold for the acute non-IRA infarcts (17.1% v 4.8%). Previous Q-wave MI was an exclusion criterion in this study but 4% had a history of previous non-STEMI and a similar number had (6% IRA-only and 5% complete revascularization groups) had chronic N-IRA MI on the acute CMR. Excluding these patients did not significantly affect the results. These data suggest that an additional 12% of patients with multivessel disease who receive CR at the time of PPCI will have evidence of additional CMR-detectable infarction compared to IRA-only revascularization. However, this proportion is less than might have been expected from previous studies in elective PCI³¹⁶ where up to 29% of patients have evidence of new infarction on CMR associated with troponin elevation²⁹. The extent of acute-NIRA infarction was also smaller (median 2.5% of LV mass) than may have been anticipated from elective PCI data given that average infarct size in those with new late enhancement on CMR was $5.0 \pm 4.8\%$ of LV mass²⁹, despite all patients in that study being pre-treated with clopidogrel for >24 hours and a glycoprotein IIb/IIIa inhibitor peri-procedurally. Importantly, in the present study, total IS was not increased acutely or at follow-up and there were no significant differences in myocardial salvage, left ventricular volumes or LVEF between the treatment groups. Peak creatine kinase was also similar in the two groups.

These findings provide reassurance that non-IRA intervention at the time of PPCI does not lead to increased total infarct size. In the main CvLPRIT trial, CR resulted in a significantly reduced hazard ratio for 12 month MACE despite the greater prevalence of CMR-detected Type 4a MI shown here. There are limited data as to whether revascularization-induced myocardial injury detected by CMR is linked to

prognosis³⁰ and none in patients presenting with STEMI. In an observational study of 152 patients undergoing elective revascularization, 32% had evidence of new LGE, which averaged 5g (4% of LV mass) and half of these patients were treated with CABG³⁰. In that study, patients with new infarction following revascularization had reduced LVEF, increased LV volumes, increased total IS and a 3-fold increase in MACE at a median of 2.9 years follow-up compared to those without new LGE³⁰. Given that the CR group in the current study had no increase in total IS, LV volumes or reduced LVEF, it seems unlikely that the short-medium term clinical benefits of CR¹⁶ will be offset in the long-term by increased heart failure or sudden cardiac deaths. However longer-term follow-up of patients in this study is needed to confirm this.

We did not observe any significant differences in myocardial salvage between the treatment groups in this study. Non-IRA revascularization at the time of PPCI could increase perfusion to watershed areas by relieving flow-limiting stenoses resulting in increased myocardial salvage³¹⁷. Alternatively, resting myocardial perfusion and flow reserve following PCI may actually be reduced, as has been shown in elective patients as a result of distal embolization, particularly when the PCI is associated with new LGE^{317, 318}. It may be that both effects are seen with non-IRA PCI resulting in no net benefit with regard to myocardial salvage in the PPCI setting.

Unexpectedly, we also observed no difference in ischemic burden between the groups undergoing follow-up stress perfusion CMR. There are several potential explanations for this finding. Firstly, it is well recognized that even severe angiographic stenoses may not cause ischemia^{22, 319}. Secondly, 11 patients in the IRA-only arm had further PCI before the stress CMR that is likely to have reduced ischemic burden in this group. Thirdly, the small number of crossovers from randomization is likely to have diminished the differences in ischemia between the groups. Finally, the stress CMR was undertaken in patients on optimal medical therapy, which may dramatically reduce post MI ischemia³²⁰ making it more difficult to detect differences between the groups, especially as there was higher use of a second anti-anginal medication in the IRA-only group. This may also explain why the overall ischemic burden in our study was small (3-4%). It remains to be determined

whether ischemia is prognostically important in the PPCI era, especially as medical therapy may result in similar clinical outcomes to a revascularization strategy even in patients treated with thrombolysis³²⁰. Further insight on this subject will be available from the CvLPRIT nuclear substudy.

5.4.1 Limitations

The optimal timing to assess infarct size post STEMI is uncertain³²¹. We chose an early timepoint to enhance participation in the CMR substudy as we felt there could have been a higher dropout rate scanning patients after discharge from hospital. MSI was only reliably measured in ~75% of patients and the use of novel T1 or T2 mapping techniques for future studies may lead to a more robust assessment. Current CMR techniques cannot reliably differentiate if a very small MI, which is not associated with wall thinning, oedema or MVO, is acute or chronic and this contributed to the slight over-reporting of acute N-IRA infarcts which were not associated with revascularization in this study.

5.4.2 Conclusions

An in-hospital CR strategy in patients with multivessel disease at the time of PPCI is associated with a small increase in Type 4a MI in non-IRA territories but total IS was not significantly different compared to an IRA-only strategy.

5.4.3 Original contribution to knowledge

At the time of writing, this is the first detailed study of acute and follow-up CMR outcomes in a RCT of IRA-only versus CR in multivessel coronary disease at PPCI.

5.4.4 My contribution

CvLPRIT-CMR was conceived by GPM and AHG with input from JPG, MF, NC, DB and MD. I was responsible for the analysis of angiographic data from Leicester, analysis of all CMR scans (supervised by GPM), coordination of the CvLPRIT-CMR substudy, data collection and construction of the substudy database, production of the statistical analysis plan (supervised by AR and GPM) and undertook the statistical

analysis. I was involved in patient recruitment at Leicester. I, GPM, JW, JPG and CP were responsible for organisation and supervision of CMR scans at the centres. I and GPM wrote the manuscript, which was reviewed for intellectual content by all authors.

CHAPTER SIX

6. CMR PREDICTORS OF SEGMENTAL FUNCTIONAL RECOVERY IN STEMI

*Relationship of myocardial strain and markers of myocardial injury to
predict segmental recovery following acute ST-segment elevation
myocardial infarction*

Published:

Khan JN, Nazir SN, Singh A, Shetye A, Lai FY, Peebles C, Wong J, Greenwood JP, McCann GP. Relationship of myocardial strain and markers of myocardial injury to predict segmental recovery following ST-segment elevation myocardial infarction. Circulation: CV Imaging. June 2016. doi: 10.1161/CIRCIMAGING.115.003457.

6.1 Background

Improvement in dysfunctional myocardium following acute ST-elevation myocardial infarction (STEMI) predicts long-term myocardial function and prognosis^{322, 323}.

Kim¹⁴¹ and Choi³²⁴ first demonstrated an inverse correlation between cardiovascular MRI (CMR)-measured segmental late gadolinium enhancement (LGE) transmuralities and functional recovery in hibernating¹⁴¹ and stunned³²⁴ myocardium, allowing the prediction of functional recovery without inotropic challenge^{322, 323}. However, the evidence base in acute STEMI is limited by a small number of single centre studies and heterogeneity of LGE assessment.^{63, 97, 98, 143, 144, 146, 325, 326} Moreover, several reports have shown that LGE, measured within days of STEMI overestimates acute infarct size and underestimates the potential for functional recovery.^{54, 321, 327} The accuracy of segmental LGE expressed as segmental extent of enhancement (SEE), defined as enhanced percentage of segmental area^{98, 143, 326, 328} rather than maximum transmuralities in predicting segmental recovery in acute STEMI has shown promise.

Several other CMR markers of myocardial injury have been associated with functional recovery following STEMI. Circumferential strain (*Ecc*)⁹⁸, myocardial salvage (MSI)¹²⁸, LGE-derived microvascular obstruction (late MVO)^{98, 128, 329} and intramyocardial haemorrhage (IMH)³²⁹ have been assessed in a few small studies. There are no studies investigating whether they offer additive value to the predictive accuracy of LGE. Feature Tracking (FT) is a novel post-processing software for the quantification of myocardial strain from steady-state free-precession (SSFP) cine images^{93, 297}. We have recently demonstrated greater robustness, reproducibility and infarct correlation with FT-derived strain compared with tagging in acute STEMI³³⁰.

We aimed to assess whether FT-derived *Ecc*, MSI, late MVO and IMH predicted segmental functional recovery in acute STEMI and whether this was of additive value to SEE.

6.2 Methods

6.2.1 Study population

This study was conducted on the 164 CvLPRIT-CMR recruits who underwent both acute and follow-up CMR scanning.

6.2.2 Cardiovascular MRI

6.2.2.1 CMR image acquisition

Acute CMR was performed at a median of 2.9 days post PPCI and was repeated at 9.4 months ('follow-up CMR') in 164 patients who comprised the cohort for this study. The acute and follow-up imaging protocols are detailed in the main Methods chapter of this thesis in Figures 19 and 25 respectively. The scans were identical apart from T2w-STIR and adenosine stress perfusion imaging performed only at the acute and follow-up CMR studies respectively.

6.2.2.2 CMR analysis

Image quality

Image quality was graded on a 4-point Likert scale: 3= excellent, 2= good, 1= moderate and 0= unanalysable.

Volumetric and functional analysis

Analysis was performed using *cvi42* v4.1 (Circle Cardiovascular Imaging, Calgary, Canada). LV volumes were calculated as described in Section 2.4.3.1.²⁹⁹ Wall motion in the 16 American Heart Association myocardial segments was assessed as described in Section 2.4.3.2 and visually graded as: 1= normokinetic, 2= hypokinetic, 3= akinetic, 4= dyskinetic and 5= aneurysmal.²⁷³ Segmental dysfunction was defined as WMS ≥ 2 at acute CMR and improvement as a WMS decrease of ≥ 1 , and normalisation where WMS returned to 1 at follow-up CMR.^{98, 143, 326, 328}

Infarct characterisation

Oedema (AAR) and infarct were assessed using *cvi42* v4.1 on T2w-STIR and LGE imaging, using Otsu's Automated Thresholding and FWHM quantification

respectively, as previously described in Sections 2.4.3.3 and 2.4.3.6³³¹. Hypointense regions within enhancement on LGE and T2w-STIR imaging were included, corresponding to MVO and IMH respectively, and expressed as present or absent for each of the 16 segments. SEE was calculated as percentage enhanced area for each myocardial segment ($SEE = 100 * [\text{segmental enhanced area} / \text{segmental area}]$)^{98, 332}. SEE was additionally classified into 5 categories: SEE 0%, SEE 1-25%, SEE 26-50%, SEE 51-75%, SEE 76-100% as previously described^{98, 326, 328}. Segmental MSI defined the proportion of the AAR that did not progress to infarction and was calculated as $[(\text{segmental AAR} - SEE) / \text{segmental AAR}] \times 100$.

Circumferential strain analysis

Segmental peak endocardial *Ecc* was measured with FT using *Diogenes Image Arena* (Tomtec, Munich, Germany). Endocardial contours were manually drawn onto the end-diastolic image and propagated. The FT algorithm has been described previously³³⁰. Suboptimally tracking segments were manually adjusted if movement of contoured borders deviated from true myocardial motion by >50%.

6.2.2.3 Statistical analysis

Normality was assessed using Kolmogorov-Smirnoff tests, histograms and Q-Q plots. Normally distributed data were expressed as mean \pm standard deviation. Non-parametric data were expressed as median (25%-75% interquartile range). ANOVA and Kruskal-Wallis analyses were used to compare mean and median values between multiple groups respectively. Spearman's Rank Correlation Coefficient assessed the correlation between the predictors and segmental function. We assessed: (1) whether SEE, *Ecc*, MVO, MSI, (presence/absence) and IMH (presence/absence) predicted improvement and normalisation of dysfunctional myocardial segments at follow-up CMR, and (2) whether *Ecc*, MVO, MSI, and IMH provided incremental improvement in predictive accuracy above SEE alone using logistic regression with random effect to account for dependence of segments from the same patient. The likely clinical benefit for differences in predictive accuracy of SEE alone compared with SEE plus each of *Ecc*, MSI, MVO and IMH was assessed for the logistic regression models using Akaike's Information Criteria (AIC)³³³ and using

Receiver-Operator Curve (ROC) analysis with the area under the curves (AUCs) compared using the method of Delong³³⁴. On AUC, predictive accuracy of >0.9 was considered excellent, 0.8-0.9 very good, 0.7-0.8 good, 0.6-0.7 average and <0.6 poor³³⁵. The optimal cut-off values of SEE, segmental *Ecc* and MSI for predicting functional recovery were identified by ROC analysis where sensitivity and specificity intersected. Intra and interobserver agreement were assessed with intraclass correlation coefficient for absolute agreement (ICC)²⁹¹ and kappa statistic on a random selection of 10 patients. Intraobserver (JNK) and interobserver agreement (JNK, SAN) are reported in Supplemental Data 1. Statistical tests were performed using SPSS v20 (IBM, New York, USA) and PROC GLIMMIX in SAS v9.4 (Statistical Analysis Systems, North Carolina, USA). $p < 0.05$ was considered significant.

6.3 Results

6.3.1 Baseline characteristics

Baseline CMR data are summarised in Table 50. Image quality was diagnostic in all cine and LGE segments (n=2624) which were analysable for WMS, SEE, *Ecc* and MVO.

Table 50: Baseline demographics and CMR characteristics

CMR characteristics	
Cine segments of diagnostic image quality (%) at acute CMR	100
LGE segments of diagnostic image quality (%) at acute CMR	100
T2w-STIR segments of diagnostic image quality (%) at acute CMR	76.8
Cine segments of diagnostic image quality (%) at follow-up CMR	100
Acute CMR time (days post STEMI)	2.9 (2.0-3.9)
Follow-up CMR time (month post STEMI)	9.4 (8.9-10.0)
Segmental characteristics	
Dysfunctional segments at acute CMR (n, %)	837/2624 (31.9)
Dysfunctional segments at follow-up CMR (n, %)	495/2624 (18.9)
Segments with LGE at acute CMR (n, %)	1186/2624 (45.2)
Segments with LGE at follow-up CMR (n, %)	1009/2624 (38.5)
Segments with MVO at acute CMR (n, %)	165/2624 (6.3%)
Segments with IMH at acute CMR (n, %)	51/2016 (2.5%)

CMR= cardiovascular magnetic resonance, LGE= late gadolinium enhancement, T2w-STIR= T2-weighted short-tau inversion recovery, MVO= microvascular obstruction, IMH= intramyocardial haemorrhage

Twenty-three percent of T2w-STIR segments (MSI, IMH) were non-analysable due to poor image quality or not being acquired due to significant breath holding and ECG gating difficulties. Thus 2020 segments were included in the assessment of CMR predictors of segmental recovery.

6.3.2 Segmental systolic function post STEMI

6.3.2.1 Wall motion scoring at acute and follow-up CMR

At acute CMR, 837 (31.9%) of segments were dysfunctional (WMS 2: 499/2624 [19.0%], WMS 3 338/2624 [12.9%], WMS 4/5: 0/2624 [0%]). At 9-month follow-up CMR, 521 (62.2%) of dysfunctional segments had improved of which 372 (44.4%) had normalised and 495 (18.8%) remained dysfunctional (WMS 2: 350/2624 [13.3%], WMS 3: 137/2624 [5.2%], WMS 4: 8/2624 [0.3%], WMS 5: 0/2624 [0%]) (Figure 47).

6.3.2.2 Segmental function according to segmental extent of LGE and strain

Acutely, with worsening function on WMS, SEE and presence of MVO and IMH increased, and segmental *Ecc* and MSI decreased (Table 51). With increasing SEE, segmental function worsened (Figure 47). Over 98% of 'SEE 76-100%' segments were dysfunctional at acute CMR. WMS correlated more strongly with SEE at acute ($r_s=0.69$, $p<0.01$) and follow-up CMR ($r_s=0.62$, $p<0.01$) than with MSI (acute: $r_s=-0.523$, <0.01 ; follow-up: $r_s=-0.514$, <0.01) and *Ecc* (acute: $r_s=0.49$, $p<0.01$; follow-up: $r_s=0.49$, $p<0.01$). At follow-up CMR, segmental function improved in each SEE grade (Figure 48). The proportion of dysfunctional segments improving or normalising decreased with increasing SEE, with 90% of 'SEE 0%' segments normalising. Of the 104 'SEE 75-100%' segments, 102 (98%) were dysfunctional. Despite this degree of SEE, 33% of 'SEE 75-100%' segments improved (34/104), however only 5% normalised (5/104) (Figure 48). The proportion of dysfunctional segments improving or normalising increased with increasing MSI. Despite this, 43% of 'MSI 0-25%' segments improved, but only 21% normalised (Figure 49).

Table 51: Segmental extent of myocardial injury according to degree of dysfunction at acute CMR

WMS at Acute CMR	1: Normal (n=1787, 68%)	2: Hypokinetic (n=499, 19%)	3: Akinetic (n=338, 13%)	p
SEE (%)	3.6±9.7	24.4±22.0	52.2±29.1	<0.001
Peak segmental <i>Ecc</i> (%)	-23.5±10.2	-14.9±9.1	-9.6±7.9	<0.001
MSI (%)	98.4 (71.2, 100.0)	58.1 (25.7, 83.2)	18.3 (0.0, 52.6)	<0.001
MVO (n, %)	7/1787 (0.4)	48/499 (9.6)	110/338 (32.5)	<0.001
IMH (n, %)	1/713 (0.1)	12/241 (4.9)	41/198 (20.7)	<0.001

SEE= segmental extent of enhancement; *Ecc*= peak segmental circumferential strain; MSI= myocardial salvage; MVO presence of microvascular obstruction (MVO) and IMH= intramyocardial haemorrhage. No segments had WMS of 4 or 5 at acute CMR

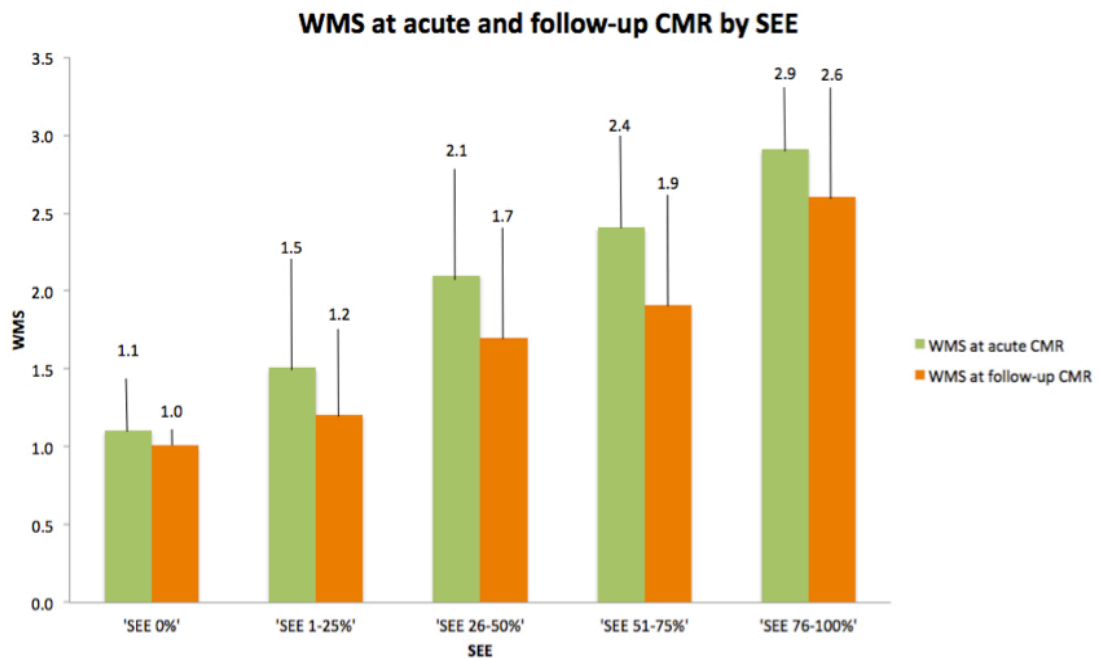


Figure 47: Wall-motion scoring at acute and follow-up CMR by segmental extent of enhancement

WMS= wall-motion score, SEE= segmental extent of enhancement

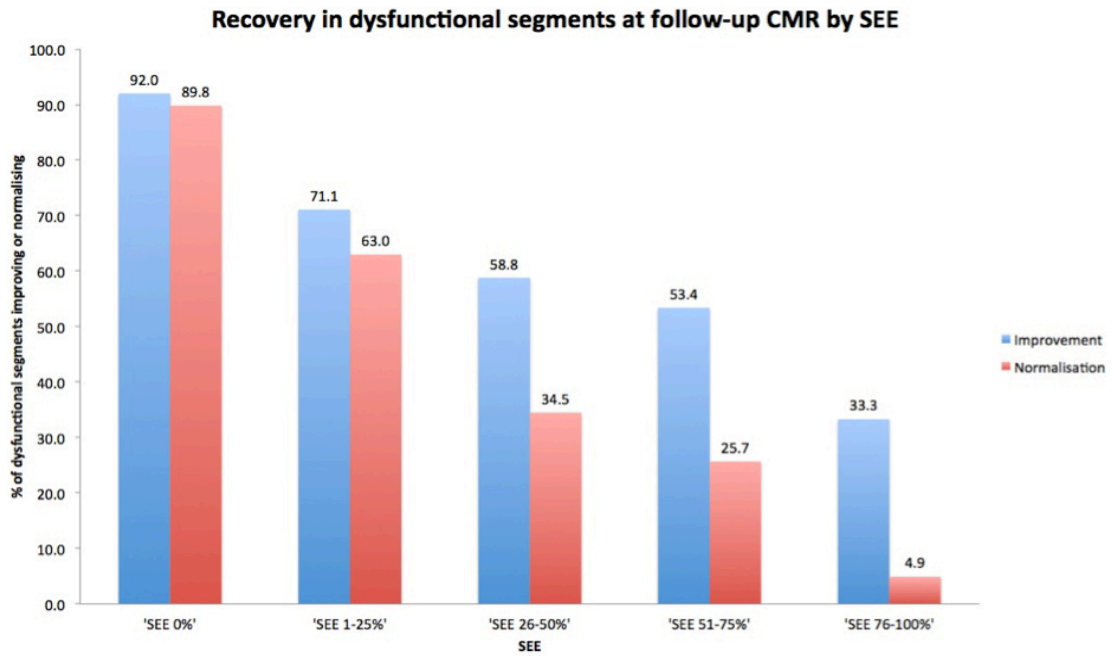


Figure 48: Recovery in dysfunctional segments at follow-up CMR by segmental extent of enhancement

SEE= segmental extent of enhancement

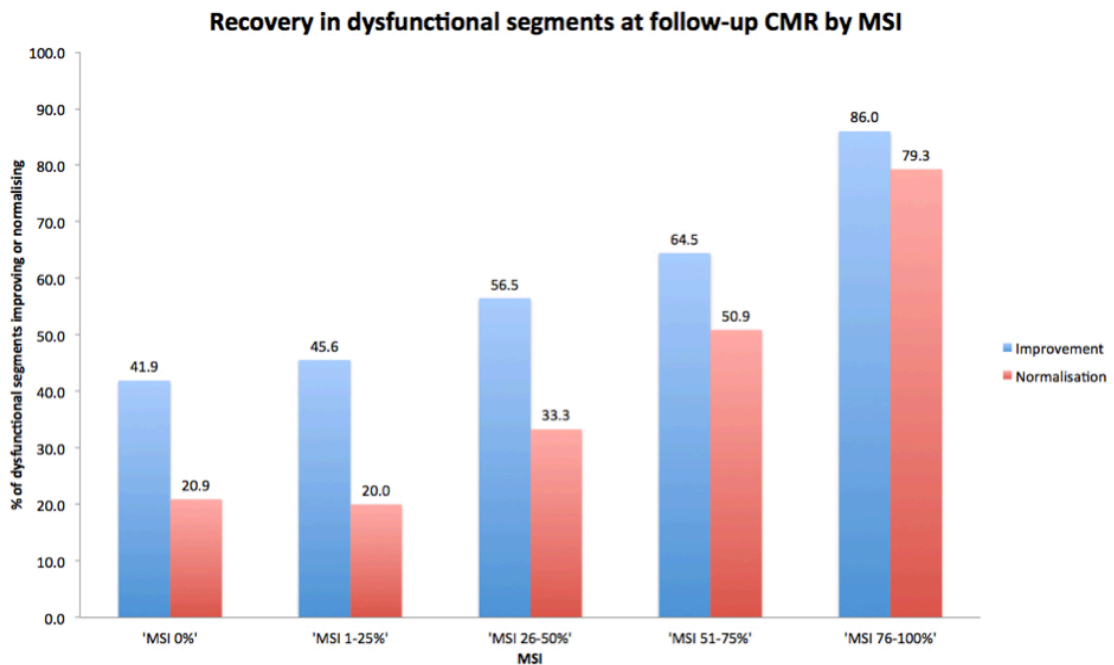


Figure 49: Recovery in dysfunctional segments at follow-up CMR by segmental myocardial salvage

MSI= myocardial salvage index

6.3.3 Predictors of segmental recovery in dysfunctional segments post STEMI

6.3.3.1 Predictors of segmental functional improvement

Individual predictors

Results are shown in Table 52. SEE was a strong predictor of functional improvement ($p<0.001$; AUC 0.840). Optimal predictive SEE cutoff was $<34\%$ (sensitivity 62%, specificity 62%). SEE predicted improvement with similar accuracy to segmental MSI ($p<0.001$; AUC 0.840; $p=0.139$ vs. MSI), *Ecc* ($p<0.001$; AUC 0.834; $p=0.613$ vs. *Ecc*) and MVO ($p=0.021$; AUC 0.826, $p=0.164$ vs. MVO). IMH was a weaker predictor of functional improvement than SEE ($p=0.004$; AUC 0.818, $p=0.041$ vs. SEE). Revascularisation strategy did not predict segmental improvement ($p=0.206$).

Predictors combined with SEE

Ecc ($p=0.027$) and MSI ($p=0.031$) added incremental predictive value to SEE. The additional incremental predictive value in the combined models was however minimal (AUC: SEE 0.846, SEE+*Ecc* 0.851, SEE+MSI 0.848; AIC: SEE 989 vs. SEE+*Ecc* 987, SEE 688 vs. SEE+MSI 686, [Figure 50]). When combined, the relative predictive value of SEE was higher than for *Ecc* (AIC: SEE 991, *Ecc* 1060) and similar to that for MSI (AIC: SEE 688, MSI: 696). MVO ($p=0.070$) and IMH ($p=0.756$) provided no incremental predictive value above SEE alone.

6.3.3.2 Predictors of segmental functional normalisation

Individual predictors

SEE was a strong predictor of functional normalisation ($p<0.001$; AUC 0.887 [Table 52]). Optimal predictive SEE cutoff was $<29\%$ (sensitivity 72%, specificity 72%). SEE was a stronger predictor than segmental MSI ($p<0.001$; AUC 0.862, $p=0.007$ vs. MSI), *Ecc* ($p<0.001$; AUC 0.844; $p=0.001$ vs. *Ecc*), MVO ($p<0.001$; AUC 0.835, $p<0.001$ vs. MVO), and segmental IMH ($p=0.001$; AUC 0.827, $p<0.001$ vs. IMH). Revascularisation strategy did not predict segmental normalisation ($p=0.463$).

Predictors combined with SEE

Ecc ($p=0.027$) and *MSI* ($p=0.027$) added incremental predictive value to *SEE*. The additional incremental predictive value in the combined models was again minimal (AUC: *SEE* 0.894, *SEE+Ecc* 0.906, *SEE+MSI* 0.892; AIC: *SEE* 890 vs. *SEE+Ecc* 880, *SEE* 622 vs. *SEE+MSI* 619 [Figure 51]). When combined, the relative predictive value of *SEE* was higher than for *Ecc* (AIC: *SEE* 890, *Ecc* 1047) and *MSI* (AIC: *SEE* 622, *MSI*: 650). *MVO* ($p=0.233$) and *IMH* ($p=0.221$) did not improve incremental predictive value above *SEE*.

6.3.4 SEE and *Ecc* as predictors of segmental functional recovery where $SEE \geq 50\%$

In dysfunctional segments with $\geq 50\%$ *SEE*, *SEE* predicted improvement ($p=0.002$) (AUC 0.924) and normalisation ($p=0.002$) (AUC 0.918, [Supplemental Data 15]). *MVO* also predicted functional normalisation ($p=0.002$) and provided incremental predictive accuracy when combined with *SEE* ($p<0.009$). *Ecc*, *MSI* and *IMH* did not predict functional recovery and were not of additive value to *SEE*.

6.3.5 CMR predictors of segmental functional recovery stratified by revascularisation strategy

Full data are presented in Supplemental Data 16. The results for all analyses were similar in patients undergoing IRA-only ($n=80$) and complete revascularisation ($n=84$), and were similar to those in the overall study cohort ($n=164$).

Table 52: CMR predictors of segmental improvement and normalisation in dysfunctional segments

<u>Improvement</u>				
Predictor	AUC	95% CI [AUC], p	Optimal cutoff	Odds-Ratio
SEE	0.840	0.814-0.867	<34% (sens 62%, spec 62%)	0.97 per +1% SEE (p<0.001)
MSI	0.840	0.809-0.872	>39% (sens 65%, spec 65%)	1.03 per +1% MSI (p<0.001)
<i>Ecc</i>	0.834	0.807-0.862	<-11.4% (sens 59%, spec 59%)	1.05 per -1% <i>Ecc</i> (p<0.001)
MVO presence	0.826	0.798-0.853	n/a	0.61 MVO present vs. absent (p=0.021)
IMH presence	0.818	0.779-0.857	n/a	0.32 IMH present vs. absent (p=0.004)
<u>Normalisation</u>				
Predictor	AUC	95% CI [AUC], p	Optimal cutoff	Odds-Ratio
SEE	0.887	0.865-0.909	<29% (sens 72%, spec 72%)	0.95 per +1% SEE (p<0.001)
MSI	0.862	0.832-0.891	>48% (sens 71%, spec 71%)	1.04 per +1% MSI (p<0.001)
<i>Ecc</i>	0.844	0.818-0.871	<-12.0% (sens 62%, spec 62%)	1.07 per -1% <i>Ecc</i> (p<0.001)
MVO presence	0.835	0.808-0.862	n/a	0.19 MVO present vs. absent (p<0.001)
IMH presence	0.827	0.789-0.865	n/a	0.08 IMH present vs. absent (p=0.001)

AUC= area under the curve, 95% CI= 95% confidence interval, sens= sensitivity, spec= specificity, SEE= segmental extent of enhancement, *Ecc*= peak segmental circumferential strain, MSI= myocardial salvage; MVO= microvascular obstruction, IMH= intramyocardial haemorrhage

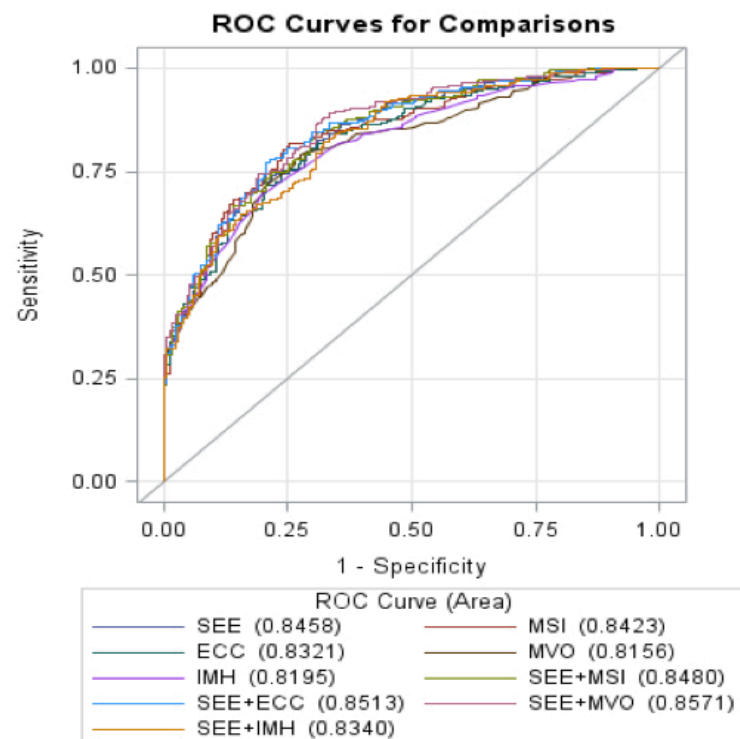


Figure 50: CMR predictors of segmental improvement assessed using Receiver Operator Curves

SEE=segmental extent of enhancement, MVO=microvascular obstruction, IMH=intramyocardial haemorrhage, Ecc=circumferential strain, MSI=myocardial salvage index

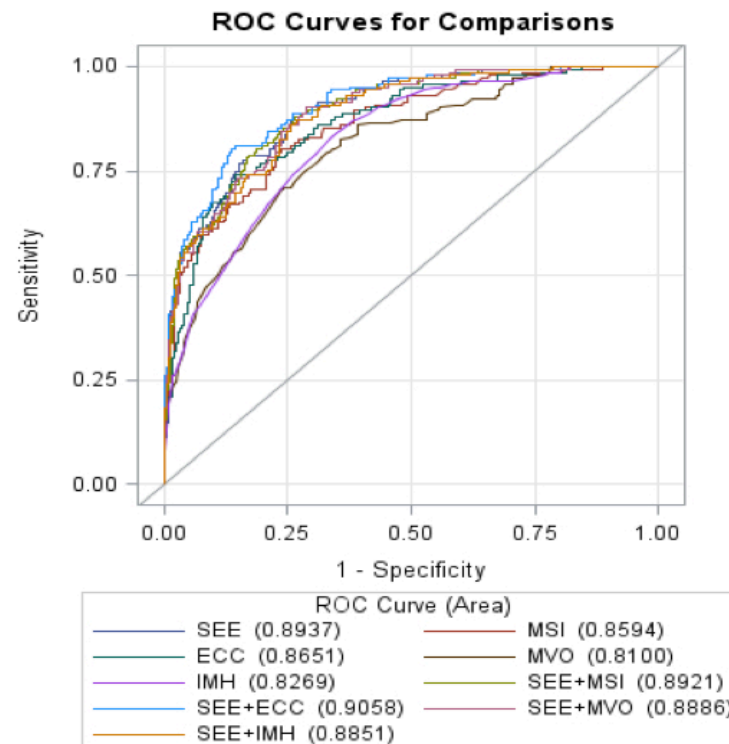


Figure 51: CMR predictors of segmental normalisation assessed using Receiver Operator Curves

SEE=segmental extent of enhancement, MVO=microvascular obstruction, IMH=intramyocardial haemorrhage, Ecc=circumferential strain, MSI=myocardial salvage index

6.4 Discussion

This is the largest study assessing CMR predictors of segmental functional recovery following acute STEMI treated with PPCI and the first to use multicentre data analysed in a core lab. We have confirmed that early after STEMI, LGE overestimates infarct size despite using FWHM quantification, which gives lower values compared with 2SD thresholding used by most previous studies^{97, 144, 146, 325, 328}. Functional improvement occurred in a significant proportion of near-transmurally enhanced segments although only 5% normalised. A key aim of conducting this study was to assess whether the accuracy of LGE to predict functional recovery following STEMI could be improved with the addition of other markers of myocardial injury. We have shown that baseline SEE is a strong predictor of recovery at 9 months. SEE was of similar predictive value to MSI, *Ecc* and MVO for improvement, and a stronger predictor than MSI, *Ecc*, MVO and IMH for normalisation. Additionally although *Ecc* and MSI provided incremental predictive value for recovery compared with SEE alone, the increase in accuracy was minimal and unlikely to be of clinical significance.

6.4.1 Prediction of segmental functional recovery with LGE

Our observed inverse correlation between SEE and functional recovery is consistent with previous studies^{63, 97, 98, 143, 144, 146, 324, 326}. The accuracy in predicting recovery was slightly lower than in the work of Kitagawa¹⁴⁴ and Orii³²⁶. LGE measured acutely overestimates necrosis by up to 30% in the first week post STEMI due to myocardial oedema^{54, 321}. We undertook acute CMR at 3 days post PPCI to assess CMR in a 'real world' setting when patients are discharged, and are less likely to undergo CMR at day 5 and 8 as in these two studies^{144, 326}. Untreated multivessel disease with potential hibernating myocardium in non-infarct artery territories in our study, differences in LGE thresholding methods^{63, 97, 143, 144, 146, 324, 326} and the smaller sample size of these studies may also have contributed to our slightly lower AUC. We used SEE^{63, 97, 98, 143} since we felt that it is a more accurate representation of segmental necrosis than transmural extent of enhancement. Transmurality can overestimate segmental necrosis since a segment may be deemed transmurally enhanced when only a small portion of segmental width demonstrates transmural extent³²⁴. Infarct

extent based on transmural extent has been compared with SEE in one study, in HCM and was 31% higher³³⁶.

The recent study by Wong⁹⁸ is the closest in design to our study. SEE and MVO were however stronger predictors of recovery in our study compared with their results (SEE: AUC 0.840 vs. 0.680, MVO: 0.836 vs. 0.670). This may be due to their small study size (n=45), the fact that they only assessed LGE on three thin (6mm) short-axis slices and hence provided incomplete LV coverage, and their later timepoint of acute CMR on day 8, by which time there may have been a degree of infarct and MVO resorption and functional recovery.

The optimal SEE cut-off for predicting recovery in our study of 34% is similar to that in the study by Becker³²⁸, who also used SEE. It may be that if transmural extent of enhancement overestimates necrosis relative to SEE, a smaller SEE cut-off predicts recovery. The commonly used arbitrary cut-off of 50% may need revising, since it has been derived from historical work in chronic coronary artery disease¹⁴¹ where LGE is unlikely to overestimate necrosis¹⁴¹. Importantly, SEE in our study was a strong predictor (AUC 0.887) of functional normalisation, which may be associated with long-term LV function and prognosis^{322, 323}.

Late MVO and IMH were moderately strong predictors of segmental recovery. This is in keeping with the work of Kidambi³²⁹ who demonstrated that infarcts with MVO had no improvement in segmental function on mid-myocardial and endocardial-strain in the infarct zone at 3 month, and that the presence of IMH further attenuated strain. Of note, MVO in our study was the only predictor of functional normalisation in segments with SEE $\geq 50\%$ in addition to SEE, and provided incremental predictive benefit. This is likely to be a reflection of the more severe myocardial injury and adverse remodelling known to accompany MVO. Indeed, Kitagawa¹⁴⁴ showed that segmental MVO extent $< 50\%$ accurately identified recovering segments with SEE $\geq 50\%$ enhancement. The lack of predictive accuracy of IMH in segments with SEE $\geq 50\%$ in our study may be due to the relatively small number of segments with IMH and SEE $\geq 50\%$ (n=41).

Our results have also shown that MSI performed equally as well as SEE to predict functional recovery. The moderate predictive accuracy of MSI is consistent with previous work highlighting that MSI may underestimate functional recovery using segmental strain.¹²⁸ The minimal incremental increase in predictive accuracy of MSI in addition to SEE is likely to result from the close relationship between SEE and MSI. Indeed, Spearman's Rank Correlation Coefficient for SEE and MSI was -0.89 ($p < 0.001$) in our study. Given that MSI significantly increases scanning time to acquire oedema images, resulted in non-analysable images in 25% of patients and provided only minimal incremental value above SEE alone, there appears to be little merit in using MSI instead of or in addition to SEE. The close interrelation between IS, MVO and IMH is also likely to account for their lack of incremental predictive accuracy in our study.

6.4.2 Prediction of segmental functional recovery with strain

We recently compared FT and tagging strain assessment in acute STEMI and showed that FT-derived endocardial *Ecc* correlated strongest with infarct characteristics³³⁰. This is likely to be a result of infarction firstly affecting the endocardium in the ischaemic cascade.¹³² This is corroborated by the fact that *Ecc* was a strong predictor of segmental recovery in this study.

Our results are in keeping with Wong who showed an almost identical predictive accuracy (AUC 0.823) to our study, of HARP-derived *Ecc* in identifying segmental recovery at 3 months⁹⁸. Unlike our study, they however demonstrated that *Ecc* was a significantly stronger predictor than SEE and MVO. This is likely to be due to methodological differences as discussed above. Our findings are similar to those of Orii³²⁶ who also showed a strong predictive accuracy of speckle-tracking echocardiographic *Ecc* (AUC 0.899) for segmental functional recovery, and similar accuracy to SEE ($p = 0.439$). On a global level, our findings are supported by the recent work of Buss⁹⁹, which showed that FT-derived global *Ecc* and LGE infarct size were moderately strong predictors of LVEF >50% at 6-months follow-up, and that *Ecc* was a non-inferior predictor compared with infarct size.

Our study is in contrast to the work of Neizel³³⁷ who used strain-encoded CMR (SENC)-derived segmental *Ecc* and LGE SEE to predict severe, persistent dysfunction at 6 months defined as segmental *Ecc* <9%. *Ecc* was only a mildly strong predictor and was a significantly weaker predictor than SEE (AUC 0.74 vs. 0.91). The weaker predictive accuracy of SENC *Ecc* compared to FT *Ecc* in their study may be due to the fact that Neizel divided the left ventricle into 10 to 12, rather than 16 segments, thus potentially reducing the accuracy of strain assessment in basal and apical segments. Indeed, no segments in their study had a strain value of zero, even those that were visually akinetic and contained MVO. In addition, SENC imaging has a lower signal-to-noise ratio than SSFP cine imaging³³⁷. However there are no data comparing SENC and FT strain assessment.

6.4.3 Limitations

Acute CMR was undertaken earlier than in some studies with potentially greater necrosis overestimation on LGE, however this allows a closer representation of 'real life' practice where acute CMR would typically be undertaken pre-discharge. All of our subjects had multivessel coronary disease, which may reduce comparability to previous studies. Approximately 25% of patients did not have satisfactory T2w-STIR images to allow diagnostic segmental data for MSI and IMH, which may be improved with newer tissue characterisation (mapping) techniques. Segmental MVO and IMH extent were not assessed due to this being currently unavailable in our analysis software. The same observer (JNK) performed all CMR analysis, however there was a 3-month gap between analysis of cine (WMS, *Ecc*), T2w-STIR (IMH, MSI) and LGE (SEE, MVO) imaging, ensuring blinded analysis of CMR predictors of segmental improvement.

6.4.4 Clinical Summary

The main benefit in being able to reliably identify patients whose LV function will recover following STEMI is to identify a lower risk group who will not require further monitoring and consideration of additional therapies such as implantable cardiac

defibrillators. Our results suggest that even patients with extensive LGE still require further imaging to assess whether LV function has recovered, with one third of patients with SEE >75% demonstrating functional recovery. This is likely to result from overestimation of necrosis on LGE in the acute phase post STEMI due to the presence of oedema. Our view on this is that measured acutely, LGE still appears to be the best method available to predict functional recovery, providing moderately strong accuracy but clinicians must be aware that a significant proportion of segments with seemingly near-transmural enhancement have the potential to recover function. If viability is the key determinant on deciding further management then the options are either to wait until oedema has settled (after 7-10 days)³²¹ or consider low-dose dobutamine assessment in patients with >50% SEE³³⁸. *Ecc* may have a role in predicting segmental recovery in patients with contraindications to gadolinium-based contrast agents.

6.4.5 Conclusions

The SEE of LGE is a strong predictor of functional recovery following PPCI but recovery occurs in a substantial proportion (33%) of dysfunctional segments with SEE >75%. FT-derived *Ecc* and MSI provide only minimal incremental benefit to SEE in predicting segmental recovery following STEMI. Further work is required to optimally identify stunned, non-necrotic myocardium following PPCI.

6.4.6 Original contribution to knowledge

At the time of writing, this is the largest study assessing CMR predictors of segmental functional recovery following acute STEMI treated with PPCI and the first to use multicentre data analysed in a core lab. In addition, this is the only study to date including SEE, *Ecc*, MSI, MVO and IMH in the same study.

6.4.7 My contribution

I and GPM conceived the idea for this study. I, GPM, JPG, CP, JW and SAN supervised study visits. I performed CMR analyses. I and FYL performed statistical analyses. I wrote the paper, which all authors critically reviewed.

CHAPTER SEVEN

7. CMR FINDINGS IN STAGED VERSUS IMMEDIATE COMPLETE REVASCULARISATION

Infarct size following complete revascularization in patients with multivessel disease at STEMI: a comparison of immediate and staged in-hospital non-infarct related artery PCI subgroups in CvLPRIT-CMR

Submitted:

Khan JN, Nazir SA, Greenwood JP, Dalby M, Curzen N, Hetherington S, Kelly DJ, Blackman D, Ring A, Peebles C, Wong J, Sasikaran T, Flather M, Swanton H, Gershlick AH, McCann GP. Infarct size following complete revascularization in patients presenting with STEMI: a comparison of immediate and staged in-hospital non-infarct related artery PCI subgroups in the CvLPRIT study.

(Submitted to Journal of Cardiovascular Magnetic Resonance, May 2016).

7.1 Background

The management of multivessel coronary artery disease in patients with STEMI at PPCI is controversial⁵. Registry data suggest that a staged outpatient CR strategy results in better clinical outcomes than immediate CR at PPCI. However three recent RCTs^{15, 16, 255} have demonstrated reduced medium-term major MACE rates with CR compared with IRA-only revascularization. These findings have resulted in the withdrawal of the American College of Cardiology 'Choosing Wisely' advice of not to undertake CR at PPCI³³⁹. In addition we have shown in the CvLPRIT-CMR study that CR is not associated with an increase in total IS assessed by in-patient CMR, despite a small increase in type 4a MI compared to IRA-only revascularization.³⁴⁰

There remains however no consensus on whether in-hospital CR should be staged (staged CR) or undertaken immediately after PPCI (Immediate CR). In the CvLPRIT study³⁴¹, there was a trend for reduced clinical events (death/MI/heart failure) in patients who had immediate (3.1%) rather than staged (11.9%) CR.

The aim of this *post-hoc* analysis of CvLPRIT-CMR³⁴⁰ was to assess IS and LV function in patients who underwent immediate compared to staged *in-hospital* CR, in order to gain insight into the likely mechanisms to explain the differences in clinical outcomes.

7.2 Methods

7.2.1 Study design, data acquisition/analysis

The Methods for this *post-hoc* analysis of the CvLPRIT-CMR substudy are identical to those of CvLPRIT-CMR and are described in detail in Section 5.2. After verbal assent patients were randomized after coronary angiography but before IRA PCI, to IRA-only or in-hospital CR. If there were no clinical contraindications, immediate CR was recommended but the non-IRA procedure could be staged, at the operator's discretion, but had to be completed during the index admission. Reasons for staging CR were not recorded. Recruitment is shown in Figure 52. Ninety-eight patients in the CMR substudy were randomised to in-hospital CR, of which 63 were performed

immediately and in 30 the procedure was staged. Five patients crossed over into the IRA-only treatment arm.

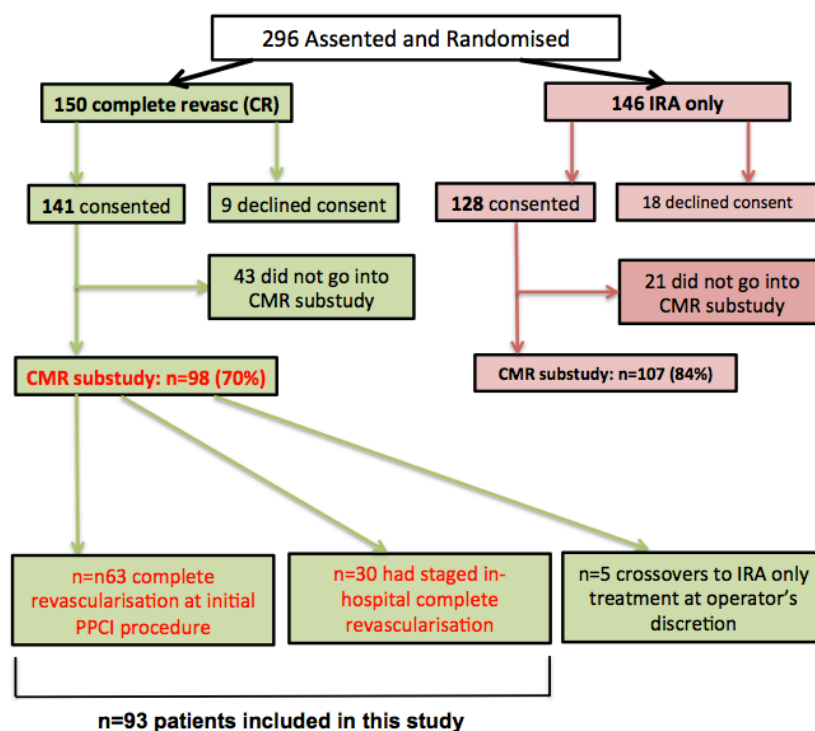


Figure 52: CONSORT diagram for patient recruitment

CONSORT diagram illustrating recruitment and patient flow. In the topmost green and red boxes are the numbers of patients randomised to each treatment arm (intention to treat) and the number who subsequently received each treatment. CR= complete revascularisation, IRA= infarct related artery

7.2.2 Outcome measures

The primary outcome was total IS measured on LGE on the acute CMR. Secondary outcomes included LVEF, presence and extent of MVO, and MSI on acute CMR. Additional secondary outcomes included inpatient and 12-month clinical events.

7.2.3 Statistical analysis

The primary outcome of acute total IS (% of LV mass) was analysed on a log-transformed scale due to right skew. This was adjusted for known baseline predictors of infarct size (anterior MI, time to revascularization, diabetes, TIMI flow

pre-PPCI) and important baseline variables that significantly differed between the two groups (TIMI flow post-PPCI, SYNTAX score, dual antiplatelet therapy choice, glycoprotein inhibitor/bivalirudin use for N-IRA PCI) using generalized mixed models. Clinical outcomes were assessed using time-to-first event survival analysis (log-rank test with right-censoring and Cox proportional hazard models were fitted to estimate hazard ratios and 95% confidence intervals for treatment comparisons.

7.3 Results

7.3.1 Baseline characteristics

Baseline characteristics and comorbidities were closely matched in the in-hospital staged CR and immediate CR subgroups and were similar to those in the overall CvLPRIT study population (Table 53). Four patients in the immediate CR group versus none in the staged group had a history of NSTEMI and previous PCI. Discharge medications were similar in the two groups.

Table 53: Baseline characteristics of the CvLPRIT and immediate vs. staged CR CMR substudy participants

Variable	CvLPRIT cohort (n=296)	Immediate CR (n=63)	Staged CR (n=30)	p
Age (y)	64.9±11.6	63.0±11.6	65.0±10.3	0.42
Male sex (%)	240/296 (81.1)	55 (87.3)	28 (93.3)	0.38
BMI (kg/m ²)	27.3 (24.4-30.2)	27.7±4.5	27.6±4.1	0.95*
Systolic BP (mmHg)	137.6±27.1	132.6±26.8	140.0±27.7	0.23
Anterior infarct (%)	106 (35.6%)	21 (33.3)	11 (36.7)	0.75
eGFR (ml/min/1.73)	95.74±34.7	96.1±30.2	101.5±41.0	0.49
Hypertension (%)	105/287 (36.6)	24 (38.1)	10 (33.3)	0.66
Hypercholesterolemia (%)	75/287 (26.1)	16 (25.4)	12 (40.0)	0.15
Diabetes Mellitus (%)	39/287 (13.6)	11 (17.5)	4 (13.3)	0.61
Current smoker (%)	87/285 (30.5)	23 (36.5)	10 (33.3)	0.77
Previous MI (%)	12/287 (4.2%)	4 (6.3)	0 (0.0)	0.16
Previous PCI (%)	9/287 (3.1%)	4 (6.3)	0 (0.0)	0.16
Anti-anginal medication (B/N)	54/287 (18.8%)	8/63 (12.7)	5/29 (17.2)	0.56
Killip Class II-III (%)	24/286 (8.4)	4 (6.3)	2 (6.7)	0.95

CR= complete revascularization, BMI= body mass index, eGFR= estimated glomerular filtration rate, CK= creatine kinase, MI= myocardial infarction, PCI= percutaneous coronary intervention. Anti-anginal medication (B/N)= beta-blocker or nitrate at admission.

*= non-normally distributed (log10 transformed)

7.3.2 Angiographic and PCI details

The median time to staged non-IRA PCI was 34.2 hours post-PPCI (IQR 24.8-48.9). There was increased visible thrombus, subsequent thrombectomy catheter use, a higher incidence of IRA no-reflow and reduced TIMI grade post-PPCI in staged CR patients (Table 54). There was a small but significant increase in CAD complexity in the staged CR group (SYNTAX score 18.3 vs. 16, $p=0.021$) involving the IRA ($p=0.043$). The prevalence of well collateralised IRA territory and LAD IRA were similar in both groups. Patients with right coronary artery IRA were more likely, and those with circumflex IRA less likely, to have a staged CR procedure. There was less glycoprotein IIb/IIIa inhibitor and bivalirudin use during the non-IRA PCI in the staged compared to the immediate CR group. When the staged and PPCI procedures were added, there was significantly increased cumulative screening time, contrast dose, number of stents (non-IRA PCI and total number of stents) and total procedure lengths in staged versus immediate CR.

Table 54: Periprocedural details in the Immediate and staged in-hospital complete revascularisation groups

Variable	Immediate CR (n=63)	Staged CR (n=30)	p
Symptom to PCI time (min)*	180 (128-307)	203 (152-296)	0.95
Radial access (%)	50 (80.6)	27 (90.0)	0.26
Aspirin	62 (98.4)	30 (100)	0.49
Second antiplatelet agent (n, %)	63 (100)	30 (100)	1.00
GPI during PPCI (n, %)	20 (31.7)	11/29 (37.9)	0.56
Bivalirudin during PPCI (n, %)	32 (53.3)	17/27 (63.0)	0.40
<i>Infarct related artery:</i>			
Left Anterior Descending (n, %)	20 (31.7)	11 (36.7)	0.64
Right Coronary (n, %)	24 (38.1)	19 (63.3)	0.022
Left Circumflex (n, %)	19 (30.2)	0 (0)	0.001
Visible thrombus (n, %)	31/62 (50.0)	26/30 (86.7)	0.001
Thrombectomy catheter (%)	39/63 (61.9)	26/30 (86.7)	0.015
Vessels with $\geq 75\%$ stenosis (n)	1.5 \pm 0.6	1.6 \pm 0.6	0.82
Stenosis in non-IRA lesions (%)	73.4	72.9	0.85
SYNTAX score (total)	16 (12-21.5)	18.3 (15-26)	0.021
SYNTAX score (IRA)	8 (5.5-11)	9.5 (8-16)	0.043
SYNTAX score (NIRAs)	6 (4-9)	7 (4.8-12)	0.24
Rentrop grade	0 (0-1)	1 (0-1)	0.35
Rentrop grade 2-3 pre PCI (n, %)	7/63 (11.1)	3/30 (10.0)	0.87
TIMI grade pre PCI*	0 (0-1)	0 (0-0)	0.47
TIMI grade post PCI*	3 (3-3), 2.92 \pm 0.4	3 (3-3), 2.77 \pm 0.5	0.023
IRA no-reflow (n, %)	1 (1.6)	7 (23.3)	<0.001
GPI at NIRA PCI (n, %)	20 (31.7)	4 (7.7)	0.06
Bivalirudin during NIRA PCI (n, %)	32/60 (53.3)	3/28 (10.7)	<0.001
GPI or Bivalirudin at NIRA PCI (n, %)	50/60 (87.7)	7/28 (25.0)	<0.001
Total Contrast dose (ml)*	295 (213-350)	390 (266-555)	0.002
Total Screening time (min)*	15.5 (12-21)	21 (17-43.3)	0.001
Total Procedure length (IRA+NIRA, min)*	58 (38.5-72.8)	91 (67-154.3)	<0.001
IRA PCI procedure length (min)*	53 (35-70.5)	55 (37.5-81.3)	0.08
Total number of stents (n)	2.8 \pm 1.1	3.4 \pm 1.4	0.034
Number of stents in IRA (n)	1.3 \pm 0.6	1.6 \pm 0.8	0.09
Number of stents in NIRAs (n)	1.5 \pm 0.8	1.8 \pm 1.0	0.026

Data presented as n/N (%), mean±SD or median (IQR). CR= complete revascularization, IRA= Infarct related artery, PCI= percutaneous coronary intervention, GPI= glycoprotein IIa/IIIb inhibitor, TIMI= thrombolysis in myocardial infarction, SYNTAX= Synergy between PCI with Taxus and Cardiac Surgery

7.3.3 CMR data

7.3.3.1 Acute CMR

Results are displayed in Table 55. Acute CMR was undertaken later in staged CR patients than in those undergoing immediate CR (4.1 [2.7-5.4] days post PPCI vs. 2.3 days [1.7-3.2], $p<0.001$). LVEF was significantly lower in staged CR patients. Median total IS was significantly greater in staged CR patients (19.7% [11.7-37.6] vs. 11.6% [6.8-18.2] LVM, $p=0.016$). This was associated with increased peak CK of borderline significance (immediate CR: 939 [627-1567] vs. staged CR: 1508 [938-2280], $p=0.05$). When corrected for important covariates, IS remained greater ($p=0.012$) in staged CR patients. In 22 patients (24%), AAR was non-quantifiable. Staged CR patients had a lower MSI and greater MVO extent ($p=0.032$).

The incidence of non-IRA territory infarcts in staged CR patients was almost three-fold that of the immediate CR group (40% vs. 14%, $p=0.006$), including when only acute non-IRA infarcts were included (30% vs. 11%, $p=0.024$). Examples are shown in Figure 53 and the location, size of infarct, expected coronary artery territory and additional non-IRA PCI are shown in Supplemental Data 17. Non-IRA territory infarcts varied considerably in size from 0.1% to 11.9% of LV mass and averaged 3.7% (immediate) and 2.9% (staged) of LV mass. Two patients (3%) in the immediate and three (10%) in the staged CR group had chronic non-IRA infarcts (evidenced by wall thinning, and absence of oedema and MVO). Excluding these patients from the analysis did not affect significantly alter the results (Supplemental Data 18).

Table 55: Acute CMR data

Variable	Immediate CR (n=63)	Staged CR (n=30)	p
Acute CMR			
Total Infarct Size (% LVM)	11.6 (6.8-18.2)	19.7 (11.7-37.6)	0.016 (0.012)*
Time from PPCI (days)	2.3 (1.7-3.2)	4.1 (2.7-5.4)	<0.001
Infarct on LGE (%)	60 (95.2)	30 (100)	0.22
Patients with >1 acute infarct	7 (11.1)	9 (30.0)	0.024
IRA Infarct size (% LVM)	11.1 (5.4-17.4)	19.1 (8.8-35.2)	0.039 (0.05)*
Non-IRA Infarct size (% LVM)	0.9±3.2	1.7±3.6	0.11 (0.65)*
Total acute infarcts (% LVM)	11.6 (6.8-17.6)	19.1 (10.2-37.1)	0.006 (0.025)*
Area at risk (% LVM)	31.4±12.5	33.1±10.8	0.57
MSI [§] (%)	61.7 (37.4-75.5)	35.1 (5.9-66.4)	0.008 (0.034)*
MVO present (n %)	34/63 (54.0)	21/30 (70.0)	0.14
MVO (% LVM)	0.07 (0.00-0.93)	0.44 (0.00-6.1)	0.032 (0.024)*
LVMl (g/m2)	52.5 (47.7-61.0)	51.5 (45.6-63.0)	0.55
LVEDVI (ml/m2)	89.9 (78.4-110.0)	89.7 (82.8-102.9)	0.43
LVEF (%)	47.4±9.4	42.2±10.2	0.019

Data presented as n/N (%), mean ±SD or median (IQR). IRA= Infarct related artery, CR= complete revascularization, LVMl= left ventricular mass index, LVEDVI= left ventricular end-diastolic volume index, LVEF= left ventricular ejection fraction, IS=infarct size, MVO= microvascular obstruction, MSI= myocardial salvage index.

* Adjusted for known predictors of IS (anterior MI, TTR, diabetes, TIMI pre-PPCI) and important baseline variables significantly varying between the groups (TIMI post-PPCI, SYNTAX score, dual antiplatelet therapy, glycoprotein inhibitor/bivalirudin use for N-IRA PCI).

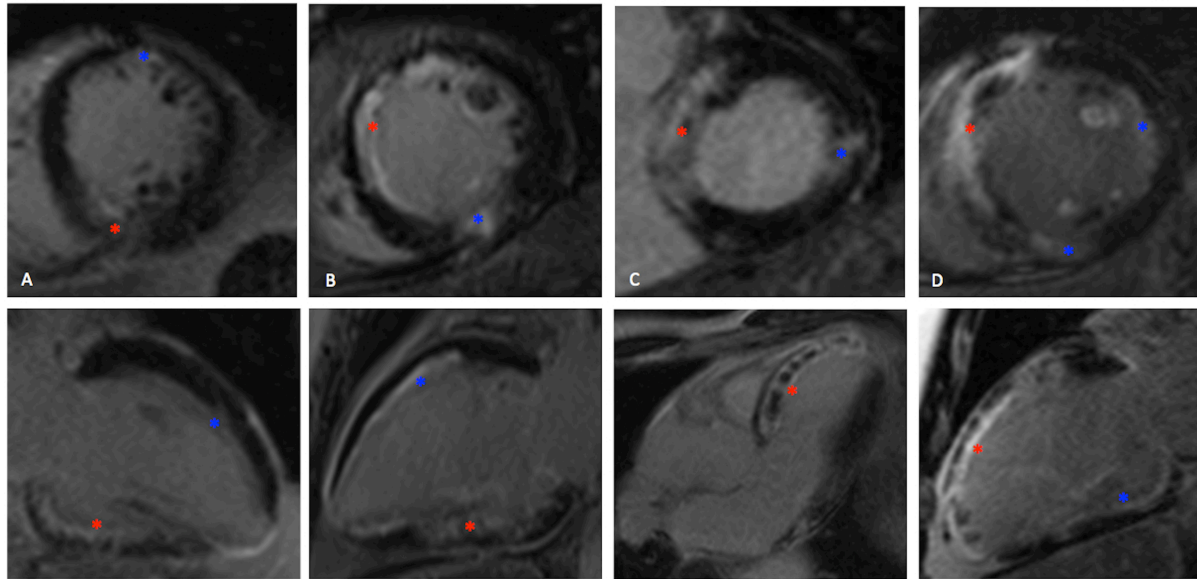


Figure 53: Examples of patients with >1 'acute' MI on CMR.

Late gadolinium enhanced short axis (top row) and long axis (bottom row). * IRA-related infarct; * NIRA-related infarct(s)

A (X511 Immediate CR): IRA (RCA) inferior infarct 19.1% LVM, NIRA (LAD) anterior infarct 3.8% LVM, total IS 22.9% LVM

B (X695 Immediate CR): IRA (RCA) inferior infarct 7.8% LVM, NIRA (LAD) anteroseptal infarct 5.0% LVM, total IS 12.8% LVM

C (X757 Staged CR): IRA (LAD) anteroseptal infarct 20.8% LVM, NIRA (LCX) lateral infarct 0.6% LVM, total IS 21.4% LVM

D (X798 Staged CR): 3 acute infarcts, IRA (LAD) anteroseptal infarct 35% LVM, NIRA-1 (RCA) inferior infarct 0.7% LVM, NIRA-2 (LCX) lateral infarct 2.0% LVM, total IS 37.6% LVM

IRA infarct size and non-IRA PCI data are shown in Supplemental Data 17.

7.3.3.2 Follow-up CMR

Results are shown in Table 56. Fifty-three patients in the immediate CR group and 26 in the staged CR group underwent follow-up CMR. There were no differences in baseline characteristics or acute CMR findings between those who did and did not undergo follow-up CMR. Total IS remained greater in staged CR patients (13.5% vs. 5.7%, $p=0.004$, corrected $p=0.044$). Reversible perfusion defects were seen in 20% of immediate CR and 27% of staged CR patients but overall ischemic burden was small (2.6 ± 6.9 and $5.2\pm12.1\%$ respectively) and not significantly different between groups.

Table 56: Follow-up CMR data

Variable	Immediate CR (n=63)	Staged CR (n=30)	p
Follow-up CMR	n=53	n=26	
LVMI (g/m ²)	45.2 (38.8-52.3)	47.4 (40.9-51.6)	0.71
LVEDVI (ml/m ²)	92.5 (80.5-105.5)	93.9 (83.3-113.6)	0.28
LVEF (%)	50.9 \pm 9.4	46.7 \pm 8.9	0.06
Infarct on LGE (n,%)	51 (96.2)	26 (100)	0.32
Patients with >1 infarct (%)	9 (17.0)	9 (34.6)	0.08
IS (% LVM)	5.7 (2.4-10.4)	13.5 (4.6-23.3)	0.004 (0.044)*

Data presented as n/N (%), mean \pm SD or median (IQR). IRA= Infarct related artery, CR= complete revascularization, LVMI= left ventricular mass index, LVEDVI= left ventricular end-diastolic volume index, LVEF= left ventricular ejection fraction, IS=infarct size, MVO= microvascular obstruction, MSI= myocardial salvage index.

* Adjusted for known predictors of IS (anterior MI, TTR, diabetes, TIMI grade pre-PPCI) and important baseline variables significantly varying between the groups (TIMI grade post-PPCI, SYNTAX score, dual antiplatelet therapy, glycoprotein inhibitor/bivalirudin use for N-IRA PCI).

7.3.4 Clinical outcomes

Discharge medication was similar between the two groups. Median follow-up was 365 days (immediate CR 365 days, staged CR 361 days, $p=0.75$). Length of inpatient stay was longer in staged CR (4.2 ± 3.2 vs. 3.1 ± 1.9 , $p=0.002$) compared to immediate

CR patient. The overall MACE rate was low (6.5%) at 1 year. The incidence of in-hospital clinical events, overall MACE and individual components were similar in the treatment arms (Table 57) apart from a higher frequency of major bleeds in staged CR patients (10.0% vs. 0.0%, $p=0.011$)

Table 57: Clinical outcomes

Variable	Immediate CR (n=63)	Staged CR (n=30)	Hazard Ratio (95% CI)	p
12 month follow-up				
MACE (n, %)	4/63 (6.3)	2/30 (6.7)	1.05 (0.18, 6.1)	0.97
Death (n, %)	0/63 (0.0)	1/30 (3.3)	**	0.15
Recurrent MI (n, %)	0/63 (0.0)	0/30 (0.0)	**	1.00
Heart failure (n, %)	2/63 (3.2)	1/30 (3.3)	0.97 (0.09, 12.1)	0.97
Revascularisation (n, %)	2/63 (3.2)	0/30 (0.0)	**	0.32
Inpatient clinical events				
Death (n, %)	1/63 (1.6)	0/30 (0.0)	**	0.49
Recurrent MI (n, %)	0/63 (0.0)	0/30 (0.0)	**	1.00
Heart failure (n, %)	2/63 (3.2)	0/30 (0.0)	**	0.32
Repeat revascularisation (n, %)	1/63 (1.6)	0/30 (0.0)	**	0.49
Safety Endpoints				
Contrast nephropathy (n, %)	1/63 (1.6)	0/30 (0.0)	**	0.49
Vascular access injury (n, %)	0/63 (0.0)	0/30 (0.0)	**	1.00
Cerebrovascular accident (n, %)	0/63 (0.0)	0/30 (0.0)	**	1.00
Major bleed (n, %)	0/63 (0.0)	3/30 (10.0)	**	0.011

CR= complete revascularization, IRA= Infarct related artery, MACE= major adverse cardiovascular events, HF= heart failure

7.4 Discussion

This *post-hoc* analysis of patients in the CvLPRIT-CMR is the first report of IS following immediate and staged CR for multivessel disease at PPCI. We have shown that patients in the CvLPRIT study who were randomized to CR, and in whom experienced interventional cardiologists chose to stage non-IRA PCI to a later timepoint in the index admission, had more visible IRA thrombus, slightly but significantly higher

SYNTAX score, lower TIMI scores and more no-flow after PPCI. These differences in baseline angiographic and PPCI results were associated with larger infarcts, less myocardial salvage and reduced LVEF compared to patients who had immediate CR. It is important to highlight that patients in this analysis were not randomized to immediate or staged CR and there were many differences in baseline characteristics between the groups. Therefore, despite adjusting for known baseline predictors of IS and other variables that significantly differed between the two groups, the results are still likely to suffer from unknown biases and we cannot conclude that staging results in larger infarcts than immediate CR. These data can be thus hypothesis generating only, but warrant further investigation in larger studies

7.4.1 Infarct size, MVO and myocardial salvage

The reduction in total IS and MVO extent, higher MSI and LVEF observed with immediate CR may be due to a number of possible factors. There could be real differences arising from treatment strategies, the staged CR group may have been having larger infarcts, and the decision to stage the procedure, at least in some cases, may have been as a direct result of poor technical success e.g. IRA no-reflow. We think it is unlikely that staged CR patients were having larger infarcts at baseline as the time to presentation, proportion having anterior MI, the area at risk and Killip Class were not significantly different from the immediate CR group and adjusting for these variables did not significantly alter results. This is also true for the degree of collateralization of the IRA that may influence IS and MVO^{342, 10}. A significant effect of ischemic preconditioning is also unlikely given the low prevalence of anti-anginal medication use in both groups³⁴³.

Immediate CR to non-IRAs could theoretically reduce IS by increasing collateral flow or by improved blood flow to the watershed region of the infarct³¹⁷. The severity of the non-IRA lesions (average diameter stenosis 73% in both groups) also indicates that these were likely to have been flow-limiting stenoses. In support of a real effect of immediate CR is the increase in MSI compared to staged CR patients. However, and most importantly, differences in angiographic and PPCI results most likely explain the reductions in MSI and increased infarct size in staged vs immediate CR patients.

The staged CR group had significantly more visible thrombus in the IRA (87% vs. 50%), subsequent thrombectomy catheter use and significantly more no-reflow (23% vs. 2%) than the immediate CR group. These factors are likely to be the main reason for the increase in IS, reduced MSI and decreased LVEF. We did not prospectively record the operators' reasons for staging the non-IRA procedures in staged CR patients but we think it is likely that a suboptimal result from the PPCI and the presence of inferior rather than lateral MI may have influenced the decision to stage the non-IRA PCI.

7.4.2 Non-IRA MI

A surprising finding in this study was that the frequency of non-IRA MI detected by CMR was considerably higher in the staged versus immediate CR groups. PCI related MI (type 4a) are well recognized,^{344, 345} although of uncertain clinical significance. In elective PCI patients up to 29%³⁴⁶ will have significant increases in troponin and a similar proportion of patients undergoing complex PCI will have evidence of type 4a MI on CMR, even when pre-treated with clopidogrel for >24 hours and a glycoprotein IIb/IIIa inhibitor periprocedurally³⁴⁶. Excluding those patients with evidence of chronic infarction, acute non-IRA MI was seen in 30% of the staged and only 11% of the immediate CR groups. Although these type 4a MI were relatively infrequent and small (3.7% and 2.8% of LV mass for immediate and staged patients respectively) there was considerable variation in size. Revascularization related injury accounting for 4% of LV mass has been associated with a three-fold increase in MACE³⁴⁷. Larger randomized studies are required to confirm whether staging CR results in more frequent non-IRA MI and poorer outcomes than immediate CR.

The explanation for the increase in type 4a MI seen with staged CR is likely to be related to greater number of stents implanted in the non-IRA of the staged patients and possibly the different use of adjunctive medication at the time of the non-IRA PCI. Glycoprotein IIb/IIIa inhibitor (8%) and bivalirudin (11%) use was low in the staged procedures compared to the immediate CR group (32% and 53% respectively), which probably reflects clinicians concerns about bleeding with a second in-patient procedure requiring additional vascular access.

7.4.3 Clinical outcomes

The clinical event rate in both groups was similar (immediate CR: 6.3% and staged CR: 6.7%) and lower than seen in the main trial for those randomized to CR (10%). The lack of other significant differences between the two groups in this *post-hoc* analysis with small numbers mean no conclusions can be drawn. Immediate CR was associated with a shorter inpatient stay of one night compared with staged CR. This finding and the reduction in catheter lab time with second procedures may suggest that an immediate CR is likely to be more cost effective than a staged CR strategy³⁴⁸. However these findings could simply be related to the fact the staged CR patients had larger MI and although cost-effectiveness will be assessed in the entire CVLPRIT population, any differences between staged and immediate CR would have to be confirmed in RCTs comparing these strategies. The increased frequency of major bleeds with staged CR is likely secondary to the need for two separate procedures and hence two arterial punctures. However, due to the small numbers, this should be confirmed in a larger study.

7.4.4 Limitations

This is a *post-hoc* analysis and patients were not randomised to immediate or staged CR. We did not systematically record the reasons for staging the procedure or use of adjunctive medication, which is a significant limitation. The marked differences in angiographic appearances at baseline, and success following PPCI, are likely to contribute to the observed differences in infarct size between the immediate and staged CR groups. The higher risk nature of CR in the staged CR cohort may hence have been a disincentive to the operator to undertake immediate CR and may be an argument in favour of randomisation of patients after successful IRA PCI, as in the PRAMI study¹⁶. However statistical significance persisted after correction for important baseline covariates. Due to the small numbers of patients in this analysis, propensity score matching was not possible. The study was not powered for clinical outcomes. Inevitably, patients who died early or who were very ill following PPCI could not participate in the CMR study which likely explains why the clinical event rates are lower than in the main study. The pre-discharge CMR was undertaken later

in staged CR patients (day 4), which is likely to have resulted in a decrease in IS and MVO extent compared with scanning at day two⁶². Hence, the observed differences in CMR outcomes in immediate and staged CR patients may have been even greater if both groups were scanned at the same timepoint. However, it was important that the CMR was performed after the staged non-IRA procedures to ensure that we captured associated type 4a MI in our results.

7.4.5 Conclusions

Patients with staged CR in the CvLPRIT-CMR substudy had more visible thrombus in the IRA, higher SYNTAX score, more stents inserted, higher incidence of no-flow and subsequently larger IS and reduced LVEF, that persisted after correction for important confounders, than patients treated with immediate CR. Prospective RCTs are needed to assess whether immediate CR results in better clinical outcomes than staged CR.

7.4.6 Original contribution to knowledge

At the time of writing, this is the first report of CMR-based markers of myocardial and microvascular injury following immediate and staged in-hospital CR for multivessel disease at PPCI.

7.4.7 My contribution

I and GPM conceived the idea for this study. I, GPM, SAN, JPG, JW and CP supervised CMR scans. I performed CMR analyses (under supervision of GPM) and QCA and SYNTAX angiographic analyses (under supervision of AHG). I performed the statistical analysis and wrote the manuscript. All authors critically reviewed the manuscript for intellectual content.

CHAPTER EIGHT

8. THESIS CONCLUSIONS AND RECOMMENDATIONS FOR FURTHER RESEARCH

8.1 Thesis conclusions and recommendations for future study

8.1.1. Semi-automated CMR methods of assessing infarct characteristics

FWHM quantification of IS is accurate compared to manual quantification, has excellent observer agreement and correlates strongly with LVEF, whereas 5SD and OAT overestimate IS. OAT accurately assesses AAR at 1.5T and with high observer agreement. Future study is required to assess:

- (1). Newer fully automated quantification techniques obviating the requirement for manual contouring.
- (2). The accuracy of the quantification methods of IS in predicting clinical outcomes, remodelling and functional improvement.
- (3) Test-retest reproducibility.
- (4) IS and AAR quantification across different platforms and vendors. This is important in contemporary, multicentre research.

8.1.2 Feature-Tracking and Tagging assessment of strain in acute STEMI

FT Global *Ecc* and *EII* measurement in acute STEMI is feasible and robust. FT-derived strain is quicker to analyse, tracks myocardium better, has better interobserver variability and correlated more strongly with infarct, area at risk (oedema), myocardial salvage and infarct transmural. Future study is required to assess:

- (1). The accuracy of CMR FT-derived strain in predicting clinical outcomes, remodelling and functional improvement.
- (2). To compare FT and newer tissue-tracking strain assessment methods which have the potential to assess transmural strain (e.g. Circle cvi42 Tissue Tracking plugin©).

8.1.3 The CvLPRIT-CMR substudy

An in-hospital CR strategy in patients with multivessel disease at the time of PPCI does not lead to increased total IS compared to an IRA-only strategy but is associated with a small increase in Type 4a MI in non-IRA territories. These findings provide further reassurance that non-IRA intervention can be considered at the time of PPCI but larger studies with long-term follow-up data for safety are required. Larger

clinical trials with longer follow-up in patients with multivessel disease presenting for PPCI are required to assess:

- (1) Whether death and MI are reduced by a CR strategy. This is particularly important given the findings of the current study, which have confirmed that CR is associated with a small increase in non-IRA MI. The ongoing COMPLETE study comparing staged in-hospital CR and IRA-only strategies is aiming for a study size of 3900 patients and median 4 years clinical follow-up.³⁴⁹
- (2). Whether functional assessment of non-IRA lesions results in similar outcomes to a pragmatic angiographic-based revascularization strategy.
- (3). The optimal timing of CR (immediate at PPCI vs. staged in-hospital CR vs. staged outpatient CR).
- (4). The cost-effectiveness of various CR strategies (immediate, staged and FFR guided) vs. an IRA-only strategy.

8.1.4 CMR predictors of segmental functional recovery in STEMI

The SEE of LGE is a strong predictor of functional recovery following PPCI but recovery occurs in a substantial proportion of dysfunctional segments with SEE >75%. FT-derived *Ecc* and MSI provide only minimal incremental benefit to SEE in predicting segmental recovery following STEMI.

- (1). Further work is required to optimally identify stunned, non-necrotic myocardium following PPCI.

8.1.5 CMR findings in staged vs. immediate complete revascularisation

Of patients randomized to in-hospital CR in the CMR substudy of CvLPRIT, those in whom the operator chose to stage revascularization had larger IS and LVEF, which persisted after adjusting for important covariates than those who underwent immediate CR.

- (1). Prospective randomized trials are needed to assess whether immediate CR results in lower infarct size and better clinical outcomes than staged CR.

CHAPTER NINE

9. APPENDICES

9. APPENDICES

Supplemental Data

Supplemental Data 1: Prospective registry studies investigating MVD revascularisation at PPCI

Study	Year	Design	n	Inclusion criteria	Exclusion criteria	Mean F/U	IRA (%)	CR (%)	SR (%)	Outcomes (primary [PO], secondary [SO])	Main findings
Manari ³⁵⁰	2014	PR/M	2061	MVD >70%	LMS, any CTO,	42m	34	18	48	PO: 30d and 2y all-cause mortality. SO: combined MACE	IRA ↑2y death, MACE. Similar in CR and Staged. CR mortality vs. Staged
Jeger ³⁵¹	2014	PR/M	1909	MVD >50%	No details	12m	77	23	0	PO: 12m all-cause mortality SO: 12m combined MACE	Similar mortality (2.7%). ↓MACE with CR driven by ↓ACS, revasc
Santos ³⁵²	2014	PR/M	257	MVD >50%	No details	Inpat	70	30	0	PO: in-hospital mortality SO: bleed, ventilation, HF, MI	Trend ↑in-hospital mortality in IRA (p=0.09). No difference for PO, SO.
Abe ³²	2013	PR/M	274	MVD >70% TTR <12h	No details	12m	80	20	0	PO: In-hospital death SO: 12m combined MACE, CIN	CR ↑in-hospital death (OR 4.7), all-cause death (OR 3.7), MACE (OR 2.0)
Jaguswski ³⁵³	2013	PR/M	4941	MVD >50%	No details	Inpat	78	22	0	PO: in-hospital mortality SO: in-hospital combined	CR ↑in-hospital mortality higher in but no diff once stratify by risk
Lee ³⁵⁴	2012	PR/M	1644	MVD >50% TTR <12h	No details	12m	67	33	0	PO: 12m combined MACE. SO: 1m MACE, individual 12m MACE	Similar outcomes but ↑revasc in CR (OR 2.5) once correct baseline diffs
Kornowski ³⁵	2011	PR/M	668	TTR <12h	Lysis, GPI, warfarin, CVA	12m	0	41	59	PO: 1y combined MACE and stent thrombosis	CR IP of 30d and 1y MACE and mortality. ↑stent thrombosis in CR

Dziewierz ⁴	2010	PR/M	777	No details	No details	12m	91	9	0	PO: 12m mortality SO: 30d mortality, revasc	CR trend ↑30d mortality (OR 2.42, p0.06) and 1y (OR 2.04, p0.09).
Hannan ¹³	2010	PR/M	4024	No details	No details	42m	81	13	6	PO: mortality in-hospital at 12m, 24m, 42m	CR ↑in-hosp mortality; trend ↑24, 42m mortality. Staged lowest
Kong ³⁵⁵	2010	PR/M	1982	MVD >70% TTR <12h	Previous MI, CABG, shock	Inpat	68	32	0	PO: in-hospital mortality	Mortality ↓with CR. CR IP for reduced mortality (OR 0.3)
Toma ⁸	2010	PR/M	2201	MVD >70% TTR <6h	Inferior MI, bleeding, LMS	3m	90	10	0	PO: 90d mortality, 90d combined MACE	CR ↑mortality and MACE at 1y. ↑procedure time in CR. Similar LOS
Cavender ³⁵⁶	2009	PR/M	28936	No details	LMS IRA, staged PCI	Inpat	89	11	0	PO: in-hospital mortality SO: PCI complications	CR ↑adjusted in-hospital mortality and only in patients with shock
Varani ⁷	2008	PR/S	399	MVD >70% TTR <24h	No details	19m	39	37	24	PO: all-cause mortality, repeat revasc	After excluded pats with shock, IRA ↑30d mortality than CR (6% v 2.8%)

***Studies highlighted in blue favour CR; yellow favour IRA-only PCI; pink favour Staged PCI; white no consensus.**

Supplemental Data 2: Retrospective studies investigating MVD revascularisation at PPCI

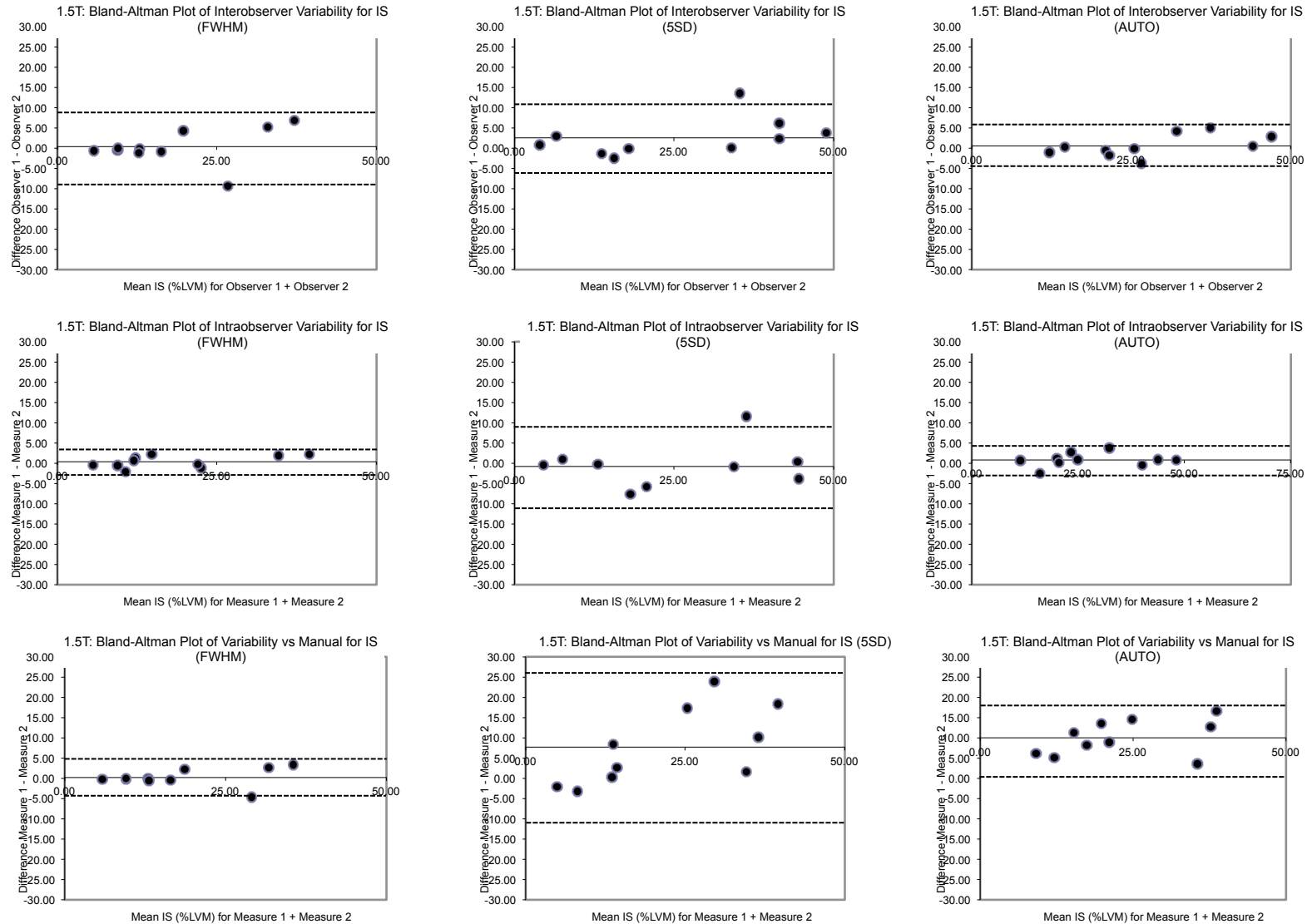
Study	Year	Design	n	Inclusion criteria	Exclusion criteria	Mean F/U	IRA (%)	CR (%)	SR (%)	Outcomes (primary [PO], secondary [SO])	Main findings
Russo ¹⁷⁹	2015	M	1038	MVD >50%	Shock, CABG, LMS	6m	75	0	25	PO: 6m mortality. SO: admission mortality; 30d MI /CVA	Staged inpat CR: ↓6m, 30d, inpat mortality; ↓PCI readmission, ↑LOS
Zhao ³⁵⁷	2014	S	326	MVD >50%	Shock, CABG	30d	46	54	0	PO: 30d CPET VO2max, VO2AT	No difference between the groups.
Mohmad ³⁵⁸	2010	S	63	MVD >70%	No details	12m	48	52	0	PO: 12m combined MACE, all-cause mortality	IRA trend for better outcome but no differences in mortality.
Han ⁴⁹	2008	S	242	MVD >70%	Shock, LMS, CKD>4	12m	62	0	38	PO: combined MACE. SO: recurrent angina, 12m LVEF	No difference MACE. ↓recurrent angina and ↑LVEF in Staged.
Qarawani ³⁵⁹	2008	S	120	MVD >70% TTR <12h	LMS, shock	12m	20	80	0	PO: in-hosp combined MACE. SO: in-hospital/12m mortality, WMS	CR: ↓in-hosp MACE, ↓LOS. Similar mortality. 15% CR pats better WMS
Rigattieri ³⁶⁰	2007	S	110	MVD >70% TTR <12h	Shock, LMS, CABG, valve	13m	46	0	54	PO: In-hospital/12m combined MACE, 12m echo LVEF	Staged PCI d6. Staged ↑in-hospital and follow-up MACE. ↓LVEF in CR
Corpus ¹⁰	2004	S	506	MVD >70% TTR <12h	CABG, LMS, ST	12m	70	5	25	PO: 12m combined MACE SO: 30d individual MACE	CR ↑reinfarction, revasc, MACE at 12m. 30d MACE and MI ↑in CR
Poyen ³⁶¹	2003	S	167	MVD >70%	No details	30d	48	52	0	PO: 30d combined MACE	CR ↓MACE (4.7% v 16.4%).
STUDIES ONLY IN CARDIOGENIC SHOCK PATIENTS											
Hussain ³⁶²	2011	M	210	MVD >70%	No details	Inpat	40	61	0	PO: In-hospital mortality	CR IP for in-hosp survival (OR 2.5)
Van Schaf ³⁶³	2010	S	161	MVD >50%	No details	12m	77	23	0	PO: 1-year mortality	No difference in 12m mortality

**Studies highlighted in blue favour CR; yellow favour IRA-only PCI; pink favour Staged PCI; white no consensus.*

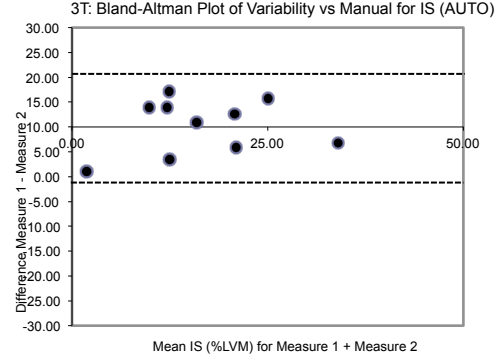
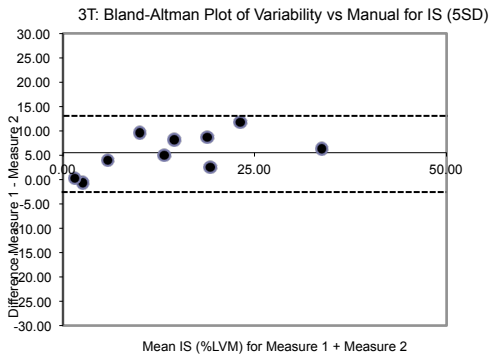
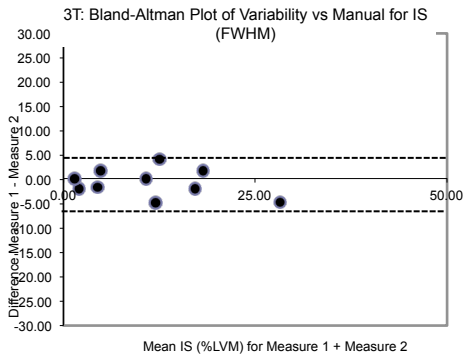
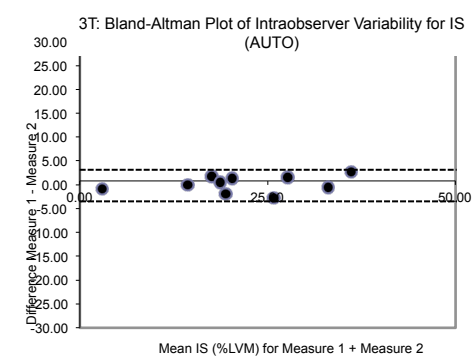
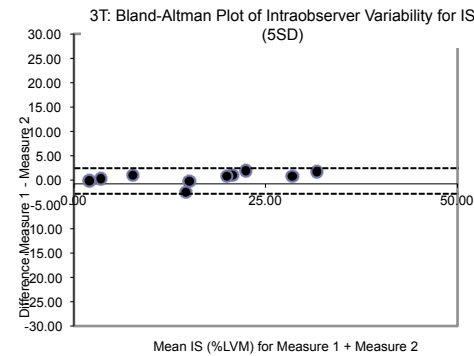
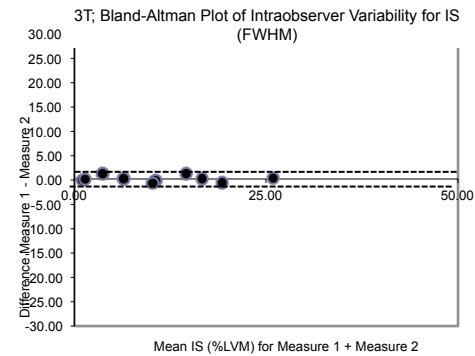
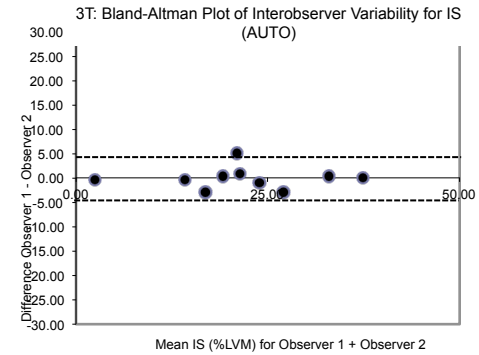
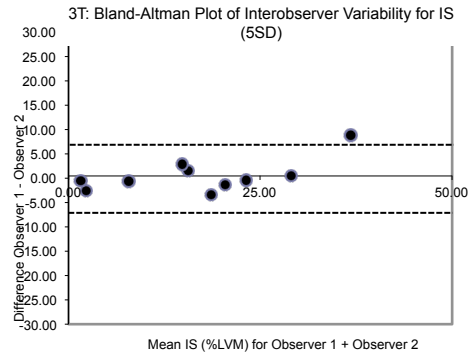
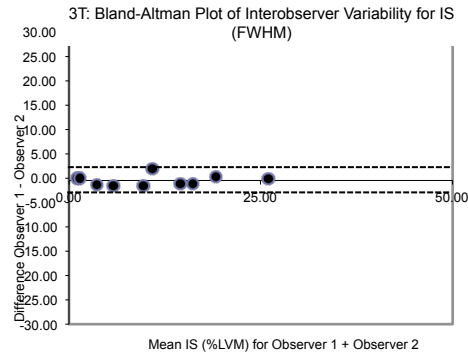
IRA= Infarct-related artery only (conventional treatment), CR= complete in-hospital revascularisation during index admission, SR= staged complete revascularisation (outpatient non-infarct related artery revascularisation)

Design: PR= prospective registry, M= multicentre, S= single-centre. *Inclusion criteria:* MVD= multivessel disease, TTR= time from symptom-onset to PPCI. *Exclusion criteria:* CABG= coronary artery bypass surgery, CTO= chronic total occlusion, CKD= chronic kidney disease, LMS= significant left-main stem disease ($\geq 50\%$), AF= atrial fibrillation. *Outcomes:* MACE= major adverse cardiovascular events, re-MI= reinfarction, CVA= cerebrovascular accident, TLR= target lesion revascularisation, TVR= target vessel revascularisation, ACS= acute coronary syndrome. *Main findings:* IRA= infarct-related artery only revascularisation, ARR= absolute risk reduction, FFR= fractional flow reserve, LVEF= left ventricular ejection fraction, LOS= length of stay, IP= independent predictor

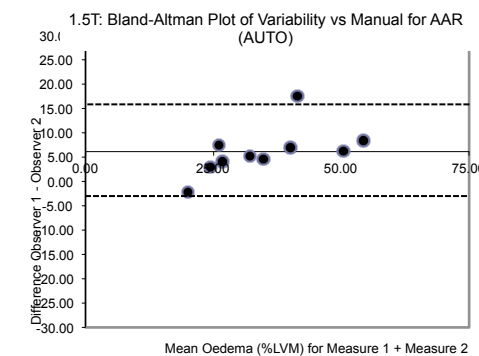
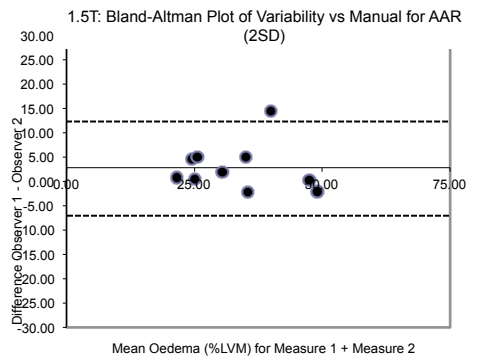
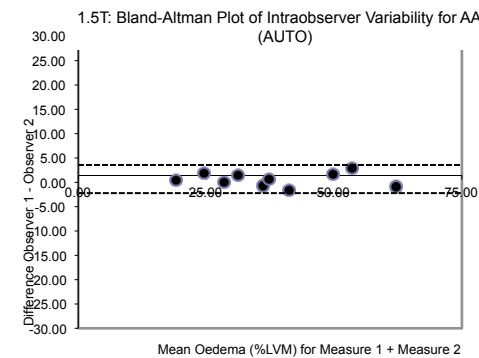
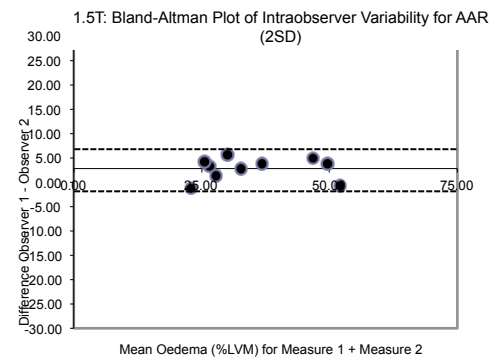
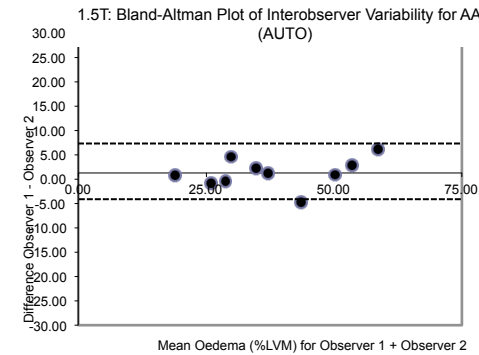
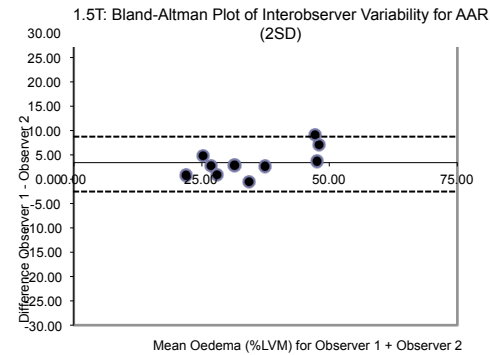
Supplemental Data 3: Bland-Altman Plots for Infarct Size (IS) Quantification at 1.5T



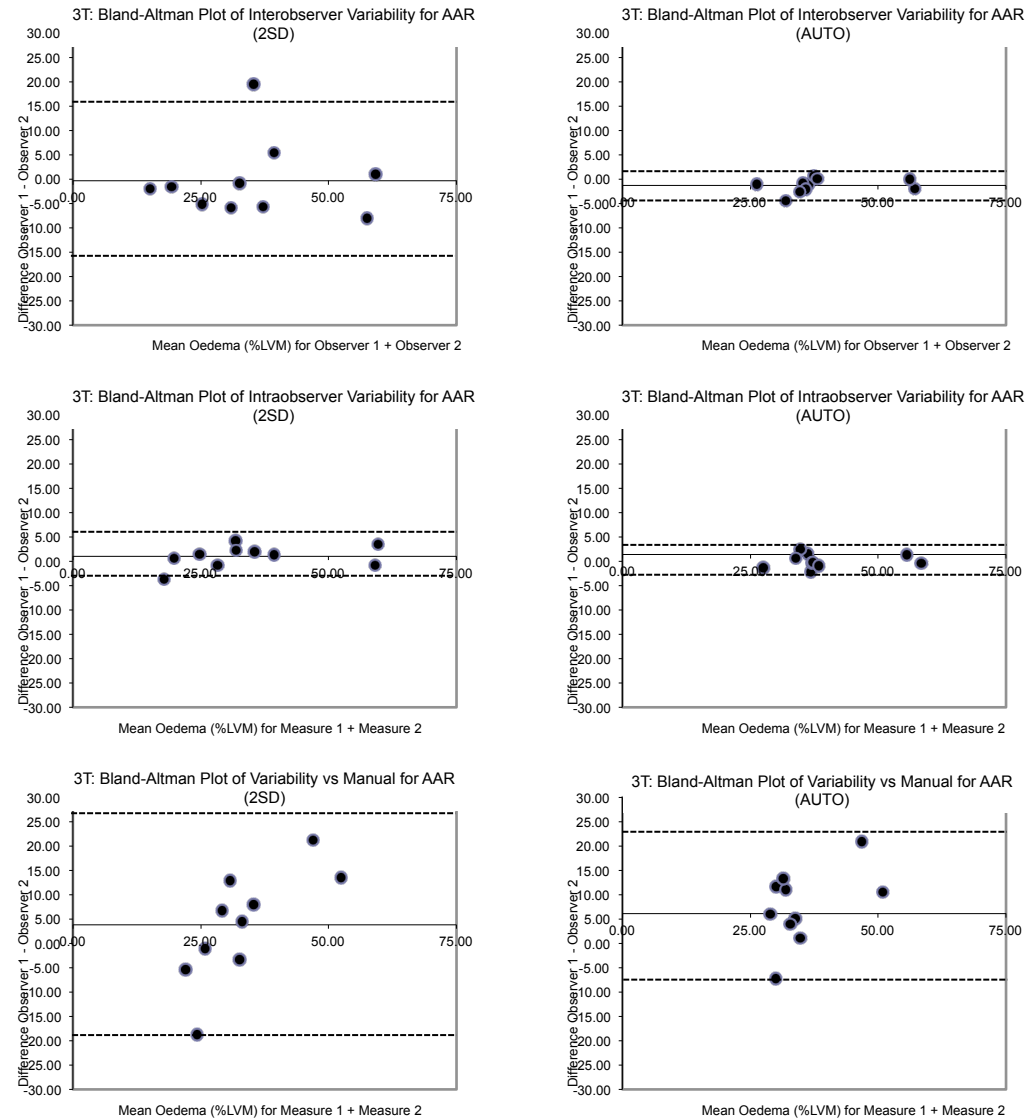
Supplemental Data 4: Bland-Altman Plots for Infarct Size (IS) Quantification at 3.0T



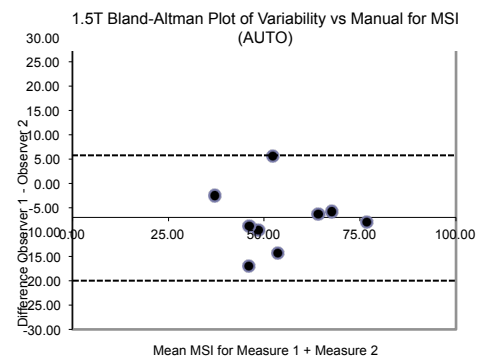
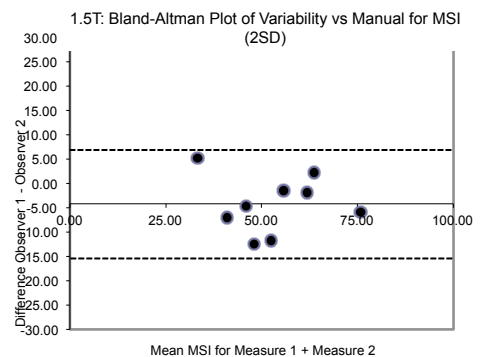
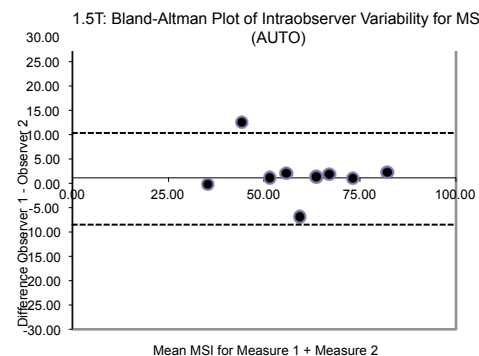
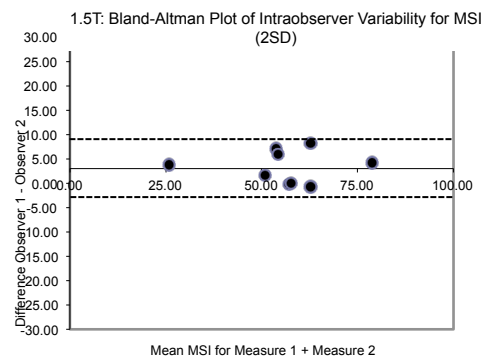
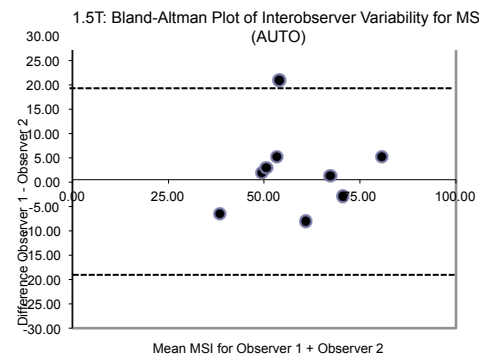
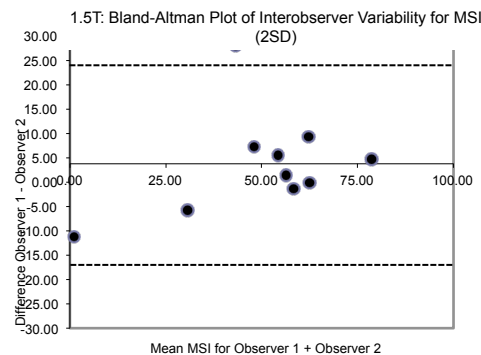
Supplemental Data 5: Bland-Altman Plots for Area At Risk (AAR) Quantification at 1.5T



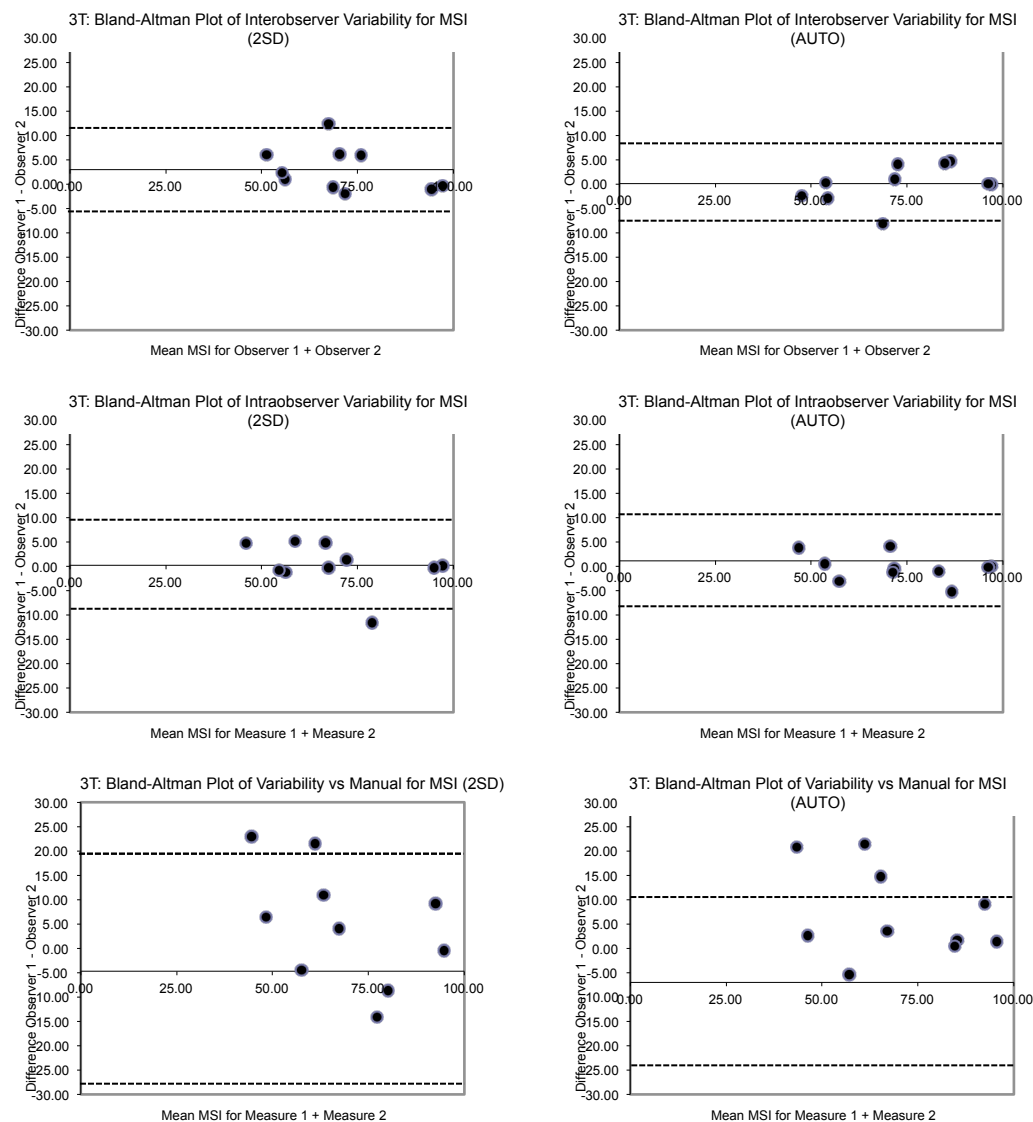
Supplemental Data 6: Bland-Altman Plots for Area At Risk (AAR) Quantification at 3.0T



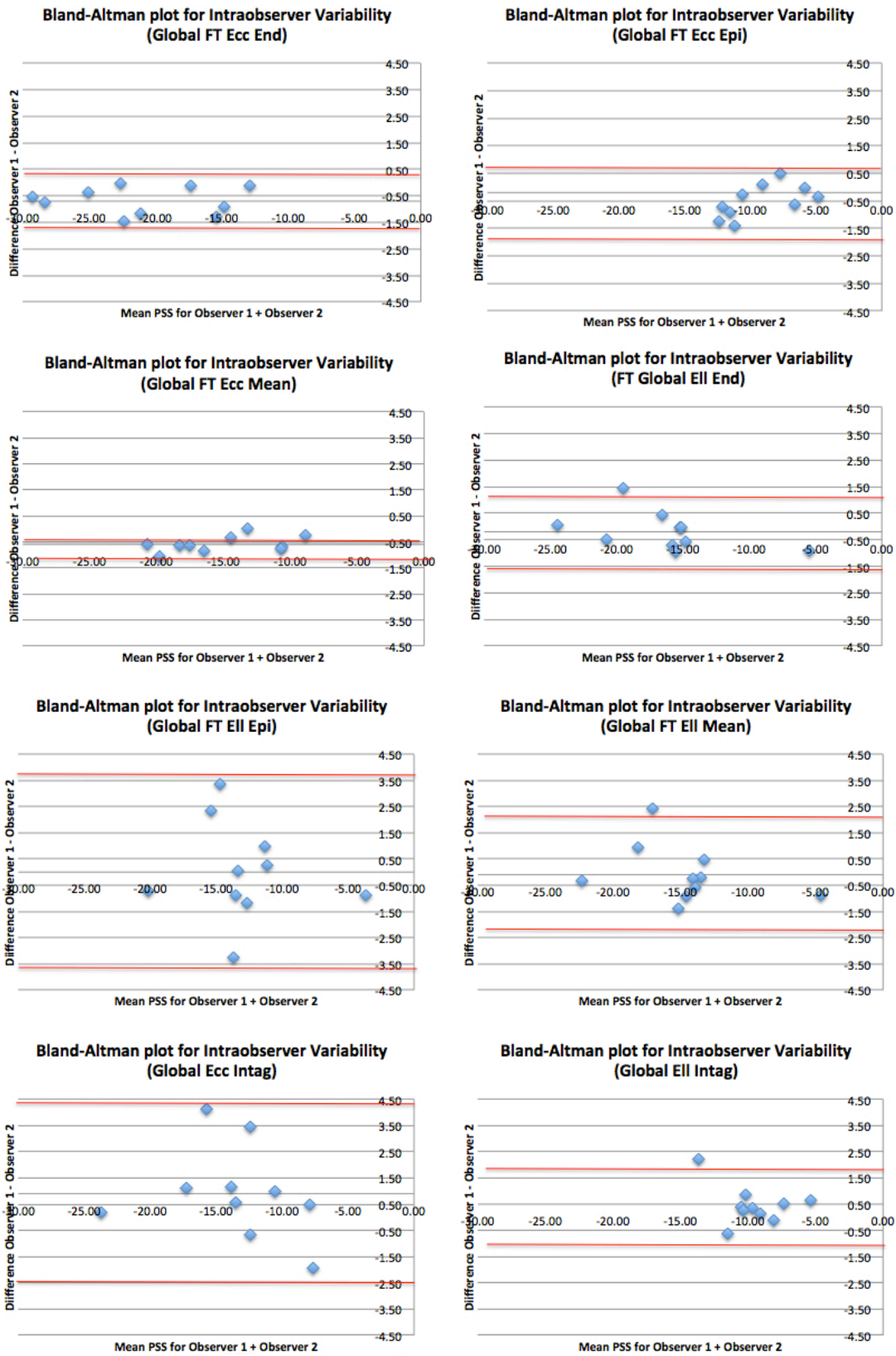
Supplemental Data 7: Bland-Altman Plots for Myocardial Salvage (MSI) Quantification at 1.5T



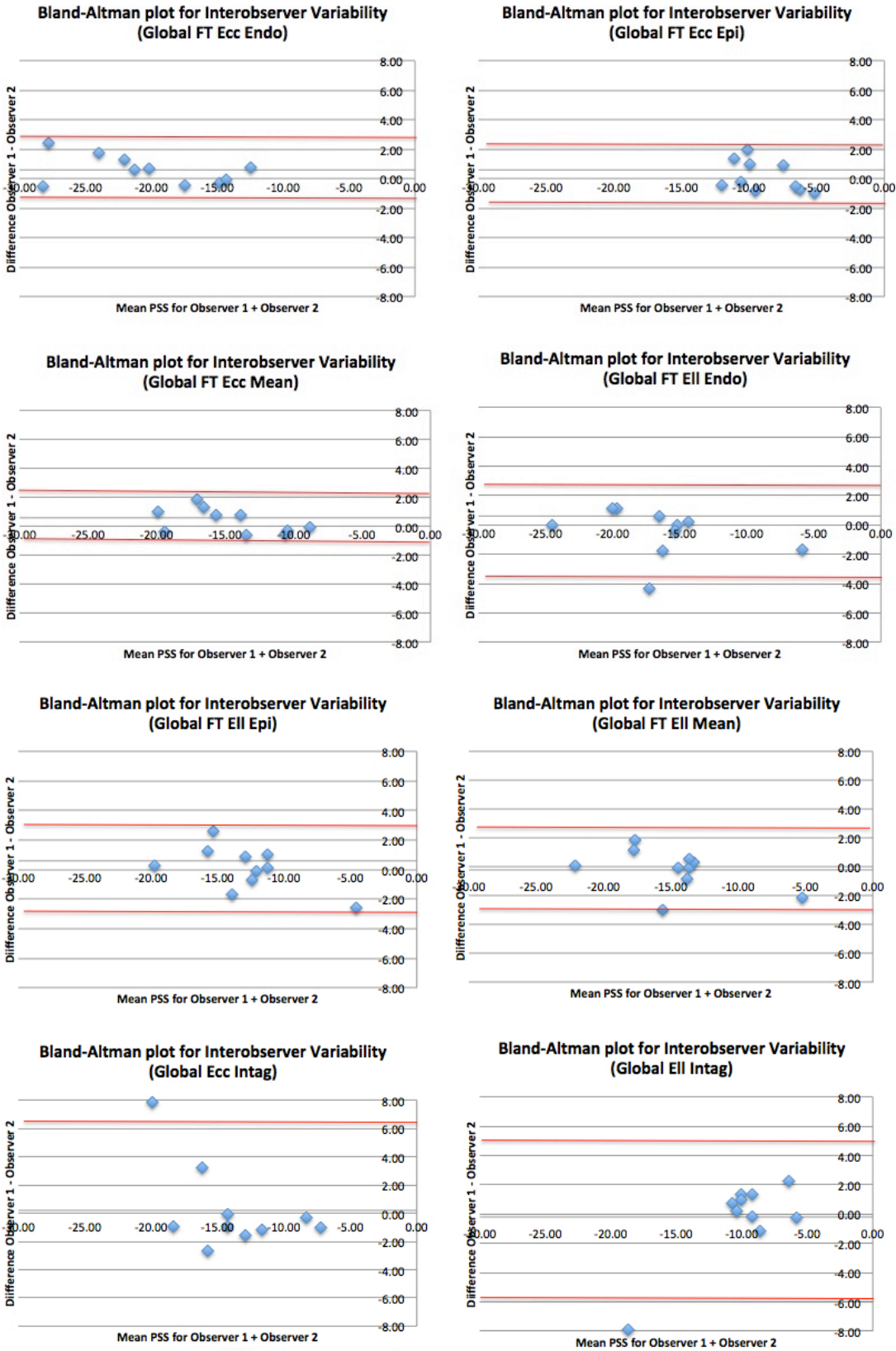
Supplemental Data 8: Bland-Altman Plots for Myocardial Salvage (MSI) Quantification at 3.0T



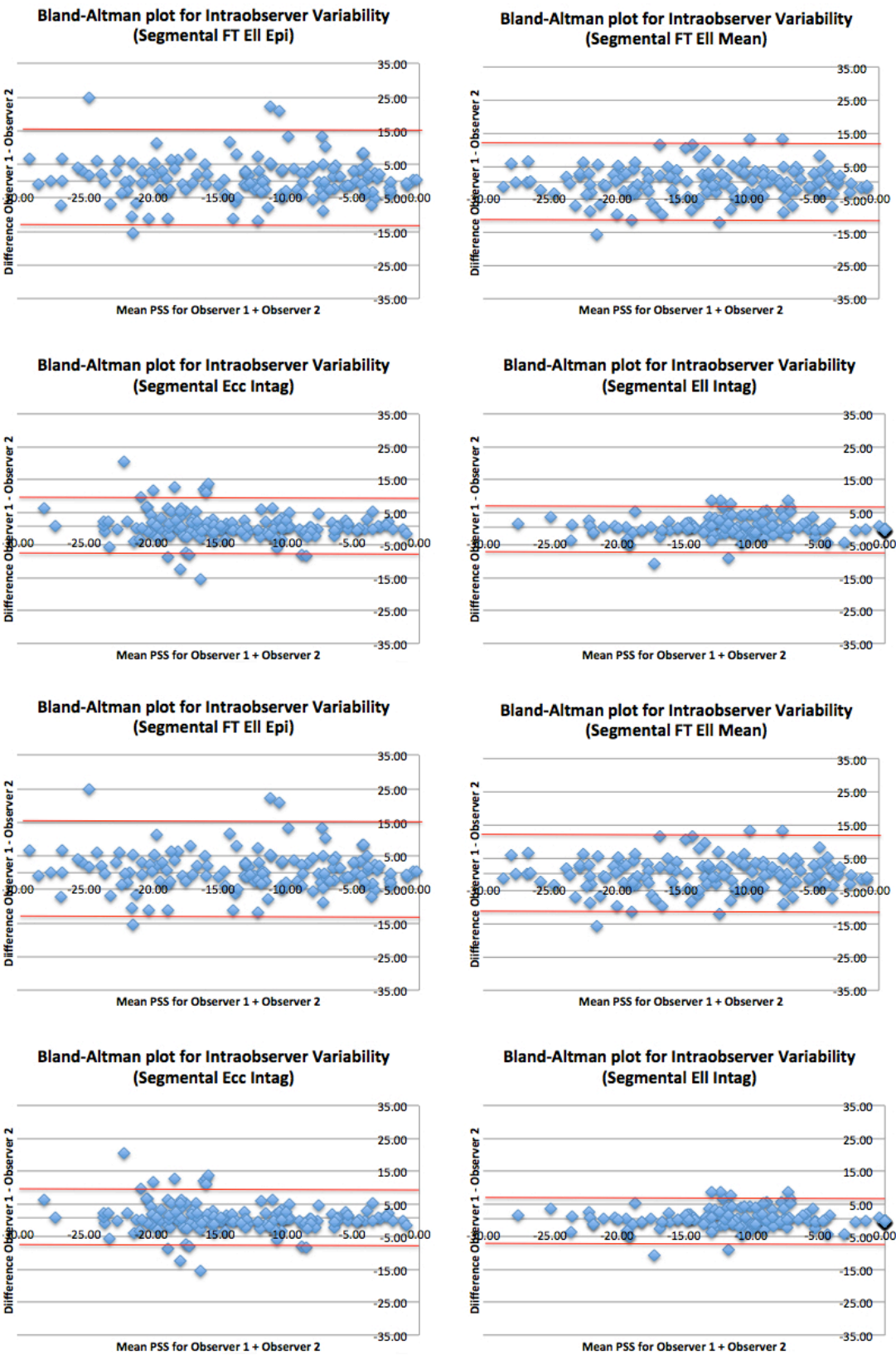
Supplemental Data 9: Bland-Altman Plots of Intraobserver Variability for Global Strain



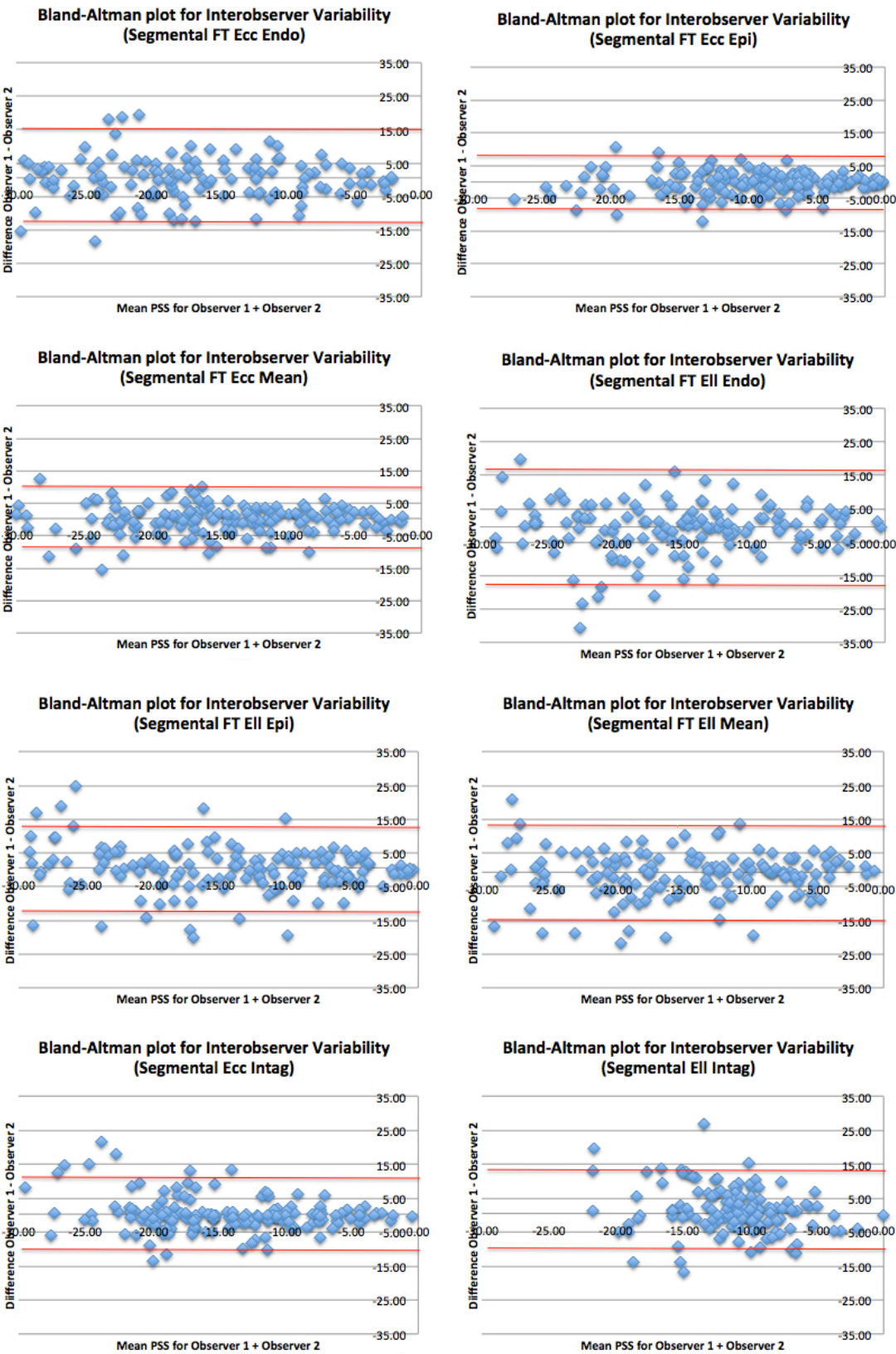
Supplemental Data 10: Bland-Altman Plots of Interobserver Variability for Global Strain



Supplemental Data 11: Bland-Altman Plots of Intraobserver Variability for Segmental Strain



Supplemental Data 12: Bland-Altman Plots of Interobserver Variability for Segmental Strain



Supplemental Data 13: Patients with ≥ 2 'acute' MI: infarct characteristics
(CvLPRIT-CMR)

ID	No. MI	IRA	MI area	IRA IS %LVM	MI 2 Area	MI 2 IS %LVM	MI 3 Area	MI 3 IS %LVM	CMR N-IRA	Actual N- IRA PCI
Complete revascularization patients										
X511	2	RCA	I	19.09	Apical	3.82	--	--	LAD	LAD
X517	2	LAD	AS	13.70	AL	0.93	--	--	Diagonal	Diagonal
X530	2	RCA	I	25.94	AS	0.06	--	--	LAD	LAD
X540	2	RCA	I	9.34	L	2.82	--	--	LCX	LAD [§]
X545	2	LAD	AS	1.56	IL	5.19	--	--	LCX	LCX
X594	3	RCA	I	4.27	AL	0.94	A	0.10	LCX+LAD	LCX+LAD
X599	3	LCX	L	9.82	I	8.93	AS	0.98	RCA+LAD	RCA+LAD
X612	2	LAD	A	42.20	I	4.37	--	--	RCA	RCA
X665	2	LCX	L	24.13	I	4.35	--	--	RCA [¶]	LAD
X695	2	RCA	I	7.75	AS	5.01	--	--	LAD	LAD
X747	2	LAD	AS	22.12	I	0.37	--	--	RCA	RCA
X757	2	LAD	AS	20.83	L	0.60	--	--	LCX	LCX
X785	2	RCA	IL	37.45	AS	0.15	--	--	LAD	LAD
X788	2	LAD	AS	4.73	IL	2.08	--	--	LCX	LCX
X791	2	LAD	AS	7.06*	IL	11.86	--	--	LCX	LCX
X798	3	LAD	AS	34.87	I	0.66	L	2.03	RCA+LCX	RCA+LCX
X808	2	LAD	AS	49.30	IL	2.85	--	--	LCX	LCX
IRA only PCI patients										
X661	2	LAD	AS	10.56	I	0.11	--	--	--	--
X709	2	LCX	IL	21.77	Apical	2.10	--	--	LAD	LAD
X716	2	RCA	I	11.25	AS	4.54	--	--	LAD	LCX
X719	2	LAD	AS	21.08	IL	4.40	--	--	--	--
X728	2	LAD	AS	24.86	I	1.50	--	--	--	--

Abbreviations: AL=Anterolateral; AS= Anteroseptal; I=inferior; IL= Inferolateral; Timing of N-IRA PCI: Index-performed at same sitting as PPCI: Staged: deferred at operator's discretion to delayed inpatient N-IRA PCI.

[§] LAD PCI crossed Diagonal; [¶] Co-dominant system.

Supplemental Data 14: CMR data excluding patients with chronic infarcts on acute CMR

Variable	CR	IRA	p
Acute CMR	n=93	n=99	
Total IS (% LVM)			
Median (IQ range)	12.5 (7.0-21.3)	12.6 (4.8-22.0)	0.48
Mean±SD	[15.5±12.3]	[15.7±13.6]	
Time from PPCI (days)	3.0 (2.0-4.2)	2.8 (1.9-3.5)	0.19
Infarct on LGE (%)	90 (96.8)	89 (89.9)	0.06
Patients with >1 infarct (%)	17 (18.3)	5 (5.1)	0.004
IRA Infarct size (% LVM)			
Median (IQ range)	12.1 (7.0-20.6)	12.4 (4.8-21.8)	0.79
Mean±SD	14.9±12.0	15.6±13.5	
Follow-up CMR	n=79	n=76	
Time to CMR (months)	9.4 (8.9-10.0)	9.3 (9.0-10.0)	0.70
Infarct on LGE (n,%)	77/79 (97.5)	67/76 (88.8)	0.024
Patients with >1 infarct (%)	15/79 (19.0)	5/76 (6.6)	0.021
Total IS (% LVM)	7.0 (3.0-13.5)	7.4 (3.0-14.7)	0.37
Perfusion	n=77	n=73	
Ischaemic burden (%)*	3.0±7.6	3.7±9.7	0.64
Ischaemia present (%)	15/77 (19.5)	15/73 (20.5)	0.87
Ischaemic burden (%) in patients with ischaemia	14.4±11.3	17.9±14.6	0.46
Ischemic burden > 20%	5 (6.5%)	5 (6.8%)	0.93

IS= infarct size, LVM= left ventricular mass, PPCI= primary percutaneous coronary intervention, IRA= infarct-related artery, LGE= late gadolinium enhancement, IS=infarct size

Acute IS corrected (age, anterior MI, TIMI pre, TTR, sex, DM, AAR, Rentrop) gives a p-value of 0.569 comparing IRA vs. CR

Supplemental Data 15: SEE and *Ecc* as predictors of segmental recovery where SEE \geq 50%

Functional improvement

In dysfunctional segments with $>50\%$ SEE (SEE 4-5), SEE strongly predicted functional improvement (model $p=0.002$, 'SEE 51-75%': OR 2.3 vs. 'SEE 76-100%', $p=0.008$). AUC was 0.924 ($p=0.002$). The other variables did not predict improvement (*Ecc*: $p=0.259$; MSI: $p=0.927$; MVO: $p=0.900$; IMH: $p=0.286$). Combining SEE *and* the other variables did not improve predictive accuracy compared with SEE alone.

Functional normalisation

Similarly, SEE was a strong predictor of functional normalisation (model $p=0.002$, 'SEE 51-75%': OR 6.7 vs. 'SEE 76-100%', $p=0.008$). AUC was 0.918 ($p=0.002$). The only other variable that predicted normalisation was MVO (MVO: $p=0.002$; *Ecc*: $p=0.427$; MSI: $p=0.837$; IMH: $p=0.117$). Combining SEE *and* MVO improve predictive accuracy compared with SEE alone ($p=0.009$).

Supplemental Data 16: Segmental function and predictors of segmental recovery by treatment

Segmental function according to segmental extent of LGE and strain stratified by revascularisation strategy

IRA-only revascularisation

WMS at Acute CMR	1: Normal (n=826)	2: Hypokinetic (n=260)	3: Akinetic (n=150)	p
SEE (%)	3.2±9.1	24.9±22.5	53.6±29.0	<0.001
Peak segmental Ecc (%)	-23.6±10.2	-15.1±8.7	-9.1±7.1	<0.001
MSI (%)	99.0 (74.5, 100.0)	57.2 (24.1, 83.5)	17.3 (0.0, 49.4)	<0.001
MVO (n, %)	4/826 (0.5)	26/260 (10.0)	44/150 (29.3)	<0.001
IMH (n, %)	1/365 (0.3)	8/118 (6.8)	14/73 (19.2)	<0.001

SEE= segmental extent of enhancement; Ecc= peak segmental circumferential strain; MSI= myocardial salvage; MVO presence of microvascular obstruction (MVO) and IMH= intramyocardial haemorrhage. No segments had WMS of 4 or 5 at acute CMR.

Correlation between SEE at acute CMR and WMS at acute CMR was $r=0.712$ ($p<0.001$), and between SEE at acute CMR and WMS at follow-up CMR was $r=0.631$ ($p<0.001$). Correlation between Ecc at acute CMR and WMS at acute CMR was $r=0.497$ ($p<0.001$), and between Ecc at acute CMR and WMS at follow-up CMR was $r=0.424$ ($p<0.01$).

Complete revascularisation

WMS at Acute CMR	1: Normal (n=961)	2: Hypokinetic (n=239)	3: Akinetic (n=188)	p
SEE (%)	4.0±10.2	23.8±21.4	51.0±29.3	<0.001
Peak segmental Ecc (%)	-23.5±10.3	-14.8±9.6	-10.0±8.6	<0.001
MSI (%)	98.4 (71.2, 100.0)	58.1 (25.7, 83.2)	18.3 (0.0, 52.6)	<0.001
MVO (n, %)	3/958 (0.3)	22/239 (9.2)	66/188 (35.1)	<0.001
IMH (n, %)	0/348 (0.0)	4/123 (3.3)	27/125 (21.6)	<0.001

SEE= segmental extent of enhancement; *Ecc*= peak segmental circumferential strain; MSI= myocardial salvage; MVO presence of microvascular obstruction (MVO) and IMH = intramyocardial haemorrhage. No segments had WMS of 4 or 5 at acute CMR.

Correlation between SEE at acute CMR and WMS at acute CMR was $r=0.676$ ($p<0.001$), and between SEE at acute CMR and WMS at follow-up CMR was $r=0.603$ ($p<0.001$). Correlation between *Ecc* at acute CMR and WMS at acute CMR was $r=0.479$ ($p<0.001$), and between *Ecc* at acute CMR and WMS at follow-up CMR was $r=0.409$ ($p<0.01$).

Predictors of segmental functional recovery in dysfunctional segments stratified by revascularisation strategy

IRA-only revascularisation

Functional improvement

All of the variables predicted segmental functional improvement with similar accuracy: SEE: $p<0.01$, AUC 0.818; MSI: $p<0.01$, AUC 0.823; *Ecc*: $p<0.01$, AUC 0.822; MVO: $p<0.01$, AUC 0.802, IMH: $p<0.01$, AUC 0.807. Only the addition of MVO to SEE improved predictive accuracy of SEE alone (SEE+MVO vs. SEE alone, $p=0.020$; AUC: 0.851 vs. 0.818).

Functional normalisation

All of the individual variables predicted segmental functional improvement with similar accuracy: SEE: $p<0.01$, AUC 0.891; MSI: $p<0.01$, AUC 0.838; *Ecc*: $p<0.01$, AUC 0.869; MVO: $p<0.01$, AUC 0.802, IMH: $p<0.01$, AUC 0.840. None of the variables provided incremental predictive accuracy when added to SEE, vs. SEE alone.

Complete revascularisation

Functional improvement

All of the individual variables predicted segmental functional improvement with similar accuracy: SEE: $p<0.01$, AUC 0.870; MSI: $p<0.01$, AUC 0.860; *Ecc*: $p<0.01$, AUC

0.846; MVO: $p < 0.01$, AUC 0.831, IMH: $p < 0.01$, AUC 0.837. None of the variables provided incremental predictive accuracy when added to SEE, vs. SEE alone.

Functional normalisation

All of the individual variables predicted segmental functional improvement with similar accuracy: SEE: $p < 0.01$, AUC 0.896; MSI: $p < 0.01$, AUC 0.874; *Ecc*: $p < 0.01$, AUC 0.866; MVO: $p < 0.01$, AUC 0.818, IMH: $p < 0.01$, AUC 0.821. None of the variables provided incremental predictive accuracy when added to SEE, vs. SEE alone.

Supplemental Data 17: Patients with ≥ 2 'acute' MI: infarct characteristics
(Staged vs Immediate)

ID	No. MI	IRA	MI area	IRA IS %LVM	MI 2 Area	MI 2 IS %LVM	MI 3 Area	MI 3 IS %LVM	CMR N-IRA	Actual N- IRA PCI
Immediate CR										
X511	2	RCA	I	19.09	Apical	3.82	--	--	LAD	LAD
X594	3	RCA	I	4.27	AL	0.94	A	0.10	LCX+LAD	LCX+LAD
X599	3	LCX	L	9.82	I	8.93	AS	0.98	RCA+LAD	RCA+LAD
X612	2	LAD	A	42.20	I	4.37	--	--	RCA	RCA
X665	2	LCX	L	24.13	I	4.35	--	--	RCA [¶]	LAD
X695	2	RCA	I	7.75	AS	5.01	--	--	LAD	LAD
X747	2	LAD	AS	22.12	I	0.37	--	--	RCA	RCA
X788	2	LAD	AS	4.73	IL	2.08	--	--	LCX	LCX
Mean						3.73		0.54		
Staged CR										
X517	2	LAD	AS	13.70	AL	0.93	--	--	Diag	Diag
X530	2	RCA	I	25.94	AS	0.06	--	--	LAD	LAD
X540	2	RCA	I	9.34	L	2.82	--	--	LCX	LAD [§]
X545	2	LAD	AS	1.56	IL	5.19	--	--	LCX	LCX
X757	2	LAD	AS	20.83	L	0.60	--	--	LCX	LCX
X785	2	RCA	IL	37.45	AS	0.15	--	--	LAD	LAD
X791	2	LAD	AS	7.06*	IL	11.86	--	--	LCX	LCX
X798	3	LAD	AS	34.87	I	0.66	L	2.03	RCA+LCX	RCA+LCX
X808	2	LAD	AS	49.30	IL	2.85	--	--	LCX	LCX
Mean						2.79				

Abbreviations: AL= Anterolateral, AS= Anteroseptal, I= Inferior, IL= Inferolateral;
Diag= Diagonal vessel, Timing of N-IRA PCI: Immediate= One-time (performed at
same sitting as PPCI), Staged: deferred at operator's discretion to delayed inpatient
N-IRA PCI.

*AS MI associated with MVO and therefore classed as the IRA. [§] LAD PCI crossed
Diagonal; [¶] Co-dominant system.

Supplemental Data 18: CMR data excluding patients with chronic infarcts on acute CMR

Variable	Immediate CR	Staged CR	p
Acute CMR	n=61	n=27	
Total IS (% LVM)			
Median (IQ range)	11.6 (6.1-16.1)	19.1 (12.2-19.1)	0.012
Mean±SD	[12.4±9.9]	[22.7±14.9]	(0.021)*
Time from PPCI (days)	2.7 (1.8-3.4)	4.1 (2.7-5.2)	0.016
Infarct on LGE (%)	58/61 (95.1)	27/27 (100)	0.24
Patients with >1 infarct (%)	7/61 (11.5)	9/27 (33.3)	0.014
IRA Infarct size (% LVM)			
Median (IQ range)	10.5 (4.9-14.9)	19.1 (9.3-36.2)	0.006
Mean±SD	11.9±9.5	21.7±14.8	(0.050)*
Acute MSI (%)	62.7 (39.4-76.2)	35.2 (4.6-67.6)	0.007
			(0.023)*
Final MSI (%)	87.0 (70.0-91.1)	64.3 (46.5-83)	0.005
			(0.06)*
Follow-up CMR	n=51	n=23	
Time to CMR (months)	9.3 (9.0-9.9)	9.4 (9.1-10.5)	0.65
Infarct on LGE (n,%)	49/51 (96.1)	23/23 (100)	0.34
Patients with >1 infarct (%)	7/51 (13.7)	6/23 (26.1)	0.20
Total IS (% LVM)	4.9 (2.3-9.7)	13.5 (5.8-24.3)	<0.001
	7.2±8.0	16.6±13.9	(<0.040)*
Perfusion	n=49	n=23	
Ischaemic burden (%)*	2.6±7.0	3.7±9.2	0.61
Ischaemia present (%)	10/49 (20.4)	5/23 (21.7)	0.90
Ischaemic burden (%) in patients with ischaemia	13.1±10.5	16.9±13.5	0.56
Ischemic burden > 20%	3/49 (6.1%)	2/23 (8.7%)	0.69

Data presented as n/N (%), mean±SD or median (IQR).

IS= infarct size, LVM= left ventricular mass, PPCI= primary percutaneous coronary intervention, IRA= infarct-related artery, CR= complete revascularization, LGE= late gadolinium enhancement, IS=infarct size, MSI= myocardial salvage index.

Analyzable oedema imaging available in 76% of patients in both groups.

* Adjusted for known predictors of IS (anterior MI, time to revascularization, diabetes, TIMI grade pre-PPCI) and important baseline variables significantly varying between the two groups (TIMI grade post-PPCI, SYNTAX score, dual antiplatelet therapy choice, glycoprotein inhibitor/bivalirudin use for N-IRA PCI)

Appendix 1: Verbal assent document inviting study participation

University Hospitals of Leicester 

NHS Trust

Glenfield Hospital
Groby Road
Leicester
LE3 9QP

Tel: 0300 303 1573
Fax: 0116 258 3950
Minicom: 0116 287 9852

VERBAL ASSENT SHEET TO INVITE PARTICIPATION IN THE CVLPRIT STUDY

“Complete Versus Lesion only Primary PCI Trial”

Version 6 (30th October 2010)

This should be read to patients and the result of the discussion documented in the clinical notes

- Your doctors have diagnosed that you are having a heart attack, which means that it is likely one of the arteries in your heart is blocked reducing blood supply to your heart muscle.
- In this hospital the usual treatment is to open the blocked artery with a balloon and stent using a procedure called angiography in which a fine tube is passed into the heart.
- Sometimes more than one artery is blocked or narrowed. At the moment we do not know if you have only one blocked artery causing your heart attack, or you have another one which is narrowed or blocked.
- We are undertaking a research study to try and find out whether it is better to treat just the artery causing the heart attack (which is a routine approach in many centres), or to treat all the arteries that look narrowed or blocked at the same time.
- The title of the study is CVLPRIT (Complete Versus Lesion only Primary PCI Trial). If we find that you have more than one artery narrowed or blocked, we would like to invite you to take part in the study.
- If you agree, we will either treat only the blocked artery causing the heart attack or we will attempt to open all the affected arteries.
- Allocation to single artery or multiple artery treatment will be performed at random (rather like tossing a coin to make the comparison fair) as we do not know which treatment is better.
- We are also asking for your permission to record simple details of your health condition and treatments in our confidential research record as part of a “registry”.
- After you have had your early treatment and are recovering, we will provide you with further information about the study and you will have another opportunity to discuss this and decide if you wish to carry on in the study or not.
- Whether you decide to take part or not is entirely up to you, and in any case you will receive the best care we can provide for your condition.

Appendix 2 Interim DSMB approval letter

ROGER J C HALL MD FRCP

**Consultant Cardiologist
Norfolk and Norwich University Hospital NHS Trust
Colney
Norwich
NR4 7UY**

**Professor of Cardiology
School of Medicine,
Health Policy and Practice
University of East Anglia
Norwich
NR4 7TJ**

RJCH/lav

**Tel: 01603 593606
Fax: 01603 259401**

Dr R H Swanton
Chairman, Trial Steering Committee
Cardiology Department
The Heart Hospital
16-18 Westmoreland Street
London
W1G 8PH

23 October 2012

Dear Howard

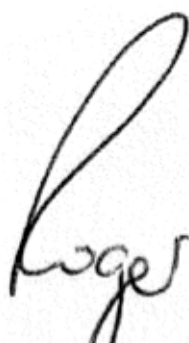
Re: CVLPRIT Trial

Further to our recent exchange of emails and letters I am pleased to say that the DMC met on 22/10/12. We reviewed the general statistics of the trial as well as the results to date. The latter review was carried out in camera by medical members of the DMC and statisticians without any members of the trial organisation present.

Review of the information to date led to the conclusion that there are no problems apparent that would prejudice the trial continuing. Under these circumstances our view is that the trial can continue safely.

The only concern of the DMC, which is not a matter that would lead to stopping the trial, is that there seems to be a significant disparity between the centres in terms of the numbers of patients entered into the registry and into the trial. The DMC is somewhat concerned that the data in the end may be biased by the fact that there seems to be a large degree of choice among operators as to which cases they should do. Clearly this is not something that can be changed at this stage and it is simply an observation.

With best wishes
Yours sincerely



COMPLETE VERSUS LESION-ONLY
PRIMARY PCI PILOT CARDIAC MRI
SUBSTUDY (CVLPRI-T-CMR)

STATISTICAL ANALYSIS PLAN FOR FINAL ANALYSIS

Study title: Complete versus lesion-only primary PCI pilot Cardiac MRI substudy

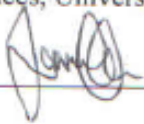
Short title: CVLPRI-t-CMR


Ethics no: EME 10/27/01

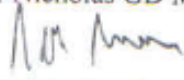
Funded by: National Institute of Health Research (NIHR) EME project grant


SAP version: v3.0

Date: 27th May 2014

Prepared by: Dr Jamal N Khan, Clinical Research Fellow, Dept. of Cardiovascular Sciences, University of Leicester
 27/5/14

Approved by: Dr Gerry P McCann, Consultant Cardiologist/NIHR Intermediate Fellow, Dept. of Cardiovascular Sciences, University of Leicester
 28/5/14

Approved by: Dr Nicholas GD Masca, BRU Statistician, University of Leicester
 28/5/14

Approved by: Prof. Arne Ring, Clinical Trials Unit Principal Statistician, University of Leicester
 28/5/14

1. INTRODUCTION

This statistical analysis plan explains the statistical analyses to be undertaken on the CvLPRI-CMR substudy data. This document is to be read in conjunction with the CVLPRI-t main study final protocol (dated 30th March 2011) and CVLPRI-t-CMR final protocol (dated August 2010). The term 'acute CMR scan' refers to the initial CMR scan performed at approximately 48 hours post Primary Percutaneous Coronary Intervention (PPCI). The term 'follow up CMR scan' refers to the second and final CMR scan performed at 9-months post PPCI.

1.1 STUDY BACKGROUND

There are >100,000 ST-elevation myocardial infarctions (STEMI) in the UK annually³⁶⁴. PPCI is the preferred revascularisation strategy for STEMI. Up to 50% of STEMI have multivessel disease (MVD) with severe coronary stenosis (>70%) in non-infarct related arteries (N-IRA's)²¹. Current guidelines recommend an infarct-related artery only ('IRA-only') revascularisation strategy rather than complete revascularisation (multivessel PCI, 'CR') unless the patient is in cardiogenic shock²⁵⁷. However these are based on limited evidence due to a lack of prospective and randomised controlled studies, which have shown conflicting results.

Benefits of CR strategy	Risks of CR strategy
Reduced infarct size, increased myocardial salvage	Infarct size may be increased by peri-procedural MI ^{29, 30}
Improve flow to remote regions, role in ventricular remodelling ³¹	Increased risk of contrast-induced nephropathy ³²
Manage unstable N-IRA lesions ³⁴	Increased procedural time and radiation exposure ⁸
Reduced overall hospital stay and total cost of care	Prothrombotic milieu risks stent thrombosis ³⁵
Reduced ischaemia burden, prognostic post MI ³⁶	Vasospasm, endothelial dysfunction overestimate N-IRA
Reduced need for outpatient ischaemia testing, revasc ¹⁶	Limited ability to discuss N-IRA treatment with patient ³⁴
Reduce risk of vascular complications (1 access site)	Complications of treating N-IRA at PPCI could be fatal ³⁴

Cardiac MRI (CMR) assessment of revascularisation following PPCI in STEMI

Previous studies have included no imaging of infarct size (other than echocardiographic ejection fraction [%EF]), microvascular obstruction or salvaged myocardium, all of which confer additional prognostic information other than that obtained by LVEF.

(a) Infarct size (IS) and left ventricular (LV) volumes

Limiting IS with reperfusion improves LV function and attenuates subsequent cardiac remodelling. CMR is the gold standard for quantification of LV volumes and function and late gadolinium contrast imaging (LGE) quantifies IS with unique precision³⁶⁵.

(b) Microvascular Obstruction (MVO) and LV remodelling

MVO on LGE imaging ('late MVO', [L-MVO]) is a strong independent predictor of LV remodelling and adverse prognosis, independently of IS, EF and cardiac volumes¹⁵⁴.

(c) Myocardial salvage index (MSI)

The MSI (proportion of non-infarcted ischaemic area at risk) is an important prognostic marker. Injured myocardium develops oedema, producing high signal intensity on T2-weighted images. The area of oedema closely approximates the AAR¹³⁵. MSI was the strongest independent predictor of 6-month MACE in a study of 208 PPCI patients²²³.

1.2 PURPOSE OF STUDY

CVLPRI-t-CMR is not funded for any additional imaging other than that driven by clinical practice. CMR offers a unique, robust assessment of revascularisation for STEMI. CMR infarct characteristics are the best-proven *surrogate* markers of medium-term outcome in patients with STEMI treated by PPCI^{81, 154, 223}. Embedding CMR in the main CVLPRI-t study will give a more robust assessment of the differences in the *efficacy* and *safety* of the revascularisation strategies being tested that may only be seen with a much larger population if there is reliance on clinical outcomes alone. We will also obtain a greater understanding of the *mechanisms* by which differences in outcome between the two groups may result. The risk of new

myocardial infarction from PCI to the N-IRA's during PPCI and the effect on MSI and LV ventricular remodelling and medium-term outcome will be well-established for the first time through the use of CMR.

1.3 STUDY OBJECTIVES

1.3.1 PRIMARY OBJECTIVES

- To determine whether infarct size (IS, expressed as a % of LV mass) is different in the CR versus IRA-only revascularisation strategies.

1.3.2 SECONDARY OBJECTIVES

- To examine whether myocardial salvage and microvascular injury (MVO, IMH) differ in the CR versus IRA-only revascularisation strategies.
- To determine whether LV function and volumes differs following the CR versus IRA-only revascularisation strategies.
- To determine whether CR reduces ischaemic burden in the medium-term.
- To determine whether medium-term (12-month) clinical outcomes differ in the CvLPRIT-CMR substudy following CR versus IRA-only revascularisation strategies.

1.4 STUDY DESIGN

1.4.1 STUDY TYPE

Multi-centre, prospective, open, randomized controlled clinical trial with blinded end-point (CMR) analysis (PROBE study design). The main analyses for primary and secondary outcomes will be according to **Intention To Treat (ITT)** where all patients will be included according to their randomization status. **Protocol violation** occurs where the revascularisation strategy received deviates from that allocated at randomisation (i.e. IRA-only randomisation but received CR; or CR randomisation but only IRA treated). If >5% of patients deviate from protocol, **per protocol analyses** will also be undertaken. This decision will be finalized by the TSC.

1.4.2 SAMPLE SIZE AND POWER

There are no published CMR data comparing the different treatment strategies.

There are however considerable data on unselected patients undergoing PPCI and CMR IS^{55, 154, 314} which is similar to that seen in our centres. 100 patients in each arm has 81% power to detect a 4% absolute difference in IS (using Cohen's d), assuming IS ~20% of LV mass and standard deviation of $\pm 10\%$, $\alpha=0.05$ and 2-tailed given that either treatment strategy may be associated with larger IS. New IS of 4% of LV mass has been shown to be associated with adverse prognosis in CAD patients with PCI-related injury³⁰.

1.4.3 STUDY POPULATION

Patients in England with acute STEMI with MVD at the time of PPCI.

1.4.4 RECRUITMENT

If patients met all inclusion criteria, they were asked to give '**assent**' to the study after reading a shortened consent form before angiography and then after angiography they were asked to give further verbal assent before randomisation. Patients were **randomised** on-table, **prior to PCI**, via a dedicated 24/7 telephone randomisation service to: **Group 1 [in-hospital CR]** or **Group 2 [in-hospital 'IRA-only' revascularization]**. Randomisation is **stratified using minimization** by anterior or non-anterior STEMI (ECG guided) and time to reperfusion ($\leq >3\text{hrs}$) since these are predictors of outcome²⁶⁴. Randomisation is run through the CTEU at the Royal Brompton Hospital and takes <90 seconds.

Those giving **consent** were given the full patient information sheets within 24 hours and asked to give full written informed consent to continued participation in the study including the optional CMR substudy. The assent process has been utilized in another trial of acute MI (STREAM) and has ethical committee approval. At all times patients were told that they are under no obligation to participate in the research study and consent can be withdrawn at any time without prejudice to their treatment.

1.4.5 ELIGIBILITY

Inclusion

- Suspected or proven acute STEMI
- Significant ST elevation or left bundle branch block (LBBB) on ECG
- < 12 hrs of symptom onset
- Scheduled for PPCI for clinical reasons
- Provision of verbal assent followed by written informed consent
- **MVD:** IRA plus ≥ 1 N-IRA with >70% stenosis in one plane or >50% in two planes. N-IRA should be >2mm diameter and be suitable for stent implantation.

Exclusion

- Any exclusion criteria for PPCI
- < 18 years age
- Clear indication for, or contraindication to multivessel PPCI according to operator
- Previous Q-wave myocardial infarction
- Patients with prior coronary artery bypass grafting (CABG) surgery
- Cardiogenic Shock
- Ventricular septal defect or moderate/severe mitral regurgitation
- Chronic kidney disease ($Cr > 200 \mu\text{mol/l}$ or $eGFR < 30\text{ml/min}$)
- Suspected or confirmed stent thrombosis
- Where the only significant N-IRA lesion is a chronic total occlusion (CTO)
- **Standard MRI contraindications (pacemaker, ICD/CRT, intracranial implant unsuitable for use in magnetic field, severe claustrophobia, weight >200kg)**

1.4.6 MONITORING

Coordinating Centre: The coordinating centre is Glenfield Hospital, Leicester (with support from Royal Brompton CTEU).

Data and Safety Monitoring Board (DSMB)/Interim Review: CVLPRI-t-CMR is overseen by an independent DSMB. An interim data review was performed by the DSMB in October 2012 (16 months after recruitment started, at which point 196 patients had been recruited and 29 had 12-months follow-up), which was satisfied

with progress to date and for the trial to continue safely (DSMB letter in Supplemental Material 1).

2. OUTCOMES

2.1 PRIMARY OUTCOME

- Infarct size (expressed as a % of LV mass)

2.2 SECONDARY OUTCOMES

- Number of discrete infarcts on CMR pre-discharge and at 9-months follow-up.
- Percentage area of each myocardial segment demonstrating infarct on LGE on CMR pre-discharge and at 9-months follow-up.
- Infarct size (expressed as a % of LV mass) at 9-months follow-up.
- Myocardial salvage index pre-discharge.
- Extent of MVO (expressed as % of LV mass, and % of infarct size) pre-discharge.
- Extent of IMH (expressed as a % LV mass, % of infarct size, and % of MVO) pre-discharge.
- LV end-diastolic volume (LVEDV), LV end-systolic volume (LVESV), LV ejection fraction, LV cardiac output, pre-discharge and at 9-months.
- Proportion of patients with LV remodeling (increase in LVEDVI >20% between acute CMR scan and 9 month follow-up CMR).
- Proportion of dysfunctional segments showing improvement at 9-months (improvement in wall-motion score of ≥ 1)
- New MI (CMR detected) at 9-months
- Proportion of patients with ischemia and extent of ischaemic burden at 9-months.
- Circumferential and longitudinal strain pre-discharge and at 9-months.
- Wall motion score assessment pre-discharge and at 9-months.

- Presence of LV thrombus, RV infarction on CMR pre-discharge and at 9-months.

2.3 SAFETY OUTCOMES

Since additional coronary interventions will be performed, safety is a major priority. Prospective monitoring of adverse and clinical events starts at randomisation and continues until hospital discharge.

2.3.1 ADVERSE EVENTS AND SERIOUS ADVERSE EVENTS

Adverse events will be recorded for the evaluation of safety and outcome measures. Serious adverse events include the following: death; serious deterioration in patient's health resulting in life-threatening injury/illness; event resulting in permanent impairment of a body structure or function; event resulting in medical or surgical intervention to prevent permanent impairment to body structure or function; event prolonging patient hospitalization. These episodes will be monitored by the coordinating centre and provided at regular intervals to the Clinical Events and DSMB. The following adverse events will be provided in a listing, overall and by treatment group: Recurrent Myocardial Infarction, Contrast-induced nephropathy, Cerebrovascular Events, Severe Heart Failure, Major Bleeding.

3. STUDY DATA

3.1 CvLPRIT-CMR DATA

CMR data will be recorded as per trial guidelines in the CRF and all CMR data will be recorded in a Research Electronic Data Capture (REDCap) database. This is a lockable, validated²⁷⁸, auditable database, which will be produced in conjunction with the Biomedical Research Unit IT team at the University of Leicester, led by Mr Nick Holden (Data Manager & Systems Architect). No clinical data will be released to Dr Gerry McCann or Dr Jamal Khan until the REDCap database is complete, checked for errors, locked and a copy provided to the CTEU. The following CMR data will be recorded (at acute CMR scan only, at *follow-up scan only (9 months post STEMI)*, all

other data taken at both scans, *=continuous/ordinal data, **=binary/categorical data (0 v 1 for N v Y).

(A full list of clinical data collected at each study time point in the main CVLPRI-t study is provided in the CVLPRI-t main study final protocol (dated 30th March 2011)).

- Infarct size (IS in g and expressed as % of LV mass)*
- Percentage area of each segment with infarct (%)*
- Number of infarcts*; if >1 then noted location, size (g, expressed as % of LV mass)*, acute vs chronic nature of each infarct, % area of segment with infarct*
- IMH (g, expressed as % of LV mass, and % of IS)*
- MVO (g, expressed as % of LV mass, and % of IS)*
- AAR (g, expressed as % of LV mass)*
- Percentage area of each segment with oedema (%)*
- Myocardial salvage index (MSI)* [expressed in 2 ways]
 - MSI-A: where IS = total IS (all infarcts) [main MSI measure]*
 - MSI-B: where IS = final total IS at 9-month CMR*
- Image quality score (0-3: for oedema, late gadolinium [LGE], cine, tagging, stress, rest, aortic magnitude and phase imaging)*
- Wall motion score as per AHA 16-segment model (WMS 1-5 per segment, total WMS (out of 80)*, WMS index (=WMS/16)*
- LV end-diastolic mass (LVEDM/I [where 'i' is indexed to body surface area in g and g/m²])*
- LVEDV/I (ml, ml/m²)*
- LVESV/I (ml, ml/m²)*
- LV stroke volume (LVSV, ml)*
- LV cardiac output (LVCO, l/min)*
- LV ejection fraction (%)*
- RVEDV/I (ml, ml/m²)*
- RVESV/I (ml, ml/m²)*
- RV stroke volume (RVSV, ml)*

- RV cardiac output (RVCO, l/min)*
- RV ejection fraction (%)*
- *Perfusion analysis using Summed Difference Score (SDS, 0-2 per segment*), total SDS (out of 32)*, global SDS ischaemic burden (%)**
- Circumferential strain (Ecc): per segment*, global (%)*
- Longitudinal strain (EII): global (%)*
- Visual presence of RV infarction (Y or N)**
- Visual presence of LV thrombus (Y or N)**

3.2 KEY TECHNICAL DETAILS ON DERIVATION OF CMR DATA

Infarct size: Measured on *cmr42* (Circle CVI, Calgary) software using Full-Width Half Maximum (FWHM) method with manual correction by removal of noise on LGE imaging. We have justified this in a pilot study. Where >1 infarct or new infarct at follow-up CMR, images will be reviewed by 2-3 readers (JNK+GPM +/- JPG).

MVO: Measured on *cmr42* as hypoenhancement within infarct core on LGE images.

AAR (oedema): Measured on *cmr42* using Otsu's Automated Method with manual correction by removal of noise and enhancement in non-IRA territories on T2w-STIR images. We have justified this in a pilot study.

IMH: Measured on *cmr42* as hypoenhancement within AAR on T2w-STIR images.

WMS: Visual wall-motion scoring assessment on short-axis cine images according to 16-segment AHA model and wall-motion scoring scheme.

LV/RV volumetrics: Endocardial and epicardial contours manually drawn excluding trabeculation and papillary muscles, on *QMass 7.1* (Leiden, NL) software.

Perfusion: Visual perfusion analysis using SDS (SDS = summed stress score [SSS] - infarct on LGE images), where segmentally SDS 0=no defect, 1=defect <50% transmural, 2=defect >50% transmural.

Strain: Measured using Tomtec Image Arena software; using Feature Tracking with contouring of endocardial contours only, on short-axis (Ecc) and long-axis (EII) images. We have justified this in a pilot study.

3.3 DATA MONITORING

Data will be monitored for quality and completeness by the CTEU. An independent DMSB will review the safety and ethics of the trial as described above in Section 1.4.6.

3.4 DATA VALIDATION

CMR data will be entered into a REDCap database. This will be automated wherever possible and using transposition of data from automatically produced data files (*.csv, *.xml, *.txt) from CMR analysis software. Manual entry of CMR data will be minimized to longitudinal strain data from the long-axis slices, 0/1 (N/Y) data on visual presence of thrombus and RV infarct, and SDS perfusion data as there are no automatically generated data files for these as data is only displayed onscreen. Five percent of data will be manually checked (randomly selected subjects). REDCap provides per-user role-based security, backup and protection from data loss. SSL encrypted web-based data entry and review, together with a mature API and data import functionality to enable data to be acquired from electronic sources. The system was developed by a multi-institutional consortium initiated at Vanderbilt University. REDCap provides user-friendly web-based case report forms, real-time data entry validation (e.g. for data types and range checks), audit trails, data retention, and a range of data visualisation and analysis tools to aid in data verification prior to export for formal statistical analysis.

3.5 MISSING DATA

CMR analyses or sequences that could not be performed (e.g. adenosine stress perfusion in asthmatics) or where image quality rendered them non-analysable will be classed as 'missing' and given a value of '999' for statistical analysis, which will be coded as missing data on SPSS. Where no infarct was seen on LGE, infarct size will be defined as 0.00g (0.00 %LV mass). Where no AAR (oedema) is seen on T2w-STIR images despite good image quality, AAR, IMH and MSI will also be classed as non-analysable.

4. STATISTICAL ANALYSIS

4.1 KEY PRINCIPLES

All statistical tests are of an exploratory nature and will be completed by presenting confidence limits and descriptive p-values.

Categorical variables will be summarised with the number and proportion of participants in each category. Continuous variables will be summarised using the number available, number missing, mean and standard deviation, median and 25th-75th quartiles, minimum and maximum values.

For the assessment of correlation, Pearson's Correlation Coefficients will be used as a default, and Spearman's Rank Correlation Coefficient where any variable is non-parametrically distributed.

Normality will be assessed using Q-Q plots. Appropriate transformations will be made to non-parametric continuous variables.

Comparison of normally distributed continuous outcomes in the treatment arms will be performed using linear mixed models.

The primary clinical outcome variable of the main CVLPRI-t study (MACE) will be analysed using the log-rank test and Cox's proportional hazards models to assess the treatment effect. Patients will be right censored. The Schoenfeld residuals output test will be used to confirm the validity of the proportional hazards model. The model will be based on time to first event for the components of the Primary Endpoint. Where the exact date (day) of the event is not recorded or known, the midpoint of the month in which the event occurred will be recorded as the date of the event. Results will be presented as Hazard ratios with their 95% confidence intervals. Kaplan-Meier survivor curves will also be produced for the 2 treatment groups. Event rates in the two treatment arms will be performed at 12 months. The primary clinical outcome variable (MACE) will be compared in patients in the main CVLPRI-t study and those in

the CMR substudy using log-rank test and Cox proportional hazards models to assess representativeness of the CMR substudy cohort.

4.2 PRIMARY ANALYSES (PRIMARY OUTCOMES)

The primary outcome for the CvLPRIT-CMR substudy is infarct size in the 2 treatment groups on the acute CMR scan. This will be expressed as % of LV mass. As this measurement is expected to be right skewed, it will be log-transformed for all analyses in order to obtain approximately normally distributed data.

Acute infarct size (expressed as % of LV mass) will be compared between the 2 treatment arms using linear mixed independent models, accounting for known predictors of infarct size using ANCOVA or generalized linear model where ordinal or N/Y categorical covariates (N/Y = 0/1). Variables that will be entered into a univariate model and adjusted for where $p < 0.1$ are: age, sex, time from symptom onset to revascularisation (TTR), infarct location (anterior vs. non-anterior), study centre, time from PPCI to CMR, Rentrop score, diabetic status and TIMI flow pre-PCI, based on the current evidence base.

4.3 SECONDARY CMR ANALYSES (KEY SECONDARY OUTCOMES)

The following outcome measures will be compared between the 2 treatment arms using the same mixed model as the primary analysis (measured at acute CMR scan only, at *follow-up scan only*, all other data taken at both scans, *=continuous/ordinal data, **=binary/categorical data (0 v 1 for N v Y)):

- The no. of patients with 1 infarct vs. >1 infarct in each treatment group will be compared using Chi-squared testing. This will be performed for all infarcts, and for acute infarcts only (excluding patients with pre-existing infarcts)
- Wall motion score index as per AHA 16-segment model*
- LVEDV/I (ml, ml/m²)*
- LVESV/I (ml, ml/m²)*
- LV ejection fraction (%)*

- LV remodelling (Y or N) defined as LVEDVI increase >20% between acute CMR scan and 9-month CMR**
- Improvement in segmental LV function in segments dysfunctional at acute CMR (improvement in wall-motion score of ≥ 1)
- RV ejection fraction (%)*
- IMH (g, expressed as a % of LV mass, and % of MVO)*
- MVO (g, expressed as a % of LV mass)*
- AAR (g, expressed as a % of LV mass)*
- Myocardial salvage index (MSI)* [expressed in 2 ways]
 - MSI-A: where IS = total IS (all infarcts)
 - MSI-B: where IS = final total IS at 9-month CMR
- Perfusion analysis using Summed Difference Score (SDS, 0-2 per segment*), total SDS (out of 32)*, global SDS ischaemic burden (%)*
- Circumferential strain (Ecc): global (%)*
- Proportion of dysfunctional segments (on WMS) showing improvement between acute CMR and follow-up CMR**
- Longitudinal strain (EII): global (%)*
- Visual presence of LV thrombus (Y or N)**

4.4 OTHER ADDITIONAL SECONDARY ANALYSES

- Bland Altman plots and two-way mixed-effect intraclass correlation coefficients for absolute agreement (ICC) to assess inter and intraobserver agreement for quantification techniques for infarct size, AAR (oedema), strain and volumetric analysis. On ICC, agreement will be defined as excellent ($ICC \geq 0.75$), good ($ICC 0.6-0.74$), fair ($ICC 0.4-0.59$), or poor ($ICC < 0.40$)²⁹³.

4.5 CURRENT PROTOCOL

This SAP is v1.0. Any updates after the approval of this will be labelled v2.0 onwards.

4.6 SOFTWARE

Data will be analysed using SPSS v20 (Statistical Package for the Social Sciences, IBM).

**COMPLETE VERSUS LESION-ONLY PRIMARY
PCI PILOT CARDIAC MRI SUBSTUDY REDCAP
DATABASE (CVLPRI-T-CMR)**

Study title: Complete versus lesion-only primary PCI pilot Cardiac MRI substudy

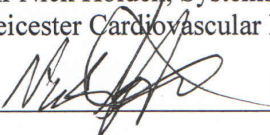
Short title: CVLPRI-t-CMR

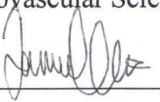
Ethics no: EME 10/27/01


Funded by: National Institute of Health Research (NIHR) EME project grant

Database: REDCap database of CVLPRIT-CMR analysis data

Date of database lock: 13th June 2014

Prepared by: Mr Nick Holden, Systems and Database Architect, NIHR
Leicester Cardiovascular BRU, Glenfield Hospital, Leicester
 13/6/2014

Data collection by: Dr Jamal Khan, Clinical Research Fellow, Dept. of
Cardiovascular Sciences, University of Leicester
 13/6/14

Approved by: Dr Gerry McCann, Consultant Cardiologist/NIHR Intermediate
Fellow, Dept. of Cardiovascular Sciences, University of Leicester
 13/6/14

5% of subjects (20 CMR studies) randomly selected had complete data check to confirm correct data entry from CMR master spreadsheet and raw CMR analysis data files (generated using QMass 7.1, CMR42, Tomtec Image Arena):

100% of data was correct. The following patients were checked:

*Acute CMR scan (x10): X549, X538, X545, X798, X624, X784, X745, X771, X782, X713.

*Follow-up CMR: (x10): X564, X797, X623, X610, X585, X716, X660, X552, X515, X733.

Publications arising from this thesis

Paper 1: Circulation: Cardiovascular Imaging (June 2016)

June 2016

Myocardial Infarction

Relationship of Myocardial Strain and Markers of Myocardial Injury to Predict Segmental Recovery After Acute ST-Segment-Elevation Myocardial Infarction

AQ1

Jamal N. Khan, MRCP, MBChB, BMedSci; Sheraz A. Nazir, MRCP, MBBChir, BSc; Anvesha Singh, MRCP, MBChB; Abhishek Shetye, BSc; Florence Y. Lai, MPhil; Charles Peebles, FRCP, MBChB; Joyce Wong, MRCP, MD; John P. Greenwood, FRCP, PhD; Gerry P. McCann, MRCP, MD

AQ3

Background—Late gadolinium-enhanced cardiovascular magnetic resonance imaging overestimates infarct size and underestimates recovery of dysfunctional segments acutely post ST-segment-elevation myocardial infarction. We assessed whether cardiovascular magnetic resonance imaging-derived segmental myocardial strain and markers of myocardial injury could improve the accuracy of late gadolinium-enhancement in predicting functional recovery after ST-segment-elevation myocardial infarction.

Methods and Results—A total of 164 ST-segment-elevation myocardial infarction patients underwent acute (median 3 days) and follow-up (median 9.4 months) cardiovascular magnetic resonance imaging. Wall-motion scoring, feature tracking-derived circumferential strain (*Ecc*), segmental area of late gadolinium-enhancement (*SEE*), microvascular obstruction, intramyocardial hemorrhage, and salvage index (*MSI*) were assessed in 2624 segments. We used logistic regression analysis to identify markers that predict segmental recovery. A percentage of 32 segments were dysfunctional acutely and 19% at follow-up. Segmental function at acute imaging and odds ratio (*OR*) for functional recovery decreased with increasing *SEE* although 33% of dysfunctional segments with *SEE* 76% to 100% improved. *SEE* was a strong predictor of functional improvement and normalization (area under the curve [*AUC*], 0.840 [95% confidence interval (*CI*), 0.814–0.867]; *OR*, 0.97 [95% *CI*, 0.97–0.98] per +1% *SEE* for improvement and *AUC*, 0.887 [95% *CI*, 0.865–0.909]; *OR*, 0.95 [95% *CI*, 0.94–0.96] per +1% *SEE* for normalization). Its predictive accuracy for improvement, as assessed by areas under the receiver operator curves, was similar to that of *MSI* (*AUC*, 0.840 [95% *CI*, 0.809–0.872]; *OR*, 1.03 [95% *CI*, 1.02–1.03] per +1% *MSI* for improvement and *AUC*, 0.862 [0.832–0.891]; *OR*, 1.04 [95% *CI*, 1.03–1.04] per +1% *SEE* for normalization) and *Ecc* (*AUC*, 0.834 [95% *CI*, 0.807–0.862]; *OR*, 1.05 [95% *CI*, 1.03–1.07] per +1% *MSI* for improvement and *AUC*, 0.844 [95% *CI*, 0.818–0.871]; *OR*, 1.07 [95% *CI*, 1.05–1.10] per +1% *SEE* for normalization), and for normalization was greater than the other predictors. *MSI* and *Ecc* remained as significant after adjustment for *SEE*, but provided no significant increase in predictive accuracy for improvement and normalization compared with *SEE* alone. *MSI* had similar predictive accuracy to *SEE* for functional recovery but was not assessable in 25% of patients. Microvascular obstruction provided no incremental predictive accuracy above *SEE*.

Conclusions—This multicentre study confirms that *SEE* is a strong predictor of functional improvement post ST-segment-elevation myocardial infarction, but recovery occurs in a substantial proportion of dysfunctional segments with *SEE* >75%. Feature tracking-derived *Ecc* and *MSI* provide minimal incremental benefit to *SEE* in predicting segmental recovery.

Clinical Trial Registration—URL: <http://www.isrctn.com>. Unique identifier: ISRCTN70913605.

(*Circ Cardiovasc Imaging*. 2016;9:e003457. DOI: 10.1161/CIRCIMAGING.115.003457.)

AQ6

Key Words: area under curve ■ cell viability ■ magnetic resonance imaging ■ myocardial infarction ■ odds ratio

Improvement in dysfunctional myocardium after acute ST-segment-elevation myocardial infarction (STEMI) predicts long-term myocardial function and prognosis.^{1,2} Kim et al³ and Choi et al⁴ first demonstrated an inverse correlation between cardiovascular magnetic resonance imaging (MRI

See Article by [Last Name] et al
See Clinical Perspective

[CMR])–measured segmental late gadolinium enhancement (LGE) transmural and functional recovery in hibernating³

Received May 18, 2015; accepted April 27, 2016.

From the Department of Cardiovascular Sciences, University of Leicester and the NIHR Leicester Cardiovascular BRU, Glenfield Hospital, Leicester, United Kingdom (J.N.K., S.A.N., A.S., F.Y.L., G.P.M.); University Hospital Southampton NHS Trust, Southampton, United Kingdom (C.P.); Royal Brompton and Harefield NHS Trust, Sydney Street, London, United Kingdom (J.W.); and Leeds Institute of Cardiovascular and Metabolic Medicine (LICAMM), University of Leeds, Leeds, United Kingdom (J.P.G.).

The Data Supplement is available at <http://circimaging.ahajournals.org/lookup/suppl/doi:10.1161/CIRCIMAGING.115.003457/-DC1>.

Correspondence to Gerry McCann, MRCP, MD, Reader in Cardiovascular Imaging, Department of Cardiovascular Sciences, University of Leicester, Glenfield Hospital, Groby Rd, Leicester LE3 9QP, United Kingdom. E-mail Gerry.McCann@uhl-tr.nhs.uk
© 2016 American Heart Association, Inc.

Circ Cardiovasc Imaging is available at <http://circimaging.ahajournals.org>

DOI: 10.1161/CIRCIMAGING.115.003457

1

AQ4

AQ5

and stunned⁴ myocardium, allowing the prediction of functional recovery without inotropic challenge.^{1,2} However, the evidence base in acute STEMI is limited by a small number of single-center studies and heterogeneity of LGE assessment.^{5–12} Moreover, several reports have shown that LGE, measured within days of STEMI, overestimates acute infarct size (IS) and underestimates the potential for functional recovery.^{13–15} The accuracy of segmental LGE expressed as segmental area of late gadolinium-enhancement (SEE) defined as enhanced percentage of segmental area,^{10–12,16} rather than maximum transmural extent in predicting segmental recovery in acute STEMI has shown promise.

Several other CMR markers of myocardial injury have been associated with functional recovery after STEMI. Circumferential strain (*Ecc*),¹¹ myocardial salvage (MSI),¹⁷ LGE-derived microvascular obstruction (late MVO),^{11,17,18} and intramyocardial hemorrhage (IMH)¹⁸ have been assessed in a few small studies. There are no studies investigating whether they offer additive value to the predictive accuracy of LGE. Feature tracking (FT) is a novel postprocessing software for the quantification of myocardial strain from steady state free-precession cine images.^{19,20} We have recently demonstrated greater robustness, reproducibility, and infarct correlation with FT-derived strain compared with tagging in acute STEMI.²¹

We aimed to assess whether FT-derived *Ecc*, MSI, late MVO, and IMH predicted segmental functional recovery in acute STEMI and whether this was of additive value to SEE.

Methods

Study Population

Two hundred and three STEMI patients with multivessel coronary disease were recruited into the CMR substudy of a multicentre, prospective, randomized controlled study assessing infarct-related artery only versus complete revascularization.²² STEMI was diagnosed according to European Society of Cardiology definitions and patients underwent primary percutaneous coronary intervention (PPCI) within 12 hours of symptoms. The study was approved by the National Research Ethics Service and was conducted according to the Declaration of Helsinki, and patients provided written informed consent.

Cardiovascular MRI

CMR was performed in 5 of the 7 centers, at a median of 2.9 days post PPCI (acute CMR) and repeated at 9.4 months (follow-up CMR) on 1.5T platforms (4 Siemens Avanto, Erlangen, Germany and 1 Philips Intera, Best, Netherlands) with dedicated cardiac receiver coils. Follow-up CMR (median, 9 months) was completed in 164 patients who comprised the final study cohort. The acute CMR was performed as previously described with the addition of T2-weighted short-tau inversion recovery (T2w-STIR) covering the entire left ventricle (LV).²³ The imaging protocol is detailed in Figure 1.

MRI Analysis

Image quality

Image quality was graded on a 4-point Likert scale: 3=excellent, 2=good, 1=moderate, and 0=unanalyzable.

Volumetric and Functional Analysis

Analysis was performed using cvi42 v4.1 (Circle Cardiovascular Imaging, Calgary, Canada). LV volumes were calculated as previously described.²² Wall motion in the 16 American Heart Association

myocardial segments was visually graded as: 1=normokinetic, 2=hypokinetic, 3=akinetic, 4=dyskinetic, and 5=aneurysmal.²⁴ Segmental dysfunction was defined as wall motion score (WMS) of ≥ 2 at acute CMR and improvement as a WMS decrease of ≥ 1 , and normalization where WMS returned to 1 at follow-up CMR.^{10–12,16}

Infarct Characterization

Edema (area-at-risk [AAR]) and infarct were quantified using cvi42 v4.1 on T2w-STIR and LGE imaging, using Otsu's Automated Method and full-width half-maximum thresholding, respectively, as previously described by our group.²⁵ Hypointense regions within enhancement on LGE and T2w-STIR imaging were included, corresponding to MVO and IMH, respectively, and expressed as present or absent for each of the 16 segments. SEE was calculated as percentage enhanced area for each myocardial segment ($SEE = 100 \times [\text{segmental enhanced area}/\text{segmental area}]$).¹¹ SEE was additionally classified into 5 categories: SEE 0%, SEE 1% to 25%, SEE 26% to 50%, SEE 51% to 75%, and SEE 76% to 100% as previously described.^{13,12,16} Segmental MSI defined the proportion of the AAR that did not progress to infarction and was calculated as $[(\text{segmental AAR} - \text{SEE})/\text{segmental AAR}] \times 100$.

Circumferential Strain Analysis

Segmental peak endocardial *Ecc* was measured with FT using *Diogenes Image Arena* (Tomtec, Munich, Germany). Endocardial contours were manually drawn onto the end-diastolic image and propagated. The FT algorithm has been described previously.²¹ Suboptimally tracking segments were manually adjusted if the movement of contoured borders deviated from true myocardial motion by $>50\%$.

Statistical Analysis

Normality was assessed using Kolmogorov-Smirnov tests, histograms, and Q-Q plots. Normally distributed data were expressed as mean \pm SD, and comparisons between groups were conducted with ANOVA. Nonparametric data were expressed as median (25%–75% interquartile range), and compared with Kruskal-Wallis testing. Spearman rank correlation coefficient assessed the correlation between the predictors and the segmental function. We assessed whether (1) SEE, *Ecc*, MVO, MSI, (presence/absence), and IMH (presence/absence) predicted improvement and normalization of dysfunctional myocardial segments at follow-up CMR using logistic regression analysis and (2) *Ecc*, MVO, MSI, and IMH provided incremental improvement in predictive accuracy above SEE alone. We developed logistic regression models with random effect to account for dependence of segments from the same patient. The likely clinical benefit for differences in predictive accuracy of SEE alone compared with SEE plus each of *Ecc*, MSI, MVO, and IMH was assessed using receiver operating characteristic curve analysis with the area under the curves (AUCs) compared using the method of DeLong.²⁶ On AUC, predictive accuracy of >0.9 was considered excellent, 0.8 to 0.9 very good, 0.7 to 0.8 good, 0.6 to 0.7 average, and <0.6 poor.²⁷ The optimal cutoff values of SEE, segmental *Ecc*, and MSI for predicting functional recovery were identified by receiver operating characteristic curve analysis where sensitivity and specificity intersected. Intra- and interobserver agreement were assessed with intraclass correlation coefficient for absolute agreement²⁸ and κ statistic on a random selection of 10 patients. Intraobserver (J.N.K.) and interobserver agreement (J.N.K., S.A.N.) are reported in the Data Supplement. Statistical tests were performed using SPSS version 20 (IBM, New York, NY) and PROC GLIMMIX in SAS version 9.4 (Statistical Analysis Systems, NC). $P < 0.05$ was considered significant.

Results

Baseline Characteristics

Demographic and CMR data are summarized in Table 1. Of the 203 enrolled patients, 164 underwent both acute and

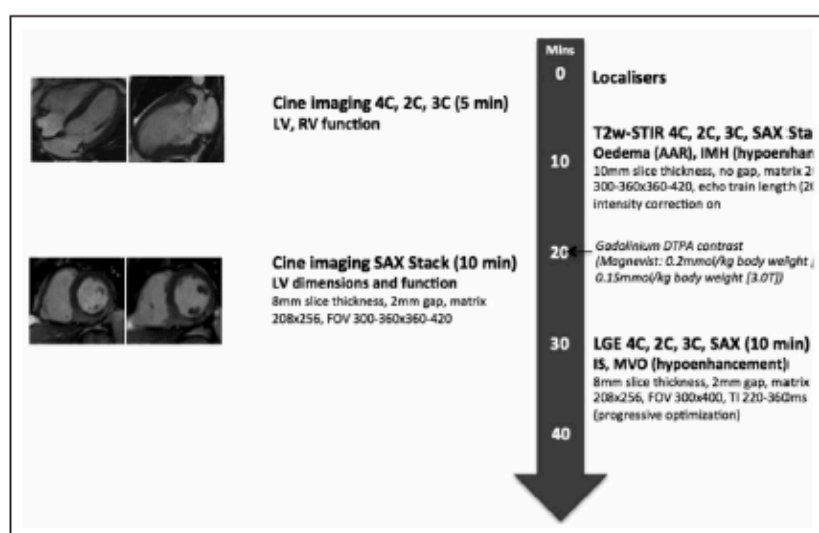


Figure 1. Magnetic resonance imaging protocol. AAR indicates area-at-risk; FOV, field of view; IMH, intramyocardial hemorrhage, IS, infarct size; LGE, late gadolinium enhancement; LV, left ventricle; MVO= microvascular obstruction; RV, right ventricle, SAX, short axis; T2w-STIR, T2-weighted short-tau inversion recovery; TE, echo time; TI, inversion time; and TR, repetition time.

follow-up CMR and hence comprised the study group. Reasons for patients not returning for follow-up CMR are shown in Figure 2. Image quality was diagnostic in all cine and LGE segments ($n=2624$), which were analyzable for WMS, SEE, Ecc, and MVO. Twenty-three percent of T2w-STIR segments (MSI, IMH) were nonanalyzable because of poor image quality or not being acquired because of significant breath holding and ECG gating difficulties. Thus 2020 segments were included in the assessment of CMR predictors of segmental recovery.

Segmental Systolic Function Post STEMI

Wall Motion Scoring at Acute and Follow-Up CMR

On WMS, at acute CMR, 837 (31.9%) segments had contractile dysfunction (WMS 2: 499/2624 [19.0%]; WMS 3: 338/2624 [12.9%]). At 9-month follow-up CMR, 521 (62.2%) dysfunctional segments had improved, of which 372 (44.4%) had normalized and 495 (18.8%) remained dysfunctional (WMS 2: 350/2624 [13.3%]; WMS 3: 137/2624 [5.2%]; and WMS 4: 8/2624 [0.3%]).

Segmental Function According to Segmental Extent of LGE and Strain

Acutely, with worsening function on WMS, SEE, Ecc and presence of MVO and IMH increased, and segmental MSI decreased (Table 2). With increasing SEE, segmental function worsened (Figure 3). More than 98% of SEE 76% to 100% segments were dysfunctional at acute CMR. WMS correlated more strongly with SEE at acute ($r_s=0.69$; $P<0.01$) and follow-up CMR ($r_s=0.62$; $P<0.01$) than with MSI (acute, $r_s=-0.523$, $P<0.01$; follow-up: $r_s=-0.514$; $P<0.01$) and Ecc (acute: $r_s=0.49$; $P<0.01$; follow-up: $r_s=0.49$; $P<0.01$). At follow-up CMR, segmental function improved in each SEE grade

(Figure 4). The proportion of dysfunctional segments improving or normalizing decreased with increasing SEE, with 90% of SEE 0% segments normalizing. Despite this, 33% of SEE 75% to 100% segments improved; however, only 5% normalized (Figure 4). The proportion of dysfunctional segments improving or normalizing increased with increasing MSI. Despite this, 43% of MSI 0% to 25% segments improved, but only 21% normalized (Figure 5).

Predictors of Segmental Recovery in Dysfunctional Segments Post STEMI

Predictors of Segmental Functional Improvement

Individual Predictors: Results are shown in Table 3. SEE ($P<0.001$), MSI ($P<0.001$), Ecc ($P<0.001$), and the presence of MVO ($P=0.021$) and IMH ($P=0.004$) predicted functional improvement. SEE was a strong predictor of functional improvement (AUC, 0.840) with optimal cutoff being $<34\%$ (sensitivity=specificity=62%). Segmental MSI (AUC, 0.840; $P=0.139$), Ecc (AUC, 0.834; $P=0.613$), and MVO (AUC, 0.826; $P=0.164$) showed similar predictive value as SEE, but IMH (AUC, 0.818; $P=0.041$) did not. Revascularization strategy did not predict segmental improvement ($P=0.206$).

Predictors Combined With SEE: When SEE and Ecc were entered into the model together for functional improvement, both remained as significant predictors ($P<0.001$ SEE and $P=0.027$ Ecc), but the predictive value for functional improvement was similar for SEE+Ecc and SEE (AUC, 0.841 and 0.840; $P=0.738$). Similarly, MSI remained a significant predictor ($P=0.031$) after adjustment for SEE; however, the addition of MSI did not improve the predictive value compared with SEE alone ($P=0.344$). MVO ($P=0.069$) and IMH ($P=0.756$) did not predict segmental improvement when added to SEE.

Table 1. Baseline Demographics and CMR Characteristics

Baseline and angiographic characteristics	
No. of patients (n)	164
Age, y	63.0±9.5
Sex (male, %)	140 (85.4)
Diabetes mellitus, n (%)	24 (14.6)
Hypertension, n (%)	60 (36.6)
Symptom to PPCI time (min)	172 (128–280)
Left anterior descending artery culprit vessel, n (%)	50 (36.6)
Infarct-related artery only PCI, n (%)	80 (48.8)
Multivessel PCI, n (%)	84 (51.2)
CMR characteristics	
Cine segments of diagnostic image quality (%) at acute CMR	100
LGE segments of diagnostic image quality (%) at acute CMR	100
T2w-STIR segments of diagnostic image quality (%) at acute CMR	76.8
Cine segments of diagnostic image quality (%) at follow-up CMR	100
Acute CMR time (d post STEMI)	2.9 (2.0–3.9)
Follow-up CMR time (mo post STEMI)	9.4 (8.9–10.0)
LV end-diastolic mass, g/m ²	52.3 (45.9–61.0)
LV end-diastolic volume, mL/m ²	89.5 (80.6–101.5)
LV end-systolic volume, mL/m ²	47.5 (39.0–58.5)
LV ejection fraction, %	46.1±9.2
Infarct size (% LV mass)	12.7 (6.9–21.5)
Myocardial salvage index, %	58.7 (35.3–76.7)
Segmental characteristics	
Dysfunctional segments at acute CMR, n (%)	837/2624 (31.9)
Dysfunctional segments at follow-up CMR, n (%)	495/2624 (18.9)
Segments with LGE at acute CMR, n (%)	1186/2624 (45.2)
Segments with LGE at follow-up CMR, n (%)	1009/2624 (38.5)
Segments with MVO at acute CMR, n (%)	165/2624 (6.3%)
Segments with IMH at acute CMR, n (%)	51/2016 (2.5%)

CMR indicates cardiovascular magnetic resonance imaging; IMH, intramyocardial hemorrhage; LGE, late gadolinium enhancement; MVO, microvascular obstruction; PPCI, primary percutaneous coronary intervention; STEMI, ST-segment-elevation myocardial infarction; and T2w-STIR, T2-weighted short-tau inversion recovery.

Predictors of Segmental Functional Normalization

Individual Predictors: SEE ($P<0.001$), MSI ($P<0.001$), *Ecc* ($P<0.001$), and the presence of MVO ($P<0.001$) and IMH ($P=0.001$) predicted functional normalization (Table 3). SEE was a strong predictor of functional normalization (AUC 0.887) with optimal predictive cutoff being $<29\%$ (sensitivity=specificity=72%). The predictive value of SEE as measured by AUC was higher than that of segmental MSI (AUC, 0.862; $P=0.007$), *Ecc* (AUC, 0.844; $P=0.001$), MVO

(AUC, 0.836; $P<0.001$), and IMH (AUC, 0.827; $P<0.001$). Revascularization strategy did not predict segmental normalization ($P=0.463$).

Predictors Combined With SEE: After adjustment for SEE, *Ecc* ($P=0.001$), and MSI ($P=0.027$) remained as significant predictors of functional normalization. However, compared with SEE alone (AUC, 0.887), the addition of these predictors did not significantly increase the predictive value for functional normalization (*Ecc*+SEE: AUC, 0.889; $P=0.379$ and MSI+SEE: AUC, 0.886; $P=0.340$). MVO ($P=0.223$) and IMH ($P=0.221$) did not predict segmental normalization when added to SEE.

SEE and *Ecc* as Predictors of Segmental Functional Recovery Where SEE $\geq 50\%$

In dysfunctional segments with $\geq 50\%$ SEE, SEE predicted improvement ($P=0.002$; AUC, 0.924) and normalization ($P=0.002$; AUC, 0.918; Data Supplement). MVO predicted functional normalization ($P=0.002$) and remained as significant after adjustment for SEE ($P<0.009$). *Ecc*, MSI, and IMH did not predict functional recovery and were not of additive value to SEE.

CMR Predictors of Segmental Functional Recovery Stratified by Revascularization Strategy

Full data are presented in the Data Supplement. The results for all analyses were similar in patients undergoing IRA only ($n=80$) and complete revascularization ($n=84$) and were similar to those in the overall study cohort ($n=164$).

Discussion

This is the largest study assessing CMR predictors of segmental functional recovery after acute STEMI treated with PPCI and the first to use multicentre data analyzed in a core laboratory. We have confirmed that early after STEMI, LGE overestimates IS despite using full-width half-maximum quantification, which gives lower values than 2 SD thresholding used by most previous studies.^{6,9,16} Functional improvement occurred in a significant proportion of near-transmurally enhanced segments although only 5% normalized. A key aim of conducting this study was to assess whether the accuracy of LGE to predict functional recovery after STEMI could be improved with the addition of other markers of myocardial injury. We have shown that baseline SEE is a strong predictor of recovery at 9 months. SEE was of similar predictive value to MSI, *Ecc*, and MVO for improvement, and a stronger predictor than MSI, *Ecc*, MVO, and IMH for normalization. In addition although *Ecc* and MSI remained as predictive after adjustment for SEE, they provided similar predictive values for recovery compared with SEE alone.

Prediction of Segmental Functional Recovery With LGE

Our observed inverse correlation between SEE and functional recovery is consistent with previous studies.^{4,5,7–12} The accuracy in predicting recovery was slightly lower than in the work of Kitagawa et al⁸ and Orii et al.¹² LGE measured acutely overestimates necrosis by up to 30% in the first week post STEMI caused by myocardial edema.^{13,15} We undertook acute CMR at

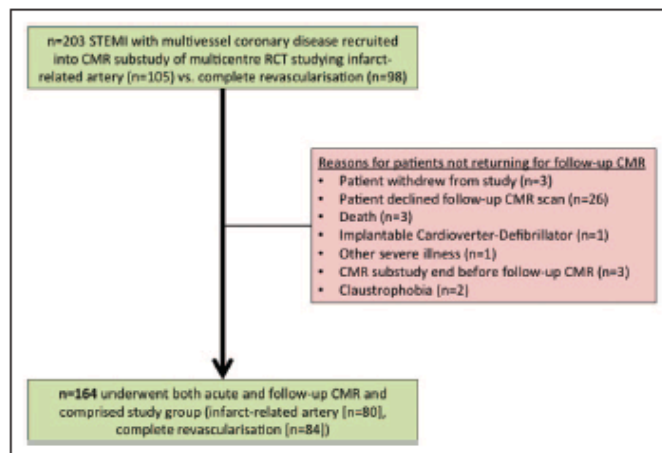


Figure 2. CONSORT diagram illustrating reasons for patients not returning for follow-up cardiovascular magnetic resonance imaging (CMR). RCT indicates randomized controlled trial; and STEMI, ST-segment-elevation myocardial infarction.

3 days post PPCI to assess CMR in a real-world setting when patients are discharged and are less likely to undergo CMR at day 5 and 8 as in these 2 studies.^{8,12} Untreated multivessel disease with potential hibernating myocardium in noninfarct artery territories in our study, differences in LGE thresholding methods,^{4,5,7-10,12} and the smaller sample size of these studies may also have contributed to our slightly lower AUC. We used SEE^{5,7,10,11} because we felt that it is a more accurate representation of segmental necrosis than transmural enhancement. Transmurality can overestimate segmental necrosis because a segment may be considered transmurally enhanced when only a small portion of segmental width demonstrates transmural enhancement.⁴ Infarct extent based on transmural enhancement has been compared with SEE in 1 study in HCM and was 31% higher.²⁹

The recent study by Wong et al¹¹ is the closest in design to our study. SEE and MVO were, however, stronger predictors

of recovery in our study than their results (SEE: AUC, 0.840 versus 0.680; MVO: AUC, 0.836 versus 0.670). This may be because of their small study size (n=45), the fact that they only assessed LGE on 3 thin (6 mm) short-axis slices and hence provided incomplete LV coverage, and their later time point of acute CMR on day 8, by which time there may have been a degree of infarct and MVO resorption and functional recovery.

The optimal SEE cutoff for predicting recovery in our study of 34% is similar to that in the study by Becker et al,¹⁶ who also used SEE. It may be that if transmural enhancement overestimates necrosis relative to SEE, a smaller SEE cutoff predicts recovery. The commonly used arbitrary cutoff of 50% may need revising because it has been derived from historical work in chronic coronary artery disease³ where LGE is unlikely to overestimate necrosis.³ Importantly, SEE in our study was a strong predictor (AUC, 0.887) of functional

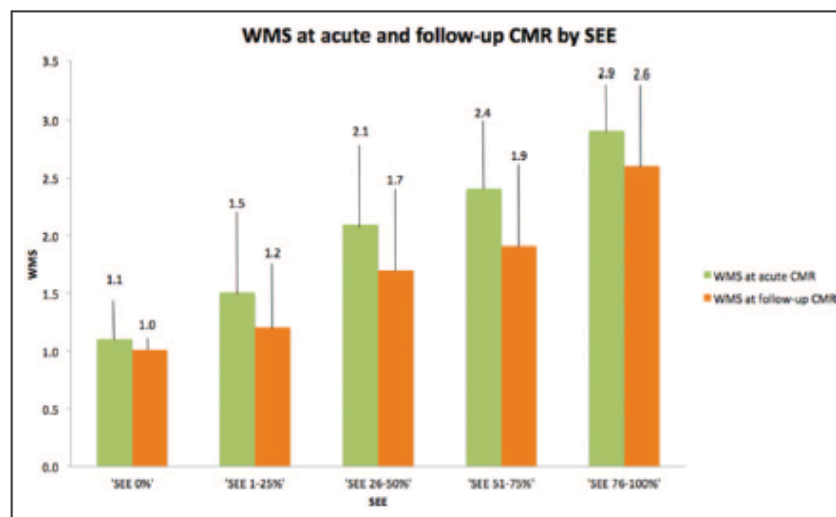


Figure 3. Wall-motion scoring (WMS) at acute and follow-up cardiovascular magnetic resonance imaging (CMR) by segmental extent of enhancement. SEE indicates segmental extent of enhancement.

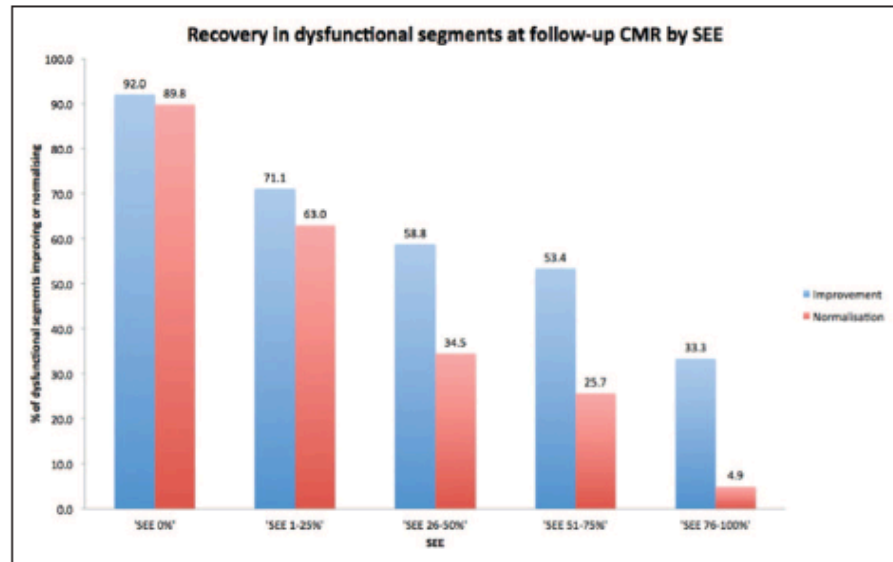


Figure 4. Recovery in dysfunctional segments at follow-up cardiovascular magnetic resonance imaging (CMR) by segmental area of late gadolinium-enhancement (SEE).

normalization, which may be associated with long-term LV function and prognosis.^{1,2}

Late MVO and IMH were moderately strong predictors of segmental recovery. This is in keeping with the work of Kidambi et al¹⁸ who demonstrated that infarcts with MVO had no improvement in segmental function on midmyocardial and endocardial-strain in the infarct zone at 3 months, and that the

presence of IMH further attenuated strain. Of note, MVO in our study was the only predictor of functional normalization in segments with SEE \geq 50% in addition to SEE and provided incremental predictive benefit. This is likely to be a reflection of the more severe myocardial injury and adverse remodeling known to accompany MVO. Indeed, Kitagawa et al⁸ showed that segmental MVO extent <50% accurately identified

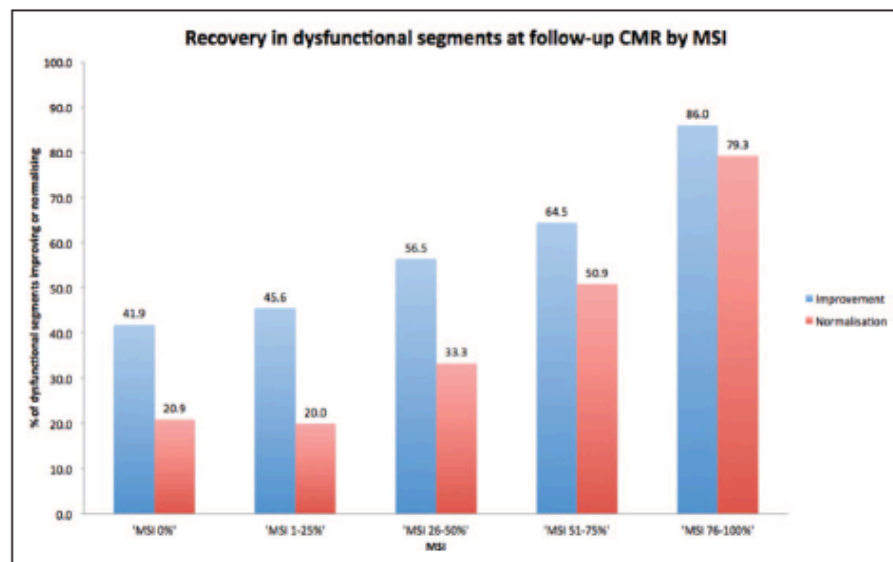


Figure 5. Recovery in dysfunctional segments at follow-up cardiovascular magnetic resonance imaging (CMR) by segmental myocardial salvage index (MSI).

Table 2. Segmental Extent of Myocardial Injury According to Degree of Dysfunction at Acute CMR

WMS at Acute CMR	1. Normal (n=1787, 68%)	2. Hypokinetic (n=499, 19%)	3. Akinetic (n=338, 13%)	P Value
SEE, %	3.6±9.7	24.4±22.0	52.2±29.1	<0.001
Peak segmental Ecc, %	-23.5±10.2	-14.9±9.1	-9.6±7.9	<0.001
MSI, %	98.4 (71.2–100.0)	58.1 (25.7–83.2)	18.3 (0.0–52.6)	<0.001
MVO, n (%)	7/1787 (0.4)	48/499 (9.6)	110/338 (32.5)	<0.001
IMH, n (%)	1/713 (0.1)	12/241 (4.9)	41/198 (20.7)	<0.001

CMR indicates cardiovascular magnetic resonance imaging; Ecc, peak segmental circumferential strain; IMH, intramyocardial hemorrhage; MSI, myocardial salvage; MVO, presence of microvascular obstruction (MVO); SEE, segmental area of late gadolinium-enhancement; and WMS, wall motion score. No segments had WMS of 4 or 5 at acute CMR.

recovering segments with SEE≥50% enhancement. The lack of predictive accuracy of IMH in segments with SEE≥50% in our study may be because of the relatively small number of segments with IMH and SEE≥50% (n=41).

Our results have also shown that MSI performed equally and SEE to predict functional recovery. The moderate predictive accuracy of MSI is consistent with previous work highlighting that MSI may underestimate functional recovery using segmental strain.¹⁷ The minimal incremental increase in predictive accuracy of MSI in addition to SEE is likely to result from the close relationship between SEE and MSI. Indeed, Spearman rank correlation coefficient for SEE and MSI was -0.89 ($P<0.001$) in our study. Given that MSI significantly increases scanning time to acquire edema images, resulted in nonanalyzable images in 25% of patients and provided only minimal incremental value above SEE alone, there seems to be little merit in using MSI instead of or in addition to SEE. The close inter-relation between IS, MVO, and IMH is also likely to account for their lack of incremental predictive accuracy in our study.

Prediction of Segmental Functional Recovery With Strain

We recently compared FT and tagging strain assessment in acute STEMI and showed that FT-derived endocardial Ecc

correlated strongest with infarct characteristics.²¹ This is likely to be a result of infarction firstly affecting the endocardium in the ischemic cascade.³⁰ This is corroborated by the fact that Ecc was a strong predictor of segmental recovery in this study.

Our results are in keeping with those of Wong et al¹¹ who showed an almost identical predictive accuracy (AUC, 0.823) to our study, of HARP-derived Ecc in identifying segmental recovery at 3 months.¹¹ Unlike our study, they however demonstrated that Ecc was a significantly stronger predictor than SEE and MVO. This is likely to be because of methodological differences as discussed above. Our findings are similar to those of Orii et al¹² who also showed a strong predictive accuracy of speckle-tracking echocardiographic Ecc (AUC, 0.899) for segmental functional recovery, and similar accuracy to SEE ($P=0.439$). On a global level, our findings are supported by the recent work of Buss et al,³¹ which showed that FT-derived global Ecc and LGE IS were moderately strong predictors of LV ejection fraction >50% at 6-month follow-up, and that Ecc was a noninferior predictor compared with IS.

Our study is in contrast to the work of Neizel et al³² who used strain-encoded CMR-derived segmental Ecc and LGE SEE to predict severe, persistent dysfunction at 6 months

Table 3. Segmental Extent of Myocardial Injury at Acute Cardiovascular Magnetic Resonance Imaging and Prediction of Functional Recovery at Follow-Up

Predictor	AUC	95% CI	Optimal Cutoff	Odds Ratio (P Value)	95% CI
Improvement					
SEE	0.840	0.814–0.867	<34% (sens 62%, spec 62%)	0.97 per +1% SEE ($P<0.001$)	0.97–0.98
MSI	0.840	0.809–0.872	>39% (sens 65%, spec 65%)	1.03 per +1% MSI ($P<0.001$)	1.02–1.03
Ecc	0.834	0.807–0.862	<-11.4% (sens 59%, spec 59%)	1.05 per -1% Ecc ($P<0.001$)	1.03–1.07
MVO presence	0.826	0.798–0.853	NA	0.61 MVO present vs absent ($P=0.021$)	0.40–0.93
IMH presence	0.818	0.779–0.857	NA	0.32 IMH present vs absent ($P=0.004$)	0.15–0.67
Normalization					
SEE	0.887	0.865–0.909	<29% (sens 72%, spec 72%)	0.95 per +1% SEE ($P<0.001$)	0.94–0.96
MSI	0.862	0.832–0.891	>48% (sens 71%, spec 71%)	1.04 per +1% MSI ($P<0.001$)	1.03–1.04
Ecc	0.844	0.818–0.871	<-12.0% (sens 62%, spec 62%)	1.07 per -1% Ecc ($P<0.001$)	1.05–1.10
MVO presence	0.835	0.808–0.862	NA	0.19 MVO present vs absent ($P<0.001$)	0.12–0.31
IMH presence	0.827	0.789–0.865	NA	0.08 IMH present vs absent ($P=0.001$)	0.02–0.30

AUC indicates area under the curve; CI, confidence interval; Ecc, peak segmental circumferential strain; IMH, intramyocardial hemorrhage; SEE, segmental area of late gadolinium-enhancement; sens, sensitivity; spec, specificity; MSI, myocardial salvage; and MVO, microvascular obstruction.

defined as segmental *Ecc* <9%. *Ecc* was only a mildly strong predictor and was a significantly weaker predictor than SEE (AUC, 0.74 versus 0.91). The weaker predictive accuracy of strain-encoded CMR *Ecc* compared with FT *Ecc* in their study may be because of the fact that Neizel divided the LV into 10 to 12, rather than 16 segments, thus potentially reducing the accuracy of strain assessment in basal and apical segments. Indeed, no segments in their study had a strain value of zero, even those that were visually akinetic and contained MVO. In addition, strain-encoded CMR has a lower signal:noise ratio than steady state free-precession cine imaging.³² However, there are no data comparing strain-encoded CMR and FT strain assessment.

Limitations

Acute CMR was undertaken earlier than in some studies with potentially greater necrosis overestimation on LGE; however, this allows a closer representation of real-life practice where acute CMR would typically be undertaken pre-discharge. All of our subjects had multivessel coronary disease, which may reduce comparability to previous studies. Only 164 of the 203 patients recruited had baseline and follow-up scans so there is a potential bias although there was no differences in clinical characteristics of those who did and did not have follow-up scans. Approximately 25% of patients did not have satisfactory T2w-STIR images to allow diagnostic segmental data for MSI and IMH, which may be improved with newer tissue characterization (mapping) techniques. Segmental MVO and IMH extent were not assessed because of this being currently unavailable in our analysis software. The same observer (J.N.K.) performed all CMR analysis; however, there was a 3-month gap between analysis of cine (WMS, *Ecc*), T2w-STIR (IMH, MSI), and LGE (SEE, MVO) imaging, ensuring blinded analysis of CMR predictors of segmental improvement.

Conclusions

The SEE of LGE is a strong predictor of functional recovery after PPCI, but recovery occurs in a substantial proportion of dysfunctional segments with SEE > 75%. FT-derived *Ecc* and MSI provide only minimal incremental benefit to SEE in predicting segmental recovery after STEMI. Further work is required to optimally identify stunned, non-necrotic myocardium after PPCI.

Acknowledgments

Dr McCann and J.N. Khan conceived the study idea. J.N. Khan and Dr Greenwood recruited patients. J.N. Khan, Dr McCann, Dr Greenwood, C. Peebles, Dr Wong, and S.A. Nazir supervised study visits. J.N. Khan and F.Y. Lai performed statistical analysis. J.N. Khan performed cardiovascular magnetic resonance imaging and statistical analyses, and wrote the article, which all authors critically reviewed and revised.

Sources of Funding

Medical Research Council and managed by the National Institute for Health Research (NIHR) Efficacy and Mechanism Evaluation programme (10-27-01). The main CvLPRIT trial was funded by the British Heart Foundation (SP/10/001) with support from the NIHR Comprehensive Local Research Networks. Dr McCann was funded by an NIHR career development research fellowship.

Disclosures

None.

References

- Baran I, Ozdemir B, Gullulu S, Kaderli AA, Senturk T, Aydinlar A. Prognostic value of viable myocardium in patients with non-Q-wave and Q-wave myocardial infarction. *J Int Med Res*. 2005;33:574–582.
- Nijland F, Kamp O, Verhorst PM, de Voogt WG, Visser CA. In-hospital and long-term prognostic value of viable myocardium detected by dobutamine echocardiography early after acute myocardial infarction and its relation to indicators of left ventricular systolic dysfunction. *Am J Cardiol*. 2001;88:949–955.
- Kim RJ, Wu E, Rafael A, Chen EL, Parker MA, Simonetti O, Klocke FJ, Bonow RO, Judd RM. The use of contrast-enhanced magnetic resonance imaging to identify reversible myocardial dysfunction. *N Engl J Med*. 2000;343:1445–1453. doi: 10.1056/NEJM200011163432003.
- Choi KM, Kim RJ, Gubernikoff G, Vargas JD, Parker M, Judd RM. Transmural extent of acute myocardial infarction predicts long-term improvement in contractile function. *Circulation*. 2001;104:1101–1107.
- Beek AM, Kuhl HP, Bondarenko O, Twisk JW, Hofman MB, van Dockum WG, Visser CA, van Rossum AC. Delayed contrast-enhanced magnetic resonance imaging for the prediction of regional functional improvement after acute myocardial infarction. *J Am Coll Cardiol*. 2003;42:895–901.
- Bodí V, Sanchis J, López-Lereu MP, Losada A, Núñez J, Pellicer M, Bertomeu V, Chorro FJ, Llácer A. Usefulness of a comprehensive cardiovascular magnetic resonance imaging assessment for predicting recovery of left ventricular wall motion in the setting of myocardial stunning. *J Am Coll Cardiol*. 2005;46:1747–1752. doi: 10.1016/j.jacc.2005.07.039.
- Gerber BL, Garot J, Bluemke DA, Wu KC, Lima JA. Accuracy of contrast-enhanced magnetic resonance imaging in predicting improvement of regional myocardial function in patients after acute myocardial infarction. *Circulation*. 2002;106:1083–1089.
- Kitagawa K, Ichikawa Y, Hirano T, Makino K, Kobayashi S, Takeda K, Sakuma H. Diagnostic value of late gadolinium-enhanced MRI and first-pass dynamic MRI for predicting functional recovery in patients after acute myocardial infarction. *Radiat Med*. 2007;25:263–271. doi: 10.1007/s11604-007-0133-7.
- Motoyasu M, Sakuma H, Ichikawa Y, Ishida N, Uemura S, Okinaka T, Isaka N, Takeda K, Nakano T. Prediction of regional functional recovery after acute myocardial infarction with low dose dobutamine stress cine MR imaging and contrast enhanced MR imaging. *J Cardiovasc Magn Reson*. 2003;5:563–574.
- Shapiro MD, Nieman K, Nasir K, Nomura CH, Sarwar A, Ferencik M, Abbura S, Hoffmann U, Hoffman U, Gold HK, Jang IK, Brady TJ, Cury RC. Utility of cardiovascular magnetic resonance to predict left ventricular recovery after primary percutaneous coronary intervention for patients presenting with acute ST-segment elevation myocardial infarction. *Am J Cardiol*. 2007;100:211–216. doi: 10.1016/j.amjcard.2007.02.079.
- Wong DT, Leong DP, Weightman MJ, Richardson JD, Dundon BK, Psaltis PJ, Leung MC, Meredith IT, Worthley MI, Worthley SG. Magnetic resonance-derived circumferential strain provides a superior and incremental assessment of improvement in contractile function in patients early after ST-segment elevation myocardial infarction. *Eur Radiol*. 2014;24:1219–1228. doi: 10.1007/s00330-014-3137-6.
- Orii M, Hirata K, Tanimoto T, Shiono Y, Shimamura K, Ishibashi K, Yamano T, Ito Y, Kitabata H, Yamaguchi T, Kubo T, Imanishi T, Akasaka T. Two-dimensional speckle tracking echocardiography for the prediction of reversible myocardial dysfunction after acute myocardial infarction: comparison with magnetic resonance imaging. *Echocardiography*. 2015;32:768–778. doi: 10.1111/echo.12726.
- Ibrahim T, Hackl T, Nekolla SG, Breuer M, Feldmair M, Schtemig A, Schwaiger M. Acute myocardial infarction: serial cardiac MR imaging shows a decrease in delayed enhancement of the myocardium during the 1st week after reperfusion. *Radiology*. 2010;254:88–97. doi: 10.1148/radiol.09090660.
- Dall'Armellina E, Karia N, Lindsay AC, Karamitsos TD, Ferreira V, Robson MD, Kellman P, Francis JM, Forfar C, Prendergast BD, Banning AP, Channon KM, Kharbada RK, Neubauer S, Choudhury RP. Dynamic changes of edema and late gadolinium enhancement after acute myocardial infarction and their relationship to functional recovery and salvage index. *Circ Cardiovasc Imaging*. 2011;4:228–236. doi: 10.1161/CIRCIMAGING.111.963421.
- Mather AN, Fairbairn TA, Artis NJ, Greenwood JP, Plein S. Timing of cardiovascular MR imaging after acute myocardial infarction: effect on

- estimates of infarct characteristics and prediction of late ventricular remodeling. *Radiology*. 2011;261:116–126. doi: 10.1148/radiol.11110228.
16. Becker M, Altiok E, Lente C, Otten S, Friedman Z, Adam D, Hoffmann R, Koos R, Krombach G, Marx N, Hoffmann R. Layer-specific analysis of myocardial function for accurate prediction of reversible ischaemic dysfunction in intermediate viability defined by contrast-enhanced MRI. *Heart*. 2011;97:748–756. doi: 10.1136/hrt.2010.210906.
 17. O'Regan DP, Ariff B, Baksi AJ, Gordon F, Durighel G, Cook SA. Salvage assessment with cardiac MRI following acute myocardial infarction underestimates potential for recovery of systolic strain. *Eur Radiol*. 2013;23:1210–1217. doi: 10.1007/s00330-012-2715-8.
 18. Kidambi A, Mather AN, Motwani M, Swoboda P, Uddin A, Greenwood JP, Plein S. The effect of microvascular obstruction and intramyocardial hemorrhage on contractile recovery in reperfused myocardial infarction: insights from cardiovascular magnetic resonance. *J Cardiovasc Magn Reson*. 2013;15:58. doi: 10.1186/1532-429X-15-58.
 19. Hor KN, Gottliebson WM, Carson C, Wash E, Cnota J, Fleck R, Wansapura J, Klimczek P, Al-Khalidi HR, Chung ES, Benson DW, Mazur W. Comparison of magnetic resonance feature tracking for strain calculation with harmonic phase imaging analysis. *JACC Cardiovasc Imaging*. 2010;3:144–151. doi: 10.1016/j.jcmg.2009.11.006.
 20. Maret E, Todt T, Brudin L, Nylander E, Swahn E, Ohlsson JL, Engvall JE. Functional measurements based on feature tracking of cine magnetic resonance images identify left ventricular segments with myocardial scar. *Cardiovasc Ultrasound*. 2009;7:53. doi: 10.1186/1476-7120-7-53.
 21. Khan JN, Singh A, Nazir SA, Kanagala P, Gershlick AH, McCann GP. Comparison of cardiovascular magnetic resonance feature tracking and tagging for the assessment of left ventricular systolic strain in acute myocardial infarction. *Eur J Radiol*. 2015;84:840–848. doi: 10.1016/j.ejrad.2015.02.002.
 22. McCann GP, Khan JN, Greenwood JP, Nazir S, Dalby M, Curzen N, Hetherington S, Kelly DJ, Blackman DJ, Ring A, Peckles C, Wong J, Sasikaran T, Flather M, Swanton H, Gershlick AH. Complete Versus Lesion-Only Primary PCI: The Randomized Cardiovascular MR CvLPRIT Substudy. *J Am Coll Cardiol*. 2015;66:2713–2724. doi: 10.1016/j.jacc.2015.09.099.
 23. Khan JN, Razvi N, Nazir SA, Singh A, Masca NG, Gershlick AH, Squire I, McCann GP. Prevalence and extent of infarct and microvascular obstruction following different reperfusion therapies in ST-elevation myocardial infarction. *J Cardiovasc Magn Reson*. 2014;16:38. doi: 10.1186/1532-429X-16-38.
 24. Lang RM, Bierig M, Devereux RB, Flachskampf FA, Foster E, Pellikka PA, Picard MH, Roman MJ, Seward J, Shanewise JS, Solomon SD, Spencer KT, Sutton MS, Stewart WJ; Chamber Quantification Writing Group; American Society of Echocardiography's Guidelines and Standards Committee; European Association of Echocardiography. Recommendations for chamber quantification: a report from the American Society of Echocardiography's Guidelines and Standards Committee and the Chamber Quantification Writing Group, developed in conjunction with the European Association of Echocardiography, a branch of the European Society of Cardiology. *J Am Soc Echocardiogr*. 2005;18:1440–1463. doi: 10.1016/j.echo.2005.10.005.
 25. Khan JN, Nazir SA, Horsfield MA, Singh A, Kanagala P, Greenwood JP, Gershlick AH, McCann GP. Comparison of semi-automated methods to quantify infarct size and area at risk by cardiovascular magnetic resonance imaging at 1.5T and 3.0T field strengths. *BMC Res Notes*. 2015;8:52. doi: 10.1186/s13104-015-1007-1.
 26. DeLong ER, DeLong DM, Clarke-Pearson DL. Comparing the areas under two or more correlated receiver operating characteristic curves: a non-parametric approach. *Biometrics*. 1988;44:837–845.
 27. Cho KH, Kim KP, Woo BC, Kim YJ, Park JY, Cho SY, Park SU, Jung WS, Park JM, Moon SK. Relationship between Blood Stasis Syndrome Score and Cardioankle Vascular Index in Stroke Patients. *Evid Based Complement Alternat Med*. 2012;2012:696983. doi: 10.1155/2012/696983.
 28. McGraw KO, Wong SP. Forming inferences about some intraclass correlation coefficients. *Psychol Methods*. 1996;1:30–46.
 29. Papavasiliu T, Flächter S, Haghi D, Stelzbeck T, Wolpert C, Dinter D, Kühl H, Borggrefe M. Extent of myocardial hyperenhancement on late gadolinium-enhanced cardiovascular magnetic resonance correlates with q waves in hypertrophic cardiomyopathy. *J Cardiovasc Magn Reson*. 2007;9:595–603. doi: 10.1080/10976640600945465.
 30. Reimer KA, Jennings RB, Cobb FR, Murdock RH, Greenfield JC Jr, Becker LC, Bulkley BH, Hutchins GM, Schwartz RP Jr, Bailey KR. Animal models for protecting ischemic myocardium: results of the NHLBI Cooperative Study. Comparison of unconscious and conscious dog models. *Circ Res*. 1985;56:651–665.
 31. Buss SJ, Krautz B, Hofmann N, Sander Y, Rust L, Giusca S, Galuschky C, Seitz S, Giannitsis E, Plegier S, Raake P, Most P, Katus HA, Korosoglou G. Prediction of functional recovery by cardiac magnetic resonance feature tracking imaging in first time ST-elevation myocardial infarction. Comparison to infarct size and transmural by late gadolinium enhancement. *Int J Cardiol*. 2015;183:162–170. doi: 10.1016/j.ijcard.2015.01.022.
 32. Neizel M, Korosoglou G, Lossnitzer D, Kühl H, Hoffmann R, Ocklenburg C, Giannitsis E, Osman NF, Katus HA, Steen H. Impact of systolic and diastolic deformation indexes assessed by strain-encoded imaging to predict persistent severe myocardial dysfunction in patients after acute myocardial infarction at follow-up. *J Am Coll Cardiol*. 2010;56:1056–1062. doi: 10.1016/j.jacc.2010.02.070.

CLINICAL PERSPECTIVE

A benefit in being able to reliably identify patients whose left ventricular function will recover after ST-segment-elevation myocardial infarction is to identify a lower risk group who will not require further monitoring and consideration of additional therapies such as implantable cardiac defibrillators. Our results suggest that even patients with extensive late gadolinium enhancement still require further imaging to assess whether left ventricular function has recovered, with one third of patients with segmental area extent of late gadolinium enhancement >75% demonstrating functional recovery. This is likely to result from overestimation of necrosis on late gadolinium enhancement in the acute phase post ST-segment-elevation myocardial infarction because of the presence of edema. Even when measured acutely, late gadolinium enhancement is still the best method available to predict functional recovery, but clinicians must be aware that some proportion of segments with near-transmural enhancement in the acute phase has the potential to recover function. If viability is the key determinant on deciding further management, then the options are either to wait until edema has settled (after 7–10 days) or consider low-dose dobutamine assessment in patients with >50% segmental area extent of late gadolinium enhancement. *Ecc* may have a role in predicting segmental recovery in patients with contraindications to gadolinium-based contrast agents.

Complete Versus Lesion-Only Primary PCI The Randomized Cardiovascular MR CvLPRIT Substudy



Gerry P. McCann, MD,* Jamal N. Khan, MScB,* John P. Greenwood, MScB, PhD,† Sheraz Nazir, MBBCh,* Miles Dalby, MD,‡ Nick Curzen, BM, PhD,§ Simon Hetherington, MD,|| Damian J. Kelly, MD,¶ Daniel J. Blackman, MD,‡ Ame Ring, PhD,*** Charles Peebles, MScB,§ Joyce Wong, MD,‡ Thiagarajah Sasikaran, PhD,†† Marcus Flather, MBBCh, PhD,‡‡ Howard Swanton, MD,§§ Anthony H. Gershlick, MBBCh*

ABSTRACT

BACKGROUND Complete revascularization may improve outcomes compared with an infarct-related artery (IRA)-only strategy in patients being treated with primary percutaneous coronary intervention (PPCI) who have multivessel disease presenting with ST-segment elevation myocardial infarction (STEMI). However, there is concern that non-IRA PCI may cause additional non-IRA myocardial infarction (MI).

OBJECTIVES This study sought to determine whether in-hospital complete revascularization was associated with increased total infarct size compared with an IRA-only strategy.

METHODS This multicenter prospective, randomized, open-label, blinded endpoint clinical trial evaluated STEMI patients with multivessel disease having PPCI within 12 h of symptom onset. Patients were randomized to either IRA-only PCI or complete in-hospital revascularization. Contrast-enhanced cardiovascular magnetic resonance (CMR) was performed following PPCI (median day 3) and stress CMR at 9 months. The pre-specified primary endpoint was infarct size on pre-discharge CMR. The study had 80% power to detect a 4% difference in infarct size with 100 patients per group.

RESULTS Of the 296 patients in the main trial, 205 participated in the CMR substudy, and 203 patients (98 complete revascularization and 105 IRA-only) completed the pre-discharge CMR. The groups were well-matched. Total infarct size (median, interquartile range) was similar to IRA-only revascularization: 13.5% (6.2% to 21.9%) versus complete revascularization, 12.6% (7.2% to 22.6%) of left ventricular mass, $p = 0.57$ (95% confidence interval for difference in geometric means 0.82 to 1.41). The complete revascularization group had an increase in non-IRA MI on the pre-discharge CMR (22 of 98 vs. 11 of 105, $p = 0.02$). There was no difference in total infarct size or ischemic burden between treatment groups at follow-up CMR.

CONCLUSIONS Multivessel PCI in the setting of STEMI leads to a small increase in CMR-detected non-IRA MI, but total infarct size was not significantly different from an IRA-only revascularization strategy. (Complete Versus Lesion-Only Primary PCI Pilot Study [CvLPRIT]; [ISRCTN70913605](https://doi.org/10.1016/j.jacc.2015.09.099)) (J Am Coll Cardiol 2015;66:2713-24)
© 2015 by the American College of Cardiology Foundation.

Listen to this manuscript's
audio summary by
JACC Editor-in-Chief
Dr. Valentin Fuster.



From the *Department of Cardiovascular Sciences, University of Leicester and the National Institute of Health Research (NIHR) Leicester Cardiovascular Biomedical Research Unit, University Hospitals of Leicester National Health Service (NHS) Trust, Glenfield Hospital, Leicester, United Kingdom; †Multidisciplinary Cardiovascular Research Centre & Division of Cardiovascular and Diabetes Research, Leeds Institute of Cardiovascular and Metabolic Medicine (LICAMM), University of Leeds, Leeds, United Kingdom; ‡Department of Cardiology, Royal Brompton and Harefield Foundation Trust, Harefield Hospital, Middlesex, United Kingdom; and the Cardiovascular Biomedical Research Unit of Royal Brompton and Harefield NHS Foundation Trust and Imperial College London, London, United Kingdom; §Department of Cardiology and Radiology, University Hospital Southampton NHS Foundation Trust and University of Southampton, Southampton, United Kingdom; ||Department of Cardiology, Kettering General Hospital, Kettering, United Kingdom; ¶Department of Cardiology, Royal Derby Hospital, Derby, United Kingdom; †Leicester Clinical Trials Unit, University of Leicester, Leicester, United Kingdom; **Department of Mathematical Statistics and Actuarial Science, University of the Free State, Bloemfontein, South Africa; ††Clinical Trials & Evaluation Unit, Royal Brompton and Harefield NHS Foundation Trust and Imperial Clinical Trials Unit, Imperial College London, London, United Kingdom; ‡‡Clinical Trials Unit, Norfolk and Norwich University Hospitals NHS Foundation Trust and Norwich Medical School, University of East Anglia, Norwich, United Kingdom; and the §§Department of Cardiology, Heart Hospital, University College London Hospitals, London, United Kingdom.

ABBREVIATIONS AND ACRONYMS

AAR	= area at risk
CMR	= cardiovascular magnetic resonance
IRA	= infarct-related artery
LGE	= late gadolinium-enhanced
LV	= left ventricle/ventricular
MACE	= major adverse cardiovascular events
MI	= myocardial infarction
MSI	= myocardial salvage index
MVO	= microvascular obstruction
PCI	= percutaneous coronary intervention
PPCI	= primary percutaneous coronary intervention
STEMI	= ST-segment elevation myocardial infarction
T2w-STIR	= T2-weighted short tau inversion recovery
TIMI	= Thrombolysis in Myocardial Infarction

Multivessel coronary artery disease is seen in approximately 40% of patients presenting with ST-segment elevation myocardial infarction (STEMI) being treated with primary percutaneous coronary intervention (PPCI). Clinical guidelines recommend percutaneous coronary intervention (PCI) to the infarct-related artery (IRA) only, largely based on registry data that have suggested increased risk of adverse events with complete revascularization (1,2) in those patients selected to receive complete revascularization. However, 2 recent prospective randomized controlled trials (PRAMI [Preventive Angioplasty in Myocardial Infarction] trial and the CvLPRIT [Complete Versus Lesion-Only Primary PCI Trial]), which compared a strategy of complete versus IRA-only revascularization in PPCI patients with multivessel disease, have shown a reduction in major adverse cardiovascular events (MACE) with complete revascularization (3,4).

SEE PAGE 2725

The mechanisms leading to improved clinical outcomes are currently unclear. However, there is concern that PCI to non-IRAs may be associated with additional procedural-related infarction (5). These well-described type 4a myocardial infarctions (MIs) (6) cannot be detected by conventional enzymatic markers at the time of PPCI because the associated increases are relatively small compared with the large rise in enzymes caused by the STEMI itself. Cardiovascular magnetic resonance (CMR) is able to precisely characterize areas of myocardial injury following myocardial ischemia. The myocardium at risk becomes edematous (7), and late gadolinium-enhanced (LGE) imaging allows the accurate detection and quantification of

infarct size and microvascular obstruction (MVO) (8). Infarct size (9) and MVO (10) measured on CMR are both strong medium-term prognostic markers following PPCI. There are no CMR data as yet in the literature on patients undergoing complete revascularization for multivessel disease at the time of PPCI.

The primary aim of the current pre-specified substudy was to assess whether a complete revascularization strategy, due to causing additional infarcts in the non-IRA territories, was associated with greater infarct size than an IRA-only strategy in patients randomized in CvLPRIT. Additionally, we aimed to assess whether myocardial salvage and myocardial ischemia at follow-up CMR were different in the 2 groups.

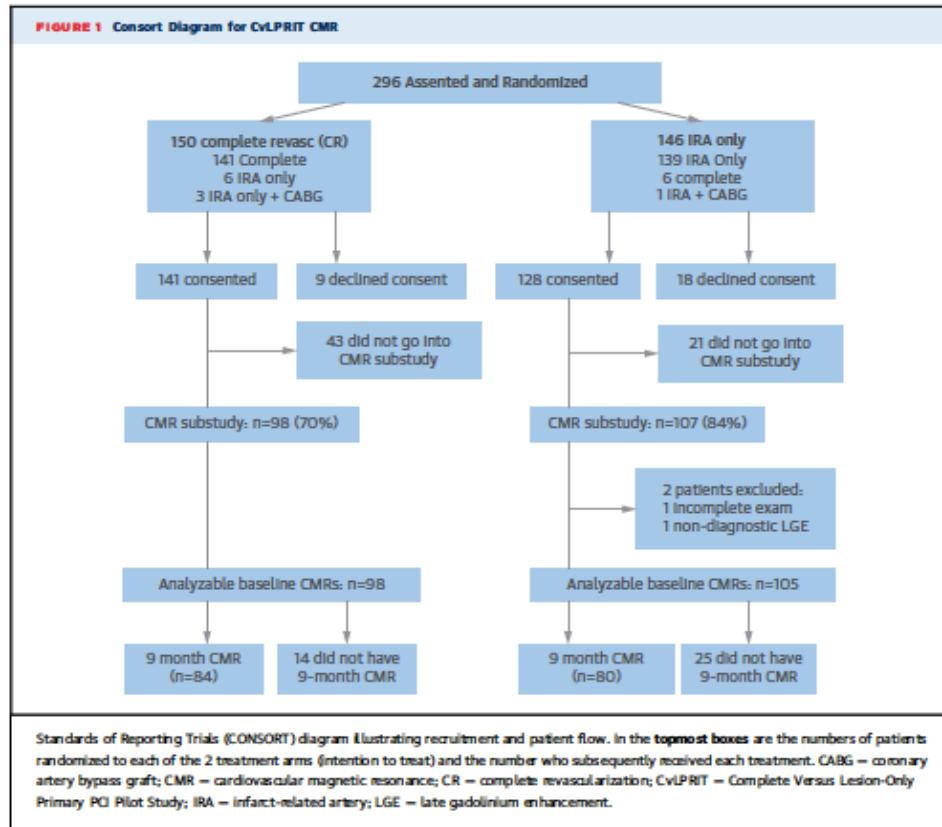
METHODS

STUDY DESIGN. The design and rationale of the study have been published previously (11). Briefly, CvLPRIT CMR was a pre-specified substudy of a multicenter, prospective, randomized, controlled, open-label clinical trial and with blinded CMR endpoint analysis (PROBE design) that was conducted in 7 U.K. centers between May 2011 and May 2014. The inclusion (PPCI <12 h from symptom onset and angiographic stenosis in the non-IRA >70% or >50% in 2 orthogonal views) and exclusion criteria were as for the main trial (4) with absolute contraindications to CMR imaging as an additional exclusion. The Trent Research Ethics Committee (Ref: 11/H0405/4) approved the study, which was conducted according to the Declaration of Helsinki. All patients gave written informed consent.

PATIENTS. The flow diagram for patient recruitment and testing is shown in Figure 1. Eligible patients from the first 286 in the main trial (4) were approached to participate in the CMR substudy until the target recruitment (200) was achieved (April 2013). Patients in the CMR substudy had similar clinical characteristics to those included in the main trial (Table 1).

The CMR substudy was funded by the Medical Research Council and managed by the NIHR Efficacy and Mechanism Evaluation programme (10-27-01). The main CvLPRIT trial was funded by the British Heart Foundation (SP/10/001) with support from the NIHR Comprehensive Local Research Networks. The views expressed in this publication are those of the author(s) and not necessarily those of the NHS, the NIHR, or the Department of Health. Dr. McCann is funded by an NIHR research fellowship. Dr. McCann has received research grants from Servier, Novartis, and Menarini International. Dr. Dalby has been a consultant for AstraZeneca, Medtronic, Boston Scientific, and Eli Lilly and Company; and has received research grants from Abbott Vascular, Daiichi Sankyo, Eli Lilly and Company, and Sanofi. Dr. Curzen has received research grants from Boston Scientific, St. Jude Medical, Haemonetics, and Medtronic; honoraria from St. Jude Medical, Haemonetics, and HeartFlow; travel sponsorship from Biosensors, Abbott Vascular, St. Jude Medical, and Haemonetics; and has also received nonfinancial support from Volcano. Dr. Ring is an employee of Medac; and has received research funding and travel grants from Boehringer Ingelheim, Novartis, and Roche. Dr. Flather has served on advisory and speakers boards for AstraZeneca and Menarini International; and has received research funding from Menarini International. Dr. Gershlick has served on advisory boards of Medtronic, Abbott Vascular, and AstraZeneca; and is on the speakers bureau of Abbott Vascular and AstraZeneca. All other authors have reported that they have no relationships relevant to the contents of this paper to disclose. Drs. McCann and Khan contributed equally to this work.

Manuscript received June 24, 2015; revised manuscript received September 2, 2015; accepted September 22, 2015.



RANDOMIZATION AND TREATMENT. Eligible patients presenting with STEMI within 12 h were randomized, after verbal assent and coronary angiography, but before PCI to the culprit lesion, to either IRA-only or in-hospital complete revascularization. Randomization was stratified by infarct location (anterior/non-anterior MI) and time to presentation (>3 or ≤3 h). PCI was performed according to current guidelines. Written informed consent for continued participation in the study was obtained on the day(s) following the PPCI, once the patient was able to understand and retain the information.

ANGIOGRAPHIC ANALYSIS. Pre- and post-PPCI epicardial coronary flow was assessed using Thrombolysis In Myocardial Infarction (TIMI) scoring (12). Collateral flow to the IRA pre-PPCI was graded using the Rentrop system (13). Quantitative coronary angiography was undertaken using QAngioXA v1.0 software (Medis, Leiden, the Netherlands).

CMR IMAGING. CMR was undertaken in 5 of the 7 hospitals recruiting to the main study, using 1.5-T platforms (4 Siemens Avanto, Erlangen, Germany, and 1 Philips Intera, Best, the Netherlands). Patients from the 2 other participating hospitals without onsite CMR (Derby and Kettering) were scanned at Glenfield Hospital.

PRE-DISCHARGE CMR. CMR was performed during the index admission and after non-IRA PCI in those patients in the complete revascularization group in whom the procedure was staged. The protocol was similar to that previously described (14) with the addition of T2-weighted short tau inversion recovery (T2w-STIR) imaging for the detection of edema and is shown in Figure 2, with typical pulse sequence parameters for the Siemens scanners. A complete T2w-STIR left ventricular (LV) short-axis stack was acquired after localizer and long-axis cine imaging. Gadolinium gadopentate (Magnevist, Bayer,

TABLE 1 Baseline Characteristics of the Main CvLPRIT and CMR Substudy Participants

	CvLPRIT (n = 296)	CMR Substudy		p Value
		CR (n = 98)	IRA (n = 105)	
Age, yrs	64.9 ± 11.6	63.1 ± 11.3	64.1 ± 10.8	0.53
Male	240/296 (81.1)	87 (88.8)	83 (79.0)	0.06
BMI, kg/m ² *	27.3 (24.4–30.2)	27.5 (24.6–29.7)	27.5 (24.7–30.6)	0.36
Systolic BP, mm Hg	137.6 ± 27.1	134.7 ± 27.3	140.0 ± 28.0	0.18
Anterior infarct	106 (35.6)	35 (35.7)	37 (37.2)	0.94
eGFR, mL/min/1.73	95.74 ± 34.7	98.2 ± 34.3	93.49 ± 30.7	0.36
Peak CK, IU/L*	1,010 (423.3–1,740)	1,025 (628–1,660)	1,057 (614–1,834)	0.37
Hypertension	105/287 (36.6)	36 (36.7)	37 (35.2)	0.82
Hypercholesterolemia	75/287 (26.1)	28 (28.6)	28 (26.7)	0.76
Diabetes mellitus	39/287 (13.6)	15 (15.3)	13 (12.4)	0.55
Current smoker	87/285 (30.5)	36 (36.7)	28 (28.0)	0.12
Previous MI	12/287 (4.2)	4 (4.1)	4 (3.8)	0.92
Previous PCI	9/287 (3.1)	4 (4.1)	3 (2.9)	0.63
Killip class II–III	24/286 (8.4)	6 (6.1)	10 (9.5)	0.37

Values are mean ± SD, n/N (%), or median (interquartile range), unless otherwise noted. *Non-normally distributed data: analyzed after log transformation with independent Student *t* testing.
BMI = body mass index; BP = blood pressure; CK = creatine kinase; CMR = cardiovascular magnetic resonance; CR = complete revascularization; CvLPRIT = Complete Versus Lesion-Only Primary PCI Pilot Study; eGFR = estimated glomerular filtration rate; IRA = infarct-related artery-only revascularization; MI = myocardial infarction; PCI = percutaneous coronary intervention.

Faversham, United Kingdom) 0.2 mmol/kg was administered before the short-axis cine stack.

FOLLOW-UP CMR. Follow-up CMR was performed at 9 months (±4 weeks) post-PPCI. The protocol for follow-up CMR was similar to the pre-discharge scan, but with T2w-STIR imaging omitted and assessment of reversible ischemia included. First-pass perfusion imaging in 3 short-axis slices was performed as previously described (15) following intravenous administration of 0.1 mmol/kg gadolinium contrast, using a breath-hold, saturation recovery gradient-echo pulse sequence. Pharmacological stress was achieved with intravenous adenosine infusion at 140 µg/kg/min for ≥3 min. Rest perfusion, with a further 0.1 mmol/kg of contrast, was performed after acquiring a short-axis cine stack covering the entire LV and ≥10 min after stress imaging. LGE imaging was acquired 10 min following rest perfusion.

CMR ANALYSIS. Physicians blinded to all clinical data, including treatment allocation, performed the CMR analyses at the University of Leicester core laboratory. Image quality was assessed on a 4-point scale: 3 = excellent; 2 = good; 1 = moderate; and 0 = unanalyzable. Additionally, for T2w-STIR sequences, if no regional variation in signal intensity within the myocardium was seen, these patients were excluded from analysis of the area at risk (AAR).

LV volumes and mass were calculated from cine images as previously described using QMass v7.1

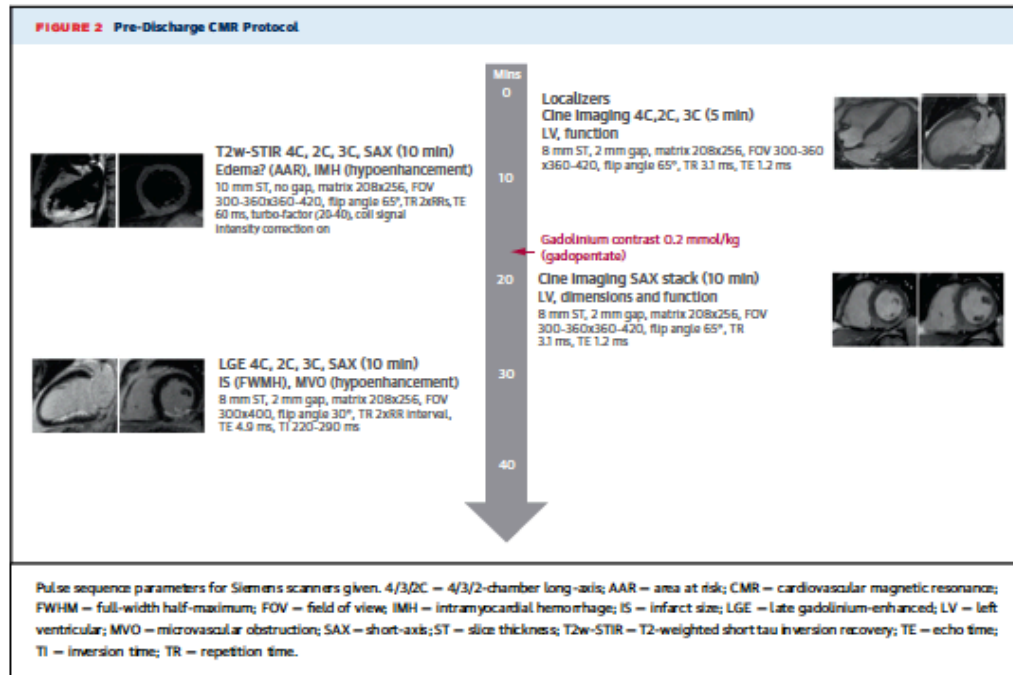
(Medis) (15). The presence of LGE was assessed by 2 observers (G.P.M., J.N.K.) and was quantitated with cvi42 (Cardiovascular Imaging, Calgary, Alberta, Canada) using the full-width half-maximum technique (16). If infarction was seen in more than 1 coronary territory in the pre-discharge CMR, this was recorded as being in the IRA territory (associated edema and/or MVO) or the non-IRA territory with the consensus of 3 observers (J.N.K., G.P.M., J.P.G.). Non-IRA infarcts were additionally classified as likely to be acute or chronic (presence of wall thinning and no edema/MVO). Infarct size was recorded for both IRA and non-IRA LGE, and total infarct size was the sum of all LGE. Edema (AAR) was quantified as hyper-enhancement on T2w-STIR imaging in cvi42 using Otsu's Automated Method (17). Areas of hypo-enhancement within infarct and edema were regarded as MVO and intramyocardial hemorrhage, respectively, and included in the infarct size and AAR, respectively. LV volumes and mass were indexed to body surface area, and infarct size was expressed as percentage of LV mass. Myocardial salvage index (MSI) was calculated as the percentage of the AAR that was not infarcted on LGE images using infarct size from both the pre-discharge (Acute MSI) and follow-up (Final MSI) CMR scan.

Perfusion images were visually assessed for defects (visible defect for ≥5 heartbeats) by the consensus of 2 observers (J.N.K., G.P.M.). Cine, stress perfusion, rest perfusion, and LGE images were studied together and assessed according to the American Heart Association 16-segment model. Rest perfusion images were used mainly to identify artifacts. Perfusion defects and areas of infarction were graded as sub-endocardial (≤50% transmural) or transmural (>50% transmural) and given a score of 1 or 2, respectively, per segment, whereas normal myocardium was scored 0. A modified summed difference score was calculated (maximum score 32) (18), defined as the difference between the sum of segmental stress perfusion defects and LGE. The summed difference score was expressed as percentage of the maximum possible to calculate ischemic burden.

INTRA- AND INTEROBSERVER VARIABILITY OF LV VOLUMETRICS AND INFARCT CHARACTERISTICS.

Ten pre-discharge and follow-up scans were randomly selected and analyzed twice by the same observer after 4 weeks (J.N.K.) and once by a further observer (S.N.). The data are shown in the Online Appendix. All intraclass correlation coefficients for intraobserver and interobserver agreement for CMR quantitative data exceeded 0.92.

CLINICAL OUTCOMES AND FOLLOW-UP. MACE comprised a composite of all-cause mortality, recurrent MI,



heart failure, and ischemia-driven revascularization. Additional secondary endpoints included cardiovascular death, individual components of the primary endpoint, and the safety endpoints stroke, major bleeding, and contrast-induced nephropathy. Data were collected by an independent clinical trials unit (Royal Brompton Hospital, London, England) and events adjudicated by blinded clinicians.

STATISTICAL ANALYSIS. The primary outcome was infarct size (expressed as a % of LV mass) on pre-discharge CMR, which was analyzed on a log-transformed scale, as it is generally right-skewed. Primary analysis was on an intention-to-treat basis of all randomized patients according to treatment group who completed the pre-discharge CMR. The result was adjusted for known predictors of infarct size (age, anterior MI, time to revascularization, diabetes, AAR, Rentrop grade, and TIMI flow grade pre-PPCI), using generalized mixed models. No adjustments for multiplicity were performed for secondary endpoints. Normally distributed continuous variables were expressed as mean \pm SD, and comparison was with Student *t* tests. Non-normally distributed data were expressed as median (25th to 75th quartiles) and

analyzed using independent Student *t* testing where log transformation normalized data, and using Mann-Whitney testing where the degree of skew rendered data nontransformable. Categorical variables were compared using chi-square testing. Clinical outcomes were assessed using time-to-first-event survival analysis (log-rank test with right censoring), and Cox proportional hazard models were fitted to estimate hazard ratios and 95% confidence intervals for treatment comparisons. One hundred patients in each arm gave 81% power to detect a 4% absolute difference in infarct size, assuming a mean of 20% of LV mass and standard deviation of 10% (19,20), using a 2-tailed test with $\alpha = 0.05$. New infarct comprising 4% of LV mass is associated with adverse prognosis in patients with revascularization-related injury (21).

RESULTS

PATIENTS. In the CMR substudy, 205 consented to participate. Of these, 2 patients were excluded: 1 patient did not complete the early CMR, and in 1 patient, the LGE images were not analyzable. The

TABLE 2 Periprocedural Details in the CR and IRA-Only Groups

	CR (n = 98)	IRA (n = 105)	p Value
Radial access	81/97 (83.5)	82/105 (78.1)	0.33
Symptom to PCI time, min*	192 (131-302)	172 (127-268)	0.20
Glycoprotein IIb/IIIa inhibitor	34/97 (35.1)	36/104 (34.6)	0.95
Bivalirudin	52/92 (56.5)	43/94 (45.7)	0.14
Thrombectomy catheter	67/97 (69.1)	79/105 (75.2)	0.33
Contrast dose, mL*	300 (220-400)	190 (150-230)	<0.001
Screening time, min*	17 (12-23)	9 (7-13)	<0.001
Procedure length, min*	66 (43-84)	42 (30-56)	<0.001
Vessels with ≥70% stenosis	1.8 ± 0.6	1.7 ± 0.6	0.82
Left anterior descending IRA	34/98 (34.7)	39/105 (37.1)	0.82
Left circumflex artery IRA	20/98 (20.4)	18/105 (17.1)	0.55
Right coronary artery IRA	44/98 (44.9)	48/105 (45.7)	0.91
Reperfusion grade			
0-1	88/98 (89.8)	102/105 (97.1)	
2-3	10/98 (10.2)	3/105 (2.9)	0.083
TIMI pre-PCI grade	0 (0-1)	0 (0-1)	0.56
TIMI grade post-PCI	3 (3-3)	3 (3-3)	0.31
IRA no-reflow	8/98 (8.2)	3/107 (2.8)	0.09
Total number of stents	3 (2-4)	1 (1-2)	<0.001
Drug-eluting stent use	97/98 (99)	96/105 (91.4)	0.013
Aspirin	97/98 (99.0)	105/105 (100)	0.30
Second antiplatelet agent	98/98 (100)	105/105 (100)	1.00
Clopidogrel	34/98 (34.7)	36/105 (34.3)	0.95
Prasugrel	49/98 (50.0)	53/104 (51.0)	0.89
Ticagrelor	15/98 (15.3)	16/105 (14.3)	0.91
Beta-blocker	93/98 (94.9)	97/105 (92.4)	0.46
ACEI or ARB	95/98 (96.9)	101/105 (96.2)	0.77
Additional antidiabetic medication	6/98 (6.1)	17/105 (16.2)	0.024
Statin	98/98 (100)	104/105 (99.1)	0.33
Loop diuretic	9/98 (9.2)	13/105 (12.4)	0.46
Alosterone inhibitor	5/98 (5.1)	5/105 (4.8)	0.91

Values are n/N (%), median (interquartile range), or mean ± SD. The bold type indicates statistically significant p values. Additional antidiabetic medication includes calcium-channel blockers, nifedipine, or nicorandil. *Non-normally distributed data analyzed after log transformation with independent Student's t testing.

ACEI = angiotensin-converting enzyme inhibitor; ARB = angiotensin receptor blocker; TIMI = Thrombolysis in Myocardial Infarction; other abbreviations as in Table 1.

complete revascularization and IRA-only groups in the CMR substudy were well-matched for characteristics, with no statistically significant differences between groups, although there was a trend for more women in the IRA-only group (Table 1).

ANGIOGRAPHIC AND PCI DETAILS. Data are shown in Table 2. Thirty patients in the complete revascularization group had a staged procedure 1.43 (interquartile range [IQR]: 1.03 to 2.04) days after the PPCI. Coronary artery disease severity was similar in the groups, although the IRA-territory collateralization grade was significantly higher in the complete revascularization group. Total screening time, contrast dose, procedure length, and number of implanted stents were significantly greater in

complete revascularization patients. The vast majority of patients in both arms received drug-eluting stents, although this was slightly higher in complete revascularization patients. Symptom-to-PCI times, antiplatelet, anticoagulant use, and post-PPCI creatine kinase rise were similar in both arms. There was a nonsignificant trend for no-reflow to be more common in the complete revascularization than the IRA group. There was greater usage of a second antianginal agent in patients in the IRA-only group.

PRE-DISCHARGE CMR. Results are displayed in Table 3. Pre-discharge CMR was undertaken at a median of 3 days post-PPCI in both treatment arms. There was no statistical difference in the primary endpoint of total infarct size between the groups: IRA-only, 13.5% (IQR: 6.2% to 21.9%) of LV mass versus complete revascularization, 12.6% (IQR: 7.2% to 22.6%) of LV mass, $p = 0.57$. The ratio of the geometric means for total infarct size in the IRA-only (15.9 ± 13.2%) and CR (16.3 ± 13.0%) arms is 0.98 (95% confidence interval: 0.82 to 1.41), confirming no difference between the 2 treatment arms. When corrected for covariates (age, sex, anterior MI, time to revascularization, TIMI flow pre-PCI, diabetic status, Reperfusion grade and AAR), there remained no difference in median infarct size (beta = 0.02, $p = 0.68$) between the 2 groups.

The prevalence of multiple territory infarcts in the complete revascularization group was double that of the IRA-only group and the number of acute non-IRA infarcts was increased 3-fold in those undergoing complete revascularization (Table 3). Examples, with corresponding edema images, are shown in Figure 3, and the location, size of infarct, expected coronary artery territory, and whether the individual patients had an additional non-IRA PCI are shown in Online Table 1. Eighteen of 20 acute non-IRA infarcts in patients in the complete revascularization group concurred with additional PCI in the relevant non-IRA coronary territory. Five patients randomized to the IRA-only group also had non-IRA acute MI. Two of these patients had treatment crossover and received non-IRA PCI. The first crossover followed ongoing ischemia post-PPCI and was associated with non-IRA MI in the relevant territory. The second crossover resulted from human error, and this patient had a small non-IRA acute MI in the anterosseptum but had non-IRA PCI of the circumflex artery. Six patients in the IRA-only and 5 in the complete revascularization group had chronic infarcts (evidenced by wall thinning). Excluding these patients from the analysis did not affect the results (Online Table 2).

MVO was present in more than one-half of all patients, although quantitatively, the amount was very low (median <0.2% of LV mass). In 52 patients (26%), AAR could not be quantified: no artifact, but no edema discernable (n = 33); not performed due to arrhythmia or suboptimal breath-holding (n = 14); or severe artifact (n = 5). AAR and MSI were lower, but not significantly, in the complete revascularization group. LV volume, mass, and ejection fraction were similar in both groups.

FOLLOW-UP CMR. Follow-up CMR was completed in 84 patients in the complete revascularization group and 80 patients in the IRA-only group (Table 3). Of the 39 patients who did not have a repeat CMR, 29 patients declined, 3 had died, 2 cited claustrophobia, 1 had an implantable cardioverter-defibrillator, 1 had a severe noncardiovascular illness, and in 3, there were logistical reasons. There were no differences in baseline characteristics or pre-discharge CMR between those who completed and did not attend the follow-up CMR (data not shown). Three patients were unable to undertake adenosine stress perfusion due to obstructive airways disease, and perfusion imaging was unanalyzable in 2 patients due to severe persistent dark-rim artefact (1 in the complete revascularization group, 1 in the IRA-only group). LV volumes and function were similar between groups. The prevalence of infarct and multiple infarcts were greater in the complete revascularization group. However, there was no significant difference in total infarct size and final MSI between the groups. Reversible perfusion defects were seen in 21% of patients in both groups, and overall ischemic burden was small. When the extent of ischemia was assessed only in patients with reversible perfusion defects, the ischemic burden was not statistically different in the complete revascularization and IRA-only groups.

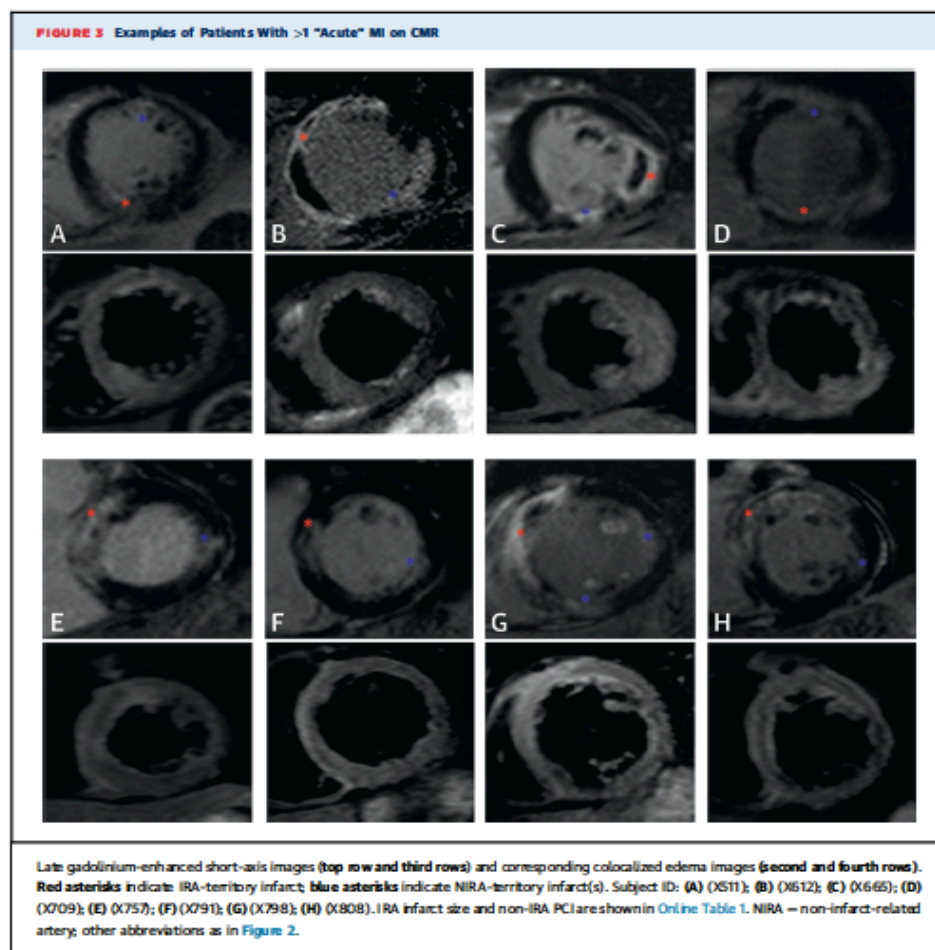
CLINICAL OUTCOMES. Median follow-up was 372 days (IRA 377 days, complete revascularization 366 days, p = 0.38). One hundred ninety-eight (98%) patients attended 12-month clinical follow-up (3 patients died before this time point, and 2 patients withdrew consent). Length of inpatient stay and incidence of in-hospital clinical events were similar in the treatment arms (Table 4). There was a borderline significant reduction in MACE in patients undergoing complete revascularization, and the corresponding events rates and hazard ratio were similar to that seen in the main trial. Thirteen patients in the IRA-only arm had 14 revascularization procedures (2 separate PCIs in 1 patient) after PPCI. All but 1 were revascularization to the non-IRAs (1 patient had acute stent thrombosis of the IRA on day 0 and had repeat PCI). The indications were

TABLE 3 Pre-Discharge and Follow-Up CMR

Pre-Discharge CMR	CR (n = 98)	IRA (n = 105)	p Value
Total infarct size, % LV mass*	12.6 (7.2-22.6), 16.3 ± 13.0	13.5 (6.2-21.9), 15.9 ± 13.2	0.57
Time from PPCI, days*	3.0 (2.0-4.3)	2.8 (1.8-3.4)	0.13
Infarct on LGE	95 (96.9)	95 (90.5)	0.06
Patients with >1 infarct	22 (22.4)	11 (10.5)	0.02
Patients >1 acute infarct	17 (17.1)	5 (4.8)	0.004
Number of acute infarcts in those with >1 infarct†	2 (2-2), 2.2 ± 0.4	2 (2-2), 2.0 ± 0.0	0.60
IRA infarct size, % LV mass*	12.1 (7.0-21.4), 15.2 ± 12.1	12.2 (6.2-21.2), 15.3 ± 13.2	0.68
Total acute IS, % LV mass*	12.5 (7.0-22.0), 15.8 ± 12.4	12.4 (6.2-21.6), 15.4 ± 13.2	0.60
Acute NIRA infarct size, % LV mass in those with >1 infarct†	2.5 (0.54-4.5), 3.2 ± 3.3	2.1 (0.81-4.5), 2.5 ± 1.9	0.004
Acute NIRA infarct size (% LV mass, per infarct†)	1.4 (0.3-2.3), 1.6 ± 1.5	1.0 (0.4-2.2), 1.3 ± 1.0	0.94
Area at risk, % LV mass‡	32.2 ± 11.8	36.0 ± 12.9	0.06
MSI§	58.5 (32.8-74.9)	60.5 (40.6-81.9)	0.14
MVO present	57/98 (58.2)	54/105 (51.4)	0.34
MVO, % LV mass†	0.19 (0.00-2.00)	0.08 (0.00-1.05)	0.63
IMH present§	22/75 (29.3)	17/77 (22.1)	0.31
RV infarction	7/98 (7.1)	4/105 (3.8)	0.29
LVMi, g/m ² *	52.3 (46.8-62.0)	52.2 (44.7-59.2)	0.33
LVEDVi, ml/m ² *	89.7 (80.7-102)	90.7 (80.4-102)	0.64
LVESVi, ml/m ² *	47.0 (38.0-58.4)	49.8 (39.7-62.1)	0.56
LVEF, %	45.9 ± 9.9	45.1 ± 9.5	0.60
Follow-Up CMR	CR (n = 84)	IRA (n = 80)	
Time to CMR, months	9.4 (9.0-10)	9.3 (8.9-9.9)	0.20
LVMi, g/m ² *	47.4 (40-52.6)	43.4 (38.0-49.3)	0.33
LVEDVi, ml/m ² *	93.3 (82.2-110)	95.0 (82.7-107)	0.63
LVESVi, ml/m ² *	45.1 (37.8-58)	43.6 (34.8-57.9)	0.33
LVEF, %	49.7 ± 9.4	50.8 ± 8.7	0.42
Infarct on LGE	82/84 (97.6)	71/80 (88.8)	0.023
Patients with >1 infarct	20/84 (23.8)	9/80 (11.2)	0.035
IS, % LV mass*	7.3 (3.0-14.4)	7.6 (3.2-15.1)	0.41
Final MSI*	82.1 (63.0-90.3)	79.4 (71.6-93.3)	0.20
Perfusion	CR (n = 82)	IRA (n = 77)	
Ischemic burden, %†	3.4 ± 8.9	4.3 ± 11.3	0.81
Ischemia present	17/82 (20.7)	16/77 (20.8)	0.99
Ischemic burden in patients with ischemia, %	15.5 ± 13.7	20.4 ± 17.1	0.37
Ischemic burden >20%	6 (7.3)	6 (7.8)	0.91

Values are n/N (%), median (interquartile range), mean ± SD, or n (%), unless otherwise noted. The bold type indicates statistically significant p values. *Nonnormally distributed data: analyzed after log transformation with independent Student t testing. †Nonnormally distributed data: analyzed using Mann-Whitney analysis. ‡Increase the median and interquartile range was 0 (0 to 0) for both IRA and CR groups, mean ± SD of the results are presented although the data are nonparametrically distributed. §Analyzable edema imaging available in 75 of the complete revascularization group and 77 of the IRA-only group. IMH = intramyocardial hemorrhage; IS = infarct size; LGE = late gadolinium enhancement; LV = left ventricle; LVEDVi = left ventricular end-diastolic volume index; LVEF = left ventricular ejection fraction; LVESVi = left ventricular end-systolic volume index; LVMi = left ventricular mass index; MSI = myocardial salvage index; MVO = microvascular obstruction; NIRA = non-infarct-related artery; PPCI = primary percutaneous coronary intervention; RV = right ventricle; other abbreviations as in Table 1.

as follows: acute coronary syndrome 7 (3 non-STEMI); 6 refractory symptoms (1 coronary artery bypass surgery); and 1 patient underwent elective PCI at the discretion of the responsible physician.



DISCUSSION

This is the first detailed study of pre-discharge and follow-up CMR outcomes in a randomized study of IRA-only versus complete revascularization in multivessel coronary disease at PPCI. The data have confirmed that non-IRA PCI is associated with additional infarction. However, these type 4a MIs (6) are relatively infrequent, generally small, and did not result in an increase in total infarct size. There is mounting evidence from randomized trials that treating multivessel disease with complete revascularization (4,22) leads to a reduction in MACE after PPCI compared with an IRA-only strategy.

The patients in the substudy had similar baseline characteristics to those in the main trial. Because time to revascularization (4) and anterior MI (23) are strongly associated with infarct size, randomization was stratified by these variables. There was a similar reduction in the hazard ratio for MACE in the complete revascularization CMR subgroup as that seen in the main study compared with IRA-only revascularization, and we believe that the CMR substudy population is representative of those in the main study.

It is well-recognized that elective PCI can cause a troponin rise in approximately 30% of patients and approximately 50% undergoing PCI for unstable angina (24). Such type 4a MIs (6) can be detected on

CMR and have been associated with adverse prognosis (21,25). In this substudy of CvLPRIT, the prevalence of >1 CMR-detected infarct in patients receiving complete revascularization was double that in the IRA-only arm (23.8% vs. 11.2%), and more than 3-fold for the acute non-IRA infarcts (17.1% vs. 4.8%) (Central Illustration). Previous Q-wave MI was an exclusion criterion in this study, but 4% had a history of previous non-STEMI, and a similar number (6% in the IRA-only and 5% in the complete revascularization groups) had chronic non-IRA MI on the pre-discharge CMR. Excluding these patients did not significantly affect the results. These data suggest that an additional 12% of patients with multivessel disease who receive complete revascularization at the time of PPCI will have evidence of additional CMR-detectable infarction compared with IRA-only revascularization. However, this proportion is less than might have been expected from previous studies in elective PCI (24), where up to 29% of patients have evidence of new infarction on CMR associated with troponin elevation (25). The extent of acute non-IRA infarction was also smaller (median 2.5% of LV mass) than may have been anticipated from elective PCI data given that average infarct size in those with new late enhancement on CMR was $5.0 \pm 4.8\%$ of LV mass (25), despite all patients in that study being pre-treated with clopidogrel for >24 h and given a glycoprotein IIb/IIIa inhibitor periprocedurally. Importantly, in the present study, total infarct size was not increased in the short term or at follow-up, and there were no significant differences in myocardial salvage, LV volumes, or ejection fraction between the treatment groups. Peak creatine kinase levels were also similar in the 2 groups.

These findings provide reassurance that non-IRA intervention at the time of PPCI does not lead to increased total infarct size. In the main CvLPRIT trial, complete revascularization resulted in a significantly reduced hazard ratio for 12-month MACE despite the greater prevalence of CMR-detected type 4a MIs shown here. There are limited data as to whether revascularization-induced myocardial injury detected by CMR is linked to prognosis (21), and none in patients presenting with STEMI. In an observational study of 152 patients undergoing elective revascularization, 32% had evidence of new LGE, which averaged 5 g (4% of LV mass), and one-half of these patients were treated with coronary artery bypass surgery (21). In that study, patients with new infarction following revascularization had reduced ejection fraction, increased LV volume, increased total infarct size, and a 3-fold increase in MACE at a median of 2.9 years follow-up compared with those without new

12-Month Follow-Up	CR (n = 98)	IRA (n = 105)	HR (95% CI)	p Value
MACE	8 (8.2)	18 (17.1)	0.43 (0.18–1.04)	0.055
Death	1 (1.0)	1 (0.9)	1.07 (0.07–17.4)	0.96
Recurrent MI	0 (0.0)	3 (2.9)	—	0.10
Heart failure	3 (3.1)	4 (3.8)	0.80 (0.17–3.7)	0.77
Revascularization	4 (4.1)	10 (9.5)	0.40 (0.12–1.3)	0.13
Inpatient Clinical Events				
OR (95% CI)				
Length of inpatient stay, days	3 (2–4), 3.5 ± 2.6	3 (2–4), 3.9 ± 2.8		0.13
Death	1 (1.0)	1 (0.9)	1.07 (0.07–17.4)	0.96
Recurrent MI	0 (0.0)	1 (0.9)	2.17 (0.19–24.3)	0.33
Heart failure	2 (2.0)	1 (1.0)	0.71 (0.12–4.3)	0.52
Repeat revascularization	2 (2.0)	3 (2.9)	—	0.71
Safety endpoints				
Contrast nephropathy	1 (1.0)	0 (0.0)	—	0.30
Vascular access injury needing repair	0 (0.0)	0 (0.0)	—	1.00
CVA/TIA	0 (0.0)	0 (0.0)	—	1.00
Major bleed	3 (3.1)	1 (1.0)	3.29 (0.34–32.1)	0.28

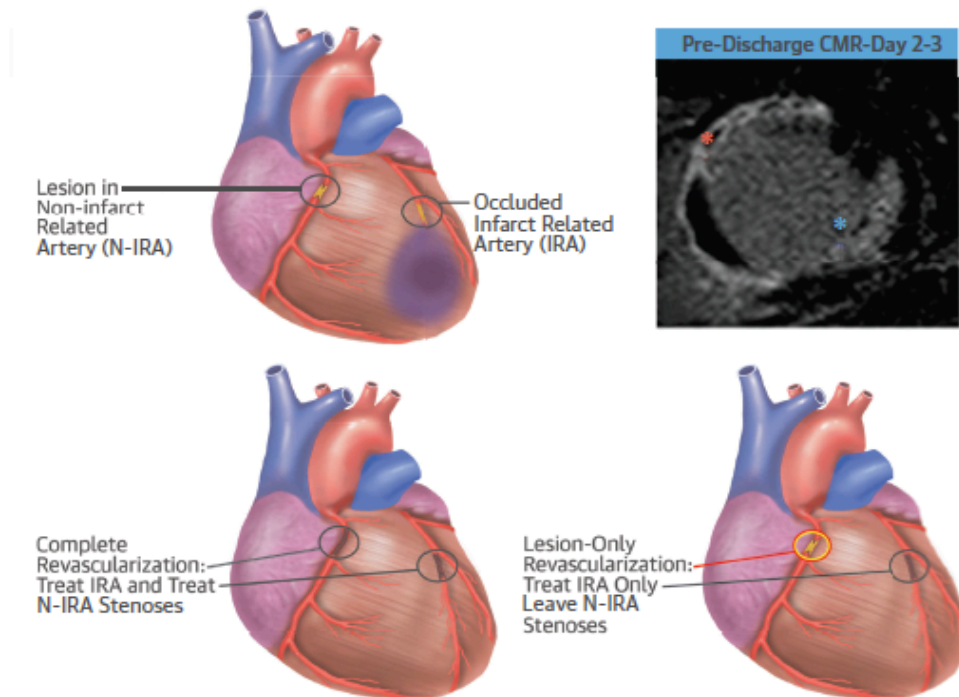
Values are n (%), median (interquartile range), or mean ± SD. A dash indicates that no HR was presentable because 1 or both treatment arms had an incidence of 0.
CI = confidence interval; CVA = cerebrovascular accident; HF = heart failure; HR = hazard ratio; MACE = major adverse cardiovascular events; OR = odds ratio; TIA = transient ischemic attack; other abbreviations as in Table 1.

LGE (21). Given that the complete revascularization group in the current study had no increase in total infarct size, LV volume, or reduced ejection fraction, it seems unlikely that the short- to medium-term clinical benefits of complete revascularization (22) will be offset in the long term by increased heart failure or sudden cardiac deaths. However, longer-term follow-up of patients in this study is needed to confirm this.

We did not observe any significant differences in myocardial salvage between the treatment groups in this study. Non-IRA revascularization at the time of PPCI could increase perfusion to watershed areas by relieving flow-limiting stenoses, resulting in increased myocardial salvage (26). Alternatively, resting myocardial perfusion and flow reserve following PCI may actually be reduced, as has been shown in elective patients as a result of distal embolization, particularly when the PCI is associated with new LGE (26,27). It may be that both effects are seen with non-IRA PCI resulting in no net benefit with regard to myocardial salvage in the PPCI setting.

Unexpectedly, we also observed no difference in ischemic burden between the groups undergoing follow-up stress perfusion CMR. There are several potential explanations for this finding. First, it is well recognized that even severe angiographic stenoses may not cause ischemia (28,29). Second, 11 patients in the IRA-only arm had further PCI before

CENTRAL ILLUSTRATION Complete Versus Lesion-Only Revascularization in Acute MI: The CMR CvLPRIT Substudy



CMR Infarcts	CR	p	IRA-only
Acute N-IRA MI	17/98 (17.1%)	0.004	5/103 (4.8%)
Total IS (% LV Mass)	12.6 (7.2-22.6)	0.57	13.5 (6.2-21.9)
IRA IS (% LV Mass)	12.1 (7.0-21.4)	0.68	12.2 (6.2-21.2)

McCann, G.P. et al. J Am Coll Cardiol. 2015; 66(24):2713-24.

Overview of the CvLPRIT CMR trial showing the randomization strategy and main results. Red asterisk indicates IRA late gadolinium enhancement; blue asterisk indicates N-IRA late gadolinium enhancement. CMR = cardiovascular magnetic resonance; CvLPRIT = Complete Versus Lesion-Only Primary PCI Pilot Study; LV = left ventricular; MI = myocardial infarction; N-IRA = non-infarct-related artery; IS = infarct size.

the stress CMR that is likely to have reduced ischemic burden in this group. Third, the small number of crossovers from randomization is likely to have diminished the differences in ischemia between the groups. Finally, the stress CMR was undertaken in patients on optimal medical therapy, which may dramatically reduce post-MI ischemia (30) making it more difficult to detect differences

between the groups, especially as there was higher use of a second antianginal medication in the IRA-only group. This may also explain why the overall ischemic burden in our study was small (3% to 4%). It remains to be determined whether ischemia is prognostically important in the PPCI era, especially because medical therapy may result in similar clinical outcomes to a revascularization strategy even in

patients treated with thrombolysis (30). Further insight on this subject will be available from the CvLPRIT nuclear substudy.

STUDY LIMITATIONS. The optimal timing to assess infarct size post-STEMI is uncertain (31). We chose an early time point to enhance participation in the CMR substudy because we felt there could have been a higher dropout rate scanning patients after hospital discharge. MSI was only reliably measured in ~75% of patients, and the use of novel T1 or T2 mapping techniques for future studies may lead to a more robust assessment. Current CMR techniques cannot reliably differentiate whether a very small MI, which is not associated with wall thinning, edema, or MVO, is acute or chronic, and this contributed to the slight overreporting of acute non-IRA MIs that were not associated with revascularization in this study.

CONCLUSIONS

An in-hospital complete revascularization strategy in patients with multivessel disease at the time of PPCI is associated with a small increase in type 4a MIs in non-IRA territories, but total infarct size

was not significantly different compared with an IRA-only strategy.

REPRINT REQUESTS AND CORRESPONDENCE: Dr. Gerry McCann, Department of Cardiovascular Sciences, University of Leicester, Glenfield Hospital, LE3 9QP Leicester, England, United Kingdom. E-mail: gpm12@le.ac.uk.

PERSPECTIVES

COMPETENCY IN MEDICAL KNOWLEDGE: In patients with STEMI and multivessel disease, a strategy of complete revascularization is associated with a small increase (12%) in the risk of type 4a MIs, but similar total infarct size, compared with a strategy addressing only the infarct-related artery.

TRANSLATIONAL OUTLOOK: Future trials should incorporate selective revascularization strategies based on coronary angiography at the time of primary PCI and functional assessments of coronary lesions to guide complete revascularization.

REFERENCES

1. Steg PG, James SK, Atar D, et al. ESC guidelines for the management of acute myocardial infarction in patients presenting with ST-segment elevation. *Eur Heart J* 2012;33:2569-619.
2. O'Gara PT, Kushner FG, Ascheim DD, et al. 2013 ACCF/AHA guideline for the management of ST-elevation myocardial infarction: a report of the American College of Cardiology Foundation/American Heart Association Task Force on Practice Guidelines. *J Am Coll Cardiol* 2013;61:e78-140.
3. Flano DS, Hillenbrand HB, Rehwald WG, et al. Infarct resorption, compensatory hypertrophy, and differing patterns of ventricular remodeling following myocardial infarctions of varying size. *J Am Coll Cardiol* 2004;43:2124-31.
4. Gershlick AH, Khan JN, Kelly DJ, et al. Randomized trial of complete versus lesion-only revascularization in patients undergoing primary percutaneous coronary intervention for STEMI and multivessel disease: the CvLPRIT trial. *J Am Coll Cardiol* 2015;65:963-72.
5. Prasad A, Rihal CS, Lennon RJ, Singh M, Jaffe AS, Holmes DR. Significance of periprocedural myonecrosis on outcomes after percutaneous coronary intervention: an analysis of preintervention and postintervention troponin T levels in 5487 patients. *Circ Cardiovasc Interv* 2008;1:10-9.
6. Thygesen K, Alpert JS, Jaffe AS, et al. Third universal definition of myocardial infarction. *Eur Heart J* 2012;33:2551-67.
7. Aletras AH, Tilak GS, Natarajan A, et al. Retrospective determination of the area at risk for reperfused acute myocardial infarction with T2-weighted cardiac magnetic resonance imaging: histopathological and displacement encoding with stimulated echoes (DENSE) functional validations. *Circulation* 2006;113:1865-70.
8. Wagner A, Mahholdt H, Holly TA, et al. Contrast-enhanced MRI and routine single photon emission computed tomography (SPECT) perfusion imaging for detection of subendocardial myocardial infarcts: an imaging study. *Lancet* 2003;361:374-9.
9. Larose E, Rodes-Cabau J, Pibarot P, et al. Predicting late myocardial recovery and outcomes in the early hours of ST-segment elevation myocardial infarction: traditional measures compared with microvascular obstruction, salvaged myocardium, and necrosis characteristics by cardiovascular magnetic resonance. *J Am Coll Cardiol* 2010;55:2459-69.
10. de Waale S, Desch S, Eitel I, Fuernau G. Impact of early vs. late microvascular obstruction assessed by magnetic resonance imaging on long-term outcome after ST-elevation myocardial infarction: a comparison with traditional prognostic markers. *Eur Heart J* 2010;31:2660-8.
11. Kelly DJ, McCann GP, Bladman D, et al. Complete Versus Culprit-Lesion Only Primary PCI Trial (CvLPRIT): a multicentre trial testing management strategies when multivessel disease is detected at the time of primary PCI: rationale and design. *EuroIntervention* 2013;8:1190-8.
12. TIMI Study Group. The Thrombolysis in Myocardial Infarction (TIMI) trial. Phase I findings. *N Engl J Med* 1985;312:932-6.
13. Rantrop KP, Cohen M, Blanke H, Phillips RA. Changes in collateral channel filling immediately after controlled coronary artery occlusion by an angioplasty balloon in human subjects. *J Am Coll Cardiol* 1985;5:587-92.
14. Khan JN, Razvi N, Nazir SA, et al. Prevalence and extent of infarct and microvascular obstruction following different reperfusion therapies in ST-elevation myocardial infarction. *J Cardiovasc Magn Reson* 2014;16:38.
15. Steadman CD, Jerosch-Herold M, Grundy B, et al. Determinants and functional significance of myocardial perfusion reserve in severe aortic stenosis. *J Am Coll Cardiol* 2012;59:182-9.
16. Amado LC, Gerber BL, Gupta SN, et al. Accurate and objective infarct sizing by contrast-enhanced magnetic resonance imaging in a canine myocardial infarction model. *J Am Coll Cardiol* 2004;44:2383-9.
17. Sjogren J, Uecker JF, Engblom H, et al. Semi-automatic segmentation of myocardium at risk in T2-weighted cardiovascular magnetic resonance. *J Cardiovasc Magn Reson* 2012;14:10.
18. Hussain ST, Paul M, Plain S, et al. Design and rationale of the MR-INFORM study: stress perfusion cardiovascular magnetic resonance imaging to guide the management of patients with stable coronary artery disease. *J Cardiovasc Magn Reson* 2012;14:65.

19. Lund GK, Stork A, Muellerleile K, et al. Prediction of left ventricular remodeling and analysis of infarct resorption in patients with reperfused myocardial infarcts by using contrast-enhanced MR imaging. *Radiology* 2007;245:95-104.
20. Wu E, Ortiz JT, Tejedor P, et al. Infarct size by contrast enhanced cardiac magnetic resonance is a stronger predictor of outcomes than left ventricular ejection fraction or end-systolic volume index: prospective cohort study. *Heart* 2008;94:730-6.
21. Rahimi K, Banning AP, Cheng AS, et al. Prognostic value of coronary revascularisation-related myocardial injury: a cardiac magnetic resonance imaging study. *Heart* 2009;95:1937-43.
22. Wald DS, Morris JK, Wald NJ, et al. Randomized trial of preventive angioplasty in myocardial infarction. *N Engl J Med* 2013;369:1115-23.
23. Masci PG, Ganame J, Francione M, et al. Relationship between location and size of myocardial infarction and their reciprocal influences on post-infarction left ventricular remodeling. *Eur Heart J* 2011;32:1640-8.
24. Alcock RF, Roy P, Adorini K, et al. Incidence and determinants of myocardial infarction following percutaneous coronary interventions according to the revised Joint Task Force definition of troponin T elevation. *Int J Cardiol* 2010;140:66-72.
25. Selvanayagam JB, Porto I, Channon K, et al. Troponin elevation after percutaneous coronary intervention directly represents the extent of irreversible myocardial injury: insights from cardiovascular magnetic resonance imaging. *Circulation* 2005;111:1027-32.
26. Selvanayagam JB, Cheng AS, Jerosch-Herold M, et al. Effect of distal embolization on myocardial perfusion reserve after percutaneous coronary intervention: a quantitative magnetic resonance perfusion study. *Circulation* 2007;116:1458-64.
27. Taylor AJ, Al-Saadi N, Abdel-Aty H, et al. Elective percutaneous coronary intervention immediately impairs resting microvascular perfusion assessed by cardiac magnetic resonance imaging. *Am Heart J* 2006;151:891.e1-7.
28. Dambitnik JH, Debrauwere JP, van't Hof AW, et al. Non-culprit lesions detected during primary PCI: treat invasively or follow the guidelines? *EuroIntervention* 2010;5:968-75.
29. De Bruyne B, Pijls NH, Kalesan B, et al. Fractional flow reserve-guided PCI versus medical therapy in stable coronary disease. *N Engl J Med* 2012;367:991-1003.
30. Mahmarian JJ, Dakik HA, Rlipchuk NG, et al. An initial strategy of intensive medical therapy is comparable to that of coronary revascularization for suppression of scintigraphic ischemia in high-risk but stable survivors of acute myocardial infarction. *J Am Coll Cardiol* 2006;48:2458-67.
31. Mather AN, Fairbairn TA, Artis NJ, Greenwood JP, Plein S. Timing of cardiovascular MR imaging after acute myocardial infarction: effect on estimates of infarct characteristics and prediction of late ventricular remodeling. *Radiology* 2011;261:116-26.

KEY WORDS CMR, complete revascularization, multivessel disease, PPCI, STEMI

APPENDIX For supplemental data and tables, please see the online version of this article.



Comparison of cardiovascular magnetic resonance feature tracking and tagging for the assessment of left ventricular systolic strain in acute myocardial infarction

Jamal N. Khan^{*}, Anvesha Singh, Sheraz A. Nazir, Prathap Kanagala, Anthony H. Gershlick, Gerry P. McCann

Department of Cardiovascular Sciences, Clinical Sciences Wing, University of Leicester and the NIHR Leicester Cardiovascular Biomedical Research Unit, Glenfield Hospital, Groby Road, Leicester LE3 9QP, UK

ARTICLE INFO

Article history:

Received 7 July 2014

Received in revised form 21 October 2014

Accepted 6 February 2015

Keywords:

Myocardial infarction
Cardiovascular magnetic resonance
Tagging
Feature tracking
Strain
Infarct size

ABSTRACT

Aims: To assess the feasibility of feature tracking (FT)-measured systolic strain post acute ST-segment elevation myocardial infarction (STEMI) and compare strain values to those obtained with tagging.

Methods: Cardiovascular MRI at 1.5T was performed in 24 patients, 2.2 days post STEMI. Global and segmental circumferential (Ecc) and longitudinal (Ell) strain were assessed using FT and tagging, and correlated with total and segmental infarct size, area at risk and myocardial salvage.

Results: All segments tracked satisfactorily with FT ($p < 0.001$ vs. tagging). Total analysis time per patient was shorter with FT (38.2 ± 3.8 min vs. 63.7 ± 10.3 min, $p < 0.001$ vs. tagging). Global Ecc and Ell were higher with FT than with tagging, apart from FT Ecc using the average of endocardial and epicardial contours (-13.45 ± 4.1 [FT] vs. -13.85 ± 3.9 [tagging], $p = 0.66$). Intraobserver and interobserver agreement for global strain were excellent for FT (ICC 0.906–0.990) but interobserver agreement for tagging was lower (ICC < 0.765). Interobserver and intraobserver agreement for segmental strain was good for both techniques (ICC > 0.7) apart from tagging Ell, which was poor (ICC = 0.15). FT-derived Ecc significantly correlated with total infarct size ($r = 0.44$, $p = 0.03$) and segmental infarct extent ($r = 0.44$, $p < 0.01$), and best distinguished transmurally infarcted segments (AUC 0.77) and infarcted from adjacent and remote segments. FT-derived Ecc correlated strongest with segmental myocardial salvage ($r_s = -0.406$).

Conclusions: FT global Ecc and Ell measurement in acute STEMI is feasible and robust. FT-derived strain is quicker to analyse, tracks myocardium better, has better interobserver variability and correlated more strongly with infarct, area at risk (oedema), myocardial salvage and infarct transmural extent.

© 2015 Elsevier Ireland Ltd. All rights reserved.

1. Introduction

Contractile dysfunction following acute ST-segment elevation myocardial infarction (STEMI) predicts prognosis [1]. Cardiovascular MRI measured myocardial strain is the gold standard measure of myocardial function [2]. It offers greater accuracy in detecting dysfunctional myocardium compared with global (ejection fraction) and regional (wall-motion scoring, wall thickening) measures of function [3]. Global strain is also an independent predictor of medium-term prognosis post STEMI [4].

Myocardial tissue tagging creates saturated lines perpendicular to the slice plane and act as tissue markers in a grid, tracking myocardial motion. Various tagging analysis techniques are available, including local sine-wave modelling (SinMod) and harmonic phase analysis (HARP), which have demonstrated close agreement [5,6]. Tagging requires the acquisition of additional sequences and time-consuming post-processing. Feature tracking (FT) tracks features of interest (tissue-cavity interfaces, tissue dishomogeneities, anatomic landmarks) along contour lines on routinely acquired steady-state free-precession (SSFP) cine images, analogous to echocardiographic speckle tracking [7,8]. FT-derived strain has been compared to tagging in muscular dystrophy patients [7] and normal volunteers [9] showing reasonable agreement although we have recently shown that FT overestimates systolic strain compared to tagging [10]. There are no published strain data using FT in acute STEMI.

^{*} Corresponding author. Tel.: +44 0116 258 3244; fax: +44 0116 258 3422.

E-mail addresses: jk211@le.ac.uk (J.N. Khan), as707@le.ac.uk (A. Singh),

sn191@le.ac.uk (S.A. Nazir), pk214@le.ac.uk (P. Kanagala), agershlick@aol.com

(A.H. Gershlick), gerry.mccann@uhl-tr.nhs.uk (G.P. McCann).

<http://dx.doi.org/10.1016/j.ejrad.2015.02.002>

0720-048X/© 2015 Elsevier Ireland Ltd. All rights reserved.

This study aimed to assess the feasibility of FT measured global and segmental peak circumferential (Ecc) and longitudinal (Ell) strain assessment post acute STEMI and compare strain values to those obtained with tagging.

2. Materials and methods

2.1. Study population

Twenty-four acute STEMI patients were recruited. STEMI was diagnosed according to European Society of Cardiology definitions [11] and patients underwent primary percutaneous coronary intervention within 12 h of symptoms. The study was approved by the local research ethics committee, conducted according to the Declaration of Helsinki and patients provided written informed consent.

2.2. Cardiovascular MRI

MRI was performed at a median of 2.2 days following STEMI presentation on a 1.5 T scanner (Siemens Avanto, Erlangen, Germany) with dedicated cardiac receiver coils. SSFP cine, T2-weighted short-tau inversion recovery (T2W-STIR) and Late Gadolinium Enhancement (LGE) imaging were performed in long-axis (2/3/4-chamber) views and contiguous short-axis slices covering the left ventricle (LV). LGE images were acquired 10 min after 0.2 mmol/kg gadolinium-DTPA (Magnevist, Bayer, Germany) using a segmented inversion-recovery gradient-echo sequence. The inversion time was progressively adjusted to null unaffected myocardium. Three pre-contrast short-axis (base, mid, apical) and long-axis tagged images were acquired using a prospectively-gated spatial modulation of magnetization (SPAMM) gradient-echo sequence. The imaging protocol is detailed in Fig. 1.

2.3. MRI analysis

2.3.1. Volumetric and LGE analysis

Analysis was performed using *cmr42* (Circle Cardiovascular Imaging, Calgary, Canada). LV volumes and function were calculated as previously described [12]. Oedema (area-at-risk, AAR) and infarct size (IS) were quantified on T2W-STIR and LGE imaging using Otsu's Automated Method [13] and Full-Width Half-Maximum technique, respectively [14]. Myocardial salvage index (MSI) defines the proportion of the AAR that does not progress to infarction and was calculated as $[(AAR - \text{infarct size})/AAR] \times 100$. Total oedema and infarct size were expressed as a percentage of LV end-diastolic mass. Segmental oedema, infarct and MSI were calculated as a percentage area for each of the 16 segments in the American Heart Association model [15,16]. Transmural enhancement was defined as >50% segmental enhanced area. Segments with <1% area of oedema or LGE were classed as having no oedema or infarct, respectively. 'Infarct' segments had LGE and oedema, 'adjacent' ('at risk') segments had oedema but no LGE, and 'remote' segments had no oedema or LGE [17].

2.3.2. Circumferential and longitudinal strain analysis

Global peak Ecc and Ell strain were calculated as the average of values obtained in the three short-axis slices and long-axis views, respectively. We recorded the time taken to: (a) analyse images, (b) post-process numerical data (generate and extract strain data on a segmental, slice and long-axis basis and paste them into a spreadsheet where segmental data are illustrated for the 16 segments in numerical order as per American Heart Association nomenclature) [15] and (c) total analysis time (sum of a and b).

2.3.2.1. Tagging analysis. Strain was measured using dedicated software (*InTag*, CREATIS, Lyon, France run as a plug-in for OsiriX

v3.8, Pixmeo, Switzerland) as described previously [5] and illustrated in Fig. 2. OsiriX functions only on Apple Mac (Cupertino, California, USA) computers. *InTag* uses the SinMod technique. Endocardial and epicardial contours were manually drawn onto the end-systolic image and automatically propagated through the cardiac cycle. Numerical data was outputted for further post-processing.

2.3.2.2. FT analysis. Strain was measured using dedicated software (*Diogenes Image Arena*, Tomtec, Munich, Germany). The FT algorithm has been described previously [18]. Short-axis cine slices were cross-referenced with the corresponding tagged image. Endocardial and epicardial contours were manually drawn onto the end-diastolic image and propagated. The software automatically places 8–12 points of interest along contours for optimal tracking (Fig. 3). Strain values were examined using three methods: (a) endocardial contours only, (b) epicardial contours only and (c) an average of both endocardial and epicardial values.

Suboptimally tracking segments using both techniques were manually adjusted and excluded from analysis if the movement of contoured borders deviated from true myocardial motion by >50% [9]. Interobserver and intraobserver variability of global and segmental strain analysis for both techniques was performed by two observers (JNK, AS) on a subset of 10 patients and repeated by a single observer (JNK) after 4 weeks, respectively.

2.4. Statistical analysis

Normality was assessed using the Shapiro–Wilk test, histograms and Q–Q plots. Normally distributed data were expressed as mean \pm standard deviation. Non-parametric data were expressed as median (25–75% interquartile range). Global and segmental Ecc and Ell using the FT and tagging methods were compared using paired *t*-testing, two-way mixed-effect intraclass correlation coefficient for absolute agreement (ICC) [19] and Bland–Altman analysis [20]. Interobserver and intraobserver variabilities were expressed using ICC, coefficient of variation (COV) and Bland–Altman analysis. On ICC, agreement was defined as excellent (ICC > 0.75), good (ICC 0.6–0.74), fair (ICC 0.4–0.59), or poor (ICC < 0.40) [21]. Strain was correlated with infarct and MSI using Spearman's Ranked Correlation Coefficient (r_s) and with oedema using Pearson's Correlation Coefficient (r). The sample size was chosen according to the table of Critical Values of the Spearman's Ranked Correlation Coefficient for $r_s \sim 0.40$ with $p < 0.05$, based on an initial pilot of 10 patients [22]. The correlation between global strain and number of transmurally-enhanced segments after correction for total IS was assessed using multiple regression. Independent *t*-testing compared segmental strain according to the presence of infarct, transmural infarction and oedema. Receiver Operating Curve (ROC) Area Under the Curve (AUC) analysis assessed the accuracy of each method in predicting transmural infarction. Statistical tests were performed using SPSS V20. $p < 0.05$ was considered significant.

3. Results

3.1. Baseline characteristics

MRI data for the 24 patients studied are summarized in Table 1. All segments tracked satisfactorily with FT despite hypoenhancement (microvascular obstruction) or hyperenhancement (contrast enhancement) in the infarct territory on cine imaging (Fig. 4). The number of segments excluded from analysis was significantly higher for tagging than FT. The time taken to contour, post-process

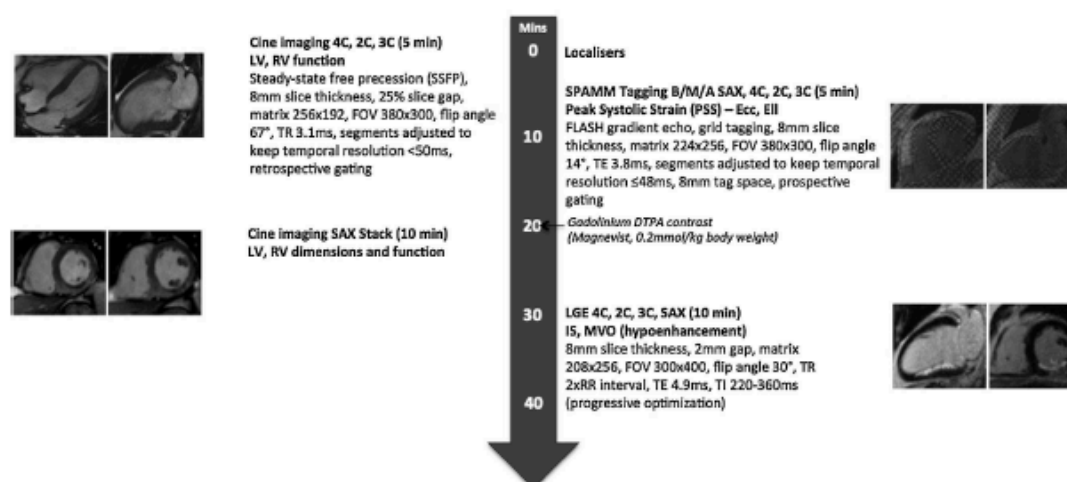


Fig. 1. MRI protocol.

Table 1
Patient characteristics and MRI data—quality and analysis time.

Number of patients (male/female)	24 (22/2)
Age (years)	63.0 ± 9.5
MRI (days post STEMI)	2.2 (1.8–3.2)
Left ventricular end-diastolic mass (g/m ²) ^a	43.7 (38.3–49.8)
Left ventricular end-diastolic volume (ml/m ²) ^a	96.4 (84.1–121.8)
Left-ventricular end-systolic volume (ml/m ²) ^a	45.9 (36.7–69.6)
Left ventricular ejection fraction (%)	49.6 ± 7.5
Infarct size (% LV mass)	13.2 (8.2–21.1)
Anterior infarct	8 (35%)
Number of segments with infarction	170
Total segments analysed	384

^a indexed for body surface area

and fully analyse each patient was significantly shorter with FT ($p < 0.001$ for all steps) (Table 2).

3.2. Global strain on FT and tagging

Global strain varied significantly with the quantification technique (Table 3). On FT, Ecc and Ell were highest using endocardial contours only, followed by the mean of endocardial and epicardial contours, and lowest using epicardial contours only ($p < 0.01$ for all comparisons). FT-derived global Ecc using endocardial contours only was higher than that derived with tagging, and lower using epicardial contours only ($p < 0.05$). Global Ecc derived using the mean of endocardial and epicardial contoured values on FT

moderately agreed with tagging but showed poor agreement using results generated from either of epicardial or endocardial contours. Global Ell was higher for all FT methods compared with tagging ($p < 0.05$).

3.3. Association with infarct extent

3.3.1. Total infarct size

There was a moderate correlation between total IS and global Ecc using all methods but statistically significant only with endocardial contours on FT (Table 4).

3.3.2. Segmental extent of infarct and transmuralty

Segmentally, Ecc and LGE moderately correlated for all FT Ecc methods, but only weakly using tagging-derived Ecc. FT and tagging-derived segmental Ell weakly correlated with segmental LGE (Table 4). The number of transmurally enhanced segments moderately correlated with global strain (Table 5). This was significant for all FT strain methods, but only for tagging-derived Ell. After correction for total IS, this correlation remained for FT methods but not for tagging-derived strain. Strain was significantly lower in transmurally-enhanced (>50%) compared with non-transmural segments using all techniques. The relative reduction in strain in transmurally-enhanced segments, and accuracy (AUC) in predicting transmural enhancement were greatest for FT-derived Ecc using endocardial contours only and FT Ecc using the mean of endocardial and epicardial contours.

Table 2
Myocardial tracking and quantification time by method.

	FT	Tagging	p
SAX cine segments excluded	0 (0%) ^a	18 (5%)	<0.001
LAX cine segments excluded	0 (0%) ^a	81 (21%)	<0.001
Number of excluded SAX segments in infarct core	0 (0%) ^a	3/18 (17%)	<0.001
Number of excluded LAX segments in infarct core	0 (0%) ^a	14/81 (17%)	<0.001
Analysis time per patient (min)	25.3 ± 3.7 ^a	33.4 ± 5.6	<0.001
Post-processing time per patient (min)	12.9 ± 2.0 ^a	30.3 ± 5.9	<0.001
Total analysis time (min)	38.2 ± 3.8 ^a	63.7 ± 10.3	<0.001

FT = feature tracking, SAX = short-axis, LAX = long-axis. Infarction defined where ≥1% segmental LGE.

^a $p < 0.001$ compared with tagging.

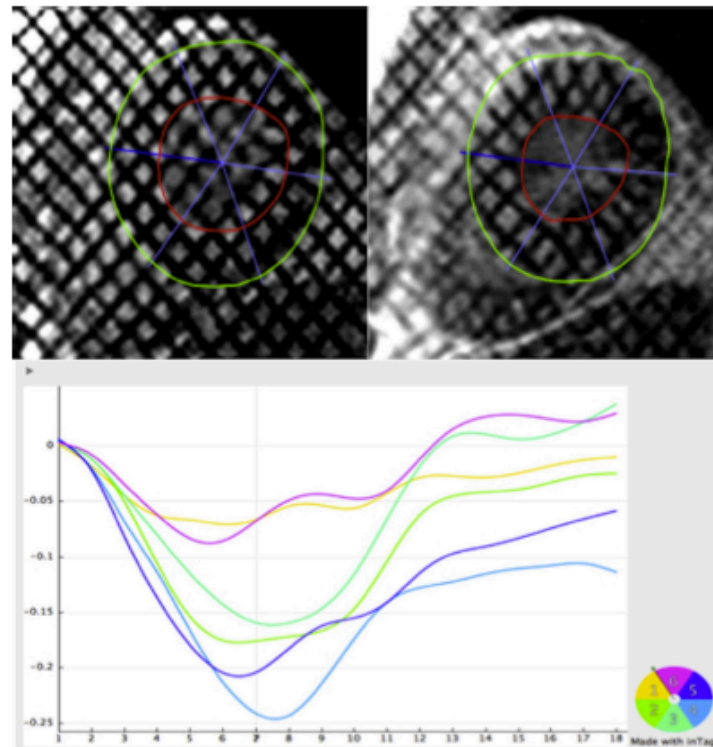


Fig. 2. Tagging strain assessment. Tagged images were analysed using *Intag* software. Top left: end-diastolic tagged image (basal short-axis slice) with endocardial and epicardial contours manually drawn and automatically propagated along the cardiac cycle per segment. Top right: corresponding end-systolic image. Bottom: segmental circumferential strain curves. Numerical data is outputted for further post-processing.

3.3.3. Infarct, adjacent and remote segments

Ecc and Ell were significantly lower in segments with infarct than in segments without, on FT and tagging. The relative reduction was greatest for FT Ecc using endocardial contours only (40% lower Ecc, Table 4). Ecc and Ell were significantly lower ($p < 0.01$ for all techniques) in 'infarct' compared with 'adjacent' segments using all techniques, except tagging-derived Ell ($p = 0.22$) (Fig. 5). The relative reduction in segmental strain was greatest for FT Ecc using endocardial contours only (41% lower Ecc in infarct vs. adjacent segments). Strain in adjacent and remote segments was similar using all techniques.

3.4. Association with oedema

Only tagging-derived global Ell significantly correlated with total oedema (AAR) (Table 4). Segmentally, there was a

significant moderate correlation between Ecc and oedema for all methods (Table 4). There was no significant correlation between segmental Ell and oedema. The relative reduction in Ecc in oedematous segments was greatest for FT Ecc using endocardial contours (29% lower in oedematous vs. non-oedematous segments).

3.5. Association with myocardial salvage index

There was a non-significant moderate correlation between global strain and total MSI using all techniques, apart from endocardially-derived FT Ell and tagging-derived Ell where there was no correlation (Table 4). Segmental strain and MSI moderately correlated using all methods, excluding tagging-derived Ell. The correlation was strongest for FT Ecc using endocardial contours

Table 3
Agreement of peak systolic strain by feature tracking and tagging.

	Ecc FT Endo	Ecc FT Epi	Ecc FT Mean	Ell FT Endo	Ell FT Epi	Ell FT mean	Ecc tagging	Ell tagging
Global strain (%)	-18.57 ± 5.4^a	-8.33 ± 3.0^a	-13.45 ± 4.1	-15.39 ± 4.5^b	-12.35 ± 3.7^b	-13.87 ± 4.0^b	-13.85 ± 3.9	-9.17 ± 2.4
ICC (FT vs. tagging)	0.271	0.159	0.417	0.137	0.297	0.200	n/a	n/a
Mean bias (%) vs. tagging (LoA)	$+4.7 (+14.9, -5.4)$	$-5.5 (+2.3, -13.3)$	$-0.4 (+8.2, -9.0)$	$+6.2 (+14.2, -1.8)$	$+3.2 (+9.6, -3.2)$	$+4.7 (+11.7, -2.3)$	n/a	n/a

Ecc = circumferential strain, Ell = longitudinal strain, FT = feature-tracking derived, Endo = endocardial contoured, Epi = epicardial contoured, IS = infarct size. Ecc (or Ell) FT Mean = Ecc (or Ell) from mean of endocardial and epicardial strain values, LoA = 95% Bland-Altman limits of agreement.

^a $p < 0.05$ Compared with Ecc tagging PSS.

^b $p < 0.05$ Compared with Ell tagging PSS.

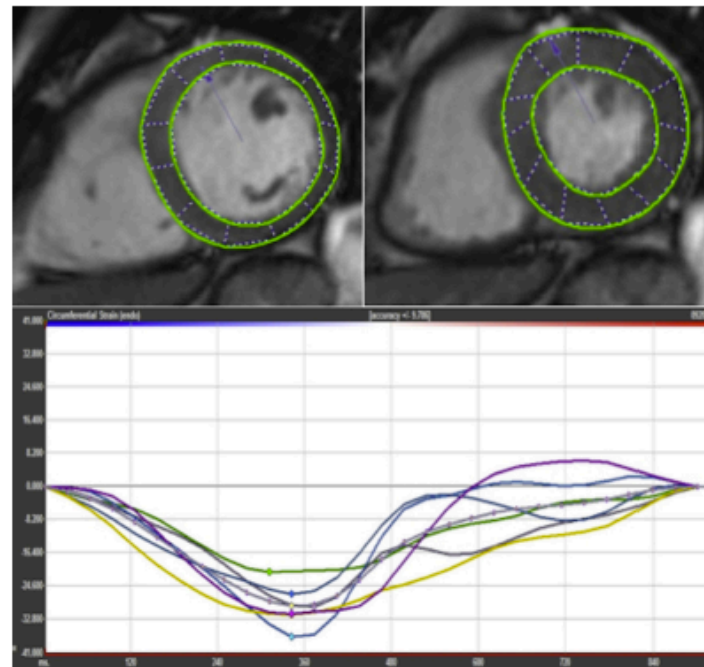


Fig. 3. Feature-tracking strain assessment. Top left: Manually drawn epicardial and endocardial contours are automatically propagated; here end-diastolic image with 12 points of analysis generated as indicated by vertical dotted lines from epicardium to endocardium. Top right: corresponding end-systolic image. Bottom: segmental circumferential strain curves, here for endocardial contour; epicardial strain curves produced separately

only ($r_s = -0.406$) and FT Ecc using the mean of endocardial and epicardial contours ($r_s = -0.402$).

3.6. Interobserver and intraobserver agreement of strain assessment

3.6.1. Global strain

All FT techniques for Ecc and Ell had excellent interobserver and intraobserver agreement (Table 6). FT strain derivation from a mean of endocardial and epicardial contours did not improve interobserver or intraobserver agreement above endocardial contouring alone. Intraobserver agreement for tagging-derived Ecc and Ell was

excellent, however interobserver agreement was lower than with FT.

3.6.2. Segmental strain

Interobserver and intraobserver agreement was lower for segmental compared with global strain for FT and tagging. Interobserver and intraobserver agreement was good for all techniques except for tagging-derived Ell where interobserver agreement was very poor (ICC 0.150, COV 58.6%). There was a trend for higher interobserver and intraobserver agreement for Ecc compared with Ell with FT (Table 6).

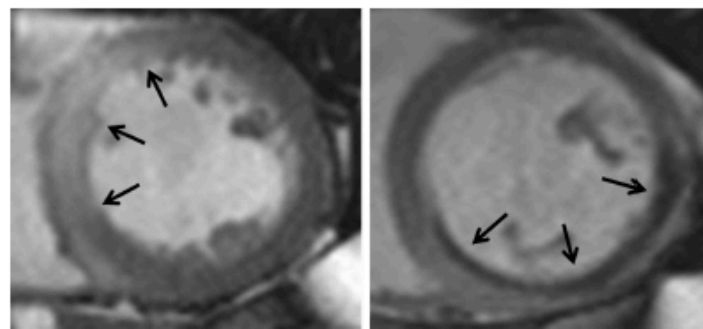


Fig. 4. Hyperenhancement and hypoenhancement on cine imaging. All segments tracked satisfactorily with FT despite hyperenhancement (contrast enhancement, left) or hypoenhancement (microvascular obstruction, right) in the infarct related territory

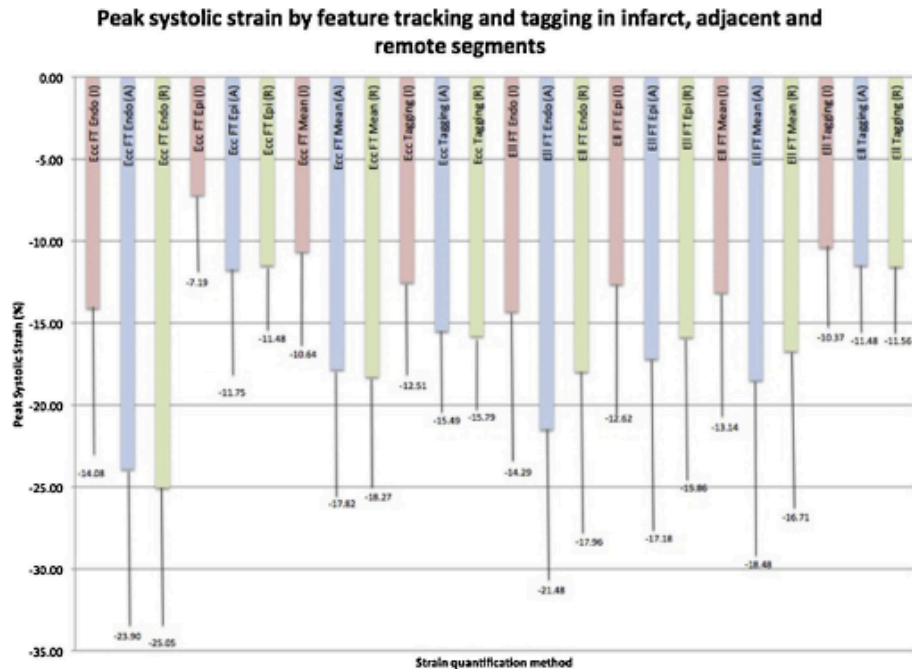


Fig. 5. Peak systolic strain by feature tracking and tagging in infarct, adjacent and remote segments.

Bland–Altman plots for intra and interobserver agreement for global and segmental strain using the techniques are in supplemental images at the end of the manuscript.

4. Discussion

In this first report of FT in acute STEMI patients, we have demonstrated the robustness of FT for the quantification of global and segmental systolic strain. Strain was higher with FT than tagging. There was excellent intraobserver agreement with FT and tagging for global strain, whereas interobserver agreement using tagging was good but remained excellent for FT. Segmental strain analysis had markedly poorer interobserver and intraobserver agreement using both techniques and was particularly poor for EII. FT-derived strain correlated more strongly with IS, AAR, MSI and infarct transmural.

Our results may have significant implications for future research studies. First, FT proved robust in our study with no non-analysable segments and a shorter analysis time compared with tagging. This was despite hypoenhancement and in particular hyperenhancement on post-contrast SSFP images, which reduces the contrast-to-noise ratio between blood-pool and myocardium. The significant number of poorly tracking, and consequently excluded tagged segments is most likely the result of image degradation due to suboptimal breath-holding and ectopy, often seen in acute STEMI. Tag fading was not a major issue as we only assessed peak systolic strain. FT requires no additional sequences to routinely acquired SSFP images, which require shorter breath-holds than tagged images. Our findings are consistent with published literature in which ~11% of tagged images have been excluded [23], whereas the majority of FT studies report no non-analysable segments [24,25]. FT thus allows faster scan times, faster

post-processing and less data are excluded due to poor contour tracking compared to tagging. In this report we quantified strain using FT by three different methods: (1) endocardial contours only, (2) epicardial contours only and (3) using the average results generated from 1 and 2. Using only one FT method dramatically speeds up the process [9].

Secondly, the method used to derive FT strain is important and investigators should be clear on which technique was used and be cautious when comparing results directly with other studies. Global Ecc using the average of endocardial and epicardial values moderately correlated with tagging in our study. We have again shown [10] that strain measured with endocardial only contouring on FT results in markedly increased values compared to the average of endocardial and epicardial values, which were similar to tagging for Ecc (with wide limits of agreement) but higher than EII. Strain values were also higher with FT than tagging in a study of healthy volunteers [9], and anteroseptal, inferior and inferoseptal Ecc were higher with FT in hypertrophic cardiomyopathy [26]. It is surprising that FT and tagging strain were reported to be very similar in patients with muscular dystrophy since it appears that endocardial contours only were used in that analysis [7]. It may be that the results of such comparisons will vary with the population and methods used, although differences in tagging analysis software are unlikely to be significant since SinMod and HARP have shown close agreement for global strain [5]. The close temporal relationship between acquisition of tagged and cine images makes true physiological differences unlikely and the temporal resolution of tagged and SSFP cine images was also very similar (~50 ms). The lower average global strain with tagging may partly result from the exclusion of segments, which contained normal non-infarcted myocardium, and this effect is likely to be greater for EII (21% of segments excluded and 83% of those non-infarcted tissue) than

Peak systolic strain by feature tracking and tagging and infarct size, area at risk and myocardial salvage.

	Ecc FT Endo	Ecc FT Epi	Ecc FT Mean	Eli FT Endo	Eli FT Epi	Eli FT Mean	Ecc Tagging	Eli Tagging
rain vs. total IS	0.438 (p=0.03)	0.385 (p=0.06)	0.395 (p=0.06)	0.314 (p=0.14)	0.326 (p=0.12)	0.368 (p=0.08)	0.303 (p=0.15)	0.396 (p=0.06)
al strain vs. segmental IS	0.437 (p<0.01)	0.368 (p<0.01)	0.445 (p<0.01)	0.176 (p=0.01)	0.171 (p=0.01)	0.184 (p<0.01)	0.266 (p<0.01)	0.078 (p=0.17)
without infarct (%)	-24.53 ± 10.8	-11.63 ± 7.1	-18.08 ± 8.2	-19.89 ± 12.2	-16.57 ± 10.3	-17.83 ± 10.7	-16.19 ± 5.8	-11.67 ± 5.4
with infarct (%)	-14.68 ± 10.5 ^a	-7.30 ± 6.0 ^a	-10.99 ± 7.7 ^a	-15.24 ± 11.0 ^a	-13.38 ± 9.8 ^a	-14.04 ± 9.4 ^a	-13.21 ± 7.1 ^a	-10.36 ± 5.3 ^a
rain vs. total AAR	0.260 (p=0.27)	0.145 (p=0.54)	0.224 (p=0.34)	0.231 (p=0.33)	0.215 (p=0.36)	0.227 (p=0.34)	0.260 (p=0.27)	0.559 (p=0.01)
al strain vs. segmental AAR	0.376 (p<0.01)	0.274 (p<0.01)	0.363 (p<0.01)	0.114 (p=0.04)	0.099 (p=0.08)	0.103 (p=0.07)	0.257 (p<0.01)	0.073 (p=0.24)
without oedema (%)	-24.81 ± 9.4	-11.47 ± 5.8	-18.13 ± 6.8	-17.75 ± 11.7	-15.87 ± 9.7	-16.61 ± 10.3	-15.64 ± 5.5	-11.43 ± 5.8
with oedema (%)	-17.51 ± 11.1 ^b	-8.75 ± 6.5 ^b	-13.13 ± 8.3 ^b	-16.85 ± 11.3	-14.18 ± 10.3	-15.01 ± 10.0	-13.56 ± 6.4 ^b	-10.81 ± 5.1
rain vs. total MSI	-0.304 (p=0.19)	-0.260 (p=0.27)	-0.294 (p=0.21)	-0.108 (p=0.65)	-0.299 (p=0.20)	-0.284 (p=0.23)	-0.224 (p=0.34)	-0.105 (p=0.66)
al strain vs. segmental MSI	-0.409 (p<0.01)	-0.332 (p<0.01)	-0.406 (p<0.01)	-0.216 (p<0.01)	-0.201 (p<0.01)	-0.226 (p<0.01)	-0.273 (p<0.01)	-0.063 (p=0.39)

with segments without infarct.

with segments without oedema. Spearman's Ranked Correlation Coefficient used for non-parametrically distributed IS and MSI. Pearson's Correlation Coefficient used for normally distributed AAR.

feature tracking and tagging and segmental transmural late gadolinium enhancement.

	Ecc FT Endo	Ecc FT Epi	Ecc FT Mean	Eli FT Endo	Eli FT Epi	Eli FT Mean	Ecc Tagging	Eli Tagging
strain vs. number of transmurally	0.463 (p=0.023)	0.442 (p=0.030)	0.436 (p=0.033)	0.397 (p=0.055)	0.414 (p=0.044)	0.441 (p=0.031)	0.334 (p=0.110)	0.487 (p=0.016)
ts								
ation between number of	+2.01 (p=0.088)	+1.17 (p=0.077)	+1.59 (p=0.076)	+2.00 (p=0.038)	+1.58 (p=0.049)	+1.79 (p=0.038)	+0.42 (p=0.619)	+0.49 (p=0.171)
inced segments and global strain								
al IS (p)								
with transmural LGE (%)	-11.61 ± 12.1 ^a	-5.90 ± 7.3 ^a	-8.76 ± 9.3 ^a	-16.03 ± 11.8 ^b	-12.32 ± 9.2 ^b	-14.21 ± 10.2 ^b	-11.77 ± 6.6 ^b	-10.63 ± 5.1 ^b
without transmural LGE (%)	-20.99 ± 11.3	-10.08 ± 6.8	-15.54 ± 8.4	-17.97 ± 11.9	-15.43 ± 10.3	-16.32 ± 10.3	-15.18 ± 6.5	-11.13 ± 5.4
strain in transmural LGE	-44.7	-41.5	-43.6	-10.8	-20.2	-12.9	-22.4	-4.5
ng segmental transmural LGE (ROC)	0.763	0.736	0.772	0.558	0.601	0.572	0.662	0.534

d with segments without transmural LGE.

with segments without transmural LGE.

change in PSS (+ is reduction in strain) with each transmurally enhanced segment.

Table 6
Interobserver and intraobserver agreement of peak systolic strain measured by feature tracking and tagging.

	Ecc FT Endo	Ecc FT Epi	Ecc FT mean	Ell FT Endo	Ell FT Epi	Ell FT mean	Ecc tagging	Ell tagging
Global strain								
Inter-observer								
ICC	0.979	0.906	0.971	0.942	0.936	0.949	0.765	0.733
Mean bias (%)	+0.6 (+2.6, −1.3)	+0.2 (+2.3, −1.9)	0.4 (+2.1, −1.3)	−0.5 (+2.7, −3.8)	+0.1 (+3.1, −2.8)	−0.2 (+2.6, −3.1)	+0.2 (+6.3, −22.2)	−0.2 (+5.4, −5.9)
LOA (±1.96SD)	4.8	12.1	6.0	10.0	11.6	9.9	22.2	28.8
Intra-observer								
ICC	0.989	0.963	0.988	0.990	0.911	0.973	0.920	0.936
Mean bias (%)	−0.7 (+0.4, −1.7)	−0.5 (+0.7, −1.7)	−0.6 (0.0, −1.2)	−0.2 (+1.3, −1.6)	0.0 (+3.7, −3.7)	−0.1 (+2.1, −2.2)	+0.9 (+4.4, −2.5)	+0.5 (+1.9, −1.0)
LOA (±1.96SD)	2.5	6.5	2.1	4.5	14.5	7.6	13.1	7.7
Segmental strain								
Inter-observer								
ICC	0.796	0.824	0.829	0.726	0.780	0.739	0.735	0.150
Mean bias (%)	+0.6 (+15.0, −13.9)	0.0 (+7.6, −7.7)	+0.3 (+9.9, −9.4)	−0.4 (+16.8, −17.7)	+0.6 (+14.3, −13.2)	−0.7 (+14.2, −15.7)	+0.3	+1.6
LOA (±1.96SD)	34.5	38.8	31.4	46.7	44.2	44.9	34.7	>(+14.7, −11.4)
Intra-observer								
ICC	0.872	0.859	0.887	0.826	0.771	0.822	0.813	0.864
Mean bias (%)	−0.6 (+10.8, −12.0)	−0.4 (+7.1, −8.0)	−0.5 (+7.5, −8.6)	−0.5 (+13.6, −14.5)	+0.7 (+15.8, −14.3)	+0.3 (+13.2, −12.6)	+0.8 (+9.2, −7.6)	+0.5 (+6.3, −5.3)
LOA (±1.96SD)	26.4	37.5	25.6	38.0	48.7	40.0	29.9	24.7

Ecc = circumferential strain, Ell = longitudinal strain, FT = feature-tracking derived, Endo = endocardial contour, Epi = epicardial contour, IS = infarct size, ICC = intraclass correlation coefficient, LOA = limits of agreement (Bland–Altman), Ecc (or Ell) FT Mean = Ecc (or Ell) derived from mean of endocardial and epicardial strain values.

for Ecc (5% of segments excluded). Our global strain Ecc values on tagging are similar to those reported previously post STEMI [3].

Thirdly, the moderate correlation between FT Ecc and infarct globally and segmentally, combined with significant differences in Ecc in segments with and without infarct provide some internal validation in the absence of 'true' strain in this clinical population. This was especially the case with FT-derived Ecc using endocardial contours only and may be because scarring and dysfunction post STEMI is greatest endocardially [27]. Ecc has correlated better with infarct size than Ell and Err on previous FT [28] (in chronic infarction) and tagging studies [3,29] and been shown to be similarly higher in adjacent and remote segments compared with infarct [30].

Furthermore, the ability of FT-derived Ecc to identify transmural enhancement offers potential for predicting functional improvement post STEMI. Ecc has also been shown to distinguish segmental transmural enhancement better than Ell using Strain-Encoded Imaging (SENC) [29]. Our findings are consistent with the only published study to date studying the influence of MSI on baseline segmental function, where O'Regan demonstrated lower Ecc on CSPAMM tagging with reducing MSI quartiles [31]. Given that quantifying strain with FT endocardial contours only is quick, requires minimal post-processing, and demonstrates moderately good agreement between Ecc and infarct size and excellent intra and interobserver agreement, this method of analysis may be preferred, even though strain values compared to tagging are markedly increased. We observed no significant relationship between segmental tagging-derived Ell and infarct. This is likely to be contributed to by the fact that 21% of long-axis tagged segments were unanalysable.

Given the tendency for LGE early after STEMI to underestimate the potential for functional recovery [31,32], it remains to be determined whether strain assessment combined with LGE more accurately predicts viable segments and clinical outcomes [33].

The excellent intraobserver agreement for global Ecc and Ell using FT and tagging is in agreement with published data, with COVs ranging from 2.8% [9] to 11.8% [28] using FT and ICCs of >0.8 using tagging [21]. The higher interobserver agreement seen with FT compared with tagging is likely related to variations in manual adjustment of poorly tracking contours, especially in end-systole where tagging may not differentiate trabeculae and papillary muscles from compact myocardium. Our interobserver and intraobserver agreement using *Intag* is lower than described by Miller [5], however they studied stable cardiomyopathy and healthy subjects who usually have good breath holding and gating. Segmental interobserver and intraobserver agreement was much poorer for FT and tagging. Our data is consistent with published literature, with reported COVs of 24–46% for FT [25,34] and ICC ~0.75 for tagging [5]. This aspect needs improving, especially when assessing changes in regional contractile function at follow-up post STEMI and it is unclear whether segmental strain assessment offers any major advantages over semi-quantitative visual wall motion scoring.

This study has a number of limitations. We have compared a single tagging sequence with FT on a single platform and the results may not be generalizable to other sequences, field strength and manufacturers. The use of a CSPAMM sequence is likely to have resulted in better tag persistence [2] but we choose to use a SPAMM sequence because of widespread availability and the likely use in multicentre clinical trials. We did not attempt to quantify diastolic strain rate due to tag fading in most patients and did not study Err since it is established that this is significantly less reproducible than Ecc and Ell. Test–retest reproducibility was not assessed and should be considered in future studies.

5. Conclusions

In conclusion, global Ecc and Ell are higher measured using FT than with tagging in patients early after STEMI. FT is more robust than SPAMM tagging in acute STEMI with better myocardial tracking, greater interobserver agreement, faster analysis and stronger correlation with IS, AAR, MSI and infarct transmural. FT strain assessment is feasible in acute STEMI and is likely to become the preferred quantification method.

Funding sources

Medical Research Council (managed by the National Institute of Health Research [NIHR] Efficacy and Mechanism Evaluation programme, 10-27-01) and The British Heart Foundation (SP/10/001) with support from the (NIHR) Comprehensive Local Research Networks.

Conflict of interest statement

There are no conflicts of interests for any of the authors.

Acknowledgments

GPM, AHG and JNK conceived the idea for the study. AHG and JNK recruited patients. JNK supervised study visits. JNK and AS performed CMR analyses. JNK wrote the paper and performed statistical analysis, which all authors critically reviewed and revised.

Appendix A. Supplementary data

Supplementary data associated with this article can be found, in the online version, at <http://dx.doi.org/10.1016/j.ejrad.2015.02.002>.

References

- [1] White HD, Norris R, Brown M, Brandt P, Whitlock R, Wild C. Left ventricular end-systolic volume as the major determinant of survival after recovery from myocardial infarction. *Circulation* 1987;76:44–51.
- [2] Ibrahim E-SH. Myocardial tagging by cardiovascular magnetic resonance: evolution of techniques—pulse sequences, analysis algorithms, and applications. *J Cardiovasc Magn Reson* 2011;13:36 (official journal of the Society for Cardiovascular Magnetic Resonance).
- [3] Gotte MJ, van Rossum AC, Twisk JWR, Kuijper JPA, Marcus JT, Visser CA. Quantification of regional contractile function after infarction: strain analysis superior to wall thickening analysis in discriminating infarct from remote myocardium. *J Am Coll Cardiol* 2001;37(3):808–17.
- [4] Antoni ML, Mollera SA, Delgado V, et al. Prognostic importance of strain and strain rate after acute myocardial infarction. *Eur Heart J* 2010;31(13):1640–7.
- [5] Miller CA, Borg A, Clark D, et al. Comparison of local sine wave modeling with harmonic phase analysis for the assessment of myocardial strain. *J Magn Reson Imaging* 2013;38(2):320–8.
- [6] Arts T, Prinzen FW, Delhaas T, Millies JR, Rossi AC, Clarysse P. Mapping displacement and deformation of the heart with local sine-wave modeling. *IEEE Trans Med Imaging* 2010;29(5):1114–23.
- [7] Hor KN, Gottlieb WM, Carson C, et al. Comparison of magnetic resonance feature tracking for strain calculation with harmonic phase imaging analysis. *JACC Cardiovasc Imaging* 2010;3(2):144–51.
- [8] Maret E, Todt T, Brudin L, et al. Functional measurements based on feature tracking of cine magnetic resonance images identify left ventricular segments with myocardial scar. *Cardiovasc Ultrasound* 2009;7:53.
- [9] Augustine D, Lewandowski AJ, Lazdam M, et al. Global and regional left ventricular myocardial deformation measures by magnetic resonance feature tracking in healthy volunteers: comparison with tagging and relevance of gender. *J Cardiovasc Magn Reson* 2013;15:8.
- [10] Singh A, Steadman CD, Khan JN, et al. Inter-technique agreement and interstudy reproducibility of strain and diastolic strain rate at 1.5 T and 3 T: a comparison of feature-tracking and tagging in patients with aortic stenosis. *J Magn Reson Imaging* 2014. <http://dx.doi.org/10.1002/jmri.24625>.
- [11] Steg PG, James SK, Atar D, et al. ESC Guidelines for the management of acute myocardial infarction in patients presenting with ST-segment elevation: the Task Force on the management of ST-segment elevation acute myocardial infarction of the European Society of Cardiology (ESC). *Eur Heart J* 2012;Oct;33(20):2569–619. <http://dx.doi.org/10.1093/eurheartj/ehs215>.
- [12] Nijveldt R, Beek AM, Hirsch A, et al. Functional recovery after acute myocardial infarction: comparison between angiography, electrocardiography, and cardiovascular magnetic resonance measures of microvascular injury. *J Am Coll Cardiol* 2008;52(3):181–9.
- [13] Sjogren J, Ubachs JF, Engblom H, Carlsson M, Arheden H, Heiberg E. Semi-automatic segmentation of myocardium at risk in T2-weighted cardiovascular magnetic resonance. *J Cardiovasc Magn Reson* 2012;14:10.
- [14] Flett AS, Hasleton J, Cook C, et al. Evaluation of techniques for the quantification of myocardial scar of differing etiology using cardiac magnetic resonance. *JACC Cardiovasc Imaging* 2011;4(2):150–6.
- [15] Cerqueira MD, Weissman NJ, Dilsizian V, et al. Standardized myocardial segmentation and nomenclature for tomographic imaging of the heart. A statement for healthcare professionals from the Cardiac Imaging Committee of the Council on Clinical Cardiology of the American Heart Association. *Circulation* 2002;105(4):539–42.
- [16] Wong DT, Leong DP, Weightman MJ, et al. Magnetic resonance-derived circumferential strain provides a superior and incremental assessment of improvement in contractile function in patients early after ST-segment elevation myocardial infarction. *Eur Radiol* 2014;Jun;24(6):1219–28. <http://dx.doi.org/10.1007/s00330-014-3137-6>.
- [17] Gerber BL, Rochitte CE, Melin JA, et al. Microvascular obstruction and left ventricular remodeling early after acute myocardial infarction. *Circulation* 2000;101:2734–41.
- [18] Hor KN, Baumann R, Pedrizzetti G, et al. Magnetic resonance derived myocardial strain assessment using feature tracking. *J Visualized Exp: JoVE* 2011;(Feb 12) 48. <http://dx.doi.org/10.3791/2356>, pii: 2356.
- [19] McGraw KO, Wong SP. Forming inferences about some intraclass correlation coefficients. *Psychol Methods* 1996;1(1):30–46.
- [20] Bland JM, Altman DG. Statistical methods for assessing agreement between two methods of clinical measurement. *Lancet* 1986;1(8476):307–10.
- [21] Castillo E, Osman NF, Rosen BD, et al. Quantitative assessment of regional myocardial function with MR-tagging in a multi-center study: interobserver and intraobserver agreement of fast strain analysis with Harmonic Phase (HARP) MRI. *J Cardiovasc Magn Reson* 2005;7(5):783–91.
- [22] Ramsey PH. Critical values for Spearman's Rank Order Correlation. *J Edu Behav Stat* 1989;14(3):245–53.
- [23] Hopp E, Lunde K, Solheim S, et al. Regional myocardial function after intracoronary bone marrow cell injection in reperfused anterior wall infarction—a cardiovascular magnetic resonance tagging study. *J Cardiovasc Magn Reson* 2011;13:22 (official journal of the Society for Cardiovascular Magnetic Resonance).
- [24] Schuster A, Kutty S, Padiyath A, et al. Cardiovascular magnetic resonance myocardial feature tracking detects quantitative wall motion during dobutamine stress. *J Cardiovasc Magn Reson* 2011;13:58.
- [25] Schuster A, Morton G, Hussain ST, et al. The intra-observer reproducibility of cardiovascular magnetic resonance myocardial feature tracking strain assessment is independent of field strength. *Eur J Radiol* 2013;82(2):296–301.
- [26] Harild DM, Han Y, Geva T, Zhou J, Marcus E, Powell AJ. Comparison of cardiac MRI tissue tracking and myocardial tagging for assessment of regional ventricular strain. *Int J Cardiovasc Imaging* 2012;28(8):2009–18.
- [27] Reimer KA, Jennings RB, Cobb FR, et al. Animal models for protecting ischemic myocardium: results of the NHLBI Cooperative Study. Comparison of unconscious and conscious dog models. *Circ Res* 1985;56(5):651–65.
- [28] Schuster A, Paul M, Bettencourt N, et al. Cardiovascular magnetic resonance myocardial feature tracking for quantitative viability assessment in ischemic cardiomyopathy. *Int J Cardiol* 2013;166(2):413–20.
- [29] Neizel M, Lossnitzer D, Korosoglou G, et al. Strain-encoded MRI for evaluation of left ventricular function and transmural infarction in acute myocardial infarction. *Circ Cardiovasc Imaging* 2009;2(2):116–22.
- [30] Ruzsics B, Suranyi P, Kiss P, et al. Myocardial strain in sub-acute peri-infarct myocardium. *Int J Cardiovasc Imaging* 2009;25(2):151–9.
- [31] O'Regan DP, Ariff B, Baksi AJ, Gordon F, Durighel G, Cook SA. Salvage assessment with cardiac MRI following acute myocardial infarction underestimates potential for recovery of systolic strain. *Eur Radiol* 2013;23(5):1210–7.
- [32] Dall'Armellina E, Karia N, Lindsay AC, et al. Dynamic changes of edema and late gadolinium enhancement after acute myocardial infarction and their relationship to functional recovery and salvage index. *Circ Cardiovasc Imaging* 2011;4:228–36.
- [33] Erbsolt M, Valeur N, Mogensen UJM, et al. Prediction of all-cause mortality and heart failure admissions from global left ventricular longitudinal strain in patients with acute myocardial infarction and preserved left ventricular ejection fraction. *J Am Coll Cardiol* 2013;61(23):2365–73.
- [34] Kempny A, Fernandez-Jimenez R, Orwat S, et al. Quantification of biventricular myocardial function using cardiac magnetic resonance feature tracking, endocardial border delineation and echocardiographic speckle tracking in patients with repaired tetralogy of Fallot and healthy controls. *J Cardiovasc Magn Reson* 2012;14:32.

RESEARCH ARTICLE

Open Access

Comparison of semi-automated methods to quantify infarct size and area at risk by cardiovascular magnetic resonance imaging at 1.5T and 3.0T field strengths

Jamal N Khan¹, Sheraz A Nazir¹, Mark A Horsfield¹, Anvesha Singh¹, Prathap Kanagala¹, John P Greenwood², Anthony H Gershlick¹ and Gerry P McCann^{1*}

Abstract

Background: There is currently no gold standard technique for quantifying infarct size (IS) and ischaemic area-at-risk (AAR [oedema]) on late gadolinium enhancement imaging (LGE) and T2-weighted short tau inversion recovery imaging (T2w-STIR) respectively. This study aimed to compare the accuracy and reproducibility of IS and AAR quantification on LGE and T2w-STIR imaging using Otsu's Automated Technique (OAT) with currently used methods at 1.5T and 3.0T post acute ST-segment elevation myocardial infarction (STEMI).

Methods: Ten patients were assessed at 1.5T and 10 at 3.0T. IS was assessed on LGE using 5–8 standard-deviation thresholding (5-8SD), full-width half-maximum (FWHM) quantification and OAT. AAR was assessed on T2w-STIR using 2SD and OAT. Accuracy was assessed by comparison with manual quantification. Interobserver and intraobserver variabilities were assessed using Intraclass Correlation Coefficients and Bland-Altman analysis. IS using each technique was correlated with left ventricular ejection fraction (LVEF).

Results: FWHM and 8SD-derived IS closely correlated with manual assessment at both field strengths (1.5T: $18.3 \pm 10.7\%$ LV Mass [LVM] with FWHM, $17.7 \pm 14.4\%$ LVM with 8SD, $16.5 \pm 10.3\%$ LVM with manual quantification; 3.0T: $10.8 \pm 8.2\%$ LVM with FWHM, $11.4 \pm 9.0\%$ LVM with 8SD, $11.5 \pm 9.0\%$ LVM with manual quantification). 5SD and OAT overestimated IS at both field strengths. OAT, 2SD and manually quantified AAR closely correlated at 1.5T, but OAT overestimated AAR compared with manual assessment at 3.0T. IS and AAR derived by FWHM and OAT respectively had better reproducibility compared with manual and SD-based quantification. FWHM IS correlated strongest with LVEF.

Conclusions: FWHM quantification of IS is accurate, reproducible and correlates strongly with LVEF, whereas 5SD and OAT overestimate IS. OAT accurately assesses AAR at 1.5T and with excellent reproducibility. OAT overestimated AAR at 3.0T and thus cannot be recommended as the preferred method for AAR quantification at 3.0T.

Keywords: Myocardial infarction, Late gadolinium enhancement, Infarct size, T2-weighted STIR, Myocardial salvage, Myocardial oedema, Ischaemic area at risk

* Correspondence: gerrymccann@uhfr.nhs.uk

¹Department of Cardiovascular Sciences, University of Leicester and the NIHR Leicester Cardiovascular Biomedical Research Unit, Glenfield Hospital, Groby Road, LE3 9QP Leicester, UK

Full list of author information is available at the end of the article



© 2015 Khan et al.; licensee BioMed Central. This is an Open Access article distributed under the terms of the Creative Commons Attribution License (<http://creativecommons.org/licenses/by/4.0/>), which permits unrestricted use, distribution, and reproduction in any medium, provided the original work is properly credited. The Creative Commons Public Domain Dedication waiver (<http://creativecommons.org/publicdomain/zero/1.0/>) applies to the data made available in this article, unless otherwise stated.

Background

Cardiovascular magnetic resonance (CMR)-measured infarct size (IS) [1,2] and myocardial salvage index (MSI) [3,4] are important measures of reperfusion success and predictors of remodelling and prognosis post acute ST-segment elevation myocardial infarction (STEMI). MSI is the proportion of reversibly injured ischaemic area-at-risk (AAR) visualised as myocardium with high signal intensity on T2-weighted images [3-5].

There is currently no gold standard technique for the quantification of IS and AAR on late gadolinium imaging (LGE) and T2-weighted short tau inversion recovery imaging (T2w-STIR) respectively.[6] Semi-automated standard deviation (SD)-based thresholding techniques [4,7], manual (visual) contouring of enhancement [1,2], the full-width half-maximum (FWHM) method [6,8], and recently, automated techniques have been used [9,10]. The heterogeneity of techniques and resulting IS and AAR values hinders comparisons between studies.

Otsu's Automated Thresholding (OAT) automatically identifies hyperenhanced areas by selecting the grayscale signal intensity threshold giving minimal intraclass variance within enhanced and normal myocardium and is largely user-independent [11]. There are very scarce published data using OAT quantification, of IS [12] and AAR [13,14].

There are no published studies assessing IS or AAR quantification at 3.0T, or using 7SD and 8SD infarct quantification thresholding at any field strength.

This study aimed to compare the accuracy and reproducibility of IS and AAR quantification on LGE and T2w-STIR using OAT with the currently used quantification methods at 1.5T and 3.0T.

Methods

Study population

Ten patients were retrospectively, randomly selected using a random number generator [15] from the cohort of a UK multicentre, prospective CMR study investigating acute STEMI management at 1.5T (Complete Versus culprit-Lesion only Primary PCI Trial) [16]. Ten further patients were identically selected from a separate multicentre study at 3.0T (Randomized Controlled Trial Comparing Intracoronary Administration of Adenosine or Sodium Nitroprusside to Control for Attenuation of Microvascular Obstruction During Primary Percutaneous Coronary Intervention) [17]. STEMI was diagnosed according to ESC definitions [18] and patients underwent primary PCI within 12 h of symptom onset. The studies were approved by Trent Research Ethics Committee, conducted according to the Declaration of Helsinki and all participants provided written informed consent.

CMR image acquisition

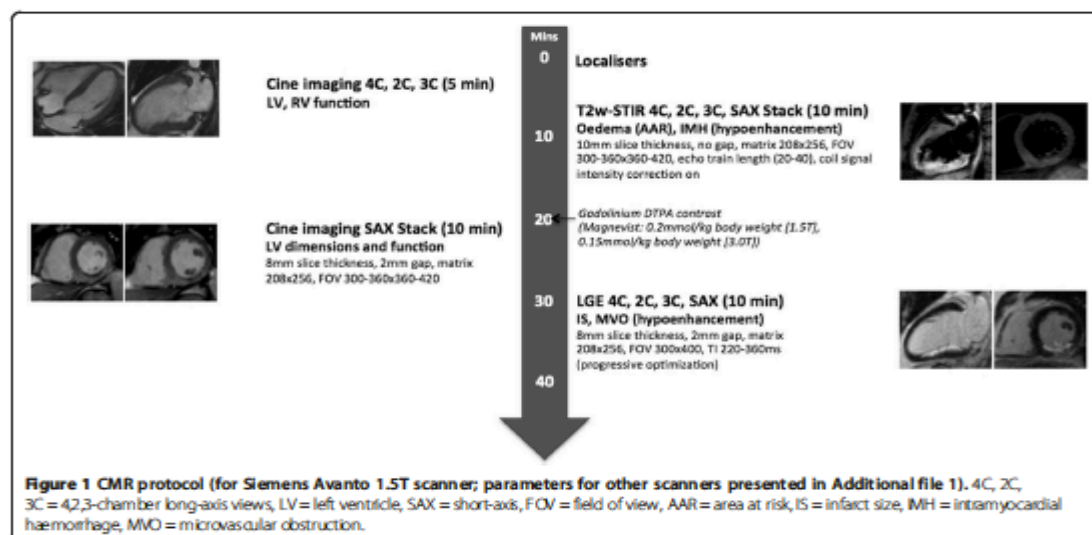
CMR was performed during the index admission on a 1.5T scanner (Siemens Avanto, Erlangen, Germany [n = 4] or Philips Intera, Best, The Netherlands [n = 6]) or 3.0T scanner (Siemens Skyra, Erlangen, Germany [n = 5]; Philips Achieva TX, Best, Netherlands [n = 4] or GE Signa HDxt, Little Chalford, UK [n = 1]) with retrospective electrocardiographic gating and dedicated cardiac receiver coils. The imaging protocol is outlined in Figure 1 and Additional file 1. T2w-STIR imaging with coil SI correction, cine imaging with steady state free precession and Late Gadolinium Enhancement (LGE) imaging were performed in long-axis views and contiguous short-axis slices covering the entire LV. LGE images were acquired 10–15 minutes after administration of 0.15 mmol/kg (3.0T) or 0.2 mmol/kg (1.5T) gadolinium-DTPA (Magnevist, Bayer, Germany) using a segmented inversion-recovery gradient-echo sequence. The inversion time was progressively adjusted to null unaffected myocardium.

IS and AAR quantification

Image quality was graded according to a 4-point scale before analysis: 3 = excellent, 2 = good, 1 = moderate and 0 = unanalysable. To remove the confounding variable of image quality on AAR quantification, 26% of studies from the total study population, where T2w-STIR images were deemed non-analysable were excluded from the random number study selection pool. Analysis was performed offline in a central core lab, blinded to patient details using *cmr42* (Circle Cardiovascular Imaging, Calgary, Canada). LGE, T2w-STIR and cine images were studied together and co-registered to allow accurate quantification based on all available data. For the assessment of LV volumes and function, IS and AAR, endocardial and epicardial borders were manually contoured on contiguous short-axis LV slices, excluding papillary muscles, trabeculae, epicardial surfaces and blood-pool artefact, and the quantification method applied. The most apical LGE and T2w-STIR slice was excluded to minimize partial volume effect. Total IS and AAR were expressed as percentage of LV mass (LVM).

IS quantification

IS was quantified on LGE magnitude images as hyperenhancement using 5/6/7/8 SD thresholding, FWHM [8] and OAT by 2 experienced readers (JNK, SN: 3 years experience each). Mean IS was compared using the techniques and with manual (visual) quantification. As there is no gold standard technique for *in vivo* IS quantification, we used the mean of 6 analyses (manual quantification undertaken twice each by observers JNK and SAN, and by an SCMR Level 3 trained reader [GPM: 10 years experience]). Manual quantification has been used in this capacity in the majority of studies comparing



quantification methods for IS [6,19,20] and AAR [13,21,22], and has high intraobserver and interobserver agreement and reproducibility [6,14]. For 5/6/7/8 SD thresholding, a region of interest (ROI) was manually drawn in remote (no enhancement, oedema or wall-motion abnormality) myocardium and the area of enhancement automatically calculated as the region with signal intensity 5/6/7/8 SD above the mean within the ROI respectively. For the FWHM technique, an ROI was manually drawn in the infarct core and enhancement calculated as pixels where signal intensity exceeded 50% of the automatically determined maximum signal intensity in the infarct core. Where it was not obvious which ROI in the infarct core had the highest maximum signal intensity, ROIs were drawn in potential regions and the ROI with the highest signal intensity selected. The ROI size for the 5/6/7/8 SD and FWHM methods was set at 2 cm². The FWHM method is unaffected by ROI size as it selects the threshold based on the single pixel with highest signal intensity. The same signal intensity threshold was set for all slices on 5/6/7/8 SD and FWHM thresholding. OAT automatically calculates a unique signal intensity threshold for each slice by dividing the greyscale signal intensity histogram in each slice into 2 groups (enhanced, normal) based on the signal intensity threshold giving the least intraclass variance (lowest sum of variances) and thus most homogeneity of signal intensities within each group (Figure 2) [11,12]. The only user input, and thus potential sources of variation are the endocardial and epicardial contours, and manual correction of noise artefact. OAT requires no

ROI selection and is thus largely user-independent compared with SD-based, FWHM and manual quantification.

AAR quantification

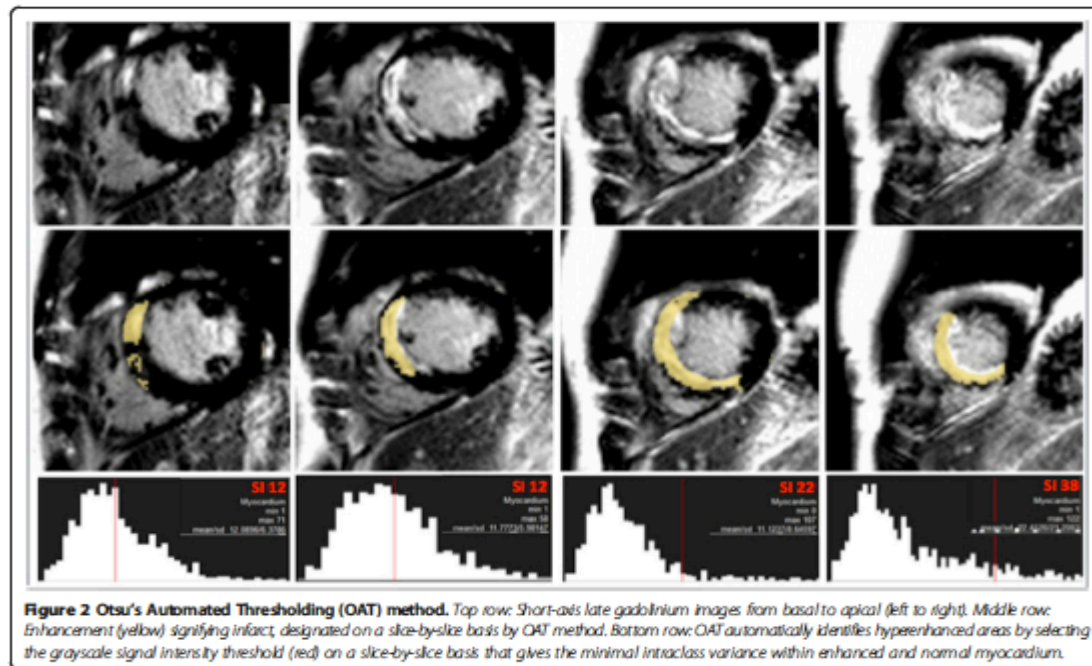
AAR was quantified on T2w-STIR as hyperenhancement using 2SD thresholding and OAT by 2 blinded readers (JNK, SAN). The ROI size for 2SD was set at 2 cm². Mean AAR was compared across the techniques and with manual quantification as described above for IS quantification.

Two manual corrections were applied to IS and AAR measurements: [a] inclusion of hypointense regions within enhancement corresponding to microvascular obstruction and intramyocardial haemorrhage in total IS and AAR respectively [4,6]; [b] exclusion of small isolated regions of enhancement without interslice continuity, in non-infarct related artery territories deemed to be noise artefact.

To assess intraobserver variability of the techniques, all images were re-quantified by a single observer after a 2-month interval. We also recorded the time taken to quantify IS and AAR using each of the methods once the endocardial and epicardial contours had been drawn (time taken for [a] quantification of AAR or IS using chosen technique + [b] inclusion of IMH or MVO where appropriate + [c] exclusion of noise artefact).

Statistical analysis

Normality was assessed using the Shapiro-Wilk test, histograms and Q-Q plots. Normally distributed data were expressed as mean \pm standard deviation. IS and AAR by



each quantification method were normally distributed and thus compared using paired t-tests, and the accuracy of each method was assessed by comparison with manual assessment using paired t-testing, two-way mixed-effect intraclass correlation coefficient for absolute agreement ICC (three, one) [23] and Bland-Altman analysis [24]. On ICC, agreement was defined as excellent ($ICC \geq 0.75$), good ($ICC 0.6-0.74$), fair ($ICC 0.4-0.59$), or poor ($ICC < 0.40$) [25]. Interobserver and intraobserver variabilities were expressed using ICC (three, one) and Bland-Altman analysis. The significance of differences in reproducibility was assessed using Wilcoxon rank comparison of the squared differences [6]. Statistical tests were performed using SPSS v20 (IBM, USA). $p < 0.05$ was considered significant.

Results

Baseline characteristics

Baseline characteristics are summarised in Table 1. Twenty patients were studied (1.5T $n = 10$, 3.0T $n = 10$). CMR was undertaken 3.7 ± 1.3 days post STEMI in the 1.5T group and 3.4 ± 2.1 days post STEMI in the 3.0T group. In total, 171 slices were analysed for IS and AAR (89 at 1.5T, at 82 at 3.0T). All LGE and STIR slices were of diagnostic image quality. Data for IS and AAR are shown in Tables 2, 3 and 4, and Figures 3 and 4.

Table 1 Baseline demographics by CMR field strength cohort

	1.5T	3.0T
n	10	10
Age (years)	56.6 ± 14.0	52.6 ± 10.6
LAD IRA (n, %)	3 (30%)	4 (40%)
LCX IRA (n, %)	2 (20%)	2 (20%)
RCA IRA (n, %)	5 (50%)	4 (40%)
Treatment strategy	IRA-only PCI: n = 3 (30%) Complete revascularisation: n = 7 (70%)	Vasodilator treatment group: n = 7 (70%) Control group: n = 3 (30%)
CMR time post STEMI (d)	3.7 ± 1.3	3.4 ± 2.1
LVEDM (g)	111.6 ± 21.9	107.1 ± 23.1
LVEDV (ml)	179.9 ± 33.8	169.3 ± 35.2
LVESV (ml)	94.7 ± 20.9	94.4 ± 32.3
LVEF (%)	47.2 ± 7.8	45.4 ± 8.1
LGE image quality	2.5 ± 0.6	2.2 ± 0.6
T2w-STIR image quality	2.6 ± 0.5	2.1 ± 0.3

Data expressed as mean \pm standard deviation. CMR = cardiovascular magnetic resonance, STEMI = ST-segment elevation myocardial infarction, LVEDM = Left ventricular end-diastolic mass, LVEDV = Left ventricular end-diastolic volume, LVESV = Left ventricular end-systolic volume, LVEF = Left ventricular ejection fraction, PCI = percutaneous coronary intervention, IRA = infarct-related artery.

Table 2 Infarct size (IS) results at 1.5T by quantification method and corresponding reproducibilities

1.5T	IS (FWHM)	IS (SSD)	IS (6SD)	IS (7SD)	IS (8SD)	IS (OAT)	IS (MANUAL)
Mean IS (%LVM)	18.3 ± 10.7	25.9 ± 16.1 ^b	22.0 ± 15.8 ^a	19.8 ± 15.3	17.7 ± 14.4	28.2 ± 11.8 ^b	16.5 ± 10.3
ICC v Manual	0.909	0.667	0.759	0.804	0.832	0.621	
Mean bias v Manual (±1.96SD LoA)	+1.84 (+10.30, -6.62)	+9.39 (+25.58, -6.81)	+5.57 (+21.65, -10.52)	+3.28 (+18.86, -12.30)	+1.21 (+15.92, -13.50)	+11.71 (+17.39, +6.03)	
Interobserver ICC	0.922	0.952	0.904	0.906	0.888	0.976	0.793
Interobserver mean bias (±1.96SD LoA)	+0.37 (+9.17, -8.43)	+2.54 (+11.62, -6.54)	+4.43 (+16.01, -7.16)	+4.00 (+15.48, -7.47)	+4.01 (+16.02, -8.01)	+0.55 (+5.82, -4.73)	+5.34 (+14.96, -4.28)
Intraobserver ICC	0.991	0.957	0.954	0.938	0.925	0.991	0.983
Intraobserver mean bias (±1.96SD LoA)	+0.36 (+3.34, -2.61)	-0.81 (+9.37, -10.99)	+0.01 (+10.28, -10.27)	+0.07 (+11.76, -11.62)	+0.42 (+13.00, -12.17)	+0.81 (+4.21, -2.50)	-1.92 (+0.64, -4.49)

IS expressed as mean ± standard deviation, FWHM = full-width half maximum, 5-8SD = >5-8 standard deviation, OAT = Otsu's Automated Thresholding, LVM = Left Ventricular Mass, ICC = Intraclass Correlation Coefficient, LoA = Limits of Agreement (Bland-Altman).

^a - p < 0.05 vs. manually quantified IS, ^b - p < 0.01 vs. manually quantified IS.

Table 3 Infarct size (IS) results at 3.0T by quantification method and corresponding reproducibilities

3 T	IS (FWHM)	IS (5SD)	IS (6SD)	IS (7SD)	IS (8SD)	IS (OAT)	IS (MANUAL)
Mean IS (%LVM)	10.8 ± 8.2	17.0 ± 11.2 ^b	14.77 ± 10.4 ^b	13.0 ± 9.7 ^a	11.4 ± 9.0	21.6 ± 9.6 ^b	11.5 ± 9.0
ICC v Manual	0.964	0.780	0.874	0.937	0.966	0.505	
Mean bias v Manual (±1.96SD LoA)	+0.22 (+5.09, -4.65)	+6.42 (+14.93, -2.09)	+4.17 (+11.05, -2.71)	+2.38 (+7.92, -3.16)	+0.81 (+5.62, -4.01)	+11.03 (+22.20, -0.15)	
Interobserver ICC	0.990	0.957	0.937	0.916	0.888	0.977	0.913
Interobserver mean bias (±1.96SD LoA)	-0.49 (+1.74, -2.72)	+0.44 (+7.23, -6.35)	+1.14 (+8.51, -6.23)	+1.40 (+9.25, -6.44)	+1.50 (+9.99, -6.98)	-0.05 (+4.35, -4.44)	+1.97 (+9.48, -5.54)
Intraobserver ICC	0.988	0.992	0.992	0.993	0.993	0.986	0.972
Intraobserver mean bias (±1.96SD LoA)	+0.20 (+1.49, -1.10)	+0.43 (+2.90, -2.03)	-0.04 (+2.42, -2.50)	+0.10 (+2.19, -1.98)	+0.32 (+2.08, -1.45)	+0.15 (+3.50, -3.21)	+1.14 (+4.35, -2.07)

IS expressed as mean ± standard deviation, FWHM = full-width half maximum, 5-8SD = >5-8 standard deviation, OAT = Otsu's Automated Thresholding, LVM = Left Ventricular Mass, ICC = Intraclass Correlation Coefficient, LoA = Limits of Agreement (Bland-Altman).

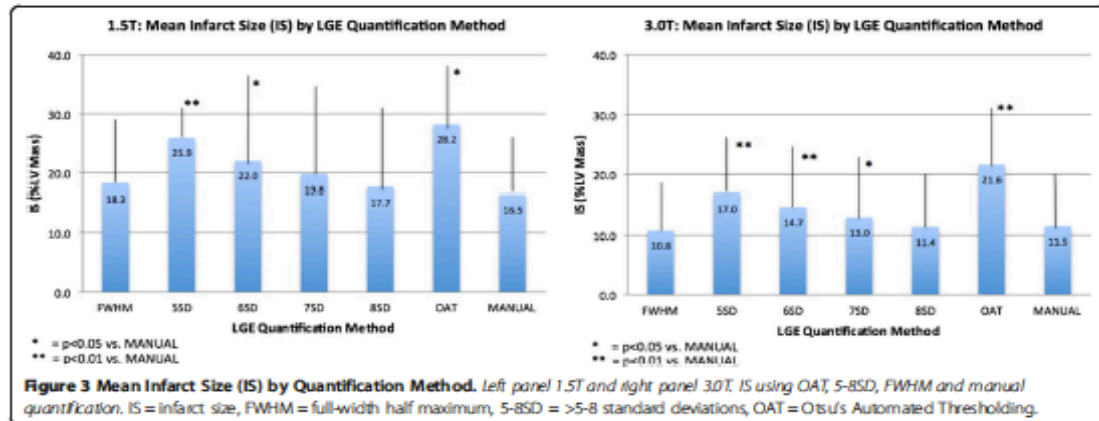
^a - p < 0.05 vs. manually quantified IS. ^b - p < 0.01 vs. manually quantified IS.

Table 4 Area at risk (AAR) by field strength and quantification method and corresponding reproducibilities

	1.5T			3.0T		
	AAR (2SD)	AAR (OAT)	AAR (MANUAL)	AAR (2SD)	AAR (OAT)	AAR (MANUAL)
Mean value (AAR [% LVM])	34.8 ± 9.8	38.1 ± 13.0	35.4 ± 11.2	35.2 ± 14.4	38.9 ± 9.9 ^a	30.0 ± 8.2
ICC v Manual	0.865	0.920		0.649	0.465	
Mean bias v Manual (±1.96SD LoA)	+0.31 (+12.20, -11.57)	+3.62 (+11.24, -4.00)		+5.13 (+22.76, -12.50)	+8.92 (+23.15, -5.31)	
Interobserver ICC	0.908	0.976	0.825	0.869	0.981	0.716
Interobserver mean bias (±1.96SD LoA)	+3.38 (+9.12, -2.37)	+1.26 (+7.20, -4.68)	+1.31 (+17.11, -14.49)	-0.34 (+15.36, -16.03)	-1.35 (+1.64, -4.33)	-5.20 (+9.54, -19.95)
Intraobserver ICC	0.948	0.995	0.977	0.987	0.990	0.826
Intraobserver mean bias (±1.96SD LoA)	+2.80 (+7.28, -1.68)	+0.58 (+3.31, -2.16)	-0.01 (+5.62, -5.64)	+1.00 (+5.50, -3.51)	+0.04 (+2.82, -2.74)	+1.46 (+14.84, -11.93)

AAR and MSI expressed as mean ± standard deviation. 2SD = >2 standard deviations, OAT = Otsu's Automated Thresholding, LVM = Left Ventricular Mass, ICC = Intraclass Correlation Coefficient, LoA = Limits of Agreement (Bland-Altman).

^a - p < 0.05 vs. manually quantified AAR.



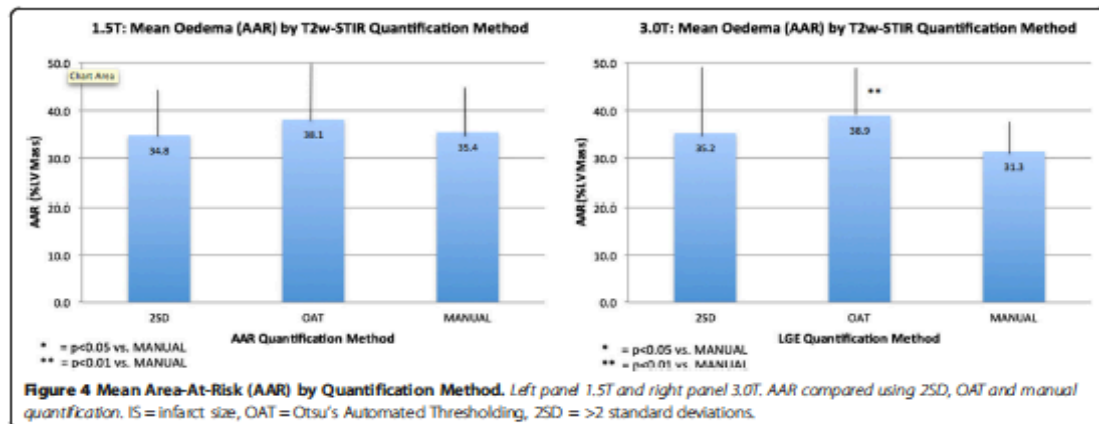
Infarct size

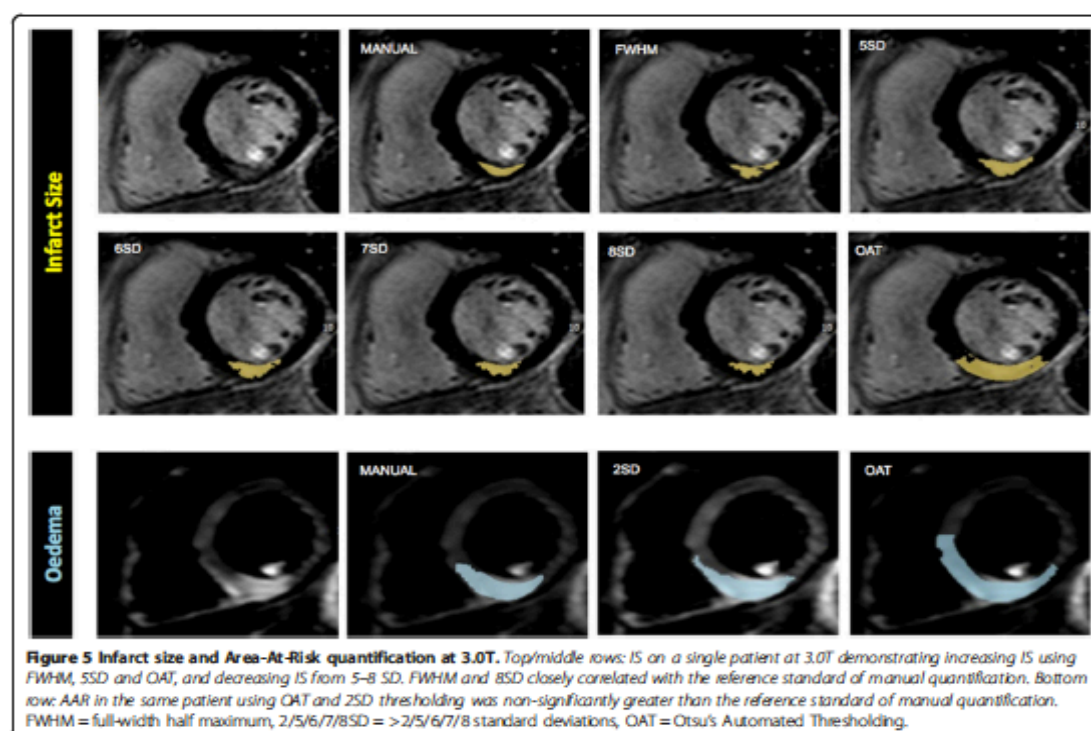
IS varied significantly with the quantification method (Tables 2 and 3 and Figures 3 and 5). FWHM, 7SD and 8SD closely agreed with manual IS quantification at 1.5T, and 6SD showed weak agreement. FWHM and 8SD closely agreed with manual quantification at 3.0T. At both field strengths, IS was significantly greater with OAT and 5SD compared with manual quantification. IS was also greater with 6SD and 7SD at 3.0T. Bland-Altman plots for agreement with manual quantification are shown in Additional file 2. There was a strong trend towards reduced IS quantification time using FWHM compared with all SD-based methods at both field strengths. The reduction in quantification time with FWHM was highly significant when compared with manual quantification at both field strengths, and when compared with 5SD and 8SD at 1.5T. There was no difference in quantification time using FWHM and OAT (Table 5).

Interobserver and intraobserver variability of IS quantification

Results are displayed in Tables 2 and 3. FWHM and OAT demonstrated extremely high interobserver and intraobserver agreement at both field strengths, with all ICC values >0.922 and mean bias $<+1.84\%$. SD-based techniques demonstrated good interobserver and intraobserver agreement at both field strengths, however lower than for FWHM and OAT, with ICC values >0.888 and mean bias $<+4.43\%$. Interobserver and intraobserver agreement for manual quantification were very high at both field strengths apart from interobserver agreement at 1.5T, which was good (ICC 0.793). Bland-Altman charts for IS are shown in Additional files 2 and 3.

Interobserver agreement for IS at 3.0T was significantly better with FWHM vs. manual quantification ($p = 0.037$). Intraobserver agreement for IS was significantly better at 1.5T with FWHM vs. 6SD ($p = 0.013$), 7SD ($p =$





0.022) and 8SD ($p = 0.037$), and at 3.0T for FWHM vs. manual ($p = 0.047$). There was a strong trend towards higher intraobserver agreement for IS at 1.5T with FWHM vs. manual ($p = 0.093$).

Correlation of myocardial injury with LV ejection fraction

At 1.5T, FWHM and manual quantification demonstrated a strong inverse correlation between IS and LVEF (FWHM: $r = -0.745$, $p = 0.013$; manual $r = -0.709$, $p = 0.022$). All other methods demonstrated moderate inverse correlation and did not reach statistical significance. At 3.0T, FWHM IS showed a significant, moderate correlation with LVEF ($r = -0.673$, $p = 0.033$). The correlation using all other techniques was weaker and not statistically significant.

AAR extent

AAR varied with the quantification method used (Figures 4 and 5). There was no significant difference between 2SD, OAT and manually quantified AAR at 1.5T. At 3.0T, AAR quantified with OAT was larger than that manually contoured ($p = 0.004$) and similar to that on 2SD. Agreement with manual quantification at 1.5T tended to be higher for OAT than 2SD, with ICC 0.920 and narrower limits of

agreement on Bland-Altman analysis. There was no difference in AAR quantification time using OAT, 2SD or manual quantification at 1.5T or 3.0T (Table 5), Additional files 4 and 5.

Interobserver and intraobserver variability of AAR and MSI quantification

OAT had extremely high interobserver and intraobserver agreement for AAR quantification at both field strengths, with all ICC values >0.976 . Good interobserver agreement was seen for 2SD quantification of AAR at both field strengths. Manual quantification demonstrated excellent interobserver agreement at 3.0T. Interobserver agreement at 1.5T and intraobserver agreement at both field strengths was good with manual quantification (ICC >0.716).

Interobserver agreement at 3.0T was significantly better for OAT vs. manual quantification ($p = 0.017$), and at 1.5T was borderline significantly higher for OAT vs. manual ($p = 0.059$). Intraobserver agreement at 3.0T was significantly better for OAT vs. manual quantification ($p = 0.007$). The raw datasets for IS and AAR quantification at 1.5T and 3.0T field strengths are available in Additional files 6 and 7.

Table 5 Time taken per patient for Infarct Size (IS) and Area at risk (AAR) quantification by field strength and quantification method

	Time (minutes)	p
-	17.1 ± 2.4 vs. 20.9 ± 5.5	0.04
1.5T: FWHM v 6SD (IS)	17.1 ± 2.4 vs. 19.4 ± 3.1	0.09
1.5T: FWHM v 7SD (IS)	17.1 ± 2.4 vs. 19.1 ± 3.7	0.13
1.5T: FWHM v 8SD (IS)	17.1 ± 2.4 vs. 19.6 ± 3.2	<0.01
1.5T: FWHM v OAT (IS)	17.1 ± 2.4 vs. 18.0 ± 2.6	0.45
1.5T: FWHM v MANUAL (IS)	17.1 ± 2.4 vs. 21.1 ± 4.7	0.01
1.5T: 5SD v OAT (IS)	20.9 ± 5.5 vs. 18.0 ± 2.6	0.21
1.5T: 2SD v OAT (AAR)	17.1 ± 2.4 vs. 16.7 ± 2.6	0.73
1.5T: 2SD v MANUAL (AAR)	17.1 ± 2.4 vs. 18.3 ± 2.6	0.14
1.5T: OAT v MANUAL (AAR)	16.7 ± 2.6 vs. 18.3 ± 2.6	0.07
3T: FWHM v 5SD (IS)	18.9 ± 2.7 vs. 24.7 ± 9.1	0.08
3T: FWHM v 6SD (IS)	18.9 ± 2.7 vs. 22.2 ± 5.2	0.07
3T: FWHM v 7SD (IS)	18.9 ± 2.7 vs. 22.5 ± 5.3	0.07
3T: FWHM v 8SD (IS)	18.9 ± 2.7 vs. 21.2 ± 3.0	0.08
3T: FWHM v OAT (IS)	18.9 ± 2.7 vs. 20.7 ± 3.2	0.11
3T: FWHM v MANUAL (IS)	18.9 ± 2.7 vs. 24.0 ± 3.7	<0.01
3T: 5SD v OAT (IS)	24.7 ± 9.1 vs. 20.7 ± 3.2	0.25
3T: 2SD v OAT (AAR)	19.6 ± 2.7 vs. 18.5 ± 2.6	0.26
3T: 2SD v MANUAL (AAR)	19.6 ± 2.7 vs. 18.3 ± 2.6	0.31
3T: OAT v MANUAL (AAR)	18.5 ± 2.6 vs. 18.3 ± 2.6	0.83

FWHM = full-width half maximum, 5/6/7/8SD = >5/6/7/8 standard deviation, OAT = Otsu's Automated Thresholding, 2SD = >2 standard deviations, p < 0.05 taken as statistically significant.

Discussion

In this study we assessed IS and AAR quantification in acute STEMI patients with currently used semi-automatic techniques at 1.5T and 3.0T. FWHM and 8SD closely agreed with the reference standard of manual IS quantification at both field strengths, whereas 5SD and OAT led to higher IS values compared to manual quantification. AAR measured by OAT and 2SD were similar to manual quantification only at 1.5T. Interobserver and intraobserver agreement for IS and AAR quantification were better with FWHM and OAT compared with manual quantification respectively, and tended to be better than with SD-based methods. There was an inverse correlation between IS and LVEF for all quantification methods and this was strongest and most significant for FWHM. Our study is the first to assess IS quantification methods using 7SD and 8SD thresholding and to assess IS and AAR quantification at 3.0T.

Mean IS using the quantification techniques

LGE IS quantification in acute MI has been validated in a small number of animal studies. FWHM [8] and manual quantification [9] of *in-vivo* images closely correlated

with IS on tetrazolium chloride stained canine hearts. Kim et al. [7] demonstrated good agreement of 2SD thresholding with tetrazolium chloride stained canine myocardium. However this was on *ex-vivo* slices with high spatial resolution and in the absence of rhythm and motion artefacts, and may not be generalizable to humans [7]. Indeed, 2SD has been shown to overestimate IS in humans based on functional improvement and IS reduction in enhanced areas [26,27]. There is no histological validation in humans and hence no 'gold standard' quantification. We thus used manual assessment as has been used previously [6,12], however derived from the mean of repeated analyses by three experienced CMR cardiologists to increase the robustness of our reference standard.

FWHM and 8SD were the only methods in our study showing good agreement with manual quantification at both field strengths. This may be because they are less prone to IS overestimation resulting from oedema and partial volume effects giving rise to intermediate signal intensities [26,28]. This resulted in negligible requirements for manual exclusion of noise artefact with FWHM and 8SD. This in conjunction with the relative ease in identification of the brightest infarct core compared with deciding on a representative remote ROI is likely to explain the shorter time required for IS quantification using FWHM compared with SD-based techniques.

The greater IS using 5SD compared with manual quantification in our study is in agreement with previous results at 1.5T [6]. These findings indicate that the good agreement between 5SD and manual quantification in chronic ischaemic heart disease [29], where infarct tends to have a higher and more homogenous SI [6], cannot be extrapolated to acute STEMI patients. The close correlation of 5SD and in particular OAT with manual assessment shown by Vermes et al. [12] is in contrast to our findings. IS quantification was only performed on slices with infarct seen visually in that study, thus potentially underestimating IS. In addition, the small remote ROI used for 5SD thresholding (0.5-1 cm²) by Vermes et al. may not adequately represent remote myocardium signal intensity, thus leading to underestimation or overestimation of IS if an excessively bright or dark, isolated region of myocardium is taken as the remote ROI respectively. By setting the ROI size at 2 cm² for all SD-based methods in our study, we aimed to ensure that the ROI was large enough to represent remote myocardium accurately. Using the same remote ROI for all SD-based methods in our study ensured consistency and removed the effect of ROI size and location when comparing IS between 5-8 SD thresholds. Hence, 6 and 5-SD and 7, 6 and 5-SD quantification overestimated IS at 1.5T and 3.0T respectively due to their intrinsically progressively lower signal intensity thresholds and not due to differences in remote ROI.

OAT has the potential to overestimate LGE IS because it calculates an individual SI threshold, and thus enhancement on *every* slice, regardless of the presence of infarct (Figure 6). Whilst small areas of enhancement in the non-infarct region were manually excluded, it is likely that OAT leads to higher values due to near transmural enhancement in the infarct area, in the presence of peri-infarct oedema [11].

We studied IS and AAR quantification early after STEMI. IS decreases with time post PPCI with a reduction of ~30% demonstrated within the first week in some studies [26,30]. The extent of necrosis is overestimated by LGE early post STEMI due to cellular disruption and oedema. As scar resorbs and remodels, IS reduces and scar may become more homogenous in signal intensity and brighter. The relative overestimation of IS by lower standard deviation thresholds and OAT compared with FWHM, 8SD and manual quantification may thus be more significant in acute compared with in chronic infarcts. We chose an early time point to minimise drop-out in the study and most importantly, all the data relating infarct size to subsequent prognosis following STEMI has been based on early measurement of infarct size (usually within 1 week) [4,31]. Whether AAR varies in the first week after STEMI has shown conflicting results [26,27]. As we have only scanned the patients in this study on a

single occasion we cannot comment on how the results would have varied if performed at later dates following presentation.

Interobserver and intraobserver variability of IS quantification

The excellent interobserver and intraobserver agreement for FWHM, 5SD and OAT quantification of IS in our study at both field strengths is in agreement with previous studies at 1.5T: FWHM, 5SD [6,27] and FWHM, OAT [12]. Consistent with the work of Flett et al. [6], we found that the FWHM technique had greater interobserver and intraobserver reproducibility compared with SD-based and manual quantification. This is expected when considering that for each patient there is a single brightest core of infarct. This is in contrast to the remote ROI, which could be drawn on any slice without complete LGE in SD-based quantification, or manual contouring of enhancement, which is completely user-dependent and in the acute phase post STEMI could potentially be affected by partial volume in infarct boundaries and oedematous myocardium.

Mean AAR and MSI using the quantification techniques

T2w-STIR AAR is typically quantified using 2SD thresholding. Validation studies are limited. 2SD-derived AAR on

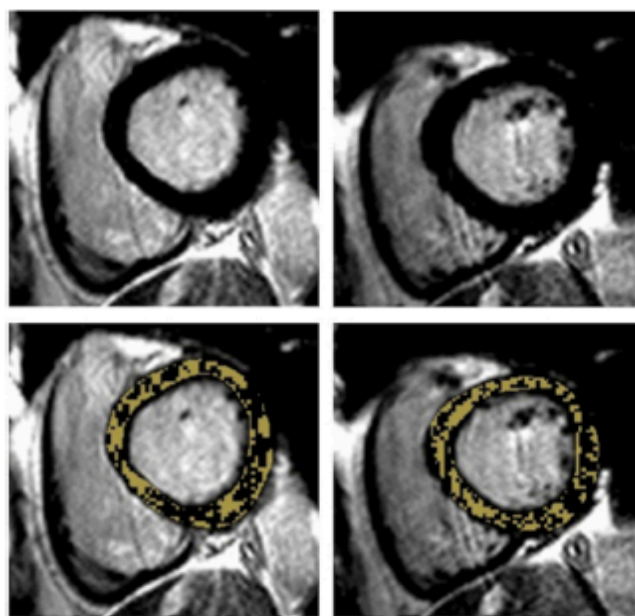


Figure 6 Hyperenhancement with OAT without obvious infarct. In this case there is no infarct present (top row), whereas OAT has calculated a significant infarct volume (bottom row). OAT = Otsu's Automated Thresholding.

T2w images *in vivo* correlated with microsphere-assessed AAR in canine myocardium ($r = 0.84$). [32] There is no gold standard AAR quantification method on T2w-STIR, hence we used manual assessment.

The close agreement between OAT and manually contoured AAR at 1.5T is consistent with the work of McAlindon et al. [14] OAT however demonstrated greater AAR compared with manual quantification at 3.0T. This is in keeping with Sjogren et al. [13] who showed overestimation of AAR using OAT with a mean bias of $+5.3 \pm 9.6\%$ compared with manual quantification [13]. The determination of an optimal threshold and quantification of enhancement on every slice with OAT, regardless of oedema is likely to contribute to this. The risk of overestimation of AAR will be greatest in slices with minimal oedema since OAT will deem a proportion of pixels enhanced. This may potentially have contributed to the overestimation of AAR at 3.0T in our study with OAT, since our 3.0T cohort had a smaller AAR than the 1.5T patients. IS was also smaller in our 3.0T cohort and may have contributed to the greater overestimation of IS using OAT at 3.0T compared with 1.5T. Conversely, underestimation of AAR is more likely in slices with complete enhancement since OAT will deem a proportion of pixels unenhanced [13]. T2w-STIR images were of diagnostic quality in all patients in our study, however mean quality control grading was slightly lower at 3.0T (2.1 ± 0.3 [3 T]) vs. 2.6 ± 0.5 [1.5T], $p = 0.05$) and may have potentially contributed to the overestimation of OAT-derived AAR if there was more noise artefact in the AAR or signal intensity drop out in remote regions by reducing the threshold. More work into automated quantification methods is required, in particular at 3.0T. Newer automated techniques, taking into account *a priori* information about the culprit artery [13] and including noise and false positive artefact exclusion [10,21] algorithms may improve the accuracy of automated IS and AAR quantification.

The relative degree of AAR overestimation in our study was, however, considerably less than for IS. The predominantly transmural pattern of OAT enhancement for IS and AAR may cause less overestimation of AAR compared with IS, since oedema has been shown to be predominantly transmural in 70-100% of oedematous segments [33,34].

Interobserver and intraobserver variability of AAR quantification

The relatively low interobserver and intraobserver agreement using 2SD compared with OAT at both field strengths is likely to result from varying manual definition of the remote ROI. The extremely high ICC's obtained with OAT are remarkable considering that these figures still take account differences in manual correction and contouring of endocardial and epicardial

borders. Given these results, quantification of AAR with OAT could minimise variability in measurement in multi-centre trials.

Limitations

The main limitation of our and previous similar studies is the lack of a gold standard for IS and AAR quantification. Different quantification techniques were studied for IS and AAR. FWHM quantification of AAR was not undertaken due to the lower CNR of T2w-STIR imaging, since the vast majority of myocardium would have signal intensity $>50\%$ of the maximum at the AAR core, leading to potentially extreme overestimation of AAR and MSI. Indeed, McAlindon et al. demonstrated that FWHM significantly overestimated AAR compared to all other quantification methods tested at 1.5T (2,3,5 SD, OAT, manual quantification) [14]. 5SD thresholding was not assessed for AAR as it has never been validated or correlated with clinical outcomes and the only study to feature it demonstrated that it significantly overestimated AAR compared to all other quantification methods tested at 1.5T (2,3 SD, FWHM, OAT, manual quantification) [14]. 2SD thresholding was not assessed for IS as it has been shown to overestimate IS [6,12] and had the lowest correlation with histological IS on tetrazolium chloride staining using Bland-Altman analysis [8] compared with all other quantification methods used in studies of IS in acute STEMI (5SD, FWHM, manual quantification). Test-retest reproducibility was not assessed and should be considered in future studies. Infarct heterogeneity and identification of peri-infarct zone (greyzone) was not assessed in this study and may be of interest to assess in future studies using OAT. We deliberately studied patients imaged at different field strengths and with different scanner vendors to represent the situation in multi-centre clinical trials and this should make the results more generalizable. Our sample size (total $n = 20$) is limited, however is comparable to similar studies in myocardial infarction [8-10,12,14,20] and our findings are supported by their consistency at both field strengths. Finally our results may not be generalizable to if patients are scanned at different time points following STEMI.

Conclusions

Inter- and intraobserver variability for the quantification of IS with FWHM is excellent at 1.5 and 3.0T and better than when using manual quantification. Only FWHM and 8SD closely agreed with manual delineation of IS at both field strengths. FWHM had better reproducibility, shorter quantification time and closer correlation with LVEF and may be the preferred method for IS quantification in future studies. AAR is similar when assessed with OAT, 2SD and manual quantification at 1.5T, however OAT has excellent intra and interobserver variability

and thus has potential in quantification of AAR at 1.5T, especially in multi-centre studies. OAT overestimated AAR at 3.0T compared with manual quantification and thus cannot currently be recommended as the preferred method for AAR quantification at 3.0T.

Additional files

Additional file 1: CMR parameters for T2-weighted STIR and late gadolinium enhanced (LGE) sequences on the scanners used.

Additional file 2: Infarct Size (IS) Quantification at 1.5T using the quantification techniques.

Additional file 3: Infarct Size (IS) Quantification at 3.0T using the quantification techniques.

Additional file 4: Area At Risk (AAR) Quantification at 1.5T using the quantification techniques.

Additional file 5: Area At Risk (AAR) Quantification at 3.0T using the quantification techniques.

Additional file 6: 1.5T dataset for IS and AAR quantification.

Additional file 7: 3.0T dataset for IS and AAR quantification.

Competing interests

The authors declare that they have no competing interests.

Authors' contributions

GPM and AHG conceived the idea for the study and developed the protocol. JNK recruited patients and was present at study visits. JNK and SAN performed the CMR analyses. JNK performed the statistical analysis and wrote the paper, which all authors critically reviewed for content. All authors read and approved the final manuscript.

Acknowledgements

GPM is supported by a NIHR Intermediate Fellowship. This study was supported by The National Institute for Health Research (funded the CMR scans and software used in image analysis, funding number BME 1027/01) and British Heart Foundation (funded recruitment of subjects, funding number SP/10/001/28194).

Author details

¹Department of Cardiovascular Sciences, University of Leicester and the NIHR Leicester Cardiovascular Biomedical Research Unit, Glenfield Hospital, Groby Road, LE3 9QP Leicester, UK. ²Division of Cardiovascular and Diabetes Research, Leeds Institute of Genetics, Health and Therapeutics, University of Leeds, LS2 9JT Leeds, UK.

Received: 30 June 2014 Accepted: 9 February 2015

Published online: 25 February 2015

References

- Klem I, Shah DJ, White RD, Pennell DJ, van Rossum AC, Regenfus M, et al. Prognostic value of routine cardiac magnetic resonance assessment of left ventricular ejection fraction and myocardial damage: an international multicenter study. *Circ Cardiovasc Imaging*. 2011;4(6):10–9.
- Hombach V, Grebe O, Merkle N, Waldenmaier S, Höher M, Kochs M, et al. Sequelae of acute myocardial infarction regarding cardiac structure and function and their prognostic significance as assessed by magnetic resonance imaging. *Eur Heart J*. 2005;26:549–57.
- Masó PG, Ganame J, Strata E, Desmet W, Aquaro GD, Dymarkowski S, et al. Myocardial Salvage by CMR Correlates With LV Remodeling and Early ST-Segment Resolution in Acute Myocardial Infarction. *JCMG*. 2010;3:45–51.
- Eikel I, Desch S, de Waha S, Fuernau G, Gutberlet M, Schuler G, et al. Long-term prognostic value of myocardial salvage assessed by cardiovascular magnetic resonance in acute reperfused myocardial infarction. *Heart (British Cardiac Soc)*. 2011;97:2038–45.
- Pennell D. Myocardial salvage: retrospection, resolution, and radio waves. *Circulation*. 2006;113:1821–3.
- Flett AS, Hasleton J, Cook C, Hausenloy D, Quarta G, Afifi C, et al. Evaluation of techniques for the quantification of myocardial scar of differing etiology using cardiac magnetic resonance. *JACC Cardiovasc Imaging*. 2011;4:150–6.
- Kim RJ, Fieno DS, Parish TB, Harris K, Chen E-J, Simonetti O, et al. Relationship of MRI Delayed Contrast Enhancement to Irreversible Injury, Infarct Age, and Contractile Function. *Circulation*. 1999;100:1992–2002.
- Amado LC, Geber BL, Gupta SN, Rettmann DW, Szarf G, Schock R, et al. Accurate and objective infarct sizing by contrast-enhanced magnetic resonance imaging in a canine myocardial infarction model. *J Am Coll Cardiol*. 2004;44:2383–9.
- Hsu LY, Natarajan A, Kellman P, Hirsch GA, Aletras AH, Arai AE. Quantitative myocardial infarction on delayed enhancement MRI. Part I: animal validation of an automated feature analysis and combined thresholding infarct sizing algorithm. *J Magn Reson Imaging*. 2006;23:298–308.
- Johnstone RI, Greenwood JP, Biglands JD, Plein S, Ridgway JP, Radjenovic A. Assessment of tissue edema in patients with acute myocardial infarction by computer-assisted quantification of triple inversion recovery prepared MRI of the myocardium. *Magn Reson Med*. 2011;66:564–73.
- Otsu N. A Threshold Selection Method from Gray-Level Histograms. *IEEE Trans Sys Man Cybern*. 1979;9:562–6.
- Vermes E, Childs H, Carbone I, Borkow P, Friedrich M. Auto-Threshold Quantification of Late Gadolinium Enhancement in Patients With Acute Heart Disease. *JMRI*. 2013;37:382–90.
- Sjogren J, Ubachs JF, Engblom H, Carlsson M, Ahlhed H, Heiberg E. Semi-automatic segmentation of myocardium at risk in T2-weighted cardiovascular magnetic resonance. *J Cardiovasc Magn Reson*. 2012;14:10.
- McAlindon E, Lawton C, Flett AS, Manghat N, Hamilton MC, Buccarelli Ducci C. Evaluation of 7 techniques for the quantification of myocardial oedema in STEMI. *JCMR*. 2013;15:P188.
- Hash M. Random.org (True Random Number Generator). <http://www.random.org>. 1998. Website (Accessed September 2013).
- Kelly DJ, McGinn GP, Blackman D, Curzen NP, Dalby M, Greenwood JP, et al. Complete Versus culprit-Lesion only Primary PCI Trial (CVLPPT): a multicentre trial testing management strategies when multivessel disease is detected at the time of primary PCI: rationale and design. *EuroIntervention*. 2013;8:1190–8.
- Nazir S, Khan JN, Mahmoud IZ, Greenwood JP, Blackman D, Kunadian V, et al. The REFLO-STEMI trial comparing intracoronary adenosine, sodium nitroprusside and standard therapy for the attenuation of infarct size and microvascular obstruction during primary percutaneous coronary intervention: study protocol for a randomised controlled trial. *Trials*. 2014;15:371.
- Sieg PG, James SK, Atar D, Badano LP, Lundqvist CB, Borger MA, et al. ESC Guidelines for the management of acute myocardial infarction in patients presenting with ST-segment elevation: The Task Force on the management of ST-segment elevation acute myocardial infarction of the European Society of Cardiology (ESC). *Eur Heart J*. 2012;33(20):2569–619.
- Heiberg E, Engblom H, Engvall J, Hedstrom E, Ugander M, Ahlhed H. Semi-automatic quantification of myocardial infarction from delayed contrast enhanced magnetic resonance imaging. *Scand Cardiovasc J*. 2005;39:267–75.
- Hsu LY, Ingkanitpong WP, Kellman P, Aletras AH, Arai AE. Quantitative myocardial infarction on delayed enhancement MRI. Part II: Clinical application of an automated feature analysis and combined thresholding infarct sizing algorithm. *J Magn Reson Imaging*. 2006;23:309–14.
- Gao H, Kadir K, Payne AR, Soraghan J, Berry C. Highly automatic quantification of myocardial oedema in patients with acute myocardial infarction using bright blood T2-weighted CMR. *J Cardiovasc Magn Reson*. 2013;15:28.
- Kadir K, Gao H, Payne A, Soraghan J, Berry C. Automatic quantification and 3D visualisation of edema in cardiac MRI. *Conf Proc IEEE Eng Med Biol Soc*. 2011;2011:8021–4.
- McGraw KO, Wong SP. Forming Inferences About Some Intraclass Correlation Coefficients. *Psychol Methods*. 1996;1:30–46.
- Bland JM, Altman DG. Statistical methods for assessing agreement between two methods of clinical measurement. *Lancet*. 1986;1:307–10.
- Castillo E, Osman NF, Rosen BD, B-Shehaby J, Pan L, Jerosch-Herold M, et al. Quantitative assessment of regional myocardial function with MR-tagging in a multi-center study: interobserver and intrasession agreement of fast strain analysis with Harmonic Phase (HARP) MRI. *J Cardiovasc Magn Reson*. 2005;7:783–91.
- Mather AN, Fairbairn TA, Ants NJ, Greenwood JP. Timing of Cardiovascular MR Imaging after Acute Myocardial Infarction: Effect on Estimates of Infarct

- Characteristics and Prediction of Late Ventricular Remodeling. *Radiology*. 2011;261:116–26.
27. Dall'Armellina E, Karia N, Lindsay AC, Karamitsos TD, Ferreira V, Robson MD, et al. Dynamic changes of edema and late gadolinium enhancement after acute myocardial infarction and their relationship to functional recovery and salvage index. *Circ Cardiovasc Imaging*. 2011;4:228–36.
 28. Kim HW, Farzaneh-Far A, Kim R.J Cardiovascular magnetic resonance in patients with myocardial infarction: current and emerging applications. *J Am Coll Cardiol*. 2009;55:1–16.
 29. Bondarenko O, Beek AM, Hofman MB, Kuhl HP, Twisk JW, van Doornum WG, et al. Standardizing the definition of hyperenhancement in the quantitative assessment of infarct size and myocardial viability using delayed contrast-enhanced CMR. *J Cardiovasc Magn Reson*. 2005;7:481–5.
 30. Ibrahim T, Hackl T, Nekolla SG, Breuer M, Feldmair M, Schömig A. Acute Myocardial Infarction : Serial Cardiac MR Imaging Shows a Decrease in Delayed Enhancement of the Myocardium during the 1st Week after Reperfusion. *Radiology*. 2010;254:88–97.
 31. Wu E, Ortiz JT, Tejedor P, Lee DC, Kansal P, Carr JC, et al. Infarct size by contrast enhanced cardiac magnetic resonance is a stronger predictor of outcomes than left ventricular ejection fraction or end-systolic volume index : prospective cohort study Infarct size by contrast enhanced cardiac magnetic resonance i. *Heart*. 2008;94:730–6.
 32. Aletras AH, Tilak GS, Natanzon A, Hsu L-Y, Gonzalez FM, Hoyt RF, et al. Retrospective determination of the area at risk for reperfused acute myocardial infarction with T2-weighted cardiac magnetic resonance imaging: histopathological and displacement encoding with stimulated echoes (DENSE) functional validations. *Circulation*. 2006;113:1865–70.
 33. Oh-ichi D, Ridgway JP, Kuehne T, Berger F, Plein S, Sivanathan M, et al. Cardiovascular magnetic resonance of myocardial edema using a short inversion time inversion recovery (STIR) black-blood technique: Diagnostic accuracy of visual and semi-quantitative assessment. *JCMR*. 2012;14:22.
 34. Friedrich MG, Abdel-Aty H, Taylor A, Schulz-Menger J, Messroghii D, Dietz R. The salvaged area at risk in reperfused acute myocardial infarction as visualized by cardiovascular magnetic resonance. *J Am Coll Cardiol*. 2008;51:1581–7.

Submit your next manuscript to BioMed Central and take full advantage of:

- Convenient online submission
- Thorough peer review
- No space constraints or color figure charges
- Immediate publication on acceptance
- Inclusion in PubMed, CAS, Scopus and Google Scholar
- Research which is freely available for redistribution

Submit your manuscript at
www.biomedcentral.com/submit



REFERENCES

10. REFERENCES

1. Steg PG, James SK, Atar D, Badano LP, Blomstrom-Lundqvist C, Borger MA, Di Mario C, Dickstein K, Ducrocq G, Fernandez-Aviles F, Gershlick AH, Giannuzzi P, Halvorsen S, Huber K, Juni P, Kastrati A, Knuuti J, Lenzen MJ, Mahaffey KW, Valgimigli M, van 't Hof A, Widimsky P, Zahger D. Esc guidelines for the management of acute myocardial infarction in patients presenting with st-segment elevation. *Eur Heart J*. 2012;33:2569-2619
2. Steg PG, James SK, Atar D, Badano LP, Blomstrom-Lundqvist C, Borger MA, Di Mario C, Dickstein K, Ducrocq G, Fernandez-Aviles F, Gershlick AH, Giannuzzi P, Halvorsen S, Huber K, Juni P, Kastrati A, Knuuti J, Lenzen MJ, Mahaffey KW, Valgimigli M, van 't Hof A, Widimsky P, Zahger D. Esc guidelines for the management of acute myocardial infarction in patients presenting with st-segment elevation. *Eur Heart J*. 2012;33:2569-2619
3. O'Gara PT, Kushner FG, Ascheim DD, Casey DE, Jr., Chung MK, de Lemos JA, Ettinger SM, Fang JC, Fesmire FM, Franklin BA, Granger CB, Krumholz HM, Linderbaum JA, Morrow DA, Newby LK, Ornato JP, Ou N, Radford MJ, Tamis-Holland JE, Tommaso CL, Tracy CM, Woo YJ, Zhao DX, Anderson JL, Jacobs AK, Halperin JL, Albert NM, Brindis RG, Creager MA, DeMets D, Guyton RA, Hochman JS, Kovacs RJ, Kushner FG, Ohman EM, Stevenson WG, Yancy CW. 2013 accf/aha guideline for the management of st-elevation myocardial infarction: A report of the american college of cardiology foundation/american heart association task force on practice guidelines. *JACC*. 2013;61:e78-140
4. Dziewierz A, Siudak Z, Rakowski T, Zasada W, Dubiel JS, Dudek D. Impact of multivessel coronary artery disease and noninfarct-related artery revascularization on outcome of patients with st-elevation myocardial infarction transferred for primary percutaneous coronary intervention (from the eurotransfer registry). *Am J Cardiol*. 2010;106:342-347
5. Sorajja P, Gersh BJ, Cox DA, McLaughlin MG, Zimetbaum P, Costantini C, Stuckey T, Tcheng JE, Mehran R, Lansky AJ, Grines CL, Stone GW. Impact of multivessel disease on reperfusion success and clinical outcomes in patients undergoing primary percutaneous coronary intervention for acute myocardial infarction. *Eur Heart J*. 2007;28:1709-1716
6. Muller DW, Topol EJ, Ellis SG, Sigmon KN, Lee K, Califf RM. Multivessel coronary artery disease: A key predictor of short-term prognosis after reperfusion therapy for acute myocardial infarction. Thrombolysis and angioplasty in myocardial infarction (tami) study group. *Am Heart J*. 1991;121:1042-1049
7. Varani E, Balducelli M, Aquilina M, Vecchi G, Hussien MN, Frassinetti V, Maresta A. Single or multivessel percutaneous coronary intervention in st-elevation myocardial infarction patients. *Catheter Cardiovasc Interv*. 2008;72:927-933
8. Toma M, Buller CE, Westerhout CM, Fu Y, O'Neill WW, Holmes DR, Hamm CW, Granger CB, Armstrong PW. Non-culprit coronary artery percutaneous coronary intervention during acute st-segment elevation myocardial infarction: Insights from the apex-ami trial. *Eur Heart J*. 2010;31:1701-1707
9. Tarantini G, Napodano M, Gasparetto N, Favaretto E, Marra MP, Cacciavillani L, Bilato C, Osto E, Cademartiri F, Musumeci G, Corbetti F, Razzolini R, Iliceto S. Impact of multivessel coronary artery disease on early ischemic injury, late clinical outcome, and remodeling in patients with acute myocardial infarction treated by primary coronary angioplasty. *Coronary artery disease*. 2010;21:78-86
10. Corpus RA, House JA, Marso SP, Grantham JA, Huber KC, Jr., Laster SB, Johnson WL, Daniels WC, Barth CW, Giorgi LV, Rutherford BD. Multivessel percutaneous coronary intervention in patients with multivessel disease and acute myocardial infarction. *Am Heart J*. 2004;148:493-500
11. Claessen BE, van der Schaaf RJ, Verouden NJ, Stegenga NK, Engstrom AE, Sjaauw KD, Kikkert WJ, Vis MM, Baan J, Jr., Koch KT, de Winter RJ, Tijssen JG, Piek JJ, Henriques JP. Evaluation of the effect of a concurrent chronic total occlusion on long-term mortality and left ventricular function in patients after primary percutaneous coronary intervention. *JACC: Cardiovasc Interv*. 2009;2:1128-1134
12. Jaski BE, Cohen JD, Trausch J, Marsh DG, Bail GR, Overlie PA, Skowronski EW, Smith SC, Jr. Outcome of urgent percutaneous transluminal coronary angioplasty in acute myocardial

- infarction: Comparison of single-vessel versus multivessel coronary artery disease. *Am Heart J*. 1992;124:1427-1433
13. Hannan EL, Samadashvili Z, Walford G, Holmes DR, Jr., Jacobs AK, Stamato NJ, Venditti FJ, Sharma S, King SB, 3rd. Culprit vessel percutaneous coronary intervention versus multivessel and staged percutaneous coronary intervention for st-segment elevation myocardial infarction patients with multivessel disease. *JACC: Cardiovasc Interv*. 2010;3:22-31
 14. Vlaar PJ, Mahmoud KD, Holmes DR, van Valkenhoef G, Hillege HL, van der Horst ICC, Zijlstra F, de Smet BJGL. Culprit vessel only versus multivessel and staged percutaneous coronary intervention for multivessel disease in patients presenting with st-segment elevation myocardial infarction: A pairwise and network meta-analysis. *JACC*. 2011;58:692-703
 15. Engstrom T, Kelbaek H, Helqvist S, Hofsten DE, Klovgaard L, Holmvang L, Jorgensen E, Pedersen F, Saunamaki K, Clemmensen P, De Backer O, Ravkilde J, Tilsted HH, Villadsen AB, Aaroe J, Jensen SE, Raungaard B, Kober L. Complete revascularisation versus treatment of the culprit lesion only in patients with st-segment elevation myocardial infarction and multivessel disease (danami-3-primulti): An open-label, randomised controlled trial. *Lancet*. 2015;386:665-671
 16. Wald DS, Morris JK, Wald NJ, Chase AJ, Edwards RJ, Hughes LO, Berry C, Oldroyd KG. Randomized trial of preventive angioplasty in myocardial infarction. *NEJM*. 2013;369:1115-1123
 17. Di Mario C, Mara S, Flavio A, Imad S, Antonio M, Anna P, Emanuela P, Stefano DS, Angelo R, Stefania C, Anna F, Carmelo C, Antonio C, Monzini N, Bonardi MA. Single vs multivessel treatment during primary angioplasty: Results of the multicentre randomised hepacoat for culprit or multivessel stenting for acute myocardial infarction (help ami) study. *International journal of cardiovascular interventions*. 2004;6:128-133
 18. Tarasov RS, Ganyukov VI, Protopopov AV, Barbarash OL, Barbarash LS. Six month results of randomized clinical trial: Multivessel stenting versus staged revascularization for st-elevation myocardial infarction patients with second generation drug eluting stents. *Clin Med Research*. 2014;3:125-129
 19. Ghani A, Dambrink JH, van 't Hof AW, Ottervanger JP, Gosselink AT, Hoorntje JC. Treatment of non-culprit lesions detected during primary pci: Long-term follow-up of a randomised clinical trial. *Netherlands heart journal : monthly journal of the Netherlands Society of Cardiology and the Netherlands Heart Foundation*. 2012;20:347-353
 20. Maamoun W, Elkhateb N, Elarasy R. Safety and feasibility of complete simultaneous revascularization during primary pci in patients with stemi and multi-vessel disease. *The Egyptian Heart Journal*. 2011;63:39-43
 21. Politi L, Sgura F, Rossi R, Monopoli D, Guerri E, Leuzzi C, Bursi F, Sangiorgi GM, Modena MG. A randomised trial of target-vessel versus multi-vessel revascularisation in st-elevation myocardial infarction: Major adverse cardiac events during long-term follow-up. *Heart*. 2010;96:662-667
 22. Dambrink JH, Debrauwere JP, van 't Hof AW, Ottervanger JP, Gosselink AT, Hoorntje JC, de Boer MJ, Suryapranata H. Non-culprit lesions detected during primary pci: Treat invasively or follow the guidelines? *EuroIntervention : journal of EuroPCR in collaboration with the Working Group on Interventional Cardiology of the European Society of Cardiology*. 2010;5:968-975
 23. Khattab AA, Abdel-Wahab M, Rother C, Liska B, Toelg R, Kassner G, Geist V, Richardt G. Multi-vessel stenting during primary percutaneous coronary intervention for acute myocardial infarction. A single-center experience. *Clin Res Cardiol*. 2008;97:32-38
 24. Ochala A, Smolka GA, Wojakowski W, Dudek D, Dziewierz A, Krolkowski Z, Gasior Z, Tendera M. The function of the left ventricle after complete multivessel one-stage percutaneous coronary intervention in patients with acute myocardial infarction. *The Journal of invasive cardiology*. 2004;16:699-702
 25. Kowalewski M, Schulze V, Berti S, Waksman R, Kubica J, Kolodziejczak M, Buffon A, Suryapranata H, Gurbel PA, Kelm M, Pawliszak W, Anisimowicz L, Navarese EP. Complete revascularisation in st-elevation myocardial infarction and multivessel disease: Meta-analysis of randomised controlled trials. *Heart*. 2015
 26. Bangalore S, Kumar S, Poddar KL, Ramasamy S, Rha SW, Faxon DP. Meta-analysis of multivessel coronary artery revascularization versus culprit-only revascularization in patients

- with st-segment elevation myocardial infarction and multivessel disease. *Am J Cardiol.* 2011;107:1300-1310
27. Eitel I, Hintze S, de Waha S, Fuernau G, Lurz P, Desch S, Schuler G, Thiele H. Prognostic impact of hyperglycemia in nondiabetic and diabetic patients with st-elevation myocardial infarction: Insights from contrast-enhanced magnetic resonance imaging. *Circulation: Cardiovascular imaging.* 2012;5:708-718
 28. Bodi V, Sanchis J, Nunez J, Mainar L, Lopez-Lereu MP, Monmeneu JV, Rumiz E, Chaustre F, Trapero I, Husser O, Forteza MJ, Chorro FJ, Llacer A. Prognostic value of a comprehensive cardiac magnetic resonance assessment soon after a first st-segment elevation myocardial infarction. *JACC: Cardiovasc Imaging.* 2009;2:835-842
 29. Selvanayagam JB, Porto I, Channon K, Petersen SE, Francis JM, Neubauer S, Banning AP. Troponin elevation after percutaneous coronary intervention directly represents the extent of irreversible myocardial injury: Insights from cardiovascular magnetic resonance imaging. *Circulation.* 2005;111:1027-1032
 30. Rahimi K, Banning AP, Cheng ASH, Pegg TJ, Karamitsos TD, Channon KM, Darby S, Taggart DP, Neubauer S, Selvanayagam JB. Prognostic value of coronary revascularisation-related myocardial injury: A cardiac magnetic resonance imaging study. *Heart.* 2009;95:1937-1943
 31. Pfeffer MA, Braunwald E. Ventricular remodeling after myocardial infarction. Experimental observations and clinical implications. *Circulation.* 1990;81:1161-1172
 32. Abe D, Sato A, Hoshi T, Takeyasu N, Misaki M, Hayashi M, Aonuma K. Initial culprit-only versus initial multivessel percutaneous coronary intervention in patients with st-segment elevation myocardial infarction: Results from the ibaraki cardiovascular assessment study registry. *Heart Vessels.* 2014;29:171-177
 33. Gibson CM, Ryan KA, Murphy SA, Mesley R, Marble SJ, Giugliano RP, Cannon CP, Antman EM, Braunwald E. Impaired coronary blood flow in nonculprit arteries in the setting of acute myocardial infarction. The timi study group. Thrombolysis in myocardial infarction. *JACC.* 1999;34:974-982
 34. Widimsky P, Holmes DR. How to treat patients with st-elevation acute myocardial infarction and multi-vessel disease? *Eur Heart J.* 2011;32:396-403
 35. Kornowski R, Mehran R, Dangas G, Nikolsky E, Assali A, Claessen BE, Gersh BJ, Wong SC, Witzenbichler B, Guagliumi G, Dudek D, Fahy M, Lansky AJ, Stone GW. Prognostic impact of staged versus "one-time" multivessel percutaneous intervention in acute myocardial infarction: Analysis from the horizons-ami (harmonizing outcomes with revascularization and stents in acute myocardial infarction) trial. *JACC.* 2011;58:704-711
 36. Erne P, Schoenenberger AW, Burckhardt D, Zuber M, Kiowski W, Buser PT, Dubach P, Resink TJ, Pfisterer M. Effects of percutaneous coronary interventions in silent ischemia after myocardial infarction: The swissii randomized controlled trial. *Journal of the American Medical Association.* 2007;297:1985-1991
 37. Hanratty CG, Koyama Y, Rasmussen HH, Nelson GI, Hansen PS, Ward MR. Exaggeration of nonculprit stenosis severity during acute myocardial infarction: Implications for immediate multivessel revascularization. *JACC.* 2002;40:911-916
 38. Babu GG, Walker JM, Yellon DM, Hausenloy DJ. Peri-procedural myocardial injury during percutaneous coronary intervention: An important target for cardioprotection. *Eur Heart J.* 2011;32:23-31
 39. Thygesen K, Alpert JS, Jaffe AS, Simoons ML, Chaitman BR, White HD, Thygesen K, Alpert JS, White HD, Jaffe AS, Katus HA, Apple FS, Lindahl B, Morrow DA, Chaitman BA, Clemmensen PM, Johanson P, Hod H, Underwood R, Bax JJ, Bonow RO, Pinto F, Gibbons RJ, Fox KA, Atar D, Newby LK, Galvani M, Hamm CW, Uretsky BF, Steg PG, Wijns W, Bassand JP, Menasche P, Ravkilde J, Ohman EM, Antman EM, Wallentin LC, Armstrong PW, Simoons ML, Januzzi JL, Nieminen MS, Gheorghiade M, Filippatos G, Luepker RV, Fortmann SP, Rosamond WD, Levy D, Wood D, Smith SC, Hu D, Lopez-Sendon JL, Robertson RM, Weaver D, Tendera M, Bove AA, Parkhomenko AN, Vasilieva EJ, Mendis S. Third universal definition of myocardial infarction. *Eur Heart J.* 2012;33:2551-2567
 40. Testa L, Van Gaal WJ, Biondi Zoccai GGL, Agostoni P, Latini Ra, Bedogni F, Porto I, Banning aP. Myocardial infarction after percutaneous coronary intervention: A meta-analysis of troponin elevation applying the new universal definition. *QJM.* 2009;102:369-378

41. Park DW, Kim YH, Yun SC, Ahn JM, Lee JY, Kim WJ, Kang SJ, Lee SW, Lee CW, Park SW, Park SJ. Frequency, causes, predictors, and clinical significance of peri-procedural myocardial infarction following percutaneous coronary intervention. *Eur Heart J*. 2013;34:1662-1669
42. Prasad A, Rihal CS, Lennon RJ, Singh M, Jaffe AS, Holmes DR. Significance of periprocedural myonecrosis on outcomes after percutaneous coronary intervention: An analysis of preintervention and postintervention troponin t levels in 5487 patients. *Circulation: Cardiovascular interventions*. 2008;1:10-19
43. Locca D, Bucciarelli-Ducci C, Ferrante G, La Manna A, Keenan NG, Grasso A, Barlis P, Del Furia F, Prasad SK, Kaski JC, Pennell DJ, Di Mario C. New universal definition of myocardial infarction applicable after complex percutaneous coronary interventions? *JACC: Cardiovasc Interv*. 2010;3:950-958
44. Ricciardi MJ, Wu E, Davidson CJ, Choi KM, Klocke FJ, Bonow RO, Judd RM, Kim RJ. Visualization of discrete microinfarction after percutaneous coronary intervention associated with mild creatine kinase-mb elevation. *Circulation*. 2001;103:2780-2783
45. Group BDW. Biomarkers and surrogate endpoints: Preferred definitions and conceptual framework. *Clinical pharmacology and therapeutics*. 2001;69:89-95
46. Desch S, Eitel I, de Waha S, Fuernau G, Lurz P, Gutberlet M, Schuler G, Thiele H. Cardiac magnetic resonance imaging parameters as surrogate endpoints in clinical trials of acute myocardial infarction. *Trials*. 2011;12:204
47. Pitcher A, Ashby D, Elliott P, Petersen SE. Cardiovascular mri in clinical trials: Expanded applications through novel surrogate endpoints. *Heart*. 2011;97:1286-1292
48. Austin PC. An introduction to propensity score methods for reducing the effects of confounding in observational studies. *Multivariate Behavioral Research*. 2011;46:399-424
49. Han YL, Wang B, Wang XZ, Li Y, Wang SL, Jing QM, Wang G, Ma YY, Luan B. Comparative effects of percutaneous coronary intervention for infarct-related artery only or for both infarct- and non-infarct-related arteries in patients with st-elevation myocardial infarction and multi-vessel disease. *Chinese medical journal*. 2008;121:2384-2387
50. Ripa RS, Nilsson JC, Wang Y, Sondergaard L, Jorgensen E, Kastrup J. Short- and long-term changes in myocardial function, morphology, edema, and infarct mass after st-segment elevation myocardial infarction evaluated by serial magnetic resonance imaging. *Am Heart J*. 2007;154:929-936
51. Hombach V, Grebe O, Merkle N, Waldenmaier S, Höher M, Kochs M, Wöhrle J, Kestler Ha. Sequelae of acute myocardial infarction regarding cardiac structure and function and their prognostic significance as assessed by magnetic resonance imaging. *Eur Heart J*. 2005;26:549-557
52. Engblom H, Hedstrom E, Heiberg E, Wagner GS, Pahlm O, Arheden H. Rapid initial reduction of hyperenhanced myocardium after reperfusion first myocardial infarction suggests recovery of the peri-infarction zone: One-year follow-up by mri. *Circulation: Cardiovascular imaging*. 2009;2:47-55
53. Ghugre NR, Ramanan V, Pop M, Yang Y, Barry J, Qiang B, Connelly KA, Dick AJ, Wright GA. Quantitative tracking of edema, hemorrhage, and microvascular obstruction in subacute myocardial infarction in a porcine model by mri. *Magn Reson Med*. 2011;66:1129-1141
54. Ibrahim T, Hackl T, Nekolla SG, Breuer M, Feldmair M, Schömig A. Acute myocardial infarction : Serial cardiac mr imaging shows a decrease in delayed enhancement of the myocardium during the 1st week after reperfusion. *Radiology*. 2010;254:88-97
55. Lund GK, Stork A, Muellerleile K, Bansmann MP, Schlichting U, Mu M, Adam G, Meinertz T. Prediction of left ventricular remodeling and analysis of infarct resorption in patients with reperfusion myocardial infarcts by using contrast-enhanced mr imaging. *Radiology*. 2007;245:95-104
56. Bolognese L, Neskovic AN, Parodi G, Cerisano G, Buonamici P, Santoro GM, Antoniucci D. Left ventricular remodeling after primary coronary angioplasty: Patterns of left ventricular dilation and long-term prognostic implications. *Circulation*. 2002;106:2351-2357
57. Ahn KT, Song YB, Choe YH, Yang JH, Hahn JY, Choi JH, Choi SH, Chang SA, Lee SC, Lee SH, Oh JK, Gwon HC. Impact of transmural necrosis on left ventricular remodeling and clinical outcomes in patients undergoing primary percutaneous coronary intervention for st-segment elevation myocardial infarction. *Int J Cardiovasc Imaging*. 2013;29:835-842

58. Masci PG, Ganame J, Francone M, Desmet W, Lorenzoni V, Iacucci I, Barison A, Carbone I, Lombardi M, Agati L, Janssens S, Bogaert J. Relationship between location and size of myocardial infarction and their reciprocal influences on post-infarction left ventricular remodelling. *Eur Heart J*. 2011;32:1640-1648
59. Wagner A, Mahrholdt H, Holly Ta, Elliott MD, Regenfus M, Parker M, Klocke FJ, Bonow RO, Kim RJ, Judd RM. Contrast-enhanced mri and routine single photon emission computed tomography (spect) perfusion imaging for detection of subendocardial myocardial infarcts: An imaging study. *Lancet*. 2003;361:374-379
60. Bellenger NG, Grothues F, Smith GC, Pennell DJ. Quantification of right and left ventricular function by cardiovascular magnetic resonance. *Herz*. 2000;25:392-399
61. Cerqueira MD, Weissman NJ, Dilsizian V, Jacobs AK, Kaul S, Laskey WK, Pennell DJ, Rumberger JA, Ryan T, Verani MS. Standardized myocardial segmentation and nomenclature for tomographic imaging of the heart. A statement for healthcare professionals from the cardiac imaging committee of the council on clinical cardiology of the american heart association. *Circulation*. 2002;105:539-542
62. Mather AN, Fairbairn TA, Artis NJ, Greenwood JP. Timing of cardiovascular mr imaging after acute myocardial infarction : Effect on estimates of infarct characteristics and prediction of late ventricular remodeling. *Radiology*. 2011;261:116-126
63. Beek AM, Ku HP, Bondarenko O, Twisk JWR, Rossum ACV. Delayed contrast-enhanced magnetic resonance imaging for the prediction of regional functional improvement after acute myocardial infarction. *JACC*. 2003;42:895-901
64. Ganame J, Messalli G, Masci PG, Dymarkowski S, Abbasi K, Van de Werf F, Janssens S, Bogaert J. Time course of infarct healing and left ventricular remodelling in patients with reperfused st segment elevation myocardial infarction using comprehensive magnetic resonance imaging. *Eur Radiol*. 2011;21:693-701
65. Dall'Armellina E, Karia N, Lindsay AC, Karamitsos TD, Ferreira V, Robson MD, Kellman P, Francis JM, Forfar C, Prendergast BD, Banning AP, Channon KM, Kharbanda RK, Neubauer S, Choudhury RP. Dynamic changes of edema and late gadolinium enhancement after acute myocardial infarction and their relationship to functional recovery and salvage index. *Circulation: Cardiovascular imaging*. 2011;4:228-236
66. Orn S, Manhenke C, Anand IS, Squire I, Nagel E, Edvardsen T, Dickstein K. Effect of left ventricular scar size, location, and transmural extent on left ventricular remodeling with healed myocardial infarction. *Am J Cardiol*. 2007;99:1109-1114
67. Husser O, Bodí V, Sanchis J, Núñez J, Mainar L, Rumiz E, López-Lereu MP, Monmeneu J, Chaustre F, Trapero I, Forteza MJ, Riegger GaJ, Chorro FJ, Llàcer A. The sum of st-segment elevation is the best predictor of microvascular obstruction in patients treated successfully by primary percutaneous coronary intervention. Cardiovascular magnetic resonance study. *Rev Esp Cardiol*. 2010;63:1145-1154
68. Beek aM, Nijveldt R, van Rossum aC. Intramyocardial hemorrhage and microvascular obstruction after primary percutaneous coronary intervention. *Int J Cardiovasc Imaging*. 2010;26:49-55
69. Ganame J, Messalli G, Dymarkowski S, Rademakers FE, Desmet W, Van de Werf F, Bogaert J. Impact of myocardial haemorrhage on left ventricular function and remodelling in patients with reperfused acute myocardial infarction. *Eur Heart J*. 2009;30:1440-1449
70. Masci PG, Ganame J, Strata E, Desmet W, Aquaro GD, Dymarkowski S, Valenti V, Janssens S, Lombardi M, Werf FVD, Abbate AL, Bogaert J. Myocardial salvage by cmr correlates with lv remodeling and early st-segment resolution in acute myocardial infarction. *JACC: Cardiovasc Imaging*. 2010;3:45-51
71. E. Canali PM, J. Bogaert, C. Bucciarelli Ducci, M. Francone, E. McAlindon, I. Carbone, M. Lombardi, W. Desmet, S. Janssens, L. Agati. Impact of gender differences on myocardial salvage and post-ischaemic left ventricular remodelling after primary coronary angioplasty : New insights from cardiovascular magnetic. *Eur Heart J: Cardiovascular Imaging*. 2012;13:948-953
72. Nijveldt R, van der Vleuten Pa, Hirsch A, Beek AM, Tio Ra, Tijssen JGP, Piek JJ, van Rossum AC, Zijlstra F. Early electrocardiographic findings and mr imaging-verified microvascular injury and myocardial infarct size. *JACC: Cardiovasc Imaging*. 2009;2:1187-1194

73. Norris RM, Barnaby PF, Brandt PW, Geary GG, Whitlock RM, Wild CJ, Barratt-Boyes BG. Prognosis after recovery from first acute myocardial infarction: Determinants of reinfarction and sudden death. *Am J Cardiol.* 1984;53:408-413
74. White HD, Norris R, Brown M, Brandt P, Whitlock R, Wild C. Left ventricular end-systolic volume as the major determinant of survival after recovery from myocardial infarction. *Circulation.* 1987;76:44-51
75. Burns RJ, Gibbons RJ, Yi Q, Roberts RS, Miller TD, Schaer GL, Anderson JL, Yusuf S. The relationships of left ventricular ejection fraction, end-systolic volume index and infarct size to six-month mortality after hospital discharge following myocardial infarction treated by thrombolysis. *JACC.* 2002;39:30-36
76. El Aidi H, Adams A, Moons KG, Den Ruijter HM, Mali WP, Doevendans PA, Nagel E, Schalla S, Bots ML, Leiner T. Cardiac magnetic resonance imaging findings and the risk of cardiovascular events in patients with recent myocardial infarction or suspected or known coronary artery disease: A systematic review of prognostic studies. *JACC.* 2014;63:1031-1045
77. Husser O, Monmeneu JV, Sanchis J, Nunez J, Lopez-Lereu MP, Bonanad C, Chaustre F, Gomez C, Bosch MJ, Hinarejos R, Chorro FJ, Riegger GA, Llacer A, Bodi V. Cardiovascular magnetic resonance-derived intramyocardial hemorrhage after stemi: Influence on long-term prognosis, adverse left ventricular remodeling and relationship with microvascular obstruction. *Int J Cardiol.* 2012
78. Eitel I, Desch S, de Waha S, Fuernau G, Gutberlet M, Schuler G, Thiele H. Long-term prognostic value of myocardial salvage assessed by cardiovascular magnetic resonance in acute reperfused myocardial infarction. *Heart.* 2011;97:2038-2045
79. Amabile N, Jacquier A, Gaudart J, Sarran A, Shuaib A, Panuel M, Moulin G, Bartoli J-m, Paganelli F. Value of a new multiparametric score for prediction of microvascular obstruction lesions in st-segment elevation myocardial infarction revascularized by percutaneous coronary intervention. *Archives of Cardiovascular Diseases.* 2010;103:512-521
80. de Waha S, Desch S, Eitel I, Fuernau G. Impact of early vs. Late microvascular obstruction assessed by magnetic resonance imaging on longterm outcome after st-elevation myocardial infarction: A comparison with traditional prognostic markers. *Eur Heart J.* 2010;31:2660-2668
81. Cochet AA, Lorgis L, Lalande A, Zeller M, Beer JC, Walker PM, Touzery C, Wolf JE, Brunotte F, Cottin Y. Major prognostic impact of persistent microvascular obstruction as assessed by contrast-enhanced cardiac magnetic resonance in reperfused acute myocardial infarction. *Eur Radiol.* 2009;19:2117-2126
82. St John Sutton M, Lee D, Rouleau JL, Goldman S, Plappert T, Braunwald E, Pfeffer MA. Left ventricular remodeling and ventricular arrhythmias after myocardial infarction. *Circulation.* 2003;107:2577-2582
83. Otterstad JE, St John Sutton M, Froland G, Skjaerpe T, Graving B, Holmes I. Are changes in left ventricular volume as measured with the biplane simpson's method predominantly related to changes in its area or long axis in the prognostic evaluation of remodelling following a myocardial infarction? *Eur J Echocardiogr.* 2001;2:118-125
84. St John Sutton M, Pfeffer MA, Plappert T, Rouleau JL, Moya LA, Dagenais GR, Lamas GA, Klein M, Sussex B, Goldman S, et al. Quantitative two-dimensional echocardiographic measurements are major predictors of adverse cardiovascular events after acute myocardial infarction. The protective effects of captopril. *Circulation.* 1994;89:68-75
85. Eitel I, Poss J, Jobs A, Eitel C, de Waha S, Barkhausen J, Desch S, Thiele H. Left ventricular global function index assessed by cardiovascular magnetic resonance for the prediction of cardiovascular events in st-elevation myocardial infarction. *J Cardiovasc Magn Reson.* 2015;17:62
86. Ibrahim E-SH. Myocardial tagging by cardiovascular magnetic resonance: Evolution of techniques--pulse sequences, analysis algorithms, and applications. *JCMR.* 2011;13:36
87. Gotte MJ, van Rossum AC, Twisk JWR, Kuijer JPA, Marcus JT, Visser CA. Quantification of regional contractile function after infarction: Strain analysis superior to wall thickening analysis in discriminating infarct from remote myocardium. *JACC.* 2001;37:808-817
88. Zerhouni EA, Parish DM, Rogers WJ, Yang A, Shapiro EP. Human heart: Tagging with mr imaging--a method for noninvasive assessment of myocardial motion. *Radiology.* 1988;169:59-63

89. Axel L, Dougherty L. Mr imaging of motion with spatial modulation of magnetization. *Radiology*. 1989;171:841-845
90. Lima JA, Jeremy R, Guier W, Bouton S, Zerhouni EA, McVeigh E, Buchalter MB, Weisfeldt ML, Shapiro EP, Weiss JL. Accurate systolic wall thickening by nuclear magnetic resonance imaging with tissue tagging: Correlation with sonomicrometers in normal and ischemic myocardium. *JACC*. 1993;21:1741-1751
91. Yeon SB, Reichek N, Tallant BA, Lima JA, Calhoun LP, Clark NR, Hoffman EA, Ho KK, Axel L. Validation of in vivo myocardial strain measurement by magnetic resonance tagging with sonomicrometry. *JACC*. 2001;38:555-561
92. Shehata ML, Cheng S, Osman NF, Bluemke Da, Lima JaC. Myocardial tissue tagging with cardiovascular magnetic resonance. *JCMR*. 2009;11:55
93. Hor KN, Gottliebson WM, Carson C, Wash E, Cnota J, Fleck R, Wansapura J, Klimeczek P, Al-Khalidi HR, Chung ES, Benson DW, Mazur W. Comparison of magnetic resonance feature tracking for strain calculation with harmonic phase imaging analysis. *JACC: Cardiovasc Imaging*. 2010;3:144-151
94. Augustine D, Lewandowski AJ, Lazdam M, Rai A, Francis J, Myerson S, Noble A, Becher H, Neubauer S, Petersen SE, Leeson P. Global and regional left ventricular myocardial deformation measures by magnetic resonance feature tracking in healthy volunteers: Comparison with tagging and relevance of gender. *JCMR*. 2013;15:8
95. Gotte MJ, van Rossum AC, Marcus JT, Kuijper JP, Axel L, Visser CA. Recognition of infarct localization by specific changes in intramural myocardial mechanics. *Am Heart J*. 1999;138:1038-1045
96. Neizel M, Lossnitzer D, Korosoglou G, Schäufele T, Peykarjou H, Steen H, Ocklenburg C, Giannitsis E, Katus Ha, Osman NF. Strain-encoded mri for evaluation of left ventricular function and transmuralty in acute myocardial infarction. *Circulation: Cardiovascular imaging*. 2009;2:116-122
97. Gerber BL. Accuracy of contrast-enhanced magnetic resonance imaging in predicting improvement of regional myocardial function in patients after acute myocardial infarction. *Circulation*. 2002;106:1083-1089
98. Wong DT, Leong DP, Weightman MJ, Richardson JD, Dundon BK, Psaltis PJ, Leung MC, Meredith IT, Worthley MI, Worthley SG. Magnetic resonance-derived circumferential strain provides a superior and incremental assessment of improvement in contractile function in patients early after st-segment elevation myocardial infarction. *Eur Radiol*. 2014;24:1219-1228
99. Buss SJ, Krautz B, Hofmann N, Sander Y, Rust L, Giusca S, Galuschky C, Seitz S, Giannitsis E, Pleger S, Raake P, Most P, Katus HA, Korosoglou G. Prediction of functional recovery by cardiac magnetic resonance feature tracking imaging in first time st-elevation myocardial infarction. Comparison to infarct size and transmuralty by late gadolinium enhancement. *Int J Cardiol*. 2015;183:162-170
100. Ersboll M, Andersen MJ, Valeur N, Mogensen UM, Fahkri Y, Thune JJ, Moller JE, Hassager C, Sogaard P, Kober L. Early diastolic strain rate in relation to systolic and diastolic function and prognosis in acute myocardial infarction: A two-dimensional speckle-tracking study. *Eur Heart J*. 2014;35:648-656
101. Ersboll M, Valeur N, Mogensen UM, Andersen MJ, Moller JE, Velazquez EJ, Hassager C, Sogaard P, Kober L. Prediction of all-cause mortality and heart failure admissions from global left ventricular longitudinal strain in patients with acute myocardial infarction and preserved left ventricular ejection fraction. *JACC*. 2013;61:2365-2373
102. Hung CL, Verma A, Uno H, Shin SH, Bourgoun M, Hassanein AH, McMurray JJ, Velazquez EJ, Kober L, Pfeffer MA, Solomon SD. Longitudinal and circumferential strain rate, left ventricular remodeling, and prognosis after myocardial infarction. *JACC*. 2010;56:1812-1822
103. Antoni ML, Mollema SA, Delgado V, Atary JZ, Borleffs CJ, Boersma E, Holman ER, van der Wall EE, Schalij MJ, Bax JJ. Prognostic importance of strain and strain rate after acute myocardial infarction. *Eur Heart J*. 2010;31:1640-1647
104. Mahrholdt H, Wagner A, Holly TA, Elliott MD, Bonow RO, Kim RJ, Judd RM. Reproducibility of chronic infarct size measurement by contrast-enhanced magnetic resonance imaging. *Circulation*. 2002;106:2322-2327

105. Nesto RW, Kowalchuk GJ. The ischemic cascade: Temporal sequence of hemodynamic, electrocardiographic and symptomatic expressions of ischemia. *Am J Cardiol.* 1987;59:23C-30C
106. Petersen S, Mohrs O, Horstick G, Oberholzer K, Abegunewardene N, Ruetzel K, Selvanayagam J, Robson M, Neubauer S, Thelen M, Meyer J, Kreitner KF. Influence of contrast agent dose and image acquisition timing on the quantitative determination of nonviable myocardial tissue using delayed contrast-enhanced magnetic resonance imaging. *JCMR.* 2004;6:541-548
107. Kim RJ, Chen EL, Lima JA, Judd RM. Myocardial gadolinium kinetics determine mri contrast enhancement and reflect the extent and severity of myocardial injury after acute reperfused infarction. *Circulation.* 1996;94:3318-3326
108. Kim RJ, Fieno DS, Parrish TB, Harris K, Chen E-I, Simonetti O, Bundy J, Finn JP, Klocke FJ, Judd RM. Relationship of mri delayed contrast enhancement to irreversible injury, infarct age, and contractile function. *Circulation.* 1999;100:1992-2002
109. Flacke SJ, Fischer SE, Lorenz CH. Measurement of the gadopentetate dimeglumine partition coefficient in human myocardium in vivo: Normal distribution and elevation in acute and chronic infarction. *Radiology.* 2001;218:703-710
110. Pennell DJ. Cardiovascular magnetic resonance. *Circulation.* 2010;121:692-705
111. Amado LC, Gerber BL, Gupta SN, Rettmann DW, Szarf G, Schock R, Nasir K, Kraitchman DL, Lima JA. Accurate and objective infarct sizing by contrast-enhanced magnetic resonance imaging in a canine myocardial infarction model. *JACC.* 2004;44:2383-2389
112. Larose E, Rodés-Cabau J, Pibarot P, Rinfret S, Proulx G, Nguyen CM, Déry J-P, Gleeton O, Roy L, Noël B, Barbeau G, Rouleau J, Boudreault J-R, Amyot M, De Larochellière R, Bertrand OF. Predicting late myocardial recovery and outcomes in the early hours of st-segment elevation myocardial infarction traditional measures compared with microvascular obstruction, salvaged myocardium, and necrosis characteristics by cardiovascular magnetic re. *JACC.* 2010;55:2459-2469
113. Zia MI, Ghugre NR, Roifman I, Strauss BH, Walcarius R, Mohammed M, Sparkes JD, Dick AJ, Wright GA, Connelly KA. Comparison of the frequencies of myocardial edema determined by cardiac magnetic resonance in diabetic versus nondiabetic patients having percutaneous coronary intervention for st elevation myocardial infarction. *Am J Cardiol.* 2014;113:607-612
114. Robbers LF, Eerenberg ES, Teunissen PF, Jansen MF, Hollander MR, Horrevoets AJ, Knaapen P, Nijveldt R, Heymans MW, Levi MM, van Rossum AC, Niessen HW, Marcu CB, Beek AM, van Royen N. Magnetic resonance imaging-defined areas of microvascular obstruction after acute myocardial infarction represent microvascular destruction and haemorrhage. *Eur Heart J.* 2013;34:2346-2353
115. Malek LA, Spiewak M, Klopotoski M, Misko J, Ruzyllo W, Witkowski A. The size does not matter - the presence of microvascular obstruction but not its extent corresponds to larger infarct size in reperfused stemi. *European journal of radiology.* 2012;81:2839-2843
116. Kim HW, Farzaneh-Far A, Kim RJ. Cardiovascular magnetic resonance in patients with myocardial infarction: Current and emerging applications. *JACC.* 2009;55:1-16
117. Flett AS, Hasleton J, Cook C, Hausenloy D, Quarta G, Ariti C, Muthurangu V, Moon JC. Evaluation of techniques for the quantification of myocardial scar of differing etiology using cardiac magnetic resonance. *JACC: Cardiovasc Imaging.* 2011;4:150-156
118. Rutt BK, Lee DH. The impact of field strength on image quality in mri. *JMRI.* 1996;6:57-62
119. Goetti R, Kozerke S, Donati O, Stolzmann P, Corti R, Manka R. Comparison of 3d and 2d acquisition of late gadolinium enhancement in patients with acute, subacute and chronic myocardial infarction. *JCMR.* 2011;13:154
120. Rosendahl L, Ahlander B-M, Björklund P-G, Blomstrand P, Brudin L, Engvall JE. Image quality and myocardial scar size determined with magnetic resonance imaging in patients with permanent atrial fibrillation: A comparison of two imaging protocols. *Clin Phys Funct Imaging.* 2010;30:122-129
121. van den Bosch HCM, Westenberg JJM, Post JC, Yo G, Verwoerd J, Kroft LJM, de Roos A. Free-breathing mri for the assessment of myocardial infarction: Clinical validation. *AJR.* 2009;192:W277-281
122. Kühl HP, Papavasiliu TS, Beek AM, Hofman MBM, Heusen NS, van Rossum AC. Myocardial viability: Rapid assessment with delayed contrast-enhanced mr imaging with three-dimensional inversion-recovery prepared pulse sequence. *Radiology.* 2004;230:576-582

123. Matsumoto H, Matsuda T, Miyamoto K, Shimada T, Hayashi A, Mikuri M, Hiraoka Y. Late gadolinium-enhanced cardiovascular mri at end-systole: Feasibility study. *AJR*. 2010;195:1088-1094
124. Peters DC, Appelbaum Ea, Nezafat R, Dokhan B, Han Y, Kissinger KV, Goddu B, Manning WJ. Left ventricular infarct size, peri-infarct zone, and papillary scar measurements: A comparison of high-resolution 3d and conventional 2d late gadolinium enhancement cardiac mr. *JMRI*. 2009;30:794-800
125. Kellman P, Arai AE, McVeigh ER, Aletras AH. Phase-sensitive inversion recovery for detecting myocardial infarction using gadolinium-delayed hyperenhancement. *Magn Reson Med*. 2002;47:372-383
126. Wildgruber M, Settles M, Kosanke K, Bielicki I, Ntziachristos V, Rummeny EJ, Botnar RM, Huber AM. Evaluation of phase-sensitive versus magnitude reconstructed inversion recovery imaging for the assessment of myocardial infarction in mice with a clinical magnetic resonance scanner. *JMRI*. 2012;36:1372-1382
127. Roujol S, Weingartner S, Foppa M, Chow K, Kawaji K, Ngo LH, Kellman P, Manning WJ, Thompson RB, Nezafat R. Accuracy, precision, and reproducibility of four t1 mapping sequences: A head-to-head comparison of molli, shmollo, sasha, and sapphire. *Radiology*. 2014;272:683-689
128. O'Regan DP, Ariff B, Baksi AJ, Gordon F, Durighel G, Cook SA. Salvage assessment with cardiac mri following acute myocardial infarction underestimates potential for recovery of systolic strain. *Eur Radiol*. 2013;23:1210-1217
129. Carrick D, Haig C, Ahmed N, McEntegart M, Petrie MC, Eteiba H, Hood S, Watkins S, Lindsay MM, Davie A, Mahrous A, Mordi I, Rauhalammi S, Sattar N, Welsh P, Radjenovic A, Ford I, Oldroyd KG, Berry C. Myocardial hemorrhage after acute reperfused st-segment-elevation myocardial infarction: Relation to microvascular obstruction and prognostic significance. *Circ Cardiovasc Imaging*. 2016;9:e004148
130. Judd RM, Lugo-Olivieri CH, Arai M, Kondo T, Croisille P, Lima JA, Mohan V, Becker LC, Zerhouni EA. Physiological basis of myocardial contrast enhancement in fast magnetic resonance images of 2-day-old reperfused canine infarcts. *Circulation*. 1995;92:1902-1910
131. Hillenbrand HB, Sandstede J, Störk S, Ramsayer B, Hahn D, Ertl G, Koestler H, Bauer W, Ritter C. Remodeling of the infarct territory in the time course of infarct healing in humans. *MAGMA*. 2011;24:277-284
132. Reimer KA, Jennings RB, Cobb FR, Murdock RH, Greenfield JC, Jr., Becker LC, Bulkley BH, Hutchins GM, Schwartz RP, Jr., Bailey KR, et al. Animal models for protecting ischemic myocardium: Results of the nhlbi cooperative study. Comparison of unconscious and conscious dog models. *Circulation research*. 1985;56:651-665
133. Fieno DS, Hillenbrand HB, Rehwald WG, Harris KR, Decker RS, Parker Ma, Klocke FJ, Kim RJ, Judd RM. Infarct resorption, compensatory hypertrophy, and differing patterns of ventricular remodeling following myocardial infarctions of varying size. *JACC*. 2004;43:2124-2131
134. Kim J-s, Ko Y-g, Yoon S-j, Moon J-y, Kim YJ, Choi BW, Choi D, Jang Y. Correlation of serial cardiac magnetic resonance imaging parameters with early resolution of st-segment elevation. 2008;72:1621-1626
135. Aletras AH, Tilak GS, Natanzon A, Hsu L-Y, Gonzalez FM, Hoyt RF, Arai AE. Retrospective determination of the area at risk for reperfused acute myocardial infarction with t2-weighted cardiac magnetic resonance imaging: Histopathological and displacement encoding with stimulated echoes (dense) functional validations. *Circulation*. 2006;113:1865-1870
136. Lowe JE, Reimer KA, Jennings RB. Experimental infarct size as a function of the amount of myocardium at risk. *The American journal of pathology*. 1978;90:363-379
137. Christian TF, Schwartz RS, Gibbons RJ. Determinants of infarct size in reperfusion therapy for acute myocardial infarction. *Circulation*. 1992;86:81-90
138. Hirsch A, Nijveldt R, Haack JDE, Beek AM, Rossum ACV, Piek JJ. Relation between the assessment of microvascular injury by cardiovascular magnetic resonance and coronary doppler flow velocity measurements in patients with acute anterior wall myocardial infarction. *JACC*. 2008;51:2330-2337
139. Francone M, Bucciarelli-Ducci C, Carbone I, Canali E, Scardala R, Calabrese Fa, Sardella G, Mancone M, Catalano C, Fedele F, Passariello R, Bogaert J, Agati L. Impact of primary coronary angioplasty delay on myocardial salvage, infarct size, and microvascular damage in

- patients with st-segment elevation myocardial infarction: Insight from cardiovascular magnetic resonance. *JACC*. 2009;54:2145-2153
140. Cochet A, Zeller M, Lalande A, L'huillier I, Walker PM, Touzery C, Verges B, Wolf J-E, Brunotte F, Cottin Y. Utility of cardiac magnetic resonance to assess association between admission hyperglycemia and myocardial damage in patients with reperfused st-segment elevation myocardial infarction. *JCMR*. 2008;10:2 doi: 10.1186/1532-1429X-1110-1182
 141. Kim R, Wu E, Rafael A, Chen E-L, Parker M, Simonetti O, Klocke FJ, Bonow RO, Judd RM. The use of contrast enhanced magnetic resonance imaging to identify reversible myocardial dysfunction. *NEJM*. 2000;343:1445-1453
 142. Natale L, Napolitano C, Bernardini A, Meduri A, Marano R, Lombardo A, Crea F, Bonomo L. Role of first pass and delayed enhancement in assessment of segmental functional recovery after acute myocardial infarction. *La Radiologia medica*. 2012;117:1294-1308
 143. Shapiro MD, Nieman K, Nasir K, Nomura CH, Sarwar A, Ferencik M, Abbata S, Hoffmann U, Gold HK, Jang IK, Brady TJ, Cury RC. Utility of cardiovascular magnetic resonance to predict left ventricular recovery after primary percutaneous coronary intervention for patients presenting with acute st-segment elevation myocardial infarction. *Am J Cardiol*. 2007;100:211-216
 144. Kitagawa K, Ichikawa Y, Hirano T, Makino K, Kobayashi S, Takeda K, Sakuma H. Diagnostic value of late gadolinium-enhanced mri and first-pass dynamic mri for predicting functional recovery in patients after acute myocardial infarction. *Radiation medicine*. 2007;25:263-271
 145. Janssens S, Dubois C, Bogaert J, Theunissen K, Deroose C, Desmet W, Kalantzi M, Herbots L, Sinnaeve P, Dens J, Maertens J, Rademakers F, Dymarkowski S, Gheysens O, Van Cleemput J, Bormans G, Nuyts J, Belmans A, Mortelmans L, Boogaerts M, Van de Werf F. Autologous bone marrow-derived stem-cell transfer in patients with st-segment elevation myocardial infarction: Double-blind, randomised controlled trial. *Lancet*. 2006;367:113-121
 146. Motoyasu M, Sakuma H, Ichikawa Y, Ishida N, Uemura S, Okinaka T, Isaka N, Takeda K, Nakano T. Prediction of regional functional recovery after acute myocardial infarction with low dose dobutamine stress cine mr imaging and contrast enhanced mr imaging. *JCMR*. 2003;5:563-574
 147. Monmeneu JV, Bodi V, Lopez-Lereu MP, Sanchis J, Nunez J, Chaustre F, Husser O, Merlos P, Bonanad C, Minana G, Chorro FJ, Llacer A. Analysis of post-infarction salvaged myocardium by cardiac magnetic resonance. Predictors and influence on adverse ventricular remodeling. *Rev Esp Cardiol*. 2012
 148. Ezekowitz JA, Armstrong PW, Granger CB, Theroux P, Stebbins A, Kim RJ, Patel MR. Predicting chronic left ventricular dysfunction 90 days after st-segment elevation myocardial infarction: An assessment of pexelizumab in acute myocardial infarction (apex-ami) substudy. *Am Heart J*. 2010;160:272-278
 149. Bodí V, Husser O, Sanchis J, Núñez J, López-lereu MP, Bosch MJ, Chorro FJ, Llácer A. Contractile reserve and extent of transmural necrosis in the setting of myocardial stunning : Methods : Results :. *Radiology*. 2010;255
 150. Wu KC, Zerhouni EA, Judd RM, Lugo-olivieri CH, Lili A, Schulman SP, Blumenthal RS, Lima JAC. Prognostic significance of microvascular obstruction by magnetic resonance imaging in patients with acute myocardial infarction. *Circulation*. 1998;97:765-772
 151. Husser O, Monmeneu JV, Bonanad C, Gomez C, Chaustre F, Nunez J, Lopez-Lereu MP, Minana G, Sanchis J, Mainar L, Ruiz V, Forteza MJ, Trapero I, Moratal D, Chorro FJ, Bodi V. Head-to-head comparison of 1 week versus 6 months cmr-derived infarct size for prediction of late events after stemi. *Int J Cardiovasc Imaging*. 2013;29:1499-1509
 152. Izquierdo M, Ruiz-Granell R, Bonanad C, Chaustre F, Gomez C, Ferrero A, Lopez-Lereu P, Monmeneu JV, Nunez J, Chorro FJ, Bodi V. Value of early cardiovascular magnetic resonance for the prediction of adverse arrhythmic cardiac events after a first noncomplicated st-segment-elevation myocardial infarction. *Circulation: Cardiovascular imaging*. 2013;6:755-761
 153. Miszalski-Jamka T, Klimeczek P, Tomala M, Krupiński M, Zawadowski G, Noelting J, Lada M, Sip K, Baniś R, Mazur W, Kereiakes DJ, Zmudka K, Pasowicz M. Extent of rv dysfunction and myocardial infarction assessed by cmr are independent outcome predictors early after stemi treated with primary angioplasty. *JACC: Cardiovasc Imaging*. 2010;3:1237-1246

154. Wu E, Ortiz JT, Tejedor P, Lee DC, Kansal P, Carr JC, Holly TA, Klocke FJ, Bonow RO. Infarct size by contrast enhanced cardiac magnetic resonance is a stronger predictor of outcomes than left ventricular ejection fraction or end-systolic volume index : Prospective cohort study infarct size by contrast enhanced cardiac magnetic resonance i. *Heart*. 2008;94:730-736
155. Reimer KA, Jennings RB. The "wavefront phenomenon" of myocardial ischemic cell death. li. Transmural progression of necrosis within the framework of ischemic bed size (myocardium at risk) and collateral flow. *Laboratory investigation; a journal of technical methods and pathology*. 1979;40:633-644
156. Kloner RA, Ganote CE, Jennings RB. The "no-reflow" phenomenon after temporary coronary occlusion in the dog. *J Clin Inv*. 1974;54:1496-1508
157. Rochitte CE, Lima JAC, Bluemke DA, Reeder SB, Elliot R, Furuta T, Becker LC, Melin JA. Magnitude and time course of microvascular obstruction and tissue injury after acute myocardial infarction. *Circulation*. 1998;98:1006-1014
158. Wong DTL, Leung MCH, Richardson JD, Puri R, Bertaso AG, Williams K, Meredith IT, Teo KSL, Worthley MI, Worthley SG. Cardiac magnetic resonance derived late microvascular obstruction assessment post st-segment elevation myocardial infarction is the best predictor of left ventricular function: A comparison of angiographic and cardiac magnetic resonance derived measurements. *Int J Cardiovasc Imaging*. 2012;28:1971-1981
159. Klug G, Mayr A, Schenk S, Esterhammer R, Schocke M, Jaschke W, Pachinger O, Metzler B. Prognostic value at 5 years of microvascular obstruction after acute myocardial infarction assessed by cardiovascular magnetic resonance. *JCMR*. 2012;14:46
160. Nijveldt R, Beek AM, Hirsch A, Stoel MG, Hofman MBM, Umans VaWM, Algra PR, Twisk JWR, van Rossum AC. Functional recovery after acute myocardial infarction: Comparison between angiography, electrocardiography, and cardiovascular magnetic resonance measures of microvascular injury. *JACC*. 2008;52:181-189
161. Bekkers SCaM, Backes WH, Kim RJ, Snoep G, Gorgels APM, Passos VL, Waltenberger J, Crijns HJGM, Schalla S. Detection and characteristics of microvascular obstruction in reperfused acute myocardial infarction using an optimized protocol for contrast-enhanced cardiovascular magnetic resonance imaging. *Eur Radiol*. 2009;19:2904-2912
162. Porto I, Burzotta F, Brancati M, Trani C, Lombardo A, Romagnoli E, Niccoli G, Natale L, Bonomo L, Crea F. Relation of myocardial blush grade to microvascular perfusion and myocardial infarct size after primary or rescue percutaneous coronary intervention. *Eur Heart J*. 2007;99:45-47
163. Appelbaum E, Abraham JM, Pride YB, Harrigan CJ, Peters DC, Biller LH, Manning WJ, Gibson CM. Imaging and diagnostic testing association of thrombolysis in myocardial infarction myocardial perfusion grade with cardiovascular magnetic resonance measures of infarct architecture after primary percutaneous coronary intervention for st-segment elevatio. *Am Heart J*. 2009;158:84-91
164. Bruder O, Barkhausen J, Naber CK, Jensen C, Erbel R, Sabin GV, Herzzinfarktverbund D. Prognostic impact of contrast- enhanced cmr early after acute st segment elevation myocardial infarction (stemi) in a regional stemi network results of the " herzzinfarktverbund essen ". *Herz*. 2008;33:136-142
165. Wu KC, Kim RJ, Bluemke DA, Rochitte CE, Zerhouni EA, Becker LC, Lima JA. Quantification and time course of microvascular obstruction by contrast-enhanced echocardiography and magnetic resonance imaging following acute myocardial infarction and reperfusion. *JACC*. 1998;32:1756-1764
166. Gerber BL, Rochitte CE, Melin JA, Mcveigh ER, Bluemke A, Wu KC, Becker LC, Lima JAC. Microvascular obstruction and left ventricular remodelling early after acute myocardial infarction. *Circulation*. 2000;101:2734-2741
167. Ørn S, Manhenke C, Greve OJ, Larsen AI, Bonarjee VVS, Edvardsen T, Dickstein K. Microvascular obstruction is a major determinant of infarct healing and subsequent left ventricular remodelling following primary percutaneous coronary intervention. *Eur Heart J*. 2009;30:1978-1985
168. Bogaert J, Kalantzi M, Rademakers FE, Dymarkowski S, Janssens S. Determinants and impact of microvascular obstruction in successfully reperfused st-segment elevation myocardial infarction. Assessment by magnetic resonance imaging. *Eur Radiol*. 2007;17:2572-2580

169. Khan JN, Razvi N, Nazir SA, Singh A, Masca NGD, Gershlick AH, Squire I, McCann GP. Prevalence and extent of infarct and microvascular obstruction following different reperfusion therapies in st-elevation myocardial infarction. *JCMR*. 2014;Accepted for publication (in print)
170. Weir RaP, Murphy CA, Petrie CJ, Martin TN, Balmain S, Clements S, Steedman T, Wagner GS, Dargie HJ, McMurray JJV. Microvascular obstruction remains a portent of adverse remodeling in optimally treated patients with left ventricular systolic dysfunction after acute myocardial infarction. *Circulation: Cardiovascular imaging*. 2010;3:360-367
171. Wong DT, Weightman MJ, Baumert M, Tayeb H, Richardson JD, Puri R, Bertaso AG, Roberts-Thomson KC, Sanders P, Worthley MI, Worthley SG. Electro-mechanical characteristics of myocardial infarction border zones and ventricular arrhythmic risk: Novel insights from grid-tagged cardiac magnetic resonance imaging. *Eur Radiol*. 2012;22:1651-1658
172. Ye YX, Basse-Lusebrink TC, Arias-Loza PA, Kocoski V, Kampf T, Gan Q, Bauer E, Sparka S, Helluy X, Hu K, Hiller KH, Boivin-Jahns V, Jakob PM, Jahns R, Bauer WR. Monitoring of monocyte recruitment in reperfused myocardial infarction with intramyocardial hemorrhage and microvascular obstruction by combined fluorine 19 and proton cardiac magnetic resonance imaging. *Circulation*. 2013;128:1878-1888
173. Kidambi A, Mather AN, Motwani M, Swoboda P, Uddin A, Greenwood JP, Plein S. The effect of microvascular obstruction and intramyocardial hemorrhage on contractile recovery in reperfused myocardial infarction: Insights from cardiovascular magnetic resonance. *JCMR*. 2013;15:58
174. Regenfus M, Schlundt C, Krahner R, Schonegger C, Adler W, Ludwig J, Daniel WG, Schmid M. Six-year prognostic value of microvascular obstruction after reperfused st-elevation myocardial infarction as assessed by contrast-enhanced cardiovascular magnetic resonance. *Am J Cardiol*. 2015;116:1022-1027
175. van Kranenburg M, Magro M, Thiele H, de Waha S, Eitel I, Cochet A, Cottin Y, Atar D, Buser P, Wu E, Lee D, Bodi V, Klug G, Metzler B, Delewi R, Bernhardt P, Rottbauer W, Boersma E, Zijlstra F, van Geuns RJ. Prognostic value of microvascular obstruction and infarct size, as measured by cmr in stemi patients. *JACC Cardiovasc Imaging*. 2014;7:930-939
176. Eitel I, de Waha S, Wohrle J, Fuernau G, Lurz P, Pauschinger M, Desch S, Schuler G, Thiele H. Comprehensive prognosis assessment by cmr imaging after st-segment elevation myocardial infarction. *J Am Coll Cardiol*. 2014;64:1217-1226
177. de Waha S, Desch S, Eitel I, Fuernau G, Lurz P, Leuschner A, Grothoff M, Gutberlet M, Schuler G, Thiele H. Relationship and prognostic value of microvascular obstruction and infarct size in st-elevation myocardial infarction as visualized by magnetic resonance imaging. *Clin Res Cardiol*. 2012
178. Bekkers SCaM, Smulders MW, Passos VL, Leiner T, Waltenberger J, Gorgels APM, Schalla S. Clinical implications of microvascular obstruction and intramyocardial haemorrhage in acute myocardial infarction using cardiovascular magnetic resonance imaging. *Eur Radiol*. 2010;20:2572-2578
179. Russo JJ, Wells GA, Chong AY, So DY, Glover CA, Froeschl MP, Hibbert B, Marquis JF, Dick A, Blondeau M, Bernick J, Labinaz M, Le May MR. Safety and efficacy of staged percutaneous coronary intervention during index admission for st-elevation myocardial infarction with multivessel coronary disease (insights from the university of ottawa heart institute stemi registry). *Am J Cardiol*. 2015;116:1157-1162
180. Lotan CS, Bouchard A, Cranney GB, Bishop SP, Pohost GM. Assessment of postreperfusion myocardial hemorrhage using proton nmr imaging at 1.5 t. *Circulation*. 1992;86:1018-1025
181. Basso C, Corbetti F, Silva C, Abudurehman A, Lacognata C, Cacciavillani L, Tarantini G, Marra MP, Ramondo A, Thiene G, Illiceto S. Morphologic validation of reperfused hemorrhagic myocardial infarction by cardiovascular magnetic resonance. *Am J Cardiol*. 2007;100:1322-1327
182. Eitel I, Kubusch K, Strohm O, Desch S, Mikami Y, de Waha S, Gutberlet M, Schuler G, Friedrich MG, Thiele H. Prognostic value and determinants of a hypointense infarct core in t2-weighted cardiac magnetic resonance in acute reperfused st-elevation-myocardial infarction. *Circulation: Cardiovascular imaging*. 2011;4:354-362

183. O'Regan DP, Ariff B, Neuwirth C, Tan Y, Durighel G, Cook Sa. Assessment of severe reperfusion injury with t2* cardiac mri in patients with acute myocardial infarction. *Heart*. 2010;96:1885-1891
184. Kali A, Tang RL, Kumar A, Min JK, Dharmakumar R. Detection of acute reperfusion myocardial hemorrhage with cardiac mr imaging: T2 versus t2. *Radiology*. 2013;269:387-395
185. Kali A, Kumar A, Cokic I, Tang RL, Tsiftaris SA, Friedrich MG, Dharmakumar R. Chronic manifestation of postreperfusion intramyocardial hemorrhage as regional iron deposition: A cardiovascular magnetic resonance study with ex vivo validation. *Circulation: Cardiovascular imaging*. 2013;6:218-228
186. Kali A, Kumar A, Cokic I, Tang R, Tsiftaris S, Friedrich M, Dharmakumar R. Chronic manifestation of post-reperfusion intramyocardial hemorrhage as regional iron deposition – a cardiovascular mr study with ex-vivo validation. *Circulation: Cardiovascular imaging*. 2012
187. Zia MI, Ghugre NR, Connelly KA, Strauss BH, Sparkes JD, Dick AJ, Wright GA. Characterizing myocardial edema and hemorrhage using quantitative t2 and t2* mapping at multiple time intervals post st elevation myocardial infarction. *Circulation: Cardiovascular imaging*. 2012
188. O'Regan DP, Ahmed R, Karunanithy N, Neuwirth C, Tan Y, Durighel G, Hajnal JV, Nadra I, Corbett SJ, Cook Sa. Reperfusion hemorrhage following acute myocardial infarction: Assessment with t2* mapping and effect on measuring the area at risk. *Radiology*. 2009;250:916-922
189. Mather AN, Fairbairn Ta, Ball SG, Greenwood JP, Plein S. Reperfusion haemorrhage as determined by cardiovascular mri is a predictor of adverse left ventricular remodelling and markers of late arrhythmic risk. *Heart*. 2011;97:453-459
190. Pedersen SF, Thrysoe S, Robich MP, Paaske WP, Ringgaard S, Botker HE, Hansen ES, Kim WY. Assessment of intramyocardial hemorrhage by t1-weighted cardiovascular magnetic resonance in reperfused acute myocardial infarction. *JCMR*. 2012;14:59
191. Amabile N, Jacquier A, Shuhab A, Gaudart J, Bartoli JM, Paganelli F, Moulin G. Incidence, predictors, and prognostic value of intramyocardial hemorrhage lesions in st elevation myocardial infarction. *Catheter Cardiovasc Interv*. 2012;79:1101-1108
192. Abdel-Aty H, Simonetti O, Friedrich MG. T2-weighted cardiovascular magnetic resonance imaging. *JMRI*. 2007;26:452-459
193. Higgins CB, Herfkens R, Lipton MJ, Sievers R, Sheldon P, Kaufman L, Crooks LE. Nuclear magnetic resonance imaging of acute myocardial infarction in dogs: Alterations in magnetic relaxation times. *Am J Cardiol*. 1983;52:184-188
194. Arai AE. Magnetic resonance imaging for area at risk, myocardial infarction, and myocardial salvage. *J Cardiov Pharm Ther*. 2012;16:313-320
195. Garcia-Dorado D, Oliveras J, Gili J, Sanz E, Perez-Villa F, Barrabes J, Carreras MJ, Solares J, Soler-Soler J. Analysis of myocardial oedema by magnetic resonance imaging early after coronary artery occlusion with or without reperfusion. *Cardiovascular research*. 1993;27:1462-1469
196. Tilak GS, Hsu LY, Hoyt RF, Jr., Arai AE, Aletras AH. In vivo t2-weighted magnetic resonance imaging can accurately determine the ischemic area at risk for 2-day-old nonreperfused myocardial infarction. *Invest Radiol*. 2008;43:7-15
197. Carlsson M, Ubachs JFa, Hedström E, Heiberg E, Jovinge S, Arheden H. Myocardium at risk after acute infarction in humans on cardiac magnetic resonance: Quantitative assessment during follow-up and validation with single-photon emission computed tomography. *JACC: Cardiovasc imaging*. 2009;2:569-576
198. Hedström E, Engblom H, Frogner F, Åström-olsson K, Öhlin H, Jovinge S, Arheden H. Infarct evolution in man studied in patients with first-time coronary occlusion in comparison to different species - implications for assessment of myocardial salvage. *JCMR*. 2009;10:1-10
199. Hadamitzky M, Langhans B, Hausleiter J, Sonne C, Kastrati A, Martinoff S, Schomig A, Ibrahim T. The assessment of area at risk and myocardial salvage after coronary revascularization in acute myocardial infarction: Comparison between cmr and spect. *JACC: Cardiovasc Imaging*. 2013;6:358-369
200. Viallon M, Mewton N, Thuny F, Guehring J, O'Donnell T, Stemmer A, Bi X, Rapacchi S, Zuehlsdorff S, Revel D, Croisille P. T2-weighted cardiac mr assessment of the myocardial area-at-risk and salvage area in acute reperfused myocardial infarction: Comparison of state-of-the-art dark blood and bright blood t2-weighted sequences. *JMRI*. 2012;35:328-339

201. Berry C, Kellman P, Mancini C, Chen MY, Bandettini WP, Lowrey T, Hsu L-Y, Aletras AH, Arai AE. Magnetic resonance imaging delineates the ischemic area at risk and myocardial salvage in patients with acute myocardial infarction. *Circulation: Cardiovascular imaging*. 2010;3:527-535
202. Versteysen MO, Bekkers SCaM, Smulders MW, Winkens B, Muhl C, Winkens MHM, Leiner T, Waltenberger JL, Kim RJ, Gorgels APM. Performance of angiographic, electrocardiographic and mri methods to assess the area at risk in acute myocardial infarction. *Heart*. 2012;98:109-115
203. Srichai MB, Lim RP, Lath N, Babb J, Axel L, Kim D. Diagnostic performance of dark-blood t2-weighted cmr for evaluation of acute myocardial injury. *Invest Radiol*. 2013;48:24-31
204. Kellman P, Aletras AH, Mancini C, McVeigh ER, Arai AE. T2-prepared ssfp improves diagnostic confidence in edema imaging in acute myocardial infarction compared to turbo spin echo. *Magn Reson Med*. 2007;57:891-897
205. Payne AR, Casey M, McClure J, McGeoch R, Murphy A, Woodward R, Saul A, Bi X, Zuehlisdruff S, Oldroyd KG, Tzemos N, Berry C. Bright-blood t2-weighted mri has higher diagnostic accuracy than dark-blood short tau inversion recovery mri for detection of acute myocardial infarction and for assessment of the ischemic area at risk and myocardial salvage. *Circulation: Cardiovascular imaging*. 2011;4:210-219
206. Goldfarb JW, Arnold S. Recent myocardial infarction : Assessment with unenhanced t1-weighted mr imaging. *Radiology*. 2007;245:245-250
207. Croisille P, Kim HW, Kim RJ. Controversies in cardiovascular mr imaging: T2-weighted imaging should not be used to delineate the area at risk in ischemic myocardial injury. *Radiology*. 2012;265:12-22
208. Simonetti OP, Kim RJ, Fieno DS, Hillenbrand HB, Wu E, Bundy JM, Finn JP, Judd RM. An improved mr imaging technique for the visualization of myocardial infarction. *Radiology*. 2001;218:215-223
209. Sörensson P, Heiberg E, Saleh N, Bouvier F, Caidahl K, Tornvall P, Rydén L, Pernow J, Arheden H. Assessment of myocardium at risk with contrast enhanced steady-state free precession cine cardiovascular magnetic resonance compared to single-photon emission computed tomography. *JCMR*. 2010;12:25
210. Ubachs JFa, Sörensson P, Engblom H, Carlsson M, Jovinge S, Pernow J, Arheden H. Myocardium at risk by magnetic resonance imaging: Head-to-head comparison of t2-weighted imaging and contrast-enhanced steady-state free precession. *Eur Heart J: Cardiovascular Imaging*. 2012
211. Verhaert D, Thavendiranathan P, Giri S, Mihai G, Rajagopalan S, Simonetti OP, Raman SV. Direct t2 quantification of myocardial edema in acute ischemic injury. *JACC: Cardiovasc Imaging*. 2011;4:269-278
212. Nassenstein K, Nensa F, Schlosser T, Bruder O, Umutlu L, Lauenstein T, Maderwald S, Ladd ME. Cardiac mri: T2-mapping versus t2-weighted dark-blood tse imaging for myocardial edema visualization in acute myocardial infarction. *RoFo : Fortschritte auf dem Gebiete der Röntgenstrahlen und der Nuklearmedizin*. 2014;186:166-172
213. Lønborg J, Engstrøm T, Mathiasen AB, Vejlstup N. Myocardial area at risk after st-elevation myocardial infarction measured with the late gadolinium enhancement after scar remodeling and t2-weighted cardiac magnetic resonance imaging. *Int J Cardiovasc Imaging*. 2011:2011
214. Ubachs JFa, Engblom H, Erlinge D, Jovinge S, Hedström E, Carlsson M, Arheden H. Cardiovascular magnetic resonance of the myocardium at risk in acute reperfused myocardial infarction: Comparison of t2-weighted imaging versus the circumferential endocardial extent of late gadolinium enhancement with transmural projection. *JCMR*. 2010;12:18
215. Kociemba A, Pyda M, Katulska K, Lanocha M, Siniawski A, Janus M, Grajek S. Comparison of diffusion-weighted with t2-weighted imaging for detection of edema in acute myocardial infarction. *JCMR*. 2013;15:90
216. Vemulapalli S, Zhou Y, Gutberlet M, Kumar AS, Mills JS, Blaxill J, Smalling R, Ohman EM, Patel MR. Importance of total ischemic time and preprocedural infarct-related artery blood flow in predicting infarct size in patients with anterior wall myocardial infarction (from the crisp-ami trial). *Am J Cardiol*. 2013;112:911-917
217. Lønborg J, Vejlstup N, Kelbaek H, Holmvang L, Jorgensen E, Helqvist S, Saunamaki K, Ahtarovski KA, Botker HE, Kim WY, Clemmensen P, Engstrom T. Final infarct size measured by

- cardiovascular magnetic resonance in patients with st elevation myocardial infarction predicts long-term clinical outcome: An observational study. *Eur Heart J: Cardiovascular Imaging*. 2013;14:387-395
218. O'Regan DP, Ahmed R, Neuwirth C, Tan Y, Durighel G, Hajnal JV, Nadra I, Corbett SJ, Cook SA. Cardiac mri of myocardial salvage at the peri-infarct border zones after primary coronary intervention. *American journal of physiology. Heart and circulatory physiology*. 2009;297:H340-346
 219. Masci PG, Andreini D, Francone M, Bertella E, De Luca L, Coceani M, Mushtaq S, Mariani M, Carbone I, Pontone G, Agati L, Bogaert J, Lombardi M. Prodromal angina is associated with myocardial salvage in acute st-segment elevation myocardial infarction. *Eur Heart J: Cardiovascular Imaging*. 2013;14:1041-1048
 220. Desch S, Engelhardt H, Meissner J, Eitel I, Sareban M, Fuernau G, S DW, Grothoff M. Reliability of myocardial salvage assessment by cardiac magnetic resonance imaging in acute reperfused myocardial infarction . 2012;28:2012
 221. Milavetz JJ, Giebel DW, Christian TF, Schwartz RS, Holmes DR, Jr., Gibbons RJ. Time to therapy and salvage in myocardial infarction. *JACC*. 1998;31:1246-1251
 222. Newby LK, Rutsch WR, Califf RM, Simoons ML, Aylward PE, Armstrong PW, Woodlief LH, Lee KL, Topol EJ, Van de Werf F. Time from symptom onset to treatment and outcomes after thrombolytic therapy. Gusto-1 investigators. *JACC*. 1996;27:1646-1655
 223. Eitel I, Desch S, Fuernau G, Hildebrand L, Bs C, Gutberlet M, Schuler G, Thiele H. Prognostic significance and determinants of myocardial salvage assessed by cardiovascular magnetic resonance in acute reperfused myocardial infarction. *JACC* 2010;55:2470-2479
 224. Friedrich MG, Abdel-Aty H, Taylor A, Schulz-Menger J, Messroghli D, Dietz R. The salvaged area at risk in reperfused acute myocardial infarction as visualized by cardiovascular magnetic resonance. *JACC*. 2008;51:1581-1587
 225. Desch S, Eitel I, Schmitt J, Sareban M, Fuernau G, Schuler G, Thiele H. Effect of coronary collaterals on microvascular obstruction as assessed by magnetic resonance imaging in patients with acute st-elevation myocardial infarction treated by primary coronary intervention. *Am J Cardiol*. 2009;104:1204-1209
 226. Phrommintikul A, Abdel-Aty H, Schulz-Menger J, Friedrich MG, Taylor AJ. Acute oedema in the evaluation of microvascular reperfusion and myocardial salvage in reperfused myocardial infarction with cardiac magnetic resonance imaging. *European journal of radiology*. 2010;74:e12-17
 227. Abdel-Aty H, Cocker M, Meek C, Tyberg JV, Friedrich MG. Edema as a very early marker for acute myocardial ischemia: A cardiovascular magnetic resonance study. *JACC*. 2009;53:1194-1201
 228. Fernandez-Jimenez R, Sanchez-Gonzalez J, Aguero J, Garcia-Prieto J, Lopez-Martin GJ, Garcia-Ruiz JM, Molina-Iracheta A, Rossello X, Fernandez-Friera L, Pizarro G, Garcia-Alvarez A, Dall'Armellina E, Macaya C, Choudhury RP, Fuster V, Ibanez B. Myocardial edema after ischemia/reperfusion is not stable and follows a bimodal pattern: Imaging and histological tissue characterization. *J Am Coll Cardiol*. 2015;65:315-323
 229. Abdel-Aty H, Zagrosek A, Schulz-Menger J, Taylor AJ, Messroghli D, Kumar A, Gross M, Dietz R, Friedrich MG. Delayed enhancement and t2-weighted cardiovascular magnetic resonance imaging differentiate acute from chronic myocardial infarction. *Circulation*. 2004;109:2411-2416
 230. Larose E, Tizon-Marcos H, Rodés-Cabau J, Rinfret S, Déry J-P, Nguyen CM, Gleeton O, Boudreault J-R, Roy L, Noël B, Proulx G, Rouleau J, Barbeau G, De Larochelière R, Bertrand OF. Improving myocardial salvage in late presentation acute st-elevation myocardial infarction with proximal embolic protection. *Catheter Cardiovasc Interv*. 2010;76:461-470
 231. Ndrepepa G, Mehilli J, Schwaiger M, Schuhlen H, Nekolla S, Martinoff S, Schmitt C, Dirschinger J, Schomig A, Kastrati A. Prognostic value of myocardial salvage achieved by reperfusion therapy in patients with acute myocardial infarction. *Journal of nuclear medicine : official publication, Society of Nuclear Medicine*. 2004;45:725-729
 232. Mewton N, Liu CY, Croisille P, Bluemke D, Lima JA. Assessment of myocardial fibrosis with cardiovascular magnetic resonance. *JACC*. 2011;57:891-903
 233. Salerno M, Kramer CM. Advances in parametric mapping with cmr imaging. *JACC: Cardiovasc Imaging*. 2013;6:806-822

234. Messroghli DR, Niendorf T, Schulz-Menger J, Dietz R, Friedrich MG. T1 mapping in patients with acute myocardial infarction. *JCMR*. 2003;5:353-359
235. Messroghli DR, Radjenovic A, Kozerke S, Higgins DM, Sivananthan MU, Ridgway JP. Modified look-locker inversion recovery (molli) for high-resolution t1 mapping of the heart. *Magn Reson Med*. 2004;52:141-146
236. O H-Ici D, Jeuthe S, Al-Wakeel N, Berger F, Kuehne T, Kozerke S, Messroghli DR. T1 mapping in ischaemic heart disease. *Eur Heart J: Cardiovascular Imaging*. 2014
237. Messroghli DR, Plein S, Higgins DM, Walters K, Jones TR, Ridgway JP, Sivananthan MU. Human myocardium: Single-breath-hold mr t1 mapping with high spatial resolution--reproducibility study. *Radiology*. 2006;238:1004-1012
238. Messroghli DR, Walters K, Plein S, Sparrow P, Friedrich MG, Ridgway JP, Sivananthan MU. Myocardial t1 mapping: Application to patients with acute and chronic myocardial infarction. *Magn Reson Med*. 2007;58:34-40
239. Giri S, Chung Y-C, Merchant A, Mihai G, Rajagopalan S, Raman SV, Simonetti OP. T2 quantification for improved detection of myocardial edema. *JCMR*. 2009;11:56
240. Ugander M, Bagi PS, Oki AJ, Chen B, Hsu LY, Aletras AH, Shah S, Greiser A, Kellman P, Arai AE. Myocardial edema as detected by pre-contrast t1 and t2 cmr delineates area at risk associated with acute myocardial infarction. *JACC: Cardiovasc Imaging*. 2012;5:596-603
241. Anderson LJ, Holden S, Davis B, Prescott E, Charrier CC, Bunce NH, Firmin DN, Wonke B, Porter J, Walker JM, Pennell DJ. Cardiovascular t2-star (t2*) magnetic resonance for the early diagnosis of myocardial iron overload. *Eur Heart J*. 2001;22:2171-2179
242. Masci PG, Francone M, Desmet W, Ganame J, Todiere G, Donato R, Siciliano V, Carbone I, Mangia M, Strata E, Catalano C, Lombardi M, Agati L, Janssens S, Bogaert J. Right ventricular ischemic injury in patients with acute st-segment elevation myocardial infarction: Characterization with cardiovascular magnetic resonance. *Circulation*. 2010;122:1405-1412
243. Puchalski MD, Williams RV, Askovich B, Minich LL, Mart C, Tani LY. Assessment of right ventricular size and function: Echo versus magnetic resonance imaging. *Congenital heart disease*. 2007;2:27-31
244. Galea N, Francone M, Carbone I, Cannata D, Vullo F, Galea R, Agati L, Fedele F, Catalano C. Utility of cardiac magnetic resonance (cmr) in the evaluation of right ventricular (rv) involvement in patients with myocardial infarction (mi). *La Radiologia medica*. 2013
245. Jensen CJ, Jochims M, Hunold P, Sabin GV, Schlosser T, Bruder O. Right ventricular involvement in acute left ventricular myocardial infarction: Prognostic implications of mri findings. *AJR*. 2010;194:592-598
246. Bonanad C, Ruiz-Sauri A, Forteza MJ, Chaustre F, Minana G, Gomez C, Diaz A, Noguera I, de Dios E, Nunez J, Mainar L, Sanchis J, Morales JM, Monleon D, Chorro FJ, Bodi V. Microvascular obstruction in the right ventricle in reperfused anterior myocardial infarction. Macroscopic and pathologic evidence in a swine model. *Thrombosis research*. 2013;132:592-598
247. Andreini D, Pontone G, Mushtaq S, Pepi M, Bogaert J, Masci PG. Microvascular obstruction complicating acute right ventricular myocardial infarction. *J Cardiovasc Med*. 2013
248. Grothoff M, Elpert C, Hoffmann J, Zachrau J, Lehmkuhl L, de Waha S, Desch S, Eitel I, Mende M, Thiele H, Gutberlet M. Right ventricular injury in st-elevation myocardial infarction: Risk stratification by visualization of wall motion, edema, and delayed-enhancement cardiac magnetic resonance. *Circulation: Cardiovascular imaging*. 2012;5:60-68
249. Bodi V, Sanchis J, Mainar L, Chorro FJ, Nunez J, Monmeneu JV, Chaustre F, Forteza MJ, Ruiz-Sauri A, Lopez-Lereu MP, Gomez C, Noguera I, Diaz A, Giner F, Llacer A. Right ventricular involvement in anterior myocardial infarction: A translational approach. *Cardiovascular research*. 2010;87:601-608
250. Larose E, Ganz P, Reynolds HG, Dorbala S, Di Carli MF, Brown Ka, Kwong RY. Right ventricular dysfunction assessed by cardiovascular magnetic resonance imaging predicts poor prognosis late after myocardial infarction. *JACC*. 2007;49:855-862
251. Kumar A, Abdel-Aty H, Kriedemann I, Schulz-Menger J, Gross CM, Dietz R, Friedrich MG. Contrast-enhanced cardiovascular magnetic resonance imaging of right ventricular infarction. *JACC*. 2006;48:1969-1976
252. Hamon M, Agostini D, Le Page O, Riddell JW, Hamon M. Prognostic impact of right ventricular involvement in patients with acute myocardial infarction: Meta-analysis. *Critical care medicine*. 2008;36:2023-2033

253. Shah PK, Maddahi J, Staniloff HM, Ellrodt AG, Pichler M, Swan HJ, Berman DS. Variable spectrum and prognostic implications of left and right ventricular ejection fractions in patients with and without clinical heart failure after acute myocardial infarction. *Am J Cardiol.* 1986;58:387-393
254. Kelly DJ, McCann GP, Blackman D, Curzen NP, Dalby M, Greenwood JP, Fairbrother K, Shipley L, Kelion A, Heatherington S, Khan JN, Nazir S, Alahmar A, Flather M, Swanton H, Schofield P, Gunning M, Hall R, Gershlick AH. Complete versus culprit-lesion only primary pci trial (cvlprit): A multicentre trial testing management strategies when multivessel disease is detected at the time of primary pci: Rationale and design. *EuroIntervention : journal of EuroPCR in collaboration with the Working Group on Interventional Cardiology of the European Society of Cardiology.* 2013;8:1190-1198
255. Gershlick AH, Khan JN, Kelly DJ, Greenwood JP, Sasikaran T, Curzen N, Blackman DJ, Dalby M, Fairbrother KL, Banya W, Wang D, Flather M, Hetherington SL, Kelion AD, Talwar S, Gunning M, Hall R, Swanton H, McCann GP. Randomized trial of complete versus lesion-only revascularization in patients undergoing primary percutaneous coronary intervention for stemi and multivessel disease: The cvlprit trial. *JACC.* 2015;65:963-972
256. Hansson L, Hedner T, Dahlof B. Prospective randomized open blinded end-point (probe) study. A novel design for intervention trials. Prospective randomized open blinded end-point. *Blood pressure.* 1992;1:113-119
257. Steg PG, James SK, Atar D, Badano LP, Lundqvist CB, Borger MA, Di Mario C, Dickstein K, Ducrocq G, Fernandez-Aviles F, Gershlick AH, Giannuzzi P, Halvorsen S, Huber K, Juni P, Kastrati A, Knuuti J, Lenzen MJ, Mahaffey KW, Valgimigli M, Van't Hof A, Widimsky P, Zahger D, Bax JJ, Baumgartner H, Ceconi C, Dean V, Deaton C, Fagard R, Funck-Brentano C, Hasdai D, Hoes A, Kirchhof P, Knuuti J, Kolh P, McDonagh T, Moulin C, Popescu BA, Reiner Z, Sechtem U, Sirnes PA, Tendera M, Torbicki A, Vahanian A, Windecker S, Hasdai D, Astin F, Astrom-Olsson K, Budaj A, Clemmensen P, Collet JP, Fox KA, Fuat A, Gustiene O, Hamm CW, Kala P, Lancellotti P, Maggioni AP, Merkely B, Neumann FJ, Piepoli MF, Van de Werf F, Verheugt F, Wallentin L. Esc guidelines for the management of acute myocardial infarction in patients presenting with st-segment elevation: The task force on the management of st-segment elevation acute myocardial infarction of the european society of cardiology (esc). *European heart journal.* 2012
258. RITA2-Investigators. Coronary angioplasty versus medical therapy for angina: The second randomised intervention treatment of angina (rita-2) trial. Rita-2 trial participants. *Lancet.* 1997;350:461-468
259. Agard A, Hermeren G, Herlitz J. Patients' experiences of intervention trials on the treatment of myocardial infarction: Is it time to adjust the informed consent procedure to the patient's capacity? *Heart.* 2001;86:632-637
260. Yuval R, Halon DA, Merdler A, Khader N, Karkabi B, Uziel K, Lewis BS. Patient comprehension and reaction to participating in a double-blind randomized clinical trial (isis-4) in acute myocardial infarction. *Archives of internal medicine.* 2000;160:1142-1146
261. Gammelgaard A. Informed consent in acute myocardial infarction research. *The Journal of medicine and philosophy.* 2004;29:417-434
262. Armstrong PW, Gershlick AH, Goldstein P, Wilcox R, Danays T, Lambert Y, Sulimov V, Ortiz FR, Ostojic M, Welsh RC, Carvalho AC, Nanas J, Arntz HR, Halvorsen S, Huber K, Grajek S, Fresco C, Bluhmki E, Regelin A, Vandenberghe K, Bogaerts K, Van de Werf F. Fibrinolysis or primary pci in st-segment elevation myocardial infarction. *NEJM.* 2013
263. Nazir S, Khan JN, Mahmoud IZ, Greenwood JP, Blackman D, Kunadian V, Been M, Abrams KR, Wilcox R, Adgey AA, McCann GP, Gershlick A. The reflo-stemi trial comparing intracoronary adenosine, sodium nitroprusside and standard therapy for the attenuation of infarct size and microvascular obstruction during primary percutaneous coronary intervention: Study protocol for a randomised controlled trial. *Trials.* 2014;15:371
264. Keeley EC, Boura JA, Grines CL. Primary angioplasty versus intravenous thrombolytic therapy for acute myocardial infarction: A quantitative review of 23 randomised trials. *Lancet.* 2003;361:13-20
265. World, Medical, Association. World medical association declaration of helsinki ethical principles for medical research involving human subjects (revision 48). *Website* (<http://www.wma.net/en/30publications/10policies/b3/17c.pdf>). 1996;Accessed June 2013

266. TIMI.Collaborators. The thrombolysis in myocardial infarction (timi) trial. Phase i findings. Timi study group. *NEJM*. 1985;312:932-936
267. Rentrop KP, Cohen M, Blanke H, Phillips RA. Changes in collateral channel filling immediately after controlled coronary artery occlusion by an angioplasty balloon in human subjects. *JACC*. 1985;5:587-592
268. Sianos G, Morel MA, Kappetein AP, Morice MC, Colombo A, Dawkins K, van den Brand M, Van Dyck N, Russell ME, Mohr FW, Serruys PW. The syntax score: An angiographic tool grading the complexity of coronary artery disease. *EuroIntervention : journal of EuroPCR in collaboration with the Working Group on Interventional Cardiology of the European Society of Cardiology*. 2005;1:219-227
269. SYNTAX-Working-Group. Syntax score calculator (version 2.11). <http://www.syntaxscore.com/> (Website). 2013;(Accessed June 2014).
270. Serruys PW, Onuma Y, Garg S, Sarno G, van den Brand M, Kappetein AP, Van Dyck N, Mack M, Holmes D, Feldman T, Morice MC, Colombo A, Bass E, Leadley K, Dawkins KD, van Es GA, Morel MA, Mohr FW. Assessment of the syntax score in the syntax study. *EuroIntervention : journal of EuroPCR in collaboration with the Working Group on Interventional Cardiology of the European Society of Cardiology*. 2009;5:50-56
271. Dizon JM, Brener SJ, Maehara A, Witzenbichler B, Biviano A, Godlewski J, Parise H, Dambrink JH, Mehran R, Gibson CM, Stone GW. Relationship between st-segment resolution and anterior infarct size after primary percutaneous coronary intervention: Analysis from the infuse-ami trial. *Eur Heart J: Acute Cardiovasc Care*. 2014;3:78-83
272. Papavassiliu T, Kuhl HP, Schroder M, Suselbeck T, Bondarenko O, Bohm CK, Beek A, Hofman MM, van Rossum AC. Effect of endocardial trabeculae on left ventricular measurements and measurement reproducibility at cardiovascular mr imaging. *Radiology*. 2005;236:57-64
273. Lang RM, Bierig M, Devereux RB, Flachskampf FA, Foster E, Pellikka PA, Picard MH, Roman MJ, Seward J, Shanewise JS, Solomon SD, Spencer KT, Sutton MS, Stewart WJ. Recommendations for chamber quantification: A report from the american society of echocardiography's guidelines and standards committee and the chamber quantification writing group, developed in conjunction with the european association of echocardiography, a branch of the european society of cardiology. *Journal of the American Society of Echocardiography : official publication of the American Society of Echocardiography*. 2005;18:1440-1463
274. Otsu N. A threshold selection method from gray-level histograms. *IEEE Trans on System, Man, and Cybernetics*. 1979;5MC-9:62-66
275. Miller CA, Borg A, Clark D, Steadman CD, McCann GP, Clarysse P, Croisille P, Schmitt M. Comparison of local sine wave modeling with harmonic phase analysis for the assessment of myocardial strain. *JMRI*. 2013;38:320-328
276. Rider OJ, Tayal U, Francis JM, Ali MK, Robinson MR, Byrne JP, Clarke K, Neubauer S. The effect of obesity and weight loss on aortic pulse wave velocity as assessed by magnetic resonance imaging. *Obesity* 2010;18:2311-2316
277. Hachamovitch R, Hayes SW, Friedman JD, Cohen I, Berman DS. Stress myocardial perfusion single-photon emission computed tomography is clinically effective and cost effective in risk stratification of patients with a high likelihood of coronary artery disease (cad) but no known cad. *JACC*. 2004;43:200-208
278. Harris PA, Taylor R, Thielke R, Payne J, Gonzalez N, Conde JG. Research electronic data capture (redcap)--a metadata-driven methodology and workflow process for providing translational research informatics support. *Journal of biomedical informatics*. 2009;42:377-381
279. Klem I, Shah DJ, White RD, Pennell DJ, van Rossum AC, Regenfus M, Sechtem U, Schwartzman PR, Hunold P, Croisille P, Parker M, Judd RM, Kim RJ. Prognostic value of routine cardiac magnetic resonance assessment of left ventricular ejection fraction and myocardial damage: An international, multicenter study. *Circulation: Cardiovascular imaging*. 2011;4:610-619
280. Pennell D. Myocardial salvage: Retrospection, resolution, and radio waves. *Circulation*. 2006;113:1821-1823
281. Hsu LY, Natanzon A, Kellman P, Hirsch GA, Aletras AH, Arai AE. Quantitative myocardial infarction on delayed enhancement mri. Part i: Animal validation of an automated feature analysis and combined thresholding infarct sizing algorithm. *JMRI*. 2006;23:298-308

282. Johnstone RI, Greenwood JP, Biglands JD, Plein S, Ridgway JP, Radjenovic A. Assessment of tissue edema in patients with acute myocardial infarction by computer-assisted quantification of triple inversion recovery prepared mri of the myocardium. *Magn Reson Med*. 2011;66:564-573
283. Vermes E, Childs H, Carbone I, Barckow P, Friedrich M. Auto-threshold quantification of late gadolinium enhancement in patients with acute heart disease. *JMRI*. 2013;37:382-390
284. Sjogren J, Ubachs JF, Engblom H, Carlsson M, Arheden H, Heiberg E. Semi-automatic segmentation of myocardium at risk in t2-weighted cardiovascular magnetic resonance. *JCMR*. 2012;14:10
285. McAlindon E, Lawton C, Flett AS, Manghat N, Hamilton MC, Bucciarelli Ducci C. Evaluation of 7 techniques for the quantification of myocardial oedema in stemi. *JCMR*. 2013;15:P188
286. Haahr M. Random.Org (true random number generator). <http://www.random.org>. 1998; Website (Accessed September 2013)
287. Heiberg E, Engblom H, Engvall J, Hedstrom E, Ugander M, Arheden H. Semi-automatic quantification of myocardial infarction from delayed contrast enhanced magnetic resonance imaging. *Scandinavian cardiovascular journal : SCJ*. 2005;39:267-275
288. Hsu LY, Ingkanisorn WP, Kellman P, Aletras AH, Arai AE. Quantitative myocardial infarction on delayed enhancement mri. Part ii: Clinical application of an automated feature analysis and combined thresholding infarct sizing algorithm. *JMRI*. 2006;23:309-314
289. Gao H, Kadir K, Payne AR, Soraghan J, Berry C. Highly automatic quantification of myocardial oedema in patients with acute myocardial infarction using bright blood t2-weighted cmr. *JCMR*. 2013;15:28
290. Kadir K, Gao H, Payne A, Soraghan J, Berry C. Automatic quantification and 3d visualisation of edema in cardiac mri. *Conference proceedings : ... Annual International Conference of the IEEE Engineering in Medicine and Biology Society. IEEE Engineering in Medicine and Biology Society. Conference*. 2011;2011:8021-8024
291. McGraw KO, Wong SP. Forming inferences about some intraclass correlation coefficients. *Psychological Methods*. 1996;1:30-46
292. Bland JM, Altman DG. Statistical methods for assessing agreement between two methods of clinical measurement. *Lancet*. 1986;1:307-310
293. Castillo E, Osman NF, Rosen BD, El-Shehaby I, Pan L, Jerosch-Herold M, Lai S, Bluemke DA, Lima JA. Quantitative assessment of regional myocardial function with mr-tagging in a multi-center study: Interobserver and intraobserver agreement of fast strain analysis with harmonic phase (harp) mri. *JCMR*. 2005;7:783-791
294. Bondarenko O, Beek AM, Hofman MB, Kuhl HP, Twisk JW, van Dockum WG, Visser CA, van Rossum AC. Standardizing the definition of hyperenhancement in the quantitative assessment of infarct size and myocardial viability using delayed contrast-enhanced cmr. *JCMR*. 2005;7:481-485
295. O H-Ici D, Ridgway JP, Kuehne T, Berger F, Plein S, Sivananthan M, Messroghli DR. Cardiovascular magnetic resonance of myocardial edema using a short inversion time inversion recovery (stir) black-blood technique: Diagnostic accuracy of visual and semi-quantitative assessment. *JCMR*. 2012;14:22
296. Arts T, Prinzen FW, Delhaas T, Milles JR, Rossi AC, Clarysse P. Mapping displacement and deformation of the heart with local sine-wave modeling. *IEEE transactions on medical imaging*. 2010;29:1114-1123
297. Maret E, Todt T, Brudin L, Nylander E, Swahn E, Ohlsson JL, Engvall JE. Functional measurements based on feature tracking of cine magnetic resonance images identify left ventricular segments with myocardial scar. *Cardiovasc Ultrasound*. 2009;7:53
298. Singh A, Steadman CD, Khan JN, Horsfield MA, Bekele S, Nazir SA, Kanagala P, Masca NGD, Clarysse P, McCann GP. Intertechnique agreement and interstudy reproducibility of strain and diastolic strain rate at 1.5t and 3t: A comparison of feature-tracking and tagging in patients with aortic stenosis. *JMRI*. 2014;doi: 10.1002/jmri.24625
299. Nijveldt R, Beek AM, Hirsch A, Stoel MG, Hofman MB, Umans VA, Algra PR, Twisk JW, van Rossum AC. Functional recovery after acute myocardial infarction: Comparison between angiography, electrocardiography, and cardiovascular magnetic resonance measures of microvascular injury. *J Am Coll Cardiol*. 2008;52:181-189

300. Ramsey PH. Critical values for spearman's rank order correlation. *J Educ and Behav Statistics*. 1989;14:245-253
301. Hopp E, Lunde K, Solheim S, Aakhus S, Arnesen H, Forfang K, Edvardsen T, Smith H-J. Regional myocardial function after intracoronary bone marrow cell injection in reperfused anterior wall infarction - a cardiovascular magnetic resonance tagging study. *JCMR*. 2011;13:22
302. Schuster A, Kutty S, Padiyath A, Parish V, Gribben P, Danford DA, Makowski MR, Bigalke B, Beerbaum P, Nagel E. Cardiovascular magnetic resonance myocardial feature tracking detects quantitative wall motion during dobutamine stress. *JCMR*. 2011;13:58
303. Schuster A, Morton G, Hussain ST, Jogiya R, Kutty S, Asrress KN, Makowski MR, Bigalke B, Perera D, Beerbaum P, Nagel E. The intra-observer reproducibility of cardiovascular magnetic resonance myocardial feature tracking strain assessment is independent of field strength. *European journal of radiology*. 2013;82:296-301
304. Harrild DM, Han Y, Geva T, Zhou J, Marcus E, Powell AJ. Comparison of cardiac mri tissue tracking and myocardial tagging for assessment of regional ventricular strain. *Int J Cardiovasc Imaging*. 2012;28:2009-2018
305. Schuster A, Paul M, Bettencourt N, Morton G, Chiribiri A, Ishida M, Hussain S, Jogiya R, Kutty S, Bigalke B, Perera D, Nagel E. Cardiovascular magnetic resonance myocardial feature tracking for quantitative viability assessment in ischemic cardiomyopathy. *Int J Cardiol*. 2013;166:413-420
306. Neizel M, Lossnitzer D, Korosoglou G, Schaufele T, Peykarjou H, Steen H, Ocklenburg C, Giannitsis E, Katus HA, Osman NF. Strain-encoded mri for evaluation of left ventricular function and transmuralty in acute myocardial infarction. *Circulation: Cardiovascular imaging*. 2009;2:116-122
307. Ruzsics B, Suranyi P, Kiss P, Brott BC, Litovsky S, Denney TS, Jr., Aban I, Lloyd SG, Simor T, Elgavish GA, Gupta H. Myocardial strain in sub-acute peri-infarct myocardium. *Int J Cardiovasc Imaging*. 2009;25:151-159
308. Kempny A, Fernandez-Jimenez R, Orwat S, Schuler P, Bunck AC, Maintz D, Baumgartner H, Diller GP. Quantification of biventricular myocardial function using cardiac magnetic resonance feature tracking, endocardial border delineation and echocardiographic speckle tracking in patients with repaired tetralogy of fallot and healthy controls. *JCMR*. 2012;14:32
309. Larose E, Rodes-Cabau J, Pibarot P, Rinfret S, Proulx G, Nguyen CM, Dery JP, Gleeton O, Roy L, Noel B, Barbeau G, Rouleau J, Boudreault JR, Amyot M, De Larochelliere R, Bertrand OF. Predicting late myocardial recovery and outcomes in the early hours of st-segment elevation myocardial infarction traditional measures compared with microvascular obstruction, salvaged myocardium, and necrosis characteristics by cardiovascular magnetic resonance. *J Am Coll Cardiol*. 2010;55:2459-2469
310. Kelion AD, Pakkal MV, Chowdhury FU, Birchall JD, Dixon KL, Lai FY, Kelly DJ, Flather M, McCann GP, Gershlick AH. Ischemia and infarction in stemi patients with multivessel disease: Insights from the cvlprit nuclear substudy. *J Am Coll Cardiol*. 2016;67:2698-2699
311. Amado LC, Gerber BL, Gupta SN, Rettmann DW, Szarf G, Schock R, Nasir K, Kraitchman DL, Lima JA. Accurate and objective infarct sizing by contrast-enhanced magnetic resonance imaging in a canine myocardial infarction model. *J Am Coll Cardiol*. 2004;44:2383-2389
312. Mehran R, Rao SV, Bhatt DL, Gibson CM, Caixeta A, Eikelboom J, Kaul S, Wiviott SD, Menon V, Nikolsky E, Serebruany V, Valgimigli M, Vranckx P, Taggart D, Sabik JF, Cutlip DE, Krucoff MW, Ohman EM, Steg PG, White H. Standardized bleeding definitions for cardiovascular clinical trials: A consensus report from the bleeding academic research consortium. *Circulation*. 2011;123:2736-2747
313. Wu E, Ortiz JT, Tejedor P, Lee DC, Bucciarelli-Ducci C, Kansal P, Carr JC, Holly TA, Lloyd-Jones D, Klocke FJ, Bonow RO. Infarct size by contrast enhanced cardiac magnetic resonance is a stronger predictor of outcomes than left ventricular ejection fraction or end-systolic volume index: Prospective cohort study. *Heart*. 2008;94:730-736
314. Hahn J-Y, Song YB, Gwon H-C, Choe YH, Kim JH, Sung J, Choi S-H, Choi JH, Kim DK, Hong KP, Park JE, Lee SH. Relation of left ventricular infarct transmuralty and infarct size after primary percutaneous coronary angioplasty to time from symptom onset to balloon inflation. *Am J Cardiol*. 2008;102:1163-1169
315. Gershlick AH, Khan JN, Kelly DJ, Greenwood JP, Sasikaran T, Curzen NP, Blackman D, Dalby M, Fairbrother K, Banya W, Wang D, Flather M, Hetherington SL, Kelion A, Talwar S, Gunning M,

- Hall R, Swanton H, McCann GP. Randomised trial of complete versus lesion only revascularisation in patients undergoing primary percutaneous coronary intervention for st elevation myocardial infarction and multi-vessel disease: The complete versus lesion-only primary pci trial (cvlprit). *Journal of the American College of Cardiology (Accepted for publication)*. 2015
316. Alcock RF, Roy P, Adorini K, Lau GT, Kritharides L, Lowe HC, Brieger DB, Freedman SB. Incidence and determinants of myocardial infarction following percutaneous coronary interventions according to the revised joint task force definition of troponin t elevation. *Int J Cardiol*. 2010;140:66-72
 317. Selvanayagam JB, Cheng aSH, Jerosch-Herold M, Rahimi K, Porto I, van Gaal W, Channon KM, Neubauer S, Banning aP. Effect of distal embolization on myocardial perfusion reserve after percutaneous coronary intervention: A quantitative magnetic resonance perfusion study. *Circulation*. 2007;116:1458-1464
 318. Taylor AJ, Al-Saadi N, Abdel-Aty H, Schulz-Menger J, Messroghli DR, Gross M, Dietz R, Friedrich MG. Elective percutaneous coronary intervention immediately impairs resting microvascular perfusion assessed by cardiac magnetic resonance imaging. *Am Heart J*. 2006;151:891 e891-897
 319. De Bruyne B, Pijls NH, Kalesan B, Barbato E, Tonino PA, Piroth Z, Jagic N, Mobius-Winkler S, Rioufol G, Witt N, Kala P, MacCarthy P, Engstrom T, Oldroyd KG, Mavromatis K, Manoharan G, Verlee P, Frobert O, Curzen N, Johnson JB, Juni P, Fearon WF. Fractional flow reserve-guided pci versus medical therapy in stable coronary disease. *NEJM*. 2012;367:991-1001
 320. Mahmarian JJ, Dakik HA, Filipchuk NG, Shaw LJ, Iskander SS, Ruddy TD, Keng F, Henzlova MJ, Allam A, Moye LA, Pratt CM. An initial strategy of intensive medical therapy is comparable to that of coronary revascularization for suppression of scintigraphic ischemia in high-risk but stable survivors of acute myocardial infarction. *JACC*. 2006;48:2458-2467
 321. Mather AN, Fairbairn TA, Artis NJ, Greenwood JP, Plein S. Timing of cardiovascular mr imaging after acute myocardial infarction: Effect on estimates of infarct characteristics and prediction of late ventricular remodeling. *Radiology*. 2011;261:116-126
 322. Baran I, Ozdemir B, Gullulu S, Kaderli AA, Senturk T, Aydinlar A. Prognostic value of viable myocardium in patients with non-q-wave and q-wave myocardial infarction. *The Journal of international medical research*. 2005;33:574-582
 323. Nijland F, Kamp O, Verhorst PM, de Voogt WG, Visser CA. In-hospital and long-term prognostic value of viable myocardium detected by dobutamine echocardiography early after acute myocardial infarction and its relation to indicators of left ventricular systolic dysfunction. *Am J Cardiol*. 2001;88:949-955
 324. Choi KM, Kim RJ, Gubernikoff G, Vargas JD, Parker M, Judd RM. Transmural extent of acute myocardial infarction predicts long-term improvement in contractile function. *Circulation*. 2001;104:1101-1107
 325. Bodi V, Sanchis J, Lopez-Lereu MP, Losada A, Nunez J, Pellicer M, Bertomeu V, Chorro FJ, Llacer A. Usefulness of a comprehensive cardiovascular magnetic resonance imaging assessment for predicting recovery of left ventricular wall motion in the setting of myocardial stunning. *JACC*. 2005;46:1747-1752
 326. Orii M, Hirata K, Tanimoto T, Shiono Y, Shimamura K, Ishibashi K, Yamano T, Ino Y, Kitabata H, Yamaguchi T, Kubo T, Imanishi T, Akasaka T. Two-dimensional speckle tracking echocardiography for the prediction of reversible myocardial dysfunction after acute myocardial infarction: Comparison with magnetic resonance imaging. *Echocardiography*. 2015;32:768-778
 327. Dall'Armellina E, Karia N, Lindsay AC, Karamitsos TD, Ferreira V, Robson MD, Kellman P, Francis JM, Forfar C, Prendergast BD, Banning AP, Channon KM, Kharbanda RK, Neubauer S, Choudhury RP. Dynamic changes of edema and late gadolinium enhancement after acute myocardial infarction and their relationship to functional recovery and salvage index. *Circulation. Cardiovascular imaging*. 2011;4:228-236
 328. Becker M, Altiok E, Lente C, Otten S, Friedman Z, Adam D, Hoffmann R, Koos R, Krombach G, Marx N, Hoffmann R. Layer-specific analysis of myocardial function for accurate prediction of reversible ischaemic dysfunction in intermediate viability defined by contrast-enhanced mri. *Heart*. 2011;97:748-756

329. Kidambi A, Mather AN, Motwani M, Swoboda P, Uddin A, Greenwood JP, Plein S. The effect of microvascular obstruction and intramyocardial hemorrhage on contractile recovery in reperfused myocardial infarction: Insights from cardiovascular magnetic resonance. *J Cardiovasc Magn Reson*. 2013;15:58
330. Khan JN, Singh A, Nazir SA, Kanagala P, Gershlick AH, McCann GP. Comparison of cardiovascular magnetic resonance feature tracking and tagging for the assessment of left ventricular systolic strain in acute myocardial infarction. *European journal of radiology*. 2015;84:840-848
331. Khan JN, Nazir SA, Horsfield MA, Singh A, Kanagala P, Greenwood JP, Gershlick AH, McCann GP. Comparison of semi-automated methods to quantify infarct size and area at risk by cardiovascular magnetic resonance imaging at 1.5t and 3.0t field strengths. *BMC Res Notes*. 2015;25:52
332. Cerqueira MD, Weissman NJ, Dilsizian V, Jacobs AK, Kaul S, Laskey WK, Pennell DJ, Rumberger JA, Ryan T, Verani MS, American Heart Association Writing Group on Myocardial S, Registration for Cardiac I. Standardized myocardial segmentation and nomenclature for tomographic imaging of the heart. A statement for healthcare professionals from the cardiac imaging committee of the council on clinical cardiology of the american heart association. *Circulation*. 2002;105:539-542
333. Harada T, Ariyoshi N, Shimura H, Sato Y, Yokoyama I, Takahashi K, Yamagata S, Imamaki M, Kobayashi Y, Ishii I, Miyazaki M, Kitada M. Application of akaike information criterion to evaluate warfarin dosing algorithm. *Thrombosis research*. 2010;126:183-190
334. DeLong ER, DeLong DM, Clarke-Pearson DL. Comparing the areas under two or more correlated receiver operating characteristic curves: A nonparametric approach. *Biometrics*. 1988;44:837-845
335. Cho KH, Kim KP, Woo BC, Kim YJ, Park JY, Cho SY, Park SU, Jung WS, Park JM, Moon SK. Relationship between blood stasis syndrome score and cardioankle vascular index in stroke patients. *Evidence-Based Complementary and Alternative Medicine*. 2012;2012:1-7
336. Papavassiliu T, Fluchter S, Haghi D, Suselbeck T, Wolpert C, Dinter D, Kuhl H, Borggrefe M. Extent of myocardial hyperenhancement on late gadolinium-enhanced cardiovascular magnetic resonance correlates with q waves in hypertrophic cardiomyopathy. *JCMR*. 2007;9:595-603
337. Neizel M, Korosoglou G, Lossnitzer D, Kuhl H, Hoffmann R, Ocklenburg C, Giannitsis E, Osman NF, Katus HA, Steen H. Impact of systolic and diastolic deformation indexes assessed by strain-encoded imaging to predict persistent severe myocardial dysfunction in patients after acute myocardial infarction at follow-up. *JACC*. 2010;56:1056-1062
338. Kramer CM, Malkowski MJ, Mankad S, Theobald TM, Pakstis DL, Rogers WJ, Jr. Magnetic resonance tagging and echocardiographic response to dobutamine and functional improvement after reperfused myocardial infarction. *Am Heart J*. 2002;143:1046-1051
339. Cardiology TACo. Choosing wisely. Five things physicians and patients should question. 2014
340. McCann GP, Khan JN, Greenwood JP, Nazir SA, Dalby M, Curzen N, Hetherington SL, Kelly DJ, Blackman D, Ring A, Peebles C, Wong J, Sasikaran T, Flather M, Swanton H, Gershlick AH. The randomised complete versus lesion-only primary pci trial: Cardiovascular mri substudy (cvlprit-cmr) *JACC*. 2015;66:2713-2724
341. Gershlick AH, Khan JN, Kelly DJ, Greenwood JP, Sasikaran T, Curzen N, Blackman DJ, Dalby M, Fairbrother KL, Banya W, Wang D, Flather M, Hetherington SL, Kelion AD, Talwar S, Gunning M, Hall R, Swanton H, McCann GP. Randomized trial of complete versus lesion-only revascularization in patients undergoing primary percutaneous coronary intervention for stemi and multivessel disease: The cvlprit trial. *Journal of the American College of Cardiology*. 2015;65:963-972
342. Ortiz-Perez JT, Lee DC, Meyers SN, Davidson CJ, Bonow RO, Wu E. Determinants of myocardial salvage during acute myocardial infarction: Evaluation with a combined angiographic and cmr myocardial salvage index. *JACC: Cardiovasc Imaging*. 2010;3:491-500
343. Reiter R, Henry TD, Traverse JH. Preinfarction angina reduces infarct size in st-elevation myocardial infarction treated with percutaneous coronary intervention. *Circulation: Cardiovasc Interv*. 2013;6:52-58
344. Prasad A, Rihal CS, Lennon RJ, Singh M, Jaffe AS, Holmes DR. Significance of periprocedural myonecrosis on outcomes after percutaneous coronary intervention: An analysis of

- preintervention and postintervention troponin t levels in 5487 patients. *Circulation. Cardiovascular interventions*. 2008;1:10-19
345. Thygesen K, Alpert JS, White HD. Universal definition of myocardial infarction. *European heart journal*. 2007;28:2525-2538
 346. Selvanayagam JB, Porto I, Channon K, Petersen SE, Francis JM, Neubauer S, Banning AP. Troponin elevation after percutaneous coronary intervention directly represents the extent of irreversible myocardial injury: Insights from cardiovascular magnetic resonance imaging. *Circulation*. 2005;111:1027-1032
 347. Rahimi K, Banning AP, Cheng AS, Pegg TJ, Karamitsos TD, Channon KM, Darby S, Taggart DP, Neubauer S, Selvanayagam JB. Prognostic value of coronary revascularisation-related myocardial injury: A cardiac magnetic resonance imaging study. *Heart*. 2009;95:1937-1943
 348. DOH. Department of health reference costs 2013-14. *Department of Health Publications*. 2014;1-125 (Website: February 2014, Accessed: June 2015)
 349. Mehta S. Complete vs culprit-only revascularization to treat multi-vessel disease after primary pci for stemi (complete, nct01740479). *ClinicalTrials.gov*. 2013;http://clinicaltrials.gov/show/NCT01740479
 350. Manari A, Varani E, Guastaroba P, Menozzi M, Valgimigli M, Menozzi A, Magnavacchi P, Franco N, Marzocchi A, Casella G. Long-term outcome in patients with st segment elevation myocardial infarction and multivessel disease treated with culprit-only, immediate, or staged multivessel percutaneous revascularization strategies: Insights from the real registry. *Catheter Cardiovasc Interv*. 2014;doi: 10.1002/ccd.25374. [Epub ahead of print]
 351. Jeger R, Jaguszewski M, Nallamothu BN, Luscher TF, Urban P, Pedrazzini GB, Erne P, Radovanovic D. Acute multivessel revascularization improves 1-year outcome in st-elevation myocardial infarction: A nationwide study cohort from the amis plus registry. *Int J Cardiol*. 2014;172:76-81
 352. Santos AR, Cordeiro Picarra B, Celeiro M, Bento A, Aguiar J. Multivessel approach in st-elevation myocardial infarction: Impact on in-hospital morbidity and mortality. *Revista portuguesa de cardiologia : orgao oficial da Sociedade Portuguesa de Cardiologia = Portuguese journal of cardiology : an official journal of the Portuguese Society of Cardiology*. 2014;33:67-73
 353. Jaguszewski M, Radovanovic D, Nallamothu BK, Luscher TF, Urban P, Eberli FR, Bertel O, Pedrazzini GB, Windecker S, Jeger R, Erne P. Multivessel versus culprit vessel percutaneous coronary intervention in st-elevation myocardial infarction: Is more worse? *EuroIntervention : journal of EuroPCR in collaboration with the Working Group on Interventional Cardiology of the European Society of Cardiology*. 2013;9:909-915
 354. Lee KH, Choi SI, Chun EJ, Kim JA, Lee MS, Yoon CH, Choi DJ. Aborted myocardial infarction: Evaluation of changes in area at risk, late gadolinium enhancement, and perfusion over time and comparison with overt myocardial infarction. *AJR*. 2012;199:328-335
 355. Kong JA, Chou ET, Minutello RM, Wong SC, Hong MK. Safety of single versus multi-vessel angioplasty for patients with acute myocardial infarction and multi-vessel coronary artery disease: Report from the new york state angioplasty registry. *Coron Artery Dis*. 2006;17:71-75
 356. Cavender MA, Milford-Beland S, Roe MT, Peterson ED, Weintraub WS, Rao SV. Prevalence, predictors, and in-hospital outcomes of non-infarct artery intervention during primary percutaneous coronary intervention for st-segment elevation myocardial infarction (from the national cardiovascular data registry). *Am J Cardiol*. 2009;104:507-513
 357. Zhao W, Bai J, Zhang F, Guo L, Gao W. Impact of completeness of revascularization by coronary intervention on exercise capacity early after acute st-elevation myocardial infarction. *Journal of cardiothoracic surgery*. 2014;9:50
 358. Mohamad T, Bernal JM, Kondur A, Hari P, Nelson K, Niraj A, Badheka A, Hassna S, Kiernan T, Elder MD, Gardi D, Schreiber T. Coronary revascularization strategy for st elevation myocardial infarction with multivessel disease: Experience and results at 1-year follow-up. *American journal of therapeutics*. 2011;18:92-100
 359. Qarawani D, Nahir M, Abboud M, Hazanov Y, Hasin Y. Culprit only versus complete coronary revascularization during primary pci. *Int J Cardiol*. 2008;123:288-292
 360. Rigattieri S, Biondi-Zoccai G, Silvestri P, Di Russo C, Musto C, Ferraiuolo G, Loschiavo P. Management of multivessel coronary disease after st elevation myocardial infarction treated by primary angioplasty. *J Interv Cardiol*. 2008;21:1-7

361. Poyen V, Labrunie P, Silvestri M, Valeix B. [complete revascularisation of multivessel coronary artery disease during acute myocardial infarction. Results following hospitalization and after 30 months. Series of 86 interventions carried out with 167 multivessel disease patients; causes of failure]. *Archives des maladies du coeur et des vaisseaux*. 2003;96:1149-1156
362. Hussain F, Philipp RK, Ducas RA, Elliott J, Dzavik V, Jassal DS, Tam JW, Roberts D, Garber PJ, Ducas J. The ability to achieve complete revascularization is associated with improved in-hospital survival in cardiogenic shock due to myocardial infarction: Manitoba cardiogenic shock registry investigators. *Catheter Cardiovasc Interv*. 2011;78:540-548
363. van der Schaaf RJ, Claessen BE, Vis MM, Hoebers LP, Koch KT, Baan J, Jr., Meuwissen M, Engstrom AE, Kikkert WJ, Tijssen JG, de Winter RJ, Piek JJ, Henriques JP. Effect of multivessel coronary disease with or without concurrent chronic total occlusion on one-year mortality in patients treated with primary percutaneous coronary intervention for cardiogenic shock. *Am J Cardiol*. 2010;105:955-959
364. BHF. British heart foundation statistics website. *BHF 9 A.D. December 16* Available from: URL: <http://www.heartstats.org/topic.asp?id=17> 2009:(Accessed 19 December 2009)
365. Kim RJ, Fieno DS, Parrish TB, Harris K, Chen EL, Simonetti O, Bundy J, Finn JP, Klocke FJ, Judd RM. Relationship of mri delayed contrast enhancement to irreversible injury, infarct age, and contractile function. *Circulation*. 1999;100:1992-2002